EPFL

Thèse n° 9897

# Adaptive algorithms for two fluids flows with anisotropic finite elements and order two time discretizations

Présentée le 27 février 2020

à la Faculté des sciences de base
Groupe Picasso
Programme doctoral en mathématiques

pour l'obtention du grade de Docteur ès Sciences

par

**Samuel DUBUIS**

Acceptée sur proposition du jury

Prof. M. Troyanov, président du jury
Prof. M. Picasso, directeur de thèse
Prof. E. Burman, rapporteur
Dr A. Loseille, rapporteur
Prof. S. Deparis, rapporteur

École
polytechnique
fédérale
de Lausanne

2020

"*I love it when a plan comes together...*"
— John "Hannibal" Smith

A mes parents et mes grands-parents...

# Remerciements

"*Happiness is only real when shared.*"
— Christopher McCandless

Il y a en général beaucoup de raisons de le dire et beaucoup de personnes à qui le dire, mais il n'y a qu'un mot pour l'exprimer : merci. 5 ans de travail de thèse, c'est avant tout de très nombreuses et belles rencontres, et encore plus de personnes sans qui ce travail n'aurait jamais abouti.

Tout d'abord, j'aimerais remercier le Prof. Marco Picasso, sans qui rien de tout cela n'aurait été possible. Il m'a offert la possibilité d'effectuer un travail de recherche dans un domaine passionnant, et malgré nos divergences sur de nombreux points de la philosophie des estimations d'erreur (blague), pour rien au monde je ne referai cette thèse sans lui.

Ensuite, je tiens du fond du coeur à remercier le Prof. Bernard Dacorogna, qui m'a accueilli au milieu de ma thèse dans son groupe, et m'a considéré comme un des ses assistants à part entière. Sans son soutien, et ses conseils, je ne serais jamais arrivé au bout de cette recherche. Finalement, combien même son impact sur ma thèse est implicite, je dois beaucoup au Prof. Philippe Metzener, qui m'a redonné le goût des mathématiques et de la recherche pendant les nombreux travaux de semestre lors desquels il m'a supervisé.

Je remercie sincèrement les membres de mon jury de thèse : le Prof. Marc Troyanov, pour son professionalisme, son calme et les conseils avisés qu'il m'a donné pour l'examen oral et les corrections du document, qui m'ont amené beaucoup de sérénité pendant le dernier rush; le Prof. Erik Burman pour le temps qu'il m'a offert à relire dans les moindres détails ma thèse; le Dr. Adrien Loseille, avec qui j'ai échangé pendant ces 5 ans et qui nous a fourni le mailleur 3D (felfo.a), sans lequel aucune des simulations tridimensionnelle présentées plus loin n'auraient été possibles; le Prof. Simone Deparis, qui a été un appui permanent pendant 5 ans et à qui je dois beaucoup pour l'implémentation des méthodes multipas.

Concernant les aspects scientifiques de mon travail de recherche, je remercie également sincèrement : le Prof. Peter Wittwer qui nous a énormément aidés pour la compréhension physique du problème du disque rigide, ainsi que le Prof. Matthieu Hillairet avec qui j'ai beaucoup échangé sur ce même sujet, des échanges qui nous ont beaucoup aidés dans la compréhension de ce même problème et du résultat qu'il a démontré; le Dr. Frédéric Alauzet qui nous a fourni le programme d'interpolation Wolf-Interpol, sans lequel nous aurions été dans l'incapacité d'implémenter notre algorithme; mon amie et ma collègue Olga, avec qui j'ai travaillé pendant un semestre sur l'adaptation de maillage pour l'équation des ondes et qui m'a amené un regard nouveau sur les estimateurs a posteriori; finalement le Prof. Assyr Abdulle qui a pris le temps de réfléchir à une question posée sur le schéma de Crank-Nicolson, et qui a levé le voile sur un problème important et qui empêchait notre code de tourner. Sans lui, aucune des simulations présentées au chapitre 4 n'auraient pu voir le jour.

Il est temps maintenant de remercier mes collègues, et avant de passer aux membres de mes groupes de recherches et d'enseignement, j'aimerais remercier avant tout les personnes sans qui rien de tout cela ne serait possible, des gens très compétents, mais dont on oublie trop souvent l'importance, les compétences et leur bienveillances. Je tiens sincèrement à remercier mes petites et grandes soeurs du campus : Sara, Virginie, Ariane, Corinne, Annick, Valérie, Carole, Marcia, Samantha, Pierrette, Catherine, Maroussia, Delphine, Anna, Karine, Nadia, Jocelyne et Marie. J'ai toujours trouvé étrange la césure habituellement faite entre personnel scientifique et personnel administratif, mais j'ai toujours considéré les secrétaires du département avant tout comme mes collègues et mes amies, et leur impact sur le bon déroulement de mes 5 ans de doctorat est tout aussi important que celui des gens avec qui j'ai eu des interactions purement mathématiques. Je profite aussi pour remercier les deux informaticiens du département, Marc et Léo, qui sont toujours disponibles et qui m'ont beaucoup aidé pour la logistique de l'examen oral de la thèse.

Puis il y a les membres de mon groupe de recherche (le GR-PI), je crois rarement avoir rencontré des gens aussi extraordinaires : le Prof. Jacques Rappaz, Diane, Thomas, Viljami, Jonathan, Sylvain, Paride, Dimitrios, Emile, Léo, Arwa, Julien, Lionel, Alexandre et Alexandre (ils se reconnaitront). Et tout aussi incroyables (mais pas pour les mêmes raisons, pour reprendre la formulation d'un célèbre mathématicien), les membres du groupe d'enseignement et de la Chaire d'Analyse Appliquée : David, Swarnendu, Saugata, Sébastien. Finalement, il y a tous les collègues et les amis: Pauline, Celia, Buro, Claudia, Bruno, Tarek, Elise, Gauthier, Quentin, Ursina, Val (bravo pour la découverte du trou noir), Orane, Nadine, Béré, Timothée, Matthieu, Adrien, Deep, Kaitlin, Alastair, Lyne, Maude, Yoan, Léo, Ana, Petar et Marie-Hélène. Tous les membres de CQFD et de QED, les Bruces, mes étudiants et les collègues de MATHICSE. Et il y aussi nos amis de Sat, que je remercie pour tous les cafés, les thés, bières qu'ils nous ont offert et qui nous ont aidé à ne pas perdre la boule : Bastien, Vincent, Sonia, Jérémiah, Jean-Luc, Lola, Sarah, Elias. Trop de gens biens pour ne pas en oublier.

Et il y a les amis des études et du collège, toujours là quand on a besoin d'eux : Aleks (merci pour le job sur l'ile), Stan, Léo, Eiichi, Sam B., Rémy "Duck", Jacques, Fabrice, Seb, Dom, Adam, Marin. Mes amies d'aventure dans le train : Rachel, Anne, Elisa et Laetitia.

Finalement, mes amis, coéquipiers, mentors du basket : Monsieur, Super Mez, Franky, Loïc, Jason, Olivier, Serge, Jean-Da, Yves, Laurent, Michel, Ed et Gianluca. Et j'adresse un merci particulier à Corinne, une toute grand dame, qui m'a permis de vivre une aventure extraordinaire en étant son assistant en ligue nationale A féminine, et qui a été très compréhensive et très souple quant à mon emploi du temps quand la fin de la thèse approchait.

Et pour terminer, ceux sans qui ma vie ne serait pas la même et qui chaque jour m'encouragent dans mes choix et me soutiennent depuis toujours : maman, papa, Vanessa, Yanick, Laetitia, Mathias et Thomas.

# Abstract

This thesis is devoted to the derivation of a posteriori error estimates for the numerical approximation of fluids flows separated by a free surface. Based on these estimates, error indicators are introduced and adaptive algorithms are proposed to solve the problem with accuracy and low computational costs. We focus on numerical methods that are combinations of anisotropic finite elements and second order methods to advance in time.

We split the technical difficulties in the derivation of the error estimates by first studying independent PDEs, and in a second time by gathering the different results to analyse the complete system of equations composed with these latter. The a posteriori error analysis for the approximation of these PDEs will be addressed in a particular and devoted chapter. The last chapter is dedicated to the study of the system describing two fluids flows.

In each chapter, we focus on two main objectives. The first is a theoretical analysis and the derivation of error estimates, the second is the description and the implementation of an algorithm to adapt meshes and time steps. Finally, numerical experiments are performed to demonstrate the efficiency of the procedure.

**Keywords:** anisotropic finite elements, second order finite differences methods, a priori and a posteriori error estimates, adaptive algorithms, elliptic equations, transport equation, Stokes and Navier-Stokes equations, non-homogeneous Navier-Stokes equations, fluids flows separated by a free surface

# Résumé

Cette thèse s'intéresse à l'estimation d'erreurs a posteriori pour l'approximation numérique d'écoulements multiphases. Basés sur ces estimations, un algorithme adaptatif est présenté avec pour but de résoudre le problème efficacement, pour le coût de calcul le plus bas possible. Nous nous concentrons sur des méthods numériques qui sont une combinaison d'éléments finits anisotropes et de schémas d'ordre deux en temps.

Nous séparons les différentes difficultés dans le calcul des estimations d'erreurs en étudiant dans un premier temps chaque équation indépendemment dans un chapitre dédié, puis en réunissant les résultats obtenus dans l'analyse du système non linéaire complet.

Dans chaque chapitre, nous nous fixons deux objectifs. Le premier est une étude théorique, le deuxième est la description et l'implémentation d'un algorithme pour adapter les maillages et les pas de temps. Des expériences numériques sont présentées pour illustrer les performances de l'algorithme.

**Mots-clefs:** éléments finis anisotropes, méthods de différences finies d'ordre deux, estimations d'erreurs a priori et a posteriori, algorithmes adaptatifs, équations elliptiques, équation du transport, équations de Stokes et Navier-Stokes, équations de Navier-Stokes non homogènes, écoulements de fluides séparés par une surface libre.

# Contents

# Introduction

### General outlook on numerical analysis, errors estimates and adaptive algorithm

Most physical phenomena can be modeled by Partial Differential Equations (PDEs). From an abstract point of view, a PDE can be written as

$$F(u) = 0, \tag{1}$$

where $u$ is an unknown that we look for in a particular functional space $V$ (in general of infinite dimension) and $F$ is a differential operator.

For instance, one may be interested in knowing the distribution of heat in a metal bar by solving the *Laplace* equation

$$-\Delta u = f,$$

in computing the transport of a chemical pollutant in a river by studying the *advection* equation

$$\frac{\partial \varphi}{\partial t} + \mathbf{u} \cdot \nabla \varphi = 0,$$

or in forecasting the flow of that same river by solving the *Navier-Stokes* equations

$$\rho \frac{\partial \mathbf{u}}{\partial t} + \rho(\mathbf{u} \cdot \nabla)\mathbf{u} - \mu \Delta \mathbf{u} + \nabla p = \mathbf{f}.$$

Of course, one may be interested also in any physical situation that is described by a dynamical system built from the above equations.

Finding the solutions of such equations, or even sometimes only proving that such solutions exist, may be a really tough work. For some problems there are still open, important and widely studied questions (1 million dollars price is promised to who can close the debate for the strong solutions to the Navier-Stokes equations). Therefore, one may use numerical methods to approximate these solutions.

A numerical method is composed with a *discretization* parameter $h$, a finite dimensional subspace (often so-called *discrete* subspace) $V_h \subset V$ and a discrete differential operator $F_h$. Rather than looking for a solution of (1), one may look for a discrete solution $u_h \in V_h$ of the finite dimensional problem

$$F_h(u_h) = 0. \tag{2}$$

The main advantage of the equation (2) compared to (1) is that it reduces in fact to a system of algebraic equations, that can be implemented and solved using a computer program and (up to wait for a couple of hours) are solvable. Its main drawback is of course that we do not obtain the *exact* solution $u$ but only an *approximation*, that we hope to be accurate.

The goal of numerical *analysis* is to study how far the approximated solution $u_h$ is from $u$. In fact, we would like to prove that if we choose $h$ such that $V_h \to V$, then $u_h \to u$. In this case, we say that the numerical method *converges*. Most of the time, we show the convergence of a numerical method by proving a so-called **a priori** error estimate. Let us equip the functional space $V$ with a norm $\|\cdot\|$. Proving an a priori error estimate between $u$ and $u_h$, that are the solutions of the equation (1) and its approximation (2), consists to show that there exists a quantity $\varepsilon = \varepsilon(u, h)$ such that

$$\|u - u_h\| \leq \varepsilon. \tag{3}$$

If $\varepsilon \to 0$ as $h \to 0$ (it is common that convergence occurs when the discretization parameter is taken smaller and smaller), then we have proven the convergence of the method (of course we must assume before that the exact solution $u$ exists, but this is an other story.)

Observe that the a priori error estimate (3) replies to the question "Does my method converge ?", but does not give any information about "How close from $u$ is $u_h$ ?" since the error $\|u - u_h\|$ is bounded by a quantity that is not computable. Indeed, $\varepsilon$ depends on $u$, that we do not know a priori. However, one may be interested to provide a *computable* estimate of the numerical error. This is the goal of the so-called **a posteriori** error estimates that consist to derive a *computable* quantity $\eta = \eta(u_h, h)$ such that $\eta \to 0$ as $h \to 0$ and

$$\|u - u_h\| \simeq \eta. \tag{4}$$

With the existence of such $\eta$ (we call it an error estimator), we can play the following game. Imagine that we would like to find an approximated solution $u_h$ that is at a distance close to a preset tolerance $TOL$ from $u$, i.e. we would like to compute $u_h$ such that

$$\|u - u_h\| \simeq TOL.$$

But in the same time, we would like that the cost of computing such as $u_h$ is the lowest possible, i.e. the size of the corresponding discrete space $V_h$ is the smallest possible. We can then proceed in the following way: let us start with a initial discretization parameter $h_0$, let us solve the discrete PDE

$$F_{h_0}(u_{h_0}) = 0$$

and then compute the error estimator $\eta_0 = \eta(u_{h_0}, h_0)$. If $\eta_0 \gg TOL$, then we may change $h_0$ and choose a smaller $h_1$ (we do not focus on how we do it at the moment) and then solve again the approximated equation (2) with $h = h_1$. If $\eta_0 \ll TOL$, then we do the same but choosing a larger $h_1$, so that the new space $V_{h_1}$ is "smaller". We can iterate the process until we reach a $h_N$ and a $u_{h_N}$ such that $\eta_N \simeq TOL$ which implies, by (4), that

$$\|u - u_{h_N}\| \simeq TOL,$$

and the size of $V_{h_N}$ is "not too large". Such an iterative process is called an **adaptive** algorithm, since the discretization parameter $h$ is adapted until we fit a certain criterion.

### Objectives of the thesis

The purpose of the present work is to propose an adaptive space-time method to compute the flow of two incompressible, immiscible and Newtonian fluids that are separated by a free surface (see equations (5) below). Many examples of two fluids flows can be found in nature: waves at the surface of the ocean, blood circulation, octopus ink jets, supernova explosion or oil flowing into water. One may also encounter such flows in industrial applications such as chemical dissolution of aluminium, see for instance [55] and [93].

Let us consider a cavity $\Omega \in \mathbb{R}^d$, $d = 2, 3$, that is filled with two incompressible, immiscible and Newtonian fluids, characterized by their respective velocity $\mathbf{u}_i \in \mathbb{R}^d$, pressure $p_i \in \mathbb{R}$, density $\rho_i \in \mathbb{R}$ and viscosity $\mu_i \in \mathbb{R}$, $i = 1, 2$. At any time $t$, $\Omega$ can be split into two subdomains $\Omega_1(t)$ and $\Omega_2(t)$ that contain each fluid and that are separated by the surface $\Sigma(t)$. The initial velocity $\mathbf{u}(0)$ as the location of $\Sigma(0)$ are known. The situation is drawn in the Figure 1.

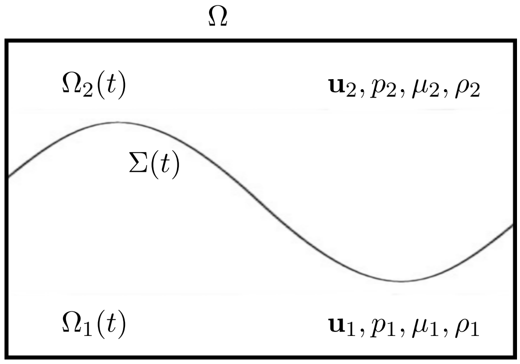


Figure 1: The two fluids flow separated by the free surface $\Sigma(t)$.

In each subdomain $\Omega_i$, the motion of the fluid is driven by the incompressible Navier-Stokes equations

$$\rho_i \frac{\partial}{\partial t}\mathbf{u}_i + \rho_i(\mathbf{u}_i \cdot \nabla)\mathbf{u}_i - \mu_i \Delta \mathbf{u}_i + \nabla p_i = \rho_i \mathbf{g}, \quad \operatorname{div} \mathbf{u}_i = 0,$$

where $\mathbf{g}$ is the gravitation field. Defining the global quantities,

$$\mathbf{u}, p, \rho, \mu = \begin{cases} \mathbf{u}_1, p_1, \rho_1, \mu_1 \text{ in } \Omega_1, \\ \mathbf{u}_2, p_2, \rho_2, \mu_2 \text{ in } \Omega_2, \end{cases}$$

one can describe the global motion of the fluids by the Navier-Stokes equations for non-homogeneous fluids

$$\rho \frac{\partial}{\partial t}\mathbf{u} + \rho(\mathbf{u} \cdot \nabla)\mathbf{u} - \operatorname{div}(2\mu D(\mathbf{u})) + \nabla p = \rho \mathbf{g}, \quad \operatorname{div} \mathbf{u} = 0.$$

These equations are coupled with boundary conditions at the interface $\Sigma$. One may require continuity of the velocity fields across the interface as the continuity of the force, which corresponds to neglect the effects of the surface tension.

In order to describe the evolution of the interface $\Sigma(t)$, we consider the piecewise constant function $\varphi$ that is defined for any $(\mathbf{x}, t) \in \Omega \times [0, \infty)$ by

$$\varphi(\mathbf{x}, t) = \begin{cases} 1, & \mathbf{x} \in \Omega_1(t), \\ 0, & \mathbf{x} \in \Omega_2(t). \end{cases}$$

$\Sigma(t)$ is identified at each time $t$ by the set of points where $\varphi$ is discontinuous. Given the initial condition $\varphi(0)$, $\varphi$ is transported by the velocity field and thus satisfies the conservative equation

$$\frac{\partial \varphi}{\partial t} + \mathbf{u} \cdot \nabla \varphi = 0.$$

In practice, one may consider a "smooth" version of $\varphi$, taking values 0 or 1, excepted in a small region where the function has strong gradients. Then, the interface $\Sigma(t)$ is approached by the set

$$\{\mathbf{x} \in \Omega : \varphi(\mathbf{x}, t) = 0.5\}.$$

The complete system of equations we are studying in this work is then

$$\begin{cases} \rho\dfrac{\partial \mathbf{u}}{\partial t} + \rho(\mathbf{u}\cdot\nabla)\mathbf{u} - \operatorname{div}(2\mu D(\mathbf{u})) + \nabla p = \rho\mathbf{g}, \\ \operatorname{div}\mathbf{u} = 0, \\ \dfrac{\partial \varphi}{\partial t} + \mathbf{u}\cdot\nabla\varphi = 0, \\ \rho = \rho_1\varphi + \rho_2(1-\varphi), \\ \mu = \mu_1\varphi + \mu_2(1-\varphi), \\ \mathbf{u}(0) = \mathbf{u}_0, \varphi(0) = \varphi_0. \end{cases} \tag{5}$$

Equations (5) are approximated by using Finite Elements to discretize the space variables and with Finite Differences to advance in time. Throughout this work, we focus on piecewise linear, continuous, **anisotropic** (we will precise the sense in a few lines) finite elements methods and **second order** advancing scheme such as the Crank-Nicolson or the BDF2 methods. We focus on the a posteriori analysis of these methods with the goal to derive space-time a posteriori error estimates. In the next paragraphs, we give a quick overview on the former contributions, and those presented in this work.

The story of a posteriori error estimation starts in the late 70's with the work of Babushka and Rheinboldt [10], where they derive a residual-based error estimate for finite elements, introducing the numerical study of error estimators [9], adaptive mesh refinements techniques [8, 95, 104] and convergence of adaptive algorithms [39, 42] to solve fine scale problems with accuracy and low computational costs. Reviews of the known techniques for a posteriori error derivations can be found for instance in the works of Verfürth [102, 105], Ainsworth and Oden [1] or in [13] in the framework of Computational Fluid Dynamics.

Most of the classical references about a posteriori error estimates for finite elements methods (or finite differences schemes) focus on linear, elliptic or parabolic equations with constant coefficients. Less works were dedicated to the cases of *nonlinear* [4, 25, 79, 103, 106] or *hyperbolic* equations [26, 36, 81, 98, 20] or PDEs with *variable* coefficients [15, 54], and, up to our knowledge, even less to problems involving these three aspects. If we look at the equations (5) and we apply to them any finite elements or finite differences methods, we can encounter, among other, four technical difficulties when performing the a posteriori error analysis. Each of them will be addressed in a particular chapter.

**A coupled nonlinear system** The system (5) is fully nonlinear, due to the coupling of the Navier-Stokes equations with the transport equation. Before deriving an a posteriori estimate that combines the errors coming from the momentum equation *and* from the conservation equation, we should study these problems separately.

**The Navier-Stokes equations** The Navier-Stokes equations are themselves nonlinear due to the convective term $(\mathbf{u}\cdot\nabla)\mathbf{u}$ that requires a particular treatment for deriving the error estimates. An other issue is the difficulty to link the pressure errors to the velocity errors for the time dependent (Navier-)Stokes equations.

**Hyperbolicity and transport** The transport equation is an hyperbolic equation that requires stabilization techniques when finite elements are used, making appear additional terms in the estimates.

**Variable coefficients** For both equations, their respective coefficients ($\rho$ and $\mu$ for Navier-Stokes equations, $\mathbf{u}$ for the transport one,) are functions that can vary in space and in time.

Most of a posteriori error estimates for time dependent problems were derived in the framework of **isotropic** finite elements and first order time advancing schemes [14, 16, 82, 101]. In this work, we propose to treat the four issues presented before when anisotropic finite elements and second order time discretization methods are used.

Isotropic meshes are a particular type of triangulation where flat triangles are not allowed. Roughly speaking, we can think of an isotropic mesh as composed with only almost equilateral triangles. The classical theory of finite elements methods was developed on such meshes [34], due to the fact that the constants involved in the standard interpolation estimates depend on the mesh aspect ratio. However, anisotropic finite elements, with very stretched triangles, are more general and are widely used in practice, but the theoretical framework is less developed. Yet the first attempt to get rid of the isotropic assumptions underlying the classical theory dates back already to the 70's [7]. Since 2000, new theoretical frameworks have been introduced [63, 44, 45], allowing to rewrite the classical finite elements theory for almost any type of meshes, with very weak hypothesis.

Anisotropic adaptive meshes have been proved to be extremely efficient for PDEs with free boundaries or boundary layers, in particular in computational fluid dynamics [6, 29, 37]. Very stretched triangles are allowed, thus accuracy is reached at lower cost. However, in most of the cases the adaptive criteria are based on heuristics or interpolation error estimates, rather than rigorous a posteriori error bounds. This is particularly the case when time dependent hyperbolic equations are involved, since few a posteriori estimates are available[36]. Lately, reliable anisotropic a posteriori error estimates were proven for a wide ranges of PDEs: elliptic equations [84, 87], parabolic equations [72, 85], convection-diffusion-reaction equations [18, 47, 90], transport and wave equations [51, 88, 20], Stokes equations [46, 86].

A posteriori error analysis for second order time discretization of parabolic problems has been proposed in [3] and [72] where, with different approaches, the authors derived a posteriori error estimates for the Crank-Nicolson method. This was extended to the case of fully discrete estimates, where both space and time discretizations are taken in account, for instance in [24] for isotropic meshes, and already in [72], where anisotropic finite elements are used. The results of [72] for anisotropic meshes and the Crank-Nicolson methods were adapted to convection-diffusion equations [90], the transport equations [41] and the wave equation [51, 73], and then used to design space-time adaptive algorithms. The techniques described in [3] and [72] were also adapted for the BDF2 method and a posteriori error estimates were derived for parabolic problems [2] and the Stokes equations [23]

## Outline

In this thesis, we approximate the solutions of (5) using a combination of continuous, piecewise linear, anisotropic finite elements and second order in time methods. Moreover, we will introduce a adaptive strategy to obtain a suitable sequences of meshes and time steps in order to maintain accuracy, while decreasing the computational cost.

The outline of the work is the following. In **Chapter 1**, we study elliptic problems with **variable coefficients**. We focus on the Poisson equation

$$-\operatorname{div}(\mu\nabla u) = f,$$

where $\mu$ is a smooth function with strong gradients. Anisotropic finite elements are used to approximate $u$. We introduce the theoretical framework of anisotropic meshes, and we prove both a priori (Theorem 1.8) and a posteriori error estimates (Theorem 1.11) for our particular numerical method. Finally, we describe the adaptive algorithm and the mesh refinement/coarsening procedure that we will be used in this thesis.

In **Chapter 2**, we focus on the **transport equation**

$$\frac{\partial \varphi}{\partial t} + \mathbf{u} \cdot \nabla \varphi = 0,$$

where the velocity field can vary in space and in time. We approximate the solution using continuous, piecewise linear, anisotropic finite elements and the Crank-Nicolson scheme and we perform the a priori and a posteriori error analysis (Theorems 2.51 and 2.55). In particular, we prove an a posteriori error estimate that involves the space and the time discretization. Then we describe the strategy to adapt the mesh and the time step.

In **Chapter 3**, we study the **Navier-Stokes equations**. We first focus on the steady Navier-Stokes equations and on the time dependent Stokes equations, before carrying our attention on the time dependent Navier-Stokes problem. We present a numerical method using anisotropic finite elements and the BDF2 method, and we prove so-called *semi-discrete* a posteriori error estimates, that is say error estimates involving the space (Theorem 3.49) **or** the time approximations (Theorem 3.57). Finally, we present for vector valued equations the equivalent of the adaptive algorithm introduced in Chapter 2.

To conclude, in **Chaper 4**, we consider the **coupled system** and perform the a posteriori error analysis of the two fluids flow equations (5). We introduce an adaptive procedure that we apply to some physical phenomena. Chapter 4 is split into two parts. First, we study the approximation of the equations (5) and we prove semi-discrete a posteriori error estimates (Theorems 4.14 and 4.21). Secondly, we focus on an example of the motion of rigid bodies into incompressible fluids, that can be seen as a limit case of (5). Other semi-discrete a posteriori error estimates are proven for this particular model (Theorems 4.31 and 4.29).

# Chapter 1

# An adaptive algorithm with anisotropic finite elements for elliptic problems with variable coefficient

In this chapter, we study an elliptic equation with variable diffusion coefficient that we will use as a toy problem to understand fluids equations with variable viscosity. We want to solve

$$-\operatorname{div}(\mu \nabla u) = f,$$

where $\mu$ is a smooth function that may exhibit strong variations in localized regions. To capture this phenomenon, we propose to use anisotropic finite elements.

The objectives of the chapter are the following:

- To introduce the theoretical framework of anisotropic meshes and finite elements.
- To present a numerical method and prove *a priori* and *a posteriori* error estimates that are valid for anisotropic meshes.
- To propose and to validate an adaptive algorithm to solve the equation.

The outline is the following: in Section 1.1, we briefly introduce the theory of anisotropic finite elements that will be used throughout this document. In particular, we present the discrepancy with the classical interpolation error estimates derived for isotropic meshes. In Section 1.2, we present a numerical method that uses continuous, piecewise linear finite elements on anisotropic meshes, and we prove error estimates. The main result is the Theorem 1.11 that contains an a posteriori error estimate.

In Section 1.3, we define an error indicator and we study its accuracy on prescribed meshes. Finally, in Section 1.4, we describe an adaptive algorithm and we check its efficiency in Sections 1.5 and 1.6 for 2D and 3D problems.

## 1.1 A brief journey through anisotropic finite elements

Let $\Omega \in \mathbb{R}^d, d = 2$ (resp. 3), be a convex polygon (resp. polyhedron). For any $h > 0$, we note $\mathcal{T}_h$ any conformal triangulation (or mesh) of $\overline{\Omega}$ into triangles (resp. tetrahedrons) $K$ of diameter $h_K \leq h$. One quantity that will be important throughout all this work is the so-called (mesh) aspect ratio $ar_K$ that is defined for every $K \in \mathcal{T}_h$ as

$$ar_K = \frac{h_K}{\rho_K}$$

where $\rho_K$ is the diameter of the largest ball inscribed in $K$. In the classical finite elements theory [34], it is assumed that $\mathcal{T}_h$ is "shape regular" that is to say the aspect ratio is uniformly bounded for all $K \in \mathcal{T}_h$. More precisely, we say that that the triangulation is shape regular if there exists a constant $c > 0$ such that for every $h > 0$ and for every $K \in \mathcal{T}_h$

$$ar_K = \frac{h_K}{\rho_K} \leq c. \tag{1.1}$$

This latter condition is equivalent and often referred to as the minimal angle condition, that is to say there exists a constant $\alpha_0 > 0$ such that, for all $h > 0$ and for every triangle (or tetrahedron) $K \in \mathcal{T}_h$, its minimum angle $\alpha_K$ satisfies $\alpha_K \geq \alpha_0$.

The condition (1.1) implies that if we refine the mesh, then it must be refined in such way that the aspect ratio remains bounded. When working with shape regular meshes, the classical finite elements theory implies that all the constants involved in interpolation error estimates depend on the aspect ratio. Therefore the interpolation error may be important if $c$ is large.

To avoid too large constants in the interpolation estimates, one may choose a particular case of shape regular meshes that is to say isotropic meshes. We say that a mesh or a triangulation is isotropic if its aspect ratio is small. This implies that the mesh size is roughly speaking the same in any directions. The main drawback of isotropic meshes is that then stretch or very flat triangles (tetrahedrons) are not allowed, which is not suited when boundary layers are involved.

However, even if they are rejected by the classical shape regular theory, in practice anisotropic meshes, that is to say meshes where some triangles can exhibit large aspect ratio, are widely used when the solution is itself anisotropic. To give a theoretical support to the use of such meshes, a new framework is introduced, in which interpolation error estimates independent of $ar_K$ can be proven. We briefly recall the theoretical aspects developped in [44, 45, 78]. Similar results can be found in [63]. For simplicity, we present it in a two dimensional framework, but the considerations that follow can be easily adapted to the three dimensional case.

Let us note $\hat{K}$ the reference triangle. For any $K \in \mathcal{T}_h$ we note $T_K : \hat{K} \to K$ the affine transformation mapping the reference triangle $\hat{K}$ into $K$ defined by

$$\mathbf{x} = T_K(\hat{\mathbf{x}}) = M_K\hat{\mathbf{x}} + \mathbf{t}_K,$$

where $M_K \in \mathbb{R}^{2\times 2}$ and $\mathbf{t}_K \in \mathbb{R}^2$. One may observe that $M_K$ is invertible, so it admits a singular value decomposition $M_K = R_K^T \Lambda_K P_K$, where $R_K$ and $P_K$ are orthogonal matrices and

$$\Lambda_K = \begin{pmatrix} \lambda_{1,K} & 0 \\ 0 & \lambda_{2,K} \end{pmatrix}, \quad \lambda_{1,K} \geq \lambda_{2,K} \geq 0, \qquad R_K = \begin{pmatrix} \mathbf{r}_{1,K}^T \\ \mathbf{r}_{2,K}^T \end{pmatrix}.$$

In the above notations, $\mathbf{r}_{1,K}, \mathbf{r}_{2,K}$ are the unit vectors corresponding to the directions of maximum and minimum stretching, respectively, so that $\lambda_{1,K}, \lambda_{2,K}$ correspond to the value of the maximum and the minimum stretching. Geometrical interpretations of the linear transformation $T_K$ and its singular values decomposition are described in Figure 1.1 when the reference triangle $\hat{K}$ is the usual reference element of vertices $(0,0), (1,0), (0,1)$ and in Figure 1.2 when $\hat{K}$ is chosen as the unit equilateral triangle.

We now give more details on the geometrical interpretation of $\lambda_{1,K}$ and $\lambda_{2,K}$. One can prove [45] that there exists constants $C_1, C_2 > 0$, that depend only on the reference

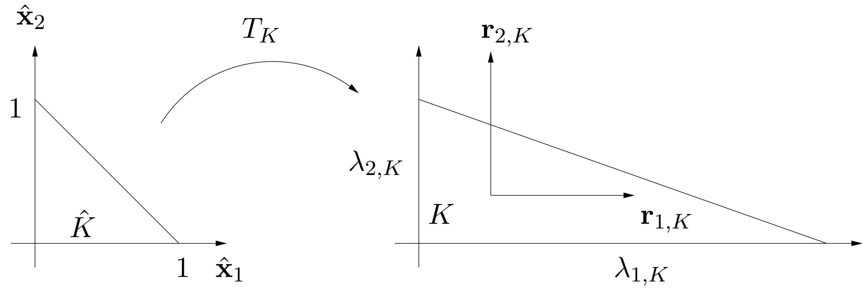


Figure 1.1: Transformation $T_K$ mapping the usual reference element $\hat{K}$ into a right triangle $K$. The reference triangle is stretched in the direction $\mathbf{r}_{1,K}$ (resp. $\mathbf{r}_{2,K}$), with an amplitude $\lambda_{1,K}$ (resp. $\lambda_{2,K}$).

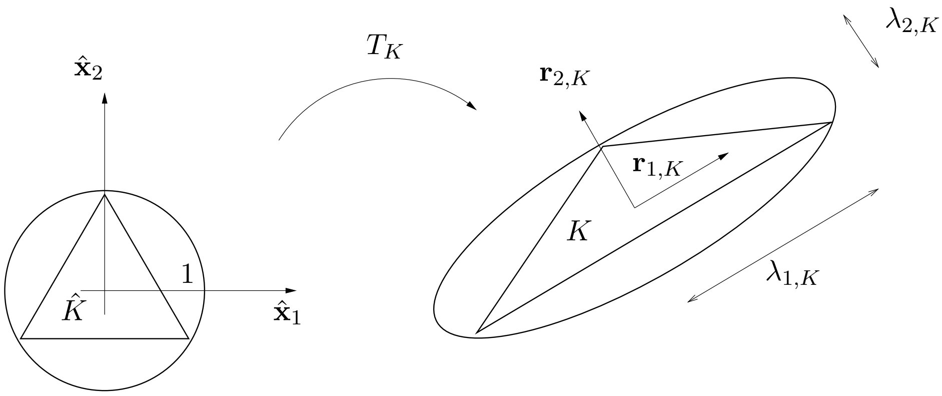


Figure 1.2: Transformation $T_K$ when the reference element $\hat{K}$ is the unit equilateral triangle. The unit circle is mapped into an ellipse of major axis, respectively minor axis, $\lambda_{1,K}\mathbf{r}_{1,K}$, respectively $\lambda_{2,K}\mathbf{r}_{2,K}$.

triangle $\hat{K}$, such that for all $K \in \mathcal{T}_h$

$$C_1 h_K \leq \lambda_{1,K} \leq C_2 h_K, \quad C_1 \rho_K \leq \lambda_{2,K} \leq C_2 \rho_K,$$

such that, roughly speaking, $\lambda_{1,K}$ is the diameter of $K$ and $\lambda_{2,K}$ is the diameter of the inscribed circle in $K$. Consequently one have that

$$\frac{C_1}{C_2}\frac{h_K}{\rho_K} \leq \frac{\lambda_{1,K}}{\lambda_{2,K}} \leq \frac{C_2}{C_1}\frac{h_K}{\rho_K},$$

and therefore the ratio $\lambda_{1,K}/\lambda_{2,K}$ can be interpreted as the aspect ratio $ar_K = h_K/\rho_K$.

Now, let $r_h$ be the linear Lagrange interpolant defined on $\mathcal{T}_h$. The following interpolation result holds.

**Proposition 1.1** (Anisotropic Lagrange interpolation error estimate [44, 45])**.**
*There exists a constant $C > 0$ depending only the reference triangle $\hat{K}$, in particular independent of the mesh aspect ratio, such that for all $K \in \mathcal{T}_h$ and for any $v \in H^2(\Omega)$*

$$\|v - r_h(v)\|^2_{L^2(K)} + \frac{\lambda^3_{2,K}}{\lambda^2_{1,K} + \lambda^2_{2,K}}\|v - r_h(v)\|^2_{L^2(\partial K)} + \lambda^2_{2,K}\|\nabla(v - r_h(v))\|^2_{L^2(K)} \leq C L^2_K(v), \quad (1.2)$$

*with*

$$L_K^2(v) = \lambda_{1,K}^4 \int_K (\mathbf{r}_{1,K}^T H(v)\mathbf{r}_{1,K})^2 d\mathbf{x} + \lambda_{1,K}^2\lambda_{2,K}^2 \int_K (\mathbf{r}_{1,K}^T H(v)\mathbf{r}_{2,K})^2 d\mathbf{x} + \lambda_{2,K}^4 \int_K (\mathbf{r}_{2,K}^T H(v)\mathbf{r}_{2,K})^2 d\mathbf{x},$$

*where $H(v)$ is the Hessian matrix given by*

$$H(v) = \begin{pmatrix} \dfrac{\partial^2 v}{\partial x_1^2} & \dfrac{\partial^2 v}{\partial x_1 \partial x_2} \\ \dfrac{\partial^2 v}{\partial x_1 \partial x_2} & \dfrac{\partial^2 v}{\partial x_2^2} \end{pmatrix}.$$

For shape regular meshes, the classical Lagrange interpolation error estimates reads

$$\|v - r_h(v)\|_{L^2(K)}^2 + h_K\|v - r_h(v)\|_{L^2(\partial K)}^2 + h_K^2\|\nabla(v - r_h(v))\|_{L^2(K)}^2 \leq Ch_K^4\|v\|_{H^2(K)}^2,$$

where the constant $C$ may depend on the aspect ratio, see [34] for instance. In the estimate (1.2), the constant depends only on the reference triangle and therefore is independent of the mesh aspect ratio. Observe moreover that the estimate (1.2) gives a theoretical explanation to the good results obtained when using anisotropic meshes for anisotropic functions. Indeed, assume that the function $v$ depends only on the $x_2$ variable, and that we align the mesh with the solution, so that $\mathbf{r}_{1,K} = (1, 0)$ and $\mathbf{r}_{2,K} = (0, 1)$ (see Figure 1.3). Then the estimate (1.2) implies that there exists $C$ independent of the aspect ratio such that

$$\|v - r_h(v)\|_{L^2(K)}^2 \leq C\lambda_{2,K}^4 \int_K (\mathbf{r}_{2,K}^T H(v)\mathbf{r}_{2,K})^2 d\mathbf{x},$$

$$\|v - r_h(v)\|_{L^2(\partial K)}^2 \leq C(\lambda_{1,K}^2 + \lambda_{2,K}^2)\lambda_{2,K} \int_K (\mathbf{r}_{2,K}^T H(v)\mathbf{r}_{2,K})^2 d\mathbf{x},$$

$$\|\nabla(v - r_h(v))\|_{L^2(K)}^2 \leq C\lambda_{2,K}^2 \int_K (\mathbf{r}_{2,K}^T H(v)\mathbf{r}_{2,K})^2 d\mathbf{x}.$$

Consequently, it is sufficient that $\max_{K\in\mathcal{T}_h} \lambda_{2,K}$ goes to 0 for $r_h(v)$ to converge to $v$.

Our work is mainly concerned with deriving a posteriori error estimates in the context of anisotropic finite elements. To this end, we will need the use of Clément's interpolant [35] and therefore some additional assumptions must be done in order to ensure that the constants involved in the interpolation estimates will not depend on the mesh aspect ratio:

***(i)*** **Number of neighbours** For each vertex of the triangulation $\mathcal{T}_h$, its number of neighbours is bounded from above, uniformly with respect to $h$.

***(ii)*** **Diameter of the reference patch** For each $K$, the diameter of $\Delta\hat{K} = T_K^{-1}(\Delta K)$, where $\Delta K$ is the union of triangles sharing a vertex with $K$, is uniformly bounded, independently of the mesh geometry.

In particular, the second hypothesis above excludes too distorted meshes as presented in Figure 1.4. In practice, this hypothesis seem to be fulfilled by the type of meshes using in our numerical experiments. For more details, we refer to [44, 45, 78, 87]. From now, all the triangulations used in this work are assumed to satisfy the two restrictions above.

Under the two above assumptions, one may prove the following interpolation error estimate for the Clément's interpolant $R_h$ on $\mathcal{T}_h$.

**Proposition 1.2** (Anisotropic Clément interpolation error estimate [44, 45, 78])**.**
*Let $\mathcal{T}_h$ be a conformal triangulation of $\Omega$ satisfying hypothesis (i) and (ii). There exists a*

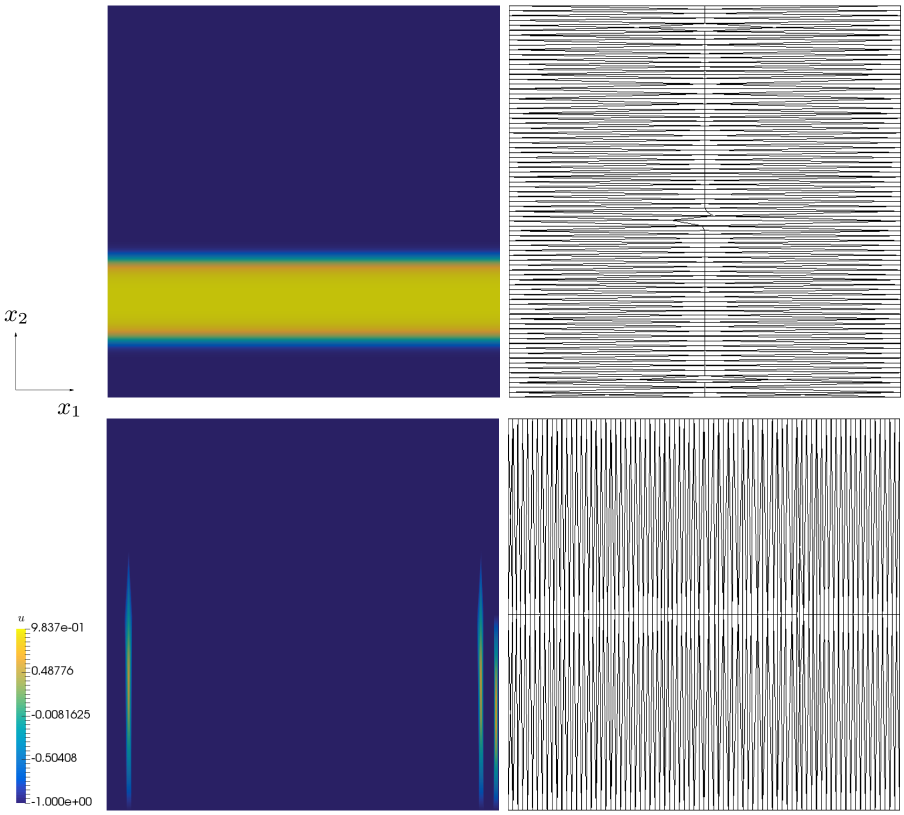


Figure 1.3: Example of a function $u(x_1, x_2)$ that depends only on the variable $x_2$. Top: the function $u$ is interpolated on the left mesh, aligned with the $x_2$ direction. Bottom: the function $u$ is interpolated on the right mesh is oriented in the $x_1$ direction (the "wrong" direction).

*constant $C > 0$ depending only on the reference triangle $\hat{K}$, in particular independent of the mesh aspect ratio, such that for all $K \in \mathcal{T}_h$ and for any $v \in H^1(\Omega)$*

$$\|v - R_h(v)\|^2_{L^2(K)} + \lambda_{2,K}\|v - R_h(v)\|^2_{L^2(\partial K)} + \lambda^2_{2,K}\|\nabla(v - R_h(v))\|^2_{L^2(K)} \leq C\omega^2_K(v), \quad (1.3)$$

*where*

$$\omega^2_K(v) = \lambda^2_{1,K}(\mathbf{r}^T_{1,K}G_K(v)\mathbf{r}_{1,K}) + \lambda^2_{2,K}(\mathbf{r}^T_{2,K}G_K(v)\mathbf{r}_{2,K}), \quad (1.4)$$

*with*

$$G_K(v) = \begin{pmatrix} \displaystyle\int_{\Delta K}\left(\frac{\partial v}{\partial x_1}\right)^2 d\mathbf{x} & \displaystyle\int_{\Delta K}\frac{\partial v}{\partial x_1}\frac{\partial v}{\partial x_2}d\mathbf{x} \\ \displaystyle\int_{\Delta K}\frac{\partial v}{\partial x_1}\frac{\partial v}{\partial x_2}d\mathbf{x} & \displaystyle\int_{\Delta K}\left(\frac{\partial v}{\partial x_2}\right)^2 d\mathbf{x} \end{pmatrix}.$$

Comparing the estimate (1.3) to the classical interpolation result valid for shape regular meshes that reads

$$\|v - R_h(v)\|^2_{L^2(K)} + h_K\|v - R_h(v)\|^2_{L^2(\partial K)} + h^2_K\|\nabla(v - R_h(v))\|^2_{L^2(K)} \leq Ch^2_K\|\nabla v\|^2_{L^2(\Delta K)},$$

where $C$ depends on the mesh aspect ratio, the same observation made for the Lagrange interpolant can be made for the Clément's one:

(i) In (1.3), the constant is independent of the mesh aspect ratio.

(ii) If the solution depends only on the $x_2$ variable and the mesh is aligned with the solution, then estimate (1.3) is sharp.

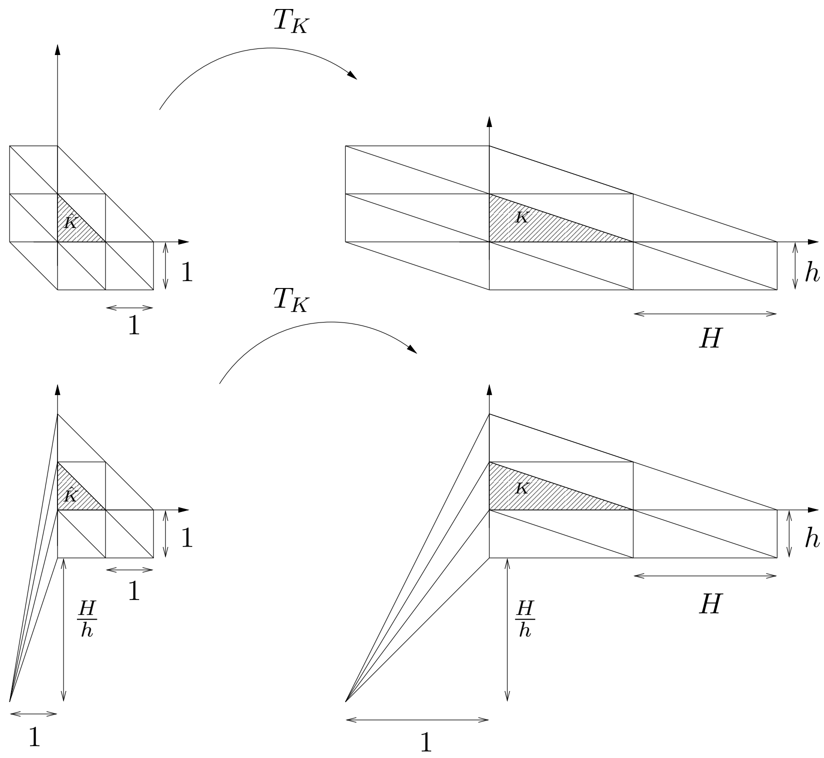


Figure 1.4: Example of a reference patch satisfying assumption (ii) (top): the size of $\Delta\hat{K}$ is independent of the aspect ratio $H/h$. Example of a reference patch that does not fulfill assumption (ii) (bottom): the size of $\Delta\hat{K}$ depends on the aspect ratio $H/h$.

The anisotropic term $\omega_K$ will appear several times throughout all this document, and therefore we list some of its properties :

- Since $\mathbf{r}_{1,K}, \mathbf{r}_{2,K}$ form an orthonormal basis, for any $v$, one can write that

$$\nabla v = (\nabla v \cdot \mathbf{r}_{1,K})\mathbf{r}_{1,K} + (\nabla v \cdot \mathbf{r}_{2,K})\mathbf{r}_{2,K}.$$

  Therefore, we have an alternative expression for $\omega_K$ given by

$$\omega_K^2(v) = \lambda_{1,K}^2 \|\nabla v \cdot \mathbf{r}_{1,K}\|_{L^2(\Delta K)}^2 + \lambda_{2,K}^2 \|\nabla v \cdot \mathbf{r}_{2,K}\|_{L^2(\Delta K)}^2.$$

- For any $K \in \mathcal{T}_h$, $\omega_K$ is a semi-norm. In particular, it satisfies the triangle inequality that is to say, for any $u, v \in H^1(\Omega)$

$$\omega_K(u+v) \leq \omega_K(u) + \omega_K(v).$$

We conclude this introductory section by two remarks.

**Remark 1.3** (Anisotropic interpolation error estimates for vector valued functions)**.** Proposition 1.1 and Proposition 1.2 can be adapted to the case of vector valued functions. The same estimates are valid if $\mathbf{v} : \Omega \to \mathbb{R}^d, d = 2, 3$, by changing the norm $L_K^2(v)$ in (1.2), respectively $\omega_K^2(v)$ in (1.3), by

$$L_K^2(\mathbf{v}) = \sum_{i=1}^{d} L_K^2(v_i), \quad \omega_K^2(\mathbf{v}) = \sum_{i=1}^{d} \omega_K^2(v_i),$$

where we denote by $v_i, 1 \leq i \leq d$, the components of $\mathbf{v}$.

**Remark 1.4** (Deriving the isotropic error estimates from the anisotropic ones)**.**
The anisotropic interpolation error estimates can be seen as a generalization of the classical finite elements theory. Indeed it is possible to recover the standard estimates by assuming that the mesh is shape regular.

(i) Observe that if we factor $\lambda_{1,K}$ out from the estimates, we obtain for the Lagrange error estimate (1.2)

$$\|v - r_h(v)\|^2_{L^2(K)} + \frac{\lambda^3_{2,K}}{\lambda^2_{1,K} + \lambda^2_{2,K}} \|v - r_h(v)\|^2_{L^2(\partial K)} \\ + \lambda^2_{2,K} \|\nabla(v - r_h(v))\|^2_{L^2(K)} \leq C \frac{\lambda^4_{1,K}}{\lambda^4_{2,K}} \lambda^4_{2,K} \|v\|^2_{H^2(K)},$$

and for the Clément's interpolant error estimate (1.3)

$$\|v - R_h(v)\|^2_{L^2(K)} + \lambda_{2,K} \|v - R_h(v)\|^2_{L^2(\partial K)} \\ + \lambda^2_{2,K} \|\nabla(v - R_h(v))\|^2_{L^2(K)} \leq C \frac{\lambda^2_{1,K}}{\lambda^2_{2,K}} \lambda^2_{2,K} |\nabla v|^2_{L^2(\Delta K)},$$

where $C > 0$ depends only on the reference triangle. Observe that we obtain expressions that are close to the classical interpolation error estimates (with respect to $\lambda_{2,K}$), but the stretching factor (that is to say the mesh aspect ratio) $\lambda_{1,K}/\lambda_{2,K}$ pops out. Therefore, to obtain a sharp estimates, we must assume that the $\lambda_{1,K}/\lambda_{2,K}$ remains bounded, that is to say there exists a constant $c$ such that for all $h > 0$ and all $K \in \mathcal{T}_h$, one have

$$\lambda_{1,K} \leq c\lambda_{2,K},$$

the best situation being when $c$ is small, that is to say when the mesh is isotropic. Under this hypothesis, we recover the classical estimates for shape regular meshes.

(ii) In the previous point, to obtain the semi-norm $H^2$ in the Lagrange interpolation estimates, respectively the semi-norm $H^1$ in the Clément's one, we use the above observation that $\mathbf{r}_{1,K}, \mathbf{r}_{2,K}$ form an orthonormal basis and that for any $v$, one can write that

$$\nabla v = (\nabla v \cdot \mathbf{r}_{1,K})\mathbf{r}_{1,K} + (\nabla \cdot \mathbf{r}_{2,K})\mathbf{r}_{2,K}.$$

Note that, compared to the anisotropic error estimates, the isotropic bounds are written in a close form, that is to say the mesh information (namely the mesh size) and the norm of the function $v$ are separated, compared for instance

$$\omega^2_K(v) = \lambda^2_{1,K}(\mathbf{r}^T_{1,K} G_K(v)\mathbf{r}_{1,K}) + \lambda^2_{2,K}(\mathbf{r}^T_{2,K} G_K(v)\mathbf{r}_{2,K}),$$

and

$$h^2_K \|\nabla v\|^2_{L^2(\Delta K)}.$$

## 1.2 Anisotropic error estimates for elliptic problems with variable coefficients

We are interested in solving the following elliptic equation, which can be seen as a toy problem to understand the two fluids flows equations (see the system (5) in the introduction). Let $\Omega \in \mathbb{R}^d, d = 2, 3$, be an open, bounded set. Given $\mu : \Omega \to \mathbb{R}$, we are looking for $u$ the solution of the Poisson equation

$$\begin{cases} -\operatorname{div}(\mu \nabla u) = f & \text{in } \Omega, \\ u = 0 & \text{on } \partial\Omega. \end{cases} \tag{1.5}$$

Integrating the previous equations with respect to a test function $v \in H_0^1(\Omega)$ yields to the following weak form

$$\int_\Omega \mu(\mathbf{x})\nabla u \cdot \nabla v d\mathbf{x} = \int_\Omega f v d\mathbf{x}, \quad \forall v \in H_0^1(\Omega). \tag{1.6}$$

Note that we explicitly write the dependence of $\mu$ on $\mathbf{x}$ under the integral sign to emphasize on its variable nature. Finally, remark that

$$\int_\Omega f v d\mathbf{x}$$

has a sense only if $f$ is a $L^2$ function. In general, $f \in H^{-1}(\Omega)$ is sufficient to have existence of a weak solution to (1.6). In this case, we should write

$$(f, v)$$

where $(\cdot, \cdot)$ stands for the duality product between $H^{-1}(\Omega)$ and $H_0^1(\Omega)$ instead of the integral over $\Omega$.

In (1.5) as in (1.6), $\mu$ is a variable coefficient (which can be interpreted as a variable viscosity) that may "jump" across an interface. We restrict ourself to the case where $\mu$ is smooth, but may have large gradient in some regions. This simplification is done since the problem (1.5) consists in a preliminary study of a two fluids flow, for which we will later on model the interface between the two phases by the mean of a smooth function. Moreover this particular choice rules out regularity issues or geometrical considerations about the meshes, that may fit the interface in order to get the optimal rates of convergence of the numerical methods. All the results that follow are adaptable to the case of non smooth coefficients, but since it is beyond the scope of our considerations, we refer to [15] for more details.

The well-posedness of (1.5) is ensured by the next proposition.

**Proposition 1.5.**
*Let $\Omega \in \mathbb{R}^d, d = 2, 3,$ be an open, bounded, connected Lipschitz set. Assume moreover that $\mu \in C^{0,1}(\overline{\Omega})$ and that there exists $\mu_{\min} > 0$ such that $\mu_{\min} \leq \mu(\mathbf{x})$ for all $\mathbf{x} \in \overline{\Omega}$. Finally, let $f \in H^{-1}(\Omega)$. Then there exists a unique $u \in H_0^1(\Omega)$ solution of (1.5) and there exists a constant $C > 0$ depending only on $\Omega$ such that the following a priori estimate holds for the energy norm*

$$\mu_{\min}\|\nabla u\|_{L^2(\Omega)} \leq C\|f\|_{H^{-1}(\Omega)}. \tag{1.7}$$

*If moreover, we assume that $\Omega$ is a smooth domain or a convex polygon (polyhedron), then $u \in H^2(\Omega)$ and there exists a constant $C' > 0$ depending only on $\Omega$ such that*

$$\mu_{\min}\|u\|_{H^2(\Omega)} \leq C'(1 + \|\nabla\mu\|_{L^\infty(\Omega)})\|f\|_{L^2(\Omega)}. \tag{1.8}$$

*Proof.* We write (1.5) in the abstract formulation

$$a(u, v) = F(v), \quad \forall v \in H_0^1(\Omega),$$

with

$$a(u, v) = \int_\Omega \mu(\mathbf{x})\nabla u \cdot \nabla v d\mathbf{x}, \quad F(v) = (f, v).$$

The well-posedness of the previous equation in $H_0^1(\Omega)$ follows directly by the use of the Lax-Milgram Lemma, observing that the bilinear form $a$ is coercive since $\mu(\mathbf{x}) \geq \mu_{\min} > 0$ and

$$a(u, u) \geq \mu_{\min}\|\nabla u\|^2_{L^2(\Omega)}.$$

The a priori estimate (1.7) is obtained by taking $v = u$.

Finally, if we assume that $\Omega$ is smooth or a convex polygon (polyhedron in 3D) and that $f \in L^2(\Omega)$, then, since $\mu \in C^{0,1}(\overline{\Omega})$, the $H^2$ regularity of $u$ follows from classical arguments [52] from elliptic PDEs theory. To derive (1.8), we observe that if $u \in H^2(\Omega)$ is a solution of

$$- \operatorname{div}(\mu \nabla u) = f,$$

then since $\mu > 0$, one have that $u$ satisfies the Laplace problem

$$-\Delta u = \frac{1}{\mu}(f + \nabla \mu \cdot \nabla u),$$

with $\frac{1}{\mu}(f + \nabla \mu \cdot \nabla u) \in L^2(\Omega)$ since $\mu$ belongs in particular to $W^{1,\infty}(\Omega)$. This implies [52] that there exists $C > 0$ depending only on $\Omega$ such that

$$\|u\|_{H^2(\Omega)} \leq C \left\| \frac{1}{\mu}(f + \nabla \mu \cdot \nabla u) \right\|_{L^2(\Omega)}.$$

The a priori bound (1.8) follows. □

**Remark 1.6.**
Note that assuming $\mu \in C^{0,1}(\overline{\Omega})$ is a sufficient condition to obtain $H^2$ solutions, but is not necessary to obtain only $H^1$ solutions. Indeed, there exists a unique $u \in H_0^1(\Omega)$ solution to (1.6) if $\mu$ is only a bounded function such that

$$0 < \mu_{\min} \leq \mu(\mathbf{x}) \leq \mu_{\max}, \quad \forall \mathbf{x} \in \Omega.$$

We now solve (1.6) with a finite elements method. We restrict ourself to the case where $\Omega$ is a convex polygons (polyhedron in $\mathbb{R}^3$) and $f \in L^2(\Omega)$, so that the domain can be completely covered by triangles and the exact solution $u$ belongs to $H^2(\Omega)$. Let $h > 0$ and $\mathcal{T}_h$ be a conformal triangulation of $\overline{\Omega}$ into triangles $K$ of diameter $h_K \leq h$. We define $V_h$ as the set of continuous piecewise linear functions on each triangle of $\mathcal{T}_h$, with zero value on $\partial\Omega$. The numerical method reads: find $u_h \in V_h$ the solution of the finite elements method

$$\int_\Omega \mu(\mathbf{x}) \nabla u_h \cdot \nabla v_h d\mathbf{x} = \int_\Omega f v_h d\mathbf{x}, \quad \forall v_h \in V_h. \tag{1.9}$$

By the same type of arguments as before, we can prove the well-posedness of (1.9) in $V_h$.

**Proposition 1.7.**
*Let $\Omega \in \mathbb{R}^d, d = 2, 3$, be an open, bounded and convex polygon. Assume moreover that $\mu \in C^{0,1}(\overline{\Omega})$ and that there exists $\mu_{\min} > 0$ such that $\mu_{\min} \leq \mu$ for all $\mathbf{x} \in \overline{\Omega}$. Finally, let $f \in L^2(\Omega)$. Then there exists a unique $u_h \in V_h$ solution of (1.9). Moreover there exists a constant $C > 0$ depending only on $\Omega$ such that the following a priori estimate holds for the energy norm*

$$\mu_{\min} \|\nabla u_h\|_{L^2(\Omega)} \leq C \|f\|_{L^2(\Omega)}. \tag{1.10}$$

We now prove the convergence of the above numerical method in the anisotropic settings presented in Section 1.1. We present the result in the 2D case, but the generalization to the third dimension follows with minor modifications. Under the same assumptions as 1.7, one can prove the following a priori error estimate.

**Theorem 1.8** (Anisotropic a priori error estimate)**.**
*Let $u \in H_0^1(\Omega) \cap H^2(\Omega)$ be the solution of (1.6) and $u_h \in V_h$ be the solution of (1.9). Then there exists a constant $C > 0$ depending only on the reference triangle $\hat{K}$, in particular*

*that is independent of the mesh aspect ratio, such that the following a priori error estimate holds*

$$\int_\Omega \mu(\mathbf{x})|\nabla(u-u_h)|^2 d\mathbf{x} \le C \sum_{K\in\mathcal{T}_h} \|\mu\|_{L^\infty(K)} \frac{L_K^2(u)}{\lambda_{2,K}^2}, \tag{1.11}$$

*where $L_K^2(u)$ is given by Proposition 1.1.*

**Remark 1.9.**
In the case of isotropic meshes, $\lambda_{1,K} \simeq \lambda_{2,K} \simeq h_K$ and $L_K^2(u) \le C h_K^4 |u|_K^2$, where $C$ is independent of the mesh size but can depend on the mesh aspect ratio. Thus, in these settings, (1.11) reduces to the standard error estimate

$$\int_\Omega \mu(\mathbf{x})|\nabla(u-u_h)|^2 d\mathbf{x} \le C\|\mu\|_{L^\infty(\Omega)} h^2 |u|_{H^2(\Omega)}^2.$$

**Remark 1.10.**
Estimate (1.11) is optimal for anisotropic meshes. Indeed, assume that the solution $u$ depends only on one variable and that the mesh is aligned with the solution, then the estimate (1.11) reduces to

$$\int_\Omega \mu(\mathbf{x})|\nabla(u-u_h)|^2 d\mathbf{x} \le C\left(\max_{K\in\mathcal{T}_h} \lambda_{2,K}\right)^2,$$

where $C$ depends on $u$, but is independent of the mesh aspect ratio. Thus $\max_{K\in\mathcal{T}_h} \lambda_{2,K} \to 0$ is sufficient to ensure the convergence of the numerical method.

*Proof.* The Galerkin orthogonality yields

$$\int_\Omega \mu(\mathbf{x})|\nabla(u-u_h)|^2 d\mathbf{x} = \int_\Omega \mu(\mathbf{x})\nabla(u-u_h)\cdot\nabla(u-u_h) d\mathbf{x} = \int_\Omega \mu(\mathbf{x})\nabla(u-u_h)\cdot\nabla(u-r_h(u)) d\mathbf{x},$$

where $r_h(u) \in V_h$ is the Lagrange interpolant on $\mathcal{T}_h$ (note that it makes sense to consider the Lagrange interpolant of $u$ since it is a $H^2$ function in $\mathbb{R}^2$, thus in particular continuous). By the Cauchy-Schwarz in $\mathbb{R}^2$ and the Young's inequality, we get

$$\int_\Omega \mu(\mathbf{x})|\nabla(u-u_h)|^2 d\mathbf{x} \le \frac{1}{2}\int_\Omega \mu(\mathbf{x})|\nabla(u-u_h)|^2 d\mathbf{x} + \frac{1}{2}\int_\Omega \mu(\mathbf{x})|\nabla(u-r_h(u))|^2 d\mathbf{x},$$

which yields

$$\int_\Omega \mu(\mathbf{x})|\nabla(u-u_h)|^2 d\mathbf{x} \le \sum_{K\in\mathcal{T}_h} \|\mu\|_{L^\infty(K)} \int_K |\nabla(u-r_h(u))|^2 d\mathbf{x}.$$

We conclude by using the interpolation error estimate of Proposition 1.1. □

Under the same assumptions as for Propositions 1.7, we now prove an a posteriori error estimate. As for the a priori error analysis, we restrict ourself to the case $\Omega \in \mathbb{R}^2$, but the result is easily generalizable to $\mathbb{R}^3$. More details will be given for the 3D situation in Section 1.6.

**Theorem 1.11** (Anisotropic a posteriori error estimate)**.**
*Let $u \in H_0^1(\Omega)$ be the solution of (1.6) and $u_h \in V_h$ be the solution of (1.9). There exists a constant $C > 0$ depending only on the reference triangle $\hat{K}$, in particular that is independent of the mesh aspect ratio, such that the following a posteriori error estimate holds*

$$\int_\Omega \mu(\mathbf{x})|\nabla(u-u_h)|^2 d\mathbf{x} \le C \sum_{K\in\mathcal{T}_h} \eta_K^2, \tag{1.12}$$

*where*

$$\eta_K^2 = \left( \|f + \mathrm{div}(\mu(\mathbf{x})\nabla u_h)\|_{L^2(K)} + \frac{\| [\mu(\mathbf{x})\nabla u_h \cdot \mathbf{n}] \|_{L^2(\partial K)}}{2\sqrt{\lambda_{2,K}}} \right) \omega_K(u - u_h), \tag{1.13}$$

*where* $\mathbf{n}$ *is the unit normal to each triangle and* $\omega_K(u - u_h)$ *is given by Proposition 1.2.*

**Remark 1.12** (Zienkiewicz–Zhu (ZZ) post-processing)**.**
Estimate 1.12 is not a standard a posteriori estimate since the exact solution $u$ is contained in $\omega_K(u - u_h)$. However, post-processing techniques can be applied in order to approximate $G_K(u - u_h)$, for instance Zienkiewicz–Zhu (ZZ) post-processing [108, 109, 110]. More precisely, we will replace the first order partial derivatives with respect to $x_i$

$$\frac{\partial(u - u_h)}{\partial x_i} \text{ by } \Pi_h^{ZZ}\frac{\partial u_h}{\partial x_i} - \frac{\partial u_h}{\partial x_i}, \qquad i = 1, 2,$$

where, for any $v_h \in V_h$, for any vertex $P$ of the mesh

$$\Pi_h^{ZZ}\frac{\partial v_h}{\partial x_i}(P) = \frac{\displaystyle\sum_{\substack{K \in \mathcal{T}_h \\ P \in K}} |K| \left.\frac{\partial v_h}{\partial x_i}\right|_K}{\displaystyle\sum_{\substack{K \in \mathcal{T}_h \\ P \in K}} |K|}$$

is an approximate $L^2(\Omega)$ projection of $\partial v_h/\partial x_i$ onto $V_h$.

To avoid to introduce too many notations, we denote the "post-processed solution" by $\Pi_h^{ZZ} u_h$. If we write $\Pi_h^{ZZ} u_h$ in an expression involving first derivatives, for instance as $\nabla(\Pi_h^{ZZ} u_h - u_h)$ and the anisotropic form $\omega_K(\Pi_h^{ZZ} u_h - u_h)$, then we take the convention that for any vertex $P$

$$\frac{\partial}{\partial x_i}(\Pi_h^{ZZ} u_h)(P) := \Pi_h^{ZZ}\frac{\partial u_h}{\partial x_i}(P), \quad i = 1, 2. \tag{1.14}$$

It is well known [110] that on structured meshes, superconvergence of the ZZ recovery occurs, implying that the post-processing is asymptotically exact, that is to say

$$\lim_{h \to 0} \frac{\|\nabla(\Pi_h^{ZZ} u_h - u_h)\|_{L^2(\Omega)}}{\|\nabla(u - u_h)\|_{L^2(\Omega)}} = 1.$$

On general meshes, it was first proven that $\|\nabla(\Pi_h^{ZZ} u_h - u_h)\|_{L^2(\Omega)}$ and the true error $\|\nabla(u - u_h)\|_{L^2(\Omega)}$ are equivalent, see for instance [64]. More recently, the superconvergence of the ZZ gradient recovery was finally shown for unstructured anisotropic meshes [27]. However, before this last result was obtained, in practice the efficiency of the ZZ post-processing was already demonstrated to be better than the theoretical predictions. We refer for instance to the numerical results presented in [84, 87, 85, 72, 88, 20] in the case of anisotropic meshes for elliptic, parabolic, and hyperbolic equations.

**Remark 1.13** (Lower bound)**.**
So far, we were not able to prove a lower bound for the numerical error $\int_\Omega \mu(\mathbf{x})|\nabla(u - u_h)|^2 d\mathbf{x}$, that is to say there exists a constant $c > 0$ independent of the mesh size, aspect ratio and $\mu$ such that

$$\sum_{K \in \mathcal{T}_h} \eta_K^2 \le c \int_\Omega \mu(\mathbf{x})|\nabla(u - u_h)|^2 d\mathbf{x}.$$

This kind of bounds seem to be difficult to reach with a variable $\mu$ in the anisotropic finite elements framework. We refer to [87] where a lower bound is proven in the anisotropic setting when $\mu$ is constant and to [15] where a proof is provided for piecewise constant $\mu$, but with isotropic finite elements.

However, numerical experiments that will be presented below demonstrate that in practice the numerical error and the a posteriori error estimator are equivalent.

*Proof of Theorem 1.11.* In what follows, we denote by $C$ any positive constant depending only on the reference triangle, which may change from line to line. Using (1.6), we have

$$\int_\Omega \mu(\mathbf{x})\nabla(u-u_h)\cdot\nabla(u-u_h)d\mathbf{x} = \int_\Omega f(u-u_h)d\mathbf{x} - \int_\Omega \nabla u_h\cdot\nabla(u-u_h)d\mathbf{x}.$$

Using the numerical scheme (1.9), we have therefore

$$\int_\Omega \mu(\mathbf{x})\nabla(u-u_h)\cdot\nabla(u-u_h)d\mathbf{x} = \int_\Omega f(u-u_h-v_h)d\mathbf{x} - \int_\Omega \mu(\mathbf{x})\nabla u_h\cdot\nabla(u-u_h-v_h)d\mathbf{x}. \tag{1.15}$$

for any $v_h \in V_h$. Integrating by parts over each triangle yields

$$\begin{aligned}\int_\Omega \mu(\mathbf{x})\nabla(u-u_h)\cdot\nabla(u-u_h)d\mathbf{x} = \sum_{K\in\mathcal{T}_h}\int_K &\left(f+\operatorname{div}(\mu(\mathbf{x})\nabla u_h)\right)(u-u_h-v_h)d\mathbf{x}\\ &+\frac{1}{2}\int_{\partial K}\left[\mu(\mathbf{x})\nabla u_h\cdot\mathbf{n}\right](u-u_h-v_h)d\mathbf{x}.\end{aligned}$$

Finally, using Cauchy-Schwarz inequality and choosing $v_h = R_h(u-u_h)$, the interpolation error estimate for Clément's interpolant of Proposition 1.2 yields

$$\begin{aligned}&\int_\Omega \mu(\mathbf{x})\nabla(u-u_h)\cdot\nabla(u-u_h)d\mathbf{x}\\ &\qquad\le C\sum_{K\in\mathcal{T}_h}\left(\|f+\operatorname{div}(\mu(\mathbf{x})\nabla u_h)\|_{L^2(K)} + \frac{\|\left[\mu(\mathbf{x})\nabla u_h\cdot\mathbf{n}\right]\|_{L^2(\partial K)}}{2\sqrt{\lambda_{2,K}}}\right)\omega_K(u-u_h).\end{aligned}$$

□

**Remark 1.14.**
We observe in the proof above that the smoothness of $\mu$ is necessary. Indeed, to be able to integrate by parts in (1.15), we must have that $\mu(\mathbf{x})\nabla\mathbf{u}_h$ is a $H^1$ function in $K$, that is clearly the case since $\mu$ is itself $C^{0,1}$, that is say $W^{1,\infty}$. If we have only assumed that $\mu$ is a bounded function (we recall that it is still sufficient for (1.6) and (1.9) to be well-posed), then we cannot conclude.

Indeed, let us consider the simple example where the domain $\Omega$ is split into two parts $\Omega_1$ and $\Omega_2$ such that $\Omega = \Omega_1\cup\Omega_2$ and let us denote by $\Gamma$ the boundary separating $\Omega_1$ and $\Omega_2$. Now we define $\mu$ as the piecewise constant function taking the constant value $\mu_1 > 0$ in $\Omega_1$ and $\mu_2 > 0$ in $\Omega_2$ with $\mu_1 \neq \mu_2$. Then there is no reason for $\mu(\mathbf{x})\nabla\mathbf{u}_h$ to be in $H^1(K)$, for instance because $\Gamma$ can cross $K$, so that $\mu$ has discontinuities in $K$. Therefore, in this case, to perform the integration by parts, it must be possible to build a mesh such that any triangle is contained either in $\Omega_1$ or in $\Omega_2$.

Based on the a posteriori error estimate of Theorem 1.11, we define the anisotropic error indicator

$$\eta^A = \left(\sum_{K\in\mathcal{T}_h}\eta_K^2\right)^{1/2}, \tag{1.16}$$

where we $\eta_K^2$ is given by

$$\eta_K^2 = \left(\|f+\operatorname{div}(\mu(\mathbf{x})\nabla u_h)\|_{L^2(K)} + \frac{\|\left[\mu(\mathbf{x})\nabla u_h\cdot\mathbf{n}\right]\|_{L^2(\partial K)}}{2\sqrt{\lambda_{2,K}}}\right)\tilde{\omega}_K(\Pi_h^{ZZ}u_h-u_h), \tag{1.17}$$

where $\Pi_h u_h$ is the ZZ post-processed solution as defined in Remark 1.12 and

$$\tilde{\omega}_K^2(v) = \lambda_{1,K}^2(\mathbf{r}_{1,K}^T \tilde{G}_K(v)\mathbf{r}_{1,K}) + \lambda_{2,K}^2(\mathbf{r}_{2,K}^T \tilde{G}_K(v)\mathbf{r}_{2,K}), \tag{1.18}$$

with

$$\tilde{G}_K(v) = \begin{pmatrix} \displaystyle\int_K \left(\frac{\partial v}{\partial x_1}\right)^2 d\mathbf{x} & \displaystyle\int_K \frac{\partial v}{\partial x_1}\frac{\partial v}{\partial x_2} d\mathbf{x} \\ \displaystyle\int_K \frac{\partial v}{\partial x_1}\frac{\partial v}{\partial x_2} d\mathbf{x} & \displaystyle\int_K \left(\frac{\partial v}{\partial x_2}\right)^2 d\mathbf{x} \end{pmatrix}.$$

We immediately make the following remark about the choice of the error indicator.

**Remark 1.15.**
The definition (1.17) of $\eta_K^2$ differs from the one of Theorem 1.11 by using the post-processed solution $\Pi_h^{ZZ} u_h$ instead of the exact solution $u$, making the error indicator computable, and by using $\tilde{\omega}_K$ instead of $\omega_K$ as obtained in the proof. The first change makes sense by the Remark 1.12 and the second one makes the implementation of $\eta_K^2$ simpler. This choice may be justified a posteriori since the goal of the adaptive algorithm will be to equidistribute the error among all the triangles $K$. Therefore putting $\tilde{\omega}_K$ instead of $\omega_K$ in the definition of the local error indicator makes the resulting global error indicator $\eta^A$ differing only by a multiplicative constant from the a posteriori error estimate of Theorem 1.11.

To investigate the sharpness of $\eta^A$, we compute the so-called effectivity index $ei^A$ defined by

$$ei^A = \frac{\eta^A}{e_{\mu,H^1}} \tag{1.19}$$

where we note

$$e_{\mu,H^1} = \left(\int_\Omega \mu|\nabla(u-u_h)|^2 d\mathbf{x}\right)^{1/2}. \tag{1.20}$$

Finally, since the local error indicator (1.17) is constructed using the ZZ post-processing, we measure the quality of this procedure by computing the true and approximated $H^1$ errors

$$e_{H^1} = \left(\int_\Omega |\nabla(u-u_h)|^2 d\mathbf{x}\right)^{1/2}, \quad \eta^{ZZ} = \left(\int_\Omega |\nabla(\Pi_h^{ZZ}u_h - u_h)|^2 d\mathbf{x}\right)^{1/2}, \tag{1.21}$$

and the ZZ effectivity index given by

$$ei^{ZZ} = \frac{\eta^{ZZ}}{e_{H^1}}. \tag{1.22}$$

## 1.3 Numerical experiments with non-adapted meshes

We are performing numerical experiments to test the quality of our error indicator (1.16) and the ZZ post-processing, as defined in Section 1.5. From our perspectives, they should satisfy the following properties :

(i) The effectivity index $ei^A$ should not depend on the exact solution $u$.

(ii) The effectivity index $ei^A$ should not depend on the mesh aspect ratio.

(iii) The effectivity index $ei^A$ should not depend on $\mu$.

(iv) The effectivity index $ei^{ZZ}$ should be close to one.

**Example 1.16** (An anisotropic solution).
The first example consists to solve (1.5) in the square $\Omega = ]0,1[\times]0,1[$ where we impose non homogeneous Dirichlet boundary conditions. We consider two cases

(1) $\mu(\mathbf{x}) = 2(0.5 + |x_1 - 0.5|)$,

(2) $\mu(\mathbf{x}) = 4x_1(x_1 - 1) + 2$.

In both cases, $\mu$ is a Lipschitz function varying between 1 and 2. We compute the right hand side $f$ such that the exact solution $u$ is given by

$$u(x_1, x_2) = 0.5x_1(1 - x_1). \tag{1.23}$$

We solve the problem on meshes with typical aspect ratio of 50 and 500. The results are reported in Tables 1.1 and 1.2, where we denote by $h_1$, respectively $h_2$, the mesh size in the $x_1$-direction, respectively the $x_2$-direction. In both cases, the effectivity index $ei^A$ stays between 3 and 3.5, and $ei^{ZZ}$ is asymptotically exact. We observe that errors and error indicators are $\simeq O(h)$ as predicted by the theory. These results seem to indicate that the effectivity indices are independent of $\mu$ and the mesh aspect ratio, as desired.

| $h_1 - h_2$ | $\eta^A$ | $e_{\mu,H^1}$ | $ei^A$ | $\eta^{ZZ}$ | $e_{H^1}$ | $ei^{ZZ}$ |
|---|---|---|---|---|---|---|
| 0.01 - 0.5 | 0.0082 | 0.0026 | 3.15 | 0.0022 | 0.0022 | 1.00 |
| 0.005 - 0.25 | 0.0045 | 0.0014 | 3.21 | 0.0011 | 0.0011 | 1.00 |
| 0.0025 - 0.125 | 0.0022 | 0.00069 | 3.19 | 0.00056 | 0.00056 | 1.00 |
| 0.00125 - 0.0625 | 0.0011 | 0.00034 | 3.24 | 0.00028 | 0.00028 | 1.00 |
| 0.001 - 0.5 | 0.0009 | 0.00025 | 3.6 | 0.00021 | 0.00021 | 1.00 |
| 0.0005 - 0.25 | 0.00046 | 0.00013 | 3.54 | 0.00011 | 0.00011 | 1.00 |
| 0.00025 - 0.125 | 0.00023 | 0.000066 | 3.48 | 0.000054 | 0.000054 | 1.00 |
| 0.000125 - 0.0625 | 0.00012 | 0.000033 | 3.64 | 0.000027 | 0.000027 | 1.00 |

Table 1.1: Numerical results for Example 1.16, case (1). The mesh aspect ratio is 50 (rows 1-4) and 500 (rows 5-8). $\mu$ is a piecewise linear function. The solution is given by (1.23).

| $h_1 - h_2$ | $\eta^A$ | $e_{\mu,H^1}$ | $ei^A$ | $\eta^{ZZ}$ | $e_{H^1}$ | $ei^{ZZ}$ |
|---|---|---|---|---|---|---|
| 0.01 - 0.5 | 0.008 | 0.0025 | 3.2 | 0.0022 | 0.0022 | 1.00 |
| 0.005 - 0.25 | 0.0044 | 0.0013 | 3.38 | 0.0011 | 0.0011 | 1.00 |
| 0.0025 - 0.125 | 0.0021 | 0.00065 | 3.23 | 0.00056 | 0.00056 | 1.00 |
| 0.00125 - 0.0625 | 0.001 | 0.00032 | 3.13 | 0.00028 | 0.00028 | 1.00 |
| 0.001 - 0.5 | 0.00086 | 0.00024 | 3.58 | 0.00021 | 0.00021 | 1.00 |
| 0.0005 - 0.25 | 0.00044 | 0.00012 | 3.67 | 0.00011 | 0.00011 | 1.00 |
| 0.00025 - 0.125 | 0.00022 | 0.000063 | 3.49 | 0.000054 | 0.000054 | 1.00 |
| 0.000125 - 0.0625 | 0.00011 | 0.000031 | 3.55 | 0.000027 | 0.000027 | 1.00 |

Table 1.2: Numerical results for Example 1.16, case (2). The mesh aspect ratio is 50 (rows 1-4) and 500 (rows 5-8). $\mu$ is a quadratic function.The solution is given by (1.23).

Finally, we check that the effectivity index $ei^A$ does not depend on the exact solution. We consider again the case (1) where this time we compute $f$ such that the exact solution is given by

$$u(x_1, x_2) = sin(\pi x_1). \tag{1.24}$$

The results are reported in Tables 1.3 and 1.4.

| $h_1 - h_2$ | $\eta^A$ | $e_{\mu,H^1}$ | $ei^A$ | $\eta^{ZZ}$ | $e_{H^1}$ | $ei^{ZZ}$ |
|---|---|---|---|---|---|---|
| 0.01 - 0.5 | 0.053 | 0.017 | 3.12 | 0.015 | 0.015 | 1.00 |
| 0.005 - 0.25 | 0.029 | 0.0089 | 3.26 | 0.0079 | 0.0079 | 1.00 |
| 0.0025 - 0.125 | 0.014 | 0.0045 | 3.11 | 0.0039 | 0.0039 | 1.00 |
| 0.00125 - 0.0625 | 0.0068 | 0.0022 | 3.09 | 0.0019 | 0.0019 | 1.00 |
| 0.001 - 0.5 | 0.0059 | 0.0016 | 3.69 | 0.0014 | 0.0014 | 1.00 |
| 0.0005 - 0.25 | 0.003 | 0.00084 | 3.57 | 0.00075 | 0.00074 | 1.00 |
| 0.00025 - 0.125 | 0.0015 | 0.00043 | 3.48 | 0.00038 | 0.00038 | 1.00 |
| 0.000125 - 0.0625 | 0.00075 | 0.00021 | 3.57 | 0.00019 | 0.00019 | 1.00 |

Table 1.3: Numerical results for Example 1.16, case (1). The mesh aspect ratio is 50 (rows 1-4) and 500 (rows 5-8). $\mu$ is a piecewise linear function. The solution is given by (1.24).

| $h_1 - h_2$ | $\eta^A$ | $e_{\mu,H^1}$ | $ei^A$ | $\eta^{ZZ}$ | $e_{H^1}$ | $ei^{ZZ}$ |
|---|---|---|---|---|---|---|
| 0.01 - 0.5 | 0.051 | 0.016 | 3.19 | 0.015 | 0.015 | 1.00 |
| 0.005 - 0.25 | 0.029 | 0.0084 | 3.45 | 0.0079 | 0.0079 | 1.00 |
| 0.0025 - 0.125 | 0.013 | 0.0042 | 3.10 | 0.0039 | 0.0039 | 1.00 |
| 0.00125 - 0.0625 | 0.0064 | 0.0021 | 3.05 | 0.0019 | 0.0019 | 1.00 |
| 0.001 - 0.5 | 0.0055 | 0.0015 | 3.67 | 0.0014 | 0.0014 | 1.00 |
| 0.0005 - 0.25 | 0.0028 | 0.00079 | 3.54 | 0.00075 | 0.00074 | 1.00 |
| 0.00025 - 0.125 | 0.0014 | 0.00040 | 3.5 | 0.00038 | 0.00038 | 1.00 |
| 0.000125 - 0.0625 | 0.00071 | 0.00020 | 3.55 | 0.00019 | 0.00019 | 1.00 |

Table 1.4: Numerical results for Example 1.16, case (2). The mesh aspect ratio is 50 (rows 1-4) and 500 (rows 5-8). $\mu$ is a quadratic function. The solution is given by (1.24).

**Example 1.17** (Coefficients with boundary layer)**.**
We now do a first step into the study of two fluids flow by solving (1.5) with $\mu$ being constant in two parts of the domain, except in a thin boundary layer. We again set $\Omega$ as the unit square and we define, for $x \in \mathbb{R}$, $H_\varepsilon(x)$ as

$$H_\varepsilon(x) = \begin{cases} 0, & 0 \leq x \leq -\varepsilon, \\ \dfrac{x+\varepsilon}{2\varepsilon} + \dfrac{1}{2\pi} sin\left(\dfrac{\pi x}{\varepsilon}\right), & -\varepsilon \leq x \leq \varepsilon, \\ 1, & \varepsilon \leq x. \end{cases} \tag{1.25}$$

The above function can be seen as a smoothing of the Heavyside function $H(x)$

$$H(x) = \begin{cases} 0, & x < 0, \\ 1, & 0 < x, \end{cases}$$

where $\varepsilon > 0$ controls the width of the boundary layer. The smooth function (1.25) was already used to describe the interface between fluids in the level set method [31]. We then define

$$\mu(\mathbf{x}) = \mu_2 H_\varepsilon(x_1 - 0.5) + \mu_1(1 - H_\varepsilon(x - 0.5)), \quad \mu_1, \mu_2 > 0, \tag{1.26}$$

such that $\mu$ is a constant except in a layer of width $2\varepsilon$ around 0.5.

We solve (1.5) where $\mu$ is defined by (1.26) and we compute the right hand side $f$ such that the exact solution $u$ is given by

$$u(x_1, x_2) = \mu_2 sin(\pi x_1) H_\varepsilon(x_1 - 0.5) + \mu_1 sin(\pi x_1) H_\varepsilon(0.5 - x_1). \tag{1.27}$$

The solution (1.27) can be seen as a smooth transition from $u_1$ to $u_2$ where $u_i$ are the solutions of

$$-\Delta u_i = -\mu_i \pi^2 sin(\pi x_1), \quad i = 1, 2.$$

The numerical results with $\mu_1 = 1$ and $\mu_2 = 2$ are reported in the Table 1.5 where we compare the convergence of the numerical scheme with the width of the boundary layer. For each value of $\varepsilon$, we built successive meshes with 1, 5, 10, 20 and 40 vertices in the boundary layer (seen in the $x_1$-direction). We observe that convergence of the numerical method and good behaviors of the effectivity indices arise when the number of vertices in the boundary layer is around 20. The numerical solution $u_h$ is plotted in Figures 1.5 and 1.6, where we choose $\varepsilon = 0.001$ and $h_1 = 0.00005, h_2 = 0.5$. An example of anisotropic mesh used in the numerical simulation is shown in Figure 1.7 for $\varepsilon = 0.1$ and $h_1 = 0.01, h_2 = 0.5$.

| $h_1 - h_2$ | $\varepsilon$ | $\eta^A$ | $e_{\mu,H^1}$ | $ei^A$ | $\eta^{ZZ}$ | $e_{H^1}$ | $ei^{ZZ}$ |
|---|---|---|---|---|---|---|---|
| 0.1 - 0.5 | 0.1 | 2.91 | 1.92 | 1.51 | 0.99 | 1.61 | 0.61 |
| 0.04 - 0.5 | 0.1 | 1.86 | 0.59 | 3.15 | 0.57 | 0.48 | 1.19 |
| 0.02 - 0.5 | 0.1 | 0.82 | 0.27 | 3.04 | 0.23 | 0.22 | 1.045 |
| 0.01 - 0.5 | 0.1 | 0.48 | 0.17 | 2.83 | 0.13 | 0.13 | 1.02 |
| 0.005 - 0.5 | 0.1 | 0.22 | 0.068 | 3.24 | 0.054 | 0.054 | 1.00 |
| 0.01 - 0.5 | 0.01 | 25.50 | 5.06 | 5.04 | 3.83 | 4.23 | 0.90 |
| 0.004 - 0.5 | 0.01 | 5.11 | 1.53 | 3.34 | 1.39 | 1.25 | 1.11 |
| 0.002 - 0.5 | 0.01 | 2.63 | 0.89 | 2.95 | 0.73 | 0.71 | 1.028 |
| 0.001 - 0.5 | 0.01 | 1.17 | 0.39 | 3.00 | 0.31 | 0.31 | 1.00 |
| 0.0005 - 0.5 | 0.01 | 0.56 | 0.19 | 2.95 | 0.16 | 0.16 | 1.00 |
| 0.001 - 0.5 | 0.001 | 102.78 | 21.37 | 4.81 | 17.10 | 19.06 | 0.90 |
| 0.0004 - 0.5 | 0.001 | 15.14 | 4.79 | 3.16 | 4.54 | 3.92 | 1.16 |
| 0.0002 - 0.5 | 0.001 | 7.52 | 2.48 | 3.03 | 2.12 | 2.026 | 1.046 |
| 0.0001 - 0.5 | 0.001 | 3.62 | 1.18 | 3.07 | 0.98 | 0.97 | 1.01 |
| 0.00005 - 0.5 | 0.001 | 1.76 | 0.59 | 2.98 | 0.48 | 0.48 | 1.00 |

Table 1.5: Numerical results for Example 1.17 with $\mu_1 = 1$ and $\mu_2 = 2$. The successive meshes contain 1,5,10,20 and 40 points in the boundary layer $2\varepsilon$ in the $x_1$-direction.

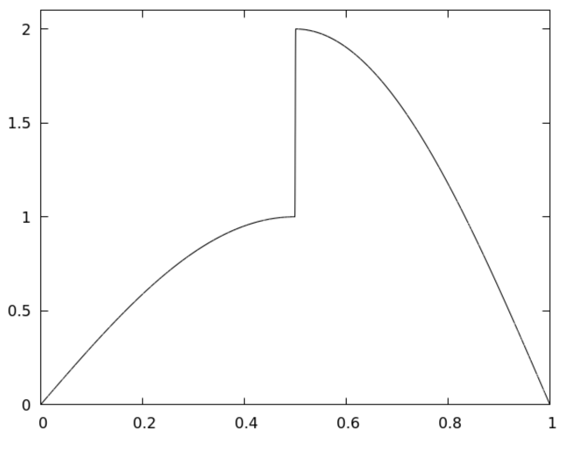


Figure 1.5: Example 1.17. Numerical solution along the $x_1$-axis computed with $\mu_1 = 1, \mu_2 = 2, \varepsilon = 0.001$. The mesh size is 0.00005 in the $x_1$-direction and 0.5 in the $x_2$-direction. The mesh aspect ratio is 10'000.

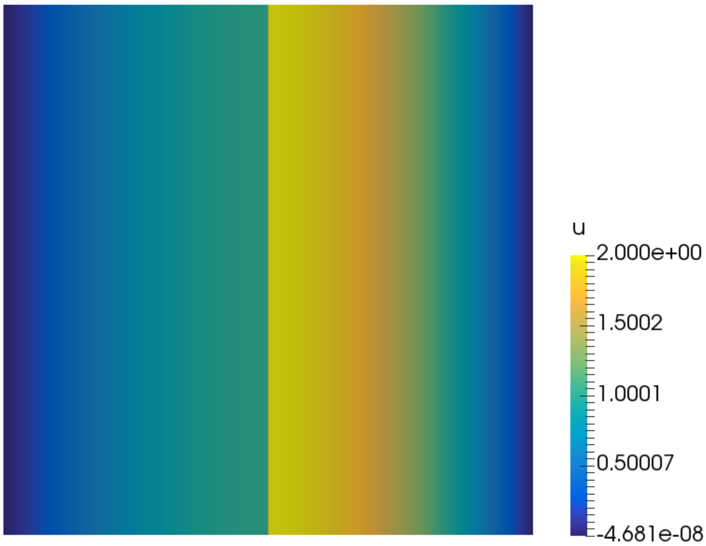


Figure 1.6: Example 1.17. Numerical solution computed with $\mu_1 = 1, \mu_2 = 2, \varepsilon = 0.001$. The mesh size is 0.00005 in the $x_1$-direction and 0.5 in the $x_2$-direction. The mesh aspect ratio is 10'000.

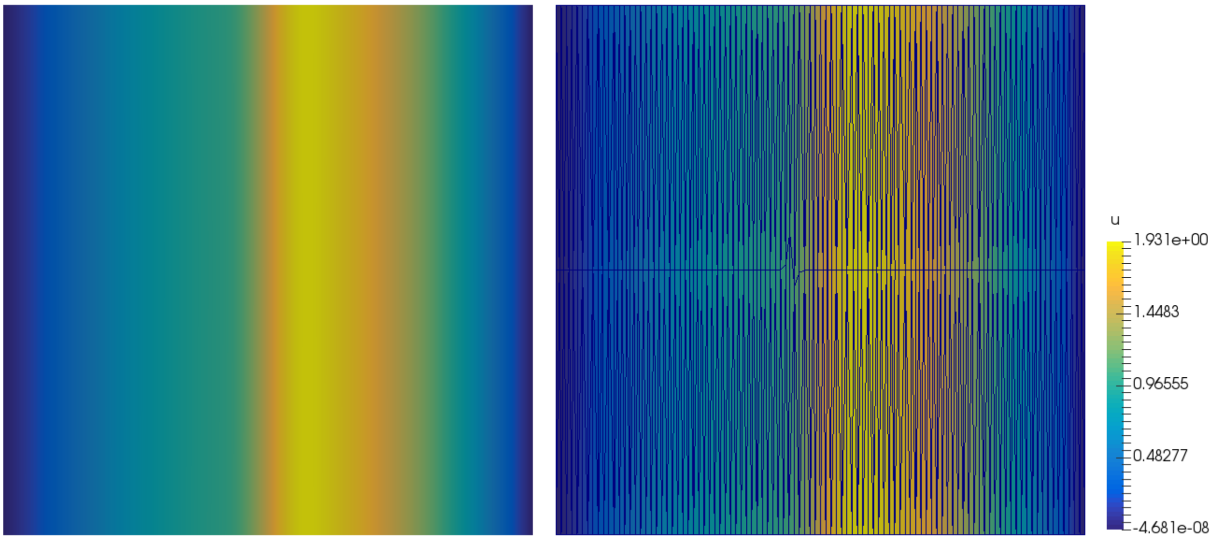


Figure 1.7: Example 1.17. Numerical solution (left) and mesh(right) computed with $\mu_1 = 1, \mu_2 = 2, \varepsilon = 0.1$. The mesh size is 0.01 in the $x_1$-direction and 0.5 in the $x_2$-direction. The mesh aspect ratio is 50.

## 1.4 An adaptive algorithm

We now present an adaptive algorithm to solve (1.5). Given a prescribed tolerance $TOL$, the goal is to build a sequence of meshes such that

$$0.75TOL \leq \left( \frac{\sum_{K \in \mathcal{T}_h} \eta_K^2}{\int_\Omega \mu(\mathbf{x}) |\nabla u_h|^2 d\mathbf{x}} \right)^{1/2} \leq 1.25TOL, \tag{1.28}$$

where we recall that the local error indicator $\eta_K^2$ is given by

$$\eta_K^2 = \left( \|f + \mathrm{div}(\mu(\mathbf{x})\nabla u_h)\|_{L^2(K)} + \frac{\| \left[\mu(\mathbf{x})\nabla u_h \cdot \mathbf{n}\right] \|_{L^2(\partial K)}}{2\sqrt{\lambda_{2,K}}} \right) \tilde{\omega}_K(\Pi_h u_h - u_h),$$

with $\Pi_h u_h$ being the ZZ post-processing of $u_h$ and $\tilde{\omega}_K$ is defined by (1.18). A sufficient condition so that (1.28) holds is to ensure that the error is equidistributed on each triangle $K$, that is to say for all $K \in \mathcal{T}_h$

$$\frac{1}{N_T} 0.75^2 TOL^2 \int_\Omega \mu(\mathbf{x})|\nabla u_h|^2 d\mathbf{x} \leq \eta_K^2 \leq \frac{1}{N_T} 1.25^2 TOL^2 \int_\Omega \mu(\mathbf{x})|\nabla u_h|^2 d\mathbf{x}, \qquad (1.29)$$

where we denote by $N_T$ the number of triangles of the mesh.

Numerical experiments performed in [85] suggest that to obtain anisotropic meshes, the error indicator should be equidistributed in both direction $x_1$ and $x_2$ (note that it is also pointed out in [87] that error equidistribution is necessary to equivalence between the posteriori error estimator and the numerical error). To do so, we remark the following fact. Since we can decompose $\tilde{\omega}_K(v), v \in H^1(\Omega)$, as

$$\tilde{\omega}_K(v) = \left(\tilde{\omega}_{1,K}^2(v) + \tilde{\omega}_{2,K}^2(v)\right)^{1/2},$$

where we set

$$\tilde{\omega}_{i,K}^2(v) = \lambda_{i,K}^2 \mathbf{r}_{i,K}^T \tilde{G}_K(v) \mathbf{r}_{i,K}, \quad i = 1, 2, \qquad (1.30)$$

observe that we have the following relation

$$\eta_K^2 = \left(\eta_{1,K}^4 + \eta_{2,K}^4\right)^{1/2}, \qquad (1.31)$$

where for $i = 1, 2$, we define the local error indicator in direction $x_i$ $\eta_{i,K}^2$ by

$$\eta_{i,K}^2 = \left( \|f + \mathrm{div}(\mu(\mathbf{x})\nabla u_h)\|_{L^2(K)} + \frac{\| \left[\mu(\mathbf{x})\nabla u_h \cdot \mathbf{n}\right] \|_{L^2(\partial K)}}{2\sqrt{\lambda_{2,K}}} \right) \tilde{\omega}_{i,K}(\Pi_h^{ZZ} u_h - u_h). \quad (1.32)$$

Consequently, to require that for all $K$ and for $i = 1, 2$,

$$\frac{1}{2N_T^2} 0.75^4 TOL^4 \left(\int_\Omega \mu(\mathbf{x})|\nabla u_h|^2 d\mathbf{x}\right)^2 \leq \eta_{i,K}^4 \leq \frac{1}{2N_T^2} 1.25^4 TOL^4 \left(\int_\Omega \mu(\mathbf{x})|\nabla u_h|^2 d\mathbf{x}\right)^2, \quad (1.33)$$

is sufficient to ensure that (1.29) holds. Observe moreover that (1.33) implies necessarely that for $i = 1, 2$,

$$\frac{1}{2^{1/4}} 0.75 TOL \leq \left( \frac{\sum_{K \in \mathcal{T}_h} \eta_{i,K}^2}{\int_\Omega \mu(\mathbf{x})|\nabla u_h|^2 d\mathbf{x}} \right)^{1/2} \leq \frac{1}{2^{1/4}} 1.25 TOL, \qquad (1.34)$$

that is to say the error is globally equidistributed in every direction.

We now describe more precisely the adaptive strategy. The goal would be to construct a mesh such that (1.33) holds. In practice, to built our meshes, we use the BL2D mesh generator [67] which needs informations on the vertices rather that on triangles. Therefore we translate the error indicator $\eta^A$ to an error indicator defined on the vertices. For every vertex $P \in \mathcal{T}_h$, we define the local error indicator $\eta_P^2$ by

$$\eta_P^2 = \sum_{\substack{K \in \mathcal{T}_h \\ P \in K}} \eta_K^2 \qquad (1.35)$$

and we have the relation

$$\sum_{P\in\mathcal{T}_h} \eta_P^2 = 3 \sum_{K\in\mathcal{T}_h} \eta_K^2. \tag{1.36}$$

To find an equivalent to the conditions (1.33), we start from the global conditions (1.28). They are equivalent to the following ones, written with the local error indicators $\eta_P^2$,

$$0.75TOL \leq \left( \frac{\sum_{P\in\mathcal{T}_h} \eta_P^2}{3\int_\Omega \mu(\mathbf{x})|\nabla u_h|^2 d\mathbf{x}} \right)^{1/2} \leq 1.25TOL. \tag{1.37}$$

A sufficient condition to ensure (1.37) is to equidistribute $\eta_P^2$ over all the vertices, that is to say to impose that for all $P \in \mathcal{T}_h$

$$\frac{3}{N_v} 0.75^2 TOL^2 \int_\Omega \mu(\mathbf{x})|\nabla u_h|^2 d\mathbf{x} \leq \eta_P^2 \leq \frac{3}{N_v} 1.25^2 TOL^2 \int_\Omega \mu(\mathbf{x})|\nabla u_h|^2 d\mathbf{x}, \tag{1.38}$$

where $N_v$ is the total number of vertices of the triangulation $\mathcal{T}_h$. Compared to (1.29), (1.38) can be interpreting as a weaker condition, consisting to equidistributing the error over the support of each basis function of $V_h$ rather than over each triangle. Finally, the final conditions are obtening by equidistributing $\eta_P^2$ in direction $x_1$ and $x_2$ observing that

$$\eta_P^2 = \sum_{\substack{K\in\mathcal{T}_h \\ P\in K}} \eta_K^2 = \sum_{\substack{K\in\mathcal{T}_h \\ P\in K}} \left(\eta_{1,K}^4 + \eta_{2,K}^4\right)^{1/2} = \frac{\sum_{\substack{K\in\mathcal{T}_h \\ P\in K}} \left(\eta_{1,K}^4 + \eta_{2,K}^4\right)^{1/2}}{\sum_{\substack{K\in\mathcal{T}_h \\ P\in K}} \eta_{1,K}^2 + \eta_{2,K}^2} \sum_{\substack{K\in\mathcal{T}_h \\ P\in K}} \left(\eta_{1,K}^2 + \eta_{2,K}^2\right).$$

Therefore, we get as sufficient conditions so that (1.37) and (1.38) hold, that $\forall P \in \mathcal{T}_h, i = 1, 2$,

$$\frac{3\sigma_P}{2N_v} 0.75^2 TOL^2 \int_\Omega \mu(\mathbf{x})|\nabla u_h|^2 d\mathbf{x} \leq \sum_{\substack{K\in\mathcal{T}_h \\ P\in K}} \eta_{i,K}^2 \leq \frac{3\sigma_P}{2N_v} 1.25^2 TOL^2 \int_\Omega \mu(\mathbf{x})|\nabla u_h|^2 d\mathbf{x}, \tag{1.39}$$

where we denote the equidistribution parameter

$$\sigma_P = \frac{\sum_{\substack{K\in\mathcal{T}_h \\ P\in K}} \left(\eta_{1,K}^2 + \eta_{2,K}^2\right)}{\sum_{\substack{K\in\mathcal{T}_h \\ P\in K}} \left(\eta_{1,K}^4 + \eta_{2,K}^4\right)^{1/2}}. \tag{1.40}$$

To build a new mesh, the BL2D software requires that at each point, we give $h_{1,P}, h_{2,P}$, that is to say the mesh size in directions $x_1$, respectively, $x_2$ and the angle $\theta_P$ between the horizontal axe and the axe $Ox_1$, see Figure 1.8. Our adaptive startegy consists to align each triangle $K$ (that is to say to align its directions of anisotropy $\mathbf{r}_{1,K}, \mathbf{r}_{2,K}$) with the eigenvectors of the gradient vector $\tilde{G}_K$ and to define a new mesh size in each direction based on (1.39). To do so, we first compute the average local gradient error matrix $G_P$ defined by

$$G_P = \sum_{\substack{K\in\mathcal{T}_h \\ P\in K}} \tilde{G}_K(\Pi_h^{ZZ} u_h - u_h). \tag{1.41}$$

We then compute the angle between the horizontal axe and the eigenvector of $G_P$ corresponding to its maximal eigenvalue (that is to say in our setting the $x_1$ direction) and we set $\theta_P$ to this angle. Moreover, to adapt the mesh size, we compute the average local stretching values $\lambda_{i,P}$ at the point $P$ defined by

$$\lambda_{i,P} = \frac{\sum_{\substack{K\in\mathcal{T}_h \\ P\in K}} \lambda_{i,K}}{\sum_{\substack{K\in\mathcal{T}_h \\ P\in K}} 1}, i = 1, 2. \tag{1.42}$$

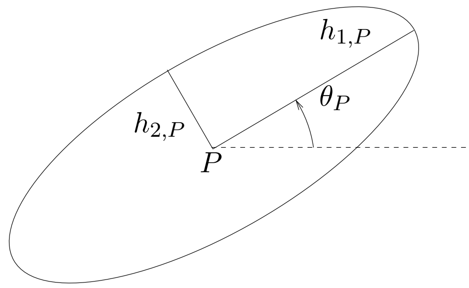


Figure 1.8: Input values of the BL2D mesh generator at a vertex $P \in \mathcal{T}_h$.

If

$$\frac{3\sigma_P}{2N_v} 0.75^2 TOL^2 \int_\Omega \mu(\mathbf{x}) |\nabla u_h|^2 d\mathbf{x} > \sum_{\substack{K \in \mathcal{T}_h \\ P \in K}} \eta_{i,K}^2 \tag{1.43}$$

then we increase the mesh size in direction $x_i$ and set $h_{i,p} = 1.5\lambda_{i,P}$. If

$$\sum_{\substack{K \in \mathcal{T}_h \\ P \in K}} \eta_{i,K}^2 > \frac{3\sigma_P}{2N_v} 1.25^2 TOL^2 \int_\Omega \mu(\mathbf{x}) |\nabla u_h|^2 d\mathbf{x}, \tag{1.44}$$

then we decrease the mesh size in direction $x_i$ and we set $h_{i,p} = \frac{\lambda_{i,P}}{1.5}$.

**Remark 1.18** (Metric based mesh generator)**.**
BL2D is a metric based mesh generator, that is to say, to generate the new mesh, we have to prescribe at each vertex $P$ a Riemannian metric $\mathcal{M}_P$. The goal of the mesh generator is then to create a cloud of points such that for every $P$ in the cloud, its neighbours are at distance one in the prescribed metric $\mathcal{M}_P$. Our algorithm provides in fact a metric given by

$$\mathcal{M}_P = \begin{pmatrix} \cos(\theta_P) & \sin(\theta_P) \\ -\sin(\theta_P) & \cos(\theta_P) \end{pmatrix} \begin{pmatrix} \frac{1}{h_{1,P}^2} & 0 \\ 0 & \frac{1}{h_{2,P}^2} \end{pmatrix} \begin{pmatrix} \cos(\theta_P) & -\sin(\theta_P) \\ \sin(\theta_P) & \cos(\theta_P) \end{pmatrix}.$$

For more details on this topic, we refer for instance to [19, 49].

The complete adaptive algorithm is summarized in Table 1.6. We note by $N_{loop}$ the number of time the adaptive procedure is repeated to build a suitable anisotropic mesh. In practice, we observe that to stop the algorithm with the criteria (1.28) or (1.34) is not sufficient to force the mesh to be highly anistropic for steady problems. This can be understand in the following way : not enough remeshings are done so that the local tests (1.39) are satisfied for must of the points. This will not be anymore a restriction in the case of transient problems, since more meshes will be built due to the evolution of the time. In the next section, numerical experiments are performed to check the efficiency of the adaptive algorithm 1.6.

| | |
|---|---|
| **For** $n = 0, 1, ..., N_{loop}$ | Max number of algorithm loops |
| Compute $u_h$ on $\mathcal{T}_h$ | |
| **For** $K \in \mathcal{T}_h$, compute | |
| $\lambda_{1,K}, \lambda_{2,K}, \mathbf{r}_{1,K}, \mathbf{r}_{2,K}$ | |
| $\tilde{G}_K(\Pi_h u_h - u_h), \eta_{1,K}^2, \eta_{2,K}^2$ | |
| **For** $P \in \mathcal{T}_h$, compute $G_P$ and $\theta_P$ | set the anisotropy directions to the eigenvectors of $G_P$ |
| **For** $i = 1, 2$ Test conditions (1.39) | |
| Compute the average mesh size $\lambda_{i,P}$ | |
| **If** the mesh size is too small in direction $x_i$, set $h_{i,P} = 3/2\lambda_{i,P}$ | Change the mesh size in direction $x_i$ |
| **If** the mesh size is too bin big in direction $x_i$, set $h_{i,P} = 2/3\lambda_{i,P}$ | |
| Build a new mesh using the BL2D software | |

Table 1.6: Anisotropic adaptive algorithm

**Remark 1.19** (Choice of $\sigma_P$)**.**
We give some motivation about the choice of $\sigma_P$ defined in (1.40).

(i) Observe that if the error (more precisely the error indicator) is zero in one direction (let us assume in direction $x_1$), then we have that

$$\eta_P^2 = \sum_{\substack{K\in\mathcal{T}_h\\P\in K}} \eta_K^2 = \sum_{\substack{K\in\mathcal{T}_h\\P\in K}} \left(\eta_{1,K}^4 + \eta_{2,K}^4\right)^{1/2} = \sum_{\substack{K\in\mathcal{T}_h\\P\in K}} \eta_{2,K}^2.$$

Consequently, it seems natural to make appear the quantities

$$\sum_{\substack{K\in\mathcal{T}_h\\P\in K}} \eta_{1,K}^2 \text{ and } \sum_{\substack{K\in\mathcal{T}_h\\P\in K}} \eta_{2,K}^2.$$

(ii) Let us assume that for any $P$, we have for all $K$ such that $P \in K$,

$$\tilde{\omega}_{1,K}(\Pi_h^{ZZ} u_h - u_h) = \tilde{\omega}_{2,K}(\Pi_h^{ZZ} u_h - u_h), \tag{1.45}$$

then we have

$$\sigma_P = \frac{2}{\sqrt{2}}.$$

Therefore, (1.39) reduces to

$$\begin{aligned} \frac{3}{\sqrt{2}N_P} 0.75^2 TOL^2 \int_\Omega \mu(\mathbf{x})|\nabla u_h|^2 d\mathbf{x} &\le \sum_{\substack{K\in\mathcal{T}_h\\P\in K}} \eta_{i,K}^2 \\ &\le \frac{3}{\sqrt{2}N_P} 1.25^2 TOL^2 \int_\Omega \mu(\mathbf{x})|\nabla u_h|^2 d\mathbf{x}, \quad i = 1, 2. \end{aligned}$$

Summing over the points, and noting that

$$\sum_{P\in\mathcal{T}_h} \sum_{\substack{K\in\mathcal{T}_h\\P\in K}} \eta_{i,K}^2 = 3 \sum_{K\in\mathcal{T}_h} \eta_{i,K}^2$$

we obtain finally that

$$\frac{1}{\sqrt{2}} 0.75^2 TOL^2 \int_\Omega \mu(\mathbf{x})|\nabla u_h|^2 d\mathbf{x} \le \sum_{K\in\mathcal{T}_h} \eta_{i,K}^2 \le \frac{1}{\sqrt{2}} 1.25^2 TOL^2 \int_\Omega \mu(\mathbf{x})|\nabla u_h|^2 d\mathbf{x} \quad i = 1, 2,$$

that is to say the error is globally equidistributed in both directions $x_1$ and $x_2$. Therefore, we think that the local tests (1.39) are the good one, since they asymptotically yield to a global error equidistribution, in addition to (1.28). (It's clear that assuming (1.45) implies in fact that $\eta_{1,K}^2 = \eta_{2,K}^2, \forall K$, yielding the stronger result that $\sum_{K\in\mathcal{T}_h} \eta_{1,K}^2 = \sum_{K\in\mathcal{T}_h} \eta_{2,K}^2$ but we were looking for a "philosophical" motivation.)

## 1.5 Numerical experiments with adapted meshes

We now analyse the efficiency of our adaptive algorithm. We first apply it to the Example 1.17 with $\mu_1 = 1, \mu_2 = 2$ and $\varepsilon = 0.1$. The initial grid is an isotropic mesh of mesh size $h = 0.1$. The convergence results are reported in Table 1.8 for $N_{loop} = 40$. In particular, we investigate the number of vertices and the value of the aspect ratio of the mesh for several values of $TOL$. The additional used notations are described in Table 1.7. We summarize our observations below:

- Both error and error indicator are $\simeq O(TOL)$.
- The number of vertices is multiplied by 2 when $TOL$ is divided by 2, like the mean aspect ratio. This validates our a priori expectation, since the solution does not depend on $x_2$.
- $ei^A$ is constant and stays close to 3.
- The ZZ post-processing is asymptotically exact.
- The necessary number of remeshings to reach the stopping criteria are independent of the tolerance.

| | |
|---|---|
| $TOL$ | Prescribed tolerance |
| $N_v$ | Number of vertices of the last generated mesh |
| $N_{v,i}$ | Number of vertices that satisfy the local test (1.39) in direction $i = 1, 2$ |
| $N_{v,i}^c$ | Number of vertices that satisfy the coarsening condition (1.43) in direction $i = 1, 2$ |
| $N_{v,i}^r$ | Number of vertices that satisfy the refinement condition (1.44) in direction $i = 1, 2$ |
| $\overline{ar}$ | Average aspect ratio of the last generated mesh |
| $ar_{max}$ | Maximum aspect ratio of the last generated mesh |
| $N_m$ | Number of remeshings such that the stopping criterion (1.28) is satisfied |
| $N_m^A$ | Number of remeshings such that the anisotropic stopping criterion (1.34) is satisfied |

Table 1.7: Additional notations for the analysis of the adaptive algorithm.

| $TOL$ | $\eta^A$ | $e_{\mu,H^1}$ | $ei^A$ | $ei^{ZZ}$ | $\overline{ar}$ | $a_{max}$ | $N_v$ | $N_m$ | $N_m^A$ |
|---|---|---|---|---|---|---|---|---|---|
| 0.1 | 0.48 | 0.16 | 3.00 | 1.02 | 57 | 246 | 122 | 4 | 4 |
| 0.05 | 0.24 | 0.078 | 3.14 | 1.00 | 110 | 638 | 233 | 4 | 15 |
| 0.025 | 0.12 | 0.038 | 3.16 | 1.00 | 224 | 1092 | 454 | 6 | 15 |
| 0.0125 | 0.061 | 0.019 | 3.18 | 1.00 | 383 | 1671 | 1025 | 7 | 17 |

Table 1.8: Convergence results for Example 1.17 with $\mu_1 = 1, \mu_2 = 2, \varepsilon = 0.1$. We run the adaptive algorithm with $N_{loop} = 40$.

Finally, we investigate the dependence on $N_{loop}$. The results are reported in the Table 1.9 where the adaptive algorithm is applied with $TOL = 0.0125$ and several values of $N_{loop}$. We compute the number of vertices that satisfy the local refinement/coarsening tests (1.39). We observe that the mesh exhibits a large aspect ratio when at least half of the total number of vertices satisfy (1.39) in each direction.

In Figure 1.9, we present the different meshes generated when $N_{loop}$ varies. It is observed that the more we force the algorithm to remesh, the more the mesh looks anisotropic.

| $N_{loop}$ | $N_v$ | $\overline{ar}$ | $N^c_{v,1}$ | $N^r_{v,1}$ | $N_{v,1}$ | $N^c_{v,2}$ | $N^r_{v,2}$ | $N_{v,2}$ |
|---|---|---|---|---|---|---|---|---|
| 1 | 378 | 2 | 35 | 312 | 31 | 41 | 313 | 24 |
| 10 | 12812 | 24 | 11119 | 8 | 1685 | 6575 | 107 | 6130 |
| 20 | 1685 | 196 | 730 | 43 | 912 | 841 | 16 | 828 |
| 30 | 1141 | 1447 | 415 | 73 | 653 | 525 | 15 | 601 |
| 40 | 1025 | 1671 | 397 | 83 | 545 | 470 | 15 | 540 |

Table 1.9: Dependence on $N_{loop}$. The results are presented for Example 1.17 with $\mu_1 = 1, \mu_2 = 2, \varepsilon = 0.1$ and $TOL = 0.0125$.

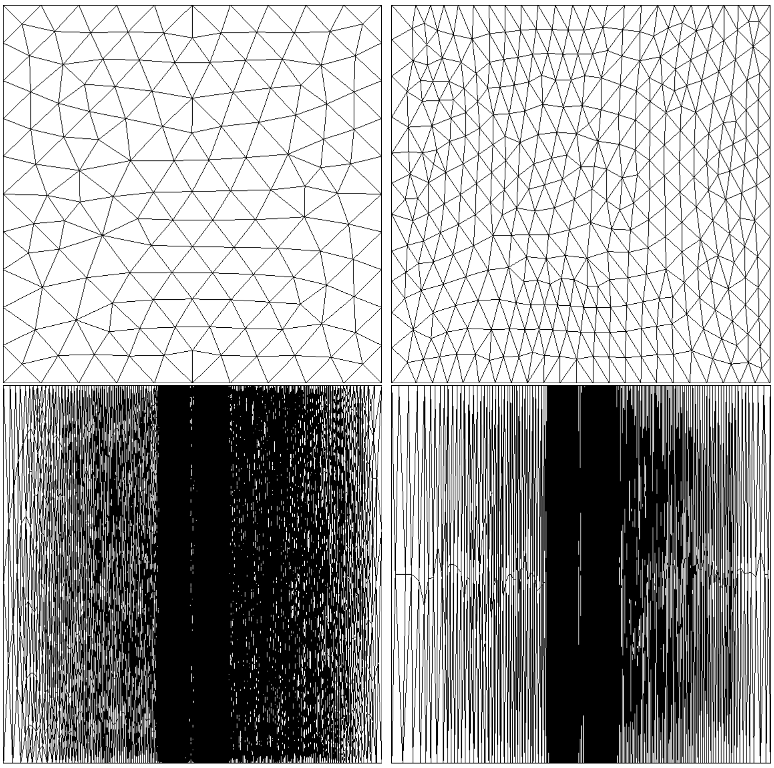

Figure 1.9: Generated meshes for Example 1.17 with $\mu_1 = 1, \mu_2 = 2, \varepsilon = 0.1, TOL = 0.0125$ and several values of $N_{loop}$. Initial grid (left top), $N_{loop} = 1$ (right top), $N_{loop} = 10$ (left bottom), $N_{loop} = 40$, (right bottom).

To conclude with the Example 1.17, we apply the adaptive algorithm to a more complex case where $\mu_1 = 1, \mu_2 = 100$ and $\varepsilon = 0.01$. The initial grid is an isotropic mesh of mesh size $h = 0.01$. The convergence results are reported in Table 1.10. The solution is represented in Figures 1.11 and 1.10 and the mesh in Figure 1.12.

| $TOL$ | $\eta^A$ | $e_{\mu,H^1}$ | $ei^A$ | $ei^{ZZ}$ | $\overline{ar}$ | $a_{max}$ | $N_v$ | $N_m$ | $N_m^A$ |
|---|---|---|---|---|---|---|---|---|---|
| 0.1 | 476.42 | 158.13 | 3.01 | 1.00 | 611 | 2184 | 156 | 9 | 9 |
| 0.05 | 258.447 | 78.48 | 3.29 | 0.96 | 1115 | 7076 | 314 | 10 | 10 |
| 0.025 | 130.42 | 40.27 | 3.23 | 0.91 | 1954 | 13815 | 651 | 11 | 11 |
| 0.0125 | 64.76 | 20.00 | 3.24 | 0.99 | 2800 | 14343 | 1619 | 12 | 12 |

Table 1.10: Convergence results for Example 1.17 with $\mu_1 = 1, \mu_2 = 100, \varepsilon = 0.01$. We run the adaptive algorithm with $N_{loop} = 40$.

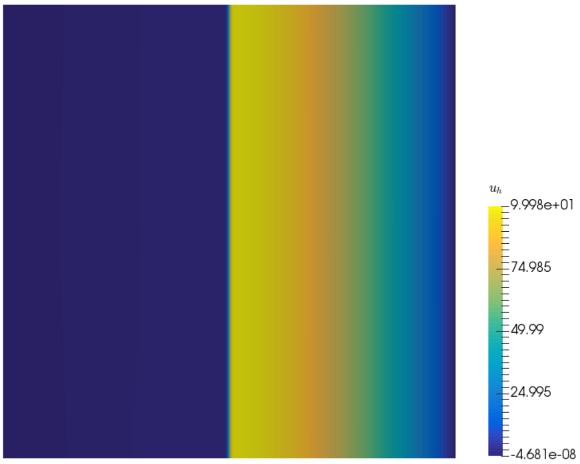


Figure 1.10: Numerical solution to Example 1.17 with $\mu_1 = 1, \mu_2 = 100$ and $\varepsilon = 0.01$. The solution is computed with $TOL = 0.0125$ and $N_{loop} = 40$.

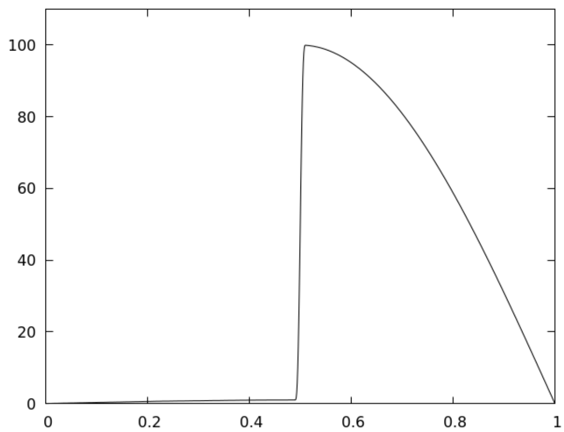


Figure 1.11: Plot along the axe $x_1$ of the numerical solution to Example 1.17 with $\mu_1 = 1, \mu_2 = 100$ and $\varepsilon = 0.01$. The solution is computed with $TOL = 0.0125$ and $N_{loop} = 40$.

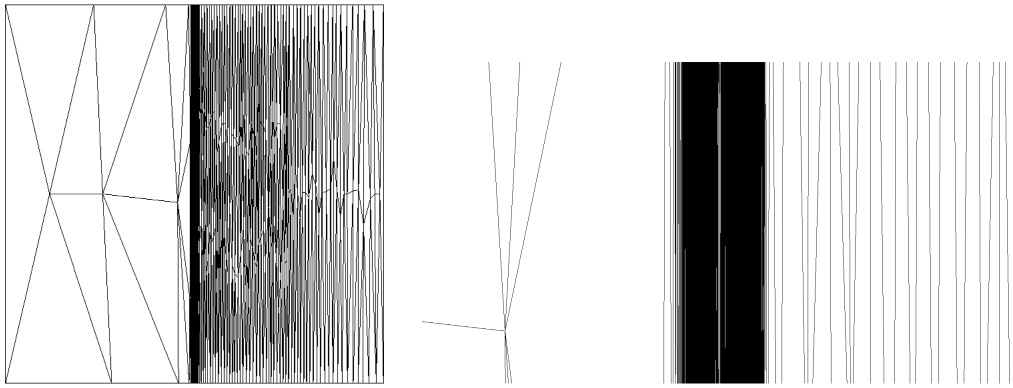

Figure 1.12: Final mesh generated when solving Example 1.17 with $\mu_1 = 1, \mu_2 = 100$, $\varepsilon = 0.01$, $TOL = 0.0125$ and $N_{loop} = 40$ (left). Zoom at the point (0.5,0.5) (right).

We conclude this analysis in the next example.

**Example 1.20.**
The goal of this example is to approximate the solution of the following problem. Let $\Omega \in \mathbb{R}^2$ be an open, convex polygon, $B$ be an open disk compactly contained in $\Omega$ and $u$ the solution of

$$\begin{cases} -\Delta u = f, & \text{in } \Omega \setminus \overline{B}, \\ \nabla u = 0, & \text{in } B, \\ u = 0, & \text{on } \partial\Omega, \end{cases} \tag{1.46}$$

with $f \in L^2(\Omega \setminus \overline{B})$. This problem can be seen as a toy version of the fluid-rigid body problem studied in the Part 2 of Chapter 4, where $B$ is interpreted as a rigid body, inside which the velocity $u$ has to be constant.

Written in weak form, the previous problem reads: find $u \in V$ such that

$$\int_{\Omega\setminus\overline{B}} \nabla u \cdot \nabla v d\mathbf{x} = \int_{\Omega\setminus\overline{B}} f v d\mathbf{x}, \quad \forall v \in V, \tag{1.47}$$

where

$$V = H_0^1(\Omega) \cap \left\{ v \in H^1(\Omega) : \nabla v = 0 \text{ in } B \right\}.$$

In [77], a penalty method is proposed to solve (1.47). Given $\delta > 0$, the method reads: find $u_\delta \in H_0^1(\Omega)$ the solution of the variational problem

$$\int_{\Omega\setminus\overline{B}} \nabla u_\delta \cdot \nabla v d\mathbf{x} + \frac{1}{\delta} \int_B \nabla u_\delta \cdot \nabla v d\mathbf{x} = \int_\Omega f v d\mathbf{x}, \quad \forall v \in H_0^1(\Omega), \tag{1.48}$$

where we extend $f$ by 0 inside $B$. It is shown [77] that (1.47) and (1.48) are well-posed and that $u_\delta$ converges to $u$ in $H_0^1(\Omega)$ as $\delta$ goes to zero, namely there exists a constant $C > 0$, independent of $\delta$ such that

$$\|\nabla(u - u_\delta)\|_{L^2(\Omega)} \leq C\delta.$$

The solution of (1.48) can be approximated by our numerical method and numerical algorithm, observing that it can be written as

$$\int_\Omega \mu_\delta(\mathbf{x}) \nabla u_\delta \cdot \nabla v d\mathbf{x} = \int_\Omega f v d\mathbf{x},$$

where

$$\mu_\delta(\mathbf{x}) = \begin{cases} 1, & \mathbf{x} \in \Omega \setminus \overline{B}, \\ \\ \dfrac{1}{\delta}, & \mathbf{x} \in B. \end{cases}$$

In order to apply our finite element scheme, we first smooth $\mu_\delta$ introducing the function

$$\mu_{\delta,\varepsilon}(\mathbf{x}) = 1 + \left(\frac{1}{\delta} - 1\right) H_\varepsilon(r(\mathbf{x})), \tag{1.49}$$

with $H_\varepsilon$ the smooth Heavyside function defined in (1.25) and $r(\mathbf{x})$ given by

$$r(\mathbf{x}) = R - \sqrt{(x_1 - c_1)^2 + (x_2 - c_2)^2},$$

where $R$ is the radius of $B$ and $(c_1, c_2)$ the coordinates of its center.

Finally, for any $h > 0$, let $\mathcal{T}_h$ be a conformal triangulation of $\Omega$ into triangles. The finite elements method used to approximate the solution of (1.46) reads: find $u_{\delta,\varepsilon,h} \in V_h$, where $V_h$ is as before the set of continuous, piecewise linear function with zero value on $\partial\Omega$, the solution of

$$\int_\Omega \mu_{\delta,\varepsilon}(\mathbf{x}) \nabla u_{\delta,\varepsilon,h} \cdot \nabla v_h d\mathbf{x} = \int_\Omega f v_h d\mathbf{x}, \quad \forall v_h \in V_h. \tag{1.50}$$

In what follows, we are not interesting in analyzing the convergence of our numerical method with respect to $\delta$ or $\varepsilon$. We will rather focus on the convergence of the adaptive algorithm 1.6 applied to (1.50), assuming that for small $\delta$ and $\varepsilon$ our solution is sufficiently close to the exact solution $u$. We choose therefore $\delta = 0.0001$ and $\varepsilon = 0.001$.

For the numerical example, we set $\Omega$ as the unit open square as before and $B$ as the disk of radius 0.1, centered at $(0.5, 0.5)$. Finally, we set $f = 1$. The initial grid is an isotropic grid of mesh size $h = 0.01$. This simulation is costly and to improve the efficiency of the adaptive algorithm we propose to proceed by continuation: we start with a tolerance $TOL = \theta$, and run the adaptive algorithm for a given $N_{loop}$. Then to compute the solution with $TOL = \theta/2$, rather than to start again from the uniform initial grid, we start from the final mesh generated with $TOL = \theta$. This procedure is reproduced to compute the solution for $TOL = \theta/4$, $\theta/8$ and so on. The algorithm is run from a starting tolerance $TOL = 0.1$ until $TOL = 0.0125$. Between each tolerance $N_{Loop}$ is set to 40.

The solution is represented in Figures 1.13 and 1.14. In Figure 1.15, we present the final meshes obtained with respect to $TOL = 0.1, 0.05, 0.025$ and 0.0125.

The convergence of the algorithm is checked in Table 1.11 and in Figure 1.17. We observe in Table 1.11 that both error indicators $\eta^A$ and $\eta^{ZZ}$ behaves asymptotically like $O(TOL)$ and that the number of vertices is approximatively multiplying by 4 when the tolerance is divided by 2 as expected since it is anticipated that the solution is an isotropic function. Note that the number of remeshings needed to reach the stopping criteria for a given tolerance are around 1 since the second tolerance. This can be explained by the fact that the algorithm starts at every tolerance with a better initial grid.

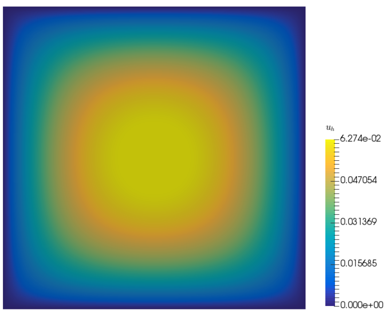


Figure 1.13: Numerical solution to Example 1.20 obtained at $TOL = 0.0125$.

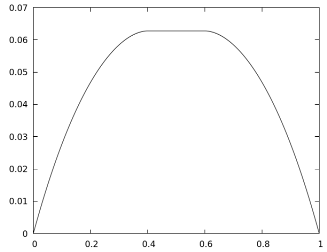


Figure 1.14: Numerical solution to Example 1.20 obtained at $TOL = 0.0125$. Plot along the $x_1$-solution.

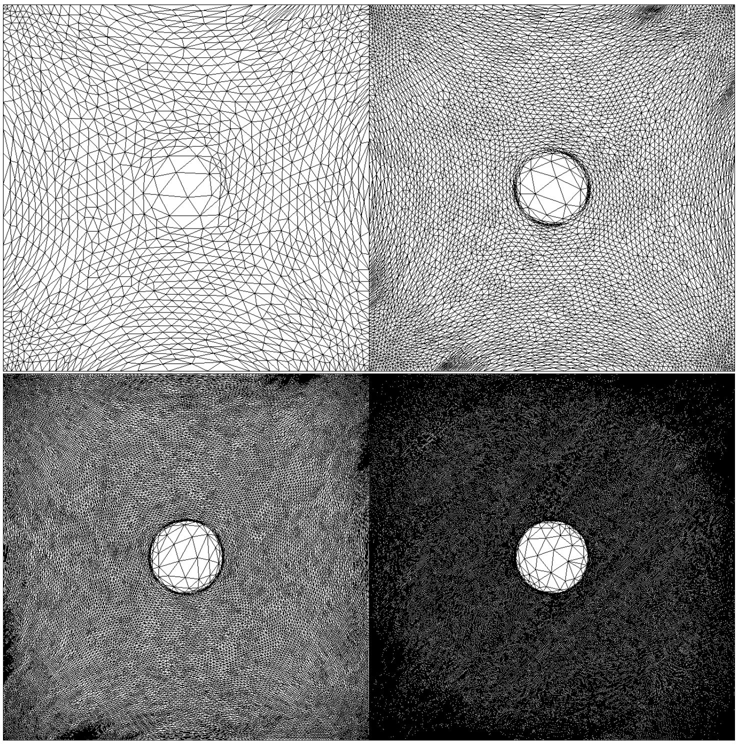

Figure 1.15: Adapted meshes obtained when solving Example 1.20. $TOL = 0.1$ (top left), $TOL = 0.05$ (top right), $TOL = 0.025$ (bottom left) and $TOL = 0.0125$ (bottom right).

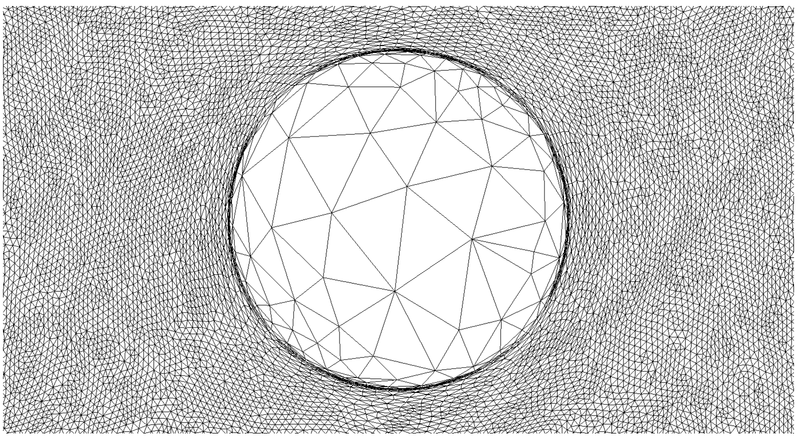

Figure 1.16: Zoom on the adapted mesh obtained when solving Example 1.20 with the adaptive algorithm at $TOL = 0.0125$.

| $TOL$ | $\eta^A$ | $\eta^{ZZ}$ | $\overline{ar}$ | $a_{max}$ | $N_v$ | $N_m$ | $N_m^A$ |
|---|---|---|---|---|---|---|---|
| 0.1 | 0.14 | 0.0055 | 3 | 22 | 1408 | 3 | 4 |
| 0.05 | 0.011 | 0.0027 | 3 | 45 | 5531 | 1 | 1 |
| 0.025 | 0.0039 | 0.0013 | 3 | 83 | 21259 | 2 | 2 |
| 0.0125 | 0.0018 | 0.00067 | 4 | 132 | 82588 | 1 | 1 |

Table 1.11: Convergence results for Example 1.20.

.

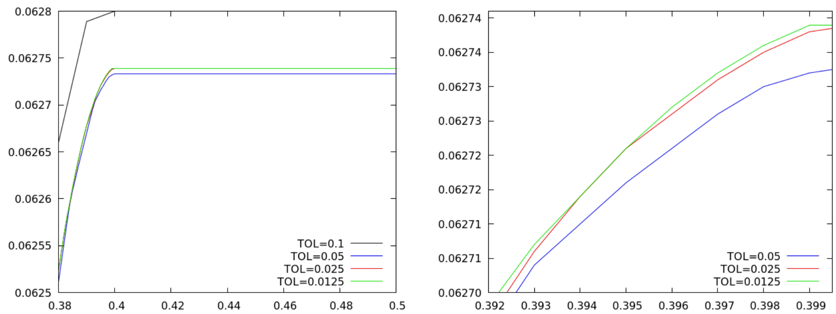


Figure 1.17: Convergence results for the adaptive algorithm apllied to Example 1.20. Plot along the $x_1$-axe. Zoom in the boudary layer.

**Remark 1.21.**
To conclude the analysis of our adaptive strategy, we make a observation on the local error indicator (1.17). We recall that $\eta_K^2$ is given by

$$\eta_K^2 = \left( \|f + \operatorname{div}(\mu(\mathbf{x})\nabla u_h)\|_{L^2(K)} + \frac{\| [\mu(\mathbf{x})\nabla u_h \cdot \mathbf{n}] \|_{L^2(\partial K)}}{2\sqrt{\lambda_{2,K}}} \right) \tilde{\omega}_K(\Pi_h^{ZZ} u_h - u_h),$$

where $\Pi_h^{ZZ} u_h$ and $\tilde{\omega}_K$ are defined as before. We can split the local error indicator in two parts, namely

$$\eta_K^2 = (\eta_K^R)^2 + (\eta_K^J)^2,$$

where we define the residual part as

$$(\eta_K^R)^2 = \|f + \operatorname{div}(\mu(\mathbf{x})\nabla u_h)\|_{L^2(K)} \tilde{\omega}_K(\Pi_h^{ZZ} u_h - u_h), \tag{1.51}$$

and the jumps part as

$$(\eta_K^J)^2 = \frac{\| [\mu(\mathbf{x})\nabla u_h \cdot \mathbf{n}] \|_{L^2(\partial K)}}{2\sqrt{\lambda_{2,K}}} \tilde{\omega}_K(\Pi_h u_h - u_h). \tag{1.52}$$

In [28], it is proven that for elliptic equations with constant coefficients, the numerical error is, up to higher order perturbations, equivalent to the error indicator $\tilde{\eta}$ defined by

$$\tilde{\eta}^2 = \sum_{K \in \mathcal{T}_h} (\eta_K^J)^2.$$

Nevertheless, numerical experiments seem to indicate that for variable coefficients the residual part cannot be neglected. We also observe that better meshes are built by the adaptive algorithm when $(\eta_K^R)^2$ is kept in the error indicator. To illustrate our comments, we do a quick and simple experiment. We fix the tolerance to $TOL = 0.025$, $N_{loop} = 10$ and we run the adaptive algorithm 1.6 with different choices for the local error estimator (without proceeding by continuation). We plot the adapted meshes obtained for Example

1.20 when we set $\eta_K^2 = (\eta_K^R)^2$ (Figure 1.18), $\eta_K^2 = (\eta_K^J)^2$ (Figure 1.19) and finally when $\eta_K^2$ is given by the full estimator (1.17) (Figure 1.20). We can notice that to obtain a suitable mesh, both parts $(\eta_K^R)^2$ and $(\eta_K^J)^2$ are necessary.

When only $(\eta_K^R)^2$ is used, the interface is well captured , but the mesh is too much refined inside the disk. On the contrary, when we used only $(\eta_K^J)^2$ as a local error indicator, the mesh is coarsen inside the disk, where the solution has no variation, but the interface is tracked with less accuracy. We conclude therefore, that for equations with variable coefficients, both parts of the local error estimator are important. In some sense, the residual part $(\eta_K^R)^2$ sees the variations of the coefficients, and the jumps part $(\eta_K^J)^2$ sees the variation of the solution. Indeed, observe in particular that the residual contains the gradient of $\mu$ since

$$\mathrm{div}(\mu(\mathbf{x})\nabla u_h) = \nabla\mu(\mathbf{x}) \cdot \nabla u_h + \mu(x)\Delta u_h = \nabla\mu(\mathbf{x}) \cdot \nabla u_h.$$

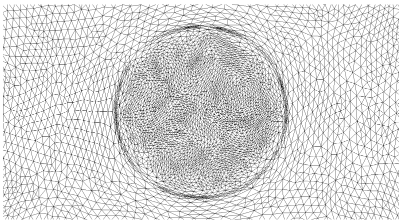

Figure 1.18: Zoom on the adapted mesh obtained when solving Example 1.20 with the adaptive algorithm with $TOL = 0.025$ and $N_{loop} = 10$. The local error estimator (1.51) is used.

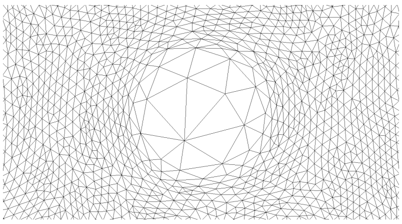

Figure 1.19: Zoom on the adapted mesh obtained when solving Example 1.20 with the adaptive algorithm with $TOL = 0.025$ and $N_{loop} = 10$. The local error estimator (1.52) is used.

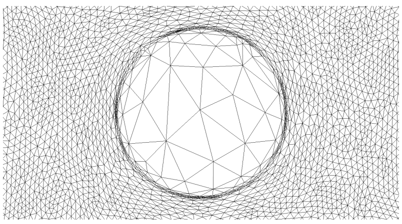

Figure 1.20: Zoom on the adapted mesh obtained when solving Example 1.20 with the adaptive algorithm with $TOL = 0.025$ and $N_{loop} = 10$. The full local error estimator (1.17) is used.

## 1.6 3D experiments

We conclude this chapter by presenting a few examples in 3D. We briefly expose the modifications in the notations used to describe our anisotropic setting. Let $\Omega$ be a convex polyhedron and $\mathcal{T}_h$ be a conformal triangulation of $\Omega$ into tetrahedrons $K$ of diameter $h_K \leq h$. We recall that, for each $K \in \mathcal{T}_h$, the affine map $T_K$ mapping the reference $\hat{K}$ into $K$ can be written as

$$\mathbf{x} = T_K(\hat{\mathbf{x}}) = M_K\hat{\mathbf{x}} + \mathbf{t}_K,$$

where $M_K \in \mathbb{R}^{3\times 3}$ and $\mathbf{t}_K \in \mathbb{R}^3$. As in the 2D case, $M_K$ can be decomposed as $M_K = R_K^T \Lambda_K P_K$ with $R_K$ and $P_K$ orthogonal matrices and $\Lambda_K$ the matrix of singular values

$$\Lambda_K = \begin{pmatrix} \lambda_{1,K} & 0 & 0 \\ 0 & \lambda_{2,K} & 0 \\ 0 & 0 & \lambda_{3,K} \end{pmatrix}, \quad \lambda_{1,K} \geq \lambda_{2,K} \geq \lambda_{3,K} \geq 0, \qquad R_K = \begin{pmatrix} \mathbf{r}_{1,K}^T \\ \mathbf{r}_{2,K}^T \\ \mathbf{r}_{3,K}^T \end{pmatrix},$$

where $\mathbf{r}_{1,K}, \mathbf{r}_{2,K}, \mathbf{r}_{3,K}$ are the three directions of anisotropy of $K$. With these notations, all the interpolation results presented in Section 1.1 can be extended. In particular, given $R_h$ the Clément's interpolant on $\mathcal{T}_h$, one can prove that there exists a constant $C > 0$ depending only on the reference tetrahedron $\hat{K}$ such that for all $v \in H^1(\Omega)$

$$\|v - R_h(v)\|_{L^2(K)}^2 + \lambda_{3,K}\|v - R_h(v)\|_{L^2(\partial K)}^2 + \lambda_{3,K}^2\|\nabla(v - R_h(v))\|_{L^2(K)}^2 \leq C\omega_K^2(v), \quad (1.53)$$

with

$$\omega_K^2(v) = \lambda_{1,K}^2(\mathbf{r}_{1,K}^T G_K(v)\mathbf{r}_{1,K}) + \lambda_{2,K}^2(\mathbf{r}_{2,K}^T G_K(v)\mathbf{r}_{2,K}) + \lambda_{3,K}^2(\mathbf{r}_{3,K}^T G_K(v)\mathbf{r}_{3,K}), \quad (1.54)$$

where $G_K(v)$ is the matrix of the first derivatives, which coefficients $G_K(v)_{ij}$ are given by

$$G_K(v)_{ij} = \int_{\Delta K} \frac{\partial v}{\partial x_i}\frac{\partial v}{\partial x_j} d\mathbf{x}, \quad i, j = 1, 2, 3.$$

The 2D a posteriori error estimate contained in Theorem 1.11 is then fully generalizable to the 3D case and we can now define the following error indicator for the numerical error $\int_\Omega \mu(\mathbf{x})|\nabla(u - u_h)|^2 d\mathbf{x}$:

$$\eta^A = \left(\sum_{K\in\mathcal{T}_h} \eta_K^2\right)^{1/2}$$

where $\eta_K^2$ is given by

$$\eta_K^2 = \left(\|f + \operatorname{div}(\mu(\mathbf{x})\nabla u_h)\|_{L^2(K)} + \frac{\|\,[\mu(\mathbf{x})\nabla u_h \cdot \mathbf{n}]\,\|_{L^2(\partial K)}}{2\sqrt{\lambda_{3,K}}}\right)\tilde{\omega}_K(\Pi_h^{ZZ}u_h - u_h), \quad (1.55)$$

where as before $\Pi_h^{ZZ}u_h$ stands for the ZZ post-processing of $u_h$ and $\tilde{\omega}_K$ is defined for $v \in H^1(\Omega)$ by

$$\tilde{\omega}_K^2(v) = \lambda_{1,K}^2(\mathbf{r}_{1,K}^T\tilde{G}_K(v)\mathbf{r}_{1,K}) + \lambda_{2,K}^2(\mathbf{r}_{2,K}^T\tilde{G}_K(v)\mathbf{r}_{2,K}) + \lambda_{3,K}^2(\mathbf{r}_{3,K}^T\tilde{G}_K(v)\mathbf{r}_{3,K})$$

with $\tilde{G}_K(v)$ being the 3D equivalent of the simplified matrix advocated in Remark 1.15 with coefficients

$$\tilde{G}_K(v)_{ij} = \int_K \frac{\partial v}{\partial x_i}\frac{\partial v}{\partial x_j} d\mathbf{x}, i, j = 1, 2, 3.$$

We focus on the 3D version of two examples presented in Section 1.5. We first perform numerical experiments on constant meshes.

**Example 1.22** (A 3D anisotropic case with non adapted meshes)**.**
We set $\Omega$ as the unit cube $]0,1[^3$ and we solve the Poisson equation (1.5) in $\Omega$. As in the 2D Example 1.17 $\mu$ is given by

$$\mu(\mathbf{x}) = \mu(x_1, x_2, x_3) = \mu_2 H_\varepsilon(x_1 - 0.5) + \mu_1(1 - H_\varepsilon(x_1 - 0.5)), \quad \mu_1, \mu_2 > 0,$$

where as before $H_\varepsilon$ is the smoothing of the Heavyside graph. We compute the right hand side $f$ such that the solution is given by

$$u(x_1, x_2, x_3) = \mu_2 sin(\pi x_1) H_\varepsilon(x_1 - 0.5) + \mu_1 sin(\pi x_1) H_\varepsilon(0.5 - x_1).$$

We report in Table 1.12 and Table 1.13 the convergence results obtained with anisotropic meshes of aspect ration 50 and 500 and several choices for $\mu_1, \mu_2$ and $\varepsilon$. The notations are the same as in the 2D numerical experiments. The numerical results imply the same conclusion as before, namely $ei^A$ is independant of $\mu$, the exact solution and the aspect ratio of the mesh and $ei^{ZZ}$ is close to one.

| $h_1 - h_2 - h_3$ | $\eta^A$ | $e_{\mu,H^1}$ | $ei^A$ | $\eta^{ZZ}$ | $e_{H^1}$ | $ei^{ZZ}$ |
|---|---|---|---|---|---|---|
| 0.01 - 0.5 - 0.5 | 0.52 | 0.18 | 2.89 | 0.15 | 0.14 | 1.07 |
| 0.005 - 0.25 - 0.25 | 0.26 | 0.081 | 3.12 | 0.065 | 0.065 | 1.00 |
| 0.0025 - 0.125 - 0.125 | 0.13 | 0.038 | 3.42 | 0.03 | 0.03 | 1.00 |
| 0.001 - 0.5 - 0.5 | 0.052 | 0.018 | 2.89 | 0.014 | 0.014 | 1.00 |
| 0.0005 - 0.25 - 0.25 | 0.026 | 0.0082 | 3.17 | 0.0065 | 0.0065 | 1.00 |

Table 1.12: Convergence results for Example 1.22 with $\mu_1 = 1, \mu_2 = 2$ and $\varepsilon = 0.1$. The mesh aspect ratio is 50 (rows 1-3) and 500 (rows 4-5).

| $h_1 - h_2 - h_3$ | $\eta^A$ | $e_{\mu,H^1}$ | $ei^A$ | $\eta^{ZZ}$ | $e_{H^1}$ | $ei^{ZZ}$ |
|---|---|---|---|---|---|---|
| 0.01 - 0.5 - 0.5 | 184.34 | 101.12 | 1.82 | 51.64 | 45.13 | 1.14 |
| 0.005 - 0.25 - 0.25 | 137.05 | 42.53 | 3.22 | 22.30 | 18.89 | 1.18 |
| 0.0025 - 0.125 - 0.125 | 67.26 | 19.15 | 3.51 | 9.06 | 8.03 | 1.13 |
| 0.001 - 0.5 - 0.5 | 26.21 | 8.95 | 2.93 | 3.88 | 3.82 | 1.02 |
| 0.0005 - 0.25 - 0.25 | 13.07 | 4.06 | 3.22 | 1.74 | 1.73 | 1.00 |

Table 1.13: Convergence results for Example 1.22 with $\mu_1 = 1, \mu_2 = 10$ and $\varepsilon = 0.01$. The mesh aspect ratio is 50 (rows 1-3) and 500 (rows 4-5).

We are now presenting numerical experiments with adapted meshes. To generate our meshes and proceed to the adaptation, we use the feflo.a software [71], which needs a local metric for every points $P \in \mathcal{T}_h$ to built a new mesh. Therefore, the 2D algorithm 1.6 is fully generalizable to the 3D case, the only step changing is that we equidistribute the error in three directions at the 4 vertices of each tetrahedron of $\mathcal{T}_h$. Therefore, the local conditions (1.39) are replaced by

$$\begin{aligned} \frac{4\sigma_P}{3N_v} 0.75^2 TOL^2 \int_\Omega \mu(\mathbf{x}) |\nabla u_h|^2 d\mathbf{x} \leq \sum_{\substack{K \in \mathcal{T}_h \\ P \in K}} \eta_{i,K}^2 \\ \leq \frac{4\sigma_P}{3N_v} 1.25^2 TOL^2 \int_\Omega \mu(\mathbf{x}) |\nabla u_h|^2 d\mathbf{x}, \forall P \in \mathcal{T}_h, i = 1, 2, 3, \quad (1.56) \end{aligned}$$

where we note the anisotropic error indicator in direction $x_i$, for $i = 1, 2, 3$,

$$\eta_{i,K}^2 = \left( \|f + \text{div}(\mu(\mathbf{x}) \nabla u_h)\|_{L^2(K)} + \frac{\| [\mu(\mathbf{x}) \nabla u_h \cdot \mathbf{n}] \|_{L^2(\partial K)}}{2\sqrt{\lambda_{3,K}}} \right) \tilde{\omega}_{i,K}(\Pi_h^{ZZ} u_h - u_h),$$

with

$$\tilde{\omega}_{i,K}^2(v) = \lambda_{i,K}^2 \mathbf{r}_{i,K}^T \tilde{G}_K(v) \mathbf{r}_{i,K},$$

and

$$\sigma_P = \frac{\sum_{\substack{K\in\mathcal{T}_h\\P\in K}} \eta_{1,K}^2 + \eta_{2,K}^2 + \eta_{3,K}^2}{\sum_{\substack{K\in\mathcal{T}_h\\P\in K}} \left(\eta_{1,K}^4 + \eta_{2,K}^4 + \eta_{3,K}^4\right)^{1/2}}.$$

For the same reason, the anisotropic stopping criterion (1.34) is replaced by

$$\frac{1}{3^{1/4}}0.75TOL \leq \left(\frac{\sum_{K\in\mathcal{T}_h} \eta_{i,K}^2}{\int_\Omega \mu(\mathbf{x})|\nabla u_h|^2 d\mathbf{x}}\right)^{1/2} \leq \frac{1}{3^{1/4}}1.25TOL, i=1,2,3. \tag{1.57}$$

**Remark 1.23.**
As for the 2D adaptive algorithm, we provide to the mesh generator a metric $\mathcal{M}_P$ given by

$$Q^T \begin{pmatrix} \frac{1}{h_{1,P}^2} & 0 & 0 \\ 0 & \frac{1}{h_{2,P}^2} & 0 \\ 0 & 0 & \frac{1}{h_{3,P}^2} \end{pmatrix} Q$$

where the column of the matrix $Q$ are the eigenvectors of $G_P$ with $G_P$ given by

$$G_P = \sum_{\substack{K\in\mathcal{T}_h\\P\in K}} \tilde{G}_K(\Pi_h^{ZZ}u_h - u_h)$$

and for $i=1,2,3$, $h_{i,P}$ is the prescribed mesh size in direction $x_i$.

We first applied our algorithm to the Example 1.22. The numerical results are reported in Tables 1.14 and 1.15 for different choices of $\mu_1, \mu_2$ and $\varepsilon$. The initial mesh is an isotropic grid of mesh size $h = 0.1$ and the number of remeshing iteration $N_{loop}$ is set to 40. $ei^A$ and $ei^{ZZ}$ stay close the value obtained on fixed grid.

| $TOL$ | $\eta^A$ | $e_{\mu,H^1}$ | $ei^A$ | $ei^{ZZ}$ | $\overline{ar}$ | $a_{max}$ | $N_v$ | $N_m$ | $N_m^A$ |
|---|---|---|---|---|---|---|---|---|---|
| 0.125 | 0.68 | 0.202 | 3.36 | 1.02 | 34 | 221 | 657 | 5 | 5 |
| 0.0625 | 0.35 | 0.11 | 3.37 | 1.00 | 54 | 347 | 1586 | 7 | 7 |
| 0.03125 | 0.18 | 0.0.54 | 3.35 | 1.00 | 83 | 578 | 4516 | 9 | 9 |

Table 1.14: Convergence results for Example 1.22 with $\mu_1 = 1, \mu_2 = 2$ and $\varepsilon = 0.1$ when using the the standard adaptive algorithm with $N_{loop} = 40$.

| $TOL$ | $\eta^A$ | $e_{\mu,H^1}$ | $ei^A$ | $ei^{ZZ}$ | $\overline{ar}$ | $a_{max}$ | $N_v$ | $N_m$ | $N_m^A$ |
|---|---|---|---|---|---|---|---|---|---|
| 1 | 160.285 | 46.64 | 3.44 | 1.00 | 22 | 146 | 1070 | 8 | 8 |
| 0.5 | 83.17 | 24.16 | 3.44 | 1.00 | 45 | 342 | 1645 | 9 | 9 |
| 0.25 | 45.19 | 13.38 | 3.38 | 0.96 | 86 | 673 | 2768 | 9 | 9 |

Table 1.15: Convergence results for Example 1.22 with $\mu_1 = 1, \mu_2 = 10$ and $\varepsilon = 0.01$ when using the the standard adaptive algorithm with $N_{loop} = 40$.

Since 3D computations are costly, to improve the efficiency of the algorithm, we can proceed by continuation. For instance, applying this strategy to Example 1.22 with $\mu_1 = 1, \mu_2 = 10$ and $\varepsilon = 0.01$, we start with a tolerance $TOL = 1$, and run the adaptive algorithm with $N_{loop} = 40$. After each 40 remeshing loops, we divide the tolerance by two, and we start from the last generated mesh until we reach $TOL = 0.125$. The meshes obtained with this procedure are represented in Figure 1.21. The solution for $TOL = 0.125$ is represented in Figure 1.22.

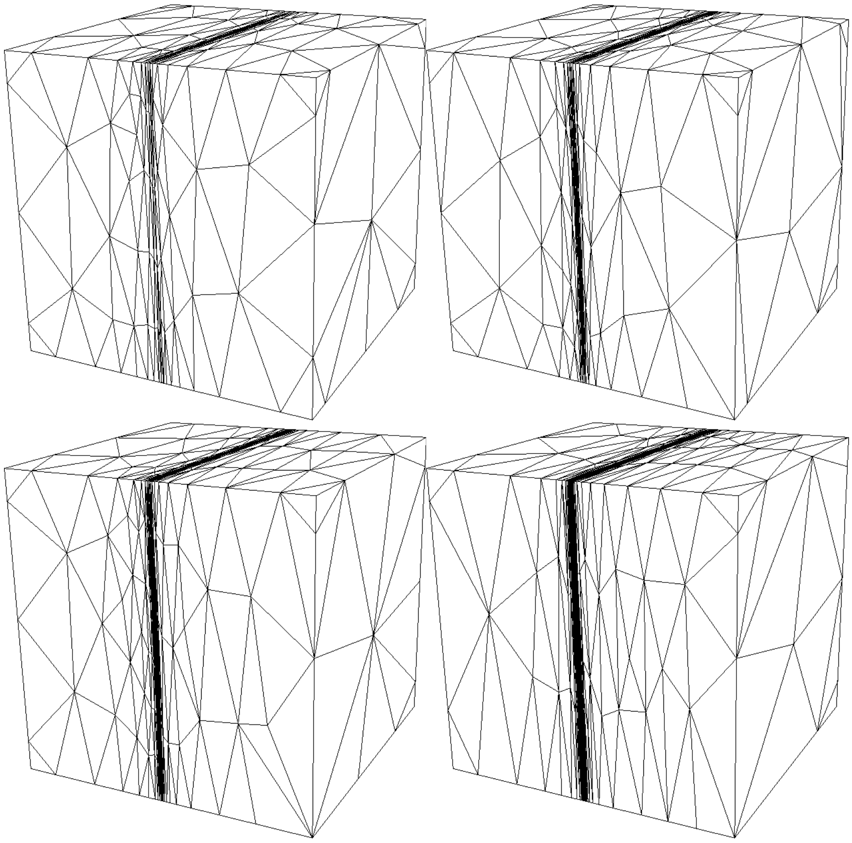

Figure 1.21: Adapted mesh generated by the adaptive algorithm when proceeding by continuation. $TOL = 1$ (top left), $TOL = 0.5$ (top right), $TOP = 0.25$ (bottom left) and $TOL = 0.125$ (bottom right).

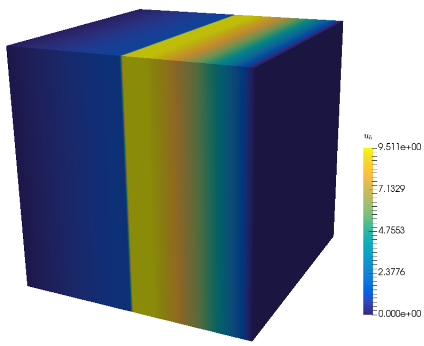


Figure 1.22: Numerical solution to Example 1.22 with $\mu_1 = 1, \mu_2 = 10, \varepsilon = 0.01$ computed with the 3D adaptive algorithm. $TOL = 0.125$.

Finally, we use our adaptive algorithm to compute an approximated solution to the 3D version of Example 1.20, where this time the solution must be constant into a sphere compactly supported in $\Omega$. We set again $f = 1$ and we choose $B$ as the sphere of radius 0.3, centered at (0.5,0.5,0.5). The smoothing parameter $\varepsilon$ is set to 0.001 and the penalty parameter $\delta$ to 10'000. As for the 2D case, we proceed by continuation: we start with a tolerance $TOL = 1$ and divide the tolerance by two until we reach $TOL = 0.125$. The number of remeshing between each tolerance is set to $N_{loop} = 40$. The solution for the finale tolerance is represented in Figure 1.23. Convergence of the adaptive algorithm is checked in Figure 1.24 and the final meshes generated at each tolerance are presented in Figures 1.25 and 1.26.

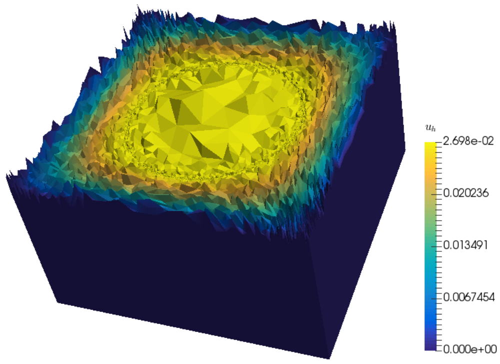


Figure 1.23: Example 1.20 in 3D. The ball has a radius of 0.3. Numerical solution at $TOL = 0.125$.

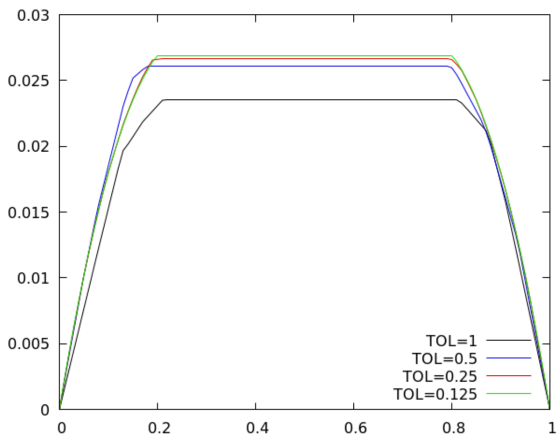


Figure 1.24: Example 1.20 in 3D. Plot of the solution along the $x_1$-axe for several tolerances.

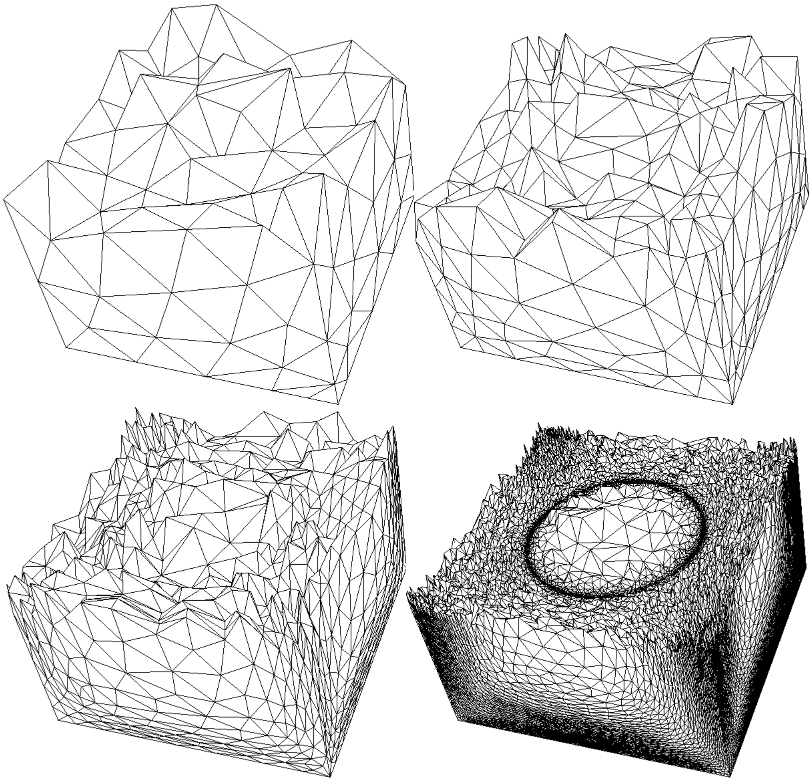

Figure 1.25: Adapted mesh obtain when solving 1.20 in 3D. $TOL = 1$ (top left), $TOL = 0.5$ (top right), $TOL = 0.25$ (bottom left) and $TOL = 0.125$ (bottom right)

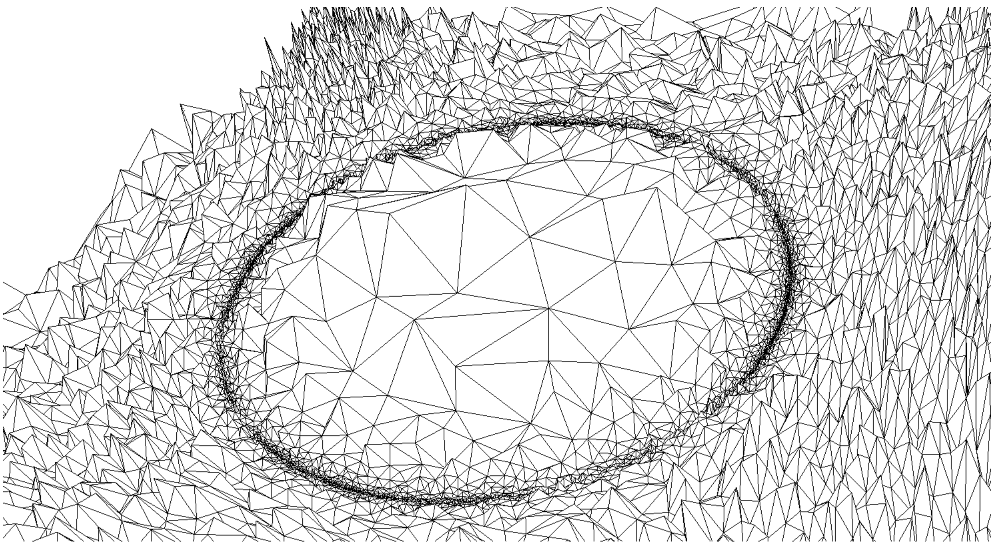

Figure 1.26: Zoom on Figure 1.25 at $TOL = 0.125$.

# Chapter 2

# An adaptive algorithm for the transport equation with anisotropic finite elements and the Crank-Nicolson method

In this chapter, we study a numerical method and we propose an adaptive algorithm to solve the transport equation

$$\frac{\partial \varphi}{\partial t} + \mathbf{u} \cdot \nabla \varphi = 0,$$

where $\mathbf{u} \in \mathbb{R}^d, d = 2, 3$, is a free divergence transport velocity field that may depend on the space and the time variables. The numerical method presented further is a combination of continuous, piecewise linear, anisotropic finite elements and the Crank-Nicolson scheme, that is an order two method in time. Since the transport equation is an hyperbolic equation, one uses a consistent stabilization to treat the advection.

The goals of the chapter are mainly:

– To prove the stability and the convergence of the method by deriving *a priori* error estimates in the most general cases possible.

– To prove an *a posteriori* error estimate that involves the spatial and the time discretization and deduce two error indicators, one for the space and one for the time, that are of optimal orders and valid for anisotropic meshes.

– To describe and implement an adaptive algorithm.

The outline of the chapter is as follows: in Section 2.1, we consider a simpler problem, that is to say the ODE

$$\frac{d\varphi(t)}{dt} + u(t)\varphi(t) = 0,$$

where here $u$ is a scalar function. This ODE can be seen as a 1D version of the transport equation. We use the Crank-Nicolson method to solve it and we show and present the techniques to derive an a posteriori error estimate that is of order two in time.

In Section 2.2, we prove a priori and a posteriori error estimates for the transport equation. We first briefly recall the known results on the semi-discrete approximation, where only the space discretization is taken in account. We then analyse the fully discrete method. We first prove all the estimates (stability, a priori and a posteriori error bounds) on the simpler case where the velocity field $\mathbf{u}$ is independent of the time. These results have already been presented and published in [41]. Then, the later estimates are generalized to the case of transient velocity field. The two main results are the Theorem 2.51, where we prove an a priori error estimate in the most general case, and the Theorem 2.55, where we demonstrate its a posteriori counterpart. All the results are presented in $\mathbb{R}^2$, but can be straightforwardly extended to $\mathbb{R}^3$.

The last sections are dedicated to the numerical experiments. In Section 2.3, we define proper error indicators and we verify the convergence of the numerical method with non-adapted meshes and constant time steps. In Section 2.4, we present an adaptive algorithm and we demonstrate its efficiency in Section 2.5 for 2D problems and in Section 2.6 for the 3D situation.

## 2.1 A posteriori error estimates for second order time discretization of ODEs: application to the Crank-Nicolson scheme

In this section, we consider the two following ODEs:

$$\begin{cases} \dfrac{d\varphi}{dt} + u\varphi = 0, \quad t \in (0,T], \\ \\ \varphi(0) = \varphi_0, \end{cases} \tag{2.1}$$

and

$$\begin{cases} \dfrac{d\varphi}{dt} + u(t)\varphi = 0, \quad t \in (0,T], \\ \\ \varphi(0) = \varphi_0, \end{cases} \tag{2.2}$$

where $T < \infty$ is the final time and we consider $u > 0$ as a constant in (2.1) and as a $C^2[0,T]$ function in (2.2). In both cases, the classical ODEs theory yields that the solution belongs at least to $C^3[0,T]$ and is given by the analytic formula

$$\varphi(t) = \varphi_0 \exp\left(-\int_0^t u(s)ds\right).$$

The two ODEs above can be interpreted as a simplified version of the transport equation

$$\frac{\partial\varphi}{\partial t} + \mathbf{u}\cdot\nabla\varphi = 0,$$

where the real function $u$ can be seen as a 1D equivalent to the velocity field $\mathbf{u}$. Observe that we differentiate the cases where $u$ is a constant (2.1) or depends on the time (2.2). The reason is that, when dealing with the transport equation, the local time error indicators that we will prove will be different and need different techniques depending on wether the vecotiy field $\mathbf{u}$ depends only on the space variables or depends also on the time variable.

The Crank-Nicolson scheme [38] applied to (2.1), respectively (2.2) reads : given $0 = t^0 < t^1 < t^2 < ... < t^N = T$ a partition of the interval $[0,T]$, starting from $\varphi^0 = \varphi_0$, find, for every $0 \le n \le N-1$, $\varphi^{n+1}$ the solution of

$$\frac{\varphi^{n+1}-\varphi^n}{\tau^{n+1}} + u\frac{\varphi^{n+1}+\varphi^n}{2} = 0, \tag{2.3}$$

respectively,

$$\frac{\varphi^{n+1}-\varphi^n}{\tau^{n+1}} + u\left(\frac{t^{n+1}+t^n}{2}\right)\frac{\varphi^{n+1}+\varphi^n}{2} = 0, \tag{2.4}$$

where we denote the time step by

$$\tau^{n+1} = t^{n+1} - t^n, \quad 0 \le n \le N-1.$$

Noting $\tau = \max_{0\le n\le N-1} \tau^{n+1}$, it is well known that the Crank-Nicolson scheme is a numerical method of order $O(\tau^2)$. We would like to derive an a posteriori error estimate for the numerical error $\varphi(T) - \varphi^N$ of optimal order, that is to say to prove that there exists a constant $C > 0$ independent of the time step and a computable quantity $\theta \simeq O(\tau^2)$ such that

$$|\varphi(T) - \varphi^N| \le C\theta. \tag{2.5}$$

A possibility [3, 82] to construct the quantity $\theta$ consists to define a piecewise smooth function $\varphi_\tau$ with the following properties:

(i) for all $0 \le n \le N$, $\varphi_\tau(t^n) = \varphi^n$, where $\varphi^n$ is the solution of (2.3) or (2.4),

(ii) $\varphi_\tau \in C^0[0,T]$,

(iii) for all $0 \le n \le N-1$, $\varphi_\tau \in C^1[t^n, t^{n+1}]$.

We say that $\varphi_\tau$ is a piecewise reconstruction of the numerical solution $(\varphi^n)_{n=0}^N$. Then, the following theorem can be used to build an a posteriori error estimate. The main idea is to plug the reconstruction $\varphi_\tau$ into the equation and to look at the remainder.

**Theorem 2.1.**
*Let $\varphi$ be the solution of (2.1), respectively (2.2), and $(\varphi^n)_{n=0}^N$ be the solution of (2.3), respectively (2.4). Let $\varphi_\tau$ be a piecewise reconstruction of $(\varphi^n)_{n=0}^N$ satisfying the properties $(i), (ii), (iii)$. Then*

$$|\varphi(T) - \varphi^N| \le \exp(1)\left(T\sum_{n=0}^{N-1}\int_{t^n}^{t^{n+1}} \theta_n^2(t)dt\right)^{1/2},$$

*where for every $0 \le n \le N-1$ and every $t \in [t^n, t^{n+1}]$, $\theta_n(t)$ is defined by*

$$\theta_n(t) = \frac{d\varphi_\tau}{dt} + u\varphi_\tau,$$

*respectively*

$$\theta_n(t) = \frac{d\varphi_\tau}{dt} + u(t)\varphi_\tau.$$

*Proof.* We only prove the theorem when considering the ODE (2.2), the computations being the same if $u$ is a constant real number. Let $0 \le n \le N-1$ and $t \in (t^n, t^{n+1})$. Noting $e(t) = \varphi(t) - \varphi_\tau(t)$, by definition of $\theta_n(t)$, we have

$$\frac{d}{dt}e(t) + u(t)e(t) = -\theta_n(t).$$

Multiplying by $e(t)$ and using that $u(t)$ is non-negative yields

$$\frac{1}{2}\frac{d}{dt}|e(t)|^2 \le -\theta_n(t)e(t).$$

Thanks to the Gronwall's inequality given by Theorem A.3, we obtain

$$e^2(T) \le \exp(1)\left(e^2(0) + T\sum_{n=0}^{N-1}\int_{t^n}^{t^{n+1}} \theta_n^2(t)dt\right).$$

We conclude using that the fact that $e(T) = \varphi(T) - \varphi_\tau(T) = \varphi(T) - \varphi^N$ and that the numerical error at initial time $e(0) = 0$ since $\varphi_\tau(0) = \varphi^0 = \varphi_0 = \varphi(0)$. □

**Remark 2.2.**
Note that we could have solved directly the ODE

$$\frac{d}{dt}e(t) + u(t)e(t) = -\theta_n(t), \quad t^n \le t \le t^{n+1},$$

in order to get the analytic expression of $e(t)$. However, we prefer to proceed as presented in the above proof, in order to stay close to the framework of estimates in a PDE framework, the multiplication by $e(t)$ corresponding to choose the test function $v = e(t)$ in the weak form of the PDE.

Using the result of Theorem 2.1, one can define $\theta$ in (2.5) as

$$\theta = \left( T \sum_{n=0}^{N-1} \int_{t^n}^{t^{n+1}} \theta_n^2(t)dt \right)^{1/2}. \tag{2.6}$$

Therefore, to achieve our goal to get an optimal order a posteriori error estimate, that is to say $\theta \simeq O(\tau^2)$, we only need to define a reconstruction $\varphi_\tau$ leading to $\theta_n(t)$ behaving as $O(\tau^2)$.

Before we discuss how to construct $\varphi_\tau$, we do the following comments. First of all observe that one can prove the a priori error estimate (where we choose to write the bound in the $L^2$ norm)

$$|\varphi(T) - \varphi^N| \le C\tau^2 \left( T \int_0^T \left| \frac{d^3\varphi(t)}{dt^3} \right|^2 dt \right)^{1/2}$$

with $C > 0$ a constant independent of the time step. Let us assume for the time being that $\theta_n \le C(\tau^{n+1})^2 \left| \frac{d^3\varphi_\tau}{dt^3} \right|$ where $C > 0$ is a positive constant independent of the time step (see Remarks 2.6 and 2.10 further). Then the global error estimator $\theta$ will behaves as

$$\theta \le C \left( T \sum_{n=0}^{N-1} \int_{t^n}^{t^{n+1}} (\tau^{n+1})^4 \left| \frac{d^3\varphi_\tau}{dt^3} \right|^2 dt \right) \le C\tau^2 \left( T \sum_{n=0}^{N-1} \int_{t^n}^{t^{n+1}} \left| \frac{d^3\varphi_\tau}{dt^3} \right|^2 dt \right).$$

Since the a posteriori bound imitates the behavior of the a priori one, we think that our construction of $\theta$ through Theorem 2.1 yields to a sharp error estimate. Finally, observe that the fact that $\theta^2$ depends linearly on the final time $T$ is due to the use of Theorem A.3, which eliminates the classical $\exp(T)$-bound coming out the estimate when using Gronwall's Lemma inequality.

Several choices for $\varphi_\tau$ were proposed in the literature. In [82], a piecewise linear reconstruction of the numerical solution is introduced in order to prove an a posteriori error estimate for the heat equation and the Backward Euler scheme. Following this paper, $\varphi_\tau$ could be defined as

$$\varphi_\tau(t) = \varphi^n + (t - t^n)\frac{\varphi^{n+1} - \varphi^n}{\tau^{n+1}}, \quad t \in [t^n, t^{n+1}], 0 \le n \le N-1.$$

Nevertheless, it is shown in [3] that this reconstruction yields to a suboptimal a posteriori error estimate for methods of order 2. In [3], the authors propose a piecewise quadratic reconstruction to achieve the optimal order of the error estimator. For instance, applied to the Cauchy problem (2.1) (we recall that in this case $u$ is a constant), the reconstruction reads

$$\varphi_\tau(t) = \varphi^n + (t - t^n)\frac{\varphi^{n+1} - \varphi^n}{\tau^{n+1}} - \frac{1}{2}(t - t^n)(t - t^{n+1})u\frac{\varphi^{n+1} - \varphi^n}{\tau^{n+1}}, \tag{2.7}$$

$t \in [t^n, t^{n+1}], 0 \leq n \leq N-1$.

In [72], an alternative quadratic reconstruction is introduced. Observe that, considering the ODE (2.1), one can think about $u\dfrac{\varphi^{n+1} - \varphi^n}{\tau^{n+1}}$ as an approximation of $u\dfrac{d\varphi}{dt} = -\dfrac{d^2\varphi}{dt^2}$. Therefore, the authors replace in (2.7) the factor $-u\dfrac{\varphi^{n+1} - \varphi^n}{\tau^{n+1}}$ by a finite difference approximation of the second derivative. So the following quadratic reconstruction is advocated

$$\varphi_\tau(t) = \varphi^n + (t - t^n)\frac{\varphi^{n+1} - \varphi^n}{\tau^{n+1}} + \frac{1}{2}(t - t^n)(t - t^{n+1})\frac{\frac{\varphi^{n+1}-\varphi^n}{\tau^{n+1}} - \frac{\varphi^n - \varphi^{n-1}}{\tau^n}}{\frac{\tau^{n+1}+\tau^n}{2}}, \tag{2.8}$$

$t \in [t^n, t^{n+1}], 1 \leq n \leq N-1$. Compared to (2.7), the only drawback of (2.8) is that it is defined only for $t \geq t^1$, forcing to use a linear reconstruction of the numerical solution on the interval $[t^0, t^1]$ (leading in general to a suboptimal local error estimator for the first iteration) or to keep the error at time $t^1$ in the estimate. In practice, this is not a restriction since $|\varphi(t^1) - \varphi^1|$ is small. Nevertheless, in what follows, we will show that for our particular problems, we are able to obtain a local error estimator achieving the order 2, even in the first interval $[t^0, t^1]$ where a linear reconstruction will be used.

In order to simplify the notations in the computations that follow, we introduce the quantities

$$\begin{aligned}
\partial\varphi^{n+1} &= \tfrac{\varphi^{n+1}-\varphi^n}{\tau^{n+1}}, && 0 \leq n \leq N-1,\\
\partial^2\varphi^{n+1} &= \frac{\frac{\varphi^{n+1}-\varphi^n}{\tau^{n+1}} - \frac{\varphi^n-\varphi^{n-1}}{\tau^n}}{\frac{\tau^{n+1}+\tau^n}{2}}, && 1 \leq n \leq N-1,\\
\varphi^{n+1/2} &= \tfrac{\varphi^{n+1}+\varphi^n}{2}, && 0 \leq n \leq N-1,\\
t^{n+1/2} &= \tfrac{t^{n+1}+t^n}{2}, && 0 \leq n \leq N-1.
\end{aligned} \tag{2.9}$$

Using the above notation, we define the reconstruction we will use in the rest of this section.

**Definition 2.3** (Piecewise quadratic numerical reconstruction)**.**
Let $(\varphi^n)_{n=0}^N$ be the solution of (2.3) or (2.4), we define the piecewise numerical reconstruction $\varphi_\tau \in C^0[0,T]$ by

$$\varphi_\tau(t) = \varphi^{n+1/2} + (t - t^{n+1/2})\partial\varphi^{n+1} + \frac{1}{2}(t - t^n)(t - t^{n+1})\partial^2\varphi^{n+1}, \tag{2.10}$$

for $t \in [t^n, t^{n+1}], 1 \leq n \leq N-1$, and by

$$\varphi_\tau(t) = \varphi^{1/2} + (t - t^{1/2})\partial\varphi^1, \tag{2.11}$$

for $t \in [t^0, t^1]$.

Observe that we write the quadratic reconstruction (2.10) in a slightly different way that one proposed in (2.8), the linear part being computed in $t^{n+1/2}$ rather than in $t^n$ (note that there are still equal). This choice is made in order to simplify the computations later on since the Crank-Nicolson method corresponds to the midpoint rule that is used to approximate the equation. As anticipated before, we use a linear reconstruction (2.11) to define the numerical solution on $[t^0, t^1]$.

We now prove that the piecewise reconstruction of Definition 2.3 yields to a local error estimator $\theta_n(t)$ of order $O(\tau^2)$. We first focus on the Cauchy problem (2.1) where $u$ is a constant. The local error estimator is contained in the proposition

**Proposition 2.4.**
*Let $(\varphi^n)_{n=0}^N$ be the solution of the numerical method (2.3). Let $0 \leq n \leq N-1$. Finally,*

*let $\varphi_\tau$ be the numerical reconstruction proposed in Definition 2.3. One have for all $t \in (t^n, t^{n+1})$*

$$\frac{d\varphi_\tau}{dt} + u\varphi_\tau = \theta_n(t)$$

*where the local error estimator $\theta_n(t)$ is given by*

$$\theta_n(t) = \begin{cases} \left(\frac{\tau^n}{2}(t - t^{n+1/2}) + \frac{1}{2}(t - t^n)(t - t^{n+1})\right) u\partial^2\varphi^{n+1}, & 1 \le n \le N-1, \\ (t - t^{1/2})u\partial\varphi^1, & n = 0. \end{cases} \tag{2.12}$$

*Proof.* We first treat the case $n \ge 1$. Let $t \in (t^n, t^{n+1})$, we have

$$\frac{d\varphi_\tau}{dt} + u\varphi_\tau = \partial\varphi^{n+1} + (t - t^{n+1/2})\partial^2\varphi^{n+1} + u\varphi^{n+1/2} + u(t - t^{n+1/2})\partial\varphi^{n+1} + \frac{u}{2}(t - t^n)(t - t^{n+1})\partial^2\varphi^{n+1}.$$

Using the numerical scheme (2.3), we have that $\partial\varphi^{n+1} + u\varphi^{n+1/2} = 0$, therefore

$$\frac{d\varphi_\tau}{dt} + u\varphi_\tau = (t - t^{n+1/2})\left(\partial^2\varphi^{n+1} + u\partial\varphi^{n+1}\right) + \frac{1}{2}(t - t^{n+1})(t - t^n)u\partial^2\varphi^{n+1}. \tag{2.13}$$

Observe that the factor $\partial^2\varphi^{n+1} + u\partial\varphi^{n+1}$ behaves as the discrete derivative of equation (2.3). So to compute it, we take the difference between (2.3) at two consecutive steps and it yields

$$\frac{\varphi^{n+1} - \varphi^n}{\tau^{n+1}} - \frac{\varphi^n - \varphi^{n-1}}{\tau^n} + u\frac{\varphi^{n+1} - \varphi^{n-1}}{2} = 0.$$

Dividing by $\frac{1}{\tau^{n+1}+\tau^n/2}$, we obtain

$$\partial^2\varphi^{n+1} + u\frac{\varphi^{n+1} - \varphi^{n-1}}{\tau^{n+1} + \tau^n} = 0. \tag{2.14}$$

Therefore one can compute that

$$\begin{aligned} \partial^2\varphi^{n+1} + u\partial\varphi^{n+1} &= u\left(\frac{\varphi^{n+1} - \varphi^n}{\tau^{n+1}} - \frac{\varphi^{n+1} - \varphi^{n-1}}{\tau^{n+1} + \tau^n}\right) \\ &= u\frac{(\varphi^{n+1} - \varphi^n)(\tau^{n+1} + \tau^n) - \tau^{n+1}(\varphi^{n+1} - \varphi^{n-1})}{\tau^{n+1}(\tau^{n+1} + \tau^n)} \\ &= u\frac{\tau^n(\varphi^{n+1} - \varphi^n) - \tau^{n+1}(\varphi^n - \varphi^{n-1})}{\tau^{n+1}(\tau^{n+1} + \tau^n)} \\ &= u\frac{\tau^{n+1}\tau^n\frac{\varphi^{n+1}-\varphi^n}{\tau^{n+1}} - \tau^{n+1}\tau^n\frac{\varphi^n-\varphi^{n-1}}{\tau^n}}{\tau^{n+1}(\tau^{n+1} + \tau^n)} \\ &= \frac{\tau^n}{2}u\frac{\frac{\varphi^{n+1}-\varphi^n}{\tau^{n+1}} - \frac{\varphi^n-\varphi^{n-1}}{\tau^n}}{\frac{\tau^{n+1}+\tau^n}{2}}. \end{aligned} \tag{2.15}$$

Finally, we obtain that

$$\partial^2\varphi^{n+1} + u\partial\varphi^{n+1} = \frac{\tau^n}{2}u\partial^2\varphi^{n+1},$$

and plug it into (2.13) yields

$$\frac{d\varphi_\tau}{dt} + u\varphi_\tau = \left(\frac{\tau^n}{2}(t - t^{n+1/2}) + \frac{1}{2}(t - t^n)(t - t^{n+1})\right) u\partial^2\varphi^{n+1}.$$

Now, for $n = 0$ and $t \in (t^0, t^1)$, we directly obtain, using the definition of $\varphi_\tau$ and the numerical method (2.3)

$$\begin{aligned}\frac{d\varphi_\tau}{dt} + u\varphi_\tau &= \frac{\varphi^1 - \varphi^0}{\tau^1} + u\varphi^{1/2} + u(t - t^{1/2})\partial\varphi^1 \\ &= (t - t^{1/2})u\partial\varphi^1.\end{aligned}$$

□

Then, the a posteriori estimate for the numerical method (2.3) is contained in the Theorem

**Theorem 2.5.**
*Let $\varphi$ be the solution of (2.1) and $(\varphi^n)_{n=0}^N$ be the solution of the numerical method (2.3). Let $0 \leq n \leq N-1$. Finally, let $\varphi_\tau$ be the numerical reconstruction proposed in Definition 2.3. Then the following a posteriori error estimate holds*

$$|\varphi(T) - \varphi^N|^2 \leq \exp(2) \sum_{n=0}^{N-1} c_n \int_{t^n}^{t^{n+1}} \theta_n^2(t)dt,$$

*where $\theta_n(t)$ is defined as in Proposition 2.4 and $c_n$ is given by*

$$c_n = \begin{cases} \tau^1, & n = 0, \\ T - t^1, & 1 \leq n \leq N-1. \end{cases}$$

*Proof.* We set $1 \leq n \leq N-1$ and $t \in (t^n, t^{n+1})$. We note $e(t) = \varphi(t) - \varphi_\tau$. Using Proposition 2.4, we have

$$\frac{d}{dt}e(t) + ue(t) = -\theta_n(t).$$

Multiplying by $e(t)$, we have

$$\frac{1}{2}\frac{d}{dt}|e(t)|^2 + u|e(t)|^2 = -\theta_n(t)e(t).$$

Using that $u$ is positive, the second term of the left hand side can be eliminated and it yields

$$\frac{1}{2}\frac{d}{dt}|e(t)|^2 \leq -\theta_n(t)e(t).$$

Using Theorem A.3 between $t^1$ and $T$, one prove that

$$|e(T)|^2 \leq \exp(1)\left(|e(t^1)|^2 + (T - t_1)\sum_{n=1}^{N-1}\int_{t^n}^{t^{n+1}} \theta_n^2(t)dt\right).$$

□

Now to estimate the error at time $t^1$, we reproduce the same computation for $t \in (0, t^1)$ and we obtain

$$\frac{1}{2}\frac{d}{dt}|e(t)|^2 \leq -\theta_1(t)e(t).$$

Using Theorem A.3 between 0 and $t^1 = \tau^1$ and using that $e(0) = 0$ yields

$$|e(t^1)|^2 \leq \exp(1)\tau^1 \int_0^{t^1} \theta_1^2(t)dt.$$

So finally, we obtain the estimate

$$|e(T)|^2 \leq \exp(1)\left(\exp(1)\tau^1 \int_0^{t^1} \theta_1^2(t)dt + (T - t_1)\sum_{n=1}^{N-1}\int_{t^n}^{t^{n+1}} \theta_n^2(t)dt\right),$$

which yields to the desired estimate by setting $c_n = \tau^1$ if $n = 0$ and $c_n = T - t^1$ otherwise.

**Remark 2.6** (Optimality of the a posteriori error estimate of Theorem 2.5). (i) Observe that for $n \geq 1$

$$\int_{t^n}^{t^{n+1}} \theta_n^2(t)dt = \frac{(\tau^n)^2(\tau^{n+1})^3}{48} + \frac{(\tau^{n+1})^5}{120} u^2 \left(\partial^2 \varphi^{n+1}\right)^2$$

which implies that

$$\sum_{n=1}^{N-1} c_n \int_{t^n}^{t^{n+1}} \theta_n^2(t)dt = O(\tau^4).$$

Moreover, for the first time step, the proof above yields as estimate for $e(t^1)$ the quantity

$$c_0 \int_{t^0}^{t^1} \theta_1^2(t)dt = \tau^1 \frac{(\tau^1)^3}{12} u^2 \left(\partial \varphi^1\right)^2 = O(\tau^4).$$

So, if we define $\theta$ by

$$\theta = \left( \sum_{n=0}^{N-1} c_n \int_{t^n}^{t^{n+1}} \theta_n^2(t)dt \right)^{1/2}$$

we have that the posteriori error estimate of Theorem 2.5 achieves the optimal order, that is to say

$$|\varphi(T) - \varphi^N| \leq C\theta = O(\tau^2).$$

(ii) Note that the result of the previous point is a consequence of the particular form of the local error estimator $\theta_n$, which approximates

$$u \frac{d^2\varphi}{dt^2} = -\frac{d^3\varphi}{dt^3}.$$

Therefore, the estimates of Theorem 2.5 mimics the a priori error estimate

$$|\varphi(T) - \varphi^N| \leq C\tau^2 \left( T \int_0^T \left| \frac{d^3\varphi(t)}{dt^3} \right|^2 dt \right)^{1/2},$$

which was one of our purposes.

**Remark 2.7.**
The computations performed (2.15) gives us in fact the identity

$$\frac{\varphi^{n+1} - \varphi^n}{\tau^{n+1}} = \frac{\varphi^{n+1} - \varphi^{n-1}}{\tau^{n+1} + \tau^n} + \frac{\tau^n}{2} \partial^2 \varphi^{n+1}$$

This is a well-known result in the framework of stabilization method, where the upwind scheme (here the left hand side) is a centered scheme stabilized by adding a diffusion term (here the right hand side).

We now treat the more general case of the Cauchy problem (2.2) where $u$ may depend on $t$. The corresponding local error indicator $\theta_n$ is contained in the Proposition

**Proposition 2.8.**
*Let $(\varphi^n)_{n=0}^N$ be the solution of the numerical method (2.4). Let $0 \leq n \leq N-1$. Finally, let $\varphi_\tau$ be the numerical reconstruction proposed in Definition 2.3. One have for all $t \in (t^n, t^{n+1})$*

$$\frac{d\varphi_\tau}{dt} + u(t)\varphi_\tau = \theta_n(t)$$

*where the local error estimator $\theta_n(t)$ is given by*

$$\theta_n(t) = \left( u(t) - u(t^{n+1/2}) - (t - t^{n+1/2}) \frac{u(t^{n+1/2}) - u(t^{n-1/2})}{\tau^{n+1}+\tau^n/2} \right) \varphi^{n+1/2} + (t - t^{n+1/2})(u(t) - u(t^{n-1/2})) \frac{\varphi^{n+1} - \varphi^{n-1}}{\tau^{n+1} + \tau^n} + \left( \frac{\tau^n}{2}(t - t^{n+1/2}) + \frac{1}{2}(t - t^n)(t - t^{n+1}) \right) u(t) \partial^2 \varphi^{n+1}, \quad 1 \leq n \leq N-1, \tag{2.16}$$

*and*

$$\theta_0(t) = \left( u(t) - u(t^{1/2}) \right) \varphi^{1/2} + (t - t^{1/2}) u(t) \partial \varphi^1. \tag{2.17}$$

*Proof.* We proceed as in Proposition 2.4. Let first $n \geq 1$ and let $t \in (t^n, t^{n+1})$. We have

$$\begin{aligned} \frac{d\varphi_\tau}{dt} + u(t)\varphi_\tau &= \partial\varphi^{n+1} + (t - t^{n+1/2})\partial^2\varphi^{n+1} \\ &\quad + u(t)\varphi^{n+1/2} + u(t)(t - t^{n+1/2})\partial\varphi^{n+1} + \frac{u(t)}{2}(t - t^n)(t - t^{n+1})\partial^2\varphi^{n+1} \\ &= \underbrace{\partial\varphi^{n+1} + u(t^{n+1/2})\varphi^{n+1/2}}_{=0\ (2.4)} + (t - t^{n+1/2}) \left( \partial^2\varphi^{n+1} + u(t)\varphi^{n+1} \right) \\ &\quad + (u(t) - u(t^{n+1/2}))\varphi^{n+1/2} + \frac{1}{2}(t - t^n)(t - t^{n+1})u(t)\partial^2\varphi^{n+1} \\ &= (t - t^{n+1/2}) \left( \partial^2\varphi^{n+1} + u(t)\varphi^{n+1} \right) + (u(t) - u(t^{n+1/2}))\varphi^{n+1/2} \\ &\quad + \frac{1}{2}(t - t^n)(t - t^{n+1})u(t)\partial^2\varphi^{n+1} \end{aligned}$$

As before, we treat the first term of the right hand side. Taking the difference between (2.4) and the same scheme at the previous step, we get

$$\partial\varphi^{n+1} + u(t^{n+1/2})\varphi^{n+1/2} - \partial\varphi^n - u(t^{n-1/2})\varphi^{n-1/2} = 0.$$

The previous equality is equivalent to

$$\partial\varphi^{n+1} - \partial\varphi^n + u(t)\frac{\varphi^{n+1} - \varphi^{n-1}}{2} + (u(t^{n+1/2}) - u(t))\varphi^{n+1/2} - (u(t^{n-1/2}) - u(t))\varphi^{n-1/2} = 0.$$

Dividing by $\frac{1}{\tau^{n+1}+\tau^n/2}$, we finally get

$$\partial^2\varphi^{n+1} + u(t)\frac{\varphi^{n+1} - \varphi^{n-1}}{\tau^{n+1} + \tau^n} + \frac{(u(t^{n+1/2}) - u(t))\varphi^{n+1/2} - (u(t^{n-1/2}) - u(t))\varphi^{n-1/2}}{\tau^{n+1}+\tau^n/2} = 0.$$

Reproducing the step (2.15), we compute that

$$\partial^2\varphi^{n+1} + u(t)\partial\varphi^{n+1} = \frac{\tau^n}{2}u(t)\partial^2\varphi^{n+1} + \frac{(u(t) - u(t^{n+1/2}))\varphi^{n+1/2} - (u(t) - u(t^{n-1/2}))\varphi^{n-1/2}}{\tau^{n+1}+\tau^n/2}.$$

Thus

$$\begin{aligned}
\frac{d\varphi_\tau}{dt} + u(t)\varphi_\tau &= (t - t^{n+1/2})\frac{(u(t) - u(t^{n+1/2}))\varphi^{n+1/2} - (u(t) - u(t^{n-1/2}))\varphi^{n-1/2}}{\tau^{n+1}+\tau^n/2} \\
&\quad + (u(t) - u(t^{n+1/2}))\varphi^{n+1/2} \\
&\quad + \left(\frac{\tau^n}{2}(t - t^{n+1/2}) + \frac{1}{2}(t - t^n)(t - t^{n+1})\right) u(t)\partial^2\varphi^{n+1} \\
&= \left(u(t) - u(t^{n+1/2}) - (t - t^{n+1/2})\frac{u(t^{n+1/2}) - u(t^{n-1/2})}{\tau^{n+1}+\tau^n/2}\right)\varphi^{n+1/2} \\
&\quad + (t - t^{n+1/2})(u(t) - u(t^{n-1/2}))\frac{\varphi^{n+1} - \varphi^{n-1}}{\tau^{n+1} + \tau^n} \\
&\quad + \left(\frac{\tau^n}{2}(t - t^{n+1/2}) + \frac{1}{2}(t - t^n)(t - t^{n+1})\right) u(t)\partial^2\varphi^{n+1}.
\end{aligned}$$

Observe that we pass to the second equality by adding and subtracting the term

$$(t - t^{n+1/2})\frac{(u(t) - u(t^{n-1/2}))\varphi^{n+1/2}}{\tau^{n+1}+\tau^n/2}.$$

For $n = 0$, we directly obtain that for any $t \in (0, t^1)$

$$\begin{aligned}
\frac{d\varphi_\tau}{dt} + u(t)\varphi_\tau &= \partial\varphi^1 + u(t)\varphi^{1/2} + u(t)(t - t^{n+1/2})\partial\varphi^1 \\
&= \underbrace{\partial\varphi^1 + u(t^{1/2})\varphi^{1/2}}_{=0} + \left(u(t) - u(t^{1/2})\right)\varphi^{1/2} + (t - t^{1/2})u(t)\partial\varphi^1 \\
&= \left(u(t) - u(t^{1/2})\right)\varphi^{1/2} + (t - t^{1/2})u(t)\partial\varphi^1.
\end{aligned}$$

□

We now state an a posteriori error estimate for the scheme (2.4), which is the final result of this section.

**Theorem 2.9.**
*Let $\varphi$ be the solution of (2.2) and $(\varphi^n)_{n=0}^N$ be the solution of the numerical method (2.4). Let $0 \le n \le N-1$. Finally, let $\varphi_\tau$ be the numerical reconstruction proposed in Definition 2.3. Then the following a posteriori error estimate holds*

$$|\varphi(T) - \varphi^N|^2 \le \exp(2)\sum_{n=0}^{N-1} c_n \int_{t^n}^{t^{n+1}} \theta_n^2(t)dt,$$

*where the local error estimator $\theta_n(t)$ is defined as in Proposition 2.8 and $c_n$ is given by*

$$c_n = \begin{cases} \tau^1, & n = 0, \\ T - t^1, & 1 \le n \le N-1. \end{cases}$$

*Proof.* The proof is exactly the same as the one of Theorem 2.5 and is not written for conciseness. □

**Remark 2.10** (Optimality of the a posteriori error estimate of Theorem 2.9)**.**
Let us note

$$M_0 = \max_{t\in[0,T]} |u(t)|, \quad M_1 = \max_{t\in[0,T]} \left|\frac{d}{dt}u(t)\right|, \quad M_2 = \max_{t\in[0,T]} \left|\frac{d^2}{dt^2}u(t)\right|.$$

Using Taylor expansion, we can prove for $n \geq 1$ that

$$|u(t) - u(t^{n-1/2})| \leq M_1 |t - t^{n-1/2}|,$$

and

$$\left| u(t) - u(t^{n+1/2}) - (t - t^{n+1/2}) \frac{u(t^{n+1/2}) - u(t^{n-1/2})}{\tau^{n+1}+\tau^{n}/2} \right| \\ \leq M_2 \left( (t - t^{n+1/2})^2 + |t - t^{n+1/2}||t - t^{n-1/2}| \right).$$

Therefore, for $n \geq 1$, we have that

$$\begin{aligned} \int_{t^n}^{t^{n+1}} \theta_n^2(t) dt &\leq 3M_2^2 |\varphi^{n+1/2}|^2 \int_{t^n}^{t^{n+1}} \left( (t - t^{n+1/2})^2 + |t - t^{n+1/2}||t - t^{n-1/2}| \right)^2 dt \\ &+ 3M_1^2 \left| \frac{\varphi^{n+1} - \varphi^{n-1}}{\tau^{n+1} + \tau^n} \right|^2 \int_{t^n}^{t^{n+1}} (t - t^{n+1/2})^2 (t - t^{n-1/2})^2 dt \\ &+ 3M_0^2 |\partial^2 \varphi^{n+1}|^2 \int_{t^n}^{t^{n+1}} \left( \frac{\tau^n}{2}(t - t^{n+1/2}) + \frac{1}{2}(t - t^n)(t - t^{n+1}) \right)^2 dt \\ &= O((\tau^{n+1})^5 + (\tau^n)^2 (\tau^{n+1})^3). \end{aligned}$$

For the same reason, we have that

$$\tau^1 \int_{t^0}^{t^1} \theta_0^2(t) dt \leq 2 \left( M_1^2 |\varphi^{1/2}|^2 + M_0^2 |\partial \varphi^2|'^2 \right) \tau^1 \int_{t^0}^{t^1} (t - t^{1/2})^2 dt = O((\tau^1)^4).$$

So, as before, if we define the error estimator

$$\theta = \left( \sum_{n=0}^{N-1} c_n \int_{t^n}^{t^{n+1}} \theta_n^2(t) dt \right)^{1/2},$$

we have finally

$$|\varphi(T) - \varphi^N| \leq C\theta = O(\tau^2).$$

**Remark 2.11.** (i) The particular form of the local error estimator $\theta_n(t)$ in Theorem 2.9 is consistent with what we learned before. Indeed, when $u$ is a constant, Theorem 2.5 means that the numerical error $\varphi - \varphi_\tau$ can be approximated by $\tau^2 u \frac{d^2}{dt^2}\varphi_\tau = \tau^2 \frac{d^2}{dt^2}(u\varphi_\tau)$. If $u$ depends on $t$ and is a $C^2$ function, then, up to Taylor expansion, the same phenomena happens and the numerical error can be approximated by

$$\tau^2 \frac{d^2}{dt^2}(u\varphi_\tau) = \tau^2 \frac{d^2 u}{dt^2}\varphi_\tau + \tau^2 \frac{du}{dt}\frac{d\varphi_\tau}{dt} + \tau^2 u \frac{d^2 \varphi_\tau}{dt^2}.$$

Therefore, the estimate of Theorem 2.9 mimics the a priori error estimate

$$|\varphi(T) - \varphi^N| \leq C\tau^2 \left( T \int_0^T \left| \frac{d^3 \varphi(t)}{dt^3} \right|^2 dt \right)^{1/2},$$

since

$$\frac{d^3 \varphi}{dt^3} = -\frac{d^2}{dt^2}(u\varphi_\tau).$$

(ii) Observe that if $u$ is a constant, then the local error estimator given by (2.16) and (2.17) is reduced to (2.12).

## 2.2 Error estimates for the time dependent transport equation with anisotropic finite elements and the Crank-Nicolson scheme

### 2.2.1 A priori and a posteriori error estimates in the case of a transport velocity independent of the time

We are now studying an anisotropic finite elements method to solve the transient transport equation. Some of the results presented below are already published in [20] and [41].

The time discretization is performed using the Crank-Nicolson method. Here we focus on the particular problem where the transport velocity $\mathbf{u}$ is independent of the time. As before, to simplify the notations, we only present the results in the 2D (spatial) case, but later on, numerical experiments will be performed to illustrate the 3D situation. Given a bounded, open set $\Omega \in \mathbb{R}^2$, a (finite) final time $T > 0$ and a divergence free velocity field $\mathbf{u} \in C^1(\overline{\Omega})$, we are looking for $\varphi : \Omega \times (0, T] \longrightarrow \mathbb{R}$ satisfying the transport problem

$$\begin{cases} \dfrac{\partial \varphi}{\partial t} + \mathbf{u} \cdot \nabla \varphi = 0, & \text{in } \Omega \times (0, T), \\ \varphi = 0, & \text{on } \Gamma^- \times (0, T), \\ \varphi(\cdot, 0) = \varphi_0, & \end{cases} \tag{2.18}$$

where $\Gamma^- = \{\mathbf{x} \in \partial\Omega : \mathbf{u} \cdot \mathbf{n} < 0\}$, with $\mathbf{n}$ being the unit outer normal of $\Omega$, and $\varphi_0 \in L^2(\Omega)$ is the initial condition. Under some reasonable assumptions on the boundary of $\Omega$, the problem (2.18) has a unique solution $\varphi \in C^0([0, T]; L^2(\Omega))$, see for instance [12]. To avoid theoretical considerations on the regularity of the domain or the solution, we will always assume that the data of the problem, that is to say $\Omega, T, \mathbf{u}$ and $\varphi_0$, are such that there exists a unique solution $\varphi$ of (2.18) that is sufficiently smooth to justify all our computations.

When discretizing the transport equation (2.18), it is well know that the classical Galerkin formulation is unsuitable and that some stabilization techniques are necessary. From now, assume that $\Omega$ is a polygon. For any $h > 0$, let $\mathcal{T}_h$ be a conformal triangulation of $\Omega$ into triangles $K$ of diameter $h_K \le h$ such that $\Gamma^-$ is the union of edges lying on $\partial\Omega$. Let $V_h$ be the set of continuous piecewise linear functions on each triangle of $\mathcal{T}_h$, with zero value on $\Gamma^-$. A possible finite element discretization in space is to search $\varphi_h : \overline{\Omega} \times [0, T] \longrightarrow \mathbb{R}$, with $\varphi_h(\cdot, t) \in V_h$ for all $t \in [0, T]$, such that $\varphi_h(\cdot, 0) = r_h(\varphi_0)$ and for all $t \in (0, T]$

$$\int_\Omega \left( \frac{\partial \varphi_h}{\partial t} + \mathbf{u} \cdot \nabla \varphi_h \right) (v_h + \delta_h \mathbf{u} \cdot \nabla v_h) d\mathbf{x} = 0, \quad \forall v_h \in V_h, \tag{2.19}$$

where $\delta_h > 0$ is a stabilization parameter that will be specified later on. The stabilized method (2.19) is an example of the Streamline-Upwind/Petrov-Galerkin method (SUPG) and is well studied in the framework of dominated convection equations. A survey of finite element methods for hyperbolic problems can be found in [60, 92]. Observe that the formulation (2.19) is consistent i.e. the exact solution $\varphi$ satisfies also

$$\int_\Omega \left( \frac{\partial \varphi}{\partial t} + \mathbf{u} \cdot \nabla \varphi \right) (v_h + \delta_h \mathbf{u} \cdot \nabla v_h) d\mathbf{x} = 0, \quad \forall v_h \in V_h.$$

Non-consistent formulations are possible, for instance asking for $\varphi_h$ satisfying

$$\int_\Omega \left( \frac{\partial \varphi_h}{\partial t} + \mathbf{u} \cdot \nabla \varphi_h \right) v_h d\mathbf{x} + \int_\Omega \delta_h (\mathbf{u} \cdot \nabla \varphi_h)(\mathbf{u} \cdot \nabla v_h) d\mathbf{x} = 0, \quad \forall v_h \in V_h.$$

However, it was observed that these types of method suffer from a lack of accuracy, even if an high order time stepping scheme is used [22]. For this reason, we choose to keep the consistent formulation, even if it leads to some technical complexity in its convergence analysis, see again [22]. In the same paper a complete convergence analysis of the method (2.19) is proposed for several choices of time discretization schemes, in particular the Backward Euler scheme and the Crank-Nicolson scheme, when linear isotropic finite elements are used. In what follows, we will propose a similar analysis for anisotropic finite elements and the Crank-Nicolson scheme, following the same ideas. Note that in [22], the analysis is done in the case of constant time step ; we extend it for variable time steps.

A numerical study of the semi-discrete method (2.19) with anisotropic finite elements has already been proposed in [20]. Our goal is to extend it, taking in account an order two in time discretization, namely the Crank-Nicolson method, as stated before. Let $N$ be a non-negative integer and consider a partition $0 = t^0 < t^1 < t^2 < ... < t^N = T$. We denote by $\tau^{n+1} = t^{n+1} - t^n$ the time step, $n = 0, 1, 2, ..., N-1$. Starting from $\varphi_h^0 = r_h(\varphi_0)$, for $n = 0, 1, 2, ..., N-1$, we are looking for $\varphi_h^{n+1} \in V_h$ such that

$$\int_\Omega \left( \frac{\varphi_h^{n+1} - \varphi_h^n}{\tau^{n+1}} + \mathbf{u} \cdot \nabla \left( \frac{\varphi_h^{n+1} + \varphi_h^n}{2} \right) \right) (v_h + \delta_h \mathbf{u} \cdot \nabla v_h) d\mathbf{x} = 0, \quad \forall v_h \in V_h. \tag{2.20}$$

#### Stability and a priori error estimates for the semi-discrete approximation in space

We briefly recall below the results previously obtained in [20] where only the space discretization is taken in account. We first state a stability result for the method (2.19). The idea of the proof, which is taken from [22] and consists to choose $\varphi_h + \delta_h \dfrac{\partial \varphi_h}{\partial t}$ as test function, is the main ingredient of all the convergence proofs that follow.

**Proposition 2.12** (Stability of the SUPG method applied to the transient transport equation)**.**
*Assume that $\delta_h > 0$ is constant and let $\varphi_h$ be the solution of (2.19). Then, for every $t \in (0, T]$ the following stability estimate holds :*

$$\|\varphi_h(t)\|^2_{L^2(\Omega)} + \delta_h^2 \|\mathbf{u} \cdot \nabla \varphi_h(t)\|^2_{L^2(\Omega)} \leq \|\varphi_h(0)\|^2_{L^2(\Omega)} + \delta_h^2 \|\mathbf{u} \cdot \nabla \varphi_h(0)\|^2_{L^2(\Omega)}. \tag{2.21}$$

**Remark 2.13.**
If no stabilization terms are added (which corresponds to set $\delta_h = 0$ in the formulation above), then we only get a control on the $L^2$-norm of the solution, that is to say for all $t \in (0, T]$, one have

$$\|\varphi_h(t)\|^2_{L^2(\Omega)} \leq \|\varphi_h(0)\|^2_{L^2(\Omega)}.$$

In particular, there is no control on the spatial derivatives of the numerical solution $\varphi_h$, meaning in practice that some spurious oscillations can arised if $h$ is not small enough. On the contrary, estimate (2.21) allows a control of the spatial derivatives, at least in the direction of the velocity field $\mathbf{u}$.

*Proof of Proposition 2.12.* We choose $v_h = \varphi_h + \delta_h \dfrac{\partial \varphi_h}{\partial t}$ in the variational formulation (2.19). We have

$$\begin{aligned}
\int_\Omega \frac{\partial \varphi_h}{\partial t} \varphi_h d\mathbf{x} + \delta_h^2 \int_\Omega (\mathbf{u} \cdot \nabla \varphi_h)(\mathbf{u} \cdot \nabla \frac{\partial \varphi_h}{\partial t}) d\mathbf{x} \\
+ \int_\Omega (\mathbf{u} \cdot \nabla \varphi_h) \varphi_h d\mathbf{x} + \delta_h^2 \int_\Omega \left( \mathbf{u} \cdot \nabla \frac{\partial \varphi_h}{\partial t} \right) \frac{\partial \varphi_h}{\partial t} d\mathbf{x} \\
+ \delta_h \int_\Omega \left( \frac{\partial \varphi_h}{\partial t} \right)^2 d\mathbf{x} + 2\delta_h \int_\Omega (\mathbf{u} \cdot \nabla \varphi_h) \frac{\partial \varphi_h}{\partial t} d\mathbf{x} + \delta_h \int_\Omega (\mathbf{u} \cdot \nabla \varphi_h)^2 d\mathbf{x} = 0.
\end{aligned}$$

We treat each line of the last equality. Since $\mathbf{u}$ is independent of the time, we can put the time derivative of the second term of the first line outside the integral sign. Therefore, we can write

$$\int_\Omega \frac{\partial \varphi_h}{\partial t}\varphi_h d\mathbf{x} + \delta_h^2 \int_\Omega (\mathbf{u}\cdot\nabla\varphi_h)(\mathbf{u}\cdot\nabla\frac{\partial \varphi_h}{\partial t})d\mathbf{x} = \frac{1}{2}\frac{d}{dt}\|\varphi_h(t)\|^2_{L^2(\Omega)} + \frac{\delta_h^2}{2}\frac{d}{dt}\|\mathbf{u}\cdot\nabla\varphi_h(t)\|^2_{L^2(\Omega)}.$$

Thanks to the divergence theorem, and since $\mathbf{u}$ is a divergence free vector field, one can write the second line as

$$\begin{aligned}
&\int_\Omega (\mathbf{u}\cdot\nabla\varphi_h)\varphi_h d\mathbf{x} + \delta_h^2 \int_\Omega \left(\mathbf{u}\cdot\nabla\frac{\partial \varphi_h}{\partial t}\right)\frac{\partial \varphi_h}{\partial t} d\mathbf{x} \\
&\qquad = \int_\Omega \mathrm{div}\left(\mathbf{u}\frac{\varphi_h^2}{2}\right)d\mathbf{x} + \frac{\delta_h^2}{2}\int_\Omega \mathrm{div}\left(\mathbf{u}\cdot\frac{1}{2}\left(\frac{\partial \varphi_h}{\partial t}\right)^2\right)d\mathbf{x} \\
&\qquad\qquad = \frac{1}{2}\int_{\partial\Omega}\mathbf{u}\cdot\mathbf{n}\varphi_h^2 d\mathbf{x} + \frac{\delta_h^2}{2}\int_{\partial\Omega}\mathbf{u}\cdot\mathbf{n}\left(\frac{\partial \varphi_h}{\partial t}\right)^2 d\mathbf{x}.
\end{aligned}$$

Finally, observe that the terms of the third line form a square, that is to say

$$\delta_h \int_\Omega \left(\frac{\partial \varphi_h}{\partial t}\right)^2 d\mathbf{x} + 2\delta_h \int_\Omega (\mathbf{u}\cdot\nabla\varphi_h)\frac{\partial \varphi_h}{\partial t}d\mathbf{x} + \delta_h\int_\Omega (\mathbf{u}\cdot\nabla\varphi_h)^2 d\mathbf{x} = \delta_h \int_\Omega \left(\frac{\partial \varphi_h}{\partial t} + \mathbf{u}\cdot\nabla\varphi_h\right)^2 d\mathbf{x}.$$

Therefore, the total equality can be written as

$$\begin{aligned}
&\frac{1}{2}\frac{d}{dt}\|\varphi_h(t)\|^2_{L^2(\Omega)} + \frac{\delta_h^2}{2}\frac{d}{dt}\|\mathbf{u}\cdot\nabla\varphi_h(t)\|^2_{L^2(\Omega)} \\
&\qquad + \frac{1}{2}\int_\Omega \mathbf{u}\cdot\mathbf{n}\varphi_h^2 d\mathbf{x} + \frac{\delta_h^2}{2}\int_\Omega \mathbf{u}\cdot\mathbf{n}\left(\frac{\partial \varphi_h}{\partial t}\right)^2 d\mathbf{x} \\
&\qquad\qquad + \delta_h \int_\Omega \left(\frac{\partial \varphi_h}{\partial t} + \mathbf{u}\cdot\nabla\varphi_h\right)^2 d\mathbf{x} = 0.
\end{aligned}$$

Thanks to the boundary conditions, both terms of the second line are non negative. Indeed we have

$$\frac{1}{2}\int_{\partial\Omega}\mathbf{u}\cdot\mathbf{n}\varphi_h^2 d\mathbf{x} + \frac{\delta_h^2}{2}\int_{\partial\Omega}\mathbf{u}\cdot\mathbf{n}\left(\frac{\partial \varphi_h}{\partial t}\right)^2 d\mathbf{x} = \frac{1}{2}\int_{\Gamma^-}\mathbf{u}\cdot\mathbf{n}\varphi_h^2 d\mathbf{x} + \frac{\delta_h^2}{2}\int_{\Gamma^-}\mathbf{u}\cdot\mathbf{n}\left(\frac{\partial \varphi_h}{\partial t}\right)^2 d\mathbf{x} \geq 0.$$

Therefore, since the third term is also positive, we finally obtain

$$\frac{1}{2}\frac{d}{dt}\|\varphi_h(t)\|^2_{L^2(\Omega)} + \frac{\delta_h^2}{2}\frac{d}{dt}\|\mathbf{u}\cdot\nabla\varphi_h(t)\|^2_{L^2(\Omega)} \leq 0,$$

which implies the result after integration between 0 and $t$. □

We now state the a priori error estimate for the numerical method (2.19) that is proved in [20]. The result is written in the anisotropic framework described in Section 1.1.

**Theorem 2.14** (An anisotropic a priori error estimate for the semi-discrete finite elements approximation of the transport equation)**.**
*Assume that* $\mathbf{u}$ *is not identically zero on* $\Omega$*. Let* $\varphi$ *be the solution of (2.18) and* $\varphi_h$ *the solution of (2.19) where we define*

$$\delta_h = \frac{\max_{K\in\mathcal{T}_h}\lambda_{2,K}}{2\|\mathbf{u}\|_{L^\infty(\Omega)}}. \tag{2.22}$$

*Assume moreover that $\varphi \in H^1(0,T;H^2(\Omega)^2)$ and let us note $e_h(t) = \varphi(t) - \varphi_h(t)$. Then there exists a constant $C > 0$ depending only on the reference triangle $\hat{K}$, in particular $C$ is independent of $\Omega, T, \mathbf{u}, \varphi$, the mesh size and aspect ratio, such that*

$$\begin{aligned}\|e_h(T)\|^2_{L^2(\Omega)} &+ \delta_h^2\|\mathbf{u}\cdot\nabla e_h(T)\|^2_{L^2(\Omega)}\\ &\leq \|e_h(0)\|^2_{L^2(\Omega)} + \delta_h^2\|\mathbf{u}\cdot\nabla e_h(0)\|^2_{L^2(\Omega)}\\ +C\Bigg(\int_0^T\Bigg(\sum_{K\in\mathcal{T}_h}&\left(\frac{1}{\delta_h}+\frac{\delta_h\|\mathbf{u}\|^2_{L^\infty(K)}}{\lambda^2_{2,K}}\right)L^2_K(\varphi)+\left(\delta_h+\frac{\delta_h^3\|\mathbf{u}\|^2_{L^\infty(K)}}{\lambda^2_{2,K}}\right)L^2_K\left(\frac{\partial\varphi}{\partial t}\right)\Bigg)dt\Bigg).\end{aligned} \tag{2.23}$$

**Remark 2.15.** (i) In the case of isotropic meshes, $\lambda_{1,K} \simeq \lambda_{2,K} \simeq h_k$ and $L^2_K(v) \leq Ch^4_K|v|^2_{H^2(K)}$ where $C$ is independent of the mesh size but may depend on the mesh aspect ratio. Thus, in this settings, (2.23) reduces to

$$\|\varphi(T) - \varphi_h(T)\|^2_{L^2(\Omega)} \leq Ch^3 + h.o.t.,$$

where *h.o.t.* stands for higher order terms.

(ii) Estimate (2.23) is optimal for anisotropic meshes. Indeed, assume that the solution $\varphi$ depends only on one variable and that the mesh is aligned with the solution, then the estimate (2.23) reduces to

$$\|\varphi(T) - \varphi_h(T)\|^2_{L^2(\Omega)} \leq C\left(\max_{K\in\mathcal{T}_h}\lambda_{2,K}\right)^3 + h.o.t.,$$

and $\max_{K\in\mathcal{T}_h}\lambda_{2,K} \to 0$ is sufficient to ensure the convergence of the numerical method.

(iii) One can also prove an a priori error estimate for the semi-norm , namely

$$\begin{aligned}&\delta_h\int_0^T\left\|\frac{\partial e_h(t)}{\partial t}+\mathbf{u}\cdot\nabla e_h(t)\right\|^2 dt\\ &\leq C\left(\int_0^T\left(\sum_{K\in\mathcal{T}_h}\left(\frac{1}{\delta_h}+\frac{\delta_h\|\mathbf{u}\|^2_{L^\infty(K)}}{\lambda^2_{2,K}}\right)L^2_K(\varphi)+\left(\delta_h+\frac{\delta_h^3\|\mathbf{u}\|^2_{L^\infty(K)}}{\lambda^2_{2,K}}\right)L^2_K\left(\frac{\partial\varphi}{\partial t}\right)\right)dt\right),\end{aligned}$$

where as before $C$ depends only on the reference triangle.

#### Stability and a priori error estimates for the fully discrete approximation

We are now studying the fully discrete method (2.20). We first state a discrete equivalent of the stability estimate of Proposition 2.12. We emphasize that, for the moment, we are still considering a divergence free velocity field $\mathbf{u}$, independent of the time. Comments about the non-divergence free case will be addressed at the end of this chapter, and a particular analysis of the time dependent case will be proposed in the next section. By sake of simplicity and clarity for the reader, we chose to present our results only in the norm $\|\cdot\|^2_{L^2(\Omega)} + \delta_h^2\|\mathbf{u}\cdot\nabla(\cdot)\|^2_{L^2(\Omega)}$. The stability estimate and the two a priori error estimates presented below can be extended to the semi-norm

$$\delta_h\int_0^T\left\|\frac{\partial\cdot}{\partial t}+\mathbf{u}\cdot\nabla(\cdot)\right\|^2_{L^2(\Omega)}dt,$$

but we refer to [22] where all the technical details are presented.

**Proposition 2.16** (Fully discrete stability estimate for the SUPG method and the Crank-Nicolson scheme applied to the transient transport equation)**.**
*Let* $(\varphi_h^n)_{n=0}^N$ *be the solution of (2.20) where* $\delta_h > 0$ *is constant. Then it holds*

$$\|\varphi_h^{n+1}\|^2_{L^2(\Omega)} + \delta_h^2 \|\mathbf{u}\cdot\nabla\varphi_h^{n+1}\|^2_{L^2(\Omega)} \leq \|\varphi_h^{n}\|^2_{L^2(\Omega)} + \delta_h^2 \|\mathbf{u}\cdot\nabla\varphi_h^{n}\|^2_{L^2(\Omega)}, \quad \forall n = 0, 1, ..., N-1. \quad (2.24)$$

**Remark 2.17.**
Observe that (2.24) implies in particular that for any $n$

$$\|\varphi_h^{n}\|^2_{L^2(\Omega)} + \delta_h^2 \|\mathbf{u}\cdot\nabla\varphi_h^{n}\|^2_{L^2(\Omega)} \leq \|\varphi_h^{0}\|^2_{L^2(\Omega)} + \delta_h^2 \|\mathbf{u}\cdot\nabla\varphi_h^{0}\|^2_{L^2(\Omega)},$$

which is exactly the discrete counterpart of (2.21).

*Proof.* We choose

$$v_h = \frac{\varphi_h^{n+1} + \varphi_h^n}{2} + \delta_h \frac{\varphi_h^{n+1} - \varphi_h^n}{\tau^{n+1}}$$

in (2.20). Following the proof of Proposition 2.12, it yields

$$\frac{1}{2\tau^{n+1}}\left(\|\varphi_h^{n+1}\|^2_{L^2(\Omega)} - \|\varphi_h^{n}\|^2_{L^2(\Omega)}\right) + \frac{1}{2}\int_\Omega \operatorname{div}\left(\mathbf{u}\left(\frac{\varphi_h^{n+1}+\varphi_h^n}{2}\right)^2\right) d\mathbf{x} + \frac{\delta_h^2}{2}\int_\Omega \operatorname{div}\left(\mathbf{u}\left(\frac{\varphi_h^{n+1}-\varphi_h^n}{\tau^{n+1}}\right)^2\right) d\mathbf{x}$$
$$+ \delta_h \int_\Omega \left(\frac{\varphi_h^{n+1}-\varphi_h^n}{\tau^{n+1}} + \mathbf{u}\cdot\nabla\left(\frac{\varphi_h^{n+1}+\varphi_h^n}{2}\right)\right)^2 d\mathbf{x} = 0.$$

As proven in Proposition 2.12, all the terms in the second and third lines have a non-negative contributions, therefore, we obtain

$$\frac{1}{2\tau^{n+1}}\left(\|\varphi_h^{n+1}\|^2_{L^2(\Omega)} - \|\varphi_h^{n}\|^2_{L^2(\Omega)}\right) + \frac{\delta_h^2}{2\tau^{n+1}}\left(\|\mathbf{u}\cdot\nabla\varphi_h^{n+1}\|^2_{L^2(\Omega)} - \|\mathbf{u}\cdot\nabla\varphi_h^{n}\|^2_{L^2(\Omega)}\right) \leq 0,$$

which yields to the desired result by multiplying by $2\tau^{n+1}$. □

We now present a first convergence result for the numerical method (2.20). The proof consists to split the numerical error at every time step $\varphi(t^n) - \varphi_h^n$ into

$$(\varphi(t^n) - \varphi_h(t^n)) + (\varphi_h(t^n) - \varphi_h^n)$$

by using the semi-discrete approximation in space. The resulting bound is not fully satisfactory since it involves time derivatives of $\varphi_h$. The curious reader can have a look at the proof, but in a first reading, it can be skipped. A better a priori error estimate is presented later on in the Theorem 2.24.

**Theorem 2.18** (A quick and first a priori error estimate for the SUPG method and the Crank-Nicolson scheme applied to the transport equation with a transport velocity field independent of the time)**.**
*Assume that* $\mathbf{u}$ *is not identically zero on* $\Omega$. *Let* $\varphi$ *be the solution of (2.18) and let* $(\varphi_h^n)_{n=0}^N$ *be the solution of (2.20) where* $\delta_h$ *is defined by*

$$\delta_h = \frac{\max\limits_{K\in\mathcal{T}_h} \lambda_{2,K}}{2\|\mathbf{u}\|_{L^\infty(\Omega)}}. \quad (2.25)$$

*Let*

$$\tau = \max_{n=0,\dots,N-1} \tau^{n+1}.$$

*Assume that* $\varphi \in H^1(0,T;H^2(\Omega))$ *and* $\dfrac{\partial^3 \varphi_h}{\partial t^3} \in L^2(0,T;L^2(\Omega))$, *where* $\varphi_h(t)$ *is the semi-discrete approximation given by (2.19). Finally, let note the numerical error* $e(t^n) = \varphi(t^n) - \varphi_h^n$. *Then, there exists* $C > 0$ *depending only on the reference triangle* $\hat{K}$, *in particular* $C$ *is independent of* $T$, $\Omega$, $\mathbf{u}$, $\varphi, N$, *the mesh size, aspect ratio and the time step, such that*

$$\|e(T)\|^2_{L^2(\Omega)} + \delta_h^2 \|\mathbf{u} \cdot \nabla e(T)\|^2_{L^2(\Omega)} \leq C\Bigg( \|e(0)\|^2_{L^2(\Omega)} + \delta_h^2 \|\mathbf{u} \cdot \nabla e(0)\|^2_{L^2(\Omega)}$$
$$+ \int_0^T \sum_{K \in \mathcal{T}_h} \left( \left( \frac{1}{\delta_h} + \frac{\delta_h \|\mathbf{u}\|_{L^\infty(K)}}{\lambda^2_{2,K}} \right) L^2_K(\varphi) + \left( \delta_h + \frac{\delta_h^3 \|\mathbf{u}\|_{L^\infty(K)}}{\lambda^2_{2,K}} \right) L^2_K\left( \frac{\partial \varphi}{\partial t} \right) \right) dt$$
$$+ \left( T\tau^4 + T\delta_h^2 \tau^2 + \delta_h \tau^4 \right) \int_0^T \left\| \frac{\partial^3 \varphi_h}{\partial t^3} \right\|^2_{L^2(\Omega)} dt \Bigg). \quad (2.26)$$

**Remark 2.19.** (i) So far, we have not been able to prove that

$$\int_0^T \left\| \frac{\partial^3 \varphi_h}{\partial t^3} \right\|^2_{L^2(\Omega)} dt$$

is bounded independently of $h$ and $\tau$. The proof is not obvious, even for parabolic problems [92]. Though this drawback, we choose to present Theorem 2.18 since its proof is fairly simple.

As announced, an other a priori error estimate (see Theorem 2.24), where only derivatives of the exact solutions appears, will be stated. The proof requires to introduce the hyperbolic projection used in [22]. Since it is only done in the isotropic settings, for completeness, we also present in our framework the a priori error estimate derived with this technique.

(ii) If we assume that

$$\int_0^T \left\| \frac{\partial^3 \varphi_h}{\partial t^3} \right\|^2_{L^2(\Omega)} dt$$

is bounded independently of $h$ and $\tau$, then the a priori error estimate (2.26) reduces (written in the isotropic settings for simplicity) to

$$e(T) = O(h^{3/2} + \tau^2) + h.o.t.,$$

as it is desired, since the Crank-Nicolson scheme is an order 2 in time numerical method.

(iii) Note that in the a priori error estimates proven in [22], the factor $T$ does not appear in the right hand side when estimating the $L^2$ norm of the error, but a different choice for the norm of $\frac{\partial^3 \varphi_h}{\partial t^3}$ has to be made. Namely, in [22], the $L^1((0,T);L^2(\Omega))$ norm is used rather than the $L^2((0,T);L^2(\Omega))$ norm that we choose here. Remark that we use the $L^2((0,T);L^2(\Omega))$ norm for consistency, since the a posteriori error estimate that we will prove later, will be expressed in the same norm.

*Proof.* The proof proceeds in two parts. For any $n = 0, 1, ..., N$, let us decompose the numerical error $e(t^n)$ as

$$e(t^n) = \varphi(t^n) - \varphi_h^n = (\varphi(t^n) - \varphi_h(t^n)) + (\varphi_h(t^n) - \varphi_h^n) = e_h(t^n) + e_h^n.$$

Observe that

$$\begin{aligned}\|e(T)\|^2_{L^2(\Omega)} &+ \delta_h^2 \|\mathbf{u} \cdot \nabla e(T)\|^2_{L^2(\Omega)} \\ &\leq \underbrace{2\|e_h(T)\|^2_{L^2(\Omega)} + 2\delta_h^2 \|\mathbf{u} \cdot \nabla e_h(T)\|^2_{L^2(\Omega)}}_{I_1} \\ &\qquad + \underbrace{2\|e_h^N\|^2_{L^2(\Omega)} + 2\delta_h^2 \|\mathbf{u} \cdot \nabla e_h^N\|^2_{L^2(\Omega)}}_{I_2}.\end{aligned}$$

We then estimate $I_1$ and $I_2$ independently. To simplify the writing, in what follows, we will denote by $\hat{C}$ any positive constants depending only on the reference triangle $\hat{K}$ and by $\tilde{C}$ any positive constant which is a pure real number (in particular independent of any datum of the problem, the mesh or any discretization parameter). Note that the values of $\hat{C}$ and $\tilde{C}$ can change from line to line.

*Part I. Estimate for $I_1$.*

We apply Theorem 2.14 on $I_1$ and we obtain

$$\begin{aligned}&\|e_h(T)\|^2_{L^2(\Omega)} + \delta_h^2 \|\mathbf{u} \cdot \nabla e_h(T)\|^2_{L^2(\Omega)} \\ &\leq \hat{C} \Bigg( \|e_h(0)\|^2_{L^2(\Omega)} + \delta_h^2 \|\mathbf{u} \cdot \nabla e_h(0)\|^2_{L^2(\Omega)} + \int_0^T \sum_{K \in \mathcal{T}_h} \Bigg( \left( \frac{1}{\delta_h} + \frac{\delta_h \|\mathbf{u}\|_{L^\infty(K)}}{\lambda_{2,K}^2} \right) L_K^2(\varphi) \\ &\qquad + \left( \delta_h + \frac{\delta_h^3 \|\mathbf{u}\|_{L^\infty(K)}}{\lambda_{2,K}^2} \right) L_K^2 \left( \frac{\partial \varphi}{\partial t} \right) \Bigg) dt \Bigg). \quad (2.27)\end{aligned}$$

*Part II. Estimate for $I_2$.*

We now have to estimate $I_2$. By using several times the Fundamental Theorem of Calculus, one can derive that

$$\frac{\varphi_h(t^{n+1}) - \varphi_h(t^n)}{\tau^{n+1}} = \frac{\partial_t \varphi_h(t^{n+1}) + \partial_t \varphi_h(t^n)}{2} + r^{n+1}, \quad (2.28)$$

where

$$r^{n+1} = \frac{1}{2\tau^{n+1}} \int_{t^n}^{t^{n+1}} \left( \int_{t^n}^{s} \int_{t^n}^{t} \frac{\partial^3 \varphi_h}{\partial t^3}(\zeta) d\zeta dt + \int_{t^{n+1}}^{s} \int_{t^n}^{t} \frac{\partial^3 \varphi_h}{\partial t^3}(\zeta) d\zeta dt \right) ds.$$

In particular, we observe that

$$|r^{n+1}|^2 \leq (\tau^{n+1})^3 \int_{t^n}^{t^{n+1}} \left( \frac{\partial^3 \varphi_h}{\partial t^3}(t) \right)^2 dt. \quad (2.29)$$

In the sequel, we will note $e_h^n = \varphi_h(t^n) - \varphi_h^n$. By using (2.19), (2.20) and (2.28), one can prove that the following relation holds for the numerical error

$$\begin{aligned}\int_\Omega \left( \frac{e_h^{n+1} - e_h^n}{\tau^{n+1}} + \mathbf{u} \cdot \nabla \left( \frac{e_h^{n+1} + e_h^n}{2} \right) \right) (v_h + \delta_h \mathbf{u} \cdot \nabla v_h)\, dx \\ = \int_\Omega r^{n+1} (v_h + \delta_h \mathbf{u} \cdot \nabla v_h)\, dx, \forall v_h \in V_h. \quad (2.30)\end{aligned}$$

Choosing

$$v_h = \frac{e_h^{n+1} + e_h^n}{2} + \delta_h \frac{e_h^{n+1} - e_h^n}{\tau^{n+1}}$$

and reproducing what we is done in the proof of Proposition 2.16, we obtain

$$\begin{aligned}
&\frac{1}{2\tau^{n+1}} \left( \|e_h^{n+1}\|_{L^2(\Omega)}^2 - \|e_h^n\|_{L^2(\Omega)}^2 \right) + \frac{\delta_h^2}{2\tau^{n+1}} \left( \|\mathbf{u} \cdot \nabla e_h^{n+1}\|_{L^2(\Omega)}^2 - \|\mathbf{u} \cdot \nabla e_h^n\|_{L^2(\Omega)}^2 \right) \\
&\qquad + \delta_h \int_\Omega \left( \frac{e_h^{n+1} - e_h^n}{\tau^{n+1}} + \mathbf{u} \cdot \nabla \left( \frac{e_h^{n+1} + e_h^n}{2} \right) \right)^2 dx \\
&\qquad \leq \int_\Omega r^{n+1} \left( \frac{e_h^{n+1} + e_h^n}{2} + \delta_h^2 \mathbf{u} \cdot \nabla \left( \frac{e_h^{n+1} - e_h^n}{\tau^{n+1}} \right) \right) dx \\
&\qquad\qquad + \delta_h \int_\Omega r^{n+1} \left( \frac{e_h^{n+1} - e_h^n}{\tau^{n+1}} + \mathbf{u} \cdot \nabla \left( \frac{e_h^{n+1} + e_h^n}{2} \right) \right) dx.
\end{aligned}$$

Recognizing that the last term of the left hand side is also present in the last term of the right hand side, we can eliminate it thanks to the Young's inequality and it yields

$$\begin{aligned}
&\frac{1}{2\tau^{n+1}} \left( \|e_h^{n+1}\|_{L^2(\Omega)}^2 - \|e_h^n\|_{L^2(\Omega)}^2 \right) + \frac{\delta_h^2}{2\tau^{n+1}} \left( \|\mathbf{u} \cdot \nabla e_h^{n+1}\|_{L^2(\Omega)}^2 - \|\mathbf{u} \cdot \nabla e_h^n\|_{L^2(\Omega)}^2 \right) \\
&\qquad \leq \left\| r^{n+1} \right\|_{L^2(\Omega)} \left\| \frac{e_h^{n+1} + e_h^n}{2} + \delta_h^2 \mathbf{u} \cdot \nabla \left( \frac{e_h^{n+1} - e_h^n}{\tau^{n+1}} \right) \right\|_{L^2(\Omega)} + \frac{\delta_h}{2} \left\| r^{n+1} \right\|_{L^2(\Omega)}^2 .
\end{aligned}$$

Multiplication by $2\tau^{n+1}$ and use of Cauchy−Schwarz, triangle and Young's inequalities imply that it holds for every $0 \leq n \leq N-1$

$$\begin{aligned}
&\|e_h^{n+1}\|_{L^2(\Omega)}^2 + \delta_h^2 \ \|\mathbf{u} \cdot \nabla e_h^{n+1}\|_{L^2(\Omega)}^2 - \|e_h^n\|_{L^2(\Omega)}^2 - \delta_h^2 \ \|\mathbf{u} \cdot \nabla e_h^n\|_{L^2(\Omega)}^2 \\
&\leq \tilde{C} \left( T\tau^{n+1} + T \frac{\delta_h^2}{\tau^{n+1}} + \delta_h \tau^{n+1} \right) \left\| r^{n+1} \right\|_{L^2(\Omega)}^2 + \frac{\tau^{n+1}}{T} \left( \|e_h^n\|_{L^2(\Omega)}^2 + \delta_h^2 \|\mathbf{u} \cdot \nabla e_h^n\|_{L^2(\Omega)}^2 \right) \\
&\qquad + \frac{\tau^{n+1}}{2T} \left( \|e_h^{n+1}\|_{L^2(\Omega)}^2 + \delta_h^2 \|\mathbf{u} \cdot \nabla e_h^{n+1}\|_{L^2(\Omega)}^2 \right).
\end{aligned}$$

Noting $\gamma_n = \dfrac{\tau^{n+1}}{T}$ and $\mu_{n+1} = \dfrac{\tau^{n+1}}{2T} < 1$, we can apply the discrete Gronwall's Lemma (see Lemma A.6 in the Appendix A.1) and we get

$$\begin{aligned}
&\|e_h^N\|_{L^2(\Omega)}^2 + \delta_h^2 \|\mathbf{u} \cdot \nabla e_h^N\|_{L^2(\Omega)}^2 \\
&\leq \tilde{C} \exp \left( \sum_{n=0}^{N-1} \frac{\mu_{n+1}}{1 - \mu_{n+1}} \right) \exp \left( \sum_{n=0}^{N-1} \gamma_n \right) \sum_{n=0}^{N-1} \left( T\tau^{n+1} + T \frac{\delta_h^2}{\tau^{n+1}} + \delta_h \tau^{n+1} \right) \left\| r^{n+1} \right\|_{L^2(\Omega)}^2 ,
\end{aligned}$$

where we use the fact that $e_h^0 = 0$. Since $\displaystyle\sum_{n=0}^{N-1} \gamma_n, \sum_{n=0}^{N-1} \frac{\mu_{n+1}}{1 - \mu_{n+1}} \leq 1$ and using (2.29), we obtain

$$I_2 \leq \tilde{C} \left( T\tau^4 + T\delta_h^2 \tau^2 + \delta_h \tau^4 \right) \int_0^T \left\| \frac{\partial^3 u_h}{\partial t^3} \right\|_{L^2(\Omega)}^2 dt. \tag{2.31}$$

Estimates (2.31) and (2.27) together yield the result. □

#### A second a priori error estimate for the fully discrete approximation

We present the alternative error estimate announced in the Remark 2.19. Rather than cutting the numerical error $\varphi(t^n) - \varphi_h^n$ into $\varphi(t^n) - \varphi_h(t^n)$ and $\varphi_h(t^n) - \varphi_h^n$, we introduce a suitable projection operator $\Pi$ and estimate the sum $(\varphi(t^n) - \Pi\varphi(t^n)) + (\Pi\varphi(t^n) - \varphi_h^n)$. This approach is the same as for parabolic problems, where $\Pi$ is chosen as the elliptic projection. The projection operator we choose for the transport equation is the hyperbolic-Ritz projection as advocated in [22] and is introduced in the next definition. At the end we will show that (up to some higher order terms and written in the isotropic setting) $\varphi(t^n) - \Pi\varphi(t^n) = O(h^{3/2})$ and $\Pi\varphi(t^n) - \varphi_h^n = O(\tau^2)$.

**Definition 2.20** (Hyperbolic-Ritz projection)**.**
Let $\mathbf{u} \in C^1(\overline{\Omega})$ such that $\operatorname{div}\mathbf{u} = 0$ and $\phi \in C^0([0,T]; H^1(\Omega))$ such that $\phi = 0$ on $\Gamma^-$. For any $t \in [0,T]$, we define the Hyperbolic-Ritz Projection (HRP) of $\phi(t)$ as the unique $\phi_h \in V_h$ solution of

$$\int_\Omega (\phi_h + \mathbf{u}\cdot\nabla\phi_h)(v_h + \delta_h \mathbf{u}\cdot\nabla v_h) d\mathbf{x} = \int_\Omega (\phi(t) + \mathbf{u}\cdot\nabla\phi(t))(v_h + \delta_h \mathbf{u}\cdot\nabla v_h) d\mathbf{x}, \quad \forall v_h \in V_h.$$

where $\delta_h > 0$. We note $\phi_h = \Pi_h^{hyp}\phi(t)$.

The projection $\Pi_h^{hyp}$ satisfies the following properties :

**Proposition 2.21.**
*Let $\phi \in C^0([0,T]; H^2(\Omega))$, $\phi = 0$ on $\Gamma^-$, and assume that $\delta_h > 0$ is a constant. There exists a constant $C > 0$ depending only on the reference triangle $\hat{K}$ such that for all $t \in [0,T]$,*

$$\|\phi(t) - \Pi_h^{hyp}\phi(t)\|_{L^2(\Omega)}^2 + \delta_h^2 \|\mathbf{u}\cdot\nabla(\phi(t) - \Pi_h^{hyp}\phi(t))\|_{L^2(\Omega)}^2 \leq C \sum_{K\in\mathcal{T}_h} \epsilon_K(\delta_h, \mathbf{u}) L_K^2(\phi(t)), \quad (2.32)$$

*where we note*

$$\epsilon_K(\delta_h, \mathbf{u}) = \left( \frac{1}{\delta_h} + \delta_h + \frac{\delta_h \|\mathbf{u}\|_{L^\infty(K)}^2}{\lambda_{2,K}^2} + \frac{\delta_h^3 \|\mathbf{u}\|_{L^\infty(K)}^2}{\lambda_{2,K}^2} \right).$$

**Remark 2.22.** (i) Observe that $\phi_h$ in the Definition 2.20 is in the fact the finite element solution of a steady advection-reaction equation, namely

$$\int_\Omega (\phi_h + \mathbf{u}\cdot\nabla\phi_h)(v_h + \delta_h \mathbf{u}\cdot\nabla v_h) d\mathbf{x} = \int_\Omega f(v_h + \delta_h \mathbf{u}\cdot\nabla v_h) d\mathbf{x}, \quad \forall v_h \in V_h,$$

where $f = \phi + \mathbf{u}\cdot\nabla\phi$.

(ii) If we choose $\delta_h = \dfrac{\max_{K\in\mathcal{T}_h} \lambda_{2,K}}{2\|\mathbf{u}\|_{L^\infty(\Omega)}}$ as in Theorem 2.14 and Theorem 2.18 and we assume that $\phi$ depends only on one spatial variable and that the mesh is taken in the right direction, then the estimate (2.32) reduces to

$$\|\phi(t) - \Pi_h^{hyp}\phi(t)\|_{L^2(\Omega)}^2 + \delta_h^2 \|\mathbf{u}\cdot\nabla(\phi(t) - \Pi_h^{hyp}\phi(t))\|_{L^2(\Omega)}^2 \leq C(\max_{K\in\mathcal{T}_h} \lambda_{2,K})^3 + h.o.t,$$

where $C > 0$ is a constant depending on $\phi$ but independent of the mesh size and the mesh aspect ratio.

(iii) In the isotropic settings, that is to say when $\lambda_{1,K} \simeq \lambda_{2,K} \simeq h_K$, then the estimate (2.32) reduces to

$$\|\phi(t) - \Pi_h^{hyp}\phi(t)\|^2_{L^2(\Omega)} + \delta_h^2 \|\mathbf{u}\cdot\nabla(\phi(t) - \Pi_h^{hyp}\phi(t))\|^2_{L^2(\Omega)} \leq Ch^3|\phi|^2_{H^2(\Omega)} + h.o.t.,$$

where $C > 0$ is independent of the mesh size but may depend on the aspect ratio.

(iv) Since $\mathbf{u}$ is independent of the time, under some smoothness hypothesis on $\phi$, one can show that the time derivative and $\Pi_h^{hyp}$ commute, that is to say

$$\frac{\partial}{\partial t}\Pi_h^{hyp}\phi(t) = \Pi_h^{hyp}\frac{\partial \phi(t)}{\partial t}, \quad \forall t \in [0,T]. \tag{2.33}$$

Indeed, assuming that we can differentiate inside the integrals, one derive immediately that

$$\int_\Omega \left(\frac{\partial}{\partial t}\phi(t) + \mathbf{u}\cdot\nabla\left(\frac{\partial}{\partial t}\phi(t)\right)\right)(v_h + \delta_h \mathbf{u}\cdot\nabla v_h)d\mathbf{x}$$
$$= \int_\Omega \left(\frac{\partial}{\partial t}\Pi_h^{hyp}\phi(t) + \mathbf{u}\cdot\nabla\left(\frac{\partial}{\partial t}\Pi_h^{hyp}\phi(t)\right)\right)(v_h + \delta_h \mathbf{u}\cdot\nabla v_h)d\mathbf{x}, \quad \forall v_h \in V_h,$$

which, by definition, implies that $\frac{\partial}{\partial t}\Pi_h^{hyp}\phi(t) = \Pi_h^{hyp}\frac{\partial\phi(t)}{\partial t}$.

*Proof of Proposition 2.21.* Let us note $e(t) = \phi(t) - \Pi_h^{hyp}\phi(t)$. Reproducing again the strategy of the proof of Proposition 2.12 (that is to say using the fact that $\mathbf{u}$ is divergence free, the fact that $\delta_h$ is constant and the boundary conditions on $\Gamma^-$), one can derive that

$$\|e(t)\|^2_{L^2(\Omega)} + \delta_h\int_\Omega (e(t) + \mathbf{u}\cdot\nabla e(t))^2 d\mathbf{x} + \delta_h^2\|\mathbf{u}\cdot\nabla e(t)\|^2_{L^2(\Omega)}$$
$$\leq \int_\Omega (e(t) + \mathbf{u}\cdot\nabla e(t))\left((e(t) + \delta_h e(t)) + \delta_h\mathbf{u}\cdot\nabla(e(t) + \delta_h e(t))\right)d\mathbf{x}.$$

Since by definition, the HRP satisfies the orthogonality property

$$\int_\Omega (e(t) + \mathbf{u}\cdot\nabla e(t))(v_h + \delta_h\mathbf{u}\cdot\nabla v_h)d\mathbf{x} = 0, \quad \forall v_h \in V_h,$$

one can subtract any test function from the right hand side. Thus, subtracting $v_h = r_h(\phi) - \Pi_h^{hyp}\phi$, where $r_h$ stands for the Lagrange interpolant, and noting $e_h(t) = \phi(t) - r_h(\phi(t))$,we obtain

$$\|e(t)\|^2_{L^2(\Omega)} + \delta_h\int_\Omega (e(t) + \mathbf{u}\cdot\nabla e(t))^2 d\mathbf{x} + \delta_h^2\|\mathbf{u}\cdot\nabla e(t)\|^2_{L^2(\Omega)}$$
$$\leq \int_\Omega (e(t) + \mathbf{u}\cdot\nabla e(t))\left((e_h(t) + \delta_h e_h(t)) + \delta_h\mathbf{u}\cdot\nabla(e_h(t) + \delta_h e_h(t))\right)d\mathbf{x}.$$

Using the Young's inequality, we get

$$\|e(t)\|^2_{L^2(\Omega)} + \delta_h\int_\Omega (e(t) + \mathbf{u}\cdot\nabla e(t))^2 d\mathbf{x} + \delta_h^2\|\mathbf{u}\cdot\nabla e(t)\|^2_{L^2(\Omega)}$$
$$\leq \frac{\delta_h}{2}\int_\Omega (e(t) + \mathbf{u}\cdot\nabla e(t))^2 d\mathbf{x} + \left(\frac{4}{\delta_h} + 2\delta_h\right)\|\phi - r_h(\phi)\|^2_{L^2(\Omega)}$$
$$+ 4(\delta_h + \delta_h^3\|\mathbf{u}\cdot\nabla(\phi - r_h(\phi))\|^2_{L^2(\Omega)}.$$

Thus, we have

$$\|e(t)\|_{L^2(\Omega)}^2 + \delta_h^2 \|\mathbf{u} \cdot \nabla e(t)\|_{L^2(\Omega)}^2$$
$$\le \sum_{K \in \mathcal{T}_h} \left( \left( \frac{4}{\delta_h} + 2\delta_h \right) \|\phi - r_h(\phi)\|_{L^2(K)}^2 + 4(\delta_h \|\mathbf{u}\|_{L^\infty(K)}^2 + \delta_h^3) \|\mathbf{u}\|_{L^\infty(K)}^2) \|\nabla(\phi - r_h(\phi))\|_K^2 \right).$$

We conclude by applying the anisotropic interpolation error estimate (1.2) for the Lagrange interpolant. □

**Remark 2.23.**
Observe that to obtain

$$\|e(t)\|_{L^2(\Omega)}^2 + \delta_h \int_\Omega (e(t) + \mathbf{u} \cdot \nabla e(t))^2 \, d\mathbf{x} + \delta_h^2 \|\mathbf{u} \cdot \nabla e(t)\|_{L^2(\Omega)}^2$$
$$\le \int_\Omega (e(t) + \mathbf{u} \cdot \nabla e(t)) \left( (e(t) + \delta_h e(t)) + \delta_h \mathbf{u} \cdot \nabla (e(t) + \delta_h e(t)) \right) d\mathbf{x}.$$

we choose $v = e(t) + \delta_h e(t)$ in the bilinear form

$$\int_\Omega (e(t) + \mathbf{u} \cdot \nabla e(t)) \, (v + \delta_h \mathbf{u} \cdot \nabla v) d\mathbf{x}.$$

by mimicking what was done for time dependent problems where we choose $v = e(t) + \delta_h \dfrac{\partial e(t)}{\partial t}$. Note that here it is not necessary since it is a steady problem and we can just choose $v = e(t)$ and get an estimate in the stronger norm

$$\| \cdot \|_{L^2(\Omega)}^2 + \delta_h \|\mathbf{u} \cdot \nabla(\cdot)\|_{L^2(\Omega)}^2.$$

And therefore, multiplication by $\delta_h$ yields an estimate in the norm

$$\| \cdot \|_{L^2(\Omega)}^2 + \delta_h^2 \|\mathbf{u} \cdot \nabla(\cdot)\|_{L^2(\Omega)}^2.$$

Note that the two estimates (the one obtained in Proposition 2.21 and the one that would be obtained following the remark above) will differ only in their higher order terms. We choose to act as in the proposed proof since it yields automatically an estimate in the norm needed for the time dependent problem .

We are now proving our second (and complete) a priori error estimate. The proof is rather technical, and a reader interested in practical purposes can go directly to the next paragraph where the a posteriori error analysis is performed.

**Theorem 2.24** (An a priori error estimate for the transport equation with anisotropic finite elements and the Crank-Nicolson scheme in the case of a transport velocity field independent of the time)**.**
*Assume that $\mathbf{u}$ is not identically zero on $\Omega$. Let $\varphi$ be the solution of (2.18) and let $(\varphi_h^n)_{n=0}^N$ be the solution of (2.20) where $\delta_h$ is defined by*

$$\delta_h = \frac{\max\limits_{K \in \mathcal{T}_h} \lambda_{2,K}}{2\|\mathbf{u}\|_{L^\infty(\Omega)}}.$$

*Let*

$$\tau = \max_{n=0,\dots,N-1} \tau^{n+1}.$$

*Assume that $\varphi \in H^3(0,T;H^2(\Omega))$ Finally, let note the numerical error $e(t^n) = \varphi(t^n) - \varphi_h^n$. Then, there exists $C > 0$ depending only on the reference triangle $\hat{K}$, in particular $C$ is independent of $T$, $\Omega$, $\mathbf{u}$, $\varphi, N$, the mesh size, aspect ratio and the time step, such that*

$$\begin{aligned}\|e(T)\|^2_{L^2(\Omega)} + \delta_h^2\|\mathbf{u}\cdot\nabla e(T)\|^2_{L^2(\Omega)} \le C \Big(\|e(0)\|^2_{L^2(\Omega)} + \delta_h^2\|\mathbf{u}\cdot\nabla e(0)\|^2_{L^2(\Omega)} \\ + \sum_{K\in\mathcal{T}_h}(1+\delta_h^2)\epsilon_K(\delta_h,\mathbf{u})(\sup_{t\in(0,T)} L_K^2(\varphi) + \sup_{t\in(0,T)} L_K^2(\partial_t\varphi)) \\ + \sum_{K\in\mathcal{T}_h}(T+\delta_h^2+T\delta_h^2)\epsilon_K(\delta_h,\mathbf{u})\left(T\sup_{t\in(0,T)} L_K^2(\varphi) + \int_0^T L_K^2(\partial_t\varphi) + L_K^2(\partial_{tt}\varphi)dt\right) \\ +(T\tau^4+\delta_h\tau^4+\delta_h^2\tau^2)\int_0^T|\partial_{ttt}\varphi|^2 dt\Big), \quad (2.34)\end{aligned}$$

*where we define $\epsilon(\delta_h,\mathbf{u})$ as in Proposition 2.21.*

*Proof.* As in the proof of Theorem 2.18, we decompose the numerical error as

$$e(t^n) = \varphi(t^n) - \varphi_h^n = (\varphi(t^n) - \Pi_h^{hyp}\varphi(t^n)) + (\Pi_h^{hyp}\varphi(t^n) - \varphi_h^n) = e_h(t^n) + e_h^n,$$

and then we separate the demonstration by estimating each part of

$$\begin{aligned}&\|e(T)\|^2_{L^2(\Omega)} + \delta_h^2\|\mathbf{u}\cdot\nabla e(T)\|^2_{L^2(\Omega)} \\ &\qquad\le \underbrace{2\|e_h(T)\|^2_{L^2(\Omega)} + 2\delta_h^2\|\mathbf{u}\cdot\nabla e_h(T)\|^2_{L^2(\Omega)}}_{I_1} + \underbrace{2\|e_h^N\|^2_{L^2(\Omega)} + 2\delta_h^2\|\mathbf{u}\cdot\nabla e_h^N\|^2_{L^2(\Omega)}}_{I_2}.\end{aligned}$$

As before, we will denote by $\hat{C}$ any positive constant depending only on the reference triangle $\hat{K}$ and by $\tilde{C}$ any positive constant which is a pure real number (in particular independent of any datum of the problem, the mesh or any discretization parameter), which values may change from line to line.

*Part I. Estimate for $I_1$.*

Using the error estimate for the HRP of Proposition 2.21, we immediately obtain that

$$I_1 \le \hat{C}\sum_{K\in\mathcal{T}_h}\epsilon_K(\delta_h,\mathbf{u})\sup_{t\in(0,T)} L_K^2(\varphi(t)).$$

*Part II. Estimate for $I_2$.*

Observe that, from the numerical scheme (2.20), we can write an error equation

$$\begin{aligned}\int_\Omega\left(\frac{e_h^{n+1}-e_h^n}{\tau^{n+1}} + \mathbf{u}\cdot\nabla\left(\frac{e_h^{n+1}+e_h^n}{2}\right)\right)(v_h+\delta_h\mathbf{u}\cdot\nabla v_h)\,dx \\ = \int_\Omega(r_1^{n+1}+r_2^{n+1})(v_h+\delta_h\mathbf{u}\cdot\nabla v_h)\,dx, \quad \forall v_h\in V_h, \quad (2.35)\end{aligned}$$

with

$$r_1^{n+1} = \frac{\varphi(t^{n+1})-\varphi(t^n)}{\tau^{n+1}} - \frac{\partial_t\varphi(t^{n+1})+\partial_t\varphi(t^n)}{2}, \quad (2.36)$$

and

$$r_2^{n+1} = (\Pi_h^{hyp}-\mathrm{Id})\frac{\varphi(t^{n+1})-\varphi(t^n)}{\tau^{n+1}} - (\Pi_h^{hyp}-\mathrm{Id})\frac{\varphi(t^{n+1})+\varphi(t^n)}{2}, \quad (2.37)$$

where Id denotes the identity operator. Observe that $r_1^{n+1}$ is a quantity involving only the time discretization and $r_2^{n+1}$ only the space discretization. Choosing in (2.35) the test function as

$$v_h = \frac{e_h^{n+1} + e_h^n}{2} + \delta_h \frac{e_h^{n+1} - e_h^n}{\tau^{n+1}},$$

we obtain similarly to the part II of Theorem 2.18

$$\begin{aligned}
&\frac{1}{2\tau^{n+1}}\left(\|e_h^{n+1}\|^2_{L^2(\Omega)} - \|e_h^n\|^2_{L^2(\Omega)}\right) + \frac{\delta_h^2}{2\tau^{n+1}}\left(\|\mathbf{u}\cdot\nabla e_h^{n+1}\|^2_{L^2(\Omega)} - \|\mathbf{u}\cdot\nabla e_h^n\|^2_{L^2(\Omega)}\right)\\
&\qquad + \delta_h \int_\Omega \left(\frac{e_h^{n+1} - e_h^n}{\tau^{n+1}} + \mathbf{u}\cdot\nabla\left(\frac{e_h^{n+1} + e_h^n}{2}\right)\right)^2 dx\\
&\qquad \le \int_\Omega (r_1^{n+1} + r_2^{n+1})\left(\frac{e_h^{n+1} + e_h^n}{2} + \delta_h^2 \mathbf{u}\cdot\nabla\left(\frac{e_h^{n+1} - e_h^n}{\tau^{n+1}}\right)\right) dx\\
&\qquad\qquad + \delta_h \int_\Omega (r_1^{n+1} + r_2^{n+1})\left(\frac{e_h^{n+1} - e_h^n}{\tau^{n+1}} + \mathbf{u}\cdot\nabla\left(\frac{e_h^{n+1} + e_h^n}{2}\right)\right) dx.
\end{aligned}$$

Before going further in the proof, we do a technical comment. If we keep on following the demonstration of Theorem 2.18, setting $r_1^{n+1} + r_2^{n+1} = r^{n+1}$, due the specific form of $r_2^{n+1}$ which contains no information on the time discretization, we will derive a priori bound containing some terms which are not bounded with respect to the time. Namely, the factor $\frac{\delta_h}{\tau^{n+1}}$ cannot be eliminated everywhere in the estimate and no uniform a priori error bound can be obtained without imposing some restrictions as $\delta_h \le \tau^{n+1}, \forall n = 0, 1, ..., N-1$. Therefore, we apply a finer treatment to the right hand side of the last inequality.

Using the Young's inequality, we can get rid of the second term in the right hand side and we have

$$\begin{aligned}
&\frac{1}{2\tau^{n+1}}\left(\|e_h^{n+1}\|^2_{L^2(\Omega)} - \|e_h^n\|^2_{L^2(\Omega)}\right) + \frac{\delta_h^2}{2\tau^{n+1}}\left(\|\mathbf{u}\cdot\nabla e_h^{n+1}\|^2_{L^2(\Omega)} - \|\mathbf{u}\cdot\nabla e_h^n\|^2_{L^2(\Omega)}\right)\\
&\qquad \le \int_\Omega (r_1^{n+1} + r_2^{n+1})\left(\frac{e_h^{n+1} + e_h^n}{2} + \delta_h^2 \mathbf{u}\cdot\nabla\left(\frac{e_h^{n+1} - e_h^n}{\tau^{n+1}}\right)\right) dx\\
&\qquad\qquad + \delta_h(\|r_1^{n+1}\|^2_{L^2(\Omega)} + \|r_2^{n+1}\|^2_{L^2(\Omega)})\\
&\qquad \le \int_\Omega (r_1^{n+1} + r_2^{n+1})\frac{e_h^{n+1} + e_h^n}{2} d\mathbf{x} + \int_\Omega r_1^{n+1}\delta_h^2 \mathbf{u}\cdot\nabla\left(\frac{e_h^{n+1} - e_h^n}{\tau^{n+1}}\right) dx\\
&\qquad\qquad + \delta_h(\|r_1^{n+1}\|^2_{L^2(\Omega)} + \|r_2^{n+1}\|^2_{L^2(\Omega)}) + \int_\Omega r_2^{n+1}\delta_h^2 \mathbf{u}\cdot\nabla\left(\frac{e_h^{n+1} - e_h^n}{\tau^{n+1}}\right) dx.
\end{aligned}$$

Let $m$ be any integer between 1 and $N$. Multiplying by $2\tau^{n+1}$ and summing up over $n = 0, 1, ..., m-1$ yields

$$\begin{aligned}
&\left(\|e_h^m\|^2_{L^2(\Omega)} - \|e_h^0\|^2_{L^2(\Omega)}\right) + \delta_h^2\left(\|\mathbf{u}\cdot\nabla e_h^m\|^2_{L^2(\Omega)} - \|\mathbf{u}\cdot\nabla e_h^0\|^2_{L^2(\Omega)}\right)\\
&\le \tilde{C}\left(\sum_{n=0}^{m-1}\tau^{n+1}\int_\Omega (r_1^{n+1} + r_2^{n+1})\frac{e_h^{n+1} + e_h^n}{2} d\mathbf{x} + \delta_h^2 \sum_{n=0}^{m-1}\int_\Omega r_1^{n+1}\mathbf{u}\cdot\nabla\left(\frac{e_h^{n+1} - e_h^n}{\tau^{n+1}}\right) dx\right.\\
&\qquad \left.\delta_h \sum_{n=0}^{m-1}\tau^{n+1}(\|r_1^{n+1}\|^2_{L^2(\Omega)} + \|r_2^{n+1}\|^2_{L^2(\Omega)}) + \delta_h^2 \sum_{n=0}^{m-1}\int_\Omega r_2^{n+1}\mathbf{u}\cdot\nabla(e_h^{n+1} - e_h^n) dx\right).
\end{aligned}$$

We now proceed to a discrete integration by parts on the last sum, and we obtain

$$\begin{aligned}
&\left(\|e_h^m\|_{L^2(\Omega)}^2 - \|e_h^0\|_{L^2(\Omega)}^2\right) + \delta_h^2\left(\|\mathbf{u}\cdot\nabla e_h^m\|_{L^2(\Omega)}^2 - \|\mathbf{u}\cdot\nabla e_h^0\|_{L^2(\Omega)}^2\right) \\
&\le \tilde{C}\left(\sum_{n=0}^{m-1}\tau^{n+1}\int_\Omega (r_1^{n+1}+r_2^{n+1})\frac{e_h^{n+1}+e_h^n}{2}d\mathbf{x} + \delta_h^2\sum_{n=0}^{m-1}\int_\Omega r_1^{n+1}\mathbf{u}\cdot\nabla\left(\frac{e_h^{n+1}-e_h^n}{\tau^{n+1}}\right)dx\right. \\
&\quad \delta_h\sum_{n=0}^{m-1}\tau^{n+1}(\|r_1^{n+1}\|_{L^2(\Omega)}^2 + \|r_2^{n+1}\|_{L^2(\Omega)}^2) + \delta_h^2\sum_{n=1}^{m-1}\tau^{n+1}\int_\Omega \frac{r_2^{n+1}-r_2^n}{\tau^{n+1}}\mathbf{u}\cdot\nabla e_h^n dx \\
&\quad \left. +\delta_h^2\int_\Omega (r_2^m\mathbf{u}\cdot\nabla e_h^m - r_2^1\mathbf{u}\cdot\nabla e_h^0)d\mathbf{x}\right).
\end{aligned}$$

Finally, using several times the Young's inequality, it holds for all $1 \le m \le N$

$$\begin{aligned}
&\|e_h^m\|_{L^2(\Omega)}^2 + \delta_h^2\|\mathbf{u}\cdot\nabla e_h^m\|_{L^2(\Omega)}^2 \\
&\le \tilde{C}\left(\|e_h^0\|_{L^2(\Omega)}^2 + \delta_h^2\|\mathbf{u}\cdot\nabla e_h^0\|_{L^2(\Omega)}^2 + \delta_h^2\sup_{0\le n\le N-1}\|r_2^n\|_{L^2(\Omega)}^2\right. \\
&\quad \sum_{n=0}^{m-1}(T\tau^{n+1} + \delta_h\tau^{n+1} + T\frac{\delta_h^2}{\tau^{n+1}})\|r_1^{n+1}\|_{L^2(\Omega)}^2 \\
&\quad \left. +(T\tau^{n+1}+\delta_h\tau^{n+1})\|r_2^{n+1}\|_{L^2(\Omega)}^2 + \sum_{n=1}^{m-1}T\delta_h^2(\tau^{n+1}+\tau^n)\left\|\frac{r_2^{n+1}-r_2^n}{\tau^{n+1}+\tau^n}\right\|_{L^2(\Omega)}^2\right) \\
&\quad + \sum_{n=0}^{m}\frac{\tau^n+\tau^{n+1}}{4T}\left(\|e_h^n\|_{L^2(\Omega)}^2 + \delta_h^2\|\mathbf{u}\cdot\nabla e_h^n\|_{L^2(\Omega)}^2\right),
\end{aligned}$$

where we set $\tau^0 = \tau^{N+1} = 0$. Applying the discrete Gronwall's Lemma A.5 and observing that $\dfrac{\tau^n+\tau^{n+1}}{4T} < 1$, we finally obtain

$$\begin{aligned}
&\|e_h^N\|_{L^2(\Omega)}^2 + \delta_h^2\|\mathbf{u}\cdot\nabla e_h^N\|_{L^2(\Omega)}^2 \\
&\le \tilde{C}\left(\|e_h^0\|_{L^2(\Omega)}^2 + \delta_h^2\|\mathbf{u}\cdot\nabla e_h^0\|_{L^2(\Omega)}^2 + \delta_h^2\sup_{0\le n\le N-1}\|r_2^n\|_{L^2(\Omega)}^2\right. \\
&\quad \sum_{n=0}^{N-1}(T\tau^{n+1} + \delta_h\tau^{n+1} + T\frac{\delta_h^2}{\tau^{n+1}})\|r_1^{n+1}\|_{L^2(\Omega)}^2 \\
&\quad \left. +(T\tau^{n+1}+\delta_h\tau^{n+1})\|r_2^{n+1}\|_{L^2(\Omega)}^2 + \sum_{n=1}^{N-1}T\delta_h^2(\tau^{n+1}+\tau^n)\left\|\frac{r_2^{n+1}-r_2^n}{\tau^{n+1}+\tau^n}\right\|_{L^2(\Omega)}^2\right).
\end{aligned}$$

Therefore, it remains to estimate $\|r_1^{n+1}\|_{L^2(\Omega)}^2, \|r_2^{n+1}\|_{L^2(\Omega)}^2, \left\|\dfrac{r_2^{n+1}-r_2^n}{\tau^{n+1}+\tau^n}\right\|_{L^2(\Omega)}^2$ and the initial error $e_h^0$ to conclude. Estimate for $r_1^{n+1}$ is straightforward using Taylor expansion or integration and reads

$$\|r_1^{n+1}\|_{L^2(\Omega)}^2 \le (\tau^{n+1})^3\int_{t^n}^{t^{n+1}}\left\|\frac{\partial^3\varphi(t)}{\partial t^3}\right\|^2 dt, \quad \forall n = 0,1,...,N-1, \tag{2.38}$$

Since $\Pi_h^{hyp}$ and the time derivative commutes, one can write

$$\begin{aligned}(\Pi_h^{hyp}-\mathrm{Id})\frac{\varphi(t^{n+1})-\varphi(t^n)}{\tau^{n+1}} &= \frac{1}{\tau^{n+1}}\int_{t^n}^{t^{n+1}}\frac{\partial}{\partial t}(\Pi_h^{hyp}-\mathrm{Id})\varphi(t)dt\\ &= \frac{1}{\tau^{n+1}}\int_{t^n}^{t^{n+1}}(\Pi_h^{hyp}-\mathrm{Id})\frac{\partial\varphi(t)}{\partial t}dt\\ &\le \frac{1}{(\tau^{n+1})^{1/2}}\left(\int_{t^n}^{t^{n+1}}\left((\Pi_h^{hyp}-\mathrm{Id})\frac{\partial\varphi(t)}{\partial t}\right)^2 dt\right)^{1/2},\end{aligned}$$

which yields using the error estimate for the HRP

$$\|r_2^{n+1}\|^2_{L^2(\Omega)} \le \hat{C}\sum_{K\in\mathcal{T}_h}\epsilon_K(\delta_h,\mathbf{u})\sup_{t\in(0,T)}L_K^2(\varphi)+\sup_{t\in(0,T)}L_K^2(\partial_t\varphi), \quad \forall n=0,1,...,N-1, \tag{2.39}$$

and

$$\sum_{n=0}^{N-1}\tau^{n+1}\|r_2^{n+1}\|^2_{L^2(\Omega)} \le \hat{C}\sum_{K\in\mathcal{T}_h}\epsilon_K(\delta_h,\mathbf{u})\left(T\sup_{t\in(0,T)}L_K^2(\varphi)+\int_0^T L_K^2(\partial_t\varphi)dt\right). \tag{2.40}$$

Reproducing the same type of computations, we derive that

$$\begin{aligned}&(\Pi_h^{hyp}-\mathrm{Id})\frac{1}{\tau^{n+1}+\tau^n}\left(\frac{\varphi(t^{n+1})-\varphi(t^n)}{\tau^{n+1}}-\frac{\varphi(t^n)-\varphi(t^{n-1})}{\tau^n}\right)\\ &\qquad\le \frac{1}{(\tau^{n+1}+\tau^n)^{1/2}}\left(\int_{t^{n-1}}^{t^{n+1}}\left((\Pi_h^{hyp}-\mathrm{Id})\frac{\partial^2\varphi(t)}{\partial t^2}\right)^2 dt\right)^{1/2},\end{aligned}$$

and

$$(\Pi_h^{hyp}-\mathrm{Id})\frac{\varphi(t^{n+1})-\varphi(t^n)}{\tau^{n+1}+\tau^n} \le \frac{1}{(\tau^{n+1}+\tau^n)^{1/2}}\left(\int_{t^{n-1}}^{t^{n+1}}\left((\Pi_h^{hyp}-\mathrm{Id})\frac{\partial\varphi(t)}{\partial t}\right)^2 dt\right)^{1/2}.$$

Thus we obtain the estimate

$$\sum_{n=1}^{N-1}(\tau^{n+1}+\tau^n)\left\|\frac{r_2^{n+1}-r_2^n}{\tau^{n+1}+\tau^n}\right\|^2_{L^2(\Omega)} \le \hat{C}\sum_{K\in\mathcal{T}_h}\epsilon_K(\delta_h,\mathbf{u})\int_0^T(L_K^2(\partial_t\varphi)+L_K^2(\partial_{tt}\varphi))dt. \tag{2.41}$$

Finally, observe that $e_h^0=\Pi_h^{hyp}\varphi(0)-\varphi_h^0=\Pi_h^{hyp}\varphi(0)-\varphi(0)+\varphi(0)-\varphi_h^0=e_h(0)+e(0)$. Thus

$$\begin{aligned}&\|e_h^0\|^2_{L^2(\Omega)}+\delta_h^2\|\mathbf{u}\cdot\nabla e_h^0\|^2_{L^2(\Omega)}\\ &\quad\le \tilde{C}\left(\|e_h(0)\|^2_{L^2(\Omega)}+\delta_h^2\|\mathbf{u}\cdot\nabla e_h(0)\|^2_{L^2(\Omega)}+\|e(0)\|^2_{L^2(\Omega)}+\delta_h^2\|\mathbf{u}\cdot\nabla e(0)\|^2_{L^2(\Omega)}\right)\\ &\qquad\le \hat{C}\left(\|e(0)\|^2_{L^2(\Omega)}+\delta_h^2\|\mathbf{u}\cdot\nabla e(0)\|^2_{L^2(\Omega)}+\sum_{K\in\mathcal{T}_h}\epsilon(\delta_h,\mathbf{u})L_K^2(\varphi(0))\right)\end{aligned} \tag{2.42}$$

Combining estimate (2.38), (2.39), (2.40), (2.41) and (2.42) yields the following bound for

$I_2$ (written in a compact form, even if we increase it a bit)

$$I_2 \leq \hat{C} \Big( \|e(0)\|^2_{L^2(\Omega)} + \delta_h^2 \|\mathbf{u}\cdot\nabla e(0)\|^2_{L^2(\Omega)} + \sum_{K\in\mathcal{T}_h} (1+\delta_h^2)\epsilon_K(\delta_h,\mathbf{u})( \sup_{t\in(0,T)} L^2_K(\varphi) + \sup_{t\in(0,T)} L^2_K(\partial_t\varphi)) + \sum_{K\in\mathcal{T}_h} (T+\delta_h^2+T\delta_h^2)\epsilon_K(\delta_h,\mathbf{u}) \left( T \sup_{t\in(0,T)} L^2_K(\varphi) + \int_0^T L^2_K(\partial_t\varphi) + L^2_K(\partial_{tt}\varphi)dt \right) + (T\tau^4 + \delta_h\tau^4 + \delta_h^2\tau^2)\int_0^T |\partial_{ttt}\varphi|^2 dt \Big).$$

The final bound is obtained by combining estimate for $I_1$ and $I_2$. □

**Remark 2.25.**
Observe that in [22], the error bound is different, in particular the fourth derivative with respect to time of the exact solution is present, whereas here time derivatives of $\varphi$ appears only up to the third one. This difference can be explained by the fact that in [22], the discrete integration by parts is applied on all the remainder $r^{n+1} = r_1^{n+1} + r_2^{n+1}$, whereas in our proof we apply it only on the spatial term, that is to say $r_2^{n+1}$. Indeed, roughly speaking, since $r_1^{n+1} \simeq \partial_{ttt}\varphi$, the integration by parts will yield to a term going as $\partial_{tttt}\varphi$.

**Remark 2.26.**
Observe that to get the estimates (2.39), (2.40) and (2.41), we strongly use the fact that $\Pi_h^{hyp}$ and $\frac{\partial}{\partial t}$ commute. This is true only when the transport field $\mathbf{u}$ does not depend on the time. However, note that it is possible to obtain similar estimates without using this commutativity property. Indeed, by a Taylor expansion, we can write that

$$\frac{\varphi(t^{n+1})-\varphi(t^n)}{\tau^{n+1}} = \frac{\partial\varphi(t^n)}{\partial t} + \frac{\tau^{n+1}}{2}\frac{\partial^2\varphi(t_*^{n+1})}{\partial t^2}, t_*^{n+1}\in(t^n,t^{n+1}).$$

By linearity of HRP, it yields that

$$(\Pi_h^{hyp}-\mathrm{Id})\frac{\varphi(t^{n+1})-\varphi(t^n)}{\tau^{n+1}} = (\Pi_h^{hyp}-\mathrm{Id})\frac{\partial\varphi(t^n)}{\partial t} + \frac{\tau^{n+1}}{2}(\Pi_h^{hyp}-\mathrm{Id})\frac{\partial^2\varphi(t_*^{n+1})}{\partial t^2},$$

implying that

$$\|r_2^{n+1}\|^2_{L^2(\Omega)} \leq \hat{C} \sum_{K\in\mathcal{T}_h} \epsilon_K(\delta_h,\mathbf{u}) \left( \sup_{t\in(0,T)} L^2_K(\varphi) + \tau^2 \sup_{t\in(0,T)} L^2_K(\partial_t\varphi) \right), \quad \forall n=0,1,...,N-1, \tag{2.43}$$

and

$$\sum_{n=0}^{N-1} \tau^{n+1}\|r_2^{n+1}\|^2_{L^2(\Omega)} \leq \hat{C}T \sum_{K\in\mathcal{T}_h} \epsilon_K(\delta_h,\mathbf{u}) \left( \sup_{t\in(0,T)} L^2_K(\varphi) + \sup_{t\in(0,T)} \tau^2 L^2_K(\partial_t\varphi)) \right). \tag{2.44}$$

For the same reason, we get

$$\sum_{n=1}^{N-1} (\tau^{n+1}+\tau^n) \left\| \frac{r_2^{n+1}-r_2^n}{\tau^{n+1}+\tau^n} \right\|^2_{L^2(\Omega)} \leq \hat{C}T \sum_{K\in\mathcal{T}_h} \epsilon_K(\delta_h,\mathbf{u}) \left( \sup_{t\in(0,T)} L^2_K(\partial_t\varphi) + \sup_{t\in(0,T)} \tau^2 L^2_K(\partial_{tt}\varphi) + \sup_{t\in(0,T)} L^2_K(\partial_{tt}\varphi) + \sup_{t\in(0,T)} \tau^2 L^2_K(\partial_{ttt}\varphi) \right). \tag{2.45}$$

**A posteriori error estimate for the fully discrete approximation**

We focus now on the *a posteriori* error analysis for the numerical method (2.20). An a posteriori error estimate is already presented in [20] where only the spatial approximation is considered. We extend this result to the time discretization and prove an a posteriori error estimate involving the time and space approximation. For the a posteriori error analysis, the stabilization parameter $\delta_h$ is not constant anymore, but piecewise constant on each triangle $K$. More precisely, for all $K \in \mathcal{T}_h$, if $\mathbf{u}$ is not identically zero on $K$, then we set

$$\delta_{h|K} = \frac{\lambda_{2,K}}{2\left\|\mathbf{u}\right\|_{L^\infty(K)}}, \tag{2.46}$$

else $\delta_{h|K}$ is set to zero. This choice is advocated in [20]. Note the analogy with the isotropic settings where $\delta_{h|K}$ is chosen as

$$\delta_{h|K} = \frac{h_K}{2\left\|\mathbf{u}\right\|_{L^\infty(K)}},$$

As it is introduced in Section 2.1, we define a piecewise quadratic reconstruction of the numerical solution in order to recover an $O(\tau^2)$ a posteriori error estimate. We shall use the following notations to simplify the future computations

$$\varphi_h^{n+1/2} = \frac{\varphi_h^{n+1} + \varphi_h^n}{2}, \quad \partial\varphi_h^{n+1} = \frac{\varphi_h^{n+1} - \varphi_h^n}{\tau^{n+1}}, \quad n = 0, 1, ..., N-1, \tag{2.47}$$

$$\partial^2\varphi_h^{n+1} = \frac{\dfrac{\varphi_h^{n+1} - \varphi_h^n}{\tau^{n+1}} - \dfrac{\varphi_h^n - \varphi_h^{n-1}}{\tau^n}}{\dfrac{\tau^{n+1} + \tau^n}{2}}, n \geq 1.$$

**Definition 2.27** (Fully discrete piecewise numerical reconstruction)**.**
Let $(\varphi_h^n)_{n=0}^N$ be the solution of (2.20), we define the piecewise numerical reconstruction $\varphi_{h\tau} \in V_h \times C^0[0,T]$ by

$$\varphi_{h\tau}(\mathbf{x}, t) = \varphi_h^{n+1/2}(\mathbf{x}) + (t - t^{n+1/2})\partial\varphi_h^{n+1}(\mathbf{x}) + \frac{1}{2}(t - t^n)(t - t^{n+1})\partial^2\varphi_h^{n+1}(\mathbf{x}), \tag{2.48}$$

for $(\mathbf{x}, t) \in \overline{\Omega} \times \left[t^n, t^{n+1}\right], n \geq 1$, and by

$$\varphi_{h\tau}(\mathbf{x}, t) = \varphi_h^{1/2}(\mathbf{x}) + (t - t^{1/2})\partial\varphi_h^1(\mathbf{x}), \tag{2.49}$$

for $(\mathbf{x}, t) \in \overline{\Omega} \times \left[t^0, t^1\right]$.

Observe that (2.48) is a Newton polynomial; for every $n \geq 1$, $\varphi_{h\tau}$ is the unique quadratic polynomial in time that equals $\varphi_h^{n-1}$, $\varphi_h^n$, $\varphi_h^{n+1}$, at time $t^{n-1}$, $t^n$, $t^{n+1}$, respectively. We show that the piecewise reconstruction introduced in the Definition 2.27 yields to an order two local time error indicator. The latter is contained in the next proposition and is derived by plugging $\varphi_{h\tau}$ into the equation and by computing the remainder.

**Proposition 2.28** (A local time error indicator for the Crank-Nicolson scheme applied to the transport equation with a velocity field independent of the time)**.**
*Let $(\varphi_h^n)_{n=0}^N$ be the solution of (2.20). Let $\varphi_{h\tau}$ be the numerical reconstruction (2.48)-(2.49) and let $0 \leq n \leq N-1$. For all $v_h \in V_h$ and for all $t \in (t^n, t^{n+1})$, one have*

$$\int_\Omega \left(\frac{\partial\varphi_{h\tau}}{\partial t} + \mathbf{u}\cdot\nabla\varphi_{h\tau}\right)(v_h + \delta_h\mathbf{u}\cdot\nabla v_h)d\mathbf{x} = \int_\Omega \theta_n(v_h + \delta_h\mathbf{u}\cdot\nabla v_h)d\mathbf{x}.$$

*where*

$$\theta_n = \begin{cases} \left(\dfrac{\tau^n}{2}(t - t^{n+1/2}) + \dfrac{1}{2}(t-t^n)(t-t^{n+1})\right) \mathbf{u} \cdot \nabla \partial^2 \varphi_h^{n+1}, & n \geq 1, \\ (t - t^{1/2}) \mathbf{u} \cdot \nabla \partial \varphi_h^1, & n = 0. \end{cases} \tag{2.50}$$

*Proof.* We reproduce the steps and the computations made in the proof of Proposition 2.4 for the ODE case. First, let $n \geq 1$. We have

$$\begin{aligned} &\int_\Omega \left(\frac{\partial \varphi_{h\tau}}{\partial t} + \mathbf{u} \cdot \nabla \varphi_{h\tau}\right)(v_h + \delta_h \mathbf{u} \cdot \nabla v_h) d\mathbf{x} \\ &= \int_\Omega \left(\partial \varphi_h^{n+1} + (t - t^{n+1/2})\partial^2 \varphi_h^{n+1} + \mathbf{u} \cdot \nabla \left(\varphi_h^{n+1/2} + (t - t^{n+1/2}) \partial \varphi_h^{n+1}\right)\right)(v_h + \delta_h \mathbf{u} \cdot \nabla v_h) d\mathbf{x} \\ &\quad + \int_\Omega \left(\frac{1}{2}(t-t^n)(t-t^{n+1}) \mathbf{u} \cdot \nabla \partial^2 \varphi_h^{n+1}\right)(v_h + \delta_h \mathbf{u} \cdot \nabla v_h) d\mathbf{x} \\ &= \int_\Omega \left(\partial \varphi_h^{n+1} + \mathbf{u} \cdot \nabla \varphi_h^{n+1/2}\right)(v_h + \delta_h \mathbf{u} \cdot \nabla v_h) d\mathbf{x} \\ &\quad + \int_\Omega (t - t^{n+1/2})(\partial^2 \varphi_h^{n+1} + \mathbf{u} \cdot \nabla \partial \varphi_h^{n+1})(v_h + \delta_h \mathbf{u} \cdot \nabla v_h) d\mathbf{x} \\ &\quad + \int_\Omega \left(\frac{1}{2}(t-t^n)(t-t^{n+1}) \mathbf{u} \cdot \nabla \partial^2 \varphi_h^{n+1}\right)(v_h + \delta_h \mathbf{u} \cdot \nabla v_h) d\mathbf{x}. \end{aligned}$$

Thanks to the numerical scheme (2.20), the first term in the last inequality is zero and it remains

$$\begin{aligned} &\int_\Omega \left(\frac{\partial \varphi_{h\tau}}{\partial t} + \mathbf{u} \cdot \nabla \varphi_{h\tau}\right)(v_h + \delta_h \mathbf{u} \cdot \nabla v_h) d\mathbf{x} \\ &= \int_\Omega (t - t^{n+1/2})(\partial^2 \varphi_h^{n+1} + \mathbf{u} \cdot \partial \varphi_h^{n+1})(v_h + \delta_h \mathbf{u} \cdot \nabla v_h) d\mathbf{x} \\ &\quad + \int_\Omega \left(\frac{1}{2}(t-t^n)(t-t^{n+1}) \mathbf{u} \cdot \nabla \partial^2 \varphi_h^{n+1}\right)(v_h + \delta_h \mathbf{u} \cdot \nabla v_h) d\mathbf{x}. \end{aligned} \tag{2.51}$$

Proceeding as in Proposition 2.4, we look for an equation for $\partial^2 \varphi_h^{n+1}$ by taking the difference between (2.20) at step $n+1$ and $n$, and we obtain

$$\int_\Omega \left(\partial^2 \varphi_h^{n+1} + \mathbf{u} \cdot \nabla \left(\frac{\varphi_h^{n+1} - \varphi_h^n}{\tau^{n+1} - \tau^n}\right)\right)(v_h + \delta_h \mathbf{u} \cdot \nabla v_h) d\mathbf{x} = 0,$$

which yields after the same transformation as the one in (2.15)

$$\int_\Omega (\partial^2 \varphi_h^{n+1} + \mathbf{u} \cdot \nabla \partial \varphi_h^{n+1})(v_h + \delta_h \mathbf{u} \cdot \nabla v_h) d\mathbf{x} = \int_\Omega \frac{\tau^n}{2} \mathbf{u} \cdot \nabla \partial^2 \varphi_h^{n+1} (v_h + \delta_h \mathbf{u} \cdot \nabla v_h) d\mathbf{x}.$$

Plugging the last relation in (2.51), we obtain the desired expression for $\theta_n$.

For $n = 0$, we obtain by a straightforward computation that

$$\begin{aligned} &\int_\Omega \left(\frac{\partial \varphi_{h\tau}}{\partial t} + \mathbf{u} \cdot \nabla \varphi_{h\tau}\right)(v_h + \delta_h \mathbf{u} \cdot \nabla v_h) d\mathbf{x} \\ &= \int_\Omega \left(\partial \varphi_h^1 + \mathbf{u} \cdot \nabla \left(\varphi_h^{1/2} + (t - t^{1/2}) \partial \varphi_h^1\right)\right)(v_h + \delta_h \mathbf{u} \cdot \nabla v_h) d\mathbf{x} \\ &= \int_\Omega (t - t^{1/2}) \mathbf{u} \cdot \nabla \partial \varphi_h^1 (v_h + \delta_h \mathbf{u} \cdot \nabla v_h) d\mathbf{x}. \end{aligned}$$

□

We are now ready to prove our a posteriori error estimate.

**Theorem 2.29** (An a posteriori error estimate for the transport equation with anisotropic finite elements and the Crank-Nicolson scheme in the case of a transport velocity field independent of the time)**.**
*Assume that* $\varphi \in L^2(0,T;H^1(\Omega)) \cap H^1(0,T;L^2(\Omega))$ *where* $\varphi$ *is the solution of (2.18). Let* $\delta_h$ *be given by (2.46),* $(\varphi_h^n)_{n=0}^N$ *be the solution of (2.20) and consider* $\varphi_{h\tau}$ *the numerical reconstruction given in Definition 2.27. Setting* $e = \varphi - \varphi_{h\tau}$*, there exists* $C > 0$ *independent of* $T, \Omega, \mathbf{u}, \varphi$*, the mesh size and aspect ratio and the time step such that*

$$\begin{aligned}
&\|e(T)\|^2_{L^2(\Omega)} \\
&\leq C\Bigg( \|e(0)\|^2_{L^2(\Omega)} + \sum_{n=0}^{N-1} \sum_{K \in \mathcal{T}_h} \int_{t^n}^{t^{n+1}} \left( \left\| \frac{\partial \varphi_{h\tau}}{\partial t} + \mathbf{u} \cdot \nabla \varphi_{h\tau} \right\|_{L^2(K)} \omega_K(e) + c_n \|\theta_n\|^2_{L^2(K)} \right) dt \Bigg) \\
&\qquad + C \sum_{n=0}^{N-1} \sum_{K \in \mathcal{T}_h} \int_{t^n}^{t^{n+1}} c_n^{-1} \omega_K^2(e) dt, \quad (2.52)
\end{aligned}$$

*where* $\omega_K$ *is the anisotropic gradient norm defined by (1.4) ,* $\theta_n$ *is given by (2.50) and we note* $c_n = \begin{cases} \tau^1, & n = 0, \\ T - \tau^1, & n \geq 1. \end{cases}$

*Proof.* In the following, we denote by $C$ any positive constant, which may depend only on the reference triangle and may change from line to line. In particular, $C$ is independent of $T$, $\Omega$,$\mathbf{u}$, $\varphi$, the mesh size, aspect ratio and the time step. Let $t \in (t^n, t^{n+1})$, $n \geq 1$. As before, one can prove that

$$\int_\Omega (\mathbf{u} \cdot \nabla e) e d\mathbf{x} \geq 0.$$

Therefore, it holds, since $e = \varphi - \varphi_{h\tau}$ and $\varphi$ satisfies (2.18)

$$\frac{1}{2}\frac{d}{dt}\int_\Omega e^2 dx \leq \int_\Omega \left( \frac{\partial e}{\partial t} e + (\mathbf{u} \cdot \nabla e) e \right) d\mathbf{x} = -\int_\Omega \left( \frac{\partial \varphi_{h\tau}}{\partial t} + \mathbf{u} \cdot \nabla \varphi_{h\tau} \right) e d\mathbf{x}.$$

By subtracting any $v_h + \delta_h \mathbf{u} \cdot \nabla v_h$ and using Proposition 2.28, we have finally

$$\begin{aligned}
&\frac{1}{2}\frac{d}{dt}\int_\Omega e^2 dx \leq \int_\Omega \left( \frac{\partial e}{\partial t} e + (\mathbf{u} \cdot \nabla e) e \right) d\mathbf{x} = -\int_\Omega \left( \frac{\partial \varphi_{h\tau}}{\partial t} + \mathbf{u} \cdot \nabla \varphi_{h\tau} \right) e d\mathbf{x} \\
&= -\int_\Omega \left( \frac{\partial \varphi_{h\tau}}{\partial t} + \mathbf{u} \cdot \nabla \varphi_{h\tau} \right) (e - v_h - \delta_h \mathbf{u} \cdot \nabla v_h) d\mathbf{x} - \int_\Omega \theta_n (v_h + \delta_h \mathbf{u} \cdot \nabla v_h) d\mathbf{x}. \quad (2.53)
\end{aligned}$$

The triangle and Cauchy-Schwarz inequalities imply then

$$\begin{aligned}
&\frac{1}{2}\frac{d}{dt}\int_\Omega e^2 dx \\
&\leq \sum_{K \in \mathcal{T}_h} \Bigg( \left( \left\| \frac{\partial \varphi_{h\tau}}{\partial t} + \mathbf{u} \cdot \nabla \varphi_{h\tau} \right\|_{L^2(K)} + \|\theta\|_{L^2(K)} \right) \left( \|e - v_h\|_{L^2(K)} + \left\| \delta_{h|K} \mathbf{u} \cdot \nabla v_h \right\|_{L^2(K)} \right) \\
&\qquad + \|\theta_n\|_{L^2(K)} \|e\|_{L^2(K)} \Bigg).
\end{aligned}$$

Choosing $v_h = R_h(e)$, one can prove that

$$\|e - R_h(e)\|_{L^2(K)} + \left\| \delta_{h|K} \mathbf{u} \cdot \nabla R_h(e) \right\|_{L^2(K)} \leq C\omega_K(e), \quad (2.54)$$

Indeed, by triangle inequality, we have

$$\|e - R_h(e)\|_{L^2(K)} + \left\|\delta_{h|K}\mathbf{u}\cdot\nabla R_h(e)\right\|_{L^2(K)}$$
$$\leq \|e - R_h(e)\|_{L^2(K)} + \left\|\delta_{h|K}\mathbf{u}\cdot\nabla(e - R_h(e))\right\|_{L^2(K)} + \left\|\delta_{h|K}\mathbf{u}\cdot\nabla e\right\|_{L^2(K)}.$$

The anisotropic Clément's interpolation error estimate (see Proposition 1.2) and the definition of $\delta_{h|K}$ imply

$$\|e - R_h(e)\|_{L^2(K)} \leq C\omega_K(e),$$

$$\left\|\delta_{h|K}\mathbf{u}\cdot\nabla(e - R_h(e))\right\|_{L^2(K)} \leq \delta_{h|K}\|\mathbf{u}\|_{L^\infty(K)}\|\nabla(e - R_h(e))\|_{L^2(K)}$$
$$\leq \frac{\lambda_{2,K}}{2}\|\nabla(e - R_h(e))\|_{L^2(K)} \leq C\omega_K(e),$$

and

$$\left\|\delta_{h|K}\mathbf{u}\cdot\nabla e\right\|_{L^2(K)} \leq \delta_{h|K}\|\mathbf{u}\|_{L^\infty(K)}\|\nabla e\|_{L^2(K)} \leq C\lambda_{2,K}\|\nabla e\|_{L^2(K)}.$$

Hence

$$\|e - R_h(e)\|_{L^2(K)} + \left\|\delta_{h|K}\mathbf{u}\cdot\nabla R_h e\right\|_{L2(K)}$$
$$\leq C(\omega_K(e) + \lambda_{2,K}\|\nabla e\|_{L^2(K)}) \leq C(\omega_K(e) + \lambda_{2,K}\|\nabla e\|_{L^2(\Delta K)}).$$

Now we recall that $\mathbf{r}_{1,K}, \mathbf{r}_{2,K}$ form an orthonormal basis and that in our anisotropic framework $\nabla e = (\nabla e\cdot\mathbf{r}_{1,K})\mathbf{r}_{1,K} + (\nabla e\cdot\mathbf{r}_{2,K})\mathbf{r}_{2,K}$ and

$$\|\nabla e\cdot\mathbf{r}_{i,K}\|^2_{L^2(\Delta K)} = \mathbf{r}^T_{i,K}G_K(e)\mathbf{r}_{i,K}, \quad i = 1,2.$$

It yields

$$\lambda^2_{2,K}\|\nabla e\|^2_{L^2(\Delta K)} = \lambda^2_{2,K}(\mathbf{r}^T_{1,K}G_K(e)\mathbf{r}_{1,K} + \mathbf{r}^T_{2,K}G_K(e)\mathbf{r}_{2,K})$$
$$\leq \lambda^2_{1,K}\mathbf{r}^T_{1,K}G_K(e)\mathbf{r}_{1,K} + \lambda^2_{2,K}\mathbf{r}^T_{2,K}G_K(e)\mathbf{r}_{2,K} = \omega^2_K(e)$$

that implies (2.54).

Thus, we have

$$\frac{1}{2}\frac{d}{dt}\|e\|^2_{L^2(\Omega)} \leq C\sum_{K\in\mathcal{T}_h}(\alpha_K + \theta_K)\,\omega_K(e) + \sum_{K\in\mathcal{T}_h}\theta_K\|e\|_{L^2(K)},$$

where we have set

$$\alpha_K = \left\|\frac{\partial\varphi_{h\tau}}{\partial t} + \mathbf{u}\cdot\nabla\varphi_{h\tau}\right\|_{L^2(K)} \qquad \text{and} \qquad \theta_K = \|\theta_n\|_{L^2(K)},$$

Using the discrete Cauchy-Schwarz, we obtain

$$\frac{1}{2}\frac{d}{dt}\|e\|^2_{L^2(\Omega)} \leq C\sum_{K\in\mathcal{T}_h}(\alpha_K + \theta_K)\,\omega_K(e) + \left(\sum_{K\in\mathcal{T}_h}\theta^2_K\right)^{1/2}\|e\|_{L^2(\Omega)}.$$

Using Theorem A.3 between time $t^1$ and $T$ yields

$$\|e(T)\|^2_{L^2(\Omega)} \leq C\left(\left\|e(t^1)\right\|^2_{L^2(\Omega)} + \sum_{n=1}^{N-1}\sum_{K\in\mathcal{T}_h}\int_{t^n}^{t^{n+1}}\left((\alpha_K + \theta_K)\,\omega_K(e) + (T - t^1)\theta^2_K\right)dt\right). \tag{2.55}$$

In order to estimate $\|e(t^1)\|^2_{L^2(\Omega}$, we proceed in the same manner to obtain

$$\left\|e(t^1)\right\|^2_{L^2(\Omega)} \leq C\Bigg( \|e(0)\|^2_{L^2(\Omega)} + \sum_{K\in\mathcal{T}_h} \int_0^{t^1} \Big( (\alpha_K + \theta_K)\omega_K(e) + \tau^1\theta_K \Big)\, dt \Bigg). \tag{2.56}$$

Plugging (2.56) into (2.55) we obtain

$$\|e(T)\|^2_{L^2(\Omega)} \leq C\Bigg( \|e(0)\|^2_{L^2(\Omega)}$$
$$+\sum_{n=0}^{N-1} \sum_{K\in\mathcal{T}_h} \int_{t^n}^{t^{n+1}} \Bigg( \Bigg( \left\| \frac{\partial\varphi_{h\tau}}{\partial t} + uex \cdot \nabla\varphi_{h\tau} \right\|_{L^2(K)} + \|\theta_n\|_{L^2(K)} \Bigg) \omega_K(e) + c_n \|\theta_n\|^2_{L^2(K)} \Bigg) \Bigg) dt. \tag{2.57}$$

Finally, thanks to Young's inequality, it holds for all $n$

$$\int_{t^n}^{t^{n+1}} \|\theta_n\|_{L^2(K)}\, \omega_K(e) dt \leq C \left( c_n \int_{t^n}^{t^{n+1}} \|\theta_n\|^2_{L^2(K)}\, dt + c_n^{-1} \int_{t^n}^{t^{n+1}} \omega_K^2(e) dt \right),$$

which yields the desired estimate by applying it to (2.57). □

**Remark 2.30.**
The estimate of Theorem 2.29 is not a standard a posteriori estimate since the exact solution $\varphi$ is contained in $\omega_K(e)$. However, as advocated in Chapter 1, the Zienkiewicz-Zhu post-processing can be applied in order to approximate $G_K(e)$ (see Remark 1.12). To obtain later on a computable error indicator, we will then replace $G_K(e) = G_K(\varphi - \varphi_{h\tau})$ by $G_K(\Pi_h^{ZZ}\varphi_{h\tau} - \varphi_{h\tau})$.

Note that for the transport equation, the use of post-processsing to recover a computable estimate is not a particularity due to the choice of working with anisotropic finite elements. Indeed, in the isotropic setting, the estimate (2.52) reads

$$\|e(T)\|^2_{L^2(\Omega)} \leq$$
$$C\Bigg( \|e(0)\|^2_{L^2(\Omega)} + \sum_{n=0}^{N-1} \sum_{K\in\mathcal{T}_h} \int_{t^n}^{t^{n+1}} \left( h_K \left\| \frac{\partial\varphi_{h\tau}}{\partial t} + \mathbf{u}\cdot\nabla\varphi_{h\tau} \right\|_{L^2(K)} \|\nabla e\|_{L^2(\Delta K)} + c_n \|\theta_n\|^2_{L^2(K)} \right) dt \Bigg)$$
$$+ C \sum_{n=0}^{N-1} \sum_{K\in\mathcal{T}_h} \int_{t^n}^{t^{n+1}} c_n^{-1} h_K^2 \|\nabla e\|^2_{L^2(\Delta K)} dt.$$

Since it is not possible to rely the $H^1$ norm of $e$ with its $L^2$ norm, we cannot obtain a computable bound without post-processing.

**Remark 2.31.**
The following a posteriori error estimate can also be proved. Starting as in the proof of Theorem 2.29, we have

$$\frac{1}{2}\frac{d}{dt}\|e\|^2_{L^2(\Omega)} \leq \int_\Omega \left( \frac{\partial e}{\partial t} e + (\beta\cdot\nabla e)e \right) dx = \int_\Omega \left( \frac{\partial\varphi_{h\tau}}{\partial t} + \mathbf{u}\cdot\nabla\varphi_{h\tau} \right) e dx.$$

Cauchy−Schwarz inequality implies that

$$\frac{1}{2}\frac{d}{dt}\|e\|^2_{L^2(\Omega)} \leq \left\| \frac{\partial\varphi_{h\tau}}{\partial t} + \mathbf{u}\cdot\nabla\varphi_{h\tau} \right\|_{L^2(\Omega)} \|e\|_{L^2(\Omega)},$$

which yields

$$\|e(T)\|_{L^2(\Omega)} \leq \|e(0)\|_{L^2(\Omega)} + \int_0^T \left\| \frac{\partial \varphi_{h\tau}}{\partial t} + \mathbf{u} \cdot \nabla \varphi_{h\tau} \right\|_{L^2(\Omega)} dt. \tag{2.58}$$

The estimate (2.58) was already pointed out in [36] and is valid even for non-smooth solutions. However, numerical experiments have shown that (2.58) is suboptimal for smooth solutions. A theoretical explanation can be put forward. Let us assume that we only consider the space approximation $\varphi_h$. Observe that, since $\varphi$ satisfies the transport equation, one has

$$\int_0^T \left\| \frac{\partial \varphi_h}{\partial t} + \mathbf{u} \cdot \nabla \varphi_h \right\|_{L^2(\Omega)} dt = \int_0^T \left\| \frac{\partial (\varphi - \varphi_h)}{\partial t} + \mathbf{u} \cdot \nabla (\varphi - \varphi_h) \right\|_{L^2(\Omega)} dt.$$

We recognize the semi-norm for which the following a priori error estimate (written in the isotropic setting for the semi-discrete approximation, see Remark 2.15 for the anisotropic version) holds

$$\int_0^T \left\| \frac{\partial (\varphi - \varphi_h)}{\partial t} + \mathbf{u} \cdot \nabla (\varphi - \varphi_h) \right\|_{L^2(\Omega)}^2 dt \leq \frac{C}{\delta_h} h^3,$$

where $C > 0$ is independent of $h$ but may depends on the aspect ratio. If $\delta_h \simeq h$ as it advocated by the a priori analysis, then the later estimate reduces to $Ch^2$.

Thus the a posteriori error indicator given by

$$\int_0^T \left\| \frac{\partial (\varphi - \varphi_{h\tau})}{\partial t} + \mathbf{u} \cdot \nabla (\varphi - \varphi_{h\tau}) \right\|_{L^2(\Omega)} dt \simeq \left( \int_0^T \left\| \frac{\partial (\varphi - \varphi_{h\tau})}{\partial t} + \mathbf{u} \cdot \nabla (\varphi - \varphi_{h\tau}) \right\|_{L^2(\Omega)}^2 dt \right)^{1/2}$$

is only a first order estimate in general.

**Remark 2.32.** (i) We have not been able to prove a lower bound corresponding to estimate (2.52), this being already difficult for parabolic problems with anisotropic finite elements [72]. For the transport equation, such a bound seems to be hardly achievable, even with isotropic finite elements.

(ii) Note the particular form of the local time error estimator $\|\theta_n\|_{L^2(K)}^2$ that behaves as

$$\mathbf{u} \cdot \nabla \frac{d^2}{dt^2} \varphi = -\frac{d^3 \varphi}{dt^3},$$

that is to say the second derivative with respect to the time of the equation. Therefore, at least from the time discretization point of view, the a posteriori error estimate of Theorem 2.29 goes as

$$\tau^2 \frac{d^3 \varphi}{dt^3}$$

that is the same as the a priori error estimate (2.34), that was one of our first goal.

(iii) Under some assumptions, one can show that the term

$$\sum_{n=0}^{N-1} \sum_{K \in \mathcal{T}_h} \int_{t^n}^{t^{n+1}} c_n^{-1} \omega_K^2(e) dt$$

is of higher order. Indeed, let us assume that (we recall that $e = \varphi - \varphi_{h\tau}$):

(1) The following a priori error estimate holds

$$\sup_{t\in(0,T)} \|\nabla e\|_{L^2(\Omega)} \leq C(\max_{K\in\mathcal{T}_h} \lambda_{2,K} + \tau^2),$$

$C > 0$ being independent of the mesh size and aspect ratio and the time step. It can be check numerically that this estimate is valid for smooth cases and when the mesh is aligned with the exact solution.

(2) The numerical error is equidistributing in both directions $\mathbf{r}_{1,K}, \mathbf{r}_{2,K}$ that is to say

$$\lambda_{1,K}^2(r_{1,K}^T G_K(e) r_{1,K}) = \lambda_{2,K}^2(r_{2,K}^T G_K(e) r_{2,K}).$$

We can give a geometrical interpretation of the second hypothesis. Indeed, it can be written as

$$\frac{\lambda_{1,K}^2}{\lambda_{2,K}^2} = \frac{r_{2,K}^T G_K(e) r_{2,K}}{r_{1,K}^T G_K(e) r_{1,K}},$$

meaning that if we build a mesh such that the second hypothesis holds, then the aspect ratio of the element $K$ is the ratio between the numerical error in direction $\mathbf{r}_{1,K}$ and $\mathbf{r}_{2,K}$. For instance, if the numerical error is nearly the same in both directions, then $\lambda_{1,K} \simeq \lambda_{2,K}$ and the mesh is an isotropic mesh. Otherwise it is anisotropic. This is precisely why the goal of the adaptive algorithm presented later on will be to fulfill (2): equidistributing the error indicator in both directions makes the mesh "naturally" anisotropic if the numerical error is large in one direction compared to the other.

Now, thanks to second hypothesis and the definition of $G_K(e)$, one proves that

$$\sum_{K\in\mathcal{T}_h} \omega_K^2(e) \leq (\max_{K\in\mathcal{T}_h} \lambda_{2,K})^2 \sum_{K\in\mathcal{T}_h} \|\nabla e\|_{L^2(\Delta K)}^2 \leq C(\max_{K\in\mathcal{T}_h} \lambda_{2,K})^2 \|\nabla e\|_{L^2(\Omega)}^2,$$

where $C$ is independent of the mesh geometry due to the hypothesis on the patch $\Delta K$ presented in Chapter 1, Section 1.1. Therefore, one have

$$\begin{aligned}
\sum_{n=0}^{N-1} \sum_{K\in\mathcal{T}_h} \int_{t^n}^{t^{n+1}} c_n^{-1} \omega_K^2(e) dt &\leq C \sum_{n=0}^{N-1} c_n^{-1} \int_{t^n}^{t^{n+1}} (\max_{K\in\mathcal{T}_h} \lambda_{2,K})^2 \|\nabla e\|_{L^2(\Omega)}^2 dt \\
&\leq C(\max_{K\in\mathcal{T}_h} \lambda_{2,K})^2((\max_{K\in\mathcal{T}_h} \lambda_{2,K})^2 + \tau^4) \sum_{n=0}^{N-1} c_n^{-1} \int_{t^n}^{t^{n+1}} dt \\
&\leq C(\max_{K\in\mathcal{T}_h} \lambda_{2,K})^2((\max_{K\in\mathcal{T}_h} \lambda_{2,K})^2 + \tau^4) \left( \frac{1}{\tau^1}\tau^1 + \sum_{n=1}^{N-1} \frac{\tau^{n+1}}{T-\tau^1} \right) \\
&\leq C(\max_{K\in\mathcal{T}_h} \lambda_{2,K})^2((\max_{K\in\mathcal{T}_h} \lambda_{2,K})^2 + \tau^4) \left( 1 + \frac{T-\tau^1}{T-\tau^1} \right) \\
&\leq C((\max_{K\in\mathcal{T}_h} \lambda_{2,K})^4 + \tau^8).
\end{aligned}$$

### 2.2.2 A priori and a posteriori error estimates in the case of transient transport velocity

We are now carrying our attention to the case where $\mathbf{u}$ depends on the time. Given $\mathbf{u} \in C^1\left(\overline{\Omega} \times [0,T]\right)$ a free divergence velocity field, we are interested in finding the solution

$\varphi : \Omega \times (0,T] \longrightarrow \mathbb{R}$ of the transport problem

$$\begin{cases} \dfrac{\partial \varphi}{\partial t} + \mathbf{u} \cdot \nabla \varphi = 0, & \text{in } \Omega \times (0,T), \\ \varphi = 0, & \text{on } \Gamma^- \times (0,T), \\ \varphi(\cdot, 0) = \varphi_0, \end{cases} \tag{2.59}$$

The transport velocity field $\mathbf{u}$ is still a divergence free vector field, but the difference with the previous section is that it can now depend on the time variable too. Observe that in this case, the inflow boundary $\Gamma^-(t) = \{\mathbf{x} \in \partial\Omega : \mathbf{u}(\mathbf{x},t) \cdot \mathbf{n}(\mathbf{x}) < 0\}$ is now moving in time. That implies in practice that the finite elements spaces used to discretize the problem should evolved in time to take in account the moving inflow boundary condition.

To keep the analysis below simple, we assume that $\Gamma^-$ does not depend on the time. That means that we allow that for any $\mathbf{x} \in \partial\Omega$ the quantity $\mathbf{u}(\mathbf{x},t) \cdot \mathbf{n}(\mathbf{x})$ varies in time, but its sign is constant. Otherwise, difficulties can arise in the proof of the error estimates, since test functions will depends on the time. Precisely, for the semi-discrete approximation in space, moving boundary conditions are not an issue since it is sufficient to define a continuous family of meshes $\mathcal{T}_h(t)$ such that $\Gamma(t)^-$ is the union of edges lying on $\partial\Omega$ and a continuous family of finite elements spaces $V_h(t)$ , that are the sets of piecewise linear continuous functions on $\mathcal{T}_h(t)$, with zero value on $\Gamma(t)^-$ and to look for a semi-discrete solution $\varphi_h(t) \in V_h(t)$, for all $t \in [0,T]$. Then all the proofs are formally the same than the ones presented below, taking care that when we interpolate a function $\phi(t)$ into a finite elements space (for instance taking its Lagrange interpolant) we do it with the interpolant defined on $V_h(t)$.

Unfortunately, when dealing with the fully discrete approximation, that is to say approximation in space and in time, the numerical scheme is not well defined anymore since it is natural to look for $\varphi_h^{n+1} \in V_h(t^{n+1})$ (as for the test function) while $\varphi_h^n$ belongs to $V_h(t^n)$, that can be a priori different subspaces. Moreover, we cannot easily determine (see for instance the proof of the Proposition 2.38 below) the sign of quantities of the type

$$\int_\Omega \mathbf{u}(t^{n+1/2}) \cdot \nabla \left( \frac{\varphi_h^{n+1} + \varphi_h^n}{2} \right) \frac{\varphi_h^{n+1} + \varphi_h^n}{2} d\mathbf{x}$$

since there is no reason that

$$\frac{\varphi_h^{n+1} + \varphi_h^n}{2} \in V_h(t^{n+1/2}),$$

that is to say we do not know if $\varphi_h^{n+1} + \varphi_h^n$ is zero in the points of $\partial\Omega$ where $\mathbf{u}(t^{n+1/2}) \cdot \mathbf{n} < 0$.

Considering now that the inflow boundary condition does not depend on the time (that is to say in practice that the finite elements space $V_h$ is fixed in time), the numerical method (2.20) is changed as follows: let $N$ be a non-negative integer and consider a partition $0 = t^0 < t^1 < t^2 < ... < t^N = T$. We denote by $\tau^{n+1} = t^{n+1} - t^n$ the time step, $n = 0,1,2,...,N-1$. Starting from $\varphi_h^0 = r_h(\varphi_0)$, for $n = 0,1,2,...,N-1$, we are looking for $\varphi_h^{n+1} \in V_h$ such that

$$\int_\Omega \left( \frac{\varphi_h^{n+1} - \varphi_h^n}{\tau^{n+1}} + \mathbf{u}(t^{n+1/2}) \cdot \nabla \left( \frac{\varphi_h^{n+1} + \varphi_h^n}{2} \right) \right) (v_h + \delta_h \mathbf{u}(t^{n+1/2}) \cdot \nabla v_h) d\mathbf{x} = 0, \forall v_h \in V_h, \tag{2.60}$$

where we recall that we note

$$t^{n+1/2} = \frac{t^{n+1} + t^n}{2}.$$

The goal is now to extend the stability and error estimates obtained in the previous section for the case of a steady transport velocity field to the case of a transient transport velocity field. We still inspire ourself from the techniques presented in [22], but note that in [22] only constant in time velocity field were considered. Therefore, the results below can be seen as a generalization.

#### Stability and a priori error estimates for the semi-discrete approximation in space

Before starting the a priori analysis of the fully discretized scheme (2.60), we first focus on the semi-discrete approximation and generalize the stability estimate (Propositon 2.12) and the semi-discrete a priori error estimate (Theorem 2.14) for a time dependent $\mathbf{u}$. Considering only the space approximation and the method reads (observe that it is substantially the same as (2.19)) : find $\varphi_h : \overline{\Omega} \times [0,T] \longrightarrow \mathbb{R}$, $\varphi_h(\cdot,t) \in V_h$ for all $t \in [0,T]$ such that $\varphi_h(\cdot,0) = r_h(\varphi_0)$ and for all $t \in (0,T]$

$$\int_\Omega \left( \frac{\partial \varphi_h}{\partial t} + \mathbf{u}(t) \cdot \nabla \varphi_h \right) (v_h + \delta_h \mathbf{u}(t) \cdot \nabla v_h) d\mathbf{x} = 0, \forall v_h \in V_h. \tag{2.61}$$

Assuming that $\delta_h$ is a constant, on can prove that the method (2.61) is stable in the norm $\| \cdot \|^2_{L^2(\Omega)} + \delta_h^2 \|\mathbf{u}(t) \cdot \nabla(\cdot)\|^2_{L^2(\Omega)}$.

**Proposition 2.33** (Stability of the SUPG method applied to the transient transport equation with a transient transport field)**.**
*Assume that $\delta_h > 0$ is constant. Let $\varphi_h$ be the solution of (2.61). Assume moreover that $\mathcal{T}_h$ satisfies the anisotropic quasi-uniformity condition: there exists $c > 0$, independent of the mesh geometry, in particular independent of the mesh size and the mesh aspect ratio such that*

$$\max_{K \in \mathcal{T}_h} \lambda_{2,K} \leq c \lambda_{2,K}, \quad \forall K \in \mathcal{T}_h. \tag{2.62}$$

*Then there exists a constant $C > 0$ independent of the mesh size and aspect ratio such that*

$$\begin{aligned} &\|\varphi_h(t)\|^2_{L^2(\Omega)} + \delta_h^2 \|\mathbf{u}(t) \cdot \nabla \varphi_h(t)\|^2_{L^2(\Omega)} \\ &\leq \exp\left( \frac{CT\delta_h^2 \|\mathbf{u}\|_{L^\infty(\Omega \times (0,T))} \|\partial_t \mathbf{u}\|_{L^\infty(\Omega \times (0,T))}}{(\max_{K \in \mathcal{T}_h} \lambda_{2,K})^2} \right) \left( \|\varphi_h(0)\|^2_{L^2(\Omega)} + \delta_h^2 \|\mathbf{u}(0) \cdot \nabla \varphi_h(0)\|^2_{L^2(\Omega)} \right). \end{aligned} \tag{2.63}$$

**Remark 2.34.** (i) Observe that if $\mathbf{u}$ does not depend on the time, then the estimate (2.63) reduces to the estimate (2.21) already derived in the case of a steady transport velocity field.

(ii) If we assume that $\mathbf{u}$ is not identically zero and, imitating what is done for the case of steady transport velocity field, we choose $\delta_h$ as

$$\delta_h = \frac{\max_{K \in \mathcal{T}_h} \lambda_{2,K}}{2\|\mathbf{u}\|_{L^\infty(\Omega \times (0,T))}}$$

then the estimate (2.63) becomes

$$\begin{aligned} &\|\varphi_h(t)\|^2_{L^2(\Omega)} + \delta_h^2 \|\mathbf{u}(t) \cdot \nabla \varphi_h(t)\|^2_{L^2(\Omega)} \\ &\leq \exp\left( \frac{CT \|\partial_t \mathbf{u}\|_{L^\infty(\Omega \times (0,T))}}{\|\mathbf{u}\|_{L^\infty(\Omega \times (0,T))}} \right) \left( \|\varphi_h(0)\|^2_{L^2(\Omega)} + \delta_h^2 \|\mathbf{u}(0) \cdot \nabla \varphi_h(0)\|^2_{L^2(\Omega)} \right), \end{aligned}$$

that is to say the numerical solution $\varphi_h$ is uniformly bounded with respect to $h$ for any time, and then the stability of the method is guaranteed.

*Proof.* We denote by $C$ any generic positive constant independent of the mesh size and aspect ratio, which value may change from line to line. We proceed as already done several times. We choose as test function $v_h = \varphi_h + \delta_h \dfrac{\partial \varphi_h}{\partial t}$ in (2.61) and get

$$\frac{1}{2}\frac{d}{dt}\|\varphi_h(t)\|^2_{L^2(\Omega)} + \delta_h^2 \int_\Omega (\mathbf{u}(t)\cdot\nabla\varphi_h(t))\left(\mathbf{u}(t)\cdot\nabla\frac{\partial\varphi_h}{\partial t}\right)d\mathbf{x}$$
$$+\int_\Omega(\mathbf{u}(t)\cdot\nabla\varphi_h)\varphi_h d\mathbf{x} + \delta_h^2\int_\Omega\left(\mathbf{u}(t)\cdot\nabla\frac{\partial\varphi_h}{\partial t}\right)\frac{\partial\varphi_h}{\partial t}d\mathbf{x}$$
$$+\delta_h\int_\Omega\left(\frac{\partial\varphi_h}{\partial t}+\mathbf{u}\cdot\nabla\varphi_h\right)^2 d\mathbf{x} = 0.$$

As in Proposition 2.12, thanks to the free divergence property and the boundary condition, we have that for all $t$

$$\int_\Omega(\mathbf{u}(t)\cdot\nabla\varphi_h)\varphi_h d\mathbf{x}, \delta_h^2\int_\Omega\left(\mathbf{u}(t)\cdot\nabla\frac{\partial\varphi_h}{\partial t}\right)\frac{\partial\varphi_h}{\partial t}d\mathbf{x} \geq 0.$$

Therefore, we have

$$\frac{1}{2}\frac{d}{dt}\|\varphi_h(t)\|^2_{L^2(\Omega)} + \delta_h^2 \int_\Omega (\mathbf{u}(t)\cdot\nabla\varphi_h(t))\left(\mathbf{u}(t)\cdot\nabla\frac{\partial\varphi_h}{\partial t}\right)d\mathbf{x} \leq 0.$$

The Leibniz rule implies

$$\frac{1}{2}\frac{d}{dt}\|\varphi_h(t)\|^2_{L^2(\Omega)} + \frac{\delta_h^2}{2}\frac{d}{dt}\|\mathbf{u}(t)\cdot\nabla\varphi_h(t)\|^2_{L^2(\Omega)} \leq \delta_h^2\int_\Omega(\mathbf{u}(t)\cdot\nabla\varphi_h(t))\left(\frac{\partial\mathbf{u}(t)}{\partial t}\cdot\nabla\varphi_h(t)\right)d\mathbf{x}.$$

Cauchy-Schwarz inequality yields

$$\frac{d}{dt}\|\varphi_h(t)\|^2_{L^2(\Omega)}+\delta_h^2\frac{d}{dt}\|\mathbf{u}(t)\cdot\nabla\varphi_h(t)\|^2_{L^2(\Omega)} \leq C\delta_h^2\|\mathbf{u}\|_{L^\infty(\Omega\times(0,T))}\|\partial_t\mathbf{u}\|_{L^\infty(\Omega\times(0,T))}\|\nabla\varphi_h\|^2_{L^2(\Omega)}.$$

We shall now use the so-called *inverse inequality*. In the framework of anisotropic finite elements, it reads [83]: there exists $C > 0$ independent of the mesh size and aspect ratio such that for all piecewise linear, continuous, $v_h$

$$\sum_{K\in\mathcal{T}_h}\int_K|\nabla v_h|^2 d\mathbf{x} \leq C\sum_{K\in\mathcal{T}_h}\frac{1}{\lambda_{2,K}^2}\int_K v_h^2 d\mathbf{x}. \tag{2.64}$$

Using the anisotropic quasi-uniformity condition (2.62), we therefore derive that

$$\frac{d}{dt}\|\varphi_h(t)\|^2_{L^2(\Omega)} + \delta_h^2\frac{d}{dt}\|\mathbf{u}(t)\cdot\nabla\varphi_h(t)\|^2_{L^2(\Omega)}$$
$$\leq C\frac{\delta_h^2}{(\max_{K\in\mathcal{T}_h}\lambda_{2,K})^2}\|\mathbf{u}\|_{L^\infty(\Omega\times(0,T))}\|\partial_t\mathbf{u}\|_{L^\infty(\Omega\times(0,T))}\|\varphi_h(t)\|^2_{L^2(\Omega)}.$$

We conclude by using the classical Gronwall's inequality. □

Before going further, we shall prove the following lemma, that gives an estimate for the numerical error in $H^1$ norm. It can be considered as a kind of inverse inequality for the numerical error. Observe that the result holds regardless if $\mathbf{u}$ depends on the time or not and the choice of $\delta_h$.

**Lemma 2.35.**
*Let $\varphi \in C^0(0,T;H^2(\Omega))$ be the solution of (2.18) and $\varphi_h$ the solution of (2.61). For every*

*$t \in [0,T]$, let us note $e_h(t) = \varphi(t) - \varphi_h(t)$. Assume that $\mathcal{T}_h$ satisfies the anisotropic quasi-uniformity condition: there exists $c > 0$, independent of the mesh geometry, in particular independent of the mesh size and the mesh aspect ratio such that*

$$\max_{K \in \mathcal{T}_h} \lambda_{2,K} \leq c\lambda_{2,K}, \quad \forall K \in \mathcal{T}_h.$$

*Then there exists a constant $C > 0$ depending only on the reference triangle $\hat{K}$, in particular $C$ is independent of $\Omega, T, \mathbf{u}, \varphi$, the mesh size and aspect ratio, such that*

$$\|\nabla e_h(t)\|^2_{L^2(\Omega)} \leq \frac{C}{(\max_{K\in\mathcal{T}_h} \lambda_{2,K})^2} \left( \sum_{K\in\mathcal{T}_h} L^2_K(\varphi(t)) + \|\varphi(t) - \varphi_h(t)\|^2_{L^2(\Omega)} \right). \tag{2.65}$$

*Proof.* In what follows, we denote by $C$ any generic positive constant, which may depend on the reference triangle only and which value may change from line to line. Triangle inequality implies that

$$\|\nabla e_h(t)\|^2_{L^2(\Omega)} \leq 2\|\nabla(\varphi(t) - r_h(\varphi(t)))\|^2_{L^2(\Omega)} + 2\|\nabla(r_h(\varphi(t)) - \varphi_h(t))\|^2_{L^2(\Omega)}.$$

Observe that $r_h(\varphi(t)) - \varphi_h(t) \in V_h$, therefore one can apply the anisotropic inverse inequality (2.64) and thanks to the quasi-uniformity of the mesh, one have

$$\|\nabla e_h(t)\|^2_{L^2(\Omega)} \leq C \left( \|\nabla(\varphi(t) - r_h(\varphi(t)))\|^2_{L^2(\Omega)} + \frac{1}{(\max_{K\in\mathcal{T}_h} \lambda_{2,K})^2} \|r_h(\varphi(t)) - \varphi_h(t)\|^2_{L^2(\Omega)} \right).$$

Using again triangle inequality, one gets

$$\begin{aligned}\|\nabla e_h(t)\|^2_{L^2(\Omega)} \leq C \Bigg( &\|\nabla(\varphi(t) - r_h(\varphi(t)))\|^2_{L^2(\Omega)} + \frac{1}{(\max_{K\in\mathcal{T}_h} \lambda_{2,K})^2} \|r_h(\varphi(t)) - \varphi(t)\|^2_{L^2(\Omega)} \\ &+ \frac{1}{(\max_{K\in\mathcal{T}_h} \lambda_{2,K})^2} \|\varphi(t) - \varphi_h(t)\|^2_{L^2(\Omega)} \Bigg).\end{aligned}$$

We then conclude by using the Lagrange interpolation error estimate for anisotropic meshes (see Proposition 1.1). □

We now prove the equivalent of Theorem 2.14 in the case $\mathbf{u}$ depends on the time.

**Theorem 2.36** (An anisotropic a priori error estimate for the semi-discrete finite elements approximation of the transport equation with a time dependent velocity field)**.**
*Assume that $\mathbf{u}$ is not identically zero on $\Omega$. Let $\varphi$ be the solution of (2.18) and $\varphi_h$ the solution of (2.61) where we define*

$$\delta_h = \frac{\max_{K\in\mathcal{T}_h} \lambda_{2,K}}{2\|\mathbf{u}\|_{L^\infty(\Omega\times(0,T))}}. \tag{2.66}$$

*Assume moreover that $\varphi \in H^1(0,T;H^2(\Omega))$ and let us note $e_h(t) = \varphi(t) - \varphi_h(t)$. Finally, assume moreover that $\mathcal{T}_h$ satisfies the anisotropic quasi-uniformity condition: there exists $c > 0$, independent of the mesh geometry, in particular independent of the mesh size and the mesh aspect ratio such that*

$$\max_{K \in \mathcal{T}_h} \lambda_{2,K} \leq c\lambda_{2,K}, \quad \forall K \in \mathcal{T}_h.$$

*Then there exists a constant $C > 0$ depending only on the reference triangle $\hat{K}$, in particular $C$ is independent of $\Omega, T, \mathbf{u}, \varphi$, the mesh size and aspect ratio, such that*

$$\begin{aligned}
&\|e_h(T)\|^2_{L^2(\Omega)} + \delta_h^2\|\mathbf{u}(T)\cdot\nabla e_h(T)\|^2_{L^2(\Omega)} \\
&\leq \exp\left(\frac{CT\delta_h^2\|\mathbf{u}\|_{L^\infty(\Omega\times(0,T))}\|\partial_t\mathbf{u}\|_{L^\infty(\Omega\times(0,T))}}{(\max_{K\in\mathcal{T}_h}\lambda_{2,K})^2}\right)\Big(\|e_h(0)\|^2_{L^2(\Omega)} + \delta_h^2\|\mathbf{u}(0)\cdot\nabla e_h(0)\|^2_{L^2(\Omega)} \\
&+C\int_0^T\left(\sum_{K\in\mathcal{T}_h}\left(\frac{1}{\delta_h} + \frac{\delta_h\|\mathbf{u}\|^2_{L^\infty(K\times(0,T))}}{\lambda_{2,K}^2} + \frac{\delta_h^2\|\mathbf{u}\|_{L^\infty(\Omega\times(0,T))}\|\partial_t\mathbf{u}\|_{L^\infty(\Omega\times(0,T))}}{(\max_{K\in\mathcal{T}_h}\lambda_{2,K})^2}\right)L_K^2(\varphi)\right. \\
&\qquad\left.+\left(\delta_h + \frac{\delta_h^3\|\mathbf{u}\|^2_{L^\infty(K\times(0,T))}}{\lambda_{2,K}^2}\right)L_K^2\left(\frac{\partial\varphi}{\partial t}\right)\right)dt\Big). \qquad (2.67)
\end{aligned}$$

**Remark 2.37.** (i) As already commented for the stability, observe that the exponential bound in the error estimate is uniformly bounded with respect to mesh size due to the choice of $\delta_h$. Also, as previously deduced for the case of non depending on time $\mathbf{u}$, the a priori error estimate of Theorem 2.36 reduces to

$$\|e_h(T)\|^2_{L^2(\Omega)} \leq Ch^3 + h.o.t.$$

in the isotropic setting (where $C$ may as usual depends on the mesh aspect ratio).

(ii) If we assume that the solution only depends on one spatial variable, and we assume moreover that the mesh is aligned with the solution, estimate (2.67) reduces to

$$\|e_h(T)\|^2_{L^2(\Omega)} \leq C(\max_{K\in\mathcal{T}_h}\lambda_{2,K})^3 + h.o.t.$$

where $C$ does not depend on the mesh aspect ratio.

*Proof.* By sake of clarity, we introduce the bilinear form $B(v_1, v_2)$ defined by

$$B(v_1,v_2) = \int_\Omega\left(\frac{\partial v_1}{\partial t} + \mathbf{u}(t)\cdot\nabla v_1\right)(v_2 + \delta_h\mathbf{u}(t)\cdot\nabla v_2)d\mathbf{x}.$$

Observe that in this notation, the Galerkin orthogonality holds for $e_h(t) = \varphi(t) - \varphi_h(t)$. It reads

$$B(e_h(t), v_h) = 0, \quad \forall v_h \in V_h, \forall t \in (0,T]. \qquad (2.68)$$

In what follows, we denote by $C$ any generic positive constant, which may depend on the reference triangle only and which value may change from line to line. The same computations that are done for the stability estimate in Proposition 2.33 yield that for all $t \in (0,T)$

$$\begin{aligned}
&\frac{1}{2}\frac{d}{dt}\|e_h(t)\|^2_{L^2(\Omega)} + \frac{\delta_h^2}{2}\frac{d}{dt}\|\mathbf{u}(t)\cdot\nabla e_h(t)\|^2_{L^2(\Omega)} + \delta_h\int_\Omega\left(\frac{\partial e_h(t)}{\partial t} + \mathbf{u}(t)\cdot\nabla e_h(t)\right)^2 d\mathbf{x} \\
&\qquad\leq B\left(e_h(t), e_h(t) + \delta_h\frac{\partial e_h(t)}{\partial t}\right) + \delta_h^2\int_\Omega(\mathbf{u}(t)\cdot\nabla e_h(t))\left(\frac{\partial\mathbf{u}(t)}{\partial t}\cdot\nabla e_h(t)\right)d\mathbf{x}.
\end{aligned}$$

Using the Galerkin orthogonality (2.68) and the Cauchy-Schwarz inequality, we obtain

$$\begin{aligned}
&\frac{1}{2}\frac{d}{dt}\|e_h(t)\|^2_{L^2(\Omega)} + \frac{\delta_h^2}{2}\frac{d}{dt}\|\mathbf{u}(t)\cdot\nabla e_h(t)\|^2_{L^2(\Omega)} + \delta_h\int_\Omega\left(\frac{\partial e_h(t)}{\partial t} + \mathbf{u}(t)\cdot\nabla e_h(t)\right)^2 d\mathbf{x} \\
&\leq B\left(e_h(t), (\varphi(t)-v_h) + \delta_h\frac{\partial(\varphi(t)-v_h)}{\partial t}\right) + C\delta_h^2\|\mathbf{u}\|_{L^\infty(\Omega\times(0,T))}\|\partial_t\mathbf{u}\|_{L^\infty(\Omega\times(0,T))}\|\nabla e_h(t)\|^2_{L^2(\Omega)},
\end{aligned}$$

for any $v_h \in V_h$. The Young's inequality yields

$$\frac{1}{2}\frac{d}{dt}\|e_h(t)\|^2_{L^2(\Omega)} + \frac{\delta_h^2}{2}\frac{d}{dt}\|\mathbf{u}(t)\cdot\nabla e_h(t)\|^2_{L^2(\Omega)} + \delta_h \int_\Omega \left(\frac{\partial e_h(t)}{\partial t} + \mathbf{u}(t)\cdot\nabla e_h(t)\right)^2 d\mathbf{x}$$

$$\leq \frac{\delta_h}{2}\int_\Omega \left(\frac{\partial e_h(t)}{\partial t} + \mathbf{u}(t)\cdot\nabla e_h(t)\right)^2 d\mathbf{x}$$

$$+ \frac{4}{2\delta_h}\left(\|\varphi(t) - v_h\|^2_{L^2(\Omega)} + \delta_h^2 \left\|\frac{\partial(\varphi(t) - v_h)}{\partial t}\right\|^2_{L^2(\Omega)} + \right.$$

$$\left. \delta_h^2\|\mathbf{u}(t)\cdot\nabla(\varphi(t) - v_h)\|^2_{L^2(\Omega)} + \delta_h^4 \left\|\mathbf{u}(t)\cdot\nabla\frac{\partial(\varphi(t) - v_h)}{\partial t}\right\|^2_{L^2(\Omega)}\right)$$

$$+ C\delta_h^2\|\mathbf{u}\|_{L^\infty(\Omega\times(0,T))}\|\partial_t\mathbf{u}\|_{L^\infty(\Omega\times(0,T))}\|\nabla e_h(t)\|^2_{L^2(\Omega)}.$$

Using Lemma 2.35, we can bound the last term as follows :

$$C\delta_h^2\|\mathbf{u}\|_{L^\infty(\Omega\times(0,T))}\|\partial_t\mathbf{u}\|_{L^\infty(\Omega\times(0,T))}\|\nabla e_h(t)\|^2_{L^2(\Omega)}$$

$$\leq C\sum_{K\in\mathcal{T}_h} \frac{\delta_h^2\|\mathbf{u}\|_{L^\infty(\Omega\times(0,T))}\|\partial_t\mathbf{u}\|_{L^\infty(\Omega\times(0,T))}}{(\max_{K\in\mathcal{T}_h}\lambda_{2,K})^2} L_K^2(\varphi(t))$$

$$+ C\frac{\delta_h^2\|\mathbf{u}\|_{L^\infty(\Omega\times(0,T))}\|\partial_t\mathbf{u}\|_{L^\infty(\Omega\times(0,T))}}{(\max_{K\in\mathcal{T}_h}\lambda_{2,K})^2}\|e_h(t)\|^2_{L^2(\Omega)}.$$

Thus

$$\frac{1}{2}\frac{d}{dt}\|e_h(t)\|^2_{L^2(\Omega)} + \frac{\delta_h^2}{2}\frac{d}{dt}\|\mathbf{u}(t)\cdot\nabla e_h(t)\|^2_{L^2(\Omega)}$$

$$\leq \frac{4}{2\delta_h}\left(\|\varphi(t) - v_h\|^2_{L^2(\Omega)} + \delta_h^2 \left\|\frac{\partial(\varphi(t) - v_h)}{\partial t}\right\|^2_{L^2(\Omega)} + \right.$$

$$\left. \delta_h^2\|\mathbf{u}(t)\cdot\nabla(\varphi(t) - v_h)\|^2_{L^2(\Omega)} + \delta_h^4 \left\|\mathbf{u}(t)\cdot\nabla\frac{\partial(\varphi(t) - v_h)}{\partial t}\right\|^2_{L^2(\Omega)}\right)$$

$$+ C\sum_{K\in\mathcal{T}_h} \frac{\delta_h^2\|\mathbf{u}\|_{L^\infty(\Omega\times(0,T))}\|\partial_t\mathbf{u}\|_{L^\infty(\Omega\times(0,T))}}{(\max_{K\in\mathcal{T}_h}\lambda_{2,K})^2} L_K^2(\varphi(t))$$

$$+ C\frac{\delta_h^2\|\mathbf{u}\|_{L^\infty(\Omega\times(0,T))}\|\partial_t\mathbf{u}\|_{L^\infty(\Omega\times(0,T))}}{(\max_{K\in\mathcal{T}_h}\lambda_{2,K})^2}\|e_h(t)\|^2_{L^2(\Omega)}.$$

Choosing $v_h = r_h(\varphi(t))$, using the commutativity between $\dfrac{\partial}{\partial t}$ and the Lagrange interpolation, and finally the anisotropic Lagrange interpolation error estimate (Proposition 1.1), we obtain

$$\frac{1}{2}\frac{d}{dt}\|e_h(t)\|^2_{L^2(\Omega)} + \frac{\delta_h^2}{2}\frac{d}{dt}\|\mathbf{u}(t)\cdot\nabla e_h(t)\|^2_{L^2(\Omega)}$$

$$\leq C\sum_{K\in\mathcal{T}_h}\left(\left(\frac{1}{\delta_h} + \frac{\delta_h\|\mathbf{u}\|^2_{L^\infty(K)}}{\lambda_{2,K}^2} + \frac{\delta_h^2\|\mathbf{u}\|_{L^\infty(\Omega\times(0,T))}\|\partial_t\mathbf{u}\|_{L^\infty(\Omega\times(0,T))}}{(\max_{K\in\mathcal{T}_h}\lambda_{2,K})^2}\right) L_K^2(\varphi(t))\right.$$

$$\left. + \left(\delta_h + \frac{\delta_h^3\|\mathbf{u}\|^2_{L^\infty(K)}}{\lambda_{2,K}^2}\right) L_K^2\left(\frac{\partial\varphi}{\partial t}(t)\right)\right)$$

$$+ C\frac{\delta_h^2\|\mathbf{u}\|_{L^\infty(\Omega\times(0,T))}\|\partial_t\mathbf{u}\|_{L^\infty(\Omega\times(0,T))}}{(\max_{K\in\mathcal{T}_h}\lambda_{2,K})^2}\|e_h(t)\|^2_{L^2(\Omega)}.$$

Applying the Gronwall's Lemma on the last relation yields the result. □

**Stability and a priori error estimates for the fully discrete approximation**

We now focus on the fully discrete scheme (2.60). We first establish a discrete (in time) equivalent to the stability estimate (2.63).

**Proposition 2.38** (Fully discrete stability estimate for the SUPG method and the Crank-Nicolson scheme applied to the transient transport equation with a time dependent transport velocity field)**.**
*Let $(\varphi_h^n)_{n=0}^N$ be the solution of (2.60) where $\delta_h > 0$ is constant. Assume moreover that $\mathcal{T}_h$ satisfies the anisotropic quasi-uniformity condition: there exists $c > 0$, independent of the mesh geometry, in particular independent of the mesh size and the mesh aspect ratio such that*

$$\max_{K\in\mathcal{T}_h} \lambda_{2,K} \le c\lambda_{2,K}, \quad \forall K \in \mathcal{T}_h.$$

*Then, there exists a constant $C > 0$ independent of $\Omega, t, n, \varphi, \varphi_h^n, \mathbf{u}$, the mesh size and aspect ratio and the time step such that for any $n > 0$ we have*

$$\begin{aligned}&\|\varphi_h^n\|^2_{L^2(\Omega)} + \delta_h^2\|\mathbf{u}(t^n)\cdot\nabla\varphi_h^n\|^2_{L^2(\Omega)}\\ &\le \exp\left(\frac{Ct^n\delta_h^2}{(\max_{K\in\mathcal{T}_h}\lambda_{2,K})^2}\|\mathbf{u}\|_{L^\infty(\Omega\times(0,T))}\|\partial_t\mathbf{u}\|_{L^\infty(\Omega\times(0,T))}\right)\left(\|\varphi_h^0\|^2_{L^2(\Omega)} + \delta_h^2\|\mathbf{u}(0)\cdot\nabla\varphi_h^0\|^2_{L^2(\Omega)}\right).\end{aligned} \tag{2.69}$$

**Remark 2.39.** (i) As stated before for the semi-discrete approximation, if $\mathbf{u}$ does not depend on the time, then the estimate (2.69) reduces to the estimate (2.24) for a non-depending on time velocity field.

(ii) If we assume that $\mathbf{u}$ is not identically zero and we choose $\delta_h$ as

$$\delta_h = \frac{\max_{K\in\mathcal{T}_h}\lambda_{2,K}}{2\|\mathbf{u}\|_{L^\infty(\Omega\times(0,T))}}$$

then the estimate (2.69) is uniformly bounded with respect to $h$ and $\tau$ for any time.

*Proof.* We again denote by $C$ any positive constant, independent of the time step, the data of the problem or the mesh geometry. We choose $v_h = \dfrac{\varphi_h^{n+1}+\varphi_h^n}{2} + \delta_h\dfrac{\varphi_h^{n+1}-\varphi_h^n}{\tau^{n+1}}$ in the weak formulation (2.60). Eliminating all the positive contributions and the terms of the form $\displaystyle\int_\Omega(\mathbf{u}\cdot\nabla\phi)\phi d\mathbf{x}$ as we do in Proposition 2.33, it remains for all $0 \le n \le N-1$

$$\begin{aligned}&\frac{1}{2\tau^{n+1}}\|\varphi_h^{n+1}\|^2_{L^2(\Omega)} - \frac{1}{2\tau^{n+1}}\|\varphi_h^n\|^2_{L^2(\Omega)}\\ &\qquad + \frac{\delta_h^2}{2\tau^{n+1}}\left\|\mathbf{u}(t^{n+1/2})\cdot\nabla\varphi_h^{n+1}\right\|^2_{L^2(\Omega)} - \frac{\delta_h^2}{2\tau^{n+1}}\left\|\mathbf{u}(t^{n+1/2})\cdot\nabla\varphi_h^n\right\|^2_{L^2(\Omega)} \le 0,\end{aligned}$$

which yields after multiplication by $2\tau^{n+1}$

$$\|\varphi_h^{n+1}\|^2_{L^2(\Omega)} - \|\varphi_h^n\|^2_{L^2(\Omega)} + \delta_h^2\left\|\mathbf{u}(t^{n+1/2})\cdot\nabla\varphi_h^{n+1}\right\|^2_{L^2(\Omega)} - \delta_h^2\left\|\mathbf{u}(t^{n+1/2})\cdot\nabla\varphi_h^n\right\|^2_{L^2(\Omega)} \le 0.$$

Observe that the last inequality will not give a telescopic sum by adding the contribution of each $n$, therefore, we first transform it in the following way

$$\begin{aligned}&\|\varphi_h^{n+1}\|^2_{L^2(\Omega)} - \|\varphi_h^n\|^2_{L^2(\Omega)} + \delta_h^2\left\|\mathbf{u}(t^{n+1/2})\cdot\nabla\varphi_h^{n+1}\right\|^2_{L^2(\Omega)} - \delta_h^2\left\|\mathbf{u}(t^{n-1/2})\cdot\nabla\varphi_h^n\right\|^2_{L^2(\Omega)}\\ &\qquad\le \delta_h^2\left\|\mathbf{u}(t^{n+1/2})\cdot\nabla\varphi_h^n\right\|^2_{L^2(\Omega)} - \delta_h^2\left\|\mathbf{u}(t^{n-1/2})\cdot\nabla\varphi_h^n\right\|^2_{L^2(\Omega)}, 0 \le n \le N-1,\end{aligned} \tag{2.70}$$

and where $t^{n-1/2} = \dfrac{t^n + t^{n-1}}{2}, n = 0, 1, ..., N+1$, and we take the convention that $t^{-1} = t^0$ such that $t^{-1/2} = t^0$. Let now $0 \leq m \leq N-1$. Observe that the last inequality is still not convenient for our purpose since for $n = m-1$ the term

$$\delta_h^2 \left\| \mathbf{u}\left(\frac{t^m + t^{m-1}}{2}\right) \cdot \nabla \varphi_h^m \right\|_{L^2(\Omega)}^2$$

appears rather than

$$\delta_h^2 \left\| \mathbf{u}\left(t^m\right) \cdot \nabla \varphi_h^m \right\|_{L^2(\Omega)}^2.$$

We then use the following trick : let us defined the auxiliary sequences $(s^n)_{n=0}^{m+1}, (\xi_h^n)_{n=0}^{m+1}$ by setting

$$\xi_h^n = \varphi_h^n, \quad s^n = t^n, \quad 0 \leq n \leq m,$$
$$\xi_h^{m+1} = \varphi_h^m, \quad s^{-1} = t^{-1} = t^0, s^{m+1} = t^m.$$

Note that we have therefore $\dfrac{s^{m+1} + s^m}{2} = t^m$. So we have then for all $n$ from 0 up to $m$ that

$$\begin{aligned}\|\xi_h^{n+1}\|_{L^2(\Omega)}^2 - \|\xi_h^n\|_{L^2(\Omega)}^2 + \delta_h^2 \left\| \mathbf{u}(s^{n+1/2}) \cdot \nabla \xi_h^{n+1} \right\|_{L^2(\Omega)}^2 - \delta_h^2 \left\| \mathbf{u}(s^{n-1/2}) \cdot \nabla \xi_h^n \right\|_{L^2(\Omega)}^2 \\ \leq \delta_h^2 \left\| \mathbf{u}(s^{n+1/2}) \cdot \nabla \xi_h^n \right\|_{L^2(\Omega)}^2 - \delta_h^2 \left\| \mathbf{u}(s^{n-1/2}) \cdot \nabla \xi_h^n \right\|_{L^2(\Omega)}^2. \quad (2.71)\end{aligned}$$

Observe that for $n = m$, (2.71) is trivially satisfied since it reduces to $0 \leq 0$. We shall use now the following inequality to bound the right hand side :

$$\begin{aligned}\|f\|_{L^2(\Omega)}^2 - \|g\|_{L^2(\Omega)}^2 &= \int_\Omega f^2 d\mathbf{x} - \int_\Omega g^2 d\mathbf{x} = \int_\Omega (f^2 - g^2) d\mathbf{x} \\ &= \int_\Omega (f-g)(f+g) d\mathbf{x} \leq \|f-g\|_{L^2(\Omega)} \|f+g\|_{L^2(\Omega)}.\end{aligned}$$

So (2.71) is equivalent to

$$\begin{aligned}&\|\xi_h^{n+1}\|_{L^2(\Omega)}^2 - \|\xi_h^n\|_{L^2(\Omega)}^2 + \delta_h^2 \left\| \mathbf{u}(s^{n+1/2}) \cdot \nabla \xi_h^{n+1} \right\|_{L^2(\Omega)}^2 - \delta_h^2 \left\| \mathbf{u}(s^{n-1/2}) \cdot \nabla \xi_h^n \right\|_{L^2(\Omega)}^2 \\ &\quad \leq \delta_h^2 \left\| \left(\mathbf{u}(s^{n+1/2}) + \mathbf{u}(s^{n-1/2})\right) \cdot \nabla \xi_h^n \right\|_{L^2(\Omega)} \left\| \left(\mathbf{u}(s^{n+1/2}) - \mathbf{u}(s^{n-1/2})\right) \cdot \nabla \xi_h^n \right\|_{L^2(\Omega)} \\ &\quad\quad \leq C\delta_h^2 (\tau^{n+1} + \tau^n) \|\mathbf{u}\|_{L^\infty(\Omega \times (0,T))} \|\partial_t \mathbf{u}\|_{L^\infty(\Omega \times (0,T))} \|\nabla \xi_h^n\|_{L^2(\Omega)}^2,\end{aligned}$$

where we use the fact that for each component $\mathbf{u}_i, i = 1, 2$ of the velocity field

$$\mathbf{u}_i(s^{n+1/2}) - \mathbf{u}_i(s^{n-1/2}) = \int_{s^{n-1/2}}^{s^{n+1/2}} \frac{\partial \mathbf{u}_i(t)}{\partial t} dt \leq \sup_{t \in (0,T)} |\partial_t \mathbf{u}_i(t)| \frac{\tau^{n+1} + \tau^n}{2}, \quad 0 \leq n \leq m,$$

where we set $\tau^0 = \tau^{m+1} = 0$. Using the anisotropic inverse inequality (2.64) and the anisotropic quasi-uniformity condition, we finally obtain for all $0 \leq n \leq m$

$$\begin{aligned}&\|\xi_h^{n+1}\|_{L^2(\Omega)}^2 - \|\xi_h^n\|_{L^2(\Omega)}^2 + \delta_h^2 \|\mathbf{u}(s^{n+1/2}) \cdot \nabla \xi_h^{n+1}\|_{L^2(\Omega)}^2 - \delta_h^2 \|\mathbf{u}(s^{n-1/2}) \cdot \nabla \xi_h^n\|_{L^2(\Omega)}^2 \\ &\quad \leq \frac{C\delta_h^2 (\tau^{n+1} + \tau^n)}{(\max_{K \in \mathcal{T}_h} \lambda_{2,K})^2} \|\mathbf{u}\|_{L^\infty(\Omega \times (0,T))} \|\partial_t \mathbf{u}\|_{L^\infty(\Omega \times (0,T))} \|\xi_h^n\|_{L^2(\Omega)}^2 \\ &\leq \frac{C\delta_h^2 (\tau^{n+1} + \tau^n)}{(\max_{K \in \mathcal{T}_h} \lambda_{2,K})^2} \|\mathbf{u}\|_{L^\infty(\Omega \times (0,T))} \|\partial_t \mathbf{u}\|_{L^\infty(\Omega \times (0,T))} \left( \|\xi_h^n\|_{L^2(\Omega)}^2 + \delta_h^2 \|\mathbf{u}(s^{n-1/2}) \cdot \nabla \xi_h^n\|_{L^2(\Omega)}^2 \right)\end{aligned}$$

Now, using for instance the discrete Gronwall's Lemma A.6, we obtain

$$\|\xi_h^{m+1}\|^2_{L^2(\Omega)} + \delta_h^2 \|\mathbf{u}(s^{m+1/2}) \cdot \nabla \xi_h^{m+1}\|^2_{L^2(\Omega)} \leq \exp\left( \frac{C s^{m+1} \delta_h^2}{(\max_{K\in\mathcal{T}_h} \lambda_{2,K})^2} \|\mathbf{u}\|_{L^\infty(\Omega\times(0,T))} \|\partial_t \mathbf{u}\|_{L^\infty(\Omega\times(0,T))} \right) \left( \|\xi_h^0\|^2_{L^2(\Omega)} + \delta_h^2 \|\mathbf{u}(s^{-1/2}) \cdot \nabla \xi_h^0\|^2_{L^2(\Omega)} \right).$$

The result is then obtained by applying the definition of the auxiliary sequences. □

We now state a first a priori error estimate for the numerical method (2.60). As for the a priori error estimate (2.26) in the case of steady velocity field $\mathbf{u}$, derivatives of the semi-discrete solution $\varphi_h(t)$ will appear in the bound. Therefore, we also propose after a alternative proof using a suitable projection (see Theorem 2.51).

**Theorem 2.40** (A quick a priori error estimate for the transport equation with anisotropic finite elements and the Crank-Nicolson scheme for the case of a time dependent velocity field)**.**
*Assume that* $\mathbf{u}$ *is not identically zero on* $\Omega$. *Let* $\varphi$ *be the solution of (2.18),*$(\varphi_h^n)_{n=0}^N$ *the solution of (2.60) where we define*

$$\delta_h = \frac{\max\limits_{K\in\mathcal{T}_h} \lambda_{2,K}}{2\|\mathbf{u}\|_{L^\infty(\Omega\times(0,T))}}. \tag{2.72}$$

*Assume moreover that* $\varphi \in H^1(0,T;H^2(\Omega))$, $\dfrac{\partial^2 \varphi_h}{\partial t^2} \in L^2(0,T;H^1(\Omega))$, $\dfrac{\partial^3 \varphi_h}{\partial t^3} \in L^2(0,T;L^2(\Omega))$ *and let us note* $e(t^n) = \varphi(t^n) - \varphi_h^n$. *Finally, assume moreover that* $\mathcal{T}_h$ *satisfies the anisotropic quasi-uniformity condition: there exists* $c > 0$*, independent of the mesh geometry, in particular independent of the mesh size and the mesh aspect ratio such that*

$$\max_{K\in\mathcal{T}_h} \lambda_{2,K} \leq c\lambda_{2,K}, \quad \forall K \in \mathcal{T}_h.$$

*Then there exists a constant* $C > 0$ *depending only on the reference triangle* $\hat{K}$*, in particular* $C$ *is independent of* $\Omega, t^n, \mathbf{u}, \varphi, \varphi_h, \varphi_h^n$*, the mesh size and aspect ratio and the time step, such that*

$$\begin{aligned}
&\|e(T)\|^2_{L^2(\Omega)} + \delta_h^2 \|\mathbf{u}(T) \cdot \nabla e(T)\|^2_{L^2(\Omega)} \\
&\leq C \exp\left( C \frac{T\delta_h^2 \|\mathbf{u}\|_{L^\infty(\Omega\times(0,T))} \|\partial_t \mathbf{u}\|_{L^\infty(\Omega\times(0,T))}}{(\max_{K\in\mathcal{T}_h} \lambda_{2,K})^2} \right) \Bigg( \|e_h(0)\|^2_{L^2(\Omega)} + \delta_h^2 \|\mathbf{u}(0) \cdot \nabla e_h(0)\|^2_{L^2(\Omega)} \\
&\quad + \int_0^T \Bigg( \sum_{K\in\mathcal{T}_h} \left( \frac{1}{\delta_h} + \frac{\delta_h \|\mathbf{u}\|^2_{L^\infty(K\times(0,T))}}{\lambda_{2,K}^2} + \frac{\delta_h^2 \|\mathbf{u}\|_{L^\infty(\Omega\times(0,T))} \|\partial_t \mathbf{u}\|_{L^\infty(\Omega\times(0,T))}}{(\max_{K\in\mathcal{T}_h} \lambda_{2,K})^2} \right) L_K^2(\varphi) \\
&\qquad + \left( \delta_h + \frac{\delta_h^3 \|\mathbf{u}\|^2_{L^\infty(K\times(0,T))}}{\lambda_{2,K}^2} \right) L_K^2\left( \frac{\partial \varphi}{\partial t} \right) \Bigg) dt \\
&\quad + (T\tau^4 + \delta_h \tau^4 + \delta_h^2 \tau^2) \left( \int_0^T \left\| \frac{\partial^3 \varphi_h}{\partial t^3} \right\|^2_{L^2(\Omega)} dt + \|\mathbf{u}\|^2_{L^\infty(\Omega\times(0,T))} \int_0^T \left\| \nabla \frac{\partial^2 \varphi_h}{\partial t^2} \right\|^2_{L^2(\Omega)} dt \right) \Bigg).
\end{aligned} \tag{2.73}$$

*Proof.* We proceed as in the proof of Theorem 2.18. We note by $\tilde{C} > 0$ generic constants independent of the data of the problem, the mesh size and aspect ratio and the time step and by $\hat{C} > 0$ any constant depending only on the reference triangle. Let us split the numerical $e(t^n) = \varphi(t^n) - \varphi_h^n$ as

$$e(t^n) = \varphi(t^n) - \varphi_h(t^n) + \varphi_h(t^n) - \varphi_h^n = e_h(t^n) - e_h^n.$$

We have at $t^N = T$,

$$\|e(T)\|^2_{L^2(\Omega)} + \delta_h^2 \|\mathbf{u}(T) \cdot \nabla e(T)\|^2_{L^2(\Omega)} \leq \underbrace{2\|e_h(T)\|^2_{L^2(\Omega)} + 2\delta_h^2 \|\mathbf{u}(T) \cdot \nabla e_h(T)\|^2_{L^2(\Omega)}}_{I_1} + \underbrace{2\|e_h^N\|^2_{L^2(\Omega)} + 2\delta_h^2 \|\mathbf{u}(T) \cdot \nabla e_h^N\|^2_{L^2(\Omega)}}_{I_2}.$$

We now estimate $I_1$ and $I_2$ independently.

*Part I. Estimate of $I_1$.*

We estimate $I_1$ directly by using the Theorem 2.36. We have

$$\begin{aligned} I_1 \leq 2\exp\left(\hat{C}\frac{T\delta_h^2 \|\mathbf{u}\|_{L^\infty(\Omega\times(0,T))}\|\partial_t \mathbf{u}\|_{L^\infty(\Omega\times(0,T))}}{(\max_{K\in\mathcal{T}_h}\lambda_{2,K})^2}\right)\Big(\|e_h(0)\|^2_{L^2(\Omega)} + \delta_h^2\|\mathbf{u}(0)\cdot\nabla e_h(0)\|^2_{L^2(\Omega)} \\ +\hat{C}\int_0^T \left(\sum_{K\in\mathcal{T}_h}\left(\frac{1}{\delta_h} + \frac{\delta_h \|\mathbf{u}\|^2_{L^\infty(K\times(0,T))}}{\lambda_{2,K}^2} + \frac{\delta_h^2 \|\mathbf{u}\|_{L^\infty(\Omega\times(0,T))}\|\partial_t \mathbf{u}\|_{L^\infty(\Omega\times(0,T))}}{(\max_{K\in\mathcal{T}_h}\lambda_{2,K})^2}\right) L_K^2(\varphi) \right. \\ \left. + \left(\delta_h + \frac{\delta_h^3 \|\mathbf{u}\|^2_{L^\infty(K\times(0,T))}}{\lambda_{2,K}^2}\right) L_K^2\left(\frac{\partial\varphi}{\partial t}\right)\right) dt\Big). \end{aligned}$$

*Part II. Estimate of $I_2$.*

Let $t = t^{n+1/2}$, we have for all $v_h$ that

$$\int_\Omega \left(\frac{\partial \varphi_h}{\partial t}(t^{n+1/2}) + \mathbf{u}(t^{n+1/2})\cdot\nabla\varphi_h(t^{n+1/2})\right)(v_h + \delta_h \mathbf{u}(t^{n+1/2})\cdot\nabla v_h)d\mathbf{x} = 0.$$

We shall now plug in the previous equality the following Taylor expansion

$$\frac{\varphi_h(t^{n+1}) - \varphi_h(t^n)}{\tau^{n+1}} = \frac{\partial\varphi_h}{\partial t}\left(t^{n+1/2}\right) + r_1^{n+1} \tag{2.74}$$

where $r_1^{n+1}$ is given by

$$r_1^{n+1} = \frac{1}{\tau^{n+1}}\int_{t^n}^{t^{n+1}}\int_{t^{n+1/2}}^{t}\int_{t^{n+1/2}}^{s}\frac{\partial^3\varphi_h}{\partial t^3}(\xi)d\xi ds dt.$$

In particular, one have

$$|r_1^{n+1}|^2 \leq (\tau^{n+1})^3\int_{t^n}^{t^{n+1}}\left|\frac{\partial^3\varphi_h}{\partial t^3}\right|^2 dt.$$

Therefore, $\varphi_h$ satisfies for all $v_h$

$$\int_\Omega\left(\frac{\varphi_h(t^{n+1}) - \varphi_h(t^n)}{\tau^{n+1}} + \mathbf{u}(t^{n+1/2})\cdot\nabla\left(\frac{\varphi_h(t^{n+1}) + \varphi_h(t^n)}{2}\right)\right)(v_h + \delta_h\mathbf{u}(t^{n+1/2})\cdot\nabla v_h)d\mathbf{x} = \int_\Omega (r_1^{n+1} + r_2^{n+1})(v_h + \delta_h \mathbf{u}(t^{n+1/2})\cdot\nabla v_h)d\mathbf{x},$$

where

$$r_2^{n+1} = \mathbf{u}(t^{n+1/2}) \cdot \nabla \left( \frac{\varphi_h(t^{n+1}) + \varphi_h(t^n)}{2} - \varphi_h(t^{n+1/2}) \right).$$

Noting that

$$\frac{\varphi_h(t^{n+1}) + \varphi_h(t^n)}{2} = \varphi_h(t^{n+1/2}) + \int_{t^{n+1/2}}^{t^{n+1}} \int_{t^{n+1/2}}^{t} \frac{\partial^2 \varphi_h}{\partial t^2}(s) ds dt + \int_{t^{n+1/2}}^{t^n} \int_{t^{n+1/2}}^{t} \frac{\partial^2 \varphi_h}{\partial t^2}(s) ds dt,$$

one have that

$$|r_2^{n+1}|^2 \leq \|\mathbf{u}\|^2_{L^\infty(\Omega\times(0,T))} (\tau^{n+1})^3 \int_{t^n}^{t^{n+1}} \left| \nabla \frac{\partial^2 \varphi_h}{\partial t^2} \right|^2 dt.$$

Thus the error $e_h^n$ satisfies the following equation

$$\int_\Omega \left( \frac{e_h^{n+1} - e_h^n}{\tau^{n+1}} + \mathbf{u}(t^{n+1/2}) \cdot \nabla \left( \frac{e_h^{n+1} + e_h^n}{2} \right) \right) (v_h + \delta_h \mathbf{u}(t^{n+1/2}) \cdot \nabla v_h) d\mathbf{x}$$
$$= \int_\Omega (r_1^{n+1} + r_2^{n+1})(v_h + \delta_h \mathbf{u}(t^{n+1/2}) \cdot \nabla v_h) d\mathbf{x}.$$

Choosing $v_h = \dfrac{e_h^{n+1} + e_h^n}{2} + \delta_h \dfrac{e_h^{n+1} - e_h^n}{\tau^{n+1}}$ and eliminating the terms of the form $\int_\Omega (\mathbf{u} \cdot \nabla\phi)\phi d\mathbf{x}$ which are positive as we state before, we obtain

$$\frac{1}{2\tau^{n+1}} \|e_h^{n+1}\|^2_{L^2(\Omega)} - \frac{1}{2\tau^{n+1}} \|e_h^n\|^2_{L^2(\Omega)}$$
$$+ \frac{\delta_h^2}{2\tau^{n+1}} \left\| \mathbf{u}(t^{n+1/2}) \cdot \nabla e_h^{n+1} \right\|^2_{L^2(\Omega)} - \frac{\delta_h^2}{2\tau^{n+1}} \left\| \mathbf{u}(t^{n+1/2}) \cdot \nabla e_h^n \right\|^2_{L^2(\Omega)}$$
$$+ \delta_h \int_\Omega \left( \frac{e_h^{n+1} - e_h^n}{\tau^{n+1}} + \mathbf{u}(t^{n+1/2}) \cdot \nabla \left( \frac{e_h^{n+1} + e_h^n}{2} \right) \right)^2 d\mathbf{x}$$
$$= \int_\Omega (r_1^{n+1} + r_2^{n+1}) \left( \frac{e_h^{n+1} + e_h^n}{2} + \delta_h^2 \mathbf{u}(t^{n+1/2}) \cdot \nabla \left( \frac{e_h^{n+1} - e_h^n}{\tau^{n+1}} \right) \right) d\mathbf{x}$$
$$+ \delta_h \int_\Omega (r_1^{n+1} + r_2^{n+1}) \left( \frac{e_h^{n+1} - e_h^n}{\tau^{n+1}} + \mathbf{u}(t^{n+1/2}) \cdot \nabla \left( \frac{e_h^{n+1} + e_h^n}{2} \right) \right) d\mathbf{x}.$$

Absorbing the last of the right hand side in the last term of the left hand side, we obtain, after multiplication by $2\tau^{n+1}$

$$\|e_h^{n+1}\|^2_{L^2(\Omega)} - \|e_h^n\|^2_{L^2(\Omega)}$$
$$+ \delta_h^2 \left\| \mathbf{u}(t^{n+1/2}) \cdot \nabla e_h^{n+1} \right\|^2_{L^2(\Omega)} - \delta_h^2 \left\| \mathbf{u}(t^{n+1/2}) \cdot \nabla e_h^n \right\|^2_{L^2(\Omega)}$$
$$\leq 2\tau^{n+1} \int_\Omega (r_1^{n+1} + r_2^{n+1}) \left( \frac{e_h^{n+1} + e_h^n}{2} + \delta_h^2 \mathbf{u}(t^{n+1/2}) \cdot \nabla \left( \frac{e_h^{n+1} - e_h^n}{\tau^{n+1}} \right) \right) d\mathbf{x}$$
$$+ \delta_h \tau^{n+1} \|r_1^{n+1} + r_2^{n+1}\|^2_{L^2(\Omega)}.$$

Rewriting the left side to obtain a telescopic expression, we have for all $0 \leq n \leq N-1$

(with the convention that $t^{-1/2} = t^0$)

$$
\begin{aligned}
&\|e_h^{n+1}\|^2_{L^2(\Omega)} - \|e_h^n\|^2_{L^2(\Omega)} \\
&\qquad + \delta_h^2 \left\|\mathbf{u}(t^{n+1/2}) \cdot \nabla e_h^{n+1}\right\|^2_{L^2(\Omega)} - \delta_h^2 \left\|\mathbf{u}(t^{n-1/2}) \cdot \nabla e_h^{n}\right\|^2_{L^2(\Omega)} \\
&\qquad \le 2\tau^{n+1} \int_\Omega (r_1^{n+1} + r_2^{n+1}) \left( \frac{e_h^{n+1} + e_h^n}{2} + \delta_h^2 \mathbf{u}(t^{n+1/2}) \cdot \nabla \left( \frac{e_h^{n+1} - e_h^n}{\tau^{n+1}} \right) \right) d\mathbf{x} \\
&\quad + \delta_h \tau^{n+1} \|r^{n+1} + s^{n+1}\|^2_{L^2(\Omega)} + \delta_h^2 \left\|\mathbf{u}(t^{n+1/2}) \cdot \nabla e_h^{n}\right\|^2_{L^2(\Omega)} - \delta_h^2 \left\|\mathbf{u}(t^{n-1/2}) \cdot \nabla e_h^{n}\right\|^2_{L^2(\Omega)} \\
&= \tau^{n+1} \int_\Omega (r_1^{n+1} + r_2^{n+1})(e_h^{n+1} + e_h^n) d\mathbf{x} + 2\delta_h^2 \int_\Omega (r^{n+1} + s^{n+1}) \mathbf{u}(t^{n+1/2}) \cdot \nabla \left(e_h^{n+1} - e_h^n\right) d\mathbf{x} \\
&\quad + \delta_h \tau^{n+1} \|r^{n+1} + s^{n+1}\|^2_{L^2(\Omega)} + \delta_h^2 \left\|\mathbf{u}(t^{n+1/2}) \cdot \nabla e_h^{n}\right\|^2_{L^2(\Omega)} - \delta_h^2 \left\|\mathbf{u}(t^{n-1/2}) \cdot \nabla e_h^{n}\right\|^2_{L^2(\Omega)}
\end{aligned}
$$

Following the idea of Proposition 2.38, we define auxiliary sequences. Since our purpose is to get an estimate at final time, it comes down to extend the sequences $t^n, \tau^n, e_h^n, r_1^n$ and $r_2^n$ up to $N+1$ by setting

$$
t^{N+1} = t^N, e_h^{N+1} = e_h^N, \tau^0 = 0, \tau^{N+1} = \tau^N, \quad r_1^{N+1} = r_2^{N+1} = 0.
$$

Observe that the last inequality still hold for $n = N+1$ since it reduces to $0 \le 0$. Note that, we do not set the last time step $\tau^{N+1} = 0$ as we did in Proposition 2.38 to avoid division by zero later. Thanks to Young's inequality, one may write

$$
\begin{aligned}
&\|e_h^{n+1}\|^2_{L^2(\Omega)} - \|e_h^n\|^2_{L^2(\Omega)} \\
&\qquad + \delta_h^2 \left\|\mathbf{u}(t^{n+1/2}) \cdot \nabla e_h^{n+1}\right\|^2_{L^2(\Omega)} - \delta_h^2 \left\|\mathbf{u}(t^{n-1/2}) \cdot \nabla e_h^{n}\right\|^2_{L^2(\Omega)} \\
&\qquad \le \tilde{C} \left( T\tau^{n+1} + \delta_h \tau^{n+1} + \frac{\delta_h^2 T}{\tau^{n+1}} \right) \|r_1^{n+1} + r_2^{n+1}\|^2_{L^2(\Omega)} \\
&\qquad + \frac{\tau^{n+1} + \tau^n}{4T} \left( \|e_h^{n+1}\|^2_{L^2(\Omega)} + \delta_h^2 \left\|\mathbf{u}(t^{n+1/2}) \cdot \nabla e_h^{n+1}\right\|^2_{L^2(\Omega)} \right) \\
&\qquad + \frac{\tau^{n+1} + \tau^n}{2T} \left( \|e_h^{n}\|^2_{L^2(\Omega)} + \delta_h^2 \left\|\mathbf{u}(t^{n-1/2}) \cdot \nabla e_h^{n}\right\|^2_{L^2(\Omega)} \right) \\
&+ \delta_h^2 \left(1 + \frac{\tau^{n+1}}{2T}\right) \left\| \left(\mathbf{u}(t^{n+1/2}) + \mathbf{u}(t^{n-1/2})\right) \cdot \nabla e_h^n \right\|_{L^2(\Omega)} \left\| \left(\mathbf{u}(t^{n+1/2}) - \mathbf{u}(t^{n-1/2})\right) \cdot \nabla e^n \right\|_{L^2(\Omega)}.
\end{aligned}
$$

The last term is estimated as before and we obtain finally, thanks to the inverse inequality (2.64) and the anisotropic quasi-uniformity condition, that it holds for all $0 \le n \le N$

$$
\begin{aligned}
&\|e_h^{n+1}\|^2_{L^2(\Omega)} - \|e_h^n\|^2_{L^2(\Omega)} \\
&\qquad + \delta_h^2 \left\|\mathbf{u}(t^{n+1/2}) \cdot \nabla e_h^{n+1}\right\|^2_{L^2(\Omega)} - \delta_h^2 \left\|\mathbf{u}(t^{n-1/2}) \cdot \nabla e_h^{n}\right\|^2_{L^2(\Omega)} \\
&\qquad \le \tilde{C} \left( T\tau^{n+1} + \delta_h \tau^{n+1} + \frac{\delta_h^2 T}{\tau^{n+1}} \right) \|r_1^{n+1} + r_2^{n+1}\|^2_{L^2(\Omega)} \\
&\qquad + \frac{\tau^{n+1} + \tau^n}{4T} \left( \|e_h^{n+1}\|^2_{L^2(\Omega)} + \delta_h^2 \left\|\mathbf{u}(t^{n+1/2}) \cdot \nabla e_h^{n+1}\right\|^2_{L^2(\Omega)} \right) \\
&\qquad + \frac{\tau^{n+1} + \tau^n}{2T} \left( \|e_h^{n}\|^2_{L^2(\Omega)} + \delta_h^2 \left\|\mathbf{u}(t^{n-1/2}) \cdot \nabla e_h^{n}\right\|^2_{L^2(\Omega)} \right) \\
&\quad + \tilde{C}\delta_h^2 \left(1 + \frac{\tau^{n+1}}{2T}\right) \frac{(\tau^{n+1} + \tau^n)}{(\max_{K \in \mathcal{T}_h} \lambda_{2,K})^2} \|\mathbf{u}\|_{L^\infty(\Omega \times (0,T))} \|\partial_t \mathbf{u}\|_{L^\infty(\Omega \times (0,T))} \\
&\qquad\qquad \left( \|e_h^n\|^2_{L^2(\Omega)} + \delta_h^2 \|\mathbf{u}(t^{n-1/2}) \cdot \nabla e_h^n\|^2_{L^2(\Omega)} \right).
\end{aligned}
$$

Using the discrete Gronwall's Lemma A.6, the fact that $e_h^0 = 0$ and the definition of the extended sequences, we obtain

$$\begin{aligned}
&\|e_h^N\|^2_{L^2(\Omega)} + \delta_h^2 \left\|\mathbf{u}(T)\cdot\nabla e_h^N\right\|^2_{L^2(\Omega)} \\
&\qquad \leq \tilde{C}\exp\left(\frac{\tilde{C}\delta_h^2 T}{(\max_{K\in\mathcal{T}_h}\lambda_{2,K})^2}\|\mathbf{u}\|_{L^\infty(\Omega\times(0,T))}\|\partial_t\mathbf{u}\|_{L^\infty(\Omega\times(0,T))}\right) \\
&\qquad\qquad \left(\sum_{n=0}^{N-1}\left(T\tau^{n+1} + \delta_h\tau^{n+1} + \frac{\delta_h^2 T}{\tau^{n+1}}\right)\|r_1^{n+1} + r_2^{n+1}\|^2_{L^2(\Omega)}\right).
\end{aligned}$$

Observe that the hypothesis needed to apply the Gronwall's Lemma are fulfilled since $\frac{\tau^{n+1}+\tau^n}{4T} < 1$. Note moreover that we bound

$$\exp\left(\sum_{n=0}^{N}\frac{\tau^{n+1}+\tau^n}{2T}\right), \exp\left(\sum_{n=0}^{N}\frac{\tau^{n+1}+\tau^n}{4T}\frac{1}{1-\frac{\tau^{n+1}+\tau^n}{4T}}\right)$$

by $\exp(3/2)$ that we absorb in $C$. Using the estimate on $r_1^{n+1}$ and $r_2^{n+1}$,we finally obtain the following estimate for $I_2$

$$\begin{aligned}
I_2 &\leq \tilde{C}\exp\left(\frac{\tilde{C}\delta_h^2 T}{(\max_{K\in\mathcal{T}_h}\lambda_{2,K})^2}\|\mathbf{u}\|_{L^\infty(\Omega\times(0,T))}\|\partial_t\mathbf{u}\|_{L^\infty(\Omega\times(0,T))}\right) \\
&(T\tau^4 + \delta_h\tau^4 + \delta_h^2\tau^2)\left(\int_0^T\left\|\frac{\partial^3\varphi_h}{\partial t^3}\right\|^2_{L^2(\Omega)} dt + \|\mathbf{u}\|^2_{L^\infty(\Omega\times(0,T))}\int_0^T\left\|\nabla\frac{\partial^2\varphi_h}{\partial t^2}\right\|^2_{L^2(\Omega)} dt\right).
\end{aligned}$$

The theorem is then proven by combining the estimates for $I_1$ and $I_2$. □

**Remark 2.41.** (i) In the isotropic settings, the above a priori error estimate reduces to

$$\|e(T)\|^2_{L^2(\Omega)} \leq C(h^3 + \tau^2) + h.o.t.$$

where $C$ does not depend on the mesh size and the time step but may depends on the aspect ratio. If the mesh is aligned with the solution and the solution depends only on one variable, then the a priori error estimate reduces to

$$\|e(T)\|^2_{L^2(\Omega)} \leq C((\max_{K\in\mathcal{T}_h}\lambda_{2,K})^3 + \tau^2) + h.o.t.$$

where $C$ does not depends on the aspect ratio either.

(ii) If $\mathbf{u}$ is independent of the time, then the exponential factor in the a above a priori error estimate is eliminated.

(iii) Observe that if $\mathbf{u}$ is independent of the time, we do not recover the a priori error estimate for a steady transport field obtained in Theorem 2.18 since the term

$$\|\mathbf{u}\|^2_{L^\infty(\Omega\times(0,T))}\int_0^T\left\|\nabla\frac{\partial^2\varphi_h}{\partial t^2}\right\|^2_{L^2(\Omega)} dt \tag{2.75}$$

appears in the bound. This is only due to a technicality (see the proof above). Indeed we must estimate the quantity

$$\mathbf{u}(t^{n+1/2})\cdot\nabla\left(\frac{\varphi_h(t^{n+1}) + \varphi_h(t^n)}{2} - \varphi_h(t^{n+1/2})\right), \tag{2.76}$$

that is to say the difference between the trapezoidal rule and the midpoint rule for squaring the integral in time. We could have made this term appear also in the a priori error estimate of Theorem 2.18 when $\mathbf{u}$ is independent of the time. But observe that in this case, the term (2.75) can be written in fact as

$$\int_0^T \left\| \mathbf{u} \cdot \nabla \frac{\partial^2 \varphi_h}{\partial t^2} \right\|^2_{L^2(\Omega)} dt,$$

which goes as $\dfrac{\partial^3 \varphi_h}{\partial t^3}$.

One can explain these technical differences by the following observation : when $\mathbf{u}$ is independent of the time, approximating in time

$$\int_{t^n}^{t^{n+1}} \int_\Omega \left( \frac{\partial \varphi_h}{\partial t} + \mathbf{u} \cdot \nabla \varphi_h \right) (v_h + \delta_h \mathbf{u} \cdot \nabla v_h) d\mathbf{x} dt = 0$$

by the midpoint rule (that is to say the Crank-Nicolson method in an finite differences framework) or the trapezoidal rule yields to the same time advancing scheme. In the proof of Theorem 2.18, we estimate the time discretized quantity $I_2$ by seeing in this case the Crank-Nicolson scheme as a trapezoidal rule (compared the Taylor expansions (2.28) and (2.74) for instance). This is why the quantity (2.76) does not come out.

#### A second a priori error estimate for the fully discrete approximation

We now state another a priori error estimate, trying to adapt the proof of Theorem 2.24 with a good choice for the projection. The discussion that follows is rather technical. The reader can go directly to the Theorem 2.51, where the resulting a priori error estimate is written in a self-contained manner, and come back later to the considerations presented below.

The first idea that comes in mind to generalize the Definition 2.20 in the framework of time dependent velocity field $\mathbf{u}$ is to define the projection of $\phi \in C^0([0,T]; H^1(\Omega))$ as the unique $\phi_h \in V_h$ solution of

$$\int_\Omega (\phi_h + \mathbf{u}(t^*) \cdot \nabla \phi_h)(v_h + \delta_h \mathbf{u}(t^*) \cdot \nabla v_h) d\mathbf{x} \\ = \int_\Omega (\phi(t) + \mathbf{u}(t^*) \cdot \nabla \phi(t)(v_h + \delta_h \mathbf{u}(t^*) \cdot \nabla v_h) d\mathbf{x}, \quad \forall v_h \in V_h. \quad (2.77)$$

where $t, t^* \in [0,T]$. We can therefore note $\phi_h = \Pi^{hyp}_{h,t^*} \phi(t)$. Observe that in this case, the projection $\Pi^{hyp}_{h,t^*}$ depends on the time $t^*$ and therefore we have in fact defined a family of projections. The proof would now consist in estimating for every $t^n$ $\varphi(t^n) - \Pi^{hyp}_{h,t^n} \varphi(t^n)$ and $\Pi^{hyp}_{h,t^n} \varphi(t^n) - \varphi^n_h$. The proof can be driven, reproducing the one of Theorem 2.24, but at the end quantities of the kind $(\Pi^{hyp}_{h,t^{n+1}} - \Pi^{hyp}_{h,t^n}) \varphi(t^n)$ (that is to say the difference in time between the projection taken at two different time steps) must be estimated. This can be down, but it yields terms that converge with a lower order, unless some restrictions on the time step and the mesh size are set, which are not observed as necessary in the numerical experiments. In fact, it turns out that the difference $(\Pi^{hyp}_{h,t^{n+1}} - \Pi^{hyp}_{h,t^n}) \varphi(t^n)$ is only $O(\tau)$, yielding to a suboptimal final estimate, since it is expected that the Crank-Nicolson scheme converges with a second order accuracy.

The problem that occurs with the definition of $\Pi^{hyp}_{h,t^*}$ is that the projection depends explicitly on the time $t^*$. To solve this issue, we introduce an iterative construction of a projected sequence of the sequence of the solutions $(\varphi(t^n))_{n=0}^N$:

**Definition 2.42** (Iterative Hyperbolic Ritz Projection (IHRP))**.**
Let $N > 0$ be a integer and $0 = t^0 < t^1 < ... < t^N = T$ a partition of $[0, T]$. Let $\phi \in C^0(0, T, H^1(\Omega))$. For any $0 \leq n \leq N$, we define $\Pi_h^{iter}\phi(t^n) \in V_h$ recursively as follows. For $n = 0$, we set

$$\Pi_h^{iter}\phi(t^0) = r_h\phi(t^0), \tag{2.78}$$

and for every $0 \leq n \leq N-1$ we define $\Pi_h^{iter}\phi(t^{n+1}) \in V_h$ as the solution of the discrete problem

$$\begin{aligned}\int_\Omega \left( \frac{\Pi_h^{iter}\phi(t^{n+1}) - \Pi_h^{iter}\phi(t^n)}{\tau^{n+1}} + \mathbf{u}(t^{n+1/2}) \cdot \nabla \left( \frac{\Pi_h^{iter}\phi(t^{n+1}) + \Pi_h^{iter}\phi(t^n)}{2} \right) \right) \\ (v_h + \delta_h \mathbf{u}(t^{n+1/2}) \cdot \nabla v_h) d\mathbf{x} \\ = \int_\Omega \left( \frac{\phi(t^{n+1}) - \phi(t^n)}{\tau^{n+1}} + \mathbf{u}(t^{n+1/2}) \cdot \nabla \left( \frac{\phi(t^{n+1}) + \phi(t^n)}{2} \right) \right) (v_h + \delta_h \mathbf{u}(t^{n+1/2}) \cdot \nabla v_h) d\mathbf{x},\end{aligned} \tag{2.79}$$

for all $v_h \in V_h$.

**Remark 2.43.** (i) Assume that we build the sequence of projected solutions $(\Pi_h^{iter}\varphi(t^n))_{n=0}^N$ where $\varphi$ is the solution of (2.18). Observe that, contrary to the classical HRP or to (2.77), we only know the projection of the solution at the discrete times $t^n$. This is not restrictive since we only need to estimate the numerical error at times $t^n$.

(ii) Let $\varphi$ be the solution of the transport equation. Then, there exists, for any $n$, a remainder $r^{n+1}$ such that

$$\frac{\varphi(t^{n+1}) - \varphi(t^n)}{\tau^{n+1}} + \mathbf{u}(t^{n+1/2}) \cdot \nabla \left( \frac{\varphi(t^{n+1}) + \varphi(t^n)}{2} \right) = r^{n+1}.$$

$r^{n+1}$ is in fact the consistency error of the Crank-Nicolson method (obtained by plugging the exact solution into the numerical scheme). Roughly speaking, building the sequence of $\Pi_h^{iter}\varphi(t^n)$ consists to project this consistency error into the finite elements space $V_h$ at every time step.

We first prove a stability result.

**Proposition 2.44** (Stability of the Iterative Hyperbolic Ritz Projection)**.**
*Let $\varphi$ be the solution of (2.18) and $(\Pi_h^{iter}\varphi(t^n))_{n=0}^N$ be the correspondent projected solution constructed in Definition 2.42 for the partition $0 = t^0 < t^1 < ... < t^N = T$ of $[0, T]$ and $\delta_h > 0$ constant. Assume moreover that $\mathcal{T}_h$ satisfies the anisotropic quasi-uniformity condition: there exists $c > 0$, independent of the mesh geometry, in particular independent of the mesh size and the mesh aspect ratio such that*

$$\max_{K \in \mathcal{T}_h} \lambda_{2,K} \leq c\lambda_{2,K}, \quad \forall K \in \mathcal{T}_h.$$

*Then, there exists a constant $C > 0$, that may depend only on the reference triangle $\hat{K}$,* *such that for all* $0 < n \leq N$ *holds*

$$\begin{aligned}
&\|\Pi_h^{iter}\varphi(t^n)\|^2_{L^2(\Omega)} + \delta_h^2\|\mathbf{u}(t^n)\cdot\nabla\Pi_h^{iter}\varphi(t^n)\|^2_{L^2(\Omega)} \\
&\qquad\leq C\Big(\|\Pi_h^{iter}\varphi(0)\|^2_{L^2(\Omega)} + \delta_h^2\|\mathbf{u}(t^0)\cdot\nabla\Pi_h^{iter}\varphi(0)\|^2_{L^2(\Omega)} \\
&\qquad+\sum_{n=0}^{n-1}(t^n\tau^{n+1} + \delta_h\tau^{n+1} + \delta_h^2(\tau^{n+1}+\tau))\|r^{n+1}\|^2_{L^2(\Omega)} \\
&\quad+\sum_{n=1}^{n-1} t^n\delta_h^2(\tau^{n+1}+\tau^n)\left\|\frac{r^{n+1}-r^n}{\tau^{n+1}+\tau^n}\right\|^2_{L^2(\Omega)} + \delta_h^2\sup_{0\leq m\leq n}\|r^m\|^2_{L^2(\Omega)}\Big) \\
&\exp\left(\frac{Ct^n\delta_h^2}{(\max_{K\in\mathcal{T}_h}\lambda_{2,K})^2}\left(\|\partial_t\mathbf{u}\|^2_{L^\infty(\Omega\times(0,T))} + \|\mathbf{u}\|_{L^\infty(\Omega\times(0,T))}\|\partial_t\mathbf{u}\|_{L^\infty(\Omega\times(0,T))}\right)\right),
\end{aligned}$$

*where we note*

$$r^{n+1} = \frac{\varphi(t^{n+1})-\varphi(t^n)}{\tau^{n+1}} + \mathbf{u}(t^{n+1/2})\cdot\nabla\left(\frac{\varphi(t^{n+1})+\varphi(t^n)}{2}\right), \quad 0\leq n\leq N-1.$$

**Remark 2.45.**
As already stated, if $\delta_h$ is given by

$$\delta_h = \frac{\max_{K\in\mathcal{T}_h}\lambda_{2,K}}{2\|\mathbf{u}\|_{L^\infty(\Omega\times(0,T))}}.$$

the estimate becomes uniform with respect to the mesh size and the time step. Moreover, if we assume that $\varphi$ is smooth enough, then all the quantities involving $r^{n+1}$ are uniformly bounded with respect to the time step.

*Proof.* As we did several times, we note by $C$ any generic positive constant independent of the data, the mesh size and aspect ratio and the time step, which may depend only on the reference triangle. Let $0 < M \leq N$ and let us recall that

$$\frac{\varphi(t^{n+1})-\varphi(t^n)}{\tau^{n+1}} + \mathbf{u}(t^{n+1/2})\cdot\nabla\left(\frac{\varphi(t^{n+1})+\varphi(t^n)}{2}\right) = r^{n+1}.$$

Choosing

$$v_h = \frac{\Pi_h^{iter}\varphi(t^{n+1})+\Pi_h^{iter}\varphi(t^n)}{2} + \delta_h\frac{\Pi_h^{iter}\varphi(t^{n+1})-\Pi_h^{iter}\varphi(t^n)}{\tau^{n+1}}$$

in the weak formulation (2.79) and eliminating all the terms of the form $\int_\Omega(\mathbf{u}\cdot\nabla v)vd\mathbf{x}$ thanks to the boundary condition, we obtain for all $0\leq n\leq M-1$

$$\begin{aligned}
&\frac{1}{2\tau^{n+1}}\|\Pi_h^{iter}\varphi(t^{n+1})\|^2_{L^2(\Omega)} - \frac{1}{2\tau^{n+1}}\|\Pi_h^{iter}\varphi(t^n)\|^2_{L^2(\Omega)} \\
&\quad+\frac{\delta_h^2}{2\tau^{n+1}}\|\mathbf{u}(t^{n+1/2})\cdot\nabla\Pi_h^{iter}\varphi(t^{n+1})\|^2_{L^2(\Omega)} - \frac{\delta_h^2}{2\tau^{n+1}}\|\mathbf{u}(t^{n+1/2})\cdot\nabla\Pi_h^{iter}\varphi(t^n)\|^2_{L^2(\Omega)} \\
&+\delta_h\int_\Omega\left(\frac{\Pi_h^{iter}\varphi(t^{n+1})-\Pi_h^{iter}\varphi(t^n)}{\tau^{n+1}} + \mathbf{u}(t^{n+1/2})\cdot\nabla\left(\frac{\Pi_h^{iter}\varphi(t^{n+1})+\Pi_h^{iter}\varphi(t^n)}{2}\right)\right)^2 d\mathbf{x} \\
&\leq\int_\Omega r^{n+1}\left(\frac{\Pi_h^{iter}\varphi(t^{n+1})+\Pi_h^{iter}\varphi(t^n)}{2} + \delta_h^2\mathbf{u}(t^{n+1/2})\cdot\nabla\left(\frac{\Pi_h^{iter}\varphi(t^{n+1})-\Pi_h^{iter}\varphi(t^n)}{\tau^{n+1}}\right)\right)d\mathbf{x} \\
&+\delta_h\int_\Omega r^{n+1}\left(\frac{\Pi_h^{iter}\varphi(t^{n+1})-\Pi_h^{iter}\varphi(t^n)}{\tau^{n+1}} + \mathbf{u}(t^{n+1/2})\cdot\nabla\left(\frac{\Pi_h^{iter}\varphi(t^{n+1})+\Pi_h^{iter}\varphi(t^n)}{2}\right)\right)d\mathbf{x}.
\end{aligned}$$

Using the Young's inequality on the second term of the right hand side yields

$$
\begin{aligned}
&\frac{1}{2\tau^{n+1}}\|\Pi_h^{iter}\varphi(t^{n+1})\|^2_{L^2(\Omega)} - \frac{1}{2\tau^{n+1}}\|\Pi_h^{iter}\varphi(t^{n})\|^2_{L^2(\Omega)} \\
&\quad + \frac{\delta_h^2}{2\tau^{n+1}}\|\mathbf{u}(t^{n+1/2})\cdot\nabla\Pi_h^{iter}\varphi(t^{n+1})\|^2_{L^2(\Omega)} - \frac{\delta_h^2}{2\tau^{n+1}}\|\mathbf{u}(t^{n+1/2})\cdot\nabla\Pi_h^{iter}\varphi(t^{n})\|^2_{L^2(\Omega)} \\
&+ \frac{\delta_h}{2}\int_\Omega \left(\frac{\Pi_h^{iter}\varphi(t^{n+1}) - \Pi_h^{iter}\varphi(t^{n})}{\tau^{n+1}} + \mathbf{u}(t^{n+1/2})\cdot\nabla\left(\frac{\Pi_h^{iter}\varphi(t^{n+1}) + \Pi_h^{iter}\varphi(t^{n})}{2}\right)\right)^2 d\mathbf{x} \\
&\leq \int_\Omega r^{n+1}\left(\frac{\Pi_h^{iter}\varphi(t^{n+1}) + \Pi_h^{iter}\varphi(t^{n})}{2} + \delta_h^2\mathbf{u}(t^{n+1/2})\cdot\nabla\left(\frac{\Pi_h^{iter}\varphi(t^{n+1}) - \Pi_h^{iter}\varphi(t^{n})}{\tau^{n+1}}\right)\right) d\mathbf{x} \\
&\qquad\qquad + \frac{\delta_h}{2}\|r^{n+1}\|^2_{L^2(\Omega)}.
\end{aligned}
$$

As for the Proposition 2.38, we multiply by $2\tau^{n+1}$ and setting $t^{-1} = t^0$, and we transform the left hand side to obtain a telescopic expression, such that for all $0 \leq n \leq M-1$ it holds

$$
\begin{aligned}
&\|\Pi_h^{iter}\varphi(t^{n+1})\|^2_{L^2(\Omega)} - \|\Pi_h^{iter}\varphi(t^{n})\|^2_{L^2(\Omega)} \\
&\quad + \delta_h^2\|\mathbf{u}(t^{n+1/2})\cdot\nabla\Pi_h^{iter}\varphi(t^{n+1})\|^2_{L^2(\Omega)} - \delta_h^2\|\mathbf{u}(t^{n-1/2})\cdot\nabla\Pi_h^{iter}\varphi(t^{n})\|^2_{L^2(\Omega)} \\
&+\tau^{n+1}\delta_h\int_\Omega \left(\frac{\Pi_h^{iter}\varphi(t^{n+1}) - \Pi_h^{iter}\varphi(t^{n})}{\tau^{n+1}} + \mathbf{u}(t^{n+1/2})\cdot\nabla\left(\frac{\Pi_h^{iter}\varphi(t^{n+1}) + \Pi_h^{iter}\varphi(t^{n})}{2}\right)\right)^2 d\mathbf{x} \\
&\leq 2\tau^{n+1}\int_\Omega r^{n+1}\left(\frac{\Pi_h^{iter}\varphi(t^{n+1}) + \Pi_h^{iter}\varphi(t^{n})}{2} + \delta_h^2\mathbf{u}(t^{n+1/2})\cdot\nabla\left(\frac{\Pi_h^{iter}\varphi(t^{n+1}) - \Pi_h^{iter}\varphi(t^{n})}{\tau^{n+1}}\right)\right) d\mathbf{x} \\
&+\tau^{n+1}\delta_h\|r^{n+1}\|^2_{L^2(\Omega)} + \delta_h^2\left(\|\mathbf{u}(t^{n+1/2})\cdot\nabla\Pi_h^{iter}\varphi(t^{n})\|^2_{L^2(\Omega)} - \|\mathbf{u}(t^{n-1/2})\cdot\nabla\Pi_h^{iter}\varphi(t^{n})\|^2_{L^2(\Omega)}\right).
\end{aligned}
$$

Finally, one may write the right hand such that for all $0 \leq n \leq M-1$

$$
\begin{aligned}
&\|\Pi_h^{iter}\varphi(t^{n+1})\|^2_{L^2(\Omega)} - \|\Pi_h^{iter}\varphi(t^{n})\|^2_{L^2(\Omega)} \\
&\quad + \delta_h^2\|\mathbf{u}(t^{n+1/2})\cdot\nabla\Pi_h^{iter}\varphi(t^{n+1})\|^2_{L^2(\Omega)} - \delta_h^2\|\mathbf{u}(t^{n-1/2})\cdot\nabla\Pi_h^{iter}\varphi(t^{n})\|^2_{L^2(\Omega)} \\
&+\tau^{n+1}\delta_h\int_\Omega \left(\frac{\Pi_h^{iter}\varphi(t^{n+1}) - \Pi_h^{iter}\varphi(t^{n})}{\tau^{n+1}} + \mathbf{u}(t^{n+1/2})\cdot\nabla\left(\frac{\Pi_h^{iter}\varphi(t^{n+1}) + \Pi_h^{iter}\varphi(t^{n})}{2}\right)\right)^2 d\mathbf{x} \\
&\qquad\leq \tau^{n+1}\int_\Omega r^{n+1}\left(\Pi_h^{iter}\varphi(t^{n+1}) + \Pi_h^{iter}\varphi(t^{n})\right) d\mathbf{x} \\
&\qquad + 2\delta_h^2\int_\Omega r^{n+1}(\mathbf{u}(t^{n+1/2})\cdot\nabla\Pi_h^{iter}\varphi(t^{n+1}) - \mathbf{u}(t^{n-1/2})\cdot\nabla\Pi_h^{iter}\varphi(t^{n}))d\mathbf{x} \\
&\qquad - 2\delta_h^2\int_\Omega r^{n+1}(\mathbf{u}(t^{n+1/2}) - \mathbf{u}(t^{n-1/2}))\cdot\nabla\Pi_h^{iter}\varphi(t^{n})d\mathbf{x} \\
&+\tau^{n+1}\delta_h\|r^{n+1}\|^2_{L^2(\Omega)} + \delta_h^2\left(\|\mathbf{u}(t^{n+1/2})\cdot\nabla\Pi_h^{iter}\varphi(t^{n})\|^2_{L^2(\Omega)} - \|\mathbf{u}(t^{n-1/2})\cdot\nabla\Pi_h^{iter}\varphi(t^{n})\|^2_{L^2(\Omega)}\right).
\end{aligned}
$$

Eliminating the positive contribution in the left hand side, we obtain

$$
\begin{aligned}
&\|\Pi_h^{iter}\varphi(t^{n+1})\|^2_{L^2(\Omega)} - \|\Pi_h^{iter}\varphi(t^n)\|^2_{L^2(\Omega)} \\
&\qquad + \delta_h^2\|\mathbf{u}(t^{n+1/2})\cdot\nabla\Pi_h^{iter}\varphi(t^{n+1})\|^2_{L^2(\Omega)} - \delta_h^2\|\mathbf{u}(t^{n-1/2})\cdot\nabla\Pi_h^{iter}\varphi(t^n)\|^2_{L^2(\Omega)} \\
&\qquad\qquad \le \tau^{n+1}\int_\Omega r^{n+1}\left(\Pi_h^{iter}\varphi(t^{n+1}) + \Pi_h^{iter}\varphi(t^n)\right)d\mathbf{x} \\
&\qquad + 2\delta_h^2\int_\Omega r^{n+1}(\mathbf{u}(t^{n+1/2})\cdot\nabla\Pi_h^{iter}\varphi(t^{n+1}) - \mathbf{u}(t^{n-1/2})\cdot\nabla\Pi_h^{iter}\varphi(t^n))d\mathbf{x} \\
&\qquad\qquad - 2\delta_h^2\int_\Omega r^{n+1}(\mathbf{u}(t^{n+1/2}) - \mathbf{u}(t^{n-1/2}))\cdot\nabla\Pi_h^{iter}\varphi(t^n)d\mathbf{x} \\
&+\tau^{n+1}\delta_h\|r^{n+1}\|^2_{L^2(\Omega)}+\delta_h^2\left(\|\mathbf{u}(t^{n+1/2})\cdot\nabla\Pi_h^{iter}\varphi(t^n)\|^2_{L^2(\Omega)} - \|\mathbf{u}(t^{n-1/2})\cdot\nabla\Pi_h^{iter}\varphi(t^n)\|^2_{L^2(\Omega)}\right).
\end{aligned}
$$

Now let $0 \le n \le m \le M$ and we sum the last inequality up to $m-1$ and proceed to a discrete integration by part on the term

$$
2\delta_h^2\int_\Omega r^{n+1}(\mathbf{u}(t^{n+1/2})\cdot\nabla\Pi_h^{iter}\varphi(t^{n+1}) - \mathbf{u}(t^{n-1/2})\cdot\nabla\Pi_h^{iter}\varphi(t^n))d\mathbf{x}.
$$

$$
\begin{aligned}
&\|\Pi_h^{iter}\varphi(t^m)\|^2_{L^2(\Omega)} - \|\Pi_h^{iter}\varphi(0)\|^2_{L^2(\Omega)} \\
&\qquad + \delta_h^2\|\mathbf{u}(t^{m-1/2})\cdot\nabla\Pi_h^{iter}\varphi(t^m)\|^2_{L^2(\Omega)} - \delta_h^2\|\mathbf{u}(t^{-1/2})\cdot\nabla\Pi_h^{iter}\varphi(0)\|^2_{L^2(\Omega)} \\
&\qquad\qquad \le \sum_{n=0}^{m-1}\tau^{n+1}\int_\Omega r^{n+1}\left(\Pi_h^{iter}\varphi(t^{n+1}) + \Pi_h^{iter}\varphi(t^n)\right)d\mathbf{x} \\
&\qquad + 2\delta_h^2\sum_{n=1}^{m-1}(\tau^{n+1}+\tau^n)\int_\Omega \frac{r^{n+1}-r^n}{\tau^{n+1}+\tau^n}\mathbf{u}(t^{n-1/2})\cdot\nabla\Pi_h^{iter}\varphi(t^n)d\mathbf{x} \\
&\qquad + 2\delta_h^2\int_\Omega r^m\mathbf{u}(t^{m+1/2}))\cdot\nabla\Pi_h^{iter}\varphi(t^m) - r^1\mathbf{u}(t^{-1/2})\cdot\nabla\Pi_h^{iter}\varphi(0)d\mathbf{x} \\
&\qquad - 2\sum_{n=0}^{m-1}\delta_h^2\int_\Omega r^{n+1}(\mathbf{u}(t^{n+1/2}) - \mathbf{u}(t^{n-1/2}))\cdot\nabla\Pi_h^{iter}\varphi(t^n)d\mathbf{x} \\
&+\sum_{n=0}^{m-1}\tau^{n+1}\delta_h\|r^{n+1}\|^2_{L^2(\Omega)}+\delta_h^2\left(\|\mathbf{u}(t^{n+1/2})\cdot\nabla\Pi_h^{iter}\varphi(t^n)\|^2_{L^2(\Omega)} - \|\mathbf{u}(t^{n-1/2})\cdot\nabla\Pi_h^{iter}\varphi(t^n)\|^2_{L^2(\Omega)}\right).
\end{aligned}
$$

We now estimate the last two terms as we did in Proposition 2.38 using the inverse inequality (2.64), and using several times Cauchy-Schwarz and the Young's inequality, one can write for all $0 \le m \le M$ (note that if $M = N$, we set $\tau^{M+1} = \tau^{N+1} = 0$)

$$
\begin{aligned}
&\|\Pi_h^{iter}\varphi(t^m)\|^2_{L^2(\Omega)} + \delta_h^2\|\mathbf{u}(t^{m-1/2})\cdot\nabla\Pi_h^{iter}\varphi(t^m)\|^2_{L^2(\Omega)} \\
&\qquad\qquad \le \|\Pi_h^{iter}\varphi(0)\|^2_{L^2(\Omega)} + \delta_h^2\|\mathbf{u}(t^{-1/2})\cdot\nabla\Pi_h^{iter}\varphi(0)\|^2_{L^2(\Omega)} \\
&\qquad\quad + C\Bigg(\sum_{n=0}^{m-1}(t^m\tau^{n+1} + \delta_h\tau^{n+1} + \delta_h^2(\tau^{n+1}+\tau^n))\|r^{n+1}\|^2_{L^2(\Omega)} \\
&\qquad\quad + \sum_{n=1}^{m-1}t^m\delta_h^2(\tau^{n+1}+\tau^n)\left\|\frac{r^{n+1}-r^n}{\tau^{n+1}+\tau^n}\right\|^2_{L^2(\Omega)} + \delta_h^2\sup_{0\le n\le m}\|r^n\|^2_{L^2(\Omega)}\Bigg) \\
&\qquad + \sum_{n=0}^{m}\frac{\tau^{n+1}+\tau^n}{4t^m}(\|\Pi_h^{iter}\varphi(t^n)\|^2_{L^2(\Omega)} + \delta_h^2\|\mathbf{u}(t^{n-1/2})\cdot\nabla\Pi_h^{iter}\varphi(t^n)\|^2_{L^2(\Omega)}) \\
&\quad + C\sum_{n=0}^{m-1}\frac{\delta_h^2(\tau^{n+1}+\tau^n)}{(\max_{K\in\mathcal{T}_h}\lambda_{2,K})^2}\left(\|\partial_t\mathbf{u}\|^2_{L^\infty(\Omega\times(0,T))} + \|\mathbf{u}\|_{L^\infty(\Omega\times(0,T))}\|\partial_t\mathbf{u}\|_{L^\infty(\Omega\times(0,T))}\right) \\
&\qquad\qquad\qquad (\|\Pi_h^{iter}\varphi(t^n)\|^2_{L^2(\Omega)} + \delta_h^2\|\mathbf{u}(t^{n-1/2})\cdot\nabla\Pi_h^{iter}\varphi(t^n)\|^2_{L^2(\Omega)}).
\end{aligned}
$$

We now conclude, up to have defined before auxiliary sequences as in Proposition 2.38 to obtain a final estimate for

$$\|\Pi_h^{iter}\varphi(t^M)\|^2_{L^2(\Omega)} + \delta_h^2\|\mathbf{u}(t^M)\cdot\nabla\Pi_h^{iter}\varphi(t^M)\|^2_{L^2(\Omega)},$$

by using the discrete Gronwall's Lemma A.5. We obtain for any $0 < M \leq N$

$$\begin{aligned}
&\|\Pi_h^{iter}\varphi(t^M)\|^2_{L^2(\Omega)} + \delta_h^2\|\mathbf{u}(t^M)\cdot\nabla\Pi_h^{iter}\varphi(t^M)\|^2_{L^2(\Omega)} \\
&\quad\leq C\Bigg(\|\Pi_h^{iter}\varphi(0)\|^2_{L^2(\Omega)} + \delta_h^2\|\mathbf{u}(t^0)\cdot\nabla\Pi_h^{iter}\varphi(0)\|^2_{L^2(\Omega)} \\
&\qquad+\sum_{n=0}^{m-1}(t^m\tau^{n+1}+\delta_h\tau^{n+1}+\delta_h^2(\tau^{n+1}+\tau))\|r^{n+1}\|^2_{L^2(\Omega)} \\
&\qquad+\sum_{n=1}^{m-1}t^m\delta_h^2(\tau^{n+1}+\tau^n)\left\|\frac{r^{n+1}-r^n}{\tau^{n+1}+\tau^n}\right\|^2_{L^2(\Omega)} + \delta_h^2\sup_{0\leq n\leq m}\|r^n\|^2_{L^2(\Omega)}\Bigg) \\
&\exp\left(\frac{Ct^m\delta_h^2}{(\max_{K\in\mathcal{T}_h}\lambda_{2,K})^2}\left(\|\partial_t\mathbf{u}\|^2_{L^\infty(\Omega\times(0,T))}+\|\mathbf{u}\|_{L^\infty(\Omega\times(0,T))}\|\partial_t\mathbf{u}\|_{L^\infty(\Omega\times(0,T))}\right)\right),
\end{aligned}$$

where we use the convention that $t^{-1/2} = t^0 = 0$. The final estimate is therefore straightforward by extending the sums in the right hand side up to $N-1$. □

We can now prove our last a priori error estimate. The strategy of the proof consists in cutting the numerical error $e^n = \varphi(t^n) - \varphi_h^n$ into $e_h(t^n) = \varphi(t^n) - \Pi_h^{iter}\varphi(t^n)$ and $e_h^n = \Pi_h^{iter}\varphi(t^n) - \varphi_h^n$. To simplify the writing of the proof, we separate it into two propositions, one containing the spatial approximation and the other the time approximation. The following lemma is needed for the first proposition.

**Lemma 2.46.**
*Let $\varphi$ be the solution of (2.18) and $(\Pi_h^{iter}\varphi(t^n))_{n=0}^N$ be the correspondent projected solution constructed in Definition 2.42 for the partition $0 = t^0 < t^1 < ... < t^N = T$ of $[0,T]$ and $\delta_h > 0$ constant. Assume moreover that $\mathcal{T}_h$ satisfies the anisotropic quasi-uniformity condition: there exists $c > 0$, independent of the mesh geometry, in particular independent of the mesh size and the mesh aspect ratio such that*

$$\max_{K\in\mathcal{T}_h}\lambda_{2,K} \leq c\lambda_{2,K}, \quad \forall K\in\mathcal{T}_h.$$

*Then, there exists a constant $C > 0$, that may depend only on the reference triangle $\hat{K}$, such that for all $0 < n \leq N$ there holds*

$$\begin{aligned}
&\|\nabla(\varphi(t^n) - \Pi_h^{iter}\varphi(t^n))\|^2_{L^2(\Omega)} \\
&\qquad\leq \frac{C}{(\max_{K\in\mathcal{T}_h}\lambda_{2,K})^2}\left(\sum_{K\in\mathcal{T}_h}L_K^2(\varphi(t^n)) + \|\varphi(t^n)-\Pi_h^{iter}\varphi(t^n)\|^2_{L^2(\Omega)}\right). \qquad (2.80)
\end{aligned}$$

*Proof.* We note by $C$ any generic positive constant which may depend only on the reference triangle. By the triangle inequality, we have

$$\|\nabla(\varphi(t^n)-\Pi_h^{iter}\varphi(t^n))\|^2_{L^2(\Omega)} \leq 2\|\nabla(\varphi(t^n)-r_h\varphi(t^n))\|^2_{L^2(\Omega)}+2\|\nabla(r_h\varphi(t^n)-\Pi_h^{iter}\varphi(t^n))\|^2_{L^2(\Omega)}.$$

Applying the anisotropic inverse inequality (2.64) on the second term of the right hand side and the anisotropic quasi-uniformity condition, one have

$$\begin{aligned}
&\|\nabla(\varphi(t^n) - \Pi_h^{iter}\varphi(t^n))\|^2_{L^2(\Omega)} \\
&\qquad\leq 2\|\nabla(\varphi(t^n) - r_h\varphi(t^n))\|^2_{L^2(\Omega)} + \frac{C}{(\max_{K\in\mathcal{T}_h}\lambda_{2,K})^2}\|r_h\varphi(t^n) - \Pi_h^{iter}\varphi(t^n)\|^2_{L^2(\Omega)}.
\end{aligned}$$

Applying again the triangle inequality yields finally

$$\|\nabla(\varphi(t^n) - \Pi_h^{iter}\varphi(t^n))\|^2_{L^2(\Omega)} \le 2\|\nabla(\varphi(t^n) - r_h\varphi(t^n))\|^2_{L^2(\Omega)}$$
$$+ \frac{C}{(\max_{K\in\mathcal{T}_h}\lambda_{2,K})^2}\left(\|r_h\varphi(t^n) - \varphi(t^n)\|^2_{L^2(\Omega)} + \|\varphi(t^n) - \Pi_h^{iter}\varphi(t^n)\|^2_{L^2(\Omega)}\right)$$

We conclude by using the interpolation error estimate (1.2). □

**Proposition 2.47** (Spatial a priori error estimate through IHRP).
*Assume that* $\mathbf{u}$ *is not identically zero. Let* $\varphi \in H^1(0,T;H^2(\Omega))$ *be the solution of (2.18). Let* $\delta_h$ *be given by*

$$\delta_h = \frac{\max_{K\in\mathcal{T}_h}\lambda_{2,K}}{2\|\mathbf{u}\|_{L^\infty(\Omega\times(0,T))}}$$

*and* $(\Pi_h^{iter}\varphi(t^n))_{n=0}^N$ *be the correspondent projected solution constructed in Definition 2.42 for the partition* $0 = t^0 < t^1 < ... < t^N = T$ *of* $[0,T]$*. Assume moreover that* $\mathcal{T}_h$ *satisfies the anisotropic quasi-uniformity condition : there exists* $c > 0$*, independent of the mesh geometry, in particular independent of the mesh size and the mesh aspect ratio such that*

$$\max_{K\in\mathcal{T}_h}\lambda_{2,K} \le c\lambda_{2,K}, \quad \forall K \in \mathcal{T}_h.$$

*Finally lets us note* $e_h(t^n) = \varphi(t^n) - \Pi_h^{iter}\varphi(t^n), n = 0,1,2,...,N$*. Then, there exists a constant* $C > 0$*, that may depend only on the reference triangle* $\hat{K}$*, such that*

$$\|e_h(T)\|^2_{L^2(\Omega)} + \delta_h^2\|\mathbf{u}(T)\cdot\nabla e_h(T)\|^2_{L^2(\Omega)}$$
$$\le \Bigg(\|e_h(0)\|^2_{L^2(\Omega)} + \delta_h^2\|\mathbf{u}(0)\cdot\nabla e_h(0)\|^2_{L^2(\Omega)}$$
$$+CT\sum_{K\in\mathcal{T}_h}\left(\frac{1}{\delta_h} + \frac{\delta_h\|\mathbf{u}\|^2_{L^\infty(\Omega\times(0,T))}}{\lambda^2_{2,K}}\right)\sup_{t\in(0,T)} L^2_K(\varphi) + \left(\delta_h + \frac{\delta_h^3\|\mathbf{u}\|^2_{L^\infty(\Omega\times(0,T))}}{\lambda^2_{2,K}}\right)\sup_{t\in(0,T)} L^2_K\left(\frac{\partial\varphi}{\partial t}\right)$$
$$+\frac{CT\delta_h^2\|\mathbf{u}\|_{L^\infty(\Omega\times(0,T))}\|\partial_t\mathbf{u}\|_{L^\infty(\Omega\times(0,T))}}{(\max_{K\in\mathcal{T}_h}\lambda_{2,K})^2}\sum_{K\in\mathcal{T}_h}\sup_{t\in(0,T)} L^2_K(\varphi)\Bigg)$$
$$\exp\left(\frac{CT\delta_h^2\|\mathbf{u}\|_{L^\infty(\Omega\times(0,T))}\|\partial_t\mathbf{u}\|_{L^\infty(\Omega\times(0,T))}}{(\max_{K\in\mathcal{T}_h}\lambda_{2,K})^2}\right).$$

**Remark 2.48.** (i) Observe that, in the isotropic setting, the error estimate of Proposition 2.47, reduces to

$$\|e_h(T)\|^2_{L^2(\Omega)} \le Ch^3 + h.o.t.$$

where $C$ may depend on the aspect ratio but is independent of the mesh size, and to

$$\|e_h(T)\|^2_{L^2(\Omega)} \le C(\max_{K\in\mathcal{T}_h}\lambda_{2,K})^3 + h.o.t.,$$

in the anisotropic setting when the mesh is aligned with the solution and this later depends on one variable only (in this case $C$ is independent of the aspect ratio).

(ii) In the case where $\mathbf{u}$ is independent of the time, the exponential bound can be eliminated, as the term

$$\frac{CT\delta_h^2\|\mathbf{u}\|_{L^\infty(\Omega\times(0,T))}\|\partial_t\mathbf{u}\|_{L^\infty(\Omega\times(0,T))}}{(\max_{K\in\mathcal{T}_h}\lambda_{2,K})^2}\sum_{K\in\mathcal{T}_h}\sup_{t\in(0,T)} L^2_K(\varphi)$$

and we recover the "classical" spatial error estimate for the transport equation.

(iii) As stated before, the exponential factor is uniformly bounded with respect to $h$ due to the choice of $\delta_h$.

*Proof.* We note by $C$ any generic positive constant independent of the data, the mesh size and aspect ratio and the time step, which may depends only on the reference triangle. The idea is to mimic in a discrete setting the proof of the semi-discrete a priori error estimate (in space) of the Theorem 2.40. As we did several times, eliminating all the positive contribution of the form $\int_\Omega (\mathbf{u}\cdot\nabla v)v d\mathbf{x}$, we have

$$\frac{\|e_h(t^{n+1})\|^2_{L^2(\Omega)} - \|e_h(t^n)\|^2_{L^2(\Omega)}}{2\tau^{n+1}} + \frac{\delta_h^2\|\mathbf{u}(t^{n+1/2})\cdot\nabla e_h(t^{n+1})\|^2_{L^2(\Omega)} - \delta_h^2\|\mathbf{u}(t^{n+1/2})\cdot\nabla e_h(t^n)\|^2_{L^2(\Omega)}}{2\tau^{n+1}}$$
$$+\delta_h\int_\Omega\left(\frac{e_h(t^{n+1})-e_h(t^n)}{\tau^{n+1}} + \mathbf{u}(t^{n+1/2})\cdot\nabla\left(\frac{e_h(t^{n+1})+e_h(t^n)}{2}\right)\right)^2 d\mathbf{x}$$
$$\le \int_\Omega\left(\frac{e_h(t^{n+1})-e_h(t^n)}{\tau^{n+1}} + \mathbf{u}(t^{n+1/2})\cdot\nabla\left(\frac{e_h(t^{n+1})+e_h(t^n)}{2}\right)\right)$$
$$(w+\delta_h\mathbf{u}(t^{n+1/2})\cdot\nabla w)d\mathbf{x}.$$

where we note $w = \dfrac{e_h(t^{n+1})+e_h(t^n)}{2} + \delta_h\dfrac{e_h(t^{n+1})-e_h(t^n)}{\tau^{n+1}}$. Since $e_h(t^n) = \varphi(t^n) - \Pi_h^{iter}\varphi(t^n)$, we have by construction (see (2.79)) that the following discrete Galerkin orthogonality holds for all $n \ge 0$

$$\int_\Omega\left(\frac{e_h(t^{n+1})-e_h(t^n)}{\tau^{n+1}} + \mathbf{u}(t^{n+1/2})\cdot\nabla\left(\frac{e_h(t^{n+1})+e_h(t^n)}{2}\right)\right)$$
$$(v_h+\delta_h\mathbf{u}(t^{n+1/2})\cdot\nabla v_h)d\mathbf{x} = 0, \quad \forall v_h \in V_h.$$

Therefore, one can subtract from the right hand side of the previous inequality the test function

$$w_h = \frac{(r_h\varphi(t^{n+1}) - \Pi_h^{iter}\varphi(t^{n+1})) + (r_h\varphi(t^n) - \Pi_h^{iter}\varphi(t^n))}{2}$$
$$+\delta_h\frac{(r_h\varphi(t^{n+1}) - \Pi_h^{iter}\varphi(t^{n+1})) - (r_h\varphi(t^n) - \Pi_h^{iter}\varphi(t^n))}{\tau^{n+1}}.$$

This yields

$$\frac{\|e_h(t^{n+1})\|^2_{L^2(\Omega)} - \|e_h(t^n)\|^2_{L^2(\Omega)}}{2\tau^{n+1}} + \frac{\delta_h^2\|\mathbf{u}(t^{n+1/2})\cdot\nabla e_h(t^{n+1})\|^2_{L^2(\Omega)} - \delta_h^2\|\mathbf{u}(t^{n+1/2})\cdot\nabla e_h(t^n)\|^2_{L^2(\Omega)}}{2\tau^{n+1}}$$
$$+\delta_h\int_\Omega\left(\frac{e_h(t^{n+1})-e_h(t^n)}{\tau^{n+1}} + \mathbf{u}(t^{n+1/2})\cdot\nabla\left(\frac{e_h(t^{n+1})+e_h(t^n)}{2}\right)\right)^2 d\mathbf{x}$$
$$\le \int_\Omega\left(\frac{e_h(t^{n+1})-e_h(t^n)}{\tau^{n+1}} + \mathbf{u}(t^{n+1/2})\cdot\nabla\left(\frac{e_h(t^{n+1})+e_h(t^n)}{2}\right)\right)$$
$$\left(\frac{(\varphi(t^{n+1}) - (r_h\varphi(t^{n+1})) + (\varphi(t^n) - r_h\varphi(t^n))}{2}\right.$$
$$+\delta_h\frac{(\varphi(t^{n+1}) - r_h\varphi(t^{n+1})) - (\varphi(t^n) - r_h\varphi(t^n))}{\tau^{n+1}}$$
$$+\delta_h\mathbf{u}(t^{n+1/2})\cdot\nabla\left(\frac{(\varphi(t^{n+1}) - (r_h\varphi(t^{n+1})) + (\varphi(t^n) - r_h\varphi(t^n))}{2}\right)$$
$$\left.+\delta_h^2\mathbf{u}(t^{n+1/2})\cdot\nabla\left(\frac{(\varphi(t^{n+1}) - r_h\varphi(t^{n+1})) - (\varphi(t^n) - r_h\varphi(t^n))}{\tau^{n+1}}\right)\right) d\mathbf{x}.$$

The Young's inequality and the fact that the time derivative and the Lagrange interpolant commutes yields

$$\frac{\|e_h(t^{n+1})\|^2_{L^2(\Omega)} - \|e_h(t^n)\|^2_{L^2(\Omega)}}{2\tau^{n+1}} + \frac{\delta_h^2\|\mathbf{u}(t^{n+1/2})\cdot\nabla e_h(t^{n+1})\|^2_{L^2(\Omega)} - \delta_h^2\|\mathbf{u}(t^{n+1/2})\cdot\nabla e_h(t^n)\|^2_{L^2(\Omega)}}{2\tau^{n+1}}$$
$$+\delta_h\int_\Omega\left(\frac{e_h(t^{n+1})-e_h(t^n)}{\tau^{n+1}} + \mathbf{u}(t^{n+1/2})\cdot\nabla\left(\frac{e_h(t^{n+1})+e_h(t^n)}{2}\right)\right)^2 d\mathbf{x}$$
$$\leq \frac{\delta_h}{2}\int_\Omega\left(\frac{e_h(t^{n+1})-e_h(t^n)}{\tau^{n+1}} + \mathbf{u}(t^{n+1/2})\cdot\nabla\left(\frac{e_h(t^{n+1})+e_h(t^n)}{2}\right)\right)^2 d\mathbf{x}$$
$$\frac{1}{\delta_h}\left(\|\varphi(t^{n+1}) - r_h\varphi(t^{n+1})\|^2_{L^2(\Omega)} + \|\varphi(t^n) - r_h\varphi(t^n)\|^2_{L^2(\Omega)]}\right)$$
$$+\frac{2\delta_h}{\tau^{n+1}}\int_{t^n}^{t^{n+1}}\left\|\frac{\partial\varphi}{\partial t} - r_h\left(\frac{\partial\varphi}{\partial t}\right)\right\|^2_{L^2(\Omega)} dt$$
$$+\delta_h\left(\|\mathbf{u}(t^{n+1/2})\cdot\nabla(\varphi(t^{n+1}) - r_h\varphi(t^{n+1})\|^2_{L^2(\Omega)} + \|\mathbf{u}(t^{n+1/2})\cdot\nabla(\varphi(t^n) - r_h\varphi(t^n)\|^2_{L^2(\Omega)}\right)$$
$$+\frac{2\delta_h^3}{\tau^{n+1}}\int_{t^n}^{t^{n+1}}\left\|\mathbf{u}(t^{n+1/2})\cdot\nabla\left(\frac{\partial\varphi}{\partial t} - r_h\left(\frac{\partial\varphi}{\partial t}\right)\right)\right\|^2_{L^2(\Omega)} dt.$$

Therefore, using the anisotropic Lagrange error interpolation estimate (1.2) and taking the supremum in time, we obtain that

$$\frac{\|e_h(t^{n+1})\|^2_{L^2(\Omega)} - \|e_h(t^n)\|^2_{L^2(\Omega)}}{2\tau^{n+1}}$$
$$+\frac{\delta_h^2\|\mathbf{u}(t^{n+1/2})\cdot\nabla e_h(t^{n+1})\|^2_{L^2(\Omega)} - \delta_h^2\|\mathbf{u}(t^{n+1/2})\cdot\nabla e_h(t^n)\|^2_{L^2(\Omega)}}{2\tau^{n+1}} \leq C\sum_{K\in\mathcal{T}_h} I_K^2,$$

where we note

$$I_K^2 = \left(\frac{1}{\delta_h} + \frac{\delta_h\|\mathbf{u}\|^2_{L^\infty(\Omega\times(0,T))}}{\lambda_{2,K}^2}\right)\sup_{t\in(0,T)} L_K^2(\varphi) + \left(\delta_h + \frac{\delta_h^3\|\mathbf{u}\|^2_{L^\infty(\Omega\times(0,T))}}{\lambda_{2,K}^2}\right)\sup_{t\in(0,T)} L_K^2\left(\frac{\partial\varphi}{\partial t}\right).$$

Then, multiplying by $2\tau^{n+1}$ and writing the left hand side as telescopic term, we get for all $n \geq 0$

$$\|e_h(t^{n+1})\|^2_{L^2(\Omega)} - \|e_h(t^n)\|^2_{L^2(\Omega)} + \delta_h^2\|\mathbf{u}(t^{n+1/2})\cdot\nabla e_h(t^{n+1})\|^2_{L^2(\Omega)} - \delta_h^2\|\mathbf{u}(t^{n-1/2})\cdot\nabla e_h(t^n)\|^2_{L^2(\Omega)}$$
$$\leq C\tau^{n+1}\sum_{K\in\mathcal{T}_h} I_K^2 + \delta_h^2\left(\|\mathbf{u}(t^{n+1/2})\cdot\nabla e_h(t^n)\|^2_{L^2(\Omega)} - \|\mathbf{u}(t^{n-1/2})\cdot\nabla e_h(t^n)\|^2_{L^2(\Omega)}\right)$$
$$\leq C\tau^{n+1}\sum_{K\in\mathcal{T}_h} I_K^2 + \delta_h^2(\tau^{n+1}+\tau^n)\|\mathbf{u}\|_{L^\infty(\Omega\times(0,T))}\|\partial_t\mathbf{u}\|_{L^\infty(\Omega\times(0,T))}\|\nabla e_h(t^n)\|^2_{L^2(\Omega)},$$

where as before we set $t^{-1} = t^0$ and $\tau^0 = 0$. By Lemma 2.46, we can write that

$$\|e_h(t^{n+1})\|^2_{L^2(\Omega)} - \|e_h(t^n)\|^2_{L^2(\Omega)} + \delta_h^2\|\mathbf{u}(t^{n+1/2})\cdot\nabla e_h(t^{n+1})\|^2_{L^2(\Omega)} - \delta_h^2\|\mathbf{u}(t^{n-1/2})\cdot\nabla e_h(t^n)\|^2_{L^2(\Omega)}$$
$$\leq C\left(\tau^{n+1}\sum_{K\in\mathcal{T}_h} I_K^2 + \frac{\delta_h^2\|\mathbf{u}\|_{L^\infty(\Omega\times(0,T))}\|\partial_t\mathbf{u}\|_{L^\infty(\Omega\times(0,T))}}{(\max_{K\in\mathcal{T}_h}\lambda_{2,K})^2}(\tau^{n+1}+\tau^n)\sum_{K\in\mathcal{T}_h} L_K^2(\varphi(t^n))\right)$$
$$+\frac{C\delta_h^2}{(\max_{K\in\mathcal{T}_h}\lambda_{2,K})^2}(\tau^{n+1}+\tau^n)\|\mathbf{u}\|_{L^\infty(\Omega\times(0,T))}\|\partial_t\mathbf{u}\|_{L^\infty(\Omega\times(0,T))}\|e_h(t^n)\|^2_{L^2(\Omega)}.$$

Up to have defined before auxiliary sequences as in Proposition 2.38, applying the discrete Gronwall's Lemma A.6, we derive that

$$
\begin{aligned}
&\|e_h(T)\|^2_{L^2(\Omega)} + \delta_h^2\|\mathbf{u}(T)\cdot\nabla e_h(T)\|^2_{L^2(\Omega)} \\
&\qquad \le \Bigg(\|e_h(0)\|^2_{L^2(\Omega)} + \delta_h^2\|\mathbf{u}(0)\cdot\nabla e_h(0)\|^2_{L^2(\Omega)} + CT\sum_{K\in\mathcal{T}_h} I_K^2 \\
&\qquad + \frac{CT\delta_h^2\|\mathbf{u}\|_{L^\infty(\Omega\times(0,T))}\|\partial_t\mathbf{u}\|_{L^\infty(\Omega\times(0,T))}}{(\max_{K\in\mathcal{T}_h}\lambda_{2,K})^2}\sum_{K\in\mathcal{T}_h}\sup_{t\in(0,T)} L_K^2(\varphi)\Bigg) \\
&\qquad\qquad \exp\left(\frac{CT\delta_h^2\|\mathbf{u}\|_{L^\infty(\Omega\times(0,T))}\|\partial_t\mathbf{u}\|_{L^\infty(\Omega\times(0,T))}}{(\max_{K\in\mathcal{T}_h}\lambda_{2,K})^2}\right),
\end{aligned}
$$

that gives the desired estimate. □

**Proposition 2.49** (Temporal a priori error estimate through IHRP)**.**
*Assume that* $\mathbf{u}$ *is not identically zero. Let* $\varphi \in H^3(0,T;L^2(\Omega)) \cap H^2(0,T;H^1(\Omega))$ *be the solution of (2.18). Let* $\delta_h$ *be given by*

$$\delta_h = \frac{\max_{K\in\mathcal{T}_h}\lambda_{2,K}}{2\|\mathbf{u}\|_{L^\infty(\Omega\times(0,T))}}.$$

*Let* $(\Pi_h^{iter}\varphi(t^n))_{n=0}^N$ *be the correspondent projected solution constructed in Definition 2.42 for the partition* $0 = t^0 < t^1 < ... < t^N = T$ *of* $[0,T]$ *and* $(\varphi_h^n)_{n=0}^N$ *be the solution of (2.60). Assume moreover that* $\mathcal{T}_h$ *satisfies the anisotropic quasi-uniformity condition: there exists* $c > 0$*, independent of the mesh geometry, in particular independent of the mesh size and the mesh aspect ratio such that*

$$\max_{K\in\mathcal{T}_h}\lambda_{2,K} \le c\lambda_{2,K}, \quad \forall K\in\mathcal{T}_h.$$

*Finally lets us note* $e_h^n = \Pi_h^{iter}\varphi(t^n) - \varphi_h^n, n = 0,1,2,...,N$*. Then, there exists a generic constant* $C > 0$*, independent of the mesh geometry, the mesh size and aspect ratio, the time step, the data of the problem and the exact solution* $\varphi$ *such that*

$$
\begin{aligned}
&\|e_h^N\|^2_{L^2(\Omega)} + \delta_h^2\left\|\mathbf{u}(T)\cdot\nabla e_h^N\right\|^2_{L^2(\Omega)} \\
&\qquad \le C\exp\left(\frac{C\delta_h^2 T}{(\max_{K\in\mathcal{T}_h}\lambda_{2,K})^2}\|\mathbf{u}\|_{L^\infty(\Omega\times(0,T))}\|\partial_t\mathbf{u}\|_{L^\infty(\Omega\times(0,T))}\right) \\
&(T\tau^4 + \delta_h\tau^4 + \delta_h^2\tau^2)\left(\int_0^T\left\|\frac{\partial^3\varphi}{\partial t^3}\right\|^2_{L^2(\Omega)} dt + \|\mathbf{u}\|^2_{L^\infty(\Omega\times(0,T))}\int_0^T\left\|\nabla\frac{\partial^2\varphi}{\partial t^2}\right\|^2_{L^2(\Omega)} dt\right).
\end{aligned} \tag{2.81}
$$

*Proof.* We note by $C$ any generic positive constant independent of the data, the mesh size and aspect ratio and the time step. Since $\varphi_h^n$ satisfies the numerical method, we have that

$$
\begin{aligned}
&\int_\Omega\left(\frac{e_h^{n+1}-e_h^n}{\tau^{n+1}} + \mathbf{u}(t^{n+1/2})\cdot\nabla\left(\frac{e_h^{n+1}+e_h^n}{2}\right)\right)(v_h + \delta_h\mathbf{u}(t^{n+1/2})\cdot\nabla v_h)d\mathbf{x} \\
&= \int_\Omega\left(\frac{\varphi(t^{n+1})-\varphi(t^n)}{\tau^{n+1}} + \mathbf{u}(t^{n+1/2})\cdot\nabla\left(\frac{\varphi(t^{n+1})+\varphi(t^n)}{2}\right)\right)(v_h + \delta_h\mathbf{u}(t^{n+1/2})\cdot\nabla v_h)d\mathbf{x}.
\end{aligned}
$$

Using the fact that $\varphi$ is the exact solution, one may write

$$\int_\Omega \left( \frac{e_h^{n+1} - e_h^n}{\tau^{n+1}} + \mathbf{u}(t^{n+1/2}) \cdot \nabla \left( \frac{e_h^{n+1} + e_h^n}{2} \right) \right) (v_h + \delta_h \mathbf{u}(t^{n+1/2}) \cdot \nabla v_h) d\mathbf{x}$$
$$= \int_\Omega \left( \partial_t \varphi(t^{n+1/2}) + \mathbf{u}(t^{n+1/2}) \cdot \nabla \varphi(t^{n+1/2}) \right) (v_h + \delta_h \mathbf{u}(t^{n+1/2}) \cdot \nabla v_h) d\mathbf{x}$$
$$+ \int_\Omega (r_1 + r_2)(v_h + \delta_h \mathbf{u}(t^{n+1/2}) \cdot \nabla v_h) d\mathbf{x}$$
$$= \int_\Omega (r_1 + r_2)(v_h + \delta_h \mathbf{u}(t^{n+1/2}) \cdot \nabla v_h) d\mathbf{x},$$

where

$$r_1 = \frac{\varphi(t^{n+1}) - \varphi(t^n)}{\tau^{n+1}} - \partial_t \varphi(t^{n+1/2}), \quad r_2 = \mathbf{u}(t^{n+1/2}) \cdot \nabla \left( \frac{\varphi(t^{n+1}) + \varphi(t^n)}{2} - \varphi(t^{n+1/2}) \right).$$

Observe that the following bounds holds (one may use several time the fundamental theorem of calculus or taylor expansion to prove them)

$$|r_1|^2 \leq (\tau^{n+1})^3 \int_{t^n}^{t^{n+1}} |\partial_{ttt} \varphi|^2 dt, \quad |r_2|^2 \leq (\tau^{n+1})^3 \|\mathbf{u}\|^2_{L^\infty(\Omega \times (0,T))} \int_{t^n}^{t^{n+1}} |\nabla \partial_{tt} \varphi|^2 dt.$$

The rest of the proof is exactly the same as the second part of Theorem 2.40. We choose

$$v_h = \frac{e_h^{n+1} + e_h^n}{2} + \delta_h \frac{e_h^{n+1} - e_h^n}{\tau^{n+1}}$$

as test function, and making the same computations as we did in Theorem 2.40, we derive that

$$\|e_h^N\|^2_{L^2(\Omega)} + \delta_h^2 \left\| \mathbf{u}(T) \cdot \nabla e_h^N \right\|^2_{L^2(\Omega)}$$
$$\leq C \exp \left( \frac{C \delta_h^2 T}{(\max_{K \in \mathcal{T}_h} \lambda_{2,K})^2} \|\mathbf{u}\|_{L^\infty(\Omega \times (0,T))} \|\partial_t \mathbf{u}\|_{L^\infty(\Omega \times (0,T))} \right)$$
$$\left( \sum_{n=0}^{N-1} \left( T \tau^{n+1} + \delta_h \tau^{n+1} + \frac{\delta_h^2 T}{\tau^{n+1}} \right) \|r_1^{n+1} + r_2^{n+1}\|^2_{L^2(\Omega)} \right).$$

We conclude by using the bounds on $r_1$ and $r_2$. □

**Remark 2.50.**
Observe that the proof of the Proposition 2.49 is formally the same as the second part of Theorem 2.40, the only difference being in the bounds of the two remainders $r_1$, $r_2$. Note indeed that in the Theorem 2.40 $r_1$ and $r_2$ contain the semi-discrete solution $\varphi_h(t)$ as in the Proposition 2.49 they contain the exact solution $\varphi$.

Combining Propositions 2.47 and 2.49, we can prove the following a priori error estimate.

**Theorem 2.51** (A fully discrete a priori error estimate for the transport equation with anisotropic finite elements and the Crank-Nicolson scheme in the case of a time dependent transport velocity field)**.**
*Assume that* $\mathbf{u}$ *is not identically zero. Asumme that the solution of (2.18)* $\varphi \in H^3(0,T;H^2(\Omega))$ *and let* $(\varphi_h^n)_{n=0}^N$ *be the solution of (2.60). Let* $\delta_h$ *be given by*

$$\delta_h = \frac{\max_{K \in \mathcal{T}_h} \lambda_{2,K}}{2\|\mathbf{u}\|_{L^\infty(\Omega \times (0,T))}}.$$

*Assume moreover that $\mathcal{T}_h$ satisfies the anisotropic quasi-uniformity condition: there exists $c > 0$, independent of the mesh geometry, in particular independent of the mesh size and the mesh aspect ratio such that*

$$\max_{K\in\mathcal{T}_h} \lambda_{2,K} \leq c\lambda_{2,K}, \quad \forall K \in \mathcal{T}_h.$$

*Let $e(t^n) = \varphi(t^n) - \varphi^n, n = 0, 1, 2, ..., N$. Then there exists a constant $C > 0$ which may depend only on the reference triangle $\hat{K}$, in particular which is independent of the mesh size and aspect ratio, the time step, $\varphi$ and the data of the problem, such that*

$$\begin{aligned}
&\|e(T)\|^2_{L^2(\Omega)} + \delta_h^2\|\mathbf{u}(T)\cdot\nabla e(T)\|^2_{L^2(\Omega)} \\
&\leq C\exp\left(C\frac{T\delta_h^2\|\mathbf{u}\|_{L^\infty(\Omega\times(0,T))}\|\partial_t\mathbf{u}\|_{L^\infty(\Omega\times(0,T))}}{(\max_{K\in\mathcal{T}_h}\lambda_{2,K})^2}\right)\Bigg(\|e_h(0)\|^2_{L^2(\Omega)} + \delta_h^2\|\mathbf{u}(0)\cdot\nabla e_h(0)\|^2_{L^2(\Omega)} \\
&+T\Bigg(\sum_{K\in\mathcal{T}_h}\left(\frac{1}{\delta_h} + \frac{\delta_h\|\mathbf{u}\|^2_{L^\infty(K\times(0,T))}}{\lambda^2_{2,K}} + \frac{T\delta_h^2\|\mathbf{u}\|_{L^\infty(\Omega\times(0,T))}\|\partial_t\mathbf{u}\|_{L^\infty(\Omega\times(0,T))}}{(\max_{K\in\mathcal{T}_h}\lambda_{2,K})^2}\right)\sup_{t\in(0,T)} L^2_K(\varphi) \\
&\qquad + \left(\delta_h + \frac{\delta_h^3\|\mathbf{u}\|^2_{L^\infty(K\times(0,T))}}{\lambda^2_{2,K}}\right)\sup_{t\in(0,T)} L^2_K\left(\frac{\partial\varphi}{\partial t}\right)\Bigg) \\
&+(T\tau^4 + \delta_h\tau^4 + \delta_h^2\tau^2)\left(\int_0^T\left\|\frac{\partial^3\varphi}{\partial t^3}\right\|^2_{L^2(\Omega)} dt + \|\mathbf{u}\|^2_{L^\infty(\Omega\times(0,T))}\int_0^T\left\|\nabla\frac{\partial^2\varphi}{\partial t^2}\right\|^2_{L^2(\Omega)} dt\right)\Bigg).
\end{aligned} \tag{2.82}$$

*Proof.* The proof is straightforward, setting

$$e(T) = e(t^N) = \varphi(t^N) - \varphi_h^N = \varphi(t^N) - \Pi_h^{iter}\varphi(t^N) + \Pi_h^{iter}\varphi(t^N) - \varphi_h^N = e_h(t^N) + e_h^N$$

and using the triangle inequality to write

$$\begin{aligned}
&\|e(T)\|^2_{L^2(\Omega)} + \delta_h^2\|\mathbf{u}(T)\cdot\nabla e(T)\|^2_{L^2(\Omega)} \\
&\qquad \leq 2\|e_h(T)\|^2_{L^2(\Omega)} + 2\delta_h^2\|\mathbf{u}(T)\cdot\nabla e_h(T)\|^2_{L^2(\Omega)} \\
&\qquad\qquad + 2\|e_h^N\|^2_{L^2(\Omega)} + 2\delta_h^2\|\mathbf{u}(T)\cdot\nabla e_h^N\|^2_{L^2(\Omega)}.
\end{aligned}$$

We then apply the Proposition 2.47 to bound the first line of the right hand side and the Proposition 2.49 for the second one. □

**Remark 2.52.**
We briefly make some final comments on the IHRP (Definition 2.42).

(i) The use of the IHRP to prove the final a priori error estimate can be trivially adapted to the case of a non depending in time $\mathbf{u}$. Moreover, the technique can be adapted to the case of other PDEs with time variable coefficients (such as parabolic equations).

(ii) Note that the proof of Theorem 2.51 is quite easy and direct, and formally the same of the Theorem 2.40.

(iii) The main difference between Theorem 2.40 and Theorem 2.51 is that in the first one, we cut the error as

$$e(t) = \varphi(t^n) - \varphi_h(t^n) + \varphi_h(t^n) - \varphi_h^n$$

rather in the second we use $\Pi_h^{iter}\varphi(t^n)$ instead. Roughly speaking, in Theorem 2.40 we first project $\varphi$ into $V_h$ through the semi-discrete approximation in space, and then we apply the time discretization to $\varphi_h$. In Theorem 2.51, we somewhere proceed in the other direction, first applying the time discretization to $\varphi$ (see the contruction of the IHRP), and projecting this discrete equation in time into $V_h$ (in fact, as already commented, projecting the consistency error).

(iv) As already explained, if we use the classical HRP, rather than the IHRP, then since $\mathbf{u}$ depends on the time, then we have to take in account the difference

$$\Pi_{h,t^2}^{hyp} - \Pi_{h,t^1}^{hyp}, \quad t^1 \neq t^2$$

in the estimate, yielding terms going as $|t^1 - t^2|$, which are then only of order one in time. So the idea behing the IHRP is that rather than we keep a time derivative to estimate (formally the time derivative of $\Pi_{h,t}^{hyp}$), we include this derivative into the projection by putting the discrete derivative

$$\frac{\varphi(t^{n+1}) - \varphi(t^n)}{\tau^{n+1}}$$

in the right hand side of (2.79).

#### A posteriori error estimate for the fully discrete approximation

We now present an a posteriori error analysis for the method (2.60). In this framework, the stabilization parameter is not kept constant and can vary in space as in time. The scheme (2.60) is then replaced by

$$\int_\Omega \left( \frac{\varphi_h^{n+1} - \varphi_h^n}{\tau^{n+1}} + \mathbf{u}(t^{n+1/2}) \cdot \nabla \left( \frac{\varphi_h^{n+1} + \varphi_h^n}{2} \right) \right) (v_h + \delta_h(t^{n+1/2}) \mathbf{u}(t^{n+1/2}) \cdot \nabla v_h) d\mathbf{x} = 0, \forall v_h \in V_h, \quad (2.83)$$

where we define, for all $t \in [0, T]$, $\delta_h(t)$ by

$$\delta_{h|K}(t) = \frac{\lambda_{2,K}}{2 \, \|\mathbf{u}(t)\|_{L^\infty(K)}}, \qquad \forall K \in \mathcal{T}_h \text{ such that } \mathbf{u}(t) \text{ is not indentically zero on } K, \quad (2.84)$$

and by $\delta_{h|K} = 0$ otherwise. To derive an a posteriori error estimate for the method (2.83), the main task consists to adapt the Proposition 2.28 to the case of a time dependent velocity field. Then, the proof of an a posteriori upper bound for the numerical error is straightforward reproducing the proof of Theorem 2.29. As for the steady transport velocity case, the idea to find a good time error indicator $\theta_n$ is to reconstruct the numerical solution using the Definition 2.48 and to plug this later into the PDE and to compute the remainder. Then, using the notations introduced in (2.47) the following Proposition can be proven

**Proposition 2.53** (An error indicator for the Crank-Nicolson method applied to the transport equation with a time dependent velocity field)**.**
*Let $(\varphi_h^n)_{n=0}^N$ be the solution of (2.83). Let $\varphi_{h\tau}$ be the numerical reconstruction (2.48)-(2.49). For $0 \leq n \leq N-1$. For all $v_h \in V_h$ and for all $t \in (t^n, t^{n+1})$, we have*

$$\int_\Omega \left( \frac{\partial \varphi_{h\tau}}{\partial t} + \mathbf{u}(t) \cdot \nabla \varphi_{h\tau} \right) (v_h + \delta_h(t) \mathbf{u}(t) \cdot \nabla v_h) d\mathbf{x} = \int_\Omega \theta_n (v_h + \delta_h(t) \mathbf{u}(t) \cdot \nabla v_h) d\mathbf{x} + \int_\Omega \boldsymbol{\zeta}_n \cdot \nabla v_h d\mathbf{x},$$

*where* $\theta_n$ *is given for* $n \geq 1$ *by*

$$\theta_n = \left(\frac{\tau^n}{2}(t - t^{n+1/2}) + \frac{1}{2}(t - t^n)(t - t^{n+1})\right)\mathbf{u}(t)\cdot\nabla\partial^2\varphi_h^{n+1}$$
$$+ (t - t^{n+1/2})(\mathbf{u}(t) - \mathbf{u}(t^{n-1/2}))\cdot\nabla\left(\frac{\varphi_h^{n+1} - \varphi_h^{n-1}}{\tau^{n+1}+\tau^n}\right)$$
$$+\left(\mathbf{u}(t) - \mathbf{u}(t^{n+1/2}) - (t - t^{n+1/2})\frac{\mathbf{u}(t^{n+1/2}) - \mathbf{u}(t^{n-1/2})}{\tau^{n+1}+\tau^n/2}\right)\cdot\nabla\varphi_h^{n+1/2}, \quad (2.85)$$

*and for* $n = 0$ *by*

$$\theta_0 = (t - t^{1/2})\mathbf{u}(t)\cdot\nabla\partial\varphi_h^1 + (\mathbf{u}(t) - \mathbf{u}(t^{1/2}))\cdot\nabla\varphi_h^{1/2}, \quad (2.86)$$

*and* $\boldsymbol{\zeta}_n$ *is given for* $n \geq 1$ *by*

$$\boldsymbol{\zeta}_n = \left(\partial\varphi_h^{n+1} + \mathbf{u}(t^{n+1/2})\cdot\nabla\varphi_h^{n+1/2}\right)$$
$$\left(\delta_h(t)\mathbf{u}(t) - \delta_h(t^{n+1/2})\mathbf{u}(t^{n+1/2}) - (t - t^{n+1/2})\frac{\delta_h(t^{n+1/2})\mathbf{u}(t^{n+1/2}) - \delta_h(t^{n-1/2})\mathbf{u}(t^{n-1/2})}{\tau^{n+1}+\tau^n/2}\right)$$
$$+(t-t^{n+1/2})\left(\partial^2\varphi_h^{n+1} + \frac{\mathbf{u}(t^{n+1/2})\cdot\nabla\varphi_h^{n+1/2} - \mathbf{u}(t^{n-1/2})\cdot\nabla\varphi_h^{n-1/2}}{\tau^{n+1}+\tau^n/2}\right)(\delta_h(t)\mathbf{u}(t) - \delta_h(t^{n-1/2})\mathbf{u}(t^{n-1/2})), \quad (2.87)$$

*and for* $n = 0$ *by*

$$\boldsymbol{\zeta}_0 = \left(\partial\varphi_h^1 + \mathbf{u}(t^{1/2})\cdot\nabla\varphi_h^{1/2}\right)(\delta_h(t)\mathbf{u}(t) - \delta_h(t^{1/2})\mathbf{u}(t^{1/2})). \quad (2.88)$$

**Remark 2.54** (Optimality of the local time error indicator)**.** (i) Assuming that $\mathbf{u}$ is two times continuously differentiable in time, then, writing $\mathbf{u} = (u_1, u_2)$, for every component $i = 1, 2$, we can write by Taylor expansion

$$u_i(t) - u_i(t^{n-1/2}) = (t - t^{n-1/2})\frac{\partial u_i(\bar{t})}{\partial t}, \bar{t} \in (t^{n-1/2}, t) \text{ or } \bar{t} \in (t, t^{n-1/2}),$$

and

$$\mathbf{u}(t) - \mathbf{u}(t^{n+1/2}) - (t - t^{n+1/2})\frac{\mathbf{u}(t^{n+1/2}) - \mathbf{u}(t^{n-1/2})}{\tau^{n+1}+\tau^n/2}$$
$$= (t - t^{n+1/2})^2\frac{\partial^2 u_i(\tilde{t})}{\partial t^2}, \tilde{t} \in (t^{n+1/2}, t) \text{ or } \tilde{t} \in (t, t^{n+1/2}).$$

Therefore, roughly speaking, $\theta_n$ (for $n \geq 1$) is approximatively given by

$$\theta_n \simeq \tau^2\mathbf{u}\cdot\nabla\partial_{tt}\varphi_{h\tau} + \tau^2\partial_t\mathbf{u}\cdot\nabla\partial_t\varphi_{h\tau} + \tau^2\partial_{tt}\mathbf{u}\cdot\nabla\varphi_{h\tau}.$$

For the same reason, we can approximate $\boldsymbol{\zeta}_n$ (for $n \geq 1$) by

$$\boldsymbol{\zeta}_n \simeq \tau^2(\partial_t\varphi_{h\tau} + \mathbf{u}\cdot\nabla\varphi_{h\tau})\partial_{tt}(\delta_h\mathbf{u}) + \tau^2(\partial_{tt}\varphi_{h\tau} + \mathbf{u}\cdot\nabla\partial_t\varphi_{h\tau})\partial_t(\delta_h\mathbf{u}).$$

Then, $\theta_n$ is $O(\tau^2)$ and, since $\delta_h \simeq h$, $\boldsymbol{\zeta}_n$ is $O(h\tau^2)$. Thus, we conclude that $\theta_n$ achieves the optimal order and that $\boldsymbol{\zeta}_n$ is of higher order.

(ii) Note that if $\mathbf{u}$ is independent of the time, then $\boldsymbol{\zeta}_n = 0, n = 0, 1, 2, ..., N-1$, and $\theta_n$ reduces to the time error indicator given in Proposition 2.28.

*Proof.* Let $n \geq 1$ and $t \in (t^n, t^{n+1})$. We compute

$$\int_\Omega \left( \frac{\partial \varphi_{h\tau}}{\partial t} + \mathbf{u}(t) \cdot \nabla \varphi_{h\tau} \right) (v_h + \delta_h(t)\mathbf{u}(t) \cdot \nabla v_h) d\mathbf{x} = I_1 + I_2 + I_3,$$

where

$$\begin{aligned} I_1 &= \int_\Omega (\partial \varphi_h^{n+1} + \mathbf{u}(t) \cdot \nabla \varphi_h^{n+1/2})(v_h + \delta_h(t)\mathbf{u}(t) \cdot \nabla v_h) d\mathbf{x}, \\ I_2 &= (t - t^{n+1/2}) \int_\Omega (\partial^2 \varphi_h^{n+1} + \mathbf{u}(t) \cdot \nabla \partial \varphi_h^{n+1})(v_h + \delta_h(t)\mathbf{u}(t) \cdot \nabla v_h) d\mathbf{x}, \\ I_3 &= \frac{1}{2}(t - t^n)(t - t^{n+1}) \int_\Omega \mathbf{u}(t) \cdot \nabla \partial^2 \varphi_h^{n+1} (v_h + \delta_h(t)\mathbf{u}(t) \cdot \nabla v_h) d\mathbf{x}. \end{aligned}$$

Observe that $I_3$ is already a quantity of order two in time. To treat $I_1$ and $I_2$, we follow the steps proposed in the Proposition 2.8 for ODEs with time dependent coefficients. It consists to add zero in a suitable way to make the numerical method (2.83) appears. A straightforward computation yields that

$$\begin{aligned} I_1 = &\int_\Omega (\partial \varphi_h^{n+1} + \mathbf{u}(t^{n+1/2}) \cdot \nabla \varphi_h^{n+1/2})(v_h + \delta_h(t^{n+1/2})\mathbf{u}(t^{n+1/2}) \cdot \nabla v_h) d\mathbf{x} \\ &+ \int_\Omega (\mathbf{u}(t) - \mathbf{u}(t^{n+1/2})) \cdot \nabla \varphi_h^{n+1/2} (v_h + \delta_h(t)\mathbf{u}(t) \cdot \nabla v_h) d\mathbf{x} \\ &+ \int_\Omega (\partial \varphi_h^{n+1} + \mathbf{u}(t^{n+1/2}) \cdot \nabla \varphi_h^{n+1/2})(\delta_h(t)\mathbf{u}(t) - \delta_h(t^{n+1/2})\mathbf{u}(t^{n+1/2})) \cdot \nabla v_h d\mathbf{x} \\ = &\int_\Omega (\mathbf{u}(t) - \mathbf{u}(t^{n+1/2})) \cdot \nabla \varphi_h^{n+1/2} (v_h + \delta_h(t)\mathbf{u}(t) \cdot \nabla v_h) d\mathbf{x} \\ &+ \int_\Omega (\partial \varphi_h^{n+1} + \mathbf{u}(t^{n+1/2}) \cdot \nabla \varphi_h^{n+1/2})(\delta_h(t)\mathbf{u}(t) - \delta_h(t^{n+1/2})\mathbf{u}(t^{n+1/2})) \cdot \nabla v_h d\mathbf{x}. \end{aligned}$$

To treat $I_2$, we first have to compute the difference between the method at two successive steps, that is to say

$$\begin{aligned} &\int_\Omega \left( \frac{\varphi_h^{n+1} - \varphi_h^n}{\tau^{n+1}} + \mathbf{u}(t^{n+1/2}) \cdot \nabla \left( \frac{\varphi_h^{n+1} + \varphi_h^n}{2} \right) \right) (v_h + \delta_h(t^{n+1/2})\mathbf{u}(t^{n+1/2}) \cdot \nabla v_h) d\mathbf{x} \\ - &\int_\Omega \left( \frac{\varphi_h^n - \varphi_h^{n-1}}{\tau^n} + \mathbf{u}(t^{n-1/2}) \cdot \nabla \left( \frac{\varphi_h^n + \varphi_h^{n-1}}{2} \right) \right) (v_h + \delta_h(t^{n-1/2})\mathbf{u}(t^{n-1/2}) \cdot \nabla v_h) d\mathbf{x} = 0. \end{aligned}$$

Dividing by ${\tau^{n+1}+\tau^n}/2$ and rewriting the last equality, we obtain that

$$\begin{aligned} &\int_\Omega \left( \partial^2 \varphi_h^{n+1} + \mathbf{u}(t) \cdot \nabla \left( \frac{\varphi_h^{n+1} - \varphi_h^{n-1}}{\tau^{n+1} + \tau^n} \right) \right) (v_h + \delta_h(t)\mathbf{u}(t) \cdot \nabla v_h) d\mathbf{x} \\ = &\frac{1}{{\tau^{n+1}+\tau^n}/2} \int_\Omega \left( (\mathbf{u}(t) - \mathbf{u}(t^{n+1/2})) \cdot \nabla \left( \frac{\varphi_h^{n+1} + \varphi_h^n}{2} \right) - (\mathbf{u}(t) - \mathbf{u}(t^{n-1/2})) \cdot \nabla \left( \frac{\varphi_h^n + \varphi_h^{n-1}}{2} \right) \right) \\ &\qquad (v_h + \delta_h(t)\mathbf{u}(t) \cdot \nabla v_h) d\mathbf{x} \\ + &\frac{1}{{\tau^{n+1}+\tau^n}/2} \int_\Omega \left( \frac{\varphi_h^{n+1} - \varphi_h^n}{\tau^{n+1}} + \mathbf{u}(t^{n+1/2}) \cdot \nabla \left( \frac{\varphi_h^{n+1} + \varphi_h^n}{2} \right) \right) (\delta_h(t)\mathbf{u}(t) - \delta_h(t^{n+1/2})\mathbf{u}(t^{n+1/2})) \cdot \nabla v_h d\mathbf{x} \\ + &\frac{1}{{\tau^{n+1}+\tau^n}/2} \int_\Omega \left( \frac{\varphi_h^n - \varphi_h^{n-1}}{\tau^{n+1}} + \mathbf{u}(t^{n-1/2}) \cdot \nabla \left( \frac{\varphi_h^n + \varphi_h^{n-1}}{2} \right) \right) (\delta_h(t)\mathbf{u}(t) - \delta_h(t^{n-1/2})\mathbf{u}(t^{n-1/2})) \cdot \nabla v_h d\mathbf{x} \end{aligned}$$

Using again the trick

$$\frac{\varphi_h^{n+1} - \varphi_h^n}{\tau^{n+1} + \tau^n} = \frac{\varphi^{n+1} - \varphi_h^n}{\tau^{n+1}} - \frac{\tau^n}{2} \partial^2 \varphi_h^{n+1}$$

we get therefore

$$\int_\Omega \left(\partial^2\varphi_h^{n+1} + \mathbf{u}(t)\cdot\nabla\partial\varphi_h^{n+1}\right)(v_h + \delta_h(t)\mathbf{u}(t)\cdot\nabla v_h)d\mathbf{x}$$
$$= \frac{\tau^n}{2}\int_\Omega \mathbf{u}(t)\nabla\partial^2\varphi_h^{n+1}(v_h + \delta_h(t)\mathbf{u}(t)\cdot\nabla v_h)d\mathbf{x}$$
$$\frac{1}{\tau^{n+1}+\tau^n/2}\int_\Omega \left((\mathbf{u}(t)-\mathbf{u}(t^{n+1/2}))\cdot\nabla\left(\frac{\varphi_h^{n+1}+\varphi_h^n}{2}\right) - (\mathbf{u}(t)-\mathbf{u}(t^{n-1/2}))\cdot\nabla\left(\frac{\varphi_h^{n}+\varphi_h^{n-1}}{2}\right)\right)$$
$$(v_h + \delta_h(t)\mathbf{u}(t)\cdot\nabla v_h)d\mathbf{x}$$
$$+\frac{1}{\tau^{n+1}+\tau^n/2}\int_\Omega \left(\frac{\varphi_h^{n+1}-\varphi_h^n}{\tau^{n+1}} + \mathbf{u}(t^{n+1/2})\cdot\nabla\left(\frac{\varphi_h^{n+1}+\varphi_h^n}{2}\right)\right)(\delta_h(t)\mathbf{u}(t)-\delta_h(t^{n+1/2})\mathbf{u}(t^{n+1/2}))\cdot\nabla v_h d\mathbf{x}$$
$$+\frac{1}{\tau^{n+1}+\tau^n/2}\int_\Omega \left(\frac{\varphi_h^{n}-\varphi_h^{n-1}}{\tau^{n+1}} + \mathbf{u}(t^{n-1/2})\cdot\nabla\left(\frac{\varphi_h^{n}+\varphi_h^{n-1}}{2}\right)\right)(\delta_h(t)\mathbf{u}(t)-\delta_h(t^{n-1/2})\mathbf{u}(t^{n-1/2}))\cdot\nabla v_h d\mathbf{x}$$

yielding for $I_2$ the following expression

$$I_2 = \frac{\tau^n}{2}(t-t^{n+1/2})\int_\Omega \mathbf{u}(t)\nabla\partial^2\varphi_h^{n+1}(v_h + \delta_h(t)\mathbf{u}(t)\cdot\nabla v_h)d\mathbf{x}$$
$$\frac{t-t^{n+1/2}}{\tau^{n+1}+\tau^n/2}\int_\Omega \left((\mathbf{u}(t)-\mathbf{u}(t^{n+1/2}))\cdot\nabla\left(\frac{\varphi_h^{n+1}+\varphi_h^n}{2}\right) - (\mathbf{u}(t)-\mathbf{u}(t^{n-1/2}))\cdot\nabla\left(\frac{\varphi_h^{n}+\varphi_h^{n-1}}{2}\right)\right)$$
$$(v_h + \delta_h(t)\mathbf{u}(t)\cdot\nabla v_h)d\mathbf{x}$$
$$+\frac{t-t^{n+1/2}}{\tau^{n+1}+\tau^n/2}\int_\Omega \left(\frac{\varphi_h^{n+1}-\varphi_h^n}{\tau^{n+1}} + \mathbf{u}(t^{n+1/2})\cdot\nabla\left(\frac{\varphi_h^{n+1}+\varphi_h^n}{2}\right)\right)(\delta_h(t)\mathbf{u}(t)-\delta_h(t^{n+1/2})\mathbf{u}(t^{n+1/2}))\cdot\nabla v_h d\mathbf{x}$$
$$+\frac{t-t^{n+1/2}}{\tau^{n+1}+\tau^n/2}\int_\Omega \left(\frac{\varphi_h^{n}-\varphi_h^{n-1}}{\tau^{n+1}} + \mathbf{u}(t^{n-1/2})\cdot\nabla\left(\frac{\varphi_h^{n}+\varphi_h^{n-1}}{2}\right)\right)(\delta_h(t)\mathbf{u}(t)-\delta_h(t^{n-1/2})\mathbf{u}(t^{n-1/2}))\cdot\nabla v_h d\mathbf{x}.$$

Adding and subtracting the terms

$$\frac{t-t^{n+1/2}}{\tau^{n+1}+\tau^n/2}\int_\Omega (\mathbf{u}(t)-\mathbf{u}(t^{n-1/2}))\cdot\nabla\varphi_h^{n+1/2}(v_h + \delta_h(t)\mathbf{u}(t)\cdot\nabla v_h)d\mathbf{x}$$

and

$$\frac{t-t^{n+1/2}}{\tau^{n+1}+\tau^n/2}\int_\Omega \left(\frac{\varphi_h^{n+1}-\varphi_h^n}{\tau^{n+1}} + \mathbf{u}(t^{n+1/2})\cdot\nabla\left(\frac{\varphi_h^{n+1}+\varphi_h^n}{2}\right)\right)(\delta_h(t)\mathbf{u}(t)-\delta_h(t^{n-1/2})\mathbf{u}(t^{n-1/2}))\cdot\nabla v_h d\mathbf{x}$$

we get as final expression for $I_2$

$$I_2 = \frac{\tau^n}{2}(t-t^{n+1/2})\int_\Omega \mathbf{u}(t)\nabla\partial^2\varphi_h^{n+1}(v_h + \delta_h(t)\mathbf{u}(t)\cdot\nabla v_h)d\mathbf{x}$$
$$+ (t-t^{n+1/2})\int_\Omega (\mathbf{u}(t)-\mathbf{u}(t^{n-1/2}))\cdot\nabla\left(\frac{\varphi_h^{n+1}-\varphi_h^{n-1}}{\tau^{n+1}+\tau^n}\right)(v_h + \delta_h(t)\mathbf{u}(t)\cdot\nabla v_h)d\mathbf{x}$$
$$- (t-t^{n+1/2})\int_\Omega \frac{\mathbf{u}(t^{n+1/2})-\mathbf{u}(t^{n-1/2})}{\tau^{n+1}+\tau^n/2}\cdot\nabla\varphi_h^{n+1/2}(v_h + \delta_h(t)\mathbf{u}(t)\cdot\nabla v_h)d\mathbf{x}$$
$$+ (t-t^{n+1/2})\int_\Omega \partial^2\varphi_h^{n+1}(\delta_h(t)\mathbf{u}(t)-\delta_h(t^{n-1/2})\mathbf{u}(t^{n-1/2}))\cdot\nabla v_h d\mathbf{x}$$
$$+(t-t^{n+1/2})\int_\Omega \frac{\mathbf{u}(t^{n+1/2})\cdot\nabla\varphi_h^{n+1/2}-\mathbf{u}(t^{n-1/2})\cdot\nabla\varphi_h^{n-1/2}}{\tau^{n+1}+\tau^n/2}(\delta_h(t)\mathbf{u}(t)-\delta_h(t^{n-1/2})\mathbf{u}(t^{n-1/2}))\cdot\nabla v_h d\mathbf{x}$$
$$-(t-t^{n+1/2})\int_\Omega \left(\partial\varphi_h^{n+1} + \mathbf{u}(t^{n+1/2})\cdot\nabla\varphi_h^{n+1/2}\right)\frac{\delta_h(t^{n+1/2})\mathbf{u}(t^{n+1/2})-\delta_h(t^{n-1/2})\mathbf{u}(t^{n-1/2})}{\tau^{n+1}+\tau^n/2}\cdot\nabla v_h d\mathbf{x}.$$

Combining the expressions for $I_1$, $I_2$ and $I_3$ yields the result for $n \geq 1$.

Finally, for $n = 0$, reproducing the steps using to compute $I_1$ here above yields that

$$\begin{aligned}
&\int_\Omega \left(\frac{\partial \varphi_{h\tau}}{\partial t} + \mathbf{u}(t)\cdot\nabla\varphi_{h\tau}\right)(v_h + \delta_h(t)\mathbf{u}(t)\cdot\nabla v_h)d\mathbf{x} \\
&= (t - t^{1/2})\int_\Omega \mathbf{u}(t)\cdot\nabla\partial\varphi_h^1(v_h + \delta_h(t)\mathbf{u}(t)\cdot\nabla v_h)d\mathbf{x} + \int_\Omega (\mathbf{u}(t) - \mathbf{u}(t^{1/2}))\cdot\nabla\varphi_h^{1/2}(v_h + \delta_h(t)\mathbf{u}(t)\cdot\nabla v_h)d\mathbf{x} \\
&\quad + \int_\Omega \left(\frac{\varphi_h^1 - \varphi_h^0}{\tau^1} + \mathbf{u}(t^{1/2})\cdot\nabla\varphi_h^{1/2}\right)(\delta_h(t)\mathbf{u}(t) - \delta_h(t^{1/2})\mathbf{u}(t^{1/2}))\cdot\nabla v_h d\mathbf{x}.
\end{aligned}$$

□

**Theorem 2.55** (An a posteriori error estimate for the transport equation with anisotropic finite elements and the Crank-Nicolson scheme with a time dependent velocity field)**.** *Assume that $\varphi \in L^2(0,T;H^1(\Omega)) \cap H^1(0,T;L^2(\Omega))$ where $\varphi$ is the solution of (2.18). Let $\delta_h$ be given by (2.84), $(\varphi_h^n)_{n=0}^N$ be the solution of (2.83) and consider $\varphi_{h\tau}$ the numerical reconstruction given in Definition 2.27. Setting $e = \varphi - \varphi_{h\tau}$, there exists $C > 0$ independent of $T, \Omega, \mathbf{u}, \varphi$, the mesh size and aspect ratio and the time step such that*

$$\begin{aligned}
\|e(T)\|^2_{L^2(\Omega)} \leq C\Bigg(\|e(0)\|^2_{L^2(\Omega)} + \sum_{n=0}^{N-1}\sum_{K\in\mathcal{T}_h}\int_{t^n}^{t^{n+1}} \Bigg(\left\|\frac{\partial\varphi_{h\tau}}{\partial t} + \mathbf{u}(t)\cdot\nabla\varphi_{h\tau}\right\|_{L^2(K)}\omega_K(e) \\
+ c_n\|\theta_n\|^2_{L^2(K)}\Bigg)dt\Bigg) \\
+ C\sum_{n=0}^{N-1}\sum_{K\in\mathcal{T}_h}\int_{t^n}^{t^{n+1}}\left(c_n\|\boldsymbol{\zeta}_n\|^2_{L^2(K)} + c_n^{-1}\omega_K^2(e)\right)dt, \quad (2.89)
\end{aligned}$$

*where $\omega_K$ is the anisotropic gradient norm defined by (1.4) , $\theta_n, \boldsymbol{\zeta}_n$ are defined in Proposition 2.53 and* $c_n = \begin{cases} \tau^1, & n = 0, \\ T - \tau^1, & n \geq 1. \end{cases}$

*Proof.* In the following, we denote by $C$ any positive constant, which may depend only on the reference triangle and may change from line to line. In particular, $C$ is independent of $T$, $\Omega$,$\mathbf{u}$, $\varphi$, the mesh size, aspect ratio and the time step. Let $t \in (t^n, t^{n+1})$, $n \geq 1$. As before, one can prove that

$$\int_\Omega (\mathbf{u}(t)\cdot\nabla e)e d\mathbf{x} \geq 0.$$

Therefore, it holds, since $e = \varphi - \varphi_{h\tau}$ and $\varphi$ is the exact solution to the transport equation,

$$\frac{1}{2}\frac{d}{dt}\int_\Omega e^2 dx \leq \int_\Omega \left(\frac{\partial e}{\partial t}e + (\mathbf{u}(t)\cdot\nabla e)e\right)d\mathbf{x} = -\int_\Omega\left(\frac{\partial\varphi_{h\tau}}{\partial t} + \mathbf{u}(t)\cdot\nabla\varphi_{h\tau}\right)e d\mathbf{x}.$$

By subtracting any $v_h + \delta_h(t)\mathbf{u}(t)\cdot\nabla v_h$ and using Proposition 2.53, we have finally

$$\begin{aligned}
\frac{1}{2}\frac{d}{dt}\int_\Omega e^2 dx &\leq -\int_\Omega\left(\frac{\partial\varphi_{h\tau}}{\partial t} + \mathbf{u}(t)\cdot\nabla\varphi_{h\tau}\right)(e - v_h - \delta_h(t)\mathbf{u}(t)\cdot\nabla v_h)d\mathbf{x} \\
&\quad - \int_\Omega \theta_n(v_h + \delta_h(t)\mathbf{u}(t)\cdot\nabla v_h)d\mathbf{x} - \int_\Omega \boldsymbol{\zeta}_n\cdot\nabla v_h d\mathbf{x} \\
&= -\int_\Omega\left(\frac{\partial\varphi_{h\tau}}{\partial t} + \mathbf{u}(t)\cdot\nabla\varphi_{h\tau} + \theta_n\right)(e - v_h - \delta_h(t)\mathbf{u}(t)\cdot\nabla v_h)d\mathbf{x} \\
&\quad - \int_\Omega \theta_n e d\mathbf{x} - \int_\Omega \boldsymbol{\zeta}_n\cdot\nabla v_h d\mathbf{x}
\end{aligned}$$

Separating the last inequality into a sum over the triangles, and using the triangle and Cauchy-Schwarz inequalities yield

$$\frac{1}{2}\frac{d}{dt}\int_\Omega e^2 dx \leq$$
$$\sum_{K\in\mathcal{T}_h}\left(\left\|\frac{\partial\varphi_{h\tau}}{\partial t}+\mathbf{u}(t)\cdot\nabla\varphi_{h\tau}\right\|_{L^2(K)}+\|\theta_n\|_{L^2(K)}\right)\left(\|e-v_h\|_{L^2(K)}+\|\delta_{h|K}(t)\mathbf{u}(t)\cdot\nabla v_h\|_{L^2(K)}\right)$$
$$+\sum_{K\in\mathcal{T}_h}\|\theta_n\|_{L^2(K)}\|e\|_{L^2(K)}+\sum_{K\in\mathcal{T}_h}\|\boldsymbol{\zeta}_n\|_{L^2(K)}\|\nabla v_h\|_{L^2(K)}.$$

We now choose $v_h = R_h e$ where we recall that $R_h$ stands for the Clément's interpolant and we proceed as in the proof of Theorem 2.29. Using the anisotropic interpolation error estimate (1.3), we can prove that

$$\|\nabla R_h e\|_{L^2(K)} \leq C\frac{\omega_K(e)}{\lambda_{2,K}}.$$

Indeed, we have

$$\|\nabla R_h e\|_{L^2(K)} \leq \|\nabla(e-R_h e)\|_{L^2(K)}+\|\nabla e\|_{L^2(K)}$$
$$\leq C\frac{\omega_K(e)}{\lambda_{2,K}}+\|\nabla e\|_{L^2(\Delta K)} = C\frac{\omega_K(e)}{\lambda_{2,K}}+\frac{\lambda_{2,K}\|\nabla e\|_{L^2(\Delta K)}}{\lambda_{2,K}}.$$

Using that $\nabla e = (\nabla e\cdot\mathbf{r}_{1,K})\mathbf{r}_{1,K}+(\nabla e\cdot\mathbf{r}_{2,K})\mathbf{r}_{2,K})$ and

$$\|\nabla e\cdot\mathbf{r}_{i,K}\|^2_{L^2(\Delta K)} = \mathbf{r}^T_{i,K}G_K(e)\mathbf{r}_{i,K},\quad i=1,2,$$

implies that

$$\lambda_{2,K}\|\nabla e\|_{L^2(\Delta K)} \leq \omega_K(e)$$

which yields the desired estimate. In the same manner, using the definition of $\delta_{h|K}(t)$, we can prove that (see Theorem 2.29 when similar computations are presented)

$$\|e-R_h e\|_{L^2(K)}+\|\delta_{h|K}(t)\mathbf{u}(t)\cdot\nabla R_h e\|_{L^2(K)} \leq C\omega_K(e).$$

So we obtain that

$$\frac{1}{2}\frac{d}{dt}\int_\Omega e^2 dx \leq C\sum_{K\in\mathcal{T}_h}(\alpha_K+\theta_K+\zeta_K)\omega_K(e)+\sum_{K\in\mathcal{T}_h}\theta_K\|e\|_{L^2(K)}$$

where we note

$$\alpha_K = \left\|\frac{\partial\varphi_{h\tau}}{\partial t}+\mathbf{u}(t)\cdot\nabla\varphi_{h\tau}\right\|_{L^2(K)},\quad \theta_K = \|\theta_n\|_{L^2(K)},\quad \text{and } \zeta_K = \|\boldsymbol{\zeta}_n\|_{L^2(K)}.$$

The discrete Cauchy-Schwarz implies then that

$$\frac{1}{2}\frac{d}{dt}\int_\Omega e^2 dx \leq C\sum_{K\in\mathcal{T}_h}(\alpha_K+\theta_K+\zeta_K)\omega_K(e)+\left(\sum_{K\in\mathcal{T}_h}\theta_K^2\right)^{1/2}\|e\|_{L^2(\Omega)}.$$

Using the Theorem A.3 between $t^1$ and $T$ yields

$$\|e(T)\|^2_{L^2(\Omega)} \leq C\left(\|e(t^1)\|^2_{L^2(\Omega)}+\sum_{n=1}^{N-1}\sum_{K\in\mathcal{T}_h}\int_{t^n}^{t^{n+1}}\left((\alpha_K+\theta_K+\zeta_K)\omega_K(e)+(T-t^1)\theta_K^2\right)dt\right).$$

Proceeding in the same manner we can obtain an estimate for $\|e(t^1)\|^2_{L^2(\Omega)}$

$$\|e(t^1)\|^2_{L^2(\Omega)} \le C\left(\|e(0)\|^2_{L^2(\Omega)} + \sum_{K\in\mathcal{T}_h}\int_0^{t^1}\left(\alpha_K + \theta_K + \zeta_K)\omega_K(e) + \tau^1\theta_K^2\right)dt\right).$$

Combining both estimates yields

$$\|e(T)\|^2_{L^2(\Omega)} \le C\Bigg(\|e(0)\|^2_{L^2(\Omega)}$$
$$+\sum_{n=0}^{N-1}\sum_{K\in\mathcal{T}_h}\int_{t^n}^{t^{n+1}}\left(\left(\left\|\frac{\partial\varphi_{h\tau}}{\partial t}+\mathbf{u}\cdot\nabla\varphi_{h\tau}\right\|_{L^2(K)} + \|\theta_n\|_{L^2(K)} + \|\boldsymbol{\zeta}_n\|_{L^2(K)}\right)\omega_K(e) + c_n\|\theta_n\|^2_{L^2(K)}\right)\Bigg)dt.$$

Finally, thanks to Young's inequality, it holds for all $n$

$$\int_{t^n}^{t^{n+1}}(\|\theta_n\|_{L^2(K)}+\|\boldsymbol{\zeta}_n\|_{L^2(K)})\omega_K(e)dt \le C\left(c_n\int_{t^n}^{t^{n+1}}\|\theta_n\|^2_{L^2(K)} + \|\boldsymbol{\zeta}_n\|^2_{L^2(K)}dt + c_n^{-1}\int_{t^n}^{t^{n+1}}\omega_K^2(e)dt\right),$$

which yields the desired final estimate. □

**Remark 2.56.** (i) As already mentioned several times, the a posteriori error estimate (2.89) is not standard since the numerical error $e$ is contained in the estimate. Post-processing techniques (as the ZZ post-processing, see Remark 2.30) are used to obtain a computable upper bound.

(ii) Observe that if $\mathbf{u}$ is independent of the time, then due to definitions of $\theta_n$ and $\boldsymbol{\zeta}_n$, the a posteriori error estimate (2.89) reduces to (2.52).

(iii) As explained in Remark 2.32, the term

$$\sum_{n=0}^{N-1}\sum_{K\in\mathcal{T}_h}\int_{t^n}^{t^{n+1}} c_n^{-1}\omega_K^2(e)dt$$

can be shown to be of higher order when the solution is smooth and aligned with the mesh.

(iv) Observe that the term

$$\sum_{n=0}^{N-1}\sum_{K\in\mathcal{T}_h}\int_{t^n}^{t^{n+1}} c_n\|\boldsymbol{\zeta}_n\|^2_{L^2(K)}dt$$

is of higher order. If $\mathbf{u}$ is smooth enough, then thanks to the definition of $\delta_h$ and Taylor expansion we have

$$\|\boldsymbol{\zeta}_n\|^2_{L^2(K)} \simeq \lambda^2_{2,K}\tau^4.$$

Therefore

$$\sum_{n=0}^{N-1}\sum_{K\in\mathcal{T}_h}\int_{t^n}^{t^{n+1}} c_n\|\boldsymbol{\zeta}_n\|^2_{L^2(K)}dt \simeq (\max_{K\in\mathcal{T}_h}\lambda_{2,K})^2\tau^4 \simeq (\max_{K\in\mathcal{T}_h}\lambda_{2,K})^4 + \tau^8.$$

### 2.2.3 Some final remarks on the proofs of the error estimates

We briefly expose some possible generalizations of the error estimates proven in this section.

(1) We only considered the case of the homogeneous transport equation, that is to say

$$\frac{\partial \varphi}{\partial t} + \mathbf{u} \cdot \nabla \varphi = 0.$$

All the stability estimates and the a priori and a posteriori error bounds can be generalized to the non-homogeneous linear case, that is to say

$$\frac{\partial \varphi}{\partial t} + \mathbf{u} \cdot \nabla \varphi = f,$$

where the right hand side $f = f(\mathbf{x}, t)$. We refer to [22] where the Euler, Crank-Nicolson and BDF2 methods are considered in the framework of isotropic finite elements and constant time steps and to [41] where the trapezoidal rule is used with anisotropic finite elements and variable time steps (note that if $f$ is linear with respect to $t$ and the velocity field does not depend on the time, the Crank-Nicolson method and the trapezoidal rule yield to the same numerical scheme). For instance, for the a posteriori error estimates, the quantity

$$\left\| \frac{\partial \varphi_{h\tau}}{\partial t} + \mathbf{u} \cdot \nabla \varphi_{h\tau} \right\|_{L^2(K)}$$

are replaced by the residual

$$\left\| f - \frac{\partial \varphi_{h\tau}}{\partial t} + \mathbf{u} \cdot \nabla \varphi_{h\tau} \right\|_{L^2(K)}.$$

Note also that the local time error indicators involve a term depending on $f$, namely

$$f(\mathbf{x}, t) - f(\mathbf{x}, t^{n+1/2}) - (t - t^{n+1/2}) \frac{f(\mathbf{x}, t^{n+1/2}) - f(\mathbf{x}, t^{n-1/2})}{\tau^{n+1} + \tau^{n}/2}.$$

(2) The analysis can also be generalized to the case of non-divergence free vector fields. In the situation, all the quantities of the type $\int_\Omega (\mathbf{u} \cdot \phi)\phi d\mathbf{x}$ can treated in the following way:

$$\begin{aligned} \int_\Omega (\mathbf{u} \cdot \phi)\phi d\mathbf{x} &= \int_\Omega \operatorname{div} \left( \mathbf{u} \frac{\phi^2}{2} \right) d\mathbf{x} - \int_\Omega \operatorname{div}(\mathbf{u}) \frac{\phi^2}{2} d\mathbf{x} \\ &= \int_{\partial\Omega} \mathbf{u} \cdot \mathbf{n} \frac{\phi^2}{2} d\mathbf{x} - \int_\Omega \operatorname{div}(\mathbf{u}) \frac{\phi^2}{2} d\mathbf{x}. \end{aligned}$$

The first term gives a non-negative contribution as already shown several times and the second one is passed in the right hand side and can be estimated by

$$\| \operatorname{div} \mathbf{u} \|_{L^\infty(\Omega \times (0,T))} \|\phi\|^2_{L^2(\Omega)}.$$

This last term can be controlled by a suitable version of the (discrete) Gronwall's Lemma and yields to a exponential factor

$$\exp(T \| \operatorname{div} \mathbf{u} \|_{L^\infty(\Omega \times (0,T))})$$

in the estimates. Note that some restrictions on the mesh size and the time step may be made in order to guarantee the validity of the bounds for the stability and the a priori error estimates [22]. For instance, in the stability analysis of the Crank-Nicolson method (the same argument can be applied to its convergence proof), we shall control the terms (we recall that $\delta_h$ is kept constant for the a priori analysis)

$$\delta_h^2 \int_\Omega \mathbf{u}(t^{n+1/2}) \cdot \nabla \left( \frac{\varphi_h^{n+1} - \varphi_h^n}{\tau^{n+1}} \right) \frac{\varphi_h^{n+1} - \varphi_h^n}{\tau^{n+1}} d\mathbf{x}$$

$$= \frac{\delta_h^2}{2} \int_\Omega \operatorname{div} \left( \mathbf{u}(t^{n+1/2}) \left( \frac{\varphi_h^{n+1} - \varphi_h^n}{\tau^{n+1}} \right)^2 \right) d\mathbf{x} - \frac{\delta_h^2}{2} \int_\Omega \operatorname{div}(\mathbf{u}(t^{n+1/2})) \left( \frac{\varphi_h^{n+1} - \varphi_h^n}{\tau^{n+1}} \right)^2 d\mathbf{x}.$$

The first term can be eliminated since it is positive, and the second one must be passed to the right hand side. Observe then that we have to bound it by

$$\frac{\delta_h^2}{(\tau^{n+1})^2} \| \operatorname{div} \mathbf{u} \|_{L^\infty(\Omega \times (0,T))} (\| \varphi_h^{n+1} \|_{L^2(\Omega)}^2 + \| \varphi_h^n \|_{L^2(\Omega)}^2).$$

To go on in the proof, we must multiply by $2\tau^{n+1}$ and use the discrete Gronwall's Lemma A.6 to control the term

$$2\tau^{n+1} \frac{\delta_h^2}{(\tau^{n+1})^2} \| \operatorname{div} \mathbf{u} \|_{L^\infty(\Omega \times (0,T))} (\| \varphi_h^{n+1} \|_{L^2(\Omega)}^2 + \| \varphi_h^n \|_{L^2(\Omega)}^2).$$

This can be done only by imposing that

$$2\tau^{n+1} \frac{\delta_h^2}{(\tau^{n+1})^2} \| \operatorname{div} \mathbf{u} \|_{L^\infty(\Omega \times (0,T))} < 1.$$

This implies the two following drawback (we recall that in practice $\delta_h \simeq \max_{K \in \mathcal{T}_h} \lambda_{2,K}$ in the anisotropic settings)

$$\max_{K \in \mathcal{T}_h} \lambda_{2,K} \simeq \min_{n=0,1,\dots,N-1} \tau^{n+1}, \quad \tau \simeq \| \operatorname{div} \mathbf{u} \|_{L^\infty(\Omega \times (0,T))}^{-1}.$$

The first condition can be interpreted as an inverse CFL condition, imposing that the mesh size must be small enough to guarantee the stability of the method. The second means that the bigger the divergence is, the smaller the time step must be taken.

(3) Note that we always prove an upper bound for the numerical error at the final time $T$. Observe however that $T$ plays an arbitrary role in all the proofs and therefore all the a priori and a posteriori error estimates can be adapted to control the numerical error at any $t^n, n \leq N$.

(4) The numerical methods as the error estimates were presented in the two dimensional case but the generalization to the third dimension is straighforward by considering the 3D anisotropic framework presented in Section 1.6 of Chapter 1. The main changes are that we must define the stabilization parameter with respect to $\lambda_{3,K}$, that is to say we set

$$\delta_{h|K}(t) = \frac{\lambda_{3,K}}{2\|\mathbf{u}(t)\|_{L^\infty(K)}},$$

and that consequently the anisotropic quasi-uniformity condition of the mesh needed for the a priori estimates when $\mathbf{u}$ depends on the time reads now

$$\max_{K \in \mathcal{T}_h} \lambda_{3,K} \leq c\lambda_{3,K}.$$

## 2.3 Numerical experiments with non-adapted meshes and constant time steps

To test the convergence of the numerical method presented above and check the sharpness of the a posteriori error estimates, we proceed to numerical experiments with non-adapted meshes and constant time steps. We consider the numerical scheme (2.83) with $\delta_h$ given by (2.84) .

We first define the following quantities. We denote by $e(T)_{L^2}$ the numerical error at final time, computed in the $L^2$ norm, that is to say

$$e(T)_{L^2} = \|\varphi(T) - \varphi_{h\tau}(T)\|_{L^2(\Omega)},$$

where we recall that $\varphi_{h\tau}$ is the numerical reconstruction given in Definition 2.27 and used to derive the a posteriori error estimates presented in the previous section.

Based on the a posteriori error estimate (2.89) contained in Theorem 2.55, we define the error indicator $\eta$ by

$$\eta = \left((\eta^A)^2 + (\eta^T)^2\right)^{1/2}, \tag{2.90}$$

where the anisotropic space error indicator $\eta^A$ is defined by

$$\eta^A = \left(\sum_{n=0}^{N-1} \sum_{K\in\mathcal{T}_h} (\eta^A_{K,n})^2\right)^{1/2}, \tag{2.91}$$

with the local space error indicator given by

$$(\eta^A_{K,n})^2 = \int_{t^n}^{t^{n+1}} \left\|\frac{\partial\varphi_{h\tau}}{\partial t} + \mathbf{u}(t)\cdot\nabla\varphi_{h\tau}\right\|_{L^2(K)} \tilde{\omega}_K(\Pi_h^{ZZ}\varphi_{h\tau} - \varphi_{h\tau})dt, \tag{2.92}$$

and the time error indicator $\eta^T$ is defined by

$$\eta^T = \left(\sum_{n=0}^{N-1} \sum_{K\in\mathcal{T}_h} (\eta^T_{K,n})^2\right)^{1/2}, \tag{2.93}$$

with the local time error indicator given by

$$(\eta^T_{K,n})^2 = c_n \int_{t^n}^{t^{n+1}} \|\theta_n\|^2_{L^2(K)} dt, \tag{2.94}$$

where we recall that

$$c_0 = \tau^1, \quad c_n = T - \tau^1, \quad n \geq 1,$$

and $\theta_n$ is defined by (2.85) and (2.86). Before going further, observe the following facts:

(1) To obtain an easy computable space error indicator, as already advocated for elliptic equation in Chapter 1, we have replaced $\omega_K$ by $\tilde{\omega}_K$ (see Remark 1.15) and applied the ZZ post-processing $\Pi_h^{ZZ}$.

(2) Note that the high orders terms of the a posteriori error estimate (2.89) (see Remark 2.56) are not taken in account in the definition of our error indicator, neither the error at initial time, which is given by $\|\varphi(0) - r_h(\varphi(0))\|_{L^2(\Omega)}$ and therefore is of higher order too (we recall that the numerical error goes as $h^{3/2} + \tau^2$ and that $\|\varphi(0) - r_h\varphi(0)\|_{L^2(\Omega)} \simeq h^2$).

(3) Observe that in the particular case where $\mathbf{u}$ is independent of the time, then the local space error indicator $(\eta_{K,n}^A)^2$ and the local time error indicator $(\eta_{K,n}^T)^2$ reduce to the corresponding one contained in the a posteriori error estimate (2.52) for a steady transport field. Therefore, we do not need to separate the cases later on and we can directly use the same indicators for a transient $\mathbf{u}$ as for a steady one.

The sharpness of the error indicator $\eta$ will be investigated by computing the effectivity index $ei$ given by

$$ei = \frac{\eta}{e(T)_{L^2}}.$$

Since the ZZ post-processing is used, we also check the efficiency of this procedure by computing the true and approximated $H^1$ error

$$e_{L^2(H^1)} = \left( \int_0^T \|\nabla(\varphi - \varphi_{h\tau})\|^2_{L^2(\Omega)} dt \right)^{1/2}, \quad \eta^{ZZ} = \left( \int_0^T \|\nabla(\Pi_h^{ZZ}\varphi - \varphi_{h\tau})\|^2_{L^2(\Omega)} dt \right)^{1/2},$$

and the ZZ effectivity index

$$ei^{ZZ} = \frac{\eta^{ZZ}}{e_{L^2(H^1)}}.$$

The numerical experiments should possibly demonstrate the following properties:

(i) The effectivity index $ei$ should not depend on the exact solution, $\mathbf{u}$, the final time or the size of the domain.

(ii) The effectivity index $ei$ should not depend on the mesh aspect ratio.

(iii) The effectivity index $ei^{ZZ}$ should be close to one.

We consider a family of "1D" problem where the initial condition is given by

$$\varphi_0(x_1, x_2) = \tanh(-C((x_1 - 0.25)^2 - 0.01)),$$

with $C > 0$ and we solve the transport problem

$$\frac{\partial \varphi}{\partial t} + \mathbf{u}(t) \cdot \nabla \varphi = 0$$

with

$$\mathbf{u}(x_1, x_2, t) = (u(t), 0),$$

where $u$ is a smooth function only depending on the time. Therefore, we trivially have that $\operatorname{div} \mathbf{u} = 0$. The exact solution is then given by

$$\varphi(x_1, x_2, t) = \varphi_0(x_1 - \int_0^t u(s) ds, x_2).$$

Observe that the solution is smooth, with small variations, except in a thin layer of width controlled by $C$.

**Example 2.57** (Numerical experiments with an horizonatal transport field)**.**
We set $u(t) = 1$ so that $\mathbf{u} = (1, 0)$ is constant. We first solve the transport equation in a square domain $\Omega = ]0,1[\times]0,1[$, where Dirichlet boundary conditions are imposed on the left side of $\Omega$, and with $T = 0.5$. The exact solution is then given by

$$\varphi(x_1, x_2, t) = \varphi_0(x_1 - t, x_2).$$

Several experiments are performed with $C = 60$ or $C = 240$, and typical mesh aspect ratio of 50 or 500. In the following tables, we denote by $h_1 - h_2$ the mesh size in directions $x_1, x_2$ and by $\tau$ the time step.

We first investigate the sharpness of the anisotropic error indicator in space $\eta^A$, choosing $\tau = O(h^2)$ so that the error due to time discretization is negligible, see Tables 2.1 and 2.2. It is observed that the $L^2(\Omega)$ error at final time is $\simeq O(h^{1.8})$ while the $L^2(0, T, H^1(\Omega))$ error is $\simeq O(h)$. The post-processed ZZ gradient is asymptotically exact, while the effectivity index $ei$ converges to a value close to 20. These results agree with those of [20].

Then, we check that the quadratic reconstruction yields an error indicator of optimal second order in time. We choose $h \simeq O(\tau^2)$ so that the error due to the space discretization is negligible. The numerical results presented in the Tables 2.3 and 2.4 show that both the $L^2(\Omega)$ error at final time and the time indicator $\eta^T$ are $\simeq O(\tau^2)$. The effectivity index tends to a value close to 2. Note that in this case, $ei^{ZZ}$ is away from 1, which implies that the post-processing included in our error indicator in space $\eta^A$ is not accurate; but this is unimportant since $\eta^A$ is much smaller than the error indicator in time $\eta^T$.

The above numerical experiments demonstrate that $ei$ does not depend on the exact solution, neither the mesh aspect ratio. In order to check that the effectivity index does not depend on $\Omega$ and $T$, we reproduce the same experiment on a domain $\Omega = (0, 10) \times (0, 1)$ for several values of the final time $T$. The corresponding results are presented in Tables 2.5 and 2.6 for $C = 60$ and meshes with aspect ratio 50. The effectivity index remains close to the values obtained previously.

In order to obtain an effectivity index close to one, we divide the space indicator $\eta^A$ by 20 and the time indicator $\eta^T$ by 2. We report the result obtain in Tables 2.7 and 2.8 where we consider the normalized error indicator

$$\sqrt{\left(\frac{\eta^A}{20}\right)^2 + \left(\frac{\eta^T}{2}\right)^2}.$$

The corresponding effectivity index (still denoted by $ei$ to avoid to many notations) is shown to be near a value of 1 when $h^{3/2} = O(\tau^2)$.

| $h_1 - h_2$ | $\tau$ | $e_{L^2(H^1)}$ | $ei^{ZZ}$ | $e(T)_{L^2}$ | $\eta^A$ | $\eta^T$ | $ei$ |
|---|---|---|---|---|---|---|---|
| 0.01 - 0.5 | 0.002 | 0.125 | 0.99 | 0.0013 | 0.0195 | 0.00078 | 14.60 |
| 0.005 - 0.25 | 0.0005 | 0.067 | 1.00 | 0.00046 | 0.0073 | 0.000049 | 15.77 |
| 0.0025 - 0.125 | 0.000125 | 0.034 | 1.00 | 0.00015 | 0.0026 | 0.0000033 | 17.22 |
| 0.00125 - 0.0625 | 0.00003125 | 0.0168 | 1.00 | 0.000044 | 0.00088 | 0.00000021 | 20.09 |
| 0.001 - 0.5 | 0.000125 | 0.012 | 1.00 | 0.0000107 | 0.00062 | 0.00000401 | 58.31 |
| 0.0005 - 0.25 | 0.00003125 | 0.0062 | 1.00 | 0.00001 | 0.00023 | 0.00000026 | 20.78 |

Table 2.1: Example 2.57. Convergence results when $\tau = O(h^2)$ with $C = 60$ and aspect ratio 50 (rows 1-4) and 500 (rows 5-6).

| $h_1 - h_2$ | $\tau$ | $e_{L^2(H^1)}$ | $ei^{ZZ}$ | $e(T)_{L^2}$ | $\eta^A$ | $\eta^T$ | $ei$ |
|---|---|---|---|---|---|---|---|
| 0.01 - 0.5 | 0.002 | 1.23 | 0.54 | 0.023 | 0.099 | 0.0094 | 4.40 |
| 0.005 - 0.25 | 0.0005 | 0.50 | 0.77 | 0.0062 | 0.041 | 0.00078 | 6.72 |
| 0.0025 - 0.125 | 0.000125 | 0.21 | 0.96 | 0.0013 | 0.015 | 0.000055 | 11.90 |
| 0.00125 - 0.0625 | 0.00003125 | 0.10 | 1.00 | 0.00028 | 0.0053 | 0.0000036 | 19.07 |
| 0.001 - 0.5 | 0.00025 | 0.072 | 0.99 | 0.00013 | 0.0037 | 0.000023 | 27.34 |
| 0.0005 - 0.25 | 0.0000625 | 0.037 | 1.00 | 0.000065 | 0.0014 | 0.000015 | 21.62 |

Table 2.2: Example 2.57. Convergence results when $\tau = O(h^2)$ with $C = 240$ and aspect ratio 50 (rows 1-4) and 500 (rows 5-6).

| $h_1 - h_2$ | $\tau$ | $e_{L^2(H^1)}$ | $ei^{ZZ}$ | $e(T)_{L^2}$ | $\eta^A$ | $\eta^T$ | $ei$ |
|---|---|---|---|---|---|---|---|
| 0.01 - 0.5 | 0.025 | 0.68 | 0.18 | 0.046 | 0.032 | 0.095 | 2.21 |
| 0.0025 - 0.125 | 0.0125 | 0.22 | 0.16 | 0.013 | 0.0063 | 0.028 | 2.09 |
| 0.000625 - 0.03125 | 0.00625 | 0.058 | 0.14 | 0.0035 | 0.0010 | 0.0072 | 2.09 |
| 0.00015625 - 0.0078125 | 0.003125 | 0.015 | 0.32 | 0.00089 | 0.00045 | 0.0018 | 2.13 |
| 0.001 - 0.5 | 0.025 | 0.68 | 0.017 | 0.046 | 0.0032 | 0.096 | 2.07 |
| 0.00025 - 0.125 | 0.0125 | 0.22 | 0.015 | 0.013 | 0.00063 | 0.028 | 2.03 |
| 0.0000625 - 0.03125 | 0.00625 | 0.058 | 0.025 | 0.0036 | 0.00018 | 0.0073 | 2.05 |

Table 2.3: Example 2.57. Convergence results when $h = O(\tau^2)$ with $C = 60$ and aspect ratio 50 (rows 1-4) and 500 (rows 5-7).

| $h_1 - h_2$ | $\tau$ | $e_{L^2(H^1)}$ | $ei^{ZZ}$ | $e(T)_{L^2}$ | $\eta^A$ | $\eta^T$ | $ei$ |
|---|---|---|---|---|---|---|---|
| 0.01 - 0.5 | 0.025 | 6.18 | 0.11 | 0.24 | 0.15 | 0.84 | 3.66 |
| 0.0025 - 0.125 | 0.0125 | 4.28 | 0.047 | 0.12 | 0.033 | 0.38 | 3.16 |
| 0.000625 - 0.03125 | 0.00625 | 2.15 | 0.048 | 0.050 | 0.0059 | 0.12 | 2.42 |
| 0.00015625 - 0.0078125 | 0.003125 | 0.75 | 0.039 | 0.016 | 0.0026 | 0.034 | 2.11 |
| 0.0000390625 - 0.001953125 | 0.0015625 | 0.21 | 0.13 | 0.042 | 0.0018 | 0.0087 | 2.11 |
| 0.001 - 0.5 | 0.025 | 6.37 | 0.011 | 0.24 | 0.015 | 0.94 | 3.9 |
| 0.00025 - 0.125 | 0.0125 | 4.30 | 0.0045 | 0.12 | 0.0034 | 0.39 | 3.17 |
| 0.0000625 - 0.03125 | 0.00625 | 2.15 | 0.0039 | 0.051 | 0.0010 | 0.12 | 2.42 |
| 0.000015612-0.0078125 | 0.003125 | 0.75 | 0.011 | 0.016 | 0.00076 | 0.034 | 2.10 |

Table 2.4: Example 2.57. Convergence results when $h = O(\tau^2)$ with $C = 240$ and aspect ratio 50 (rows 1-5) and 500 (rows 6-8).

| $T$ | $e_{L^2(H^1)}$ | $ei^{ZZ}$ | $e(T)_{L^2}$ | $\eta^A$ | $\eta^T$ | $ei$ |
|---|---|---|---|---|---|---|
| 0.5 | 0.014 | 1.00 | 0.000031 | 0.00070 | 0.000015 | 22.63 |
| 1 | 0.0205 | 1.00 | 0.000043 | 0.00099 | 0.000019 | 22.87 |
| 1.5 | 0.024 | 1.00 | 0.000052 | 0.0012 | 0.000023 | 23.31 |
| 5 | 0.045 | 1.00 | 0.000085 | 0.0022 | 0.000041 | 26.25 |
| 9.5 | 0.073 | 1.00 | 0.00013 | 0.0031 | 0.000056 | 23.12 |

Table 2.5: Example 2.57. Convergence results when $\Omega = (0, 10) \times (0, 1)$ and $T$ varies; $h_1 = 0.000625$, $h_2 = 0.03125$, $\tau = 0.000125$.

| $T$ | $e_{L^2(H^1)}$ | $ei^{ZZ}$ | $e(T)_{L^2}$ | $\eta^A$ | $\eta^T$ | $ei$ |
|---|---|---|---|---|---|---|
| 0.5 | 0.059 | 0.24 | 0.0036 | 0.0018 | 0.0073 | 2.11 |
| 1 | 0.16 | 0.12 | 0.0071 | 0.0025 | 0.014 | 2.08 |
| 1.5 | 0.29 | 0.084 | 0.011 | 0.0031 | 0.021 | 2.08 |
| 5 | 1.59 | 0.028 | 0.032 | 0.0057 | 0.073 | 2.21 |
| 9.5 | 3.60 | 0.017 | 0.057 | 0.0079 | 0.14 | 2.43 |

Table 2.6: Example 2.57. Convergence results when $\Omega = (0, 10) \times (0, 1)$ and $T$ varies; $h_1 = 0.000625$, $h_2 = 0.03125$, $\tau = 0.00625$.

| $h_1 - h_2$ | $\tau$ | $e_{L^2(H^1)}$ | $ei^{ZZ}$ | $e(T)_{L^2}$ | $\eta^A/20$ | $\eta^T/2$ | $ei$ |
|---|---|---|---|---|---|---|---|
| 0.01 - 0.05 | 0.005 | 0.13 | 0.96 | 0.0025 | 0.001 | 0.0024 | 1.02 |
| 0.004 - 0.2 | 0.0025 | 0.049 | 0.98 | 0.0007 | 0.00015 | 0.00060 | 0.93 |
| 0.0016 - 0.08 | 0.00125 | 0.022 | 1.00 | 0.00016 | 0.000077 | 0.00015 | 1.03 |
| 0.00064 - 0.032 | 0.000625 | 0.0084 | 1.00 | 0.000038 | 0.00002 | 0.000038 | 1.12 |
| 0.001 - 0.5 | 0.0005 | 0.012 | 1.00 | 0.000020 | 0.000040 | 0.000027 | 1.7 |
| 0.0004 - 0.2 | 0.00025 | 0.0047 | 1.00 | 0.000010 | 0.0000086 | 0.0000068 | 1.16 |
| 0.00016 - 0.08 | 0.000125 | 0.0021 | 1.00 | 0.00000304 | 0.0000026 | 0.0000017 | 1.01 |

Table 2.7: Example 2.57. Convergence results with the normalized error indicator when $h^{3/2} = O(\tau^2)$ with $C = 60$ and aspect ratio 50 (rows 1-4) and 500 (rows 5-7). Here $ei = \sqrt{\left(\frac{\eta^A}{20}\right)^2 + \left(\frac{\eta^T}{2}\right)^2} / e(T)_{L^2}$.

| $h_1 - h_2$ | $\tau$ | $e_{L^2(H^1)}$ | $ei^{ZZ}$ | $e(T)_{L^2}$ | $\eta^A/20$ | $\eta^T/2$ | $ei$ |
|---|---|---|---|---|---|---|---|
| 0.01 - 0.05 | 0.005 | 1.43 | 0.47 | 0.031 | 0.0053 | 0.028 | 0.91 |
| 0.004 - 0.2 | 0.0025 | 0.55 | 0.52 | 0.010 | 0.0014 | 0.01 | 1.01 |
| 0.0016 - 0.08 | 0.00125 | 0.18 | 0.703 | 0.0027 | 0.00045 | 0.0028 | 1.03 |
| 0.00064 - 0.032 | 0.000625 | 0.06 | 0.83 | 0.00069 | 0.00012 | 0.00070 | 1.04 |
| 0.001 - 0.5 | 0.0005 | 0.075 | 0.96 | 0.00044 | 0.00020 | 0.00046 | 1.12 |
| 0.0004 - 0.2 | 0.00025 | 0.029 | 0.98 | 0.00012 | 0.000051 | 0.00011 | 1.04 |
| 0.00016 - 0.08 | 0.000125 | 0.013 | 1.00 | 0.000032 | 0.000015 | 0.000029 | 1.1 |

Table 2.8: Example 2.57. Convergence results with the normalized error indicator when $h^{3/2} = O(\tau^2)$ with $C = 240$ and aspect ratio 50 (rows 1-4) and 500 (rows 5-7). Here $ei = \sqrt{\left(\frac{\eta^A}{20}\right)^2 + \left(\frac{\eta^T}{2}\right)^2} / e(T)_{L^2}$.

**Example 2.58** (Numerical example with a time dependent transport field)**.**
We now consider the same situation as in Example 2.57 but with $u(t) = 10 + 10t^2$. We still impose Dirichlet boundary conditions on the left side of $\Omega$ and set $T = 0.05$. The numerical results are reported in Tables 2.9 and 2.10 where we choose $\tau = O(h^2)$. Both $ei$ and $ei^{ZZ}$ behaves as in the steady transport velocity case. The numerical errors are respectively $\simeq O(h^{1.8})$ for the $L^2$ error at final time and $\simeq O(h)$ for the $L^2(0, T; H^1(\Omega))$. When we choose $h = O(\tau^2)$, the effectivity index is close to 2 as before and we note that both numerical errors goes as $O(\tau^2)$, see Tables 2.11 and 2.12. We finally perform numerical experiments with the normalized error estimator

$$\sqrt{\left(\frac{\eta^A}{20}\right)^2 + \left(\frac{\eta^T}{2}\right)^2}.$$

The corresponding effectivity index is near a value of 1 when $h^{3/2} = O(\tau^2)$.

| $h_1 - h_2$ | $\tau$ | $e_{L^2(H^1)}$ | $ei^{ZZ}$ | $e(T)_{L^2}$ | $\eta^A$ | $\eta^T$ | $ei$ |
|---|---|---|---|---|---|---|---|
| 0.01 - 0.5 | 0.0002 | 0.039 | 1.00 | 0.0013 | 0.019 | 0.0.00079 | 14.57 |
| 0.005 - 0.25 | 0.00005 | 0.021 | 1.00 | 0.00047 | 0.0074 | 0.000049 | 15.77 |
| 0.0025 - 0.125 | 0.0000125 | 0.011 | 1.00 | 0.00015 | 0.0026 | 0.0000033 | 17.22 |
| 0.00125 - 0.0625 | 0.000003125 | 0.0052 | 1.00 | 0.000043 | 0.00085 | 0.00000021 | 19.65 |
| 0.001 - 0.5 | 0.0000125 | 0.0039 | 1.00 | 0.000011 | 0.00063 | 0.00000402 | 58.37 |
| 0.0005 - 0.25 | 0.000003125 | 0.0019 | 1.00 | 0.000012 | 0.00024 | 0.00000026 | 20.79 |

Table 2.9: Example 2.58. Convergence results when $\tau = O(h^2)$ with $C = 60$ and aspect ratio 50 (rows 1-4) and 500 (rows 5-6).

| $h_1 - h_2$ | $\tau$ | $e_{L^2(H^1)}$ | $ei^{ZZ}$ | $e(T)_{L^2}$ | $\eta^A$ | $\eta^T$ | $ei$ |
|---|---|---|---|---|---|---|---|
| 0.01 - 0.5 | 0.0002 | 0.39 | 0.54 | 0.023 | 0.098 | 0.0094 | 4.39 |
| 0.005 - 0.25 | 0.00005 | 0.16 | 0.77 | 0.0062 | 0.041 | 0.000 78 | 6.72 |
| 0.0025 - 0.125 | 0.0000125 | 0.067 | 0.96 | 0.0012 | 0.015 | 0.000054 | 11.89 |
| 0.00125 - 0.0625 | 0.000003125 | 0.032 | 1.00 | 0.00027 | 0.0053 | 0.0000036 | 19.077 |
| 0.001 - 0.5 | 0.0000125 | 0.023 | 1.00 | 0.000064 | 0.0036 | 0.000059 | 42.75 |
| 0.0005 - 0.25 | 0.000003125 | 0.012 | 1.00 | 0.000065 | 0.0014 | 0.0000037 | 21.62 |

Table 2.10: Example 2.58. Convergence results when $\tau = O(h^2)$ with $C = 240$ and aspect ratio 50 (rows 1-4) and 500 (rows 5-6).

| $h_1 - h_2$ | $\tau$ | $e_{L^2(H^1)}$ | $ei^{ZZ}$ | $e(T)_{L^2}$ | $\eta^A$ | $\eta^T$ | $ei$ |
|---|---|---|---|---|---|---|---|
| 0.01 - 0.5 | 0.0025 | 0.22 | 0.18 | 0.046 | 0.032 | 0.095 | 2.19 |
| 0.0025 - 0.125 | 0.00125 | 0.069 | 0.15 | 0.013 | 0.0063 | 0.027 | 2.08 |
| 0.000625 - 0.03125 | 0.000625 | 0.018 | 0.14 | 0.0035 | 0.00103 | 0.0073 | 2.07 |
| 0.00015625 - 0.0078125 | 0.0003125 | 0.0048 | 0.32 | 0.0009 | 0.00045 | 0.0018 | 2.13 |
| 0.001 - 0.5 | 0.0025 | 0.22 | 0.017 | 0.046 | 0.0032 | 0.096 | 2.07 |
| 0.00025 - 0.125 | 0.00125 | 0.069 | 0.015 | 0.013 | 0.00063 | 0.027 | 2.03 |
| 0.0000625 - 0.03125 | 0.000625 | 0.018 | 0.025 | 0.0035 | 0.00018 | 0.0073 | 2.05 |

Table 2.11: Example 2.58. Convergence results when $h = O(\tau^2)$ with $C = 60$ and aspect ratio 50 (rows 1-4) and 500 (rows 5-7).

| $h_1 - h_2$ | $\tau$ | $e_{L^2(H^1)}$ | $ei^{ZZ}$ | $e(T)_{L^2}$ | $\eta^A$ | $\eta^T$ | $ei$ |
|---|---|---|---|---|---|---|---|
| 0.01 - 0.5 | 0.0025 | 1.95 | 0.11 | 0.23 | 0.15 | 0.84 | 3.63 |
| 0.0025 - 0.125 | 0.00125 | 1.35 | 0.047 | 0.12 | 0.033 | 0.39 | 3.16 |
| 0.000625 - 0.03125 | 0.000625 | 0.68 | 0.023 | 0.051 | 0.0059 | 0.15 | 2.43 |
| 0.00015625 - 0.0078125 | 0.0003125 | 0.23 | 0.039 | 0.016 | 0.0026 | 0.034 | 2.11 |
| 0.0000390625 - 0.001953125 | 0.00015625 | 0.066 | 0.13 | 0.0042 | 0.0018 | 0.0087 | 2.11 |
| 0.001 - 0.5 | 0.0025 | 2.017 | 0.012 | 0.24 | 0.063 | 0.94 | 3.89 |
| 0.00025 - 0.125 | 0.00125 | 1.36 | 0.0045 | 0.12 | 0.0034 | 0.39 | 3.17 |
| 0.0000625 - 0.03125 | 0.000625 | 0.68 | 0.0039 | 0.051 | 0.0011 | 0.12 | 2.42 |
| 0.000015612-0.0078125 | 0.0003125 | 0.24 | 0.011 | 0.016 | 0.00076 | 0.034 | 2.10 |

Table 2.12: Example 2.58. Convergence results when $h = O(\tau^2)$ with $C = 240$ and aspect ratio 50 (rows 1-5) and 500 (rows 6-8).

| $h_1 - h_2$ | $\tau$ | $e_{L^2(H^1)}$ | $ei^{ZZ}$ | $e(T)_{L^2}$ | $\eta^A/20$ | $\eta^T/2$ | $ei$ |
|---|---|---|---|---|---|---|---|
| 0.01 - 0.05 | 0.0005 | 0.041 | 0.96 | 0.0025 | 0.0011 | 0.0033 | 1.38 |
| 0.004 - 0.2 | 0.00025 | 0.015 | 0.98 | 0.0007 | 0.00025 | 0.00085 | 1.26 |
| 0.0016 - 0.08 | 0.000125 | 0.0069 | 1.00 | 0.00016 | 0.000077 | 0.00021 | 1.38 |
| 0.00064 - 0.032 | 0.0000625 | 0.0026 | 1.00 | 0.000038 | 0.00002 | 0.000054 | 1.49 |
| 0.001 - 0.5 | 0.00005 | 0.0038 | 1.00 | 0.000025 | 0.000034 | 0.000037 | 1.99 |
| 0.0004 - 0.2 | 0.000025 | 0.0015 | 1.00 | 0.000011 | 0.0000087 | 0.0000096 | 1.22 |
| 0.00016 - 0.08 | 0.0000125 | 0.00067 | 1.00 | 0.0000034 | 0.0000026 | 0.0000024 | 1.03 |

Table 2.13: Example 2.58. Convergence results with the normalized error indicator when $h^{3/2} = O(\tau^2)$ with $C = 60$ and aspect ratio 50 (rows 1-4) and 500 (rows 5-7). Here $ei = \sqrt{\left(\frac{\eta^A}{20}\right)^2 + \left(\frac{\eta^T}{2}\right)^2} / e(T)_{L^2}$.

| $h_1 - h_2$ | $\tau$ | $e_{L^2(H^1)}$ | $ei^{ZZ}$ | $e(T)_{L^2}$ | $\eta^A/20$ | $\eta^T/2$ | $ei$ |
|---|---|---|---|---|---|---|---|
| 0.01 - 0.05 | 0.0005 | 0.45 | 0.47 | 0.031 | 0.0053 | 0.041 | 1.30 |
| 0.004 - 0.2 | 0.00025 | 0.17 | 0.52 | 0.010 | 0.0014 | 0.015 | 1.42 |
| 0.0016 - 0.08 | 0.000125 | 0.058 | 0.703 | 0.0028 | 0.00045 | 0.0039 | 1.44 |
| 0.00064 - 0.032 | 0.0000625 | 0.018 | 0.83 | 0.00069 | 0.00012 | 0.001 | 1.46 |
| 0.001 - 0.5 | 0.00005 | 0.024 | 0.96 | 0.00044 | 0.00019 | 0.00065 | 1.52 |
| 0.0004 - 0.2 | 0.000025 | 0.0091 | 0.98 | 0.00012 | 0.000051 | 0.00016 | 1.4 |
| 0.00016 - 0.08 | 0.0000125 | 0.004 | 1.00 | 0.000032 | 0.000015 | 0.000041 | 1.35 |

Table 2.14: Example 2.58. Convergence results with the normalized error indicator when $h^{3/2} = O(\tau^2)$ with $C = 240$ and aspect ratio 50 (rows 1-4) and 500 (rows 5-7). Here $ei = \sqrt{\left(\frac{\eta^A}{20}\right)^2 + \left(\frac{\eta^T}{2}\right)^2} / e(T)_{L^2}$.

## 2.4 A space-time adaptive algorithm

We now present a space-time adaptive algorithm to solve the transport equation. The remeshing procedure is similar to the one presented in Chapter 1, Section 1.4. The goal is to control the numerical error over the time, therefore given a prescribed tolerance $TOL$, we want to build a sequence of meshes and time steps such that

$$0.75TOL \leq \left(\frac{\eta^2}{T}\right)^{1/2} \leq 1.25TOL. \tag{2.95}$$

Since

$$\eta^2 = \sum_{n=0}^{N-1} \sum_{K \in \mathcal{T}_h} \left( (\eta^A_{K,n})^2 + (\eta^T_{K,n})^2 \right), \quad T = \sum_{n=0}^{N-1} \tau^{n+1},$$

a sufficient condition to ensure the above criterion is that for any $n = 0, 1, ..., N-1$ it holds

$$0.75^2 TOL^2 \tau^{n+1} \leq \sum_{K \in \mathcal{T}_h} \left( (\eta^A_{K,n})^2 + (\eta^T_{K,n})^2 \right) \leq 1.25^2 TOL^2 \tau^{n+1}.$$

A simple and natural idea consists to equidistribute the error between the space and the time discretization, therefore to ensure that (2.95) holds, we check at every $n = 0, 1, ..., N-1$ that

$$\frac{0.75^2 TOL^2 \tau^{n+1}}{2} \leq \sum_{K \in \mathcal{T}_h} (\eta^A_{K,n})^2 \leq \frac{1.25^2 TOL^2 \tau^{n+1}}{2}, \tag{2.96}$$

and

$$\frac{0.75^2 TOL^2 \tau^{n+1}}{2} \leq \sum_{K \in \mathcal{T}_h} (\eta^T_{K,n})^2 \leq \frac{1.25^2 TOL^2 \tau^{n+1}}{2}. \tag{2.97}$$

As already presented in the Chapter 1 for elliptic problem, we translate the spatial error indicator from triangles to vertices. We define

$$(\eta^A_{P,n})^2 = \sum_{\substack{K \in \mathcal{T}_h \\ P \in K}} (\eta^A_{K,n})^2, \quad n = 0, 1, ..., N-1,$$

so that

$$\sum_{P \in \mathcal{T}_h} (\eta^A_{P,n})^2 = 3 \sum_{K \in \mathcal{T}_h} (\eta^A_{K,n})^2, \quad n = 0, 1, ..., N-1.$$

Therefore, a sufficient conditions to obtain (2.96) is to ensure that for all $P \in \mathcal{T}_h$

$$\frac{3}{N_P} \frac{0.75^2 TOL^2 \tau^{n+1}}{2} \leq (\eta^A_{P,n})^2 \leq \frac{3}{N_P} \frac{1.25^2 TOL^2 \tau^{n+1}}{2}, \tag{2.98}$$

where $N_P$ stands for the number vertices. The goal is now to equidistribute the spatial error between the two directions of anisotropy. Note that here we have to take in account the integral in time. Indeed, observe that

$$(\eta_{K,n}^A)^2 = \int_{t^n}^{t^{n+1}} \left\| \frac{\partial \varphi_{h\tau}}{\partial t} + \mathbf{u}(t) \cdot \nabla \varphi_{h\tau} \right\|_{L^2(K)} \tilde{\omega}_K(\Pi_h^{ZZ} \varphi_{h\tau} - \varphi_{h\tau}) dt,$$

where we recall that (see (1.30))

$$\tilde{\omega}_K(v) = \left( \tilde{\omega}_{1,K}^2(v) + \tilde{\omega}_{2,K}^2(v) \right)^{1/2}.$$

It seem therefore natural to define the local spatial error indicator in direction $x_i, i = 1, 2$ by

$$(\eta_{i,K,n}^A)^2 = \int_{t^n}^{t^{n+1}} \left\| \frac{\partial \varphi_{h\tau}}{\partial t} + \mathbf{u}(t) \cdot \nabla \varphi_{h\tau} \right\|_{L^2(K)} \tilde{\omega}_{i,K}(\Pi_h^{ZZ} \varphi_{h\tau} - \varphi_{h\tau}) dt,$$

and its pointwise version

$$(\eta_{i,P,n}^A)^2 = \sum_{\substack{K \in \mathcal{T}_h \\ P \in K}} (\eta_{i,K,n}^A)^2.$$

Note that the definition of $(\eta_{i,K,n}^A)^2$ is motivated by the following observation : let us assume that the error is zero in one direction (for instance the $x_1$ direction), then automatically, the following equality holds

$$(\eta_{K,n}^A)^2 = (\eta_{2,K,n}^A)^2.$$

Observe now, that

$$(\eta_P^A)^2 = ((\eta_{1,P,n}^A)^2 + (\eta_{2,P,n}^A)^2) \sigma_P^{-1},$$

where we define the scaling factor

$$\sigma_P = \frac{(\eta_{1,P,n}^A)^2 + (\eta_{2,P,n}^A)^2}{(\eta_P^A)^2}.$$

Therefore, sufficient conditions to satisfy (2.98) is that for all $P \in \mathcal{T}_h$

$$\frac{3\sigma_P}{2N_P} \frac{0.75^2 TOL^2 \tau^{n+1}}{2} \leq (\eta_{i,P,n}^A)^2 \leq \frac{3\sigma_P}{2N_P} \frac{1.25^2 TOL^2 \tau^{n+1}}{2}, \quad i = 1, 2. \tag{2.99}$$

The adaptive algorithm goes as follows ans is summarized in Table 2.15: at each time step, we compute the errors indicators and we check the conditions (2.97) and (2.99). Whenever it is needed we change the time step and build a new mesh. Note that, if a new mesh has to be built, then the finite elements problem

$$\int_\Omega \left( \frac{\varphi_h^{n+1} - \varphi_h^n}{\tau^{n+1}} + \mathbf{u}(t^{n+1/2}) \cdot \nabla \left( \frac{\varphi_h^{n+1} + \varphi_h^n}{2} \right) \right) (v_h + \delta_h(t^{n+1/2}) \mathbf{u}(t^{n+1/2}) \cdot \nabla v_h) d\mathbf{x} = 0, \forall v_h \in V_h,$$

is not well defined since a priori $\varphi_h^n$ will not belong to $V_h$. Therefore, the previous finite element approximation, $\varphi_h^n$, has to be interpolated on the current mesh. More precisely, if we denote by $\mathcal{T}_{h,i}^n$ and $\mathcal{T}_{h,i+1}^n$ two successive meshes generated at time $t^{n+1}$, and by $V_{h,i}^n$, $V_{h,i+1}^n$ the associated finite elements spaces, we consider the interpolation operator

$$\pi_{h,i+1}^n : V_{h,i}^n \longrightarrow V_{h,i+1}^n.$$

If a new mesh has to be built, then we interpolate the values of $\varphi_h^n$ from $V_{h,i}^n$ to $V_{h,i+1}^n$ and compute $\varphi_h^{n+1} \in V_{h,i+1}^n$ such that

$$\int_\Omega \left( \frac{\varphi_h^{n+1} - \pi_{h,i+1}^n \varphi_h^n}{\tau^{n+1}} + \mathbf{u}(t^{n+1/2}) \cdot \nabla \left( \frac{\varphi_h^{n+1} + \pi_{h,i+1}^n \varphi_h^n}{2} \right) \right) \left( v_h + \delta_h(t^{n+1/2}) \mathbf{u}(t^{n+1/2}) \cdot \nabla v_h \right) = 0, \quad (2.100)$$

for all $v_h \in V_{h,i+1}^n$. In practice, several choices are proposed for the interpolation operator $\pi_{h,i+1}^n$. More comments will be addressed on the interpolation error in the part dedicated to the numerical experiments with adapted meshes. Note that the analysis of the interpolation process is not covered by our theory since we only study the a priori and a posteriori errors on a single mesh in order to simplify the discussion. Several examples can be found in the literature where moving meshes are taking in account in the a posteriori analysis, see for instance [11, 65, 79] for parabolic problems or [16] for the Stokes equations.

To build a new mesh, we proceed as presented in Chapter 1. We first compute the average local gradient error matrix $G_P$ defined by

$$G_P = \sum_{\substack{K \in \mathcal{T}_h \\ P \in K}} \tilde{G}_K(\Pi_h^{ZZ} \varphi_h^{n+1} - \varphi_h^{n+1}) \quad (2.101)$$

where $\tilde{G}_K$ is given by (1.18) and the two direction of anisotropy are aligned with the eigenvectors of $G_P$. In practice, as already presented in Section 1.4 we compute the angle $\theta_P$ between the horizontal axe and the $x_1$ direction. To adapt the mesh size, as before, we compute the average local stretching values $\lambda_{i,P}$ at the point $P$ defined by

$$\lambda_{i,P} = \frac{\sum_{\substack{K \in \mathcal{T}_h \\ P \in K}} \lambda_{i,K}}{\sum_{\substack{K \in \mathcal{T}_h \\ P \in K}} 1}, i = 1, 2. \quad (2.102)$$

If

$$\frac{3\sigma_P}{2N_v} 0.75^2 TOL^2 \tau^{n+1} > (\eta_{i,P,n})^2$$

then we increase $h_{i,P}$ ( that is to say the mesh size in direction $x_i$) by setting set $h_{i,p} = 1.5\lambda_{i,P}$. If

$$(\eta_{i,P,n})^2 > \frac{3\sigma_P}{2N_v} 1.25^2 TOL^2 \tau^{n+1},$$

then we decrease the mesh size in direction $x_i$ by setting $h_{i,p} = \frac{\lambda_{i,P}}{1.5}$. Finally, for every $P \in \mathcal{T}_{h,i}^n$, we pass to the remeshing software $\theta_P$ and the two mesh size $h_{1,P}, h_{2,P}$.

In the 2D numerical experiments presented later, the meshes are generated with the BL2D software [67]. The interpolation between meshes is done with the BL2D interpolation modules and the Wolf-Interpol program [5].

| | |
|---|---|
| Set $\mathcal{T}_{h,0}^0, \varphi_h^0, n = 0, \tau^1, i = 0$. | Initialization |
| **While** $t < T$ | Time loop |
| $t = t + \tau^{n+1}$ | Increment next time step |
| Compute $\varphi_h^{n+1}$ on $\mathcal{T}_{h,i}^n$ by solving (2.100) | |
| **For** $K \in \mathcal{T}_{h,i}^n$, compute | |
| $(\eta_{K,n}^A)^2, (\eta_{K,n}^T)^2$ | compute the space and time error indicators |
| **If** (2.96) and (2.97) are satisfied **then** | Mesh and time step are correct |
| $\mathcal{T}_{h,0}^{n+1} = \mathcal{T}_{h,i}^n, \tau^{n+2} = \tau^{n+1}$ | |
| $i = 0, n = n + 1$ | |
| **else** | |
| $t = t - \tau^{n+1}$ | |
| **If** (2.96) is not satisfied | Adapt the mesh |
| **For** $P \in \mathcal{T}_{h,i}^n$, compute $G_P$ and $\theta_P$ | set the anisotropy directions to the eigenvectors of $G_P$ |
| **For** $i = 1, 2$ Test conditions (2.99) | |
| Compute the average mesh size $\lambda_{i,P}$ | |
| **If** the mesh size is too small in direction $x_i$, set $h_{i,P} = 3/2\lambda_{i,P}$ | Change the mesh size in direction $x_i$ |
| **If** the mesh size is too bin big in direction $x_i$, set $h_{i,P} = 2/3\lambda_{i,P}$ | |
| Build a new mesh $\mathcal{T}_{h,i+1}^n$ using the BL2D software | |
| **If** $n > 0$ | |
| $\varphi_h^n = \pi_{h,i+1}^n \varphi_h^n, \varphi_h^{n-1} = \pi_{h,i+1}^n \varphi_h^{n-1}$ | interpolate the old solutions on the new mesh |
| $i = i + 1$ | |
| **If** (2.97) is not satisfied | Adapt the time step |
| **If** $\sum_{K \in \mathcal{T}_h} (\eta_{K,n}^T)^2$ is too big, set $\tau^{n+1} = \tau^{n+1}/2$ | |
| **If** $\sum_{K \in \mathcal{T}_h} (\eta_{K,n}^T)^2$ is too small, set $\tau^{n+1} = 3/2\tau^{n+1}$ | |
| **If** $\tau^{n+1} > T - t$ set $\tau^{n+1} = T - t$ | Check that final time is not exceeded and stop time step adaptation |

Table 2.15: Time space adaptive algorithm

## 2.5 Numerical experiments with adapted meshes and adapted time steps

We now perform numerical experiments using the space-time adaptive algorithm presented in Section 2.4. We investigate the number of vertices, aspect ratio, number of time steps and remeshings, for various values of the prescribed tolerance $TOL$. The notations are summarized in Table 2.16.

| | |
|---|---|
| $N_v$ : | Number of vertices of the mesh at final time |
| $N_\tau$ : | Number of time steps |
| $N_m$ : | Number of remeshings |
| $N_c$ : | Number of time step changes |
| $ar$ : | Maximum aspect ratio at final time, the aspect ratio on an element $K$ being $\lambda_{1,K}/\lambda_{2,K}$ |
| $\overline{ar}$ : | Average aspect ratio at final time |

Table 2.16: Additional notations for the analysis of the adaptive algorithm

As briefly commented in Section 2.4, the main issue to the space-time algorithm is the interpolation between meshes. We recall that at each time $t^{n+1}$ (see Table 2.15 for the description of the algorithm), if a new mesh as to be built, then we have to interpolate $\varphi_n^n$ from the old mesh to the new one. More precisely, if $\mathcal{T}_{h,i}^n$ and $\mathcal{T}_{h,i+1}^n$ are two successive meshes built at the step $n+1$, and we denote by $V_{h,i}^{n+1}, V_{h,i+1}^{n+1}$ the respective associated finite elements spaces, then to compute $\varphi_h^{n+1} \in V_{h,i+1}^{n+1}$ by solving (2.100), we first have to interpolate $\varphi_h^n$ from $V_{h,i}^n$ to $V_{h,i+1}^n$ by computing $\pi_{h,i+1}^n \varphi_h^n$ where $\pi_{h,i+1}^n : V_{h,i}^n \to V_{h,i+1}^{n+1}$. In [20, 41] several choices for $\pi_{h,i+1}^n$ were proposed in practice, in particular :

- the Lagrange interpolation from $V_{h,i}^n$ to $V_{h,i+1}^n$,
- the exact $L^2$ projection [43], where $\pi_{h,i+1}^n \varphi_h^n$ is the unique element of $V_{h,i+1}^n$ satisfying

$$\int_\Omega \pi_{h,i+1}^n \varphi_h^n v_h d\mathbf{x} = \int_\Omega \varphi_h^n v_h d\mathbf{x}, \quad \forall v_h \in V_{h,i+1}^n,$$

- the conservative algorithm of [5].

The goal is to find an operator that minimizes the error due to the interpolation from one mesh to the other. It was observed that the interpolation error does not have a significant effect on the numerical results for parabolic problems [72], but is a crucial issue for hyperbolic problem [20, 51]. The best results were obtained when the conservative algorithm [5] is used. The Lagrange interpolation seems to be less accurate. Note that in [20], the exact $L^2$ was shown to be as efficient as the conservative algorithm proposed in [5]. Numerical experiments showed that the $H^1$ projection can also be a good alternative for hyperbolic equations [51].

From a theoretical point of view, we would like to prove some stability estimate for the scheme (2.100). Let us demonstrate this fact in a more simpler case where we assume that $\mathbf{u}$ is independent of the time and that $\delta_h$ is constant in time and space. One can easily show, by taking

$$v_h = \frac{\varphi_h^{n+1} + \pi_{h,i+1}^n \varphi_h^n}{2} + \delta_h \frac{\varphi_h^{n+1} - \pi_{h,i}^n \varphi_h^n}{\tau^{n+1}}$$

as test function and performing the same computation as in Proposition 2.16, that

$$\|\varphi_h^{n+1}\|_{L^2(\Omega)}^2 + \delta_h^2 \|\mathbf{u} \cdot \nabla \varphi_h^{n+1}\|_{L^2(\Omega)}^2 \leq \|\pi_{h,i+1}^n \varphi_h^n\|_{L^2(\Omega)}^2 + \delta_h^2 \|\mathbf{u} \cdot \nabla \pi_{h,i+1}^n \varphi_h^n\|_{L^2(\Omega)}^2.$$

Then, if we assume that the projection $\pi_{h,i+1}^n$ satisfies for any $g \in H^1(\Omega)$ that

$$\|\pi_{h,i+1}^n g\|_{L^2(\Omega)}^2 + \delta_h^2 \|\mathbf{u} \cdot \nabla \pi_{h,i+1}^n g\|_{L^2(\Omega)}^2 \leq \|g\|_{L^2(\Omega)}^2 + \delta_h^2 \|\mathbf{u} \cdot \nabla g\|_{L^2(\Omega)}^2, \tag{2.103}$$

then one will have that

$$\|\varphi_h^{n+1}\|_{L^2(\Omega)}^2 + \delta_h^2 \|\mathbf{u} \cdot \nabla \varphi_h^{n+1}\|_{L^2(\Omega)}^2 \leq \|\varphi_h^n\|_{L^2(\Omega)}^2 + \delta_h^2 \|\mathbf{u} \cdot \nabla \varphi_h^n\|_{L^2(\Omega)}^2.$$

Unfortunately, none of the projections proposed above satisfies such properties. In [41], it was proposed to chose $\pi^n_{h,i+1} : H^1(\Omega) \longrightarrow V^n_{h,i+1}$ as the modified $L^2$ projection

$$\int_\Omega \pi^n_{h,i+1} g v_h d\mathbf{x} + \int_\Omega (\delta_h \mathbf{u} \cdot \nabla \pi^n_{h,i+1} g)(\delta_h \mathbf{u} \cdot \nabla v_h) d\mathbf{x} \\ = \int_\Omega g v_h d\mathbf{x} + \int_\Omega (\delta_h \mathbf{u} \cdot \nabla g)(\delta_h \mathbf{u} \cdot \nabla v_h) dx, \forall v_h \in V^n_{h,i+1}, \quad (2.104)$$

which satisfies (2.103). However, this has a little interest in practice since the stability result is guaranteed only for constant $\delta_h$. Moreover, the numerical experiments showed that this choice was not the best one. Therefore, we present below the tests performed with the conservative algorithm [5] that yields the best results. For comparison, we also present the results obtained with the classical Lagrange interpolation between meshes. A theoretical study should be conducted to give a proper answer to our empiric observations.

We first run the adaptive algorithm with Example 2.57. The initial grid is an isotropic mesh of mesh size $h = 0.1$ and the initial time step is taken as $\tau^1 = 0.001$. The solution and meshes are represented in Figures 2.1 and 2.2 for $C = 240$. The numerical results are presented in Table 2.17 where we compare Lagrange interpolation to the conservative algorithm [5]. When the latter is used, the following conclusions can be observed:

- The error at final time is approximatively divided by 2 when $TOL$ is divided by 2.
- Both effectivity indices $ei$ and $ei^{ZZ}$ are close to one.
- The number of remeshing depends on the exact solution $u$ (in particular the larger $C$, the larger $N_m$).
- The total number of vertices at final time is doubled as the tolerance is divided by two.
- The total number of time steps is multiplied by $\sqrt{2}$ as the tolerance is divided by 2, which confirms the second order convergence of the error indicator in time $\eta^T$.

All these conclusions are satisfactory, except the final number of vertices. Indeed, since the solution depends only on the $x_1$ variable, it is expected that $N_v \simeq h^{-1}$. Therefore $N_v$ should be rather multiplied by $2^{2/3}$ ($\simeq 1.6$) when the tolerance is divided by 2, since the $L^2$ error a final time is $O(h^{3/2})$. We have no precise explanation, but this lost can maybe be attributed to the interpolation error.

Note that for all the numerical experiments presented below, we consider the normalized error indicators

$$\frac{\eta^A}{20}, \quad \frac{\eta^T}{2},$$

and the corresponding effectivity index

$$ei = \sqrt{\left(\frac{\eta^A}{20}\right)^2 + \left(\frac{\eta^T}{2}\right)^2} / e(T)_{L^2}.$$

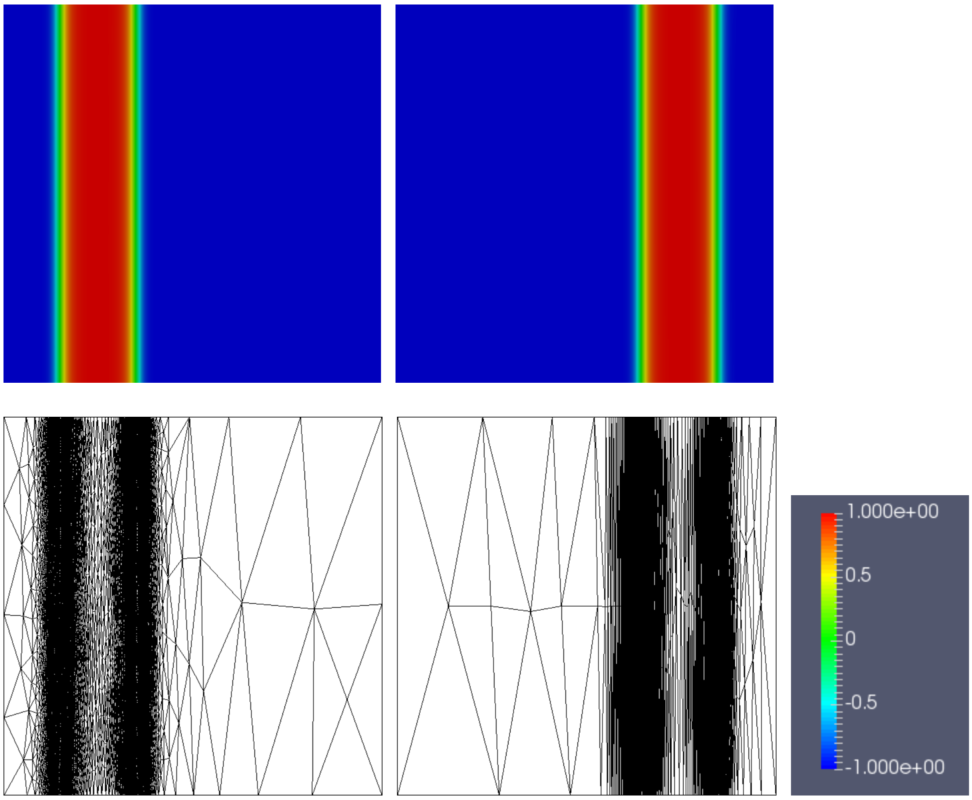


Figure 2.1: Example 2.57. Mesh and solution with $C = 240$ and $TOL = 0.001$ at $t = 0$ (left) and $t = 0.5$ (right). Conservative interpolation between meshes is used.

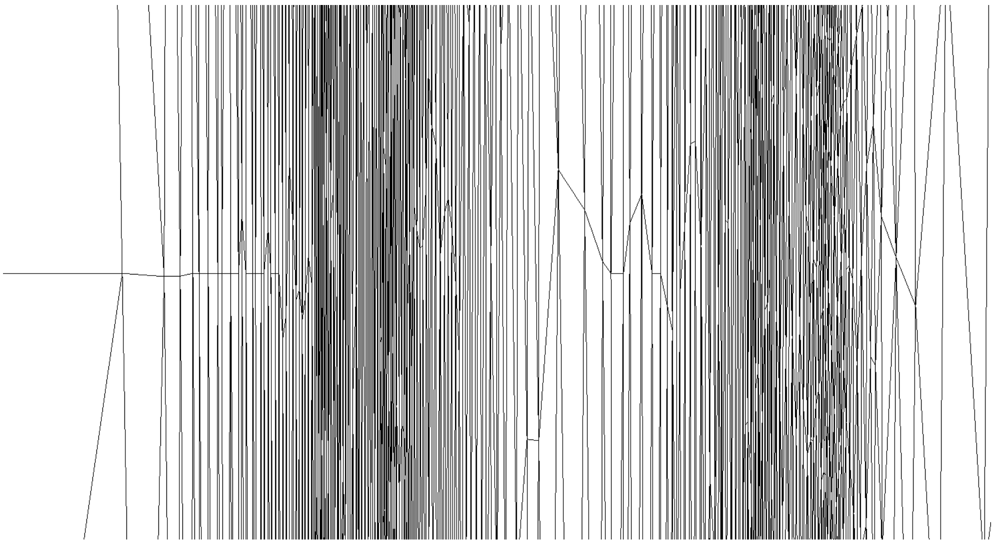

Figure 2.2: Example 2.57. Zoom of Figure 2.1 at final time.

| $TOL$ | $e(T)_{L^2}$ | $ei$ | $e_{L^2(H^1)}$ | $ei^{ZZ}$ | $\eta^A$ | $\eta^T$ | $ar$ | $\bar{ar}$ | $N_v$ | $N_\tau$ | $N_m$ | $N_c$ |
|---|---|---|---|---|---|---|---|---|---|---|---|---|
| 0.001 | 0.0055 | 0.12 | 0.096 | 0.79 | 0.00048 | 0.00046 | 284 | 65 | 567 | 361 | 31 | 286 |
| 0.0005 | 0.0025 | 0.13 | 0.055 | 0.85 | 0.00024 | 0.00022 | 800 | 85 | 1020 | 538 | 35 | 366 |
| 0.00025 | 0.00096 | 0.17 | 0.032 | 0.91 | 0.00012 | 0.00011 | 752 | 106 | 2236 | 769 | 36 | 379 |
| 0.000125 | 0.00039 | 0.21 | 0.019 | 0.96 | 0.000061 | 0.000057 | 1157 | 151 | 3958 | 1197 | 37 | 375 |
| 0.001 | 0.012 | 0.057 | 0.29 | 0.45 | 0.00048 | 0.00045 | 1399 | 173 | 825 | 1597 | 89 | 1170 |
| 0.0005 | 0.0045 | 0.072 | 0.14 | 0.59 | 0.00024 | 0.00022 | 1560 | 244 | 1605 | 2297 | 90 | 1414 |
| 0.00025 | 0.0017 | 0.094 | 0.069 | 0.76 | 0.00012 | 0.00011 | 2615 | 372 | 2513 | 3399 | 98 | 1605 |
| 0.000125 | 0.0011 | 0.073 | 0.043 | 0.77 | 0.000061 | 0.000055 | 4274 | 203 | 14544 | 7943 | 104 | 911 |
| 0.001 | 0.00083 | 0.802 | 0.077 | 0.98 | 0.00049 | 0.00045 | 335 | 81 | 444 | 344 | 37 | 229 |
| 0.0005 | 0.00036 | 0.92 | 0.047 | 0.99 | 0.00024 | 0.00022 | 584 | 89 | 1197 | 503 | 40 | 361 |
| 0.00025 | 0.00017 | 0.98 | 0.029 | 1.00 | 0.00012 | 0.00011 | 1034 | 135 | 1649 | 712 | 42 | 379 |
| 0.000125 | 0.000008 | 1.04 | 0.018 | 1.00 | 0.000062 | 0.000056 | 1978 | 200 | 3287 | 1003 | 45 | 546 |
| 0.001 | 0.00088 | 0.75 | 0.14 | 0.93 | 0.00048 | 0.00045 | 801 | 159 | 998 | 1498 | 94 | 965 |
| 0.0005 | 0.00036 | 0.89 | 0.086 | 0.97 | 0.00024 | 0.00022 | 1860 | 278 | 1521 | 2124 | 89 | 1059 |
| 0.00025 | 0.00017 | 0.95 | 0.053 | 0.99 | 0.00012 | 0.00011 | 2539 | 365 | 2696 | 3028 | 95 | 1462 |
| 0.000125 | 0.000086 | 0.99 | 0.033 | 1.00 | 0.000061 | 0.000059 | 4215 | 489 | 5214 | 4259 | 100 | 1732 |

Table 2.17: Example 2.57. Convergence results for the adaptive algorithm with linear interpolation (row 1-8) $C = 60$ (row 1-4) $C = 240$ (row 5-8) and conservative interpolation (row 9-16) $C = 60$ (row 9-12) $C = 240$ (row 13-16).

**Example 2.59** (An example with a strong variation in time)**.**
We now consider $u(t) = 1 + 9H_{0.03}(t - 0.25)$ such that the solution moves along the $x_1$ axis at a constant velocity 1 until $t = 0.25$ and then quickly accelerate to reach a velocity of 10 until $T = 0.3$. For a given $\varepsilon > 0$, we recall that $H_\varepsilon$ is the smoothing of the Heaviside function given by

$$H_\varepsilon(x) = \begin{cases} 0, & x \leq -\varepsilon, \\ \dfrac{x+\varepsilon}{2\varepsilon} + \dfrac{1}{2\pi}\sin\left(\dfrac{\pi x}{\varepsilon}\right), & -\varepsilon \leq x \leq \varepsilon, \\ 1, & x \geq \varepsilon. \end{cases}$$

We choose the initial condition as in Example 2.57, with $C = 60$. We are mainly concerned to check if our adaptive algorithm can capture the quick acceleration of the solution around $t = 0.25$. In Table 2.18, we present the converge results for several values of TOL. We observe the same conclusions as previously. In Figure 2.3, we check the evolution of the time step. We observe that, up to some oscillations occurring when the adaptive algorithm refuses the current time step, that the time step follows the evolution of $\mathbf{u}$. In particular, when $\mathbf{u}$ is 10 times larger, the adaptive algorithm selects a time step that is approximatively 10 times smaller.

| $TOL$ | $e(T)_{L^2}$ | $ei$ | $e_{L^2(H^1)}$ | $ei^{ZZ}$ | $\eta^A$ | $\eta^T$ | $ar$ | $\bar{ar}$ | $N_v$ | $N_\tau$ | $N_m$ | $N_c$ |
|---|---|---|---|---|---|---|---|---|---|---|---|---|
| 0.005 | 0.0024 | 1.086 | 0.17 | 0.95 | 0.0018 | 0.0019 | 164 | 53 | 106 | 459 | 42 | 245 |
| 0.0025 | 0.00094 | 1.39 | 0.102 | 0.97 | 0.00093 | 0.00091 | 272 | 78 | 244 | 667 | 42 | 328 |
| 0.00125 | 0.000051 | 1.29 | 0.065 | 0.98 | 0.00047 | 0.00046 | 429 | 118 | 390 | 942 | 44 | 414 |

Table 2.18: Example 2.59. Convergence results for the adaptive algorithm. Conservative interpolation between meshes is used.

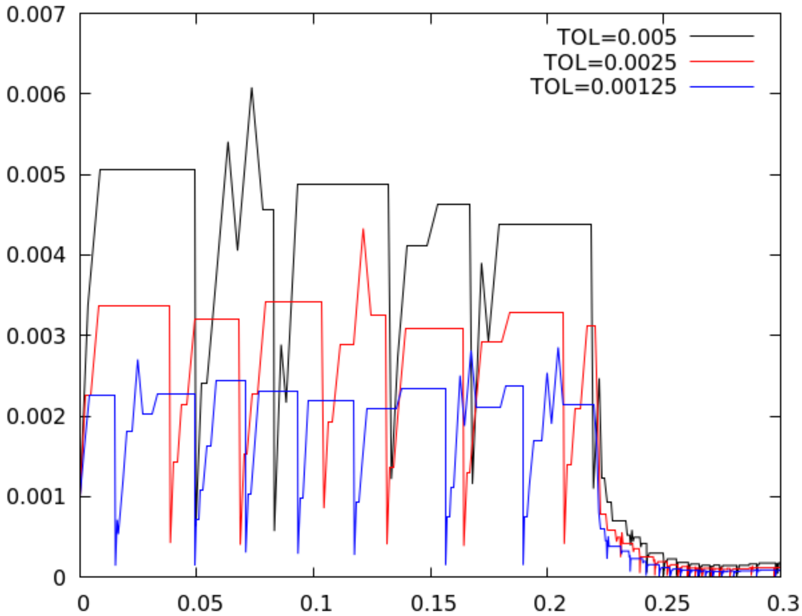


Figure 2.3: Example 2.59. Evolution of the current time step for several values of $TOL$. Conservative interpolation between meshes is used.

**Example 2.60** (Stretching of a circle in a vortex flow)**.**
The last test case is the stretching of a circle in a vortex flow. We set $\Omega = ]0,1[^2, T = 4$. The initial condition is given by

$$\varphi_0(x_1, x_2) = \tanh\left(-C(\sqrt{(x_1-0.5)^2 + (x_2-0.75)^2} - 0.15)\right),$$

where $C = 60$ or $C = 240$. No boundary conditions along $\partial\Omega$ are prescribed. The velocity field is defined by

$$\mathbf{u}(x_1, x_2, t) = \begin{pmatrix} -2\sin(\pi x_2)\cos(\pi x_2)\sin^2(\pi x_1)\cos(0.25\pi t) \\ 2\sin(\pi x_1)\cos(\pi x_1)\sin^2(\pi x_2)\cos(0.25\pi t) \end{pmatrix}.$$

The exact solution is not known, however, since the flow is reversed at $t = 2$, we must have $\varphi(x_1, x_2, 4) = \varphi_0(x_1, x_2)$ and therefore the $L^2$ error at final time is computable.

We start the adaptive algorithm with an initial grid of mesh size $h = 0.1$ and an initial time step $\tau^1 = 0.001$. Several meshes and numerical solutions are presented in Figures 2.4 and 2.5 when $TOL = 0.00125$ and conservative interpolation is used. In Figures 2.6 and 2.8 and Table 2.19 we have checked convergence of the computed solution at final time for several values of $TOL$. For comparison, we present in Table 2.20 results with non-adapted uniform meshes and constant time steps. In Figure 2.10, we compare the solution computed on a non-adapted meshes with the one obtained with $TOL = 0.005$ of the adaptive algorithm. Clearly, the adapted solution is more accurate than the finest non-adapted one. Note that the number of vertices of the non-adapted mesh is 200 larger than that of adapted meshes.

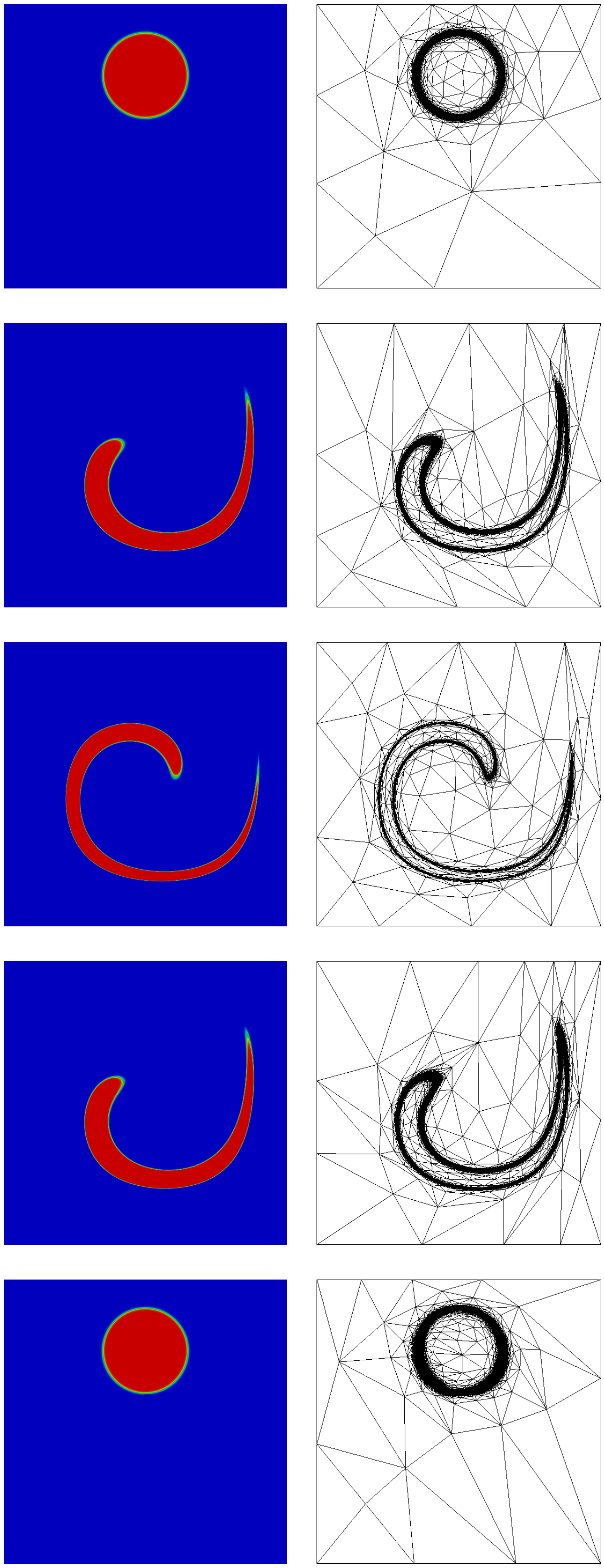

Figure 2.4: Example 2.60. Mesh and solution at time $t = 0, 1, 2, 3, 4$, with $C = 240$ and $TOL = 0.00125$. Conservative interpolation between meshes is used.

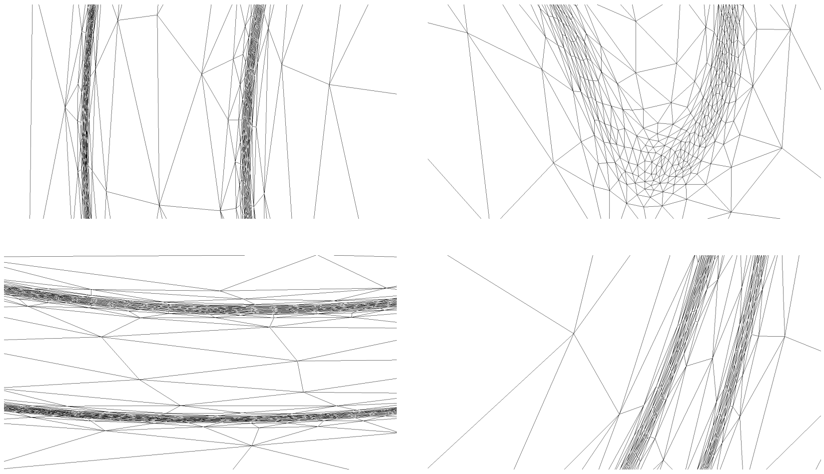

Figure 2.5: Example 2.60. Zoom on the mesh at time $t = 2$ with $C = 240$ and $TOL = 0.00125$. Conservative interpolation between meshes is used.

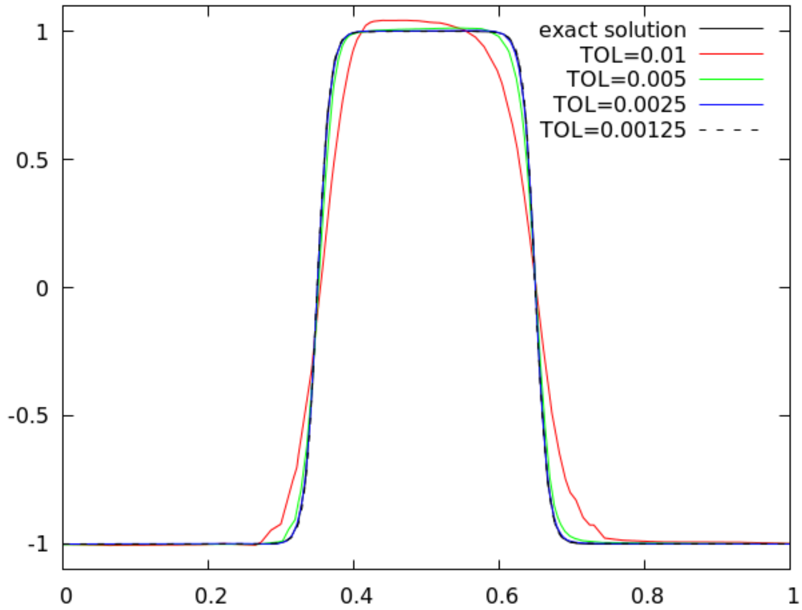


Figure 2.6: Example 2.60. Exact and numerical solutions at time $T = 4$ with $C = 60$. Plot of $\varphi_{h\tau}$ with respect to $x_1$ along the line $x_2 = 0.75$. Conservative interpolation between meshes is used.

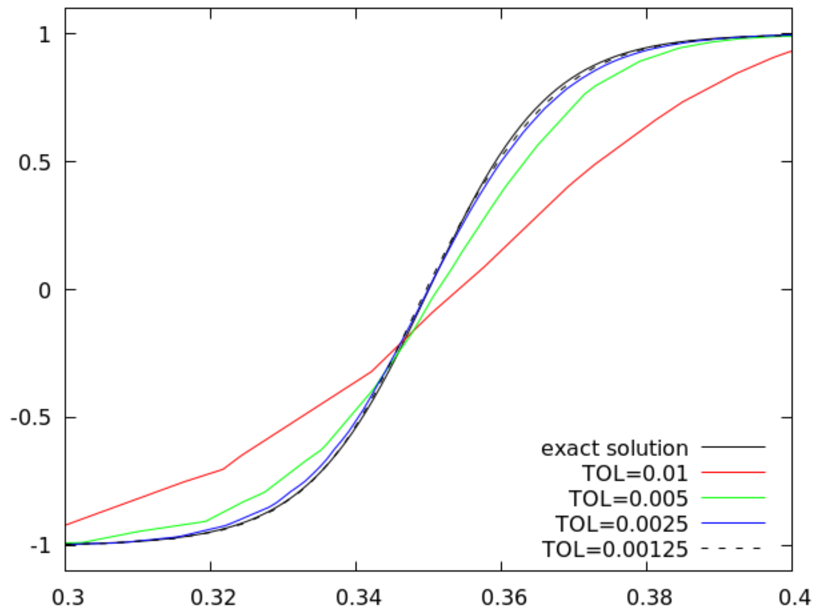


Figure 2.7: Example 2.60. Zoom at Figure 2.6.

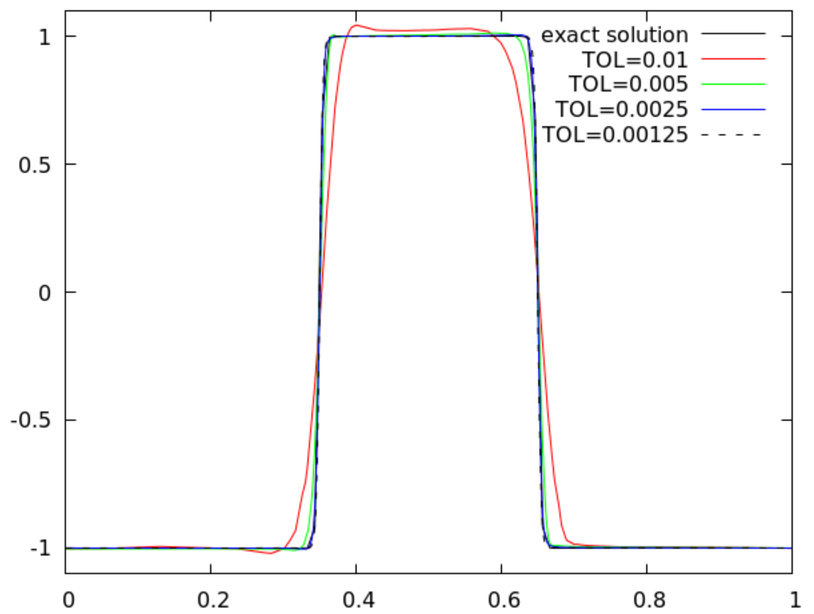


Figure 2.8: Example 2.60. Exact and numerical solutions at time $T = 4$ with $C = 240$. Plot of $\varphi_{h\tau}$ with respect to $x_1$ along the line $x_2 = 0.75$. Conservative interpolation between meshes is used.

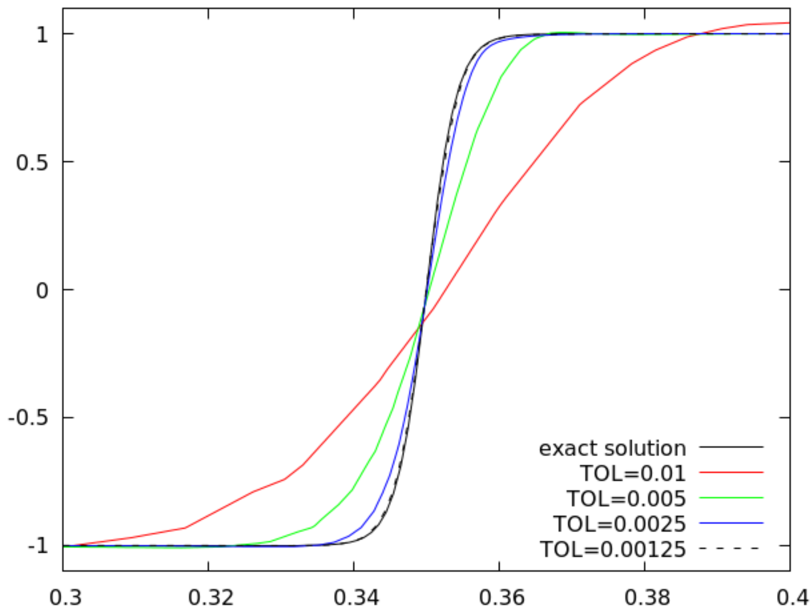


Figure 2.9: Example 2.60. Zoom at Figure 2.8.

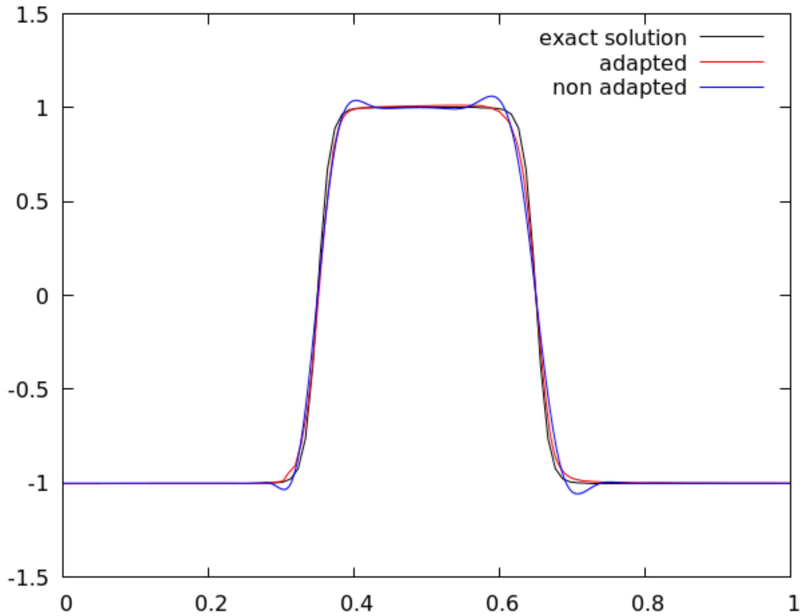


Figure 2.10: Example 2.60. Comparison between numerical solutions at time $T = 4$ with $C = 60$. Plot of $\varphi_{h\tau}$ with respect to $x_1$ along the line $x_2 = 0.75$. The adapted solution is computed with the adaptive algorithm with $TOL = 0.005$. The non-adapted solution is computed on a fix uniform mesh with constant time steps ($h = 0.0025, \tau = 0.00016$).

| $TOL$ | $e(T)_{L^2}$ | $N_v$ | $N_\tau$ |
|---|---|---|---|
| 0.01 | 0.074 | 438 | 1238 |
| 0.005 | 0.023 | 949 | 2572 |
| 0.0025 | 0.0075 | 3510 | 4397 |
| 0.00125 | 0.00404 | 10276 | 7169 |
| 0.01 | 0.090 | 753 | 3407 |
| 0.005 | 0.038 | 2148 | 9247 |
| 0.0025 | 0.0011 | 6666 | 20282 |
| 0.00125 | 0.00038 | 15534 | 36840 |

Table 2.19: Exemple 2.60. Stretching of a circle in a vortex flow. Convergence results for the adaptive algorithm with $C = 60$ (rows 1-4), $C = 240$, (rows 4-6). Conservative interpolation between meshes is used.

| $h$ | $\tau$ | $e(T)_{L^2}$ | $N_v$ | $N_\tau$ |
|---|---|---|---|---|
| 0.01 | 0.001 | 0.11 | 12191 | 4000 |
| 0.005 | 0.0004 | 0.057 | 48354 | 10000 |
| 0.0025 | 0.00016 | 0.025 | 192657 | 25000 |
| 0.01 | 0.001 | 0.15 | 12191 | 4000 |
| 0.005 | 0.0004 | 0.1 | 48354 | 10000 |
| 0.0025 | 0.00016 | 0.071 | 192657 | 25000 |

Table 2.20: Exemple 2.60. Stretching of a circle in a vortex flow. Convergence results with non-adapted meshes and constant time steps ($\tau^2 = O(h^{3/2})$) with $C = 60$ (rows 1-3), $C = 240$, (rows 4-6).

## 2.6 3D experiments

We now briefly present the generalization of our a posteriori results for $\mathbb{R}^3$ using the notations already presented in the Section 1.6 of Chapter 1. The numerical method (2.83) reads the same of the 2D case, except for the stabilization parameter that is choosen now as

$$\delta_{h|K} = \frac{\lambda_{3,K}}{2\,\|\mathbf{u}(t)\|_{L^\infty(K)}}, \qquad \forall K \in \mathcal{T}_h \text{ such that } \mathbf{u} \text{ is not indentically zero on } K, \quad (2.105)$$

and by $\delta_{h|K} = 0$ otherwise. Then, the a posteriori error estimate contained in the Theorem 2.55 is generalized to the 3D case and follows the same proof, the only change being that we have to consider the 3D definition of $\omega_K$ as described in Chapter 1, Section 1.6. For the same reason, the error indicators $\eta^A$ and $\eta^T$ defined before for the 2D case are directly extended to the 3D situation (by replacing the two dimensional definition of $\tilde{\omega}$ by its three dimensional one as presented in Section 1.6). Note that the time error indicator $\eta^T$ remains unchanged.

As for the 2D case, the goal of the adaptive algorithm is to build a sequence of time steps and meshes such that, roughly speaking ,

$$\eta = \sqrt{(\eta^A)^2 + (\eta^T)^2} \simeq TOL$$

for a prescribed tolerance. We here ask that

$$0.875\,TOL \leq \left(\frac{\eta^2}{T}\right)^{1/2} \leq 1.125\,TOL.$$

Observe that the lower and the upper bound are slightly closer than in the 2D case. This will a priori increase the number of remeshing / time steps changes, but will yield more accurate results. The adaptive algorithm (2.15) reads the same, the only difference being in the conditions (2.99) that are written as

$$\frac{4\sigma_P}{3N_P}\frac{0.875^2 TOL^2\tau^{n+1}}{2} \leq (\eta^A_{i,P,n})^2 \leq \frac{4\sigma_P}{3N_P}\frac{1.125^2 TOL^2\tau^{n+1}}{2}, \quad i=1,2,3.$$

since we now consider tetrahedron and three directions. Here above $\sigma_P$ is given by

$$\sigma_P = \frac{(\eta^A_{1,P,n})^2 + (\eta^A_{3,P,n})^2 + (\eta^A_{3,P,n})^2}{(\eta^A_{P,n})^2}$$

where we construct $(\eta^A_{P,n})^2$ and $(\eta^A_{i,P,n})^2, i = 1,2,3$, as before as

$$(\eta^A_{P,n})^2 = \sum_{\substack{K\in\mathcal{T}_h\\ P\in K}} \eta^2_{K,n}$$

with

$$(\eta^A_{K,n})^2 = \int_{t^n}^{t^{n+1}} \left\| \frac{\partial\varphi_{h\tau}}{\partial t} + \mathbf{u}(t)\cdot\nabla\varphi_{h\tau}\right\|_{L^2(K)} \tilde{\omega}_K(\Pi_h^{ZZ}\varphi_{h\tau} - \varphi_{h\tau})dt.$$

and for $i = 1,2,3$

$$(\eta^A_{i,P,n})^2 = \sum_{\substack{K\in\mathcal{T}_h\\ P\in K}} \eta^2_{i,K,n}$$

with

$$(\eta^A_{i,K,n})^2 = \int_{t^n}^{t^{n+1}} \left\| \frac{\partial\varphi_{h\tau}}{\partial t} + \mathbf{u}(t)\cdot\nabla\varphi_{h\tau}\right\|_{L^2(K)} \tilde{\omega}_{i,K}(\Pi_h^{ZZ}\varphi_{h\tau} - \varphi_{h\tau})dt.$$

All the meshes are generated with the 3D mesh generator feflo.a [71]. Interpolation between meshes are done with the Wolf-Interpol program [5], that allows us to perform both the Lagrange and conservative interpolation.

We choose the domain $\Omega$ to be the unique cube $]0,1[^3$. We first solve the 3D version of Example 2.57 to test the convergence of the numerical method on non-adapted meshes and constant time steps. The numerical results are reported in Table 2.21 where we compute in particular the effectivity index

$$ei = \frac{\eta}{e(T)_{L^2}}.$$

We observe the same conclusions as in the 2D case:

- When the numerical error is mainly due to the space discretization, $ei$ is close to 20 and $ei^{ZZ}$ is close to 1.
- When the numerical error is mainly due to the time discretization, $ei$ is close to 2.

| $h_1 - h_2 - h_3$ | $\tau$ | $e_{L^2(H^1)}$ | $ei^{ZZ}$ | $e(T)_{L^2}$ | $\eta^A$ | $\eta^T$ | $ei$ |
|---|---|---|---|---|---|---|---|
| 0.01 - 0.5 -0.5 | 0.002 | 0.13 | 0.98 | 0.0019 | 0.018 | 0.0013 | 9.02 |
| 0.005 - 0.25 -0.25 | 0.0005 | 0.074 | 0.99 | 0.00072 | 0.0069 | 0.00014 | 9.62 |
| 0.0025 - 0.125 -0.125 | 0.000125 | 0.038 | 0.99 | 0.00022 | 0.0025 | 0.000016 | 11.29 |
| 0.00125 - 0.0625 - 0.0625 | 0.00003125 | 0.019 | 0.99 | 0.000064 | 0.0012 | 0.0000019 | 18.75 |
| 0.02 - 0.1 -0.1 | 0.05 | 1.5 | 0.14 | 0.12 | 0.038 | 0.26 | 2.26 |
| 0.005 - 0.025 -0.025 | 0.025 | 0.69 | 0.101 | 0.046 | 0.0066 | 0.099 | 2.16 |
| 0.00125 - 0.06125 -0.06125 | 0.0125 | 0.22 | 0.089 | 0.014 | 0.000092 | 0.031 | 2.23 |

Table 2.21: 3D version of Example 2.57 with $C = 60$. Convergence results when $\tau = O(h^2)$ (rows 1-3) and $h = O(\tau^2)$(rows 4-6). The mesh aspect ratio is 50.

We then run the adaptive algorithm where we choose the normalized error indicators

$$\frac{\eta^A}{20}, \quad \frac{\eta^T}{2},$$

and the corresponding effectivity index

$$ei = \sqrt{\left(\frac{\eta^A}{20}\right)^2 + \left(\frac{\eta^T}{2}\right)^2} / e(T)_{L^2}.$$

As in 2D, we do not introduce new notations, and we opt for the convention that error indicators and the effectivity index are always divided by their respective weight, unless we clearly indicate the contrary. The results are reported in Table 2.22, and the mesh and the solutions are represented in Figure 2.11 for $TOL = 0.0005$ . The same conclusions as in 2D are made when we use the linear Lagrange interpolation or the conservative algorithm to perform meshes interpolations, the Lagrange interpolation yielding very poor results. We start the algorithm with an initial uniform grid of mesh size $h = 0.1$ and with an initial time step $\tau^1 = 0.001$. Since 3D computations are costly, we improve a bit our method by generating a first good grid by forcing the algorithm to remesh several times at the first iteration, even if we satisfy the stopping criterion.

| $TOL$ | $e(T)_{L^2}$ | $ei$ | $e_{L^2(H^1)}$ | $ei^{ZZ}$ | $\eta^A$ | $\eta^T$ | $ar$ | $\bar{ar}$ | $N_v$ | $N_\tau$ | $N_m$ | $N_c$ |
|---|---|---|---|---|---|---|---|---|---|---|---|---|
| 0.001 | 0.0012 | 0.57 | 0.101 | 0.91 | 0.00051 | 0.00048 | 967 | 135 | 870 | 363 | 60 | 898 |
| 0.0005 | 0.00049 | 0.71 | 0.063 | 0.93 | 0.00026 | 0.00024 | 2321 | 223 | 1245 | 569 | 78 | 1519 |
| 0.00025 | 0.00021 | 0.85 | 0.038 | 0.96 | 0.00013 | 0.00012 | 3336 | 348 | 2164 | 805 | 86 | 1781 |
| 0.000125 | 0.000082 | 1.06 | 0.023 | 0.97 | 0.000064 | 0.000059 | 6742 | 710 | 3147 | 1164 | 94 | 2210 |

Table 2.22: Example 2.57. Convergence results for the adaptive algorithm. Conservative interpolation is used.

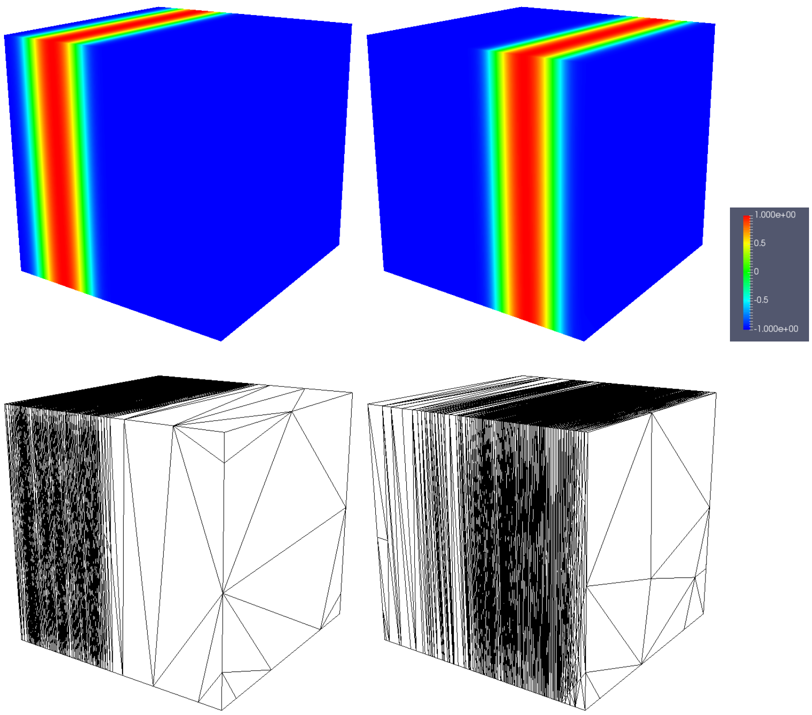


Figure 2.11: Example 2.57. Mesh and solution with $C = 60$ and $TOL = 0.0005$ at $t = 0$ (left) and $t = 0.5$ (right). Conservative interpolation between meshes is used.

Finally, we test our adaptive agorithm for 3D versions of Example 2.60. To avoid too small time steps and shorten the simulation, we present the results obtained with the non-normalized error indicators, that allow us to take large tolerances. The first test consists to solve the deformation of the sphere of radius 0.15 centered at $(0.7, 0.5, 0.5)$ where $\mathbf{u}$ is given by

$$\mathbf{u}(x_1, x_2, x_3, t) = \begin{pmatrix} \sin^2(\pi x_1) cos(\pi t/3) \left(\sin(\pi(x_2 - 0.5)) - \sin(\pi(x_3 - 0.5))\right) \\ \sin^2(\pi x_2) cos(\pi t/3) \left(\sin(\pi(x_3 - 0.5)) - \sin(\pi(x_1 - 0.5))\right) \\ \sin^2(\pi x_3) cos(\pi t/3) \left(\sin(\pi(x_1 - 0.5)) - \sin(\pi(x_2 - 0.5))\right) \end{pmatrix}.$$

The solution is represented for $t = 0, 0.75, 1.5, 2.25, 3$ in Figure 2.12 where we choose $TOL = 0.05$.

The last case is the Leveque-Enright's test case, that was proposed in the framework of conservative methods for advection equations. We start with an initial sphere of radius 0.15 centered at $(0.35, 0.35, 0.35)$ that is deformed through the incompressible flow $\mathbf{u}$ given by

$$\mathbf{u}(x_1, x_2, x_3, t) = \begin{pmatrix} 2\sin^2(\pi x_1)\sin(2\pi x_2)\sin(2\pi x_3)\cos(\pi t/3) \\ -\sin(2\pi x_1)\sin^2(\pi x_2)\sin(2\pi x_3)\cos(\pi t/3) \\ -\sin(2\pi x_1)\sin(2\pi x_2)\sin^2(\pi x_3)\cos(\pi t/3) \end{pmatrix}.$$

The solution is represented in Figure 2.13 where we choose $TOL = 0.05$.

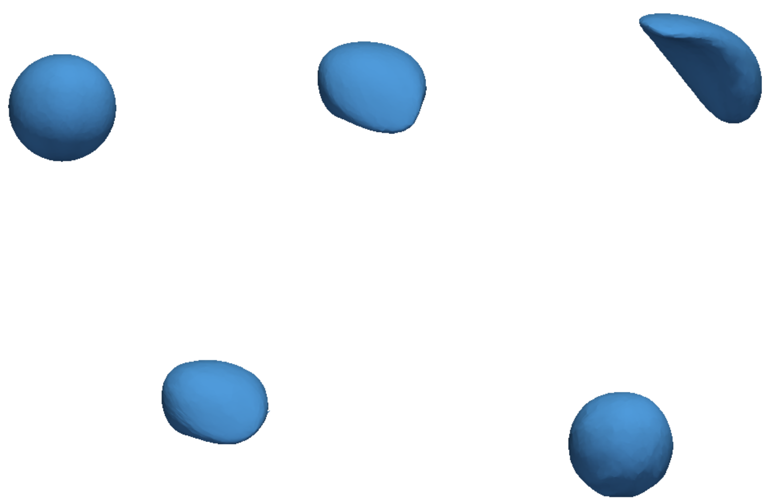

Figure 2.12: Stretching of a sphere in a vortex flow. Solution at time $t = 0, 0.75, 1.5, 2.25, 3$, with $TOL = 0.05$. Conservative interpolation between meshes is used.

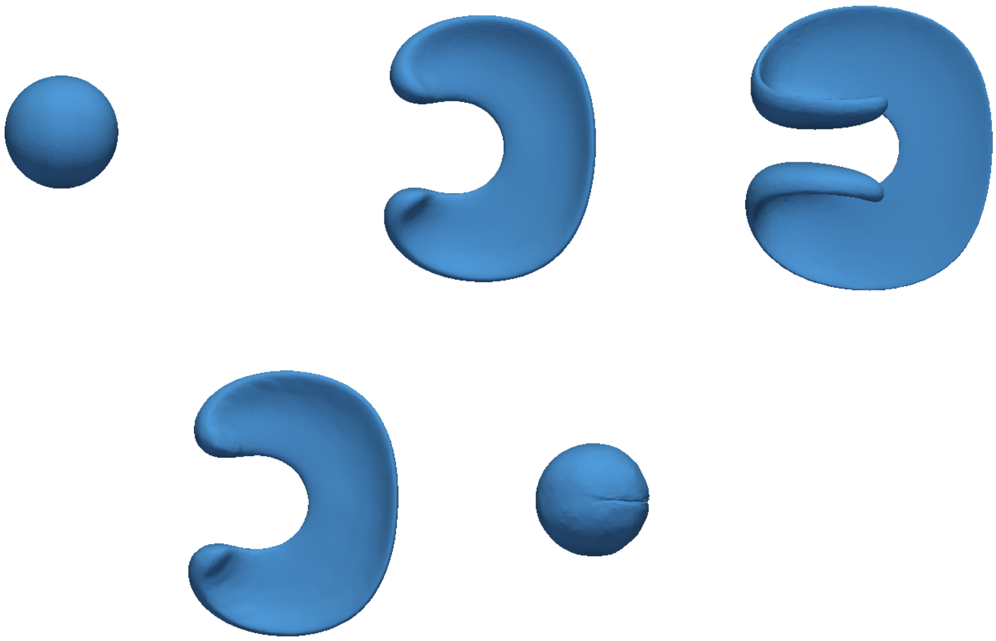

Figure 2.13: Leveque-Enright's test case. Solution at time $t = 0, 0.75, 1.5, 2.25, 3$, with $TOL = 0.05$. Conservative interpolation between meshes is used.

# Chapter 3

# A posteriori error estimates for the time dependent incompressible Stokes and Navier-Stokes equations with constant coefficients

In this chapter, we study a numerical method and prove a posteriori error estimates for the incompressible (Navier-)Stokes equations with constant density and viscosity. The spatial approximation is performed with continuous, piecewise linear, anisotropic stabilized finite elements while the time is discretized with Backward Differentiation Formula (BDF), namely the Backward Euler method, that is an order one scheme, and the BDF2 method, which is of second order accuracy.

To split the technical difficulties, we first focus on the steady Navier-Stokes equations

$$\rho(\mathbf{u} \cdot \nabla)\mathbf{u} - \mu\Delta\mathbf{u} + \nabla p = \mathbf{f}$$

and we prove an a posteriori error estimate. Then, we prove a posteriori error estimates for transient fluids equations by first considering the simpler and linear case of the time dependent Stokes equations

$$\rho\frac{\partial\mathbf{u}}{\partial t} - \mu\Delta\mathbf{u} + \nabla p = \mathbf{f},$$

and we extend the results to the time dependent Navier-Stokes equations

$$\rho\frac{\partial\mathbf{u}}{\partial t} + \rho(\mathbf{u} \cdot \nabla)\mathbf{u} - \mu\Delta\mathbf{u} + \nabla p = \mathbf{f}.$$

The objectives of this chapter are the followings :

- To present a numerical methods to solve fluids motion equations with anisotropic finite elements and a time advancing scheme.
- To prove a posteriori error estimates involving the space and the time discretizations.
- To present and to study an adaptive algorithm.

The outline of the Chapter is as follows: in Section 3.1, we present the numerical method used to solve the steady Navier-Stokes equations and we demonstrate an anisotropic a posteriori error estimate. In Section 3.2 and 3.3, numerical experiments are perfomed with fix and adapted meshes.

In Section 3.4 and 3.5, we study the time dependent Stokes equations and we prove a posteriori error estimates involving only the spatial approximation (Section 3.4) and involving both space and time discretization (Section 3.5).

Finally, in Sections 3.6, 3.7 and 3.8, we extend the previous results to the nonlinear case and we perform numerical experiments with fix meshes and time step in Section 3.9. In Section 3.10, we present the adaptive algorithm and we perform numerical experiments with adapted meshes and time steps.

The main theorems of this chapter are: the Theorem 3.6 that contains an anisotropic a posteriori error estimates for the steady Navier-Stokes equations; the Theorem 3.41 that proves a an posteriori error bound for the fully discrete time dependent Stokes equations; finally the Theorem 3.49, resp. 3.57 that contain a semi-discrete a posteriori error estimate for the space, resp. the time, approximation of the time dependent Navier-Stokes equations.

Throughout all this chapter, we mainly focus on the 2D situation and we comment on the differences in the three dimensional case whenever it is appropriate.

## 3.1 A posteriori error estimates for the steady incompressible Navier-Stokes equations

In this section, we study a numerical method to solve the steady Navier-Stokes equations. We focus on the a posteriori error analysis when using anisotropic meshes. Existing results for isotropic finite elements can be found for instance in [25], where an a posteriori error estimate is deriving using the Inverse Function Theorem, or in [17] where an error indicator is proposed based on the study of linearized equations.

Let $\Omega$ be an open, bounded, Lipschitz set of $\mathbb{R}^2$, $\rho, \mu > 0$ standing respectively for the density and the viscosity, and $\mathbf{f} \in (L^2(\Omega))^2$, then we are looking for $(\mathbf{u}, p)$ the solution of the incompressible steady Navier-Stokes equation

$$\begin{cases} \rho(\mathbf{u}\cdot\nabla)\mathbf{u} - \mu\Delta\mathbf{u} + \nabla p = \mathbf{f}, & \text{in } \Omega, \\ \operatorname{div}\mathbf{u} = 0, & \text{in } \Omega, \\ \mathbf{u} = 0, & \text{on } \partial\Omega. \end{cases} \tag{3.1}$$

One key to solve the Navier-Stokes equations is to find a functional space for the velocity and a functional space for the pressure that satisfy the so-called inf-sup condition (also known as the Ladyzhenskaya-Babuska-Brezzi condition). For instance, it's well known that

$$\inf_{\substack{p\in L^2_0(\Omega)\\ p\neq 0}} \left( \sup_{\substack{\mathbf{v}\in (H^1_0(\Omega))^2\\ \mathbf{v}\neq 0}} \frac{\int_\Omega p \operatorname{div}\mathbf{v} d\mathbf{x}}{\|p\|_{L^2(\Omega)}\|\mathbf{v}\|_{H^1(\Omega)}} \right) > 0. \tag{3.2}$$

One can observe two important properties that result from (3.2). First of all, for any $F \in (H^{-1}(\Omega))^2$, there exists a unique $p \in L^2_0(\Omega)$ such that

$$-\int_\Omega p \operatorname{div}\mathbf{v} d\mathbf{x} = F(\mathbf{v}), \forall \mathbf{v} \in (H^1_0(\Omega))^2.$$

This is a fundamental result used to prove the existence (and uniqueness) of a pressure that solves the Navier-Stokes equations. On the other hand, (3.2) implies also that the divergence operator is surjective from $(H^1_0(\Omega))^2$ to $L^2_0(\Omega)$. In particular, that means that there exists a constant $C > 0$ depending only on $\Omega$ such that for all $r \in L^2_0(\Omega)$, there exists $\mathbf{w} \in (H^1_0(\Omega))^2$ such that

$$\operatorname{div}\mathbf{w} = r, \quad \|\nabla\mathbf{w}\|_{L^2(\Omega)} \leq C\|q\|_{L^2(\Omega)}.$$

This last fact will be used to derive the error estimates.

In a weak formulation, the equations (3.1) reads: find $(\mathbf{u}, p) \in (H^1_0(\Omega))^2 \times L^2_0(\Omega)$ such that

$$\begin{aligned} \rho\int_\Omega(\mathbf{u}\cdot\nabla)\mathbf{u}\cdot\mathbf{v}d\mathbf{x} + \mu\int_\Omega\nabla\mathbf{u}\cdot\nabla\mathbf{v}d\mathbf{x} - \int_\Omega p\operatorname{div}\mathbf{v}d\mathbf{x} &= \int_\Omega\mathbf{f}\cdot\mathbf{v}d\mathbf{x}, \quad \forall\mathbf{v}\in(H^1_0(\Omega))^2,\\ -\int_\Omega q\operatorname{div}\mathbf{u}d\mathbf{x} &= 0, \quad \forall q\in L^2_0(\Omega). \end{aligned} \tag{3.3}$$

We know [21, 99] that there exists at least one solution $(\mathbf{u}, p) \in (H^1_0(\Omega))^2 \times L^2_0(\Omega)$ to the equations (3.3). Moreover, the velocity satisfies the following a priori estimate that we shall use later :

**Proposition 3.1.**
*Let $(\mathbf{u}, p) \in (H^1_0(\Omega))^2 \times L^2_0(\Omega)$ be a solution of (3.3). Then the following a priori estimate holds*

$$\|\nabla\mathbf{u}\|_{L^2(\Omega)} \leq \frac{C_P\|\mathbf{f}\|_{L^2(\Omega)}}{\mu}, \tag{3.4}$$

*where $C_P$ is the Poincaré constant of the domain.*

*Proof.* By choosing $\mathbf{v} = \mathbf{u}$ in (3.3) yields

$$\rho\int_\Omega((\mathbf{u}\cdot\nabla)\mathbf{u})\cdot\mathbf{u}d\mathbf{x} + \mu\|\nabla\mathbf{u}\|^2_{L^2(\Omega)} = \int_\Omega\mathbf{f}\cdot\mathbf{u}d\mathbf{x}.$$

Reproducing the same computation performed in the framework of the transport equation, one can show that

$$\rho\int_\Omega((\mathbf{u}\cdot\nabla)\mathbf{u})\cdot\mathbf{u}d\mathbf{x} = 0.$$

Indeed, since $\mathbf{u}$ is divergence free

$$\rho\int_\Omega((\mathbf{u}\cdot\nabla)\mathbf{u}))\cdot\mathbf{u}d\mathbf{x} = \rho\int_\Omega\operatorname{div}\left(\mathbf{u}\frac{|\mathbf{u}|^2}{2}\right)d\mathbf{x} = \rho\int_{\partial\Omega}\mathbf{u}\cdot\mathbf{n}\frac{|\mathbf{u}|^2}{2}d\mathbf{x} = 0,$$

where we use the divergence theorem and the boundary condition to conclude. Therefore it remains that

$$\mu\|\nabla\mathbf{u}\|^2_{L^2(\Omega)} = \int_\Omega\mathbf{f}\cdot\mathbf{u}d\mathbf{x}$$

which yields the result after using the Cauchy-Schwarz and Poincaré inequality on the right hand side. ☐

**Remark 3.2.** (i) One important step to prove an energy estimate, that we will use to prove the error bounds, is the fact that

$$\rho\int_\Omega((\mathbf{u}\cdot\nabla)\mathbf{u})\cdot\mathbf{u}d\mathbf{x} = \rho\int_{\partial\Omega}\mathbf{u}\cdot\mathbf{n}\frac{|\mathbf{u}|^2}{2}d\mathbf{x} = 0,$$

since $\mathbf{u}$ has zero trace on $\partial\Omega$. Another condition that yields to the same results is for instance that $\mathbf{u}\cdot\mathbf{n} = 0$ on $\partial\Omega$.

(ii) Requiring that $\mathbf{f} \in (L^2(\Omega))^2$ is too much for (3.3) to be well-posed in $(H_0^1(\Omega))^2 \times L_0^2(\Omega)$ since both existence and uniqueness hold for a more general case where $\mathbf{f} \in (H^{-1}(\Omega))^2$. To simplify the discussion, we directly assume that $\mathbf{f}$ is square integrable since it is necessary to give a sense to our numerical method and estimates.

If we assume that the force term $\mathbf{f}$ is small enough, then we can moreover show that the solutions of (3.1) are unique. This well-known result is presented in the next proposition.

**Proposition 3.3** (Uniqueness for small data).
*Let us denote by $C_P$ the Poincaré constant of $\Omega$ and by $C_{SOB}$ the Sobolev embedding constant of Proposition A.8 in the Appendix. Define*

$$C_{NS} = \frac{C_P C_{SOB} \rho \|\mathbf{f}\|_{L^2(\Omega)}}{\mu^2}.$$

*If*

$$C_{NS} < 1 \tag{3.5}$$

*then there exists a unique $(\mathbf{u}, p) \in (H_0^1(\Omega))^2 \times L_0^2(\Omega)$ satisfying (3.1).*

*Proof.* Assume that $(\mathbf{u}_1, p_1), (\mathbf{u}_2, p_2) \in (H_0^1(\Omega))^2 \times L_0^2(\Omega)$ are two different solutions of (3.3). Taking the difference between the equations for each solution, we obtain

$$\rho \int_\Omega ((\mathbf{u}_1 \cdot \nabla)\mathbf{u}_1 - (\mathbf{u}_2 \cdot \nabla)\mathbf{u}_2) \cdot \mathbf{v} d\mathbf{x} + \mu \int_\Omega \nabla(\mathbf{u}_1 - \mathbf{u}_2) \cdot \nabla \mathbf{v} d\mathbf{x} - \int_\Omega (p_1 - p_2) \operatorname{div} \mathbf{v} d\mathbf{x} = 0.$$

Choosing $\mathbf{v} = \mathbf{u}_1 - \mathbf{u}_2$ in the last formulation yields

$$\mu \|\nabla(\mathbf{u}_1 - \mathbf{u}_2)\|_{L^2(\Omega)}^2 = -\rho \int_\Omega ((\mathbf{u}_1 \cdot \nabla)\mathbf{u}_1 - (\mathbf{u}_2 \cdot \nabla)\mathbf{u}_2) \cdot (\mathbf{u}_1 - \mathbf{u}_2) d\mathbf{x}.$$

Observe that the non linear part can be written as

$$-\rho \int_\Omega ((\mathbf{u}_1 \cdot \nabla)(\mathbf{u}_1 - \mathbf{u}_2) + ((\mathbf{u}_1 - \mathbf{u}_2) \cdot \nabla)\mathbf{u}_2) \cdot (\mathbf{u}_1 - \mathbf{u}_2) d\mathbf{x}.$$

Note that since $\operatorname{div} \mathbf{u}_1 = 0$, we have as in Proposition 3.1 that

$$-\rho \int_\Omega ((\mathbf{u}_1 \cdot \nabla)(\mathbf{u}_1 - \mathbf{u}_2)) \cdot (\mathbf{u}_1 - \mathbf{u}_2) d\mathbf{x} = 0.$$

Therefore it remains that

$$\mu \|\nabla(\mathbf{u}_1 - \mathbf{u}_2)\|_{L^2(\Omega)}^2 = -\rho \int_\Omega ((\mathbf{u}_1 - \mathbf{u}_2) \cdot \nabla)\mathbf{u}_2) \cdot (\mathbf{u}_1 - \mathbf{u}_2) d\mathbf{x}.$$

Using Proposition A.8, the right hand side can be bounded by

$$\rho C_{SOB} \|\nabla \mathbf{u}_2\|_{L^2(\Omega)} \|\nabla(\mathbf{u}_1 - \mathbf{u}_2)\|_{L^2(\Omega)}^2.$$

Using moreover the a priori estimate (3.4), we have finally that

$$\mu \|\nabla(\mathbf{u}_1 - \mathbf{u}_2)\|_{L^2(\Omega)}^2 \leq \frac{C_P C_{SOB} \rho \|\mathbf{f}\|_{L^2(\Omega)}}{\mu} \|\nabla(\mathbf{u}_1 - \mathbf{u}_2)\|_{L^2(\Omega)}^2 = C_{NS} \mu \|\nabla(\mathbf{u}_1 - \mathbf{u}_2)\|_{L^2(\Omega)}^2.$$

Since we assume that $C_{NS} < 1$, we obtain that

$$(1 - C_{NS}) \mu \|\nabla(\mathbf{u}_1 - \mathbf{u}_2)\|_{L^2(\Omega)}^2 \leq 0$$

implying that $\mathbf{u}_1 = \mathbf{u}_2$. By the inf-sup condition (3.2), we necessarily have that $p_1 = p_2$. □

To approximate the equations (3.3) with finite elements, we may first check that the inf-sup condition holds also between the discrete space for the velocity and the discrete space for the pressure. This is the case when $\mathbb{P}^2$ continuous finite elements are used to approximate the velocity and $\mathbb{P}^1$ for the pressure. When $\mathbb{P}^1-\mathbb{P}^1$ elements are used, the inf-sup condition does not hold and some alternative techniques have to be used to guarantee the solvability of the numerical scheme. We focus on stabilization techniques, namely the so-called PSPG methods (Pressure Stabilized Petrov-Galerkin), see for instance [92] for the case of isotropic finite elements. The idea is to add a residual term to the standard finite elements discretization of the mass conservation equation. From now, we assume that $\Omega$ is a convex polygon in $\mathbb{R}^2$. The numerical method reads: for all $h>0$, let $\mathcal{T}_h$ be a conformal triangulation of $\Omega$ into triangles $K$ of diameter $h_K \le h$. Let us note by $W_h$ the classical finite elements set of all continuous, piecewise linear functions, and by $W_{h,0}$ the subset of $W_h$ which elements have zero value on $\partial\Omega$. Finally let $V_h=(W_{h,0})^2$ and $Q_h = W_h \cap L^2_0(\Omega)$ be respectively the discrete velocity space and pressure space. Then, we are looking for $(\mathbf{u}_h, p_h) \in V_h \times Q_h$ such that

$$\begin{aligned}
&\rho \int_\Omega (\mathbf{u}_h \cdot \nabla)\mathbf{u}_h \cdot \mathbf{v}_h d\mathbf{x} + \mu \int_\Omega \nabla \mathbf{u}_h \cdot \nabla \mathbf{v}_h d\mathbf{x} - \int_\Omega p_h \operatorname{div} \mathbf{v}_h d\mathbf{x} \\
&\qquad + \sum_{K\in\mathcal{T}_h} \alpha_K \int_K (\mathbf{f} - \rho(\mathbf{u}_h\cdot\nabla)\mathbf{u}_h + \mu\Delta\mathbf{u}_h - \nabla p_h)\cdot(\rho(\mathbf{u}_h\cdot\nabla)\mathbf{v}_h - \mu\Delta\mathbf{v}_h)\, d\mathbf{x} \\
&\qquad\qquad = \int_\Omega \mathbf{f}\cdot\mathbf{v}_h d\mathbf{x}, \quad \forall \mathbf{v}_h \in V_h, \\
&-\int_\Omega q_h \operatorname{div} \mathbf{u}_h d\mathbf{x} + \sum_{K\in\mathcal{T}_h} \alpha_K \int_K (\mathbf{f} - \rho(\mathbf{u}_h\cdot\nabla)\mathbf{u}_h + \mu\Delta\mathbf{u}_h - \nabla p_h)\cdot\nabla q_h d\mathbf{x} = 0, \quad \forall q_h \in Q_h,
\end{aligned} \tag{3.6}$$

where $\alpha_K$ (in the isotropic setting) is given by

$$\alpha_K = \frac{\alpha h_K^2}{\mu \xi(Re_K)}$$

with $\alpha > 0$ and

$$\xi(Re_K) = \begin{cases} 1 & \text{if } Re_K \le 1, \\ Re_K & \text{if } Re_K \ge 1, \end{cases}$$

where we define the local Reynolds number $Re_K$ by

$$Re_K = \frac{\rho \|\mathbf{u}_h\|_{L^\infty(K)} h_K}{\mu}.$$

Analysis of the above method was proposed in [48]. Observe that the above method is the equivalent of the SUPG method for advection-diffusion equation and that the stabilization technique proposed is a consistent stabilization. Indeed all the terms of the equation are put into the stabilization part, and therefore the exact solution $(\mathbf{u}, p)$ satisfies also the numerical method (3.27).

For the anisotropic case, we follow the idea advocated in [78] for the steady Stokes equations and we choose $\alpha_K$ as

$$\alpha_K = \frac{\alpha \lambda_{2,K}^2}{\mu \xi(Re_K)} \tag{3.7}$$

where the anisotropic local Reynolds number is given by

$$Re_K = \frac{\rho \|\mathbf{u}_h\|_{L^\infty(K)} \lambda_{2,K}}{\mu}. \tag{3.8}$$

Note that if we consider $\Omega \in \mathbb{R}^3$, the numerical method reads the same, the only difference being that we replace $\lambda_{2,K}$ by $\lambda_{3,K}$ in the definitions of $\alpha_K$ and $Re_K$.

We prove, under the assumption that the numerical method converges, an a posteriori error estimate. We always work under the small data hypothesis, implying that the problem (3.1) has a unique solution. The a posteriori error estimate is contained in the next theorem. The result is not fully satisfactory in our framework since isotropic terms remain in the estimator. Later on, we will prove a better estimate, more convenient for anisotropic meshes (see Theorem 3.6).

**Theorem 3.4** (A first anisotropic a posteriori error estimate for the steady Navier-Stokes equations)**.**
*Let us assume that the small data hypothesis (3.5) is fullfilled, that is to say*

$$C_{NS} < 1,$$

*and let* $(\mathbf{u}, p) \in (H_0^1(\Omega))^2 \times L_0^2(\Omega)$ *be the solution of (3.1). Assume that there exists a unique* $(\mathbf{u}_h, p_h) \in V_h \times Q_h$ *that is solution of (3.6), where* $\alpha_K$ *is given by its anisotropic version (3.7) and that moreover* $\|\nabla(\mathbf{u} - \mathbf{u}_h)\|_{L^2(\Omega)} \to 0$ *as* $h \to 0$*. Then, there exists* $h_0 > 0$ *and a constant* $C > 0$ *depending only on* $\Omega$ *and the reference triangle* $K$ *such that if* $h \leq h_0$ *we have:*

$$\mu\|\nabla(\mathbf{u} - \mathbf{u}_h)\|^2_{L^2(\Omega)} + \frac{1}{\mu}\|p - p_h\|^2_{L^2(\Omega)} \leq \frac{C}{(1 - C_{NS})^2} \sum_{K\in\mathcal{T}_h} (\eta^A_{K,\mathbf{u}})^2 + (\eta^I_{K,p})^2 + (\eta^{\mathrm{div}}_K)^2, \quad (3.9)$$

*where*

$$(\eta^A_{K,\mathbf{u}})^2 = \left(\|\mathbf{f} - \rho(\mathbf{u}_h \cdot \nabla)\mathbf{u}_h + \mu\Delta\mathbf{u}_h - \nabla p_h\|_{L^2(K)} + \frac{1}{2\sqrt{\lambda_{2,K}}}\|[\mu\nabla\mathbf{u}_h \cdot \mathbf{n}]\|_{L^2(\partial K)}\right)\omega_K(\mathbf{u}{-}\mathbf{u}_h),$$

$$(\eta^I_{K,p})^2 = \frac{1}{\mu}(\lambda^2_{1,K}{+}\lambda^2_{2,K})\left(\|\mathbf{f} - \rho(\mathbf{u}_h \cdot \nabla)\mathbf{u}_h + \mu\Delta\mathbf{u}_h - \nabla p_h\|_{L^2(K)} + \frac{1}{2\sqrt{\lambda_{2,K}}}\|[\mu\nabla\mathbf{u}_h \cdot \mathbf{n}]\|_{L^2(\partial K)}\right)^2$$

$$(\eta^{\mathrm{div}}_K)^2 = \mu\|\operatorname{div}\mathbf{u}_h\|^2_{L^2(K)}.$$

*Proof.* In what follows, we denote by $C > 0$ any positive constant that may depend only on the reference triangle or the domain $\Omega$, which value may change from line to line. When it is necessary, we denote by $C_{SOB}$ the Sobolev constant of Proposition A.8.

*Step 1. A first estimate for the velocity.*

We first derive an estimate for the velocity. Observe that

$$\begin{aligned}\mu\|\nabla(\mathbf{u} - \mathbf{u}_h)\|^2_{L^2(\Omega)} &= \mu\int_\Omega \nabla(\mathbf{u} - \mathbf{u}_h)\cdot\nabla(\mathbf{u} - \mathbf{u}_h)d\mathbf{x}\\ &+ \int_\Omega (p - p_h)\operatorname{div}(\mathbf{u} - \mathbf{u}_h)d\mathbf{x} - \int_\Omega (p - p_h)\operatorname{div}(\mathbf{u} - \mathbf{u}_h)d\mathbf{x}\\ &+ \rho\int_\Omega ((\mathbf{u}\cdot\nabla)\mathbf{u})\cdot(\mathbf{u} - \mathbf{u}_h)d\mathbf{x} - \rho\int_\Omega ((\mathbf{u}\cdot\nabla)\mathbf{u})\cdot(\mathbf{u} - \mathbf{u}_h)d\mathbf{x}\\ &+ \rho\int_\Omega ((\mathbf{u}_h\cdot\nabla)\mathbf{u}_h)\cdot(\mathbf{u} - \mathbf{u}_h)d\mathbf{x} - \rho\int_\Omega ((\mathbf{u}_h\cdot\nabla)\mathbf{u}_h)\cdot(\mathbf{u} - \mathbf{u}_h)d\mathbf{x}.\end{aligned}$$

Since $(\mathbf{u}, p)$ are the exact solutions to the Navier-Stokes equations, we have in fact

$$\begin{aligned}\mu\|\nabla(\mathbf{u}-\mathbf{u}_h)\|^2_{L^2(\Omega)} = &\int_\Omega \mathbf{f}\cdot(\mathbf{u}-\mathbf{u}_h)d\mathbf{x} - \rho\int_\Omega((\mathbf{u}_h\cdot\nabla)\mathbf{u}_h)\cdot(\mathbf{u}-\mathbf{u}_h)d\mathbf{x}\\ &-\mu\int_\Omega \nabla\mathbf{u}_h\cdot\nabla(\mathbf{u}-\mathbf{u}_h)d\mathbf{x} + \int_\Omega p_h \operatorname{div}(\mathbf{u}-\mathbf{u}_h)d\mathbf{x}\\ &+\int_\Omega(p-p_h)\operatorname{div}\mathbf{u}_h d\mathbf{x} - \rho\int_\Omega((\mathbf{u}\cdot\nabla)\mathbf{u}-(\mathbf{u}_h\cdot\nabla)\mathbf{u}_h)\cdot(\mathbf{u}-\mathbf{u}_h)d\mathbf{x}.\end{aligned}$$

Using (3.6), we can remove any couple of test functions $(\mathbf{v}_h, q_h)\in V_h\times Q_h$ and it yields

$$\begin{aligned}\mu\|\nabla(\mathbf{u}-\mathbf{u}_h)\|^2_{L^2(\Omega)} = &\int_\Omega \mathbf{f}\cdot(\mathbf{u}-\mathbf{u}_h-\mathbf{v}_h)d\mathbf{x} - \rho\int_\Omega((\mathbf{u}_h\cdot\nabla)\mathbf{u}_h)\cdot(\mathbf{u}-\mathbf{u}_h-\mathbf{v}_h)d\mathbf{x}\\ &-\mu\int_\Omega \nabla\mathbf{u}_h\cdot\nabla(\mathbf{u}-\mathbf{u}_h-\mathbf{v}_h)d\mathbf{x} + \int_\Omega p_h \operatorname{div}(\mathbf{u}-\mathbf{u}_h-\mathbf{v}_h)d\mathbf{x}\\ &+\int_\Omega(p-p_h-q_h)\operatorname{div}\mathbf{u}_h d\mathbf{x}\\ &+\sum_{K\in\mathcal{T}_h}\alpha_K\int_K(\mathbf{f}-\rho(\mathbf{u}_h\cdot\nabla)\mathbf{u}_h+\mu\Delta\mathbf{u}_h-\nabla p_h)\cdot(\rho\mathbf{u}_h\cdot\nabla\mathbf{v}_h-\mu\Delta\mathbf{v}_h+\nabla q_h)\\ &-\rho\int_\Omega((\mathbf{u}\cdot\nabla)\mathbf{u}-(\mathbf{u}_h\cdot\nabla)\mathbf{u}_h)\cdot(\mathbf{u}-\mathbf{u}_h)d\mathbf{x}.\end{aligned}$$

An integration by parts over each triangle yields finally

$$\begin{aligned}\mu\|\nabla(\mathbf{u}-\mathbf{u}_h)\|^2_{L^2(\Omega)} = &\sum_{K\in\mathcal{T}_h}\Big(\int_K(\mathbf{f}-\rho(\mathbf{u}_h\cdot\nabla)\mathbf{u}_h+\mu\Delta u_h-\nabla p_h)(\mathbf{u}-\mathbf{u}_h-\mathbf{v}_h)d\mathbf{x}\\ &+\frac{1}{2}\int_{\partial K}[\mu\nabla\mathbf{u}_h\cdot\mathbf{n}]\cdot(\mathbf{u}-\mathbf{u}_h-\mathbf{v}_h)d\mathbf{x}\Big)\\ &+\int_\Omega(p-p_h-q_h)\operatorname{div}\mathbf{u}_h d\mathbf{x}\\ &+\sum_{K\in\mathcal{T}_h}\alpha_K\int_K(\mathbf{f}-\rho(\mathbf{u}_h\cdot\nabla)\mathbf{u}_h+\mu\Delta\mathbf{u}_h-\nabla p_h)\cdot(\rho(\mathbf{u}_h\cdot\nabla)\mathbf{v}_h-\mu\Delta\mathbf{v}_h+\nabla q_h)\,d\mathbf{x}\\ &-\rho\int_\Omega((\mathbf{u}\cdot\nabla)\mathbf{u}-(\mathbf{u}_h\cdot\nabla)\mathbf{u}_h)\cdot(\mathbf{u}-\mathbf{u}_h)d\mathbf{x}.\end{aligned}$$

Choosing $\mathbf{v}_h = R_h(\mathbf{u}-\mathbf{u}_h)$ and $q_h = 0$, and applying the Cauchy-Schwarz inequality, we obtain, using the anisotropic interpolation error estimates for the Clément's interpolant of Proposition 1.2 (note that we use the fact $\Delta\mathbf{v}_h = 0$ on each $K$)

$$\begin{aligned}&\mu\|\nabla(\mathbf{u}-\mathbf{u}_h)\|^2_{L^2(\Omega)}\\ &\le C\sum_{K\in\mathcal{T}_h}\left(\|\mathbf{f}-\rho(\mathbf{u}_h\cdot\nabla)\mathbf{u}_h+\mu\Delta u_h-\nabla p_h\|_{L^2(K)}+\frac{1}{2\sqrt{\lambda_{2,K}}}\|[\mu\nabla\mathbf{u}_h\cdot\mathbf{n}]\|_{L^2(\partial K)}\right)\omega_K(\mathbf{u}-\mathbf{u}_h)\\ &\qquad+\|p-p_h\|_{L^2(\Omega)}\|\operatorname{div}\mathbf{u}_h\|_{L^2(\Omega)}\\ &\quad+\sum_{K\in\mathcal{T}_h}\alpha_K\,\|\mathbf{f}-\rho(\mathbf{u}_h\cdot\nabla)\mathbf{u}_h+\mu\Delta\mathbf{u}_h-\nabla p_h\|_{L^2(K)}\,\|\rho(\mathbf{u}_h\cdot\nabla)R_h(\mathbf{u}-\mathbf{u}_h)\|_{L^2(K)}\\ &\qquad-\rho\int_\Omega((\mathbf{u}\cdot\nabla)\mathbf{u}-(\mathbf{u}_h\cdot\nabla)\mathbf{u}_h)\cdot(\mathbf{u}-\mathbf{u}_h)d\mathbf{x}. \quad (3.10)\end{aligned}$$

We first bound the third term of the right hand side. Observe that

$$\alpha_K\,\|\rho(\mathbf{u}_h\cdot\nabla)R_h(\mathbf{u}-\mathbf{u}_h)\|_{L^2(K)} \le \alpha_K\rho\|\mathbf{u}_h\|_{L^\infty(K)}\|\nabla R_h(\mathbf{u}-\mathbf{u}_h)\|_{L^2(K)}.$$

Note that

$$\alpha_K \rho \|\mathbf{u}_h\|_{L^\infty(K)} = \frac{\alpha \lambda_{2,K}^2 \rho \|\mathbf{u}_h\|_{L^\infty(K)}}{\mu \xi(Re_K)} = \alpha \lambda_{2,K} \frac{Re_K}{\xi(Re_K)} \leq \alpha \lambda_{2,K}$$

since we clearly have that $\dfrac{Re_K}{\xi(Re_K)} \leq 1$. It yields

$$\alpha_K \left\| \rho(\mathbf{u}_h \cdot \nabla) R_h(\mathbf{u} - \mathbf{u}_h) \right\|_{L^2(K)} \leq \alpha \lambda_{2,K} \left\| \nabla R_h(\mathbf{u} - \mathbf{u}_h) \right\|_{L^2(K)}.$$

The same computations made to derive an a posteriori error estimate for the transport (see Theorem 2.29, inequality (2.54)) yield

$$\alpha \lambda_{2,K} \left\| \nabla R_h(\mathbf{u} - \mathbf{u}_h) \right\|_{L^2(K)} \leq C \omega_K(\mathbf{u} - \mathbf{u}_h).$$

Therefore, putting all together, we have that

$$\alpha_K \left\| \rho(\mathbf{u}_h \cdot \nabla) R_h(\mathbf{u} - \mathbf{u}_h) \right\|_{L^2(K)} \leq C \omega_K(\mathbf{u} - \mathbf{u}_h)$$

implying that the stabilization term

$$\sum_{K \in \mathcal{T}_h} \alpha_K \left\| \mathbf{f} - \rho(\mathbf{u}_h \cdot \nabla)\mathbf{u}_h + \mu \Delta \mathbf{u}_h - \nabla p_h \right\|_{L^2(K)} \left\| \rho(\mathbf{u}_h \cdot \nabla) R_h(\mathbf{u} - \mathbf{u}_h) \right\|_{L^2(K)}$$

is bounded by

$$C \sum_{K \in \mathcal{T}_h} \left\| \mathbf{f} - \rho(\mathbf{u}_h \cdot \nabla)\mathbf{u}_h + \mu \Delta \mathbf{u}_h - \nabla p_h \right\|_{L^2(K)} \omega_K(\mathbf{u} - \mathbf{u}_h)$$

and therefore can be absorbed in the first term of (3.10). To conclude this first step, we have still to bound the last term of (3.10) involving the nonlinear terms. Formally, observe that

$$\begin{aligned}(\mathbf{u} \cdot \nabla)\mathbf{u} - (\mathbf{u}_h \cdot \nabla)\mathbf{u}_h &= (\mathbf{u} \cdot \nabla)\mathbf{u} - (\mathbf{u} \cdot \nabla)\mathbf{u}_h + (\mathbf{u} \cdot \nabla)\mathbf{u}_h - (\mathbf{u}_h \cdot \nabla)\mathbf{u}_h \\ &= (\mathbf{u} \cdot \nabla)(\mathbf{u} - \mathbf{u}_h) + ((\mathbf{u} - \mathbf{u}_h) \cdot \nabla)\mathbf{u}_h.\end{aligned}$$

Therefore we have

$$\begin{aligned}&\rho \int_\Omega ((\mathbf{u} \cdot \nabla)\mathbf{u} - (\mathbf{u}_h \cdot \nabla)\mathbf{u}_h) \cdot (\mathbf{u} - \mathbf{u}_h) d\mathbf{x} \\ &\qquad = \rho \int_\Omega ((\mathbf{u} \cdot \nabla)(\mathbf{u} - \mathbf{u}_h)) \cdot (\mathbf{u} - \mathbf{u}_h) d\mathbf{x} + \rho \int_\Omega (((\mathbf{u} - \mathbf{u}_h) \cdot \nabla)\mathbf{u}_h) \cdot (\mathbf{u} - \mathbf{u}_h) d\mathbf{x}.\end{aligned}$$

The first term can be shown to be zero. Since $\mathbf{u}$ is divergence free and vanishes on $\partial\Omega$

$$\rho \int_\Omega ((\mathbf{u} \cdot \nabla)(\mathbf{u} - \mathbf{u}_h)) \cdot (\mathbf{u} - \mathbf{u}_h) d\mathbf{x} = \rho \int_\Omega \operatorname{div}\left( \mathbf{u} \frac{|\mathbf{u} - \mathbf{u}_h|^2}{2} \right) d\mathbf{x} = \rho \int_{\partial\Omega} \mathbf{u} \cdot \mathbf{n} \frac{|\mathbf{u} - \mathbf{u}_h|^2}{2} d\mathbf{x} = 0.$$

So we finally have, using Proposition A.8 of the Appendix that

$$\begin{aligned}\rho \int_\Omega ((\mathbf{u} \cdot \nabla)\mathbf{u} - (\mathbf{u}_h \cdot \nabla)\mathbf{u}_h) \cdot (\mathbf{u} - \mathbf{u}_h) d\mathbf{x} &= \rho \int_\Omega (((\mathbf{u} - \mathbf{u}_h) \cdot \nabla)\mathbf{u}_h) \cdot (\mathbf{u} - \mathbf{u}_h) d\mathbf{x} \\ &\leq \rho C_{SOB} \|\nabla \mathbf{u}_h\|_{L^2(\Omega)} \|\nabla(\mathbf{u} - \mathbf{u}_h)\|_{L^2(\Omega)}^2 \\ &\leq \left( \rho C_{SOB} \|\nabla(\mathbf{u} - \mathbf{u}_h)\|_{L^2(\Omega)} + \rho C_{SOB} \|\nabla \mathbf{u}\|_{L^2(\Omega)} \right) \|\nabla(\mathbf{u} - \mathbf{u}_h)\|_{L^2(\Omega)}^2.\end{aligned}$$

Using the a priori estimate (3.4), we have finally that

$$\rho \int_\Omega ((\mathbf{u}\cdot\nabla)\mathbf{u} - (\mathbf{u}_h\cdot\nabla)\mathbf{u}_h)\cdot(\mathbf{u}-\mathbf{u}_h)d\mathbf{x}$$
$$\leq \left( \frac{\rho C_{SOB}\|\nabla(\mathbf{u}-\mathbf{u}_h)\|_{L^2(\Omega)}}{\mu} + \frac{\rho C_P C_{SOB}\|\mathbf{f}\|_{L^2(\Omega)}}{\mu^2} \right) \mu\|\nabla(\mathbf{u}-\mathbf{u}_h)\|^2_{L^2(\Omega)}$$
$$= \left( \frac{\rho C_{SOB}\|\nabla(\mathbf{u}-\mathbf{u}_h)\|_{L^2(\Omega)}}{\mu} + C_{NS} \right) \mu\|\nabla(\mathbf{u}-\mathbf{u}_h)\|^2_{L^2(\Omega)}$$

Since $1 - C_{NS} > 0$ and we assume that $\|\nabla(\mathbf{u}-\mathbf{u}_h)\|_{L^2(\Omega)} \to 0$ as $h \to 0$, there exists $h_0 > 0$ such that if $h \leq h_0$ then

$$\frac{\rho C_{SOB}\|\nabla(\mathbf{u}-\mathbf{u}_h)\|_{L^2(\Omega)}}{\mu} \leq \frac{1-C_{NS}}{2}$$

implying that

$$\frac{\rho C_{SOB}\|\nabla(\mathbf{u}-\mathbf{u}_h)\|_{L^2(\Omega)}}{\mu} + C_{NS} \leq \frac{1-C_{NS}}{2} + C_{NS} = \frac{1+C_{NS}}{2} < 1.$$

In conclusion, we can pass the term

$$\left( \frac{\rho C_{SOB}\|\nabla(\mathbf{u}-\mathbf{u}_h)\|_{L^2(\Omega)}}{\mu} + C_{NS} \right) \mu\|\nabla(\mathbf{u}-\mathbf{u}_h)\|^2_{L^2(\Omega)}$$

to the left hand side, and obtain that

$$\frac{1-C_{NS}}{2}\mu\|\nabla(\mathbf{u}-\mathbf{u}_h)\|^2_{L^2(\Omega)}$$
$$\leq C \sum_{K\in\mathcal{T}_h} \left( \|\mathbf{f} - \rho(\mathbf{u}_h\cdot\nabla)\mathbf{u}_h + \mu\Delta u_h - \nabla p_h\|_{L^2(K)} + \frac{1}{2\sqrt{\lambda_{2,K}}}\|[\mu\nabla\mathbf{u}_h\cdot\mathbf{n}]\|_{L^2(\partial K)} \right) \omega_K(\mathbf{u}-\mathbf{u}_h)$$
$$+ \|p-p_h\|_{L^2(\Omega)}\|\operatorname{div}\mathbf{u}_h\|_{L^2(\Omega)},$$

which yields (since again $1 - C_{NS} > 0$)

$$\mu\|\nabla(\mathbf{u}-\mathbf{u}_h)\|^2_{L^2(\Omega)}$$
$$\leq \frac{C}{1-C_{NS}} \sum_{K\in\mathcal{T}_h} \left( \|\mathbf{f} - \rho(\mathbf{u}_h\cdot\nabla)\mathbf{u}_h + \mu\Delta u_h - \nabla p_h\|_{L^2(K)} + \frac{1}{2\sqrt{\lambda_{2,K}}}\|[\mu\nabla\mathbf{u}_h\cdot\mathbf{n}]\|_{L^2(\partial K)} \right) \omega_K(\mathbf{u}-\mathbf{u}_h)$$
$$+ \frac{2}{1-C_{NS}}\|p-p_h\|_{L^2(\Omega)}\|\operatorname{div}\mathbf{u}_h\|_{L^2(\Omega)}.$$

*Step 2. Estimate for the pressure.*

To finish the proof, we have to estimate $\|p-p_h\|_{L^2(\Omega)}$. To do so, we use the inf-sup condition (3.2) that implies that there exists $\mathbf{w} \in (H^1_0(\Omega))^2$ such that

$$\operatorname{div}\mathbf{w} = p_h - p, \quad \|\nabla\mathbf{w}\|_{L^2(\Omega)} \leq C\|p-p_h\|_{L^2(\Omega)}.$$

We have then

$$\|p-p_h\|^2_{L^2(\Omega)} = -\int_\Omega (p-p_h)\operatorname{div}\mathbf{w}d\mathbf{x} = -\int_\Omega p\operatorname{div}\mathbf{w}d\mathbf{x} + \int_\Omega p_h\operatorname{div}\mathbf{w}d\mathbf{x}$$
$$= \int_\Omega \mathbf{f}\cdot\mathbf{w} - \rho((\mathbf{u}\cdot\nabla)\mathbf{u})\cdot\mathbf{w} - \mu\nabla\mathbf{u}\nabla\mathbf{w}d\mathbf{x} + \int_\Omega p_h\operatorname{div}\mathbf{w}d\mathbf{x}$$
$$= \int_\Omega \mathbf{f}\cdot\mathbf{w} - \rho((\mathbf{u}_h\cdot\nabla)\mathbf{u}_h)\cdot\mathbf{w} - \mu\nabla\mathbf{u}_h\nabla\mathbf{w} + p_h\operatorname{div}\mathbf{w}d\mathbf{x}$$
$$- \rho\int_\Omega ((\mathbf{u}\cdot\nabla)\mathbf{u} - (\mathbf{u}_h\cdot\nabla)\mathbf{u}_h)\cdot\mathbf{w}d\mathbf{x} - \mu\int_\Omega \nabla(\mathbf{u}-\mathbf{u}_h)\cdot\nabla\mathbf{w}d\mathbf{x}.$$

Using (3.6), we can remove any $\mathbf{v}_h \in V_h$ and we get

$$\|p-p_h\|^2_{L^2(\Omega)} = \int_\Omega \mathbf{f}\cdot(\mathbf{w}-\mathbf{v}_h)-\rho((\mathbf{u}_h\cdot\nabla)\mathbf{u}_h)\cdot(\mathbf{w}-\mathbf{v}_h)-\mu\nabla\mathbf{u}_h\nabla(\mathbf{w}-\mathbf{v}_h)+p_h \operatorname{div}(\mathbf{w}-\mathbf{v}_h)d\mathbf{x}$$
$$+\sum_{K\in\mathcal{T}_h}\alpha_K\int_K(\mathbf{f}-\rho(\mathbf{u}_h\cdot\nabla)\mathbf{u}_h+\mu\Delta\mathbf{u}_h-\nabla p_h)\cdot(\rho(\mathbf{u}_h\cdot\nabla)\mathbf{v}_h-\mu\Delta\mathbf{v}_h)\,d\mathbf{x}$$
$$-\rho\int_\Omega((\mathbf{u}\cdot\nabla)\mathbf{u}-(\mathbf{u}_h\cdot\nabla)\mathbf{u}_h)\cdot\mathbf{w}d\mathbf{x}-\mu\int_\Omega\nabla(\mathbf{u}-\mathbf{u}_h)\cdot\nabla\mathbf{w}d\mathbf{x}.$$

We finish as we did in the first step. We integrate by parts and use the Cauchy-Schwarz inequality to obtain

$$\|p-p_h\|^2_{L^2(\Omega)}$$
$$\leq \sum_{K\in\mathcal{T}_h}\|\mathbf{f}-\rho(\mathbf{u}_h\cdot\nabla)\mathbf{u}_h+\mu\Delta\mathbf{u}_h+\nabla p_h\|_{L^2(K)}\|\mathbf{w}-\mathbf{v}_h\|_{L^2(K)}+\frac{1}{2}\|\,[\mu\nabla\mathbf{u}_h\cdot\mathbf{n}]\,\|_{L^2(\partial K)}\|\mathbf{w}-\mathbf{v}_h\|_{L^2(\partial K)}$$
$$+\sum_{K\in\mathcal{T}_h}\alpha_K\,\|\mathbf{f}-\rho(\mathbf{u}_h\cdot\nabla)\mathbf{u}_h+\mu\Delta\mathbf{u}_h-\nabla p_h\|_{L^2(K)}\,\|\rho(\mathbf{u}_h\cdot\nabla)\mathbf{v}_h-\mu\Delta\mathbf{v}_h\|_{L^2(\Omega)}$$
$$-\rho\int_\Omega((\mathbf{u}\cdot\nabla)\mathbf{u}-(\mathbf{u}_h\cdot\nabla)\mathbf{u}_h)\cdot\mathbf{w}d\mathbf{x}-\mu\int_\Omega\nabla(\mathbf{u}-\mathbf{u}_h)\cdot\nabla\mathbf{w}d\mathbf{x}.$$

Choosing $\mathbf{v}_h = R_h(\mathbf{w})$ and using the anisotropic Clément's interpolation error estimate, we obtain, after bounding the terms coming from the stabilization in the same manner as we did in the first step,

$$\|p-p_h\|^2_{L^2(\Omega)}$$
$$\leq C\sum_{K\in\mathcal{T}_h}\left(\|\mathbf{f}-\rho(\mathbf{u}_h\cdot\nabla)\mathbf{u}_h+\mu\Delta\mathbf{u}_h+\nabla p_h\|_{L^2(K)}+\frac{1}{2\sqrt{\lambda_{2,K}}}\|\,[\mu\nabla\mathbf{u}_h\cdot\mathbf{n}]\,\|_{L^2(\partial K)}\right)\omega_K(\mathbf{w})$$
$$-\rho\int_\Omega((\mathbf{u}\cdot\nabla)\mathbf{u}-(\mathbf{u}_h\cdot\nabla)\mathbf{u}_h)\mathbf{w}d\mathbf{x}-\mu\int_\Omega\nabla(\mathbf{u}-\mathbf{u}_h)\cdot\nabla\mathbf{w}d\mathbf{x}. \quad (3.11)$$

To simplify the rest of the proof, we note

$$\nu_K = \|\mathbf{f}-\rho(\mathbf{u}_h\cdot\nabla)\mathbf{u}_h+\mu\Delta\mathbf{u}_h+\nabla p_h\|_{L^2(K)}+\frac{1}{2\sqrt{\lambda_{2,K}}}\|\,[\mu\nabla\mathbf{u}_h\cdot\mathbf{n}]\,\|_{L^2(\partial K)}.$$

We now treat each of the three terms of the right hand side. Since $\mathbf{r}_{1,K},\mathbf{r}_{2,K}$ form an orthonormal basis, we recall that

$$(\mathbf{r}^T_{1,K}G_K(\mathbf{w})\mathbf{r}_{1,K}+\mathbf{r}^T_{2,K}G_K(\mathbf{w})\mathbf{r}_{2,K})^{1/2} = \|\nabla\mathbf{w}\|_{L^2(\Delta K)}.$$

Therefore, one have

$$\omega_K(\mathbf{w}) \leq \sqrt{\lambda^2_{1,K}+\lambda^2_{2,K}}(\mathbf{r}^T_{1,K}G_K(\mathbf{w})\mathbf{r}_{1,K}+\mathbf{r}^T_{2,K}G_K(\mathbf{w})\mathbf{r}_{2,K})^{1/2} = \sqrt{\lambda^2_{1,K}+\lambda^2_{2,K}}\|\nabla\mathbf{w}\|_{L^2(\Delta K)}.$$

The discrete Cauchy-Swchwarz inequality implies then

$$\sum_{K\in\mathcal{T}_h}\nu_K\omega_K(\mathbf{w}) \leq \left(\sum_{K\in\mathcal{T}_h}(\lambda^2_{1,K}+\lambda^2_{2,K})\nu^2_K\right)^{1/2}\left(\sum_{K\in\mathcal{T}_h}\|\nabla\mathbf{w}\|^2_{L^2(\Delta K)}\right)^{1/2}.$$

We recall (see the hypothesis *(i)* presented in Section 1.1) that for all vertices in $\mathcal{T}_h$, its number of neighbors is uniformly bounded by above with respect to the mesh size. Therefore one may bound

$$\left(\sum_{K\in\mathcal{T}_h}\|\nabla\mathbf{w}\|^2_{L^2(\Delta K)}\right)^{1/2} \leq C\|\nabla\mathbf{w}\|_{L^2(\Omega)}$$

implying that the first term of (3.11) is bounded by

$$C\left(\sum_{K\in\mathcal{T}_h}(\lambda_{1,K}^2+\lambda_{2,K}^2)\nu_K^2\right)^{1/2}\|\nabla\mathbf{w}\|_{L^2(\Omega)},$$

where $C$ is in particular independent of the aspect ratio. The last term of (3.11) can be bounded directly by

$$-\mu\int_\Omega\nabla(\mathbf{u}-\mathbf{u}_h)\cdot\nabla\mathbf{w}d\mathbf{x}\leq\mu\|\nabla(\mathbf{u}-\mathbf{u}_h)\|_{L^2(\Omega)}\|\nabla\mathbf{w}\|_{L^2(\Omega)}.$$

The nonlinear term is estimated in the following way. Note that

$$\begin{aligned}-\rho\int_\Omega&((\mathbf{u}\cdot\nabla)\mathbf{u}-(\mathbf{u}_h\cdot\nabla)\mathbf{u}_h)\cdot\mathbf{w}d\mathbf{x}\\&=-\rho\int_\Omega((\mathbf{u}\cdot\nabla)(\mathbf{u}-\mathbf{u}_h)+((\mathbf{u}-\mathbf{u}_h)\cdot\nabla)\mathbf{u}_h)\cdot\mathbf{w}d\mathbf{x}.\end{aligned}$$

Using the Proposition A.8, we obtain

$$\begin{aligned}-\rho\int_\Omega&((\mathbf{u}\cdot\nabla)\mathbf{u}-(\mathbf{u}_h\cdot\nabla)\mathbf{u}_h)\cdot\mathbf{w}d\mathbf{x}\\&\leq C_{SOB}\rho\left(\|\nabla\mathbf{u}\|_{L^2(\Omega)}+\|\nabla\mathbf{u}_h\|_{L^2(\Omega)}\right)\|\nabla(\mathbf{u}-\mathbf{u}_h)\|_{L^2(\Omega)}\|\nabla\mathbf{w}\|_{L^2(\Omega)}.\end{aligned}$$

Using the triangle inequality and the a priori estimate (3.4), we have that

$$\begin{aligned}C_{SOB}\rho\left(\|\nabla\mathbf{u}\|_{L^2(\Omega)}+\|\nabla\mathbf{u}_h\|_{L^2(\Omega)}\right)&\leq C_{SOB}\rho\left(2\|\nabla\mathbf{u}\|_{L^2(\Omega)}+\|\nabla(\mathbf{u}-\mathbf{u}_h)\|_{L^2(\Omega)}\right)\\&\leq\left(\frac{2\rho C_{SOB}C_P\|\mathbf{f}\|_{L^2(\Omega)}}{\mu^2}+\frac{\rho C_{SOB}\|\nabla(\mathbf{u}-\mathbf{u}_h)\|_{L^2(\Omega)}}{\mu}\right)\mu\\&=\left(2C_{NS}+\frac{\rho C_{SOB}\|\nabla(\mathbf{u}-\mathbf{u}_h)\|_{L^2(\Omega)}}{\mu}\right)\mu.\end{aligned}$$

We recall that we choose in the Step 1 $h_0$ such that if $h\leq h_0$ we have

$$\frac{\rho C_{SOB}\|\nabla(\mathbf{u}-\mathbf{u}_h)\|_{L^2(\Omega)}}{\mu}\leq\frac{1-C_{NS}}{2}.$$

Therefore we finally have that

$$\begin{aligned}-\rho\int_\Omega&((\mathbf{u}\cdot\nabla)\mathbf{u}-(\mathbf{u}_h\cdot\nabla)\mathbf{u}_h)\cdot\mathbf{w}d\mathbf{x}\\&\leq\left(2C_{NS}+\frac{1-C_{NS}}{2}\right)\mu\|\nabla(\mathbf{u}-\mathbf{u}_h)\|_{L^2(\Omega)}\|\nabla\mathbf{w}\|_{L^2(\Omega)}\\&\frac{3C_{NS}+1}{2}\mu\|\nabla(\mathbf{u}-\mathbf{u}_h)\|_{L^2(\Omega)}\|\nabla\mathbf{w}\|_{L^2(\Omega)}\leq2\mu\|\nabla(\mathbf{u}-\mathbf{u}_h)\|_{L^2(\Omega)}\|\nabla\mathbf{w}\|_{L^2(\Omega)}\end{aligned}$$

since $C_{NS}<1$. Putting all together into (3.11), we finally obtain

$$\|p-p_h\|_{L^2(\Omega)}^2\leq\left(C\left(\sum_{K\in\mathcal{T}_h}(\lambda_{1,K}^2+\lambda_{2,K}^2)\nu_K^2\right)^{1/2}+3\mu\|\nabla(\mathbf{u}-\mathbf{u}_h)\|_{L^2(\Omega)}\right)\|\nabla\mathbf{w}\|_{L^2(\Omega)}.$$

Using that $\|\nabla\mathbf{w}\|_{L^2(\Omega)}\leq C\|p-p_h\|_{L^2(\Omega)}$ yields

$$\|p-p_h\|_{L^2(\Omega)}\leq C\left(\left(\sum_{K\in\mathcal{T}_h}(\lambda_{1,K}^2+\lambda_{2,K}^2)\nu_K^2\right)^{1/2}+3\mu\|\nabla(\mathbf{u}-\mathbf{u}_h)\|_{L^2(\Omega)}\right).\tag{3.12}$$

*Step 3. Put estimates for velocity and pressure together.*

We recall that we note

$$\nu_K = \|\mathbf{f} - \rho(\mathbf{u}_h \cdot \nabla)\mathbf{u}_h + \mu\Delta\mathbf{u}_h + \nabla p_h\|_{L^2(K)} + \frac{1}{2\sqrt{\lambda_{2,K}}}\| [\mu\nabla\mathbf{u}_h \cdot \mathbf{n}] \|_{L^2(\partial K)}.$$

From the step 1, we have

$$\mu\|\nabla(\mathbf{u} - \mathbf{u}_h)\|^2_{L^2(\Omega)} \leq \frac{C}{1 - C_{NS}} \sum_{K\in\mathcal{T}_h} \nu_K\omega_K(\mathbf{u} - \mathbf{u}_h) + \frac{2}{1 - C_{NS}}\|p - p_h\|_{L^2(\Omega)}\| \operatorname{div} \mathbf{u}_h\|_{L^2(\Omega)}.$$

Using the estimate for $\|p - p_h\|_{L^2(\Omega)}$ obtained through the step 2, we have

$$\mu\|\nabla(\mathbf{u} - \mathbf{u}_h)\|^2_{L^2(\Omega)} \leq \frac{C}{1 - C_{NS}} \sum_{K\in\mathcal{T}_h} \nu_K\omega_K(\mathbf{u} - \mathbf{u}_h) + \frac{C}{1 - C_{NS}}\left(\left(\sum_{K\in\mathcal{T}_h} (\lambda^2_{1,K} + \lambda^2_{2,K})\nu^2_K\right)^{1/2} + \mu\|\nabla(\mathbf{u} - \mathbf{u}_h)\|_{L^2(\Omega)}\right)\| \operatorname{div} \mathbf{u}_h\|_{L^2(\Omega)}.$$

Using the Young's inequality, one can prove the desired a posteriori error estimate for the velocity

$$\mu\|\nabla(\mathbf{u}-\mathbf{u}_h)\|^2_{L^2(\Omega)} \leq \frac{C}{(1 - C_{NS})^2} \sum_{K\in\mathcal{T}_h} \left(\nu_K\omega_K(\mathbf{u} - \mathbf{u}_h) + (\lambda^2_{1,K} + \lambda^2_{2,K})\frac{\nu^2_K}{\mu} + \mu\| \operatorname{div} \mathbf{u}_h\|^2_{L^2(K)}\right). \tag{3.13}$$

Note that we use the bound

$$\frac{1}{1 - C_{NS}} \leq \frac{1}{(1 - C_{NS})^2}$$

to put the constance in front of the estimate. Finally, plugging the last estimate into (3.12) yields

$$\|p-p_h\|^2_{L^2(\Omega)} \leq \frac{C}{(1 - C_{NS})^2} \sum_{K\in\mathcal{T}_h} \left(\mu\nu_K\omega_K(\mathbf{u} - \mathbf{u}_h) + (\lambda^2_{1,K} + \lambda^2_{2,K})\nu^2_K + \mu^2\| \operatorname{div} \mathbf{u}_h\|^2_{L^2(K)}\right).$$

Dividing by $\mu$ on both sides, we finally obtain as estimate for the pressure

$$\frac{1}{\mu}\|p-p_h\|^2_{L^2(\Omega)} \leq \frac{C}{(1 - C_{NS})^2} \sum_{K\in\mathcal{T}_h} \left(\nu_K\omega_K(\mathbf{u} - \mathbf{u}_h) + (\lambda^2_{1,K} + \lambda^2_{2,K})\frac{\nu^2_K}{\mu} + \mu\| \operatorname{div} \mathbf{u}_h\|^2_{L^2(K)}\right).$$

Summing this last estimate with (3.13) yields the result. □

**Remark 3.5.** (i) As already mentioned, the a posteriori error estimate of Theorem 3.4 is not standard since the exact velocity $\mathbf{u}$ is contained in the estimate. We shall use the ZZ post-processed solution $\Pi^{ZZ}_h\mathbf{u}_h$ to obtain a computable bound as presented in the previous chapters. Note that the post-processing of a vector field is the post-processing of each components.

(ii) Note that the a posteriori error estimate (3.9) is valid only asymptotically (since $h$ must be small enough) and under the assumption that the numerical method converges. This last hypothesis seems reasonable and not too constraining since we only ask for the convergence in the $H^1$ semi-norm without requiring any order of convergence. This condition is quite natural when dealing with nonlinear problem.

The a posteriori error estimate presented in Theorem 3.4 is not strictly anisotropic, the main issue being to derive an anisotropic error estimate for the pressure. Indeed, estimating the pressure requires to make appears the quantity

$$(\lambda_{1,K}^2+\lambda_{2,K}^2)\left(\|\mathbf{f}-\rho(\mathbf{u}_h\cdot\nabla)\mathbf{u}_h+\mu\Delta u_h-\nabla p_h\|_{L^2(K)}+\frac{1}{2\sqrt{\lambda_{2,K}}}\|[\mu\nabla\mathbf{u}_h\cdot\mathbf{n}]\|_{L^2(\partial K)}\right)^2.$$

The term $(\lambda_{1,K}^2+\lambda_{2,K}^2)$ can be bounded either by $2\lambda_{1,K}^2$, which yields a very bad estimate for stretch triangles, or by $\left(\frac{\lambda_{1,K}^2}{\lambda_{2,K}^2}+1\right)\lambda_{2,K}^2$ which makes appear the aspect ratio, forcing to use isotropic finite elements to control it. This is a really bad drawback, since it completely annihilates our goal and the main advantage of the anisotropic framework we use, that is to say proving estimates that do not depend on the mesh aspect ratio, that gives a theoretical justification to the use of anisotropic meshes.

To circumvent this drawback, in [86] the author propose to solve a dual problem rather than using the inf-sup condition to recover a pressure estimate. Let $p$ be the pressure solution in (3.1) and $p_h$ its finite elements approximation obtained by solving (3.6) with $\alpha_K$ given by (3.7). We look for $(\mathbf{w},r)\in(H_0^1(\Omega))^2\times L_0^2(\Omega)$ the weak solution of

$$\begin{cases}-\mu\Delta\mathbf{w}+\nabla r=0, & \text{in } \Omega,\\ \operatorname{div}\mathbf{w}=p_h-p, & \text{in } \Omega,\\ \mathbf{w}=0, & \text{on } \partial\Omega.\end{cases}\tag{3.14}$$

Note that (3.14) is a standard Stokes problem, and its well-posedness in $(H_0^1(\Omega))^2\times L_0^2(\Omega)$ is ensured by the inf-sup condition [21], leading to the following a priori estimate :

$$\|\nabla\mathbf{w}\|_{L^2(\Omega)}+\frac{1}{\mu}\|r\|_{L^2(\Omega)}\le C\|p-p_h\|_{L^2(\Omega)},\tag{3.15}$$

where $C>0$ is a constant depending only on $\Omega$. Using the dual solution, one can derive the same a posteriori estimates as the one presented in Theorem 3.4, excepted that one may replace the quantity $(\eta_{K,p}^I)^2$ by

$$\left(\|\mathbf{f}-\rho(\mathbf{u}_h\cdot\nabla)\mathbf{u}_h+\mu\Delta u_h-\nabla p_h\|_{L^2(K)}+\frac{1}{2\sqrt{\lambda_{2,K}}}\|[\mu\nabla\mathbf{u}_h\cdot\mathbf{n}]\|_{L^2(\partial K)}\right)\omega_K(\mathbf{w}).$$

The proof follows exactly the same arguments as those presented in the demonstration of Theorem 3.4, the only difference being that in (3.12) we keep $\omega_K(\mathbf{w})$ rather than bound it by $\sqrt{\lambda_{1,K}^2+\lambda_{2,K}^2}\|\nabla\mathbf{w}\|_{L^2(\Delta K)}$. By sake of completeness, we write down below the Theorem and its proof that uses the dual problem rather than the inf-sup condition to derive the pressure estimate.

**Theorem 3.6** (An anisotropic a posteriori error estimate for the steady Navier-Stokes equatiosn: a second estimate)**.**
*Let us assume that the small data hypothesis (3.5) is fullfilled, that is to say*

$$C_{NS}<1,$$

*and let* $(\mathbf{u},p)\in(H_0^1(\Omega))^2\times L_0^2(\Omega)$ *be the solution of (3.1). Assume that there exists a unique* $(\mathbf{u}_h,p_h)\in V_h\times Q_h$ *that is solution of (3.6), where* $\alpha_K$ *is given by its anisotropic version (3.7), and moreover that* $\|\nabla(\mathbf{u}-\mathbf{u}_h)\|_{L^2(\Omega)}\to 0$ *as* $h\to 0$*. Finally, let* $(\mathbf{w},r)\in(H_0^1(\Omega))^2\times L_0^2(\Omega)$ *the solution of the dual problem (3.14). Then, there exists* $h_0>0$ *small* *enough and a constant $C > 0$ depending only on $\Omega$ and the reference triangle $K$ such that if $h \leq h_0$*

$$\mu\|\nabla(\mathbf{u}-\mathbf{u}_h)\|^2_{L^2(\Omega)} + \frac{1}{\mu}\|p-p_h\|^2_{L^2(\Omega)} \leq \frac{C}{(1-C_{NS})^2}\sum_{K\in\mathcal{T}_h}(\eta^A_{K,\mathbf{u}})^2 + (\eta^A_{K,p})^2 + (\eta^{\text{div}}_K)^2, \quad (3.16)$$

*where*

$$(\eta^A_{K,\mathbf{u}})^2 = \left(\|\mathbf{f}-\rho(\mathbf{u}_h\cdot\nabla)\mathbf{u}_h + \mu\Delta\mathbf{u}_h - \nabla p_h\|_{L^2(K)} + \frac{1}{2\sqrt{\lambda_{2,K}}}\|[\mu\nabla\mathbf{u}_h\cdot\mathbf{n}]\|_{L^2(\partial K)}\right)\omega_K(\mathbf{u}-\mathbf{u}_h),$$

$$(\eta^A_{K,p})^2 = \frac{1}{\mu}\left(\|\mathbf{f}-\rho(\mathbf{u}_h\cdot\nabla)\mathbf{u}_h + \mu\Delta\mathbf{u}_h - \nabla p_h\|_{L^2(K)} + \frac{1}{2\sqrt{\lambda_{2,K}}}\|[\mu\nabla\mathbf{u}_h\cdot\mathbf{n}]\|_{L^2(\partial K)}\right)\omega_K(\mathbf{w})$$

$$(\eta^{\text{div}}_K)^2 = \mu\|\operatorname{div}\mathbf{u}_h\|^2_{L^2(K)}.$$

*Proof.* We proceed as in the Theorem 3.4 and separate the proof into three steps. Below, we will denote by $C$ any constants that depend only on the reference triangle and $\Omega$. We keep the notation

$$\nu_K = \|\mathbf{f}-\rho(\mathbf{u}_h\cdot\nabla)\mathbf{u}_h + \mu\Delta u_h - \nabla p_h\|_{L^2(K)} + \frac{1}{2\sqrt{\lambda_{2,K}}}\|[\mu\nabla\mathbf{u}_h\cdot\mathbf{n}]\|_{L^2(\partial K)}.$$

*Step 1 : estimate for the velocity.*

Following exactly the same computation as in the Step 1 of Theorem 3.4, we derive that

$$\mu\|\nabla(\mathbf{u}-\mathbf{u}_h)\|^2_{L^2(\Omega)} \leq \frac{C}{1-C_{NS}}\sum_{K\in\mathcal{T}_h}\nu_K\omega_K(\mathbf{u}-\mathbf{u}_h) + \frac{2}{1-C_{NS}}\|p-p_h\|_{L^2(\Omega)}\|\operatorname{div}\mathbf{u}_h\|_{L^2(\Omega)}.$$

Using the Young's inequality, the last estimate is equivalent to

$$\mu\|\nabla(\mathbf{u}-\mathbf{u}_h)\|^2_{L^2(\Omega)} \leq \frac{C}{1-C_{NS}}\sum_{K\in\mathcal{T}_h}\left(\|\mathbf{f}-\rho(\mathbf{u}_h\cdot\nabla)\mathbf{u}_h + \mu\Delta u_h - \nabla p_h\|_{L^2(K)} + \frac{1}{2\sqrt{\lambda_{2,K}}}\|[\mu\nabla\mathbf{u}_h\cdot\mathbf{n}]\|_{L^2(\partial K)}\right)\omega_K(\mathbf{u}-\mathbf{u}_h) + \frac{2}{1-C_{NS}}\left(\frac{1}{2\varepsilon}\|p-p_h\|^2_{L^2(\Omega)} + \frac{\varepsilon}{2}\|\operatorname{div}\mathbf{u}_h\|^2_{L^2(\Omega)}\right),$$

where $\varepsilon > 0$ has to be chosen at the end of the proof.

*Step 2 : estimate for the pressure.*

Since $\operatorname{div}\mathbf{w} = p_h - p$, we have

$$\|p-p_h\|^2_{L^2(\Omega)} = -\int_\Omega (p-p_h)\operatorname{div}\mathbf{w}d\mathbf{x}.$$

Therefore, by following the same steps as in Theorem 3.4, we obtain

$$\|p-p_h\|^2_{L^2(\Omega)} \leq C\sum_{K\in\mathcal{T}_h}\nu_K\omega_K(\mathbf{w}) + 3\mu\|\nabla(\mathbf{u}-\mathbf{u}_h)\|_{L^2(\Omega)}\|\nabla\mathbf{w}\|_{L^2(\Omega)}.$$

Using the fact that

$$\|\nabla \mathbf{w}\|_{L^2(\Omega)} \leq C\|p - p_h\|_{L^2(\Omega)}$$

we obtain, by using the Young's inequality, that there exists $\tilde{C} > 0$ depending only on the reference triangle and $\Omega$ such that

$$\|p - p_h\|^2_{L^2(\Omega)} \leq \tilde{C} \left( \sum_{K \in \mathcal{T}_h} \nu_K \omega_K(\mathbf{w}) + \mu^2 \|\nabla(\mathbf{u} - \mathbf{u}_h)\|^2_{L^2(\Omega)} \right). \tag{3.17}$$

*Step 3 : put all together.*

Combining the estimates obtained in the steps 1 and 2, we have for the velocity

$$\mu\|\nabla(\mathbf{u} - \mathbf{u}_h)\|^2_{L^2(\Omega)} \leq \frac{C}{1 - C_{NS}} \sum_{K \in \mathcal{T}_h} \nu_K \omega_K(\mathbf{u} - \mathbf{u}_h)$$
$$+ \frac{2}{1 - C_{NS}} \left( \frac{\tilde{C}}{2\varepsilon} \sum_{K \in \mathcal{T}_h} \nu_K \omega_K(\mathbf{w}) + \frac{\tilde{C}}{2\varepsilon} \mu^2 \|\nabla(\mathbf{u} - \mathbf{u}_h)\|^2_{L^2(\Omega)} + \frac{\varepsilon}{2} \|\operatorname{div} \mathbf{u}_h\|^2_{L^2(\Omega)} \right). \tag{3.18}$$

We finish the proof by choosing $\varepsilon = \frac{\tilde{C}\mu}{2(1-C_{NS})}$ and plugging again (3.18) into (3.17), and conclude as in Theorem 3.4 by summing the estimates for the velocity and the pressure. □

As already commented, the main difference between Theorem 3.4 and 3.6 is that we choose to write the anisotropic error indicator $(\eta^A_{K,p})^2$ in Theorem 3.6 rather than the isotropic quantity $(\eta^I_{K,p})^2$ of Theorem 3.4. Since $\mathbf{w}$ is the solution of the system of equations (3.14), in practice, to obtain a computable bound, we can replace $\mathbf{w}$ in (3.16) by its finite elements approximation $\mathbf{w}_h$. To do so, we first have to find a superconvergent approximation $P_h$ of the pressure $p$ and then approximate the problem

$$\begin{cases} -\mu\Delta\mathbf{w} + \nabla r = 0, & \text{in } \Omega, \\ \operatorname{div} \mathbf{w} = p_h - P_h, & \text{in } \Omega, \\ \mathbf{w} = 0, & \text{on } \partial\Omega. \end{cases}$$

Finding this $P_h$ is not an obvious task and out of the scope of our work. We can however convince ourself that if $p - p_h$ converges, then the error indicator $(\eta^A_{K,p})^2$ is at least of the right order since $\|\nabla\mathbf{w}\|_{L^2(\Omega)}$ goes as $\|p - p_h\|_{L^2(\Omega)}$. Therefore, in the numerical experiments and in particular in the adaptive framework, we will not consider the pressure estimates and choose heuristically only $\sum_{K \in \mathcal{T}_h} (\eta^A_{K,\mathbf{u}})^2$ as an error indicator for the velocity.

**Remark 3.7** (3D anisotropic a posteriori error estimates)**.**
Both Theorems 3.4 and 3.6 are easily generalizable to $\mathbb{R}^3$. In this case, we have

$$(\eta^A_{K,\mathbf{u}})^2 = \nu_K \omega_K(\mathbf{u} - \mathbf{u}_h), \quad (\eta^A_{K,p})^2 = \frac{1}{\mu} \nu_K \omega_K(\mathbf{w}), \quad (\eta^I_{K,p})^2 = \frac{1}{\mu} (\lambda^2_{1,K} + \lambda^2_{2,K} + \lambda^2_{3,K}) \nu^2_K,$$

with

$$\nu_K = \|\mathbf{f} - \rho(\mathbf{u}_h \cdot \nabla)\mathbf{u}_h + \mu\Delta\mathbf{u}_h - \nabla p_h\|_{L^2(K)} + \frac{1}{2\sqrt{\lambda_{3,K}}} \|[\mu\nabla\mathbf{u}_h \cdot \mathbf{n}]\|_{L^2(\partial K)}$$

and where for $\mathbf{v} \in (H^1(\Omega))^3$

$$\omega_K(\mathbf{v}) = \left( \lambda^2_{1,K} \mathbf{r}^T_{1,K} G_K(\mathbf{v}) \mathbf{r}_{1,K} + \lambda^2_{2,K} \mathbf{r}^T_{2,K} G_K(\mathbf{v}) \mathbf{r}_{2,K} + \lambda^2_{3,K} \mathbf{r}^T_{3,K} G_K(\mathbf{v}) \mathbf{r}_{3,K} \right)^{1/2}.$$

## 3.2 Numerical experiments for the steady incompressible Navier-Stokes equations with non-adapted meshes

We now perform numerical experiments on non-adapted meshes to check the convergence of the method (3.6), where the stabilization parameter $\alpha_K$ is chosen as the anisotropic version (3.7) i.e.

$$\alpha_K = \frac{\alpha \lambda_{2,K}^2}{\mu \xi(Re_K)}$$

with the anisotropic local Reynolds number given by

$$Re_K = \frac{\rho \|\mathbf{u}_h\|_{L^\infty(K)} \lambda_{2,K}}{\mu}.$$

Based on the results obtained in [86, 89] for similar problems, we set $\alpha = 0.01$. A Newton method is applied to solve the nonlinearity issue.

We now present our choice for an error indicator. As already mentioned above, we only consider the velocity. Based on the a posteriori error estimate contained in Theorem 3.6, we define $\eta^A$ the velocity error indicator as

$$\eta^A = \left( \sum_{K \in \mathcal{T}_h} (\eta_K)^2 \right)^{1/2} \tag{3.19}$$

with

$$(\eta_K)^2 = \left( \|\mathbf{f} - \rho(\mathbf{u}_h \cdot \nabla)\mathbf{u}_h + \mu \Delta \mathbf{u}_h - \nabla p_h\|_{L^2(K)} + \frac{1}{2\sqrt{\lambda_{2,K}}} \|[\mu \nabla \mathbf{u}_h \cdot \mathbf{n}]\|_{L^2(\partial K)} \right) \tilde{\omega}_K(\Pi_h^{ZZ}\mathbf{u}_h - \mathbf{u}_h),$$

where we recall that $\Pi_h^{ZZ}$ stands for the Zienkiewicz-Zhu post-processing and $\tilde{\omega}_K$ is the simplified anisotropic form (1.18) given for vector valued functions by

$$\tilde{\omega}_K^2(\mathbf{v}) = \tilde{\omega}_K^2(v_1) + \tilde{\omega}_K^2(v_2), \quad \mathbf{v} = (v_1, v_2) \in (H^1(\Omega))^2.$$

Observe that we do not put in our indicator the divergence part of the estimate (3.16), the reason being that the quantity

$$\mu^{1/2} \| \operatorname{div} \mathbf{u}_h \|_{L^2(\Omega)}$$

is small compared to the rest of the estimate, as it will be verified in the numerical experiments.

As we did in the framework of elliptic problem, we are mainly interested in the effectivity indices $ei$ and $ei^{ZZ}$ that stand respectively for

$$\frac{\eta^A}{e_{\mu,H^1}}, \quad \frac{\|\nabla(\Pi_h^{ZZ}\mathbf{u}_h - \mathbf{u}_h)\|_{L^2(\Omega)}}{e_{H^1}},$$

where the numerical errors for the velocity are defined by

$$e_{\mu,H^1} = \mu^{1/2} \|\nabla(\mathbf{u} - \mathbf{u}_h)\|_{L^2(\Omega)}, \quad e_{H^1} = \|\nabla(\mathbf{u} - \mathbf{u}_h)\|_{L^2(\Omega)}.$$

To check the convergence of the pressure, we also compute the $L^2$ norm of $p - p_h$ denoted $e_p$ and the quantity

$$e_{\text{div}} = \mu^{1/2} \| \operatorname{div} \mathbf{u}_h \|_{L^2(\Omega)}.$$

**Example 3.8** (An anisotropic solution to the steady incompressible Navier-Stokes equations: an example with a boundary layer)**.**
We consider $\Omega$ as the rectangle $(0, 0.15)\times(0, 0.03)$ and we compute $\mathbf{f}$ such that the solutions of the Navier-Stokes equations (3.1) are given by

$$\mathbf{u}(x_1, x_2) = (u_\varepsilon(x_2), 0), \quad p(x_1, x_2) = 10(0.15 - x_1),$$

where

$$u_\varepsilon(x_2) = \begin{cases} 1, \quad 0 \le x_2 \le 0.005, \\ \exp\left(\frac{(x_2-0.005)^2}{(x_2-0.005)^2-\varepsilon^2}\right), \quad 0.005 \le x_2 \le 0.005+\varepsilon, \\ 0, \quad 0.005+\varepsilon \le x_2 \le 0.03. \end{cases}$$

The vector field $\mathbf{u}$ is trivially divergence free and has a strong variation in a region of height $\varepsilon$. We impose Dirichlet boundary conditions for the velocity on $\partial\Omega$ and to simplify the implementation, we fix the pressure on the right side of $\Omega$ rather than to impose the zero mean value condition. To check that the error indicator is independent of the data of the problem, we define the Reynolds number associated to this example by $Re = \frac{\rho 0.03}{\mu}$. For all the experiments, we set $\rho = 1$ and we vary the viscosity.

For our purposes, we would like to observe the following facts:

- $ei$ is close to a constant and in particular is independent of the mesh aspect ratio, the solution of the problem and the Reynolds number $Re$.
- $ei^{ZZ}$ is close to 1.

We first solve this example with $\varepsilon = 0.02$ for meshes of typical aspect ratio $10, 50$ and 500 and Reynolds number 1 and 100. The results are reported in the Table 3.1. $ei$ stays close to a value of 3 and the ZZ post-processing is asymptotically exact. To check that the effectivity index is independent of the solution we solve the same example with $\varepsilon = 0.005$. The results are reported in the Table 3.2.

| $h_1 - h_2$ | $e_{\mu,H^1}$ | $ei^A$ | $e_{H^1}$ | $ei^{ZZ}$ | $e_p$ | $e_{\text{div}}$ |
|---|---|---|---|---|---|---|
| 0.05 - 0.005 | 0.15 | 3.26 | 0.88 | 1.11 | 0.027 | 0.011 |
| 0.025 - 0.0025 | 0.082 | 2.78 | 0.47 | 1.12 | 0.011 | 0.0042 |
| 0.0125 - 0.00125 | 0.043 | 2.84 | 0.24 | 1.08 | 0.0037 | 0.0024 |
| 0.05 - 0.005 | 0.015 | 3.31 | 0.88 | 1.09 | 0.00034 | 0.00101 |
| 0.025 - 0.0025 | 0.0082 | 2.79 | 0.48 | 1.11 | 0.00015 | 0.00047 |
| 0.0125 - 0.00125 | 0.0043 | 2.84 | 0.25 | 1.08 | 0.000052 | 0.00025 |
| 0.05 - 0.001 | 0.041 | 2.81 | 0.23 | 1.04 | 0.0079 | 0.00086 |
| 0.025 - 0.0005 | 0.017 | 3.02 | 0.099 | 1.03 | 0.0033 | 0.00035 |
| 0.0125 - 0.00025 | 0.0087 | 2.79 | 0.051 | 1.00 | 0.0013 | 0.00024 |
| 0.05 - 0.001 | 0.0041 | 2.84 | 0.23 | 1.05 | 0.00029 | 0.000085 |
| 0.025 - 0.0005 | 0.0017 | 3.03 | 0.099 | 1.03 | 0.000091 | 0.000041 |
| 0.0125 - 0.00025 | 0.00087 | 2.81 | 0.051 | 1.00 | 0.000038 | 0.000028 |
| 0.05 - 0.0001 | 0.0029 | 2.97 | 0.017 | 0.99 | 0.0027 | 0.00018 |
| 0.025 - 0.00005 | 0.0017 | 2.91 | 0.01005 | 1.00 | 0.0033 | 0.000066 |
| 0.05 - 0.0001 | 0.00029 | 2.97 | 0.017 | 0.99 | 0.000036 | 0.000019 |
| 0.025 - 0.00005 | 0.00017 | 2.94 | 0.01006 | 1.00 | 0.000015 | 0.0000098 |

Table 3.1: Numerical results for Example 3.9 with $\varepsilon = 0.02$. The mesh aspect ratio is 10 (rows 1-6), 50 (rows 7-12) and 500 (rows 13-16) . The Reynolds number is set to 1 (rows 1-3, 7-9 and 13-14) and 100 (rows 4-6,10-12 and 15-16).

| $h_1 - h_2$ | $e_{\mu,H^1}$ | $ei^A$ | $e_{H^1}$ | $ei^{ZZ}$ | $e_p$ | $e_{\text{div}}$ |
|---|---|---|---|---|---|---|
| 0.025 - 0.0005 | 0.15 | 2.82 | 0.86 | 1.07 | 0.081 | 0.0078 |
| 0.0125 - 0.00025 | 0.074 | 2.82 | 0.43 | 1.06 | 0.014 | 0.0021 |
| 0.00625 - 0.000125 | 0.035 | 2.84 | 0.21 | 1.02 | 0.0025 | 0.0017 |
| 0.025 - 0.0005 | 0.015 | 2.82 | 0.86 | 1.07 | 0.00083 | 0.00066 |
| 0.0125 - 0.00025 | 0.0074 | 2.83 | 0.43 | 1.06 | 0.00017 | 0.00021 |
| 0.00625 - 0.000125 | 0.0035 | 2.84 | 0.21 | 1.02 | 0.000022 | 0.00011 |
| 0.05 - 0.0001 | 0.023 | 2.83 | 0.13 | 1.00 | 0.0079 | 0.00072 |
| 0.025 - 0.00005 | 0.014 | 2.81 | 0.081 | 1.00 | 0.0064 | 0.00032 |
| 0.05 - 0.0001 | 0.0023 | 2.83 | 0.13 | 1.00 | 0.000086 | 0.000073 |
| 0.025 - 0.00005 | 0.0014 | 2.81 | 0.081 | 1.00 | 0.000061 | 0.000032 |

Table 3.2: Numerical results for Example 3.9 with $\varepsilon = 0.005$. The mesh aspect ratio is 50 (rows 1-6) and 500 (rows 7-10) . The Reynolds number is set to 1 (rows 1-3 and 7-8) and 100 (rows 4-6 and 8-9).

## 3.3 Numerical experiments for the steady incompressible Navier-Stokes equations with adapted meshes

In this section, we apply the adaptive algorithm 1.6 to solve the steady Navier-Stokes equations with the numerical method (3.6). As for fixed grid, we choose the anisotropic stabilization (3.7) with $\alpha = 0.01$.

The adaptive algorithm reads the same as the one proposed for elliptic problems, using the error indicator (3.19) instead. Since now we are dealing with vector valued functions, we define the local error indicators $\eta_{i,K}^2$ in direction $x_i, i = 1, 2$ by

$$(\eta_{i,K}^A)^2 = \left( \|\mathbf{f} - \rho(\mathbf{u}_h \cdot \nabla)\mathbf{u}_h + \mu\Delta\mathbf{u}_h - \nabla p_h\|_{L^2(K)} + \frac{1}{2\sqrt{\lambda_{2,K}}} \|[\mu\nabla\mathbf{u}_h \cdot \mathbf{n}]\|_{L^2(\partial K)} \right) \tilde{\omega}_{i,K}(\Pi_h^{ZZ}\mathbf{u}_h - \mathbf{u}_h),$$

where the directional anisotropic form $\omega_{i,K}$ given by (1.30) is adapted to vector valued functions by setting

$$\tilde{\omega}_{i,K}^2(\mathbf{v}) = \tilde{\omega}_{i,K}^2(v_1) + \tilde{\omega}_{i,K}^2(v_2), \quad \mathbf{v} = (v_1, v_2) \in (H^1(\Omega))^2.$$

**Example 3.9** (An anisotropic solution to the steady incompressible Navier-Stokes equations: an example with a boundary layer)**.**
We first apply the adaptive algorithm to the previous example with $\varepsilon = 0.02$ and $Re = 1$. The initial grid is an isotropic mesh of size $h = 0.01$. We first check the convergence of our algorithm with respect to the number of remeshing $N_{loop}$. In Figure 3.9, we present the different grids obtained when applying the adaptive algorithm with $TOL = 0.25$ and several values of $N_{loop}$. As for elliptic problems, we observe that an anisotropic grid is generated after 10 remeshings, and we push the process until 40 to obtain a high average aspect ratio.

In Table 3.3, we present the convergence results for several value of $TOL$ and $N_{loop}$ fixed to 40. We keep the same notations as the on introduced in Chapter 1, Section 1.5, Table 1.7. Our observations are the following:

- Both velocity and pressure errors are $O(TOL)$.
- The number of vertices is multiplied by two as the tolerance is divided by two. This is the expected and desired result. Indeed, since the velocity depends only on $x_2$, we have that the numerical error $e_{\mu,H^1}$ behaves as $O(h) = O(N_v^{-1})$ on anisotropic meshes.
- The number of remeshings needed to satisfy the stopping criteria are independent of $TOL$.
- Both $ei$ is close the value of 3 obtained on fix grids and $ei^{ZZ}$ is asymptotically 1.

In Figure 3.9, we present the mesh and solution obtained with $N_{loop} = 40$ and $TOL = 0.03125$. As it is observed in [86], since we only use the velocity error indicator, the mesh is strongly anisotropic, but instabilities for the pressure occur. We refer to [86] for practical solutions to solve this issue. To not involve a pressure indicator in the adaptive algorithm is clearly a bad drawback for such cases where the pressure is "orthogonal" to the velocity variations. Nevertheless, for the more "real" situations we will investigate later on, the meshes generated by our adaptive algorithm seem satisfactory to capture a good approximation of the pressure.

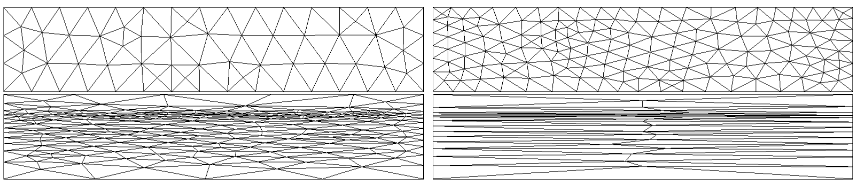

Figure 3.1: Example 3.9 with $\varepsilon = 0.02$ and $Re = 1$. Final meshes generated by the adaptive algorithm with $TOL = 0.25$. Initial grid (top left), $N_{loop} = 1$ (top right), $N_{loop} = 10$ (bottom left) and $N_{loop} = 40$ (bottom right).

| $TOL$ | $e_{\mu,H^1}$ | $ei^A$ | $ei^{ZZ}$ | $e_p$ | $e_{\text{div}}$ | $\overline{ar}$ | $ar_{\max}$ | $N_v$ | $N_m$ | $N_m^A$ |
|---|---|---|---|---|---|---|---|---|---|---|
| 0.25 | 0.037 | 3.02 | 1.00 | 0.023 | 0.0012 | 79 | 385 | 45 | 3 | 3 |
| 0.125 | 0.0202 | 2.87 | 1.01 | 0.0063 | 0.00026 | 140 | 640 | 77 | 5 | 5 |
| 0.0625 | 0.0098 | 3.12 | 1.00 | 0.014 | 0.00022 | 318 | 1414 | 143 | 6 | 6 |
| 0.03125 | 0.0049 | 3.00 | 1.00 | 0.0064 | 0.00011 | 616 | 3183 | 293 | 7 | 7 |

Table 3.3: Example 3.9 with $\varepsilon = 0.02$ and $Re = 1$. Convergence results obtained for several value of $TOL$ and $N_{loop} = 40$.

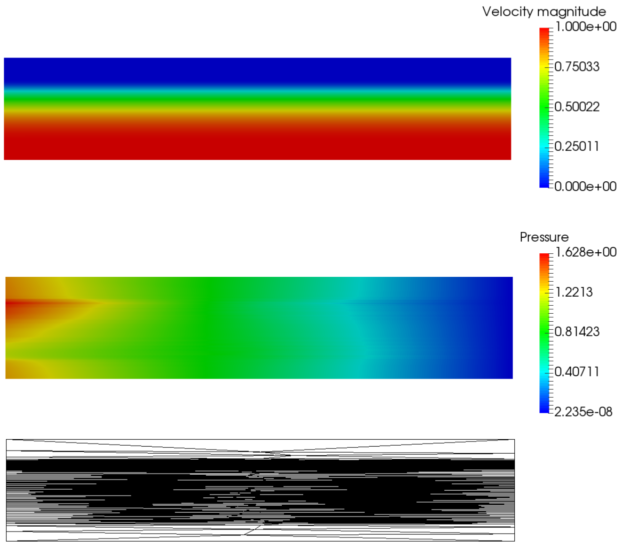


Figure 3.2: Numerical solution obtained with the adaptive algorithm with $N_{loop} = 40$ and $TOL = 0.03125$.

**Example 3.10** (Two-walls driven square cavity flow: steady solutions)**.**
The next example is famous in the framework of Navier-Stokes equations and is a version of the driven cavity test case. We are interested in solving in the square $\Omega = (0,1) \times (0,1)$ the Navier-Stokes equations

$$\begin{cases} \rho \dfrac{\partial \mathbf{u}}{\partial t} + \rho(\mathbf{u} \cdot \nabla)\mathbf{u} - \mu \Delta \mathbf{u} + \nabla p = 0, & \text{in } \Omega \times (0, +\infty), \\ \operatorname{div} \mathbf{u} = 0, & \text{in } \Omega \times (0, +\infty), \end{cases} \tag{3.20}$$

where we impose the following non-homogeneous boundary conditions

$$\begin{cases} \mathbf{u}(x_1, 1, t) = (1, 0), & 0 \leq x_1 \leq 1, t \in (0, +\infty) \\ \mathbf{u}(0, x_2, t) = (0, -1), & 0 \leq x_2 \leq 1, t \in (0, +\infty) \\ \mathbf{u}(x_1, x_2, t) = 0, & \text{otherwise.} \end{cases} \tag{3.21}$$

For this particular problem, the Reynolds number is given by $Re = \rho/\mu$ and it was numerically observed that until $Re = 4000$ [50] the problem (3.136), (3.137) admits a steady solution. Therefore, we focus on a steady version that reads

$$\begin{cases} (\mathbf{u} \cdot \nabla)\mathbf{u} - \mu \Delta \mathbf{u} + \nabla p = 0, & \text{in } \Omega, \\ \operatorname{div} \mathbf{u} = 0, & \text{in } \Omega, \end{cases} \tag{3.22}$$

coupled with the boundary conditions

$$\begin{cases} \mathbf{u}(x_1, 1) = (1, 0), & 0 \le x_1 \le 1, \\ \mathbf{u}(0, x_2) = (0, -1), & 0 \le x_2 \le 1, \\ \mathbf{u}(x_1, x_2) = 0, & \text{otherwise} . \end{cases} \tag{3.23}$$

Note that we choose $\rho = 1$ so that the Reynolds number is given by $^1/_\mu$. We approximate the problem (3.22), (3.24) with the numerical method (3.6) and the anisotropic stabilization (3.7) where we fix $\alpha = 0.01$. Since the boundary conditions are discontinuous, we smooth them by setting

$$\begin{cases} \mathbf{u}(x_1, 1) = (16x_1^2(1 - x_1)^2, 0), & 0 \le x_1 \le 1, \\ \mathbf{u}(0, x_2) = (0, -16x_2^2(1 - x_2)^2), & 0 \le x_2 \le 1, \\ \mathbf{u}(x_1, x_2) = 0, & \text{otherwise} . \end{cases} \tag{3.24}$$

Finally, we impose the pressure to be zero at the corner $(1, 0)$ instead of imposing its mean value.

We first apply the adaptive algorithm with a Reynolds number of 100. The initial grid is an isotropic mesh of mesh size $h = 0.0125$. In Figures 3.3, 3.4 and 3.5, we show the solutions and the meshes obtained for several values of $TOL$ after 10 remeshings.

In Figure 3.6, we present plots of the velocity magnitude $|\mathbf{u}_h|$ and $p_h$ along the diagonal line $(0, 0) - (1, 1)$. We observe that the smaller the tolerance is, the more symmetric is the solution. Oscillations in the pressure also disappear when the tolerance is sufficiently small.

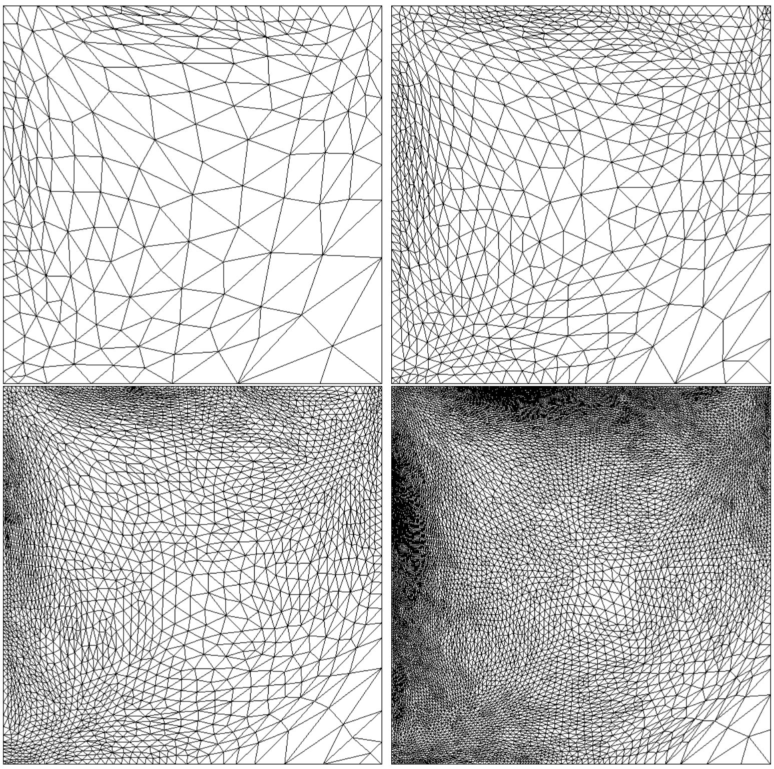

Figure 3.3: Example 3.10 with $Re = 100$. Meshes generated by the adaptive algorithm for several values of $TOL$ and $N_{loop} = 10$. $TOL = 0.5$ (top left), $TOL = 0.25$ (top right), $TOL = 0.125$ (bottom left) and $TOL = 0.0625$ (bottom right).

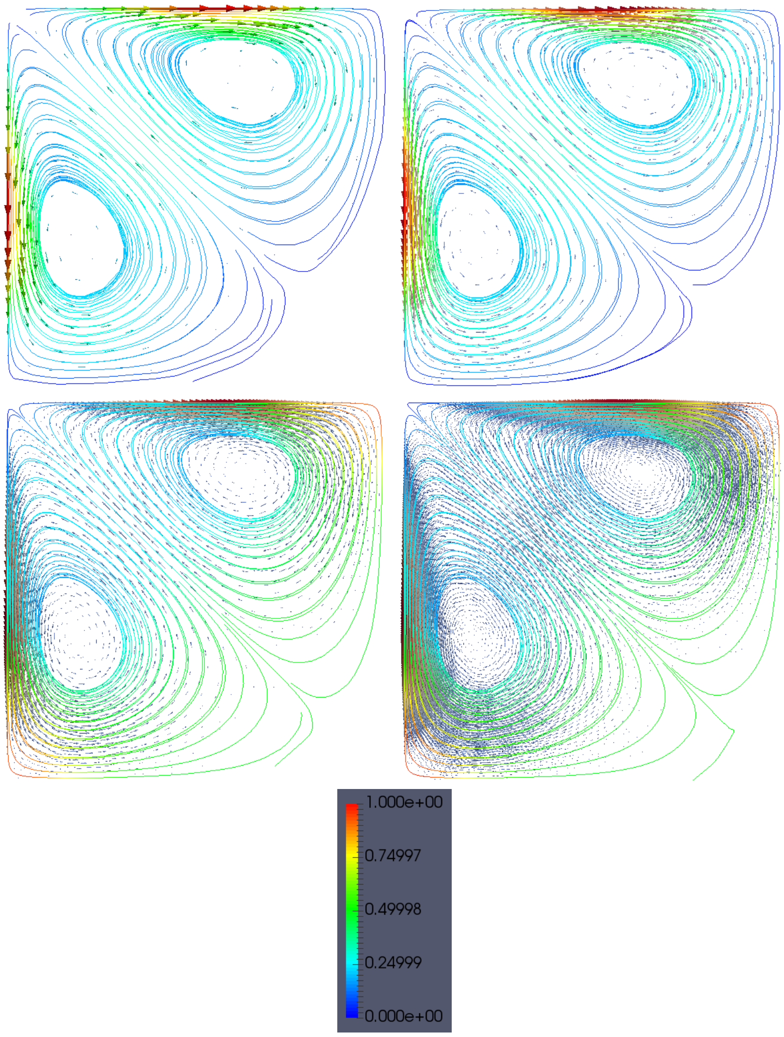


Figure 3.4: Example 3.10 with $Re = 100$. Velocity streamlines for several values of $TOL$ and $N_{loop} = 10$. $TOL = 0.5$ (top left), $TOL = 0.25$ (top right), $TOL = 0.125$ (bottom left) and $TOL = 0.0625$ (bottom right).

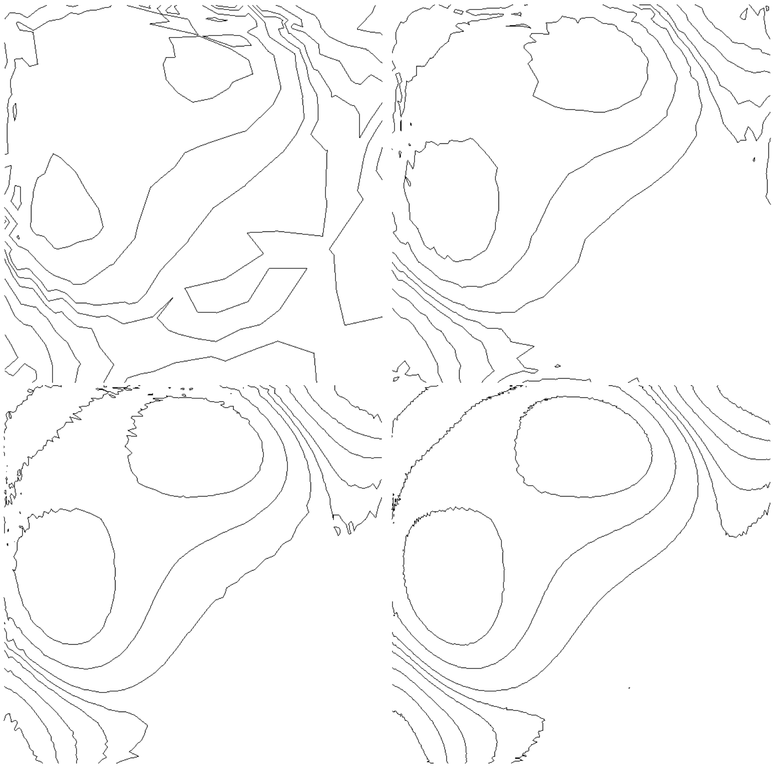

Figure 3.5: Example 3.10 with $Re = 100$. Pressure isolines for several values of $TOL$ and $N_{loop} = 10$. $TOL = 0.5$ (top left), $TOL = 0.25$ (top right), $TOL = 0.125$ (bottom left) and $TOL = 0.0625$ (bottom right).

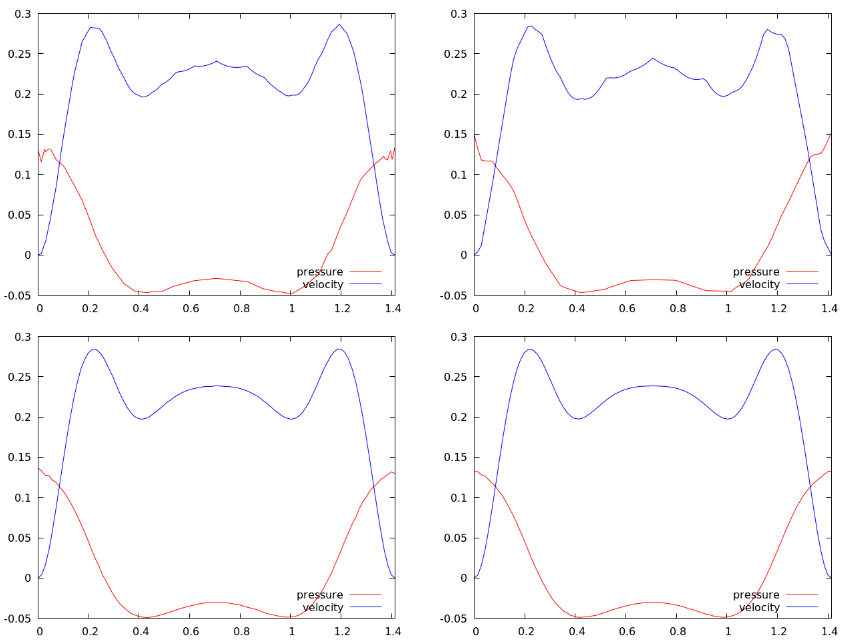


Figure 3.6: Example 3.10 with $Re = 100$. Plots of $|\mathbf{u}_h|$ and $p_h$ along the diagonal line $(0,0)-(1,1)$ for several values of $TOL$ and $N_{loop} = 10$. $TOL = 0.5$ (top left), $TOL = 0.25$ (top right), $TOL = 0.125$ (bottom left) and $TOL = 0.0625$ (bottom right).

We now compute the solution for several Reynolds number up to 4000. We run the algorithm with $TOL = 0.125$ and $N_{loop} = 10$. To reach the solution for $Re = 4000$, we proceed by continuation, computing the solution for $Re = 100$ and then using it as initial guess for the solution at $Re = 200$. The sequence of Reynolds number are: 100, 200, 300, 400, 500, 600, 700, 800, 900, 1000, 2000, 3000 and 4000. In Figures 3.7, 3.9 and 3.10, we present the meshes and the solution obtained for $Re = 1000, 2000, 3000$ and 4000. In Figure 3.8, we zoom on the mesh obtained for $Re = 4000$. For this case, elements that are close to the left and top side of $\Omega$ becomes anisotropic.

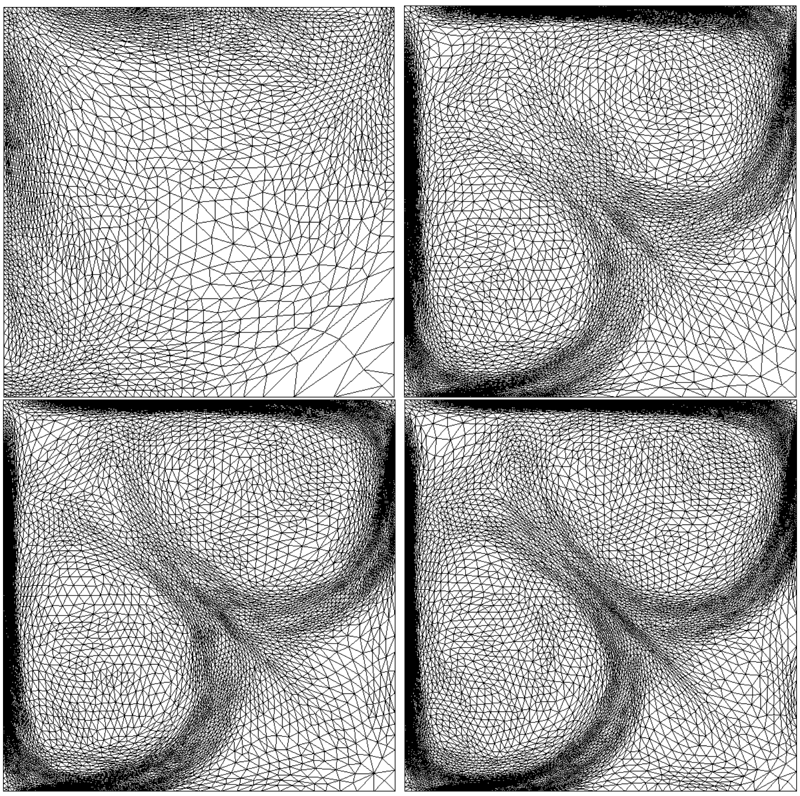

Figure 3.7: Example 3.10. Meshes generated by the adaptive algorithm with $TOL = 0.125$ and $N_{loop} = 10$. $Re = 1000$ (top left), $Re = 2000$ (top right), $Re = 3000$ (bottom left) and $Re = 4000$ (bottom right).

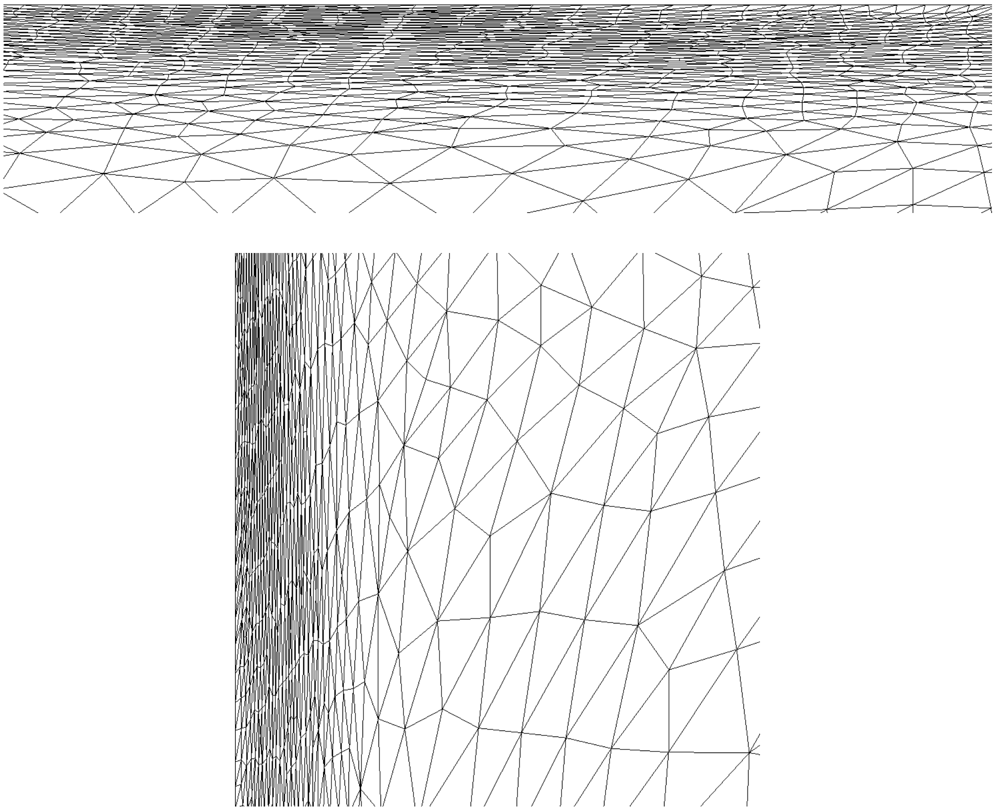

Figure 3.8: Example 3.10. Mesh generated by the adaptive algorithm with $TOL = 0.125$ and $N_{loop} = 10$ and $Re = 4000$. Zoom on the top of $\Omega$ (top) and on the left side of $\Omega$ (bottom).

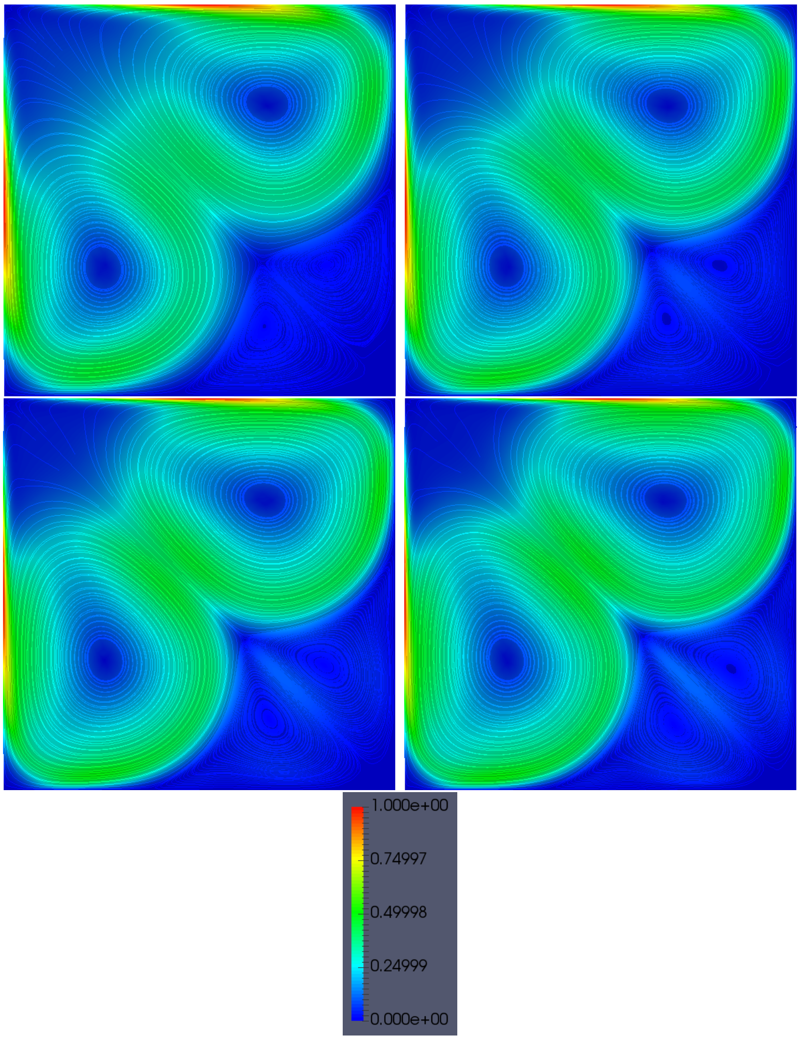


Figure 3.9: Example 3.10. Velocity streamlines with $TOL = 0.125$ and $N_{loop} = 10$. $Re = 1000$ (top left), $Re = 2000$ (top right), $Re = 3000$ (bottom left) and $Re = 4000$ (bottom right).

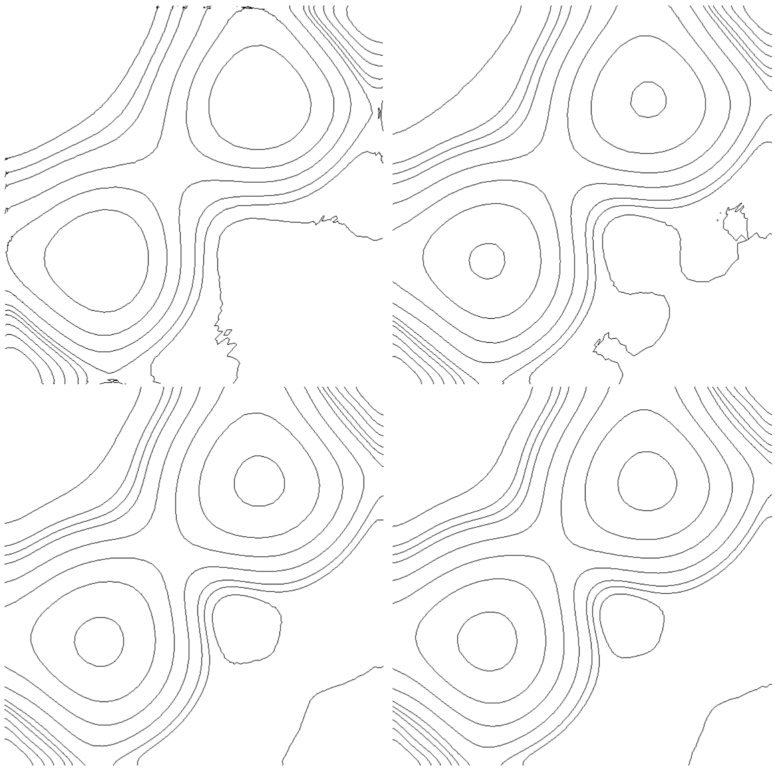

Figure 3.10: Example 3.10. Pressure isolines with $TOL = 0.125$ and $N_{loop} = 10$. $Re = 1000$ (top left), $Re = 2000$ (top right), $Re = 3000$ (bottom left) and $Re = 4000$ (bottom right).

## 3.4 A posteriori error estimates for the unsteady Stokes equations with constant coefficients: space approximation

In this section, we focus on the posteriori error analysis of the unsteady Stokes equations. The problem to be solved is the following: let $\Omega$ be an open, bounded, Lipschitz set of $\mathbb{R}^2$, $T > 0$ the final time, $\rho, \mu > 0$ standing respectively for the density and the viscosity, the force term $\mathbf{f} \in L^2(0, T; (L^2(\Omega))^2)$, and an initial condition $\mathbf{u}_0 \in (H_0^1(\Omega))^2$ such that $\operatorname{div} \mathbf{u}_0 = 0$. We are looking for $(\mathbf{u}, p)$ the solution of the incompressible unsteady Stokes equations

$$\begin{cases} \rho \dfrac{\partial \mathbf{u}}{\partial t} - \mu \Delta \mathbf{u} + \nabla p = \mathbf{f}, & \text{in } \Omega \times (0, T), \\ \operatorname{div} \mathbf{u} = 0, & \text{in } \Omega \times (0, T), \\ \mathbf{u} = 0, & \text{on } \partial\Omega \times (0, T), \\ \mathbf{u}(\cdot, 0) = \mathbf{u}_0, & \text{in } \Omega. \end{cases} \tag{3.25}$$

The existence and uniqueness of weak solutions of (3.25) are established for instance in [99] or [21]. In particular, the following regularity is achieved

$$\mathbf{u} \in C^0([0, T]; (L^2(\Omega))^2) \cap L^2(0, T; (H_0^1(\Omega))^2), \quad \frac{\partial \mathbf{u}}{\partial t} \in L^2(0, T; L^2(\Omega)^2),$$

$$p \in L^2(0, T; L_0^2(\Omega)).$$

If moreover we assume that $\Omega$ is smooth or a convex polygon, then one can even prove [99] the higher regularity in space

$$\mathbf{u} \in L^2(0,T;(H^2(\Omega))^2), \quad p \in L^2(0,T;H^1(\Omega)).$$

The corresponding weak-form reads: find $\mathbf{u} \in H^1(0,T;(L^2(\Omega))^2) \cap L^2(0,T;(H^1_0(\Omega))^2$ and $p \in L^2(0,T;L^2_0(\Omega))$ such that $\mathbf{u}(\cdot,0) = \mathbf{u}_0$ almost everywhere in $\Omega$ and for almost every $t \in (0,T)$

$$\begin{aligned} \rho \int_\Omega \frac{\partial \mathbf{u}}{\partial t} \cdot \mathbf{v} d\mathbf{x} + \mu \int_\Omega \nabla \mathbf{u} : \nabla \mathbf{v} d\mathbf{x} - \int_\Omega p \operatorname{div} \mathbf{v} d\mathbf{x} = \int_\Omega \mathbf{f} \cdot \mathbf{v} d\mathbf{x}, \quad \forall \mathbf{v} \in (H^1_0(\Omega))^2, \\ - \int_\Omega q \operatorname{div} \mathbf{u} d\mathbf{x} = 0, \quad \forall q \in L^2_0(\Omega). \end{aligned} \tag{3.26}$$

We first focus on the spatial approximation of (3.26). The numerical method we shall use to solve (3.26) is a pressure stabilized finite elements methods, which convergence is for instance numerically studied in [75]. From now we assume that $\Omega$ is a convex. Moreover, we assume that $\mathbf{f} \in C^0\left([0,T];(L^2(\Omega))^2\right)$ so that it makes sense to evaluate the force term, and later on the equations, pointwise with respect to the time variable. We use the same notation as in Section 3.1. For any $h > 0$, let $\mathcal{T}_h$ be a conformal triangulation of $\Omega$ into triangles $K$ of diameter $h_K \leq h$. We still denote by $W_h$ the classical finite elements set of all continuous, piecewise linear functions, and by $W_{h,0}$ the subset of $W_h$ which elements have zero value on $\partial\Omega$. Finally we recall that the discrete velocity space and pressure space are given by $V_h = (W_{h,0})^2$ and $Q_h = W_h \cap L^2_0(\Omega)$. Assuming that $\mathbf{u}_0 \in (H^1_0(\Omega))^2 \cap (H^2(\Omega))^2$, we are looking, for $(\mathbf{u}_h, p_h) : \overline{\Omega} \times [0,T] \longrightarrow \mathbb{R}^2 \times \mathbb{R}$ such that $\forall t \in [0,T]$, $\mathbf{u}_h(\cdot,t), \in V_h$ and $p_h(\cdot,t) \in Q_h$, where $\mathbf{u}_h(\cdot,0) = r_h(\mathbf{u}_0)$, and for all $t \in (0,T]$

$$\begin{aligned} &\rho \int_\Omega \frac{\partial \mathbf{u}_h}{\partial t} \cdot \mathbf{v}_h d\mathbf{x} + \mu \int_\Omega \nabla \mathbf{u}_h : \nabla \mathbf{v}_h d\mathbf{x} - \int_\Omega p_h \operatorname{div} \mathbf{v}_h d\mathbf{x} = \int_\Omega \mathbf{f} \cdot \mathbf{v}_h d\mathbf{x}, \quad \forall \mathbf{v}_h \in V_h, \\ &- \int_\Omega q_h \operatorname{div} \mathbf{u}_h d\mathbf{x} + \sum_{K \in \mathcal{T}_h} \alpha_K \int_K \left( \mathbf{f} - \rho \frac{\partial \mathbf{u}_h}{\partial t} + \mu \Delta \mathbf{u}_h - \nabla p_h \right) \cdot \nabla q_h d\mathbf{x} = 0, \quad \forall q_h \in Q_h, \end{aligned} \tag{3.27}$$

with the stabilization parameter $\alpha_K$ given by

$$\alpha_K = \frac{\alpha \lambda_{2,K}^2}{\mu} \tag{3.28}$$

where $\alpha > 0$ is a prescribed dimensionless positive value.

**Remark 3.11.**
Imposing an initial condition for the pressure is not needed to solve (3.26) or (3.27). In particular, we only ask that (3.27) holds for any $t > 0$. However, for future discussions, we must be able to evaluate the momentum equation also at $t = 0$, in particular to obtain informations on

$$\frac{\partial \mathbf{u}_h}{\partial t}(0) \text{ and } p_h(0).$$

This implies to give a meaning to $p_h(0)$. We propose two choices. A first idea is to assume that $p(\cdot,0) = p_0$ is known and sufficiently regular (for instant belonging to $C^0(\Omega)$) such that we can define $p_h(0) = r_h(p_0)$. Otherwise, we can also solve (3.27) at $t = 0$ and define $\left(\frac{\partial \mathbf{u}_h}{\partial t}(0), p_h(0)\right)$ as the solution of

$$\begin{aligned} &\rho \int_\Omega \frac{\partial \mathbf{u}_h}{\partial t}(0) \cdot \mathbf{v}_h d\mathbf{x} - \int_\Omega p_h(0) \operatorname{div} \mathbf{v}_h d\mathbf{x} = \int_\Omega \mathbf{f}(0) \cdot \mathbf{v}_h d\mathbf{x} - \mu \int_\Omega \nabla r_h \mathbf{u}_0 : \nabla \mathbf{v}_h d\mathbf{x}, \quad \forall \mathbf{v}_h \in V_h, \\ &- \int_\Omega q_h \operatorname{div} r_h \mathbf{u}_0 d\mathbf{x} + \sum_{K \in \mathcal{T}_h} \alpha_K \int_K \left( \mathbf{f} - \rho \frac{\partial \mathbf{u}_h}{\partial t}(0) + \mu \Delta r_h \mathbf{u}_0 - \nabla p_h(0) \right) \cdot \nabla q_h d\mathbf{x} = 0, \quad \forall q_h \in Q_h. \end{aligned}$$

We are mainly concerned in the a posteriori error analysis of the semi-discrete method (3.27). Some references about the a priori error analysis will be pointed out when we will study the fully discrete method where both space and time approximation will be considered. For the rest of this section, it will be assumed that both the exact and the finite elements solutions exist and are smooth enough to justify the computations. Note finally that the stabilization technique proposed above is a consistent stabilization, since all the terms of the equation are put into the stabilization terms, and therefore the exact solution $(\mathbf{u}, p)$ satisfies also the numerical method (3.27).

Proving an a posteriori error for the unsteady Stokes equation could be at first view an "easy" process, since the unsteady Stokes equation can be seen as a parabolic problem for the velocity (and the a posteriori analysis of parabolic problem is well known) and we know how to tackle the pressure error estimate for steady case. We could therefore think that deriving an a posteriori bound is a straightforward combination of parabolic problems techniques and treatment of the pressure through the inf-sup condition or a duality argument (see Section 3.1). Unfortunately, contrary to the steady (Navier-)Stokes equations, eliminating the pressure error from the treatment of the velocity is not an obvious task since it is not possible to relate $\|p - p_h\|_{L^2(\Omega)}$ to $\|\nabla(\mathbf{u} - \mathbf{u}_h)\|_{L^2(\Omega)}$. Below, we propose several possible a posteriori error estimates and their proofs, and comment their different advantages and drawbacks. Note that the problem with relating the pressure error to the velocity one is not a particularity due to the use of anisotropic finite elements. The same assessment is already observed with standard finite elements, and the different approaches to tackle this issue were originally introduced in the isotropic settings. In the next two paragraphs, we propose preliminary a posteriori error estimates that are not fully satisfactory for our purposes since they involve isotropic low order terms. In a first reading, we can go directly to Theorems 3.27 and 3.29 that contain the best a posteriori estimates we were able to prove for the time being.

**Parabolic a posteriori error estimate**

The first a posteriori error estimate can be seen as a "parabolic" estimate. As for the steady Navier-Stokes equations, it requires the use of the following dual problem to derive a anisotropic pressure estimate: for any $t \in [0, T]$, we consider $(\mathbf{w}(t), r(t)) \in (H_0^1(\Omega))^2 \times L_0^2(\Omega)$ the weak solution of

$$\begin{cases} -\mu\Delta\mathbf{w}(t) + \nabla r(t) = 0, & \text{in } \Omega, \\ \operatorname{div}\mathbf{w}(t) = p_h(t) - p(t), & \text{in } \Omega, \\ \mathbf{w}(t) = 0, & \text{on } \partial\Omega. \end{cases} \tag{3.29}$$

We recall that the following a priori estimate holds:

$$\|\nabla\mathbf{w}(t)\|_{L^2(\Omega)} + \frac{1}{\mu}\|r(t)\|_{L^2(\Omega)} \le C\|p(t) - p_h(t)\|_{L^2(\Omega)}, \tag{3.30}$$

where $C$ depends only on $\Omega$. Observe that the above dual problem is well defined for any $t \in [0, T]$ by assuming the extra regularity for the pressure and its finite elements approximation

$$p, p_h \in C^0\left([0, T]; L_0^2(\Omega)\right).$$

Note that it is a bit too much, since in fact we need for our proof that the dual problem is well-posed for almost every $t$ only. Therefore it is sufficient that $p, p_h \in L^2\left(0, T; L_0^2(\Omega)\right)$.

We do not want to go into too much details and always assume, for all the theorems and proofs presented below, that all the computations and the involved quantities are *punctually* well-defined for *every* $t$. For simplification, we will only indicate the necessary regularity of the solutions so that our error estimates have a sense, but maybe not sufficient for the computations to be justified for all $t \in [0,T]$.

For the next theorem, we assume that

$$\mathbf{u}, \mathbf{u}_h \in H^1\left(0,T;(L^2(\Omega))^2\right) \cap C^0\left([0,T];(H_0^1(\Omega))^2\right),$$

$$\mathbf{w}, p_h \in L^2\left(0,T;H^1(\Omega)\right).$$

**Theorem 3.12** (A first and simple a posteriori estimate for the semi-approximation of the unsteady Stokes equations)**.**
*Let* $(\mathbf{u},p)$ *be the solution of (3.26),* $(\mathbf{u}_h,p_h)$ *the solution of the finite elements scheme (3.27) and* $(\mathbf{w},r)$ *the solution of the dual problem (3.29). There exists a constant* $C>0$ *that depends only on the reference triangle and the domain* $\Omega$ *such that*

$$\begin{aligned}
\rho\|(\mathbf{u}-\mathbf{u}_h)(T)\|^2_{L^2(\Omega)} &+ \mu\int_0^T \|\nabla(\mathbf{u}-\mathbf{u}_h)(t)\|^2_{L^2(\Omega)}dt \\
&+\rho\int_0^T\left\|\frac{\partial \mathbf{u}}{\partial t}(t)-\frac{\partial \mathbf{u}_h}{\partial t}(t)\right\|^2_{L^2(\Omega)}dt+\mu\|\nabla(\mathbf{u}-\mathbf{u}_h)(T)\|^2_{L^2(\Omega)}\\
\leq \rho\|(\mathbf{u}-\mathbf{u}_h)(0)\|^2_{L^2(\Omega)}&+\mu\|\nabla(\mathbf{u}-\mathbf{u}_h)(0)\|^2_{L^2(\Omega)}+C\int_0^T\sum_{K\in\mathcal{T}_h}(\eta^A_{K,\mathbf{u}})^2(t)+(\eta^A_{K,p})^2(t)+(\eta^{\mathrm{div}}_K)^2(t)dt,
\end{aligned} \tag{3.31}$$

*where*

$$\begin{aligned}
(\eta^A_{K,\mathbf{u}})^2(t) = \Bigg(\left\|\mathbf{f}(t)-\rho\frac{\partial \mathbf{u}_h}{\partial t}(t)+\mu\Delta\mathbf{u}_h(t)-\nabla p_h(t)\right\|_{L^2(K)}+\frac{1}{2\sqrt{\lambda_{2,K}}}\|[\mu\nabla\mathbf{u}_h(t)\cdot\mathbf{n}]\|_{L^2(\partial K)}\Bigg)\\
\left(\omega_K(\mathbf{u}(t)-\mathbf{u}_h(t))+\omega_K\left(\frac{\partial \mathbf{u}}{\partial t}(t)-\frac{\partial \mathbf{u}_h}{\partial t}(t)\right)\right),
\end{aligned}$$

$$\begin{aligned}
&(\eta^A_{K,p})^2(t)\\
&=\left(\left\|\mathbf{f}(t)-\rho\frac{\partial \mathbf{u}_h}{\partial t}(t)+\mu\Delta\mathbf{u}_h(t)-\nabla p_h(t)\right\|_{L^2(K)}+\frac{1}{2\sqrt{\lambda_{2,K}}}\|[\mu\nabla\mathbf{u}_h(t)\cdot\mathbf{n}]\|_{L^2(\partial K)}\right)\frac{\omega_K(\mathbf{w}(t))}{\max(\mu,\rho)}
\end{aligned}$$

$$(\eta^{\mathrm{div}}_K)^2 = \max(\mu,\rho)\left(\|\operatorname{div}\mathbf{u}_h(t)\|^2_{L^2(K)}+\left\|\operatorname{div}\frac{\partial \mathbf{u}_h}{\partial t}(t)\right\|^2_{L^2(K)}\right),$$

*and*

$$\begin{aligned}
\int_0^T\|p-p_h\|^2_{L^2(\Omega)}dt \leq C\max(\mu,\rho)\Big(\rho\|\mathbf{u}-\mathbf{u}_h(0)\|^2_{L^2(\Omega)}+\mu\|\nabla(\mathbf{u}-\mathbf{u}_h)(0)\|^2_{L^2(\Omega)}+\\
\int_0^T\sum_{K\in\mathcal{T}_h}(\eta^A_{K,p})^2(t)+(\eta^A_{K,\mathbf{u}})^2(t)+(\eta^{\mathrm{div}}_K)^2(t)dt\Big).
\end{aligned} \tag{3.32}$$

*Proof.* Let $t\in(0,T)$. We denote by $C$ any constant that depends on the reference triangle or $\Omega$, by $\hat{C}>0$ any positive constant that may depend only on the reference triangle and by $\tilde{C}$ any constant depending only on $\Omega$. The value of these constants may change from line to line. To lighten the notations, we omit to note the explicit dependence on time of the functions.

*Step 1. Estimate for the velocity.*

We have

$$\frac{\rho}{2}\frac{d}{dt}\|\mathbf{u}-\mathbf{u}_h\|^2_{L^2(\Omega)}+\mu\|\nabla(\mathbf{u}-\mathbf{u}_h)\|^2_{L^2(\Omega)}+\rho\left\|\frac{\partial\mathbf{u}}{\partial t}-\frac{\partial\mathbf{u}_h}{\partial t}\right\|^2_{L^2(\Omega)}+\frac{\mu}{2}\frac{d}{dt}\|\nabla(\mathbf{u}-\mathbf{u}_h)\|^2_{L^2(\Omega)}$$
$$=\rho\int_\Omega\frac{\partial}{\partial t}(\mathbf{u}-\mathbf{u}_h)\cdot\left(\mathbf{u}-\mathbf{u}_h+\frac{\partial}{\partial t}(\mathbf{u}-\mathbf{u}_h)\right)d\mathbf{x}+\mu\int_\Omega\nabla(\mathbf{u}-\mathbf{u}_h):\nabla\left(\mathbf{u}-\mathbf{u}_h+\frac{\partial}{\partial t}(\mathbf{u}-\mathbf{u}_h)\right)d\mathbf{x}$$
$$=\rho\int_\Omega\frac{\partial}{\partial t}(\mathbf{u}-\mathbf{u}_h)\cdot\left(\mathbf{u}-\mathbf{u}_h+\frac{\partial}{\partial t}(\mathbf{u}-\mathbf{u}_h)\right)d\mathbf{x}+\mu\int_\Omega\nabla(\mathbf{u}-\mathbf{u}_h):\nabla\left(\mathbf{u}-\mathbf{u}_h+\frac{\partial}{\partial t}(\mathbf{u}-\mathbf{u}_h)\right)d\mathbf{x}$$
$$-\int_\Omega(p-p_h)\operatorname{div}\left(\mathbf{u}-\mathbf{u}_h+\frac{\partial}{\partial t}(\mathbf{u}-\mathbf{u}_h)\right)d\mathbf{x}+\int_\Omega(p-p_h)\operatorname{div}\left(\mathbf{u}-\mathbf{u}_h+\frac{\partial}{\partial t}(\mathbf{u}-\mathbf{u}_h)\right)d\mathbf{x}$$
$$=\int_\Omega\mathbf{f}\cdot\left(\mathbf{u}-\mathbf{u}_h+\frac{\partial}{\partial t}(\mathbf{u}-\mathbf{u}_h)\right)d\mathbf{x}-\rho\int_\Omega\frac{\partial\mathbf{u}_h}{\partial t}\cdot\left(\mathbf{u}-\mathbf{u}_h+\frac{\partial}{\partial t}(\mathbf{u}-\mathbf{u}_h)\right)d\mathbf{x}$$
$$-\mu\int_\Omega\nabla\mathbf{u}_h:\nabla\left(\mathbf{u}-\mathbf{u}_h+\frac{\partial}{\partial t}(\mathbf{u}-\mathbf{u}_h)\right)d\mathbf{x}+\int_\Omega p_h\operatorname{div}\left(\mathbf{u}-\mathbf{u}_h+\frac{\partial}{\partial t}(\mathbf{u}-\mathbf{u}_h)\right)d\mathbf{x}$$
$$+\int_\Omega(p-p_h)\operatorname{div}\left(\mathbf{u}-\mathbf{u}_h+\frac{\partial}{\partial t}(\mathbf{u}-\mathbf{u}_h)\right)d\mathbf{x}.$$

Using the numerical method (3.27), we can remove any test function $\mathbf{v}_h$. Note tat we only use the momentum equation so that the stabilization term does not appear.

$$\frac{\rho}{2}\frac{d}{dt}\|\mathbf{u}-\mathbf{u}_h\|^2_{L^2(\Omega)}+\mu\|\nabla(\mathbf{u}-\mathbf{u}_h)\|^2_{L^2(\Omega)}+\rho\left\|\frac{\partial\mathbf{u}}{\partial t}-\frac{\partial\mathbf{u}_h}{\partial t}\right\|^2_{L^2(\Omega)}+\frac{\mu}{2}\frac{d}{dt}\|\nabla(\mathbf{u}-\mathbf{u}_h)\|^2_{L^2(\Omega)}$$
$$=\int_\Omega\mathbf{f}\cdot\left(\mathbf{u}-\mathbf{u}_h+\frac{\partial}{\partial t}(\mathbf{u}-\mathbf{u}_h)-\mathbf{v}_h\right)d\mathbf{x}-\rho\int_\Omega\frac{\partial\mathbf{u}_h}{\partial t}\cdot\left(\mathbf{u}-\mathbf{u}_h+\frac{\partial}{\partial t}(\mathbf{u}-\mathbf{u}_h)-\mathbf{v}_h\right)d\mathbf{x}$$
$$-\mu\int_\Omega\nabla\mathbf{u}_h:\nabla\left(\mathbf{u}-\mathbf{u}_h+\frac{\partial}{\partial t}(\mathbf{u}-\mathbf{u}_h)-\mathbf{v}_h\right)d\mathbf{x}+\int_\Omega p_h\operatorname{div}\left(\mathbf{u}-\mathbf{u}_h+\frac{\partial}{\partial t}(\mathbf{u}-\mathbf{u}_h)-\mathbf{v}_h\right)d\mathbf{x}$$
$$+\int_\Omega(p-p_h)\operatorname{div}\left(\mathbf{u}-\mathbf{u}_h+\frac{\partial}{\partial t}(\mathbf{u}-\mathbf{u}_h)\right)d\mathbf{x}.$$

Integration by parts over each triangles and the Cauchy-Schwarz inequality implies then

$$\frac{\rho}{2}\frac{d}{dt}\|\mathbf{u}-\mathbf{u}_h\|^2_{L^2(\Omega)}+\mu\|\nabla(\mathbf{u}-\mathbf{u}_h)\|^2_{L^2(\Omega)}+\rho\left\|\frac{\partial\mathbf{u}}{\partial t}-\frac{\partial\mathbf{u}_h}{\partial t}\right\|^2_{L^2(\Omega)}+\frac{\mu}{2}\frac{d}{dt}\|\nabla(\mathbf{u}-\mathbf{u}_h)\|^2_{L^2(\Omega)}$$
$$\leq\sum_{K\in\mathcal{T}_h}\left\|\mathbf{f}-\rho\frac{\partial\mathbf{u}_h}{\partial t}+\mu\Delta\mathbf{u}_h-\nabla p_h\right\|_{L^2(K)}\left\|\mathbf{u}-\mathbf{u}_h+\frac{\partial}{\partial t}(\mathbf{u}-\mathbf{u}_h)-\mathbf{v}_h\right\|_{L^2(\Omega)}$$
$$+\frac{1}{2}\|\,[\mu\nabla\mathbf{u}_h\cdot\mathbf{n}]\,\|_{L^2(\partial K)}\left\|\mathbf{u}-\mathbf{u}_h+\frac{\partial}{\partial t}(\mathbf{u}-\mathbf{u}_h)-\mathbf{v}_h\right\|_{L^2(\partial K)}$$
$$+\|p-p_h\|_{L^2(\Omega)}\left(\|\operatorname{div}\mathbf{u}_h\|_{L^2(\Omega)}+\left\|\operatorname{div}\frac{\partial\mathbf{u}_h}{\partial t}\right\|_{L^2(\Omega)}\right).$$

Choosing $\mathbf{v}_h=R_h\left(\mathbf{u}-\mathbf{u}_h+\frac{\partial}{\partial t}(\mathbf{u}-\mathbf{u}_h)\right)$, the anisotropic Clément's interpolation error estimate yields finally

$$\frac{\rho}{2}\frac{d}{dt}\|\mathbf{u}-\mathbf{u}_h\|^2_{L^2(\Omega)}+\mu\|\nabla(\mathbf{u}-\mathbf{u}_h)\|^2_{L^2(\Omega)}+\rho\left\|\frac{\partial\mathbf{u}}{\partial t}-\frac{\partial\mathbf{u}_h}{\partial t}\right\|^2_{L^2(\Omega)}+\frac{\mu}{2}\frac{d}{dt}\|\nabla(\mathbf{u}-\mathbf{u}_h)\|^2_{L^2(\Omega)}$$
$$\leq\hat{C}\sum_{K\in\mathcal{T}_h}\left(\left\|\mathbf{f}-\rho\frac{\partial\mathbf{u}_h}{\partial t}+\mu\Delta\mathbf{u}_h-\nabla p_h\right\|_{L^2(K)}+\frac{1}{2\sqrt{\lambda_{2,K}}}\|\,[\mu\nabla\mathbf{u}_h\cdot\mathbf{n}]\,\|_{L^2(\partial K)}\right)$$
$$\omega_K\left(\mathbf{u}-\mathbf{u}_h+\frac{\partial}{\partial t}(\mathbf{u}-\mathbf{u}_h)\right)$$
$$+\frac{1}{\varepsilon}\|p-p_h\|^2_{L^2(\Omega)}+\varepsilon\|\operatorname{div}\mathbf{u}_h\|^2_{L^2(\Omega)}+\varepsilon\left\|\operatorname{div}\frac{\partial\mathbf{u}_h}{\partial t}\right\|^2_{L^2(\Omega)},\quad(3.33)$$

where we use the Young's inequaliy on the last term to conclude.

*Step 2. Estimate for the pressure.*

We use $\mathbf{w}$ the dual solution obtained in (3.29). Proceeding as in Theorem 3.6, we have

$$\begin{aligned}\|p-p_h\|^2_{L^2(\Omega)} &= -\int_\Omega (p-p_h)\operatorname{div}\mathbf{w}d\mathbf{x} = \int_\Omega \mathbf{f}\cdot\mathbf{w}-\rho\frac{\partial\mathbf{u}}{\partial t}\cdot\mathbf{w}-\mu\nabla\mathbf{u}:\nabla\mathbf{w}d\mathbf{x}+\int_\Omega p_h\operatorname{div}\mathbf{w}d\mathbf{x}\\ &= \int_\Omega \mathbf{f}\cdot\mathbf{w}-\rho\frac{\partial\mathbf{u}_h}{\partial t}\cdot\mathbf{w}-\mu\nabla\mathbf{u}_h:\nabla\mathbf{w}d\mathbf{x}+\int_\Omega p_h\operatorname{div}\mathbf{w}d\mathbf{x}\\ &\qquad -\rho\int_\Omega\frac{\partial}{\partial t}(\mathbf{u}-\mathbf{u}_h)\cdot\mathbf{w}d\mathbf{x}-\mu\int_\Omega\nabla(\mathbf{u}-\mathbf{u}_h):\nabla\mathbf{w}d\mathbf{x}.\end{aligned}$$

Removing any test function $v_h$, we have after using an integration by parts and the Cauchy-Schwarz inequality

$$\begin{aligned}\|p-p_h\|^2_{L^2(\Omega)} &= -\int_\Omega (p-p_h)\operatorname{div}\mathbf{w}d\mathbf{x} = \int_\Omega \mathbf{f}\cdot\mathbf{w}-\rho\frac{\partial\mathbf{u}}{\partial t}\cdot\mathbf{w}-\mu\nabla\mathbf{u}:\nabla\mathbf{w}d\mathbf{x}+\int_\Omega p_h\operatorname{div}\mathbf{w}d\mathbf{x}\\ &= \sum_{K\in\mathcal{T}_h}\left\|\mathbf{f}-\rho\frac{\partial\mathbf{u}_h}{\partial t}+\mu\Delta\mathbf{u}_h-\nabla p_h\right\|_{L^2(K)}\|\mathbf{w}-\mathbf{v}_h\|_{L^2(\Omega)}\\ &\qquad +\frac{1}{2}\|\,[\mu\nabla\mathbf{u}_h\cdot\mathbf{n}]\,\|_{L^2(\partial K)}\|\mathbf{w}-\mathbf{v}_h\|_{L^2(\partial K)}\\ &\qquad -\rho\int_\Omega\frac{\partial}{\partial t}(\mathbf{u}-\mathbf{u}_h)\cdot\mathbf{w}d\mathbf{x}-\mu\int_\Omega\nabla(\mathbf{u}-\mathbf{u}_h):\nabla\mathbf{w}d\mathbf{x}.\end{aligned}$$

Choosing $\mathbf{v}_h = R_h(\mathbf{w})$ and using the Young's and Poincaré inequalities with the a priori estimate (3.30), we have finally

$$\begin{aligned}\|p-p_h\|^2_{L^2(\Omega)} &= -\int_\Omega (p-p_h)\operatorname{div}\mathbf{w}d\mathbf{x} = \int_\Omega \mathbf{f}\cdot\mathbf{w}-\rho\frac{\partial\mathbf{u}}{\partial t}\cdot\mathbf{w}-\mu\nabla\mathbf{u}:\nabla\mathbf{w}d\mathbf{x}+\int_\Omega p_h\operatorname{div}\mathbf{w}d\mathbf{x}\\ &\le \hat{C}\sum_{K\in\mathcal{T}_h}\left(\left\|\mathbf{f}-\rho\frac{\partial\mathbf{u}_h}{\partial t}+\mu\Delta\mathbf{u}_h-\nabla p_h\right\|_{L^2(K)}+\frac{1}{2\sqrt{\lambda_{2,K}}}\|\,[\mu\nabla\mathbf{u}_h\cdot\mathbf{n}]\,\|_{L^2(\partial K)}\right)\omega_K(\mathbf{w})\\ &\qquad +\tilde{C}\rho^2\left\|\frac{\partial}{\partial t}(\mathbf{u}-\mathbf{u}_h)\right\|^2_{L^2(\Omega)}+\tilde{C}\mu^2\|\nabla(\mathbf{u}-\mathbf{u}_h)\|^2_{L^2(\Omega)},\end{aligned}\tag{3.34}$$

where we denote by $C_P$ the Poincaré constant of $\Omega$ and by $\tilde{C}$ the constant in the a priori estimate (3.30).

*Step 3. Putting all together.*

By plugging (3.34) into (3.33) and choosing $\varepsilon = 2\tilde{C}\max(\mu,\rho)$, we obtain

$$\begin{aligned}&\frac{\rho}{2}\frac{d}{dt}\|\mathbf{u}-\mathbf{u}_h\|^2_{L^2(\Omega)}+\frac{\mu}{2}\|\nabla(\mathbf{u}-\mathbf{u}_h)\|^2_{L^2(\Omega)}+\frac{\rho}{2}\left\|\frac{\partial\mathbf{u}}{\partial t}-\frac{\partial\mathbf{u}_h}{\partial t}\right\|^2_{L^2(\Omega)}+\frac{\mu}{2}\frac{d}{dt}\|\nabla(\mathbf{u}-\mathbf{u}_h)\|^2_{L^2(\Omega)}\\ &\quad\le C\sum_{K\in\mathcal{T}_h}\left(\left\|\mathbf{f}-\rho\frac{\partial\mathbf{u}_h}{\partial t}+\mu\Delta\mathbf{u}_h-\nabla p_h\right\|_{L^2(K)}+\frac{1}{2\sqrt{\lambda_{2,K}}}\|\,[\mu\nabla\mathbf{u}_h\cdot\mathbf{n}]\,\|_{L^2(\partial K)}\right)\\ &\qquad\left(\omega_K\left(\mathbf{u}-\mathbf{u}_h+\frac{\partial}{\partial t}(\mathbf{u}-\mathbf{u}_h)\right)+\frac{1}{\max(\mu,\rho)}\omega_K(\mathbf{w})\right)\\ &\qquad +C\max(\mu,\rho)\left(\|\operatorname{div}\mathbf{u}_h\|^2_{L^2(\Omega)}+\left\|\operatorname{div}\frac{\partial\mathbf{u}_h}{\partial t}\right\|^2_{L^2(\Omega)}\right).\end{aligned}$$

Since $\omega_K$ satisfies the triangle inequality, we can bound $\omega_K\left(\mathbf{u}-\mathbf{u}_h+\frac{\partial}{\partial t}(\mathbf{u}-\mathbf{u}_h)\right)$ by

$$\omega_K(\mathbf{u}-\mathbf{u}_h)+\omega_K\left(\frac{\partial}{\partial t}(\mathbf{u}-\mathbf{u}_h)\right)$$

and integrating from 0 to $T$ yields the desired estimate for the velocity error. Combining it with (3.34) yields the estimate for the pressure. □

One can make the three following observations about the a posteriori upper bounds of Theorem 3.12:

(1) The proof is quite simple, since it generalizes the one for steady (Navier-)Stokes equations. Compared to a classical parabolic problem, where we would estimate the velocity error in the norm

$$\rho\|\mathbf{v}(T)\|^2_{L^2(\Omega)} + \int_0^T \mu\|\nabla \mathbf{v}\|^2_{L^2(\Omega)}dt,$$

here it is necessary to estimate it in the norm

$$\rho\|\mathbf{v}(T)\|^2_{L^2(\Omega)} + \int_0^T \mu\|\nabla \mathbf{v}\|^2_{L^2(\Omega)}dt + \rho\int_0^T \left\|\frac{\partial \mathbf{v}}{\partial t}\right\|^2_{L^2(\Omega)} dt + \mu\|\nabla \mathbf{v}(T)\|^2_{L^2(\Omega)}.$$

This is the only important difference with the common a posteriori error estimate derived in the classical theory.

(2) Since $\mathbf{u}_h(0) = r_h(\mathbf{u}_0) = r_h(\mathbf{u}(0))$, both terms

$$\rho\|(\mathbf{u}-\mathbf{u}_h)(0)\|^2_{L^2(\Omega)}, \quad \mu\|\nabla(\mathbf{u}-\mathbf{u}_h(0))\|^2_{L^2(\Omega)}$$

can be bounded using the anisotropic Lagrange interpolation error estimate of Proposition 1.1 since we assumed that $\mathbf{u}_0 \in (H^2(\Omega))^2$. Therefore, there are known quantities. In the isotropic setting, we will have that

$$\rho\|(\mathbf{u}-\mathbf{u}_h)(0)\|^2_{L^2(\Omega)} = O(h^4), \quad \mu\|\nabla(\mathbf{u}-\mathbf{u}_h(0))\|^2_{L^2(\Omega)} = O(h^2).$$

(3) To obtain a computable bound, we should apply a post-processing in order to replace not only the gradient of $\mathbf{u}$ but also its time derivative, that are contained in $\omega_K$. Note that even in the isotropic settings, we cannot avoid to post-process $\nabla\dfrac{\partial \mathbf{u}}{\partial t}$. Indeed, the a posteriori error estimate will read (note that $C$ depends here on the mesh aspect ratio)

$$\begin{aligned}
\rho\|(\mathbf{u}-\mathbf{u}_h)(T)\|^2_{L^2(\Omega)} &+ \mu\int_0^T \|\nabla(\mathbf{u}-\mathbf{u}_h)\|^2_{L^2(\Omega)}dt \\
&+ \rho\int_0^T \left\|\frac{\partial \mathbf{u}}{\partial t} - \frac{\partial \mathbf{u}_h}{\partial t}\right\|^2_{L^2(\Omega)} dt + \mu\|\nabla(\mathbf{u}-\mathbf{u}_h)(T)\|^2_{L^2(\Omega)} \\
&\le \rho\|(\mathbf{u}-\mathbf{u}_h)(0)\|^2_{L^2(\Omega)} + \mu\|\nabla(\mathbf{u}-\mathbf{u}_h)(0)\|^2_{L^2(\Omega)} \\
&\qquad + C\int_0^T \sum_{K\in\mathcal{T}_h} \left((\eta^I_{K,\mathbf{u},1})^2 + (\eta^I_{K,\mathbf{u},2})^2 + (\eta^{\mathrm{div}}_K)^2\right) dt,
\end{aligned}$$

where

$$(\eta^I_{K,\mathbf{u},1})^2 \quad = \quad h_K^2 \left\|\mathbf{f} - \rho\frac{\partial \mathbf{u}_h}{\partial t} + \mu\Delta\mathbf{u}_h - \nabla p_h\right\|^2_{L^2(K)} \; + \; h_K \,\|[\mu\nabla\mathbf{u}_h\cdot\mathbf{n}]\|^2_{L^2(\partial K)},$$

$$\begin{aligned}
(\eta^I_{K,\mathbf{u},2})^2 = \left(h_K \left\|\mathbf{f} - \rho\frac{\partial \mathbf{u}_h}{\partial t} + \mu\Delta\mathbf{u}_h - \nabla p_h\right\|_{L^2(K)} + h_K^{1/2}\,\|[\mu\nabla\mathbf{u}_h\cdot\mathbf{n}]\|_{L^2(\partial K)}\right) \\
\left\|\nabla\left(\frac{\partial \mathbf{u}}{\partial t} - \frac{\partial \mathbf{u}_h}{\partial t}\right)\right\|_{L^2(\Delta K)},
\end{aligned}$$

$$(\eta_K^{\text{div}})^2 = \max(\mu, \rho) \left( \|\operatorname{div} \mathbf{u}_h\|^2_{L^2(K)} + \left\|\operatorname{div} \frac{\partial \mathbf{u}_h}{\partial t}\right\|^2_{L^2(K)} \right),$$

and the norm $\left\| \nabla \left( \frac{\partial \mathbf{u}}{\partial t} - \frac{\partial \mathbf{u}_h}{\partial t} \right) \right\|_{L^2(\Omega)}$ is not present in the left hand side. Therefore it is not possible to write the estimate in a close form and we shall use post-processing that approximate the norm

$$\left\| \nabla \left( \frac{\partial \mathbf{u}}{\partial t} - \frac{\partial \mathbf{u}_h}{\partial t} \right) \right\|_{L^2(\Omega)}.$$

To obtain an estimate in a close form, it will require to derive the equations with respect to the time, but it will yield to the necessity to estimate $\left\| \frac{\partial p}{\partial t} - \frac{\partial p_h}{\partial t} \right\|_{L^2(\Omega)}$ that will generate a term containing the second derivatives with respect to time of the velocity etc. etc..

(4) It is not clear a priori that both errors

$$\left\| \nabla \left( \frac{\partial \mathbf{u}}{\partial t} - \frac{\partial \mathbf{u}_h}{\partial t} \right) \right\|_{L^2(\Omega)}, \left\| \operatorname{div} \frac{\partial \mathbf{u}_h}{\partial t} \right\|_{L^2(\Omega)}$$

converge with the right orders, especially when a time advancing scheme will be applied later on and we were not able to clearly verifiy it in the numerical experiments. This lowers considerably the interest of the upper bounds presented in the Theorem 3.12.

**A posteriori error estimate through Stokes projection**

To counter the drawbacks of Theorem 3.12, up to our knowledge, two approaches can be found in the literature, both based on the observation that if $\mathbf{u}_h$ is divergence free, then $\operatorname{div}(\mathbf{u} - \mathbf{u}_h) = 0$ and it is therefore possible to obtain an estimate for the velocity error without the need to estimate the pressure error $p - p_h$ since the term

$$\int_\Omega (p - p_h) \operatorname{div}(\mathbf{u} - \mathbf{u}_h) d\mathbf{x}$$

will naturally disappear. Both approaches were developed for isotropic finite elements, and we propose below to extend them to the anisotropic case.

It was first proposed in [16] to use the Stokes projection $\Pi^{\text{div}} : (H_0^1(\Omega))^2 \longrightarrow (H_0^1(\Omega))^2$ where for $\mathbf{v} \in (H_0^1(\Omega))^2$, we define $\Pi^{\text{div}}\mathbf{v}$ as the (unique) weak solution of

$$\begin{cases} -\Delta \Pi^{\text{div}}\mathbf{v} + \nabla s = 0, & \text{in } \Omega, \\ \operatorname{div} \Pi^{\text{div}}\mathbf{v} = \operatorname{div} \mathbf{v}, & \text{in } \Omega, \\ \Pi^{\text{div}}\mathbf{v} = 0, & \text{on } \partial\Omega. \end{cases} \tag{3.35}$$

The problem (3.35) is a standard Stokes problem which well-posedness is ensured, in a weak sense, in $(H_0^1(\Omega))^2 \times L_0^2(\Omega)$ provided $\operatorname{div} \mathbf{v} \in L_0^2(\Omega)$ [21]. Observe that the last condition is verified. Since $\mathbf{v} \in (H_0^1(\Omega))^2$, it implies that $\operatorname{div} \mathbf{v} \in L^2(\Omega)$ and, thanks to the divergence theorem and the fact that the trace of $\mathbf{v}$ is zero, one has

$$\int_\Omega \operatorname{div} \mathbf{v} d\mathbf{x} = \int_{\partial\Omega} \mathbf{v} \cdot \mathbf{n} d\mathbf{x} = 0,$$

so that $\operatorname{div} \mathbf{v}$ has zero mean value.

Moreover, there exists a constant $C > 0$ depending only on $\Omega$ such that

$$\|\nabla \Pi^{\mathrm{div}} \mathbf{v}\|_{L^2(\Omega)} + \|s\|_{L^2(\Omega)} \leq C \| \operatorname{div} \mathbf{v}\|_{L^2(\Omega)}. \tag{3.36}$$

The Stokes projection $\Pi^{\mathrm{div}}$ satisfies the following properties, that we gather in the next lemma. The proofs can be found in [16], Lemma 4.2. For the last property, we recall that we assume $\Omega$ convex, and that, given $\mathcal{T}_h$ a conformal triangulation of $\Omega$ into triangles of diameter less than $h$, we denote by $V_h$ the set of piecewise linear continuous (vector valued) functions with zero value on $\partial\Omega$.

**Lemma 3.13.** *(i) For all* $\mathbf{v} \in (H_0^1(\Omega))^2$, *if* $\operatorname{div} \mathbf{v} = 0$, *then* $\Pi^{\mathrm{div}} \mathbf{v} = 0$.

*(ii) For all* $\mathbf{v} \in (H_0^1(\Omega))^2$,

$$\|\nabla \left(\mathbf{v} - \Pi^{\mathrm{div}} \mathbf{v}\right) \|_{L^2(\Omega)} \leq \|\nabla \mathbf{v}\|_{L^2(\Omega)}.$$

*(iii) There exists* $C > 0$ *depending only on* $\Omega$ *and the mesh aspect ratio such that for all* $\mathbf{v}_h \in V_h$

$$\|\Pi^{\mathrm{div}} \mathbf{v}_h\|^2_{L^2(\Omega)} \leq C \sum_{K \in \mathcal{T}_h} h_K^2 \| \operatorname{div} \mathbf{v}_h\|^2_{L^2(K)}.$$

We also observe, under some smoothness assumptions, that if $\mathbf{v}$ also depends on the time and is sufficiently smooth, then the fact that (3.35) is uniquely solvable implies that $\frac{\partial}{\partial t}$ and $\Pi^{\mathrm{div}}$ commutes i.e.

$$\frac{\partial}{\partial t} \Pi^{\mathrm{div}} \mathbf{v} = \Pi^{\mathrm{div}} \frac{\partial}{\partial t} \mathbf{v}.$$

Using the Stokes projection, it is possible to derive an a posteriori error estimate for the velocity error $\mathbf{u} - \mathbf{u}_h$ avoiding to estimate the pressure error $p - p_h$. Note that an estimate for the pressure is after that available but one have to consider the norm

$$\left\| \frac{\partial}{\partial t}(\mathbf{u} - \mathbf{u}_h) + \nabla(p - p_h) \right\|_{H^{-1}(\Omega)}$$

which has a low interest from a practical point of view in a adaptive framework. Therefore, in what follows, we will only prove the corresponding a posteriori error estimate for the velocity, and we refer to [16] for more details on the treatment of the pressure.

For the next theorem, we assume in particular the following regularity:

$$\mathbf{u}_h \in C^0\left([0,T]; (L^2(\Omega))^2\right) \cap L^2\left(0,T; (H_0^1(\Omega))^2\right), \frac{\partial \mathbf{u}_h}{\partial t} \in C^0\left([0,T]; (H^1(\Omega))^2\right),$$

$$p_h \in L^2\left([0,T]; H^1(\Omega)\right).$$

**Theorem 3.14** (An a posteriori error estimate for the unsteady Stokes equations using the Stokes projection)**.**
*Let* $(\mathbf{u}, p)$ *be the solution of (3.26),* $(\mathbf{u}_h, p_h)$ *the solution of the finite elements scheme (3.27) and* $\Pi^{\mathrm{div}} \mathbf{u}_h$ *the Stokes projection of the finite elements approximation of the velocity. There exists a constant* $C_1 > 0$ *that depends only on the reference triangle and the domain* $\Omega$ *and a constant* $C_2 > 0$ *that depends on* $\Omega$ *and the mesh aspect ratio such that*

$$\begin{aligned} \rho\|\mathbf{u} - \mathbf{u}_h(T)\|^2_{L^2(\Omega)} &+ \mu \int_0^T \|\nabla(\mathbf{u} - \mathbf{u}_h)(t)\|^2_{L^2(\Omega)} dt \\ &\leq C_1 \left( \rho\|\mathbf{u} - \mathbf{u}_h(0)\|^2_{L^2(\Omega)} + \int_0^T \sum_{K \in \mathcal{T}_h} (\eta^A_{K,\mathbf{u}})^2(t) + (\eta^{\mathrm{div}}_K)^2(t) dt \right) \\ &\qquad + C_2 \sum_{K \in \mathcal{T}_h} (\varepsilon^I_{K,1})^2 + C_2 \int_0^T \sum_{K \in \mathcal{T}_h} (\varepsilon^I_{K,2})^2(t) dt, \end{aligned} \tag{3.37}$$

*where we note*

$$(\eta^A_{K,\mathbf{u}})^2(t) = \left(\left\|\mathbf{f}(t) - \rho\frac{\partial \mathbf{u}_h}{\partial t}(t) + \mu\Delta\mathbf{u}_h(t) - \nabla p_h(t)\right\|_{L^2(K)} + \frac{1}{2\sqrt{\lambda_{2,K}}}\|[\mu\nabla\mathbf{u}_h(t)\cdot\mathbf{n}]\|_{L^2(\partial K)}\right)$$
$$\omega_K\left(\left(\mathbf{u} - \mathbf{u}_h - \Pi^{\text{div}}(\mathbf{u} - \mathbf{u}_h)\right)(t)\right),$$

$$(\eta^{\text{div}}_K)^2(t) = \mu\|\operatorname{div}\mathbf{u}_h(t)\|^2_{L^2(K)},$$

$$(\varepsilon^I_{K,1})^2 = \rho h_K^2\left(\|\operatorname{div}\mathbf{u}_h(T)\|^2_{L^2(K)} + \|\operatorname{div}\mathbf{u}_h(0)\|^2_{L^2(K)}\right),$$

$$(\varepsilon^I_{K,2})^2(t) = \frac{\rho^2}{\mu}h_K^2\left\|\operatorname{div}\frac{\partial}{\partial t}\mathbf{u}_h(t)\right\|^2_{L^2(K)}.$$

*Proof.* Let $t \in (0,T)$. In the following, we will denote by $\hat{C}$ any positive constant that depends on the reference triangle only and by $\tilde{C}$ any constant that depends only on $\Omega$. Since we will use the estimate contained in Lemma 3.13, (*iii*), we will note the corresponding constant by $D$. Note that $D$ depends on $\Omega$ and the mesh aspect ratio.

Using the fact that for any $\mathbf{v} \in (H^1_0(\Omega))^2$, we have $\operatorname{div}\left(\mathbf{v} - \Pi^{\text{div}}\mathbf{v}\right) = 0$, one can write that

$$\begin{aligned}
&\frac{\rho}{2}\frac{d}{dt}\|\mathbf{u} - \mathbf{u}_h\|^2_{L^2(\Omega)} + \mu\|\nabla(\mathbf{u} - \mathbf{u}_h)\|^2_{L^2(\Omega)}\\
&\quad = \rho\int_\Omega \frac{\partial}{\partial t}(\mathbf{u} - \mathbf{u}_h)\cdot(\mathbf{u} - \mathbf{u}_h)d\mathbf{x} + \mu\int_\Omega \nabla(\mathbf{u} - \mathbf{u}_h) : \nabla(\mathbf{u} - \mathbf{u}_h)d\mathbf{x}\\
&\quad = \rho\int_\Omega \frac{\partial}{\partial t}(\mathbf{u} - \mathbf{u}_h)\cdot(\mathbf{u} - \mathbf{u}_h)d\mathbf{x} + \mu\int_\Omega \nabla(\mathbf{u} - \mathbf{u}_h) : \nabla(\mathbf{u} - \mathbf{u}_h)d\mathbf{x}\\
&\qquad - \int_\Omega (p - p_h)\operatorname{div}\left(\mathbf{u} - \mathbf{u}_h - \Pi^{\text{div}}(\mathbf{u} - \mathbf{u}_h)\right)d\mathbf{x}\\
&= \rho\int_\Omega \frac{\partial}{\partial t}(\mathbf{u}-\mathbf{u}_h)\cdot\left(\mathbf{u} - \mathbf{u}_h - \Pi^{\text{div}}(\mathbf{u} - \mathbf{u}_h)\right)d\mathbf{x} + \mu\int_\Omega \nabla(\mathbf{u}-\mathbf{u}_h) : \nabla\left(\mathbf{u} - \mathbf{u}_h - \Pi^{\text{div}}(\mathbf{u} - \mathbf{u}_h)\right)d\mathbf{x}\\
&\qquad - \int_\Omega (p - p_h)\operatorname{div}\left(\mathbf{u} - \mathbf{u}_h - \Pi^{\text{div}}(\mathbf{u} - \mathbf{u}_h)\right)d\mathbf{x}\\
&\qquad + \rho\int_\Omega \frac{\partial}{\partial t}(\mathbf{u} - \mathbf{u}_h)\cdot\Pi^{\text{div}}(\mathbf{u} - \mathbf{u}_h)d\mathbf{x} + \mu\int_\Omega \nabla(\mathbf{u} - \mathbf{u}_h) : \Pi^{\text{div}}(\mathbf{u} - \mathbf{u}_h)d\mathbf{x}\\
&= \int_\Omega \left(\mathbf{f} - \rho\frac{\partial \mathbf{u}_h}{\partial t}\right)\cdot\left(\mathbf{u} - \mathbf{u}_h - \Pi^{\text{div}}(\mathbf{u} - \mathbf{u}_h)\right)d\mathbf{x} - \mu\int_\Omega \nabla\mathbf{u}_h : \nabla\left(\mathbf{u} - \mathbf{u}_h - \Pi^{\text{div}}(\mathbf{u} - \mathbf{u}_h)\right)d\mathbf{x}\\
&\qquad + \int_\Omega p_h\operatorname{div}\left(\mathbf{u} - \mathbf{u}_h - \Pi^{\text{div}}(\mathbf{u} - \mathbf{u}_h)\right)d\mathbf{x}\\
&\qquad + \rho\int_\Omega \frac{\partial}{\partial t}(\mathbf{u} - \mathbf{u}_h)\cdot\Pi^{\text{div}}(\mathbf{u} - \mathbf{u}_h)d\mathbf{x} + \mu\int_\Omega \nabla(\mathbf{u} - \mathbf{u}_h) : \nabla\Pi^{\text{div}}(\mathbf{u} - \mathbf{u}_h)d\mathbf{x}.
\end{aligned}$$

As we already did several times, thanks to the numerical method (3.27), we can remove any test function $\mathbf{v}_h$ from the residual part

$$\int_\Omega \left(\mathbf{f} - \rho\frac{\partial \mathbf{u}_h}{\partial t}\right)\cdot\left(\mathbf{u} - \mathbf{u}_h - \Pi^{\text{div}}(\mathbf{u} - \mathbf{u}_h)\right)d\mathbf{x} - \mu\int_\Omega \nabla\mathbf{u}_h : \nabla\left(\mathbf{u} - \mathbf{u}_h - \Pi^{\text{div}}(\mathbf{u} - \mathbf{u}_h)\right)d\mathbf{x}$$
$$+ \int_\Omega p_h\operatorname{div}\left(\mathbf{u} - \mathbf{u}_h - \Pi^{\text{div}}(\mathbf{u} - \mathbf{u}_h)\right)d\mathbf{x}$$

and choosing $\mathbf{v}_h = R_h\left(\mathbf{u} - \mathbf{u}_h - \Pi^{\text{div}}(\mathbf{u} - \mathbf{u}_h)\right)$, we obtain after an integration by parts and applying the Cauchy-Schwarz and the interpolation error estimates for the Clément's interpolant

$$\begin{aligned}\frac{\rho}{2}\frac{d}{dt}\|\mathbf{u}-\mathbf{u}_h\|^2_{L^2(\Omega)} + \mu\|\nabla(\mathbf{u}-\mathbf{u}_h)\|^2_{L^2(\Omega)} \\ \leq \hat{C}\sum_{K\in\mathcal{T}_h}\nu_K\omega_K\left(\mathbf{u}-\mathbf{u}_h-\Pi^{\mathrm{div}}(\mathbf{u}-\mathbf{u}_h)\right) \\ +\rho\int_\Omega\frac{\partial}{\partial t}(\mathbf{u}-\mathbf{u}_h)\cdot\Pi^{\mathrm{div}}(\mathbf{u}-\mathbf{u}_h)d\mathbf{x}+\mu\int_\Omega\nabla(\mathbf{u}-\mathbf{u}_h):\nabla\Pi^{\mathrm{div}}(\mathbf{u}-\mathbf{u}_h)d\mathbf{x},\end{aligned}$$

where we use the notation

$$\nu_K = \left\|\mathbf{f}-\rho\frac{\partial\mathbf{u}_h}{\partial t}+\mu\Delta\mathbf{u}_h-\nabla p_h\right\|_{L^2(K)}+\frac{1}{2\sqrt{\lambda_{2,K}}}\|[\mu\nabla\mathbf{u}_h\cdot\mathbf{n}]\|_{L^2(\partial K)}.$$

The Leibniz rule and the commutativity of $\Pi^{\mathrm{div}}$ with the time derivative imply

$$\begin{aligned}\frac{\partial}{\partial t}\left((\mathbf{u}-\mathbf{u}_h)\cdot\Pi^{\mathrm{div}}(\mathbf{u}-\mathbf{u}_h)\right) &= \frac{\partial}{\partial t}(\mathbf{u}-\mathbf{u}_h)\cdot\Pi^{\mathrm{div}}(\mathbf{u}-\mathbf{u}_h)+(\mathbf{u}-\mathbf{u}_h)\cdot\frac{\partial}{\partial t}\Pi^{\mathrm{div}}(\mathbf{u}-\mathbf{u}_h) \\ &= \frac{\partial}{\partial t}(\mathbf{u}-\mathbf{u}_h)\cdot\Pi^{\mathrm{div}}(\mathbf{u}-\mathbf{u}_h)+(\mathbf{u}-\mathbf{u}_h)\cdot\Pi^{\mathrm{div}}\frac{\partial}{\partial t}(\mathbf{u}-\mathbf{u}_h).\end{aligned}$$

Therefore, the last inequality can be written as

$$\begin{aligned}\frac{\rho}{2}\frac{d}{dt}\|\mathbf{u}-\mathbf{u}_h\|^2_{L^2(\Omega)} + \mu\|\nabla(\mathbf{u}-\mathbf{u}_h)\|^2_{L^2(\Omega)} \\ \leq \hat{C}\sum_{K\in\mathcal{T}_h}\nu_K\omega_K\left(\mathbf{u}-\mathbf{u}_h-\Pi^{\mathrm{div}}(\mathbf{u}-\mathbf{u}_h)\right) \\ +\rho\frac{d}{dt}\int_\Omega(\mathbf{u}-\mathbf{u}_h)\cdot\Pi^{\mathrm{div}}(\mathbf{u}-\mathbf{u}_h)d\mathbf{x}-\rho\int_\Omega(\mathbf{u}-\mathbf{u}_h)\cdot\Pi^{\mathrm{div}}\frac{\partial}{\partial t}(\mathbf{u}-\mathbf{u}_h)d\mathbf{x} \\ +\mu\int_\Omega\nabla(\mathbf{u}-\mathbf{u}_h):\nabla\Pi^{\mathrm{div}}(\mathbf{u}-\mathbf{u}_h)d\mathbf{x}.\end{aligned}$$

Integration from 0 to $T$ and Cauchy-Schwarz yield

$$\begin{aligned}\frac{\rho}{2}\|\mathbf{u}-\mathbf{u}_h(T)\|^2_{L^2(\Omega)}+\mu\int_0^T\|\nabla(\mathbf{u}-\mathbf{u}_h)\|^2_{L^2(\Omega)}dt \\ \leq\frac{\rho}{2}\|\mathbf{u}-\mathbf{u}_h(0)\|^2_{L^2(\Omega)}+\hat{C}\int_0^T\sum_{K\in\mathcal{T}_h}\nu_K\omega_K\left(\mathbf{u}-\mathbf{u}_h-\Pi^{\mathrm{div}}(\mathbf{u}-\mathbf{u}_h)\right)dt \\ +\rho\|\mathbf{u}-\mathbf{u}_h(T)\|_{L^2(\Omega)}\|\Pi^{\mathrm{div}}(\mathbf{u}-\mathbf{u}_h)(T)\|_{L^2(\Omega)}+\rho\|\mathbf{u}-\mathbf{u}_h(0)\|_{L^2(\Omega)}\|\Pi^{\mathrm{div}}(\mathbf{u}-\mathbf{u}_h)(0)\|_{L^2(\Omega)} \\ +\rho\int_0^T\|\mathbf{u}-\mathbf{u}_h\|_{L^2(\Omega)}\left\|\Pi^{\mathrm{div}}\frac{\partial}{\partial t}(\mathbf{u}-\mathbf{u}_h)\right\|_{L^2(\Omega)}dt+\mu\int_0^T\|\nabla(\mathbf{u}-\mathbf{u}_h)\|_{L^2(\Omega)}\|\nabla\Pi^{\mathrm{div}}(\mathbf{u}-\mathbf{u}_h)\|_{L^2(\Omega)}dt.\end{aligned}$$

Using the Young's inequality, one may write

$$\begin{aligned}\frac{\rho}{4}\|\mathbf{u}-\mathbf{u}_h(T)\|^2_{L^2(\Omega)}+\frac{\mu}{2}\int_0^T\|\nabla(\mathbf{u}-\mathbf{u}_h)\|^2_{L^2(\Omega)}dt \\ \leq\rho\|\mathbf{u}-\mathbf{u}_h(0)\|^2_{L^2(\Omega)}+\hat{C}\int_0^T\sum_{K\in\mathcal{T}_h}\nu_K\omega_K\left(\mathbf{u}-\mathbf{u}_h-\Pi^{\mathrm{div}}(\mathbf{u}-\mathbf{u}_h)\right)dt \\ +\rho\|\Pi^{\mathrm{div}}(\mathbf{u}-\mathbf{u}_h)(T)\|^2_{L^2(\Omega)}+\frac{\rho}{2}\|\Pi^{\mathrm{div}}(\mathbf{u}-\mathbf{u}_h)(0)\|^2_{L^2(\Omega)} \\ +\frac{\rho}{2\varepsilon}\int_0^T\|\mathbf{u}-\mathbf{u}_h\|^2_{L^2(\Omega)}dt+\frac{\rho\varepsilon}{2}\int_0^T\left\|\Pi^{\mathrm{div}}\frac{\partial}{\partial t}(\mathbf{u}-\mathbf{u}_h)\right\|^2_{L^2(\Omega)}dt+\frac{\mu}{2}\int_0^T\|\nabla\Pi^{\mathrm{div}}(\mathbf{u}-\mathbf{u}_h)\|^2_{L^2(\Omega)}dt.\end{aligned} \tag{3.38}$$

Using the Poincaré inequality and choosing $\varepsilon = 2\frac{\rho C_P^2}{\mu}$, where $C_P$ is Poincaré constant of $\Omega$, one can bound the first term in the last line of (3.38) in the following way

$$\frac{\rho}{2\varepsilon}\int_0^T \|\mathbf{u}-\mathbf{u}_h\|^2_{L^2(\Omega)}dt \leq \frac{\mu}{4}\int_0^T \|\nabla(\mathbf{u}-\mathbf{u}_h)\|^2_{L^2(\Omega)}dt$$

and then pass it to the left hand side. Finally, using the properties of $\Pi^{\mathrm{div}}$ (in particular we recall that $\Pi^{\mathrm{div}}\mathbf{u} = 0$), it yields

$$\begin{aligned}
&\frac{\rho}{4}\|\mathbf{u}-\mathbf{u}_h(T)\|^2_{L^2(\Omega)} + \frac{\mu}{4}\int_0^T \|\nabla(\mathbf{u}-\mathbf{u}_h)\|^2_{L^2(\Omega)}dt \\
&\qquad \leq \rho\|\mathbf{u}-\mathbf{u}_h(0)\|^2_{L^2(\Omega)} + \hat{C}\int_0^T \sum_{K\in\mathcal{T}_h} \nu_K\omega_K\left(\mathbf{u}-\mathbf{u}_h-\Pi^{\mathrm{div}}(\mathbf{u}-\mathbf{u}_h)\right)dt \\
&\qquad\quad + \rho D\sum_{K\in\mathcal{T}_h} h_K^2\left(\|\operatorname{div}\mathbf{u}_h(T)\|^2_{L^2(K)} + \|\operatorname{div}\mathbf{u}_h(0)\|^2_{L^2(K)}\right) \\
&\qquad\quad + \frac{\rho^2 C_P^2 D}{\mu}\int_0^T \sum_{K\in\mathcal{T}_h} h_K^2\left\|\operatorname{div}\frac{\partial}{\partial t}\mathbf{u}_h\right\|^2_{L^2(K)}dt + \frac{\mu\tilde{C}}{2}\int_0^T \|\operatorname{div}\mathbf{u}_h\|^2_{L^2(\Omega)}dt,
\end{aligned}$$

that concludes the proof. □

**Remark 3.15.**
Note that in (3.38) we control the term

$$\frac{\rho}{2\varepsilon}\int_0^T \|\mathbf{u}-\mathbf{u}_h\|^2_{L^2(\Omega)}dt$$

by using the Poincaré inequality so that we can absorb it into the $H^1$ semi-norm in the left hand side. We could also keep it and control it by a Gronwall's type argument (in integral form) since

$$\rho\|\mathbf{u}-\mathbf{u}_h(T)\|^2_{L^2(\Omega)}$$

is present also in the left hand side. This would yield at the end to the following a posteriori error estimate

$$\begin{aligned}
&\rho\|\mathbf{u}-\mathbf{u}_h(T)\|^2_{L^2(\Omega)} + \mu\int_0^T \|\nabla(\mathbf{u}-\mathbf{u}_h)\|^2_{L^2(\Omega)}dt \\
&\qquad \leq \exp\left(\frac{2\rho T}{\varepsilon}\right)C_1\left(\rho\|\mathbf{u}-\mathbf{u}_h(T)\|^2_{L^2(\Omega)} + \int_0^T \sum_{K\in\mathcal{T}_h}(\eta^A_{K,\mathbf{u}})^2 + (\eta^{\mathrm{div}}_K)^2 dt\right) \\
&\qquad\quad + \exp\left(\frac{2\rho T}{\varepsilon}\right)C_2\sum_{K\in\mathcal{T}_h}(\varepsilon^I_{K,1})^2 + \exp\left(\frac{2\rho T}{\varepsilon}\right)C_2\int_0^T\sum_{K\in\mathcal{T}_h}(\varepsilon^I_{K,2})^2 dt,
\end{aligned}$$

with as before

$$\begin{aligned}
(\eta^A_{K,\mathbf{u}})^2 = &\left(\left\|\mathbf{f}-\rho\frac{\partial\mathbf{u}_h}{\partial t}+\mu\Delta\mathbf{u}_h-\nabla p_h\right\|_{L^2(K)} + \frac{1}{2\sqrt{\lambda_{2,K}}}\|[\mu\nabla\mathbf{u}_h\cdot\mathbf{n}]\|_{L^2(\partial K)}\right) \\
&\qquad\qquad \omega_K\left(\mathbf{u}-\mathbf{u}_h-\Pi^{\mathrm{div}}(\mathbf{u}-\mathbf{u}_h)\right),
\end{aligned}$$

$$(\eta^{\mathrm{div}}_K)^2 = \mu\|\operatorname{div}\mathbf{u}_h\|^2_{L^2(K)},$$

$$(\varepsilon^I_{K,1})^2 = \rho h_K^2\left(\|\operatorname{div}\mathbf{u}_h(T)\|^2_{L^2(K)} + \|\operatorname{div}\mathbf{u}_h(0)\|^2_{L^2(K)}\right),$$

but this time $(\varepsilon^I_{K,2})^2$ is given by

$$(\varepsilon^I_{K,2})^2 = \rho\varepsilon h_K^2 \left\| \operatorname{div} \frac{\partial}{\partial t}\mathbf{u}_h \right\|^2_{L^2(K)}.$$

Choosing $\varepsilon = \frac{T}{2\rho}$ eliminates the exponential in time. So we endow finally (up to a pure numeric constant) with the same a posteriori error estimate as the one in Theorem 3.12, except that we replace $\dfrac{\rho^2}{\mu}$ by $\rho T$ in the definition of $(\varepsilon^I_{K,2})^2$.

The main advantage of Theorem 3.14 and the use of the Stokes projection $\Pi^{\text{div}}$ is that an estimate for the velocity is reachable without the need of estimating the pressure. Moreover, even if some parts of the estimate (3.37) contain a constant that may depend on the mesh aspect ratio, mainly the isotropic error estimators $\varepsilon^I_{K,1}$ and $\varepsilon^I_{K,2}$, we have good reason to think that they are *a priori* of higher orders. Indeed, it is natural to hope $\|\operatorname{div}\mathbf{u}_h\|_{L^2(\Omega)} = O(h)$ and that at least $\|\operatorname{div}\partial_t\mathbf{u}_h\|_{L^2(\Omega)} = O(h^k)$ for $0 < k \leq 1$. This implies that

$$\sum_{K\in\mathcal{T}_h} (\varepsilon^I_{K,1})^2 = O(h^4) \text{ and } \sum_{K\in\mathcal{T}_h} (\varepsilon^I_{K,1})^2 = O(h^{2(k+1)}).$$

Therefore, even if the constant $C_2$ in Theorem 3.14 depends on the aspect ratio, the corresponding terms are of higher order (with respect to the $H^1$ semi-norm that is numerically checked to be $O(h)$). Compared to the Theorem 3.12, the problem of having the term $\operatorname{div}\frac{\partial}{\partial t}\mathbf{u}_h$ in the estimate is then solved by the Theorem 3.14.

However, the drawback of the a posteriori error estimate of Theorem 3.14 is the presence of the factor

$$\omega_K\left(\mathbf{u} - \mathbf{u}_h - \Pi^{\text{div}}(\mathbf{u} - \mathbf{u}_h)\right).$$

Note that in the isotropic settings, see [16], the error indicator $(\eta^A_{K,\mathbf{u}})^2$ is replaced by

$$\left( h_K \left\| \mathbf{f} - \rho\frac{\partial \mathbf{u}_h}{\partial t} + \mu\Delta\mathbf{u}_h - \nabla p_h \right\|_{L^2(K)} + h_K^{1/2} \|[\mu\nabla\mathbf{u}_h\cdot\mathbf{n}]\|_{L^2(\partial K)} \right) \left\| \nabla\left(\mathbf{u} - \mathbf{u}_h - \Pi^{\text{div}}(\mathbf{u} - \mathbf{u}_h)\right)\right\|_{L^2(\Delta K)},$$

and therefore, summing over the triangle and using the discrete Cauchy-Schwartz inequality, it will yield (up to a constant)

$$\left( \sum_{K\in\mathcal{T}_h} h_K^2 \left\| \mathbf{f} - \rho\frac{\partial \mathbf{u}_h}{\partial t} + \mu\Delta\mathbf{u}_h - \nabla p_h \right\|^2_{L^2(K)} + h_K \|[\mu\nabla\mathbf{u}_h\cdot\mathbf{n}]\|^2_{L^2(\partial K)} \right)^{1/2} \left\| \nabla\left(\mathbf{u} - \mathbf{u}_h - \Pi^{\text{div}}(\mathbf{u} - \mathbf{u}_h)\right)\right\|_{L^2(\Omega)},$$

and the factor $\left\| \nabla\left(\mathbf{u} - \mathbf{u}_h - \Pi^{\text{div}}(\mathbf{u} - \mathbf{u}_h)\right)\right\|_{L^2(\Omega)}$ can be absorbed in the left hand side using the property (see Lemma 3.13)

$$\left\| \nabla\left(\mathbf{u} - \mathbf{u}_h - \Pi^{\text{div}}(\mathbf{u} - \mathbf{u}_h)\right)\right\|_{L^2(\Omega)} \leq \|\nabla(\mathbf{u} - \mathbf{u}_h)\|_{L^2(\Omega)}.$$

This manipulation is unfortunately not possible in general in the anisotropic settings, since there is no reason a priori that

$$\omega_K\left(\mathbf{u} - \mathbf{u}_h - \Pi^{\text{div}}(\mathbf{u} - \mathbf{u}_h)\right) \text{ is bounded by } \omega_K(\mathbf{u} - \mathbf{u}_h). \tag{3.39}$$

Indeed, we only have a global control over all $\Omega$

$$\left\|\nabla\left(\mathbf{v}-\Pi^{\mathrm{div}}\mathbf{v}\right)\right\|_{L^2(\Omega)} \leq \|\nabla\mathbf{v}\|_{L^2(\Omega)}$$

and to obtain an estimate as (3.39), we should be able to prove that on every patch and in every direction, it holds

$$\|\nabla\left(\mathbf{u}-\mathbf{u}_h-\Pi^{\mathrm{div}}(\mathbf{u}-\mathbf{u}_h)\right)\cdot\mathbf{r}_{i,K}\|_{L^2(\Delta K)} \leq \|\nabla\left(\mathbf{u}-\mathbf{u}_h\right)\cdot\mathbf{r}_{i,K}\|_{L^2(\Delta K)}, \quad i=1,2.$$

So far, we do not know if such an inequality is valid or can be demonstrated. What can be done is to use that $\Pi^{\mathrm{div}}\mathbf{u}=0$ and to apply the triangle inequality

$$\omega_K\left(\mathbf{u}-\mathbf{u}_h-\Pi^{\mathrm{div}}(\mathbf{u}-\mathbf{u}_h)\right) \leq \omega_K(\mathbf{u}-\mathbf{u}_h)+\omega_K\left(\Pi^{\mathrm{div}}\mathbf{u}_h\right)$$

and then bound

$$\left(\left\|\mathbf{f}-\rho\frac{\partial\mathbf{u}_h}{\partial t}+\mu\Delta\mathbf{u}_h-\nabla p_h\right\|_{L^2(K)}+\frac{1}{2\sqrt{\lambda_{2,K}}}\|[\mu\nabla\mathbf{u}_h\cdot\mathbf{n}]\|_{L^2(\partial K)}\right)\omega_K\left(\Pi^{\mathrm{div}}\mathbf{u}_h\right)$$

by

$$\left(\lambda_{1,K}^2+\lambda_{2,K}^2\right)^{1/2}$$
$$\left(\left\|\mathbf{f}-\rho\frac{\partial\mathbf{u}_h}{\partial t}+\mu\Delta\mathbf{u}_h-\nabla p_h\right\|_{L^2(K)}+\frac{1}{2\sqrt{\lambda_{2,K}}}\|[\mu\nabla\mathbf{u}_h\cdot\mathbf{n}]\|_{L^2(\partial K)}\right)\left\|\nabla\Pi^{\mathrm{div}}\mathbf{u}_h\right\|_{L^2(\Delta K)}.$$

Thanks to the discrete Cauchy-Schwarz inequality and the Young's inequality, we obtain finally for the sum over triangles that

$$\sum_{K\in\mathcal{T}_h}\left(\left\|\mathbf{f}-\rho\frac{\partial\mathbf{u}_h}{\partial t}+\mu\Delta\mathbf{u}_h-\nabla p_h\right\|_{L^2(K)}+\frac{1}{2\sqrt{\lambda_{2,K}}}\|[\mu\nabla\mathbf{u}_h\cdot\mathbf{n}]\|_{L^2(\partial K)}\right)\omega_K\left(\Pi^{\mathrm{div}}\mathbf{u}_h\right)$$

is controlled (up to a constant) by

$$\sum_{K\in\mathcal{T}_h}(\lambda_{1,K}^2+\lambda_{2,K}^2)\left(\left\|\mathbf{f}-\rho\frac{\partial\mathbf{u}_h}{\partial t}+\mu\Delta\mathbf{u}_h-\nabla p_h\right\|_{L^2(K)}+\frac{1}{2\sqrt{\lambda_{2,K}}}\|[\mu\nabla\mathbf{u}_h\cdot\mathbf{n}]\|_{L^2(\partial K)}\right)^2 + \left\|\nabla\Pi^{\mathrm{div}}\mathbf{u}_h\right\|_{L^2(\Omega)}^2.$$

Finally we use that

$$\left\|\nabla\Pi^{\mathrm{div}}\mathbf{u}_h\right\|_{L^2(\Omega)}^2$$

is controlled by $\|\operatorname{div}\mathbf{u}_h\|_{L^2(\Omega)}^2$ to obtain an estimate that does not involve $\Pi^{\mathrm{div}}\mathbf{u}_h$. As already explained before, the term

$$\sum_{K\in\mathcal{T}_h}(\lambda_{1,K}^2+\lambda_{2,K}^2)\left(\left\|\mathbf{f}-\rho\frac{\partial\mathbf{u}_h}{\partial t}+\mu\Delta\mathbf{u}_h-\nabla p_h\right\|_{L^2(K)}+\frac{1}{2\sqrt{\lambda_{2,K}}}\|[\mu\nabla\mathbf{u}_h\cdot\mathbf{n}]\|_{L^2(\partial K)}\right)^2$$

is suboptimal for anisotropic meshes, since it is a low order term (it goes as $O(h)$ after taking the square root) but

$$\lambda_{1,K}^2+\lambda_{2,K}^2$$

cannot be bounded independently of the mesh aspect ratio.

**A posteriori error estimates through Stokes reconstruction**

The second approach to correct the issues of Theorem 3.12 is presented in [61]. The authors propose to use the so-called Stokes reconstruction, that is an extension to the Stokes equations of the elliptic reconstruction introduced in [74] for parabolic problems. The proofs of the final a posteriori error estimates obtained with this technique are a combination of several propositions (Propositions 3.19, 3.21, 3.23 and 3.25) that are presented independently and reassemble in the Theorems 3.27 and 3.29. In a first reading, the proofs of these propositions can be skipped and the reader can go directly to the Theorems 3.27 and 3.29.

Let $t \in [0, T]$ and let $(\mathbf{u}_h(t), p_h(t))$ be the discrete (in space) approximation of the velocity and pressure given by (3.27). We define the Stokes reconstruction of $(\mathbf{u}_h(t), p_h(t))$ as the unique solution $(\mathbf{U}(t), P(t))$ of the steady Stokes equations

$$\begin{cases} -\mu\Delta\mathbf{U}(t) + \nabla P(t) = \mathbf{f}(t) - \rho\dfrac{\partial \mathbf{u}_h}{\partial t}(t), & \text{in } \Omega, \\ \operatorname{div}\mathbf{U}(t) = 0, & \text{in } \Omega, \\ \mathbf{U}(t) = 0, & \text{on } \partial\Omega. \end{cases} \tag{3.40}$$

We recall that we assume for any $t \in [0, T], \mathbf{f}(t) \in (L^2(\Omega))^2$. If moreover we assume for instance that for any $t \in [0, T]$, $\dfrac{\partial \mathbf{u}_h}{\partial t}(t) \in (L^2(\Omega))^2$ too, then there exists for all $t \in [0, T]$ a unique pair $(\mathbf{U}(t), P(t)) \in (H_0^1(\Omega))^2 \times L_0^2(\Omega)$ that is a weak solution of (3.40). Since the domain $\Omega$ is a convex polygon, it is also sufficient to obtain that for every $t \in [0, T]$ $(\mathbf{U}(t), P(t)) \in (H^2(\Omega))^2 \times H^1(\Omega)$, see [62]. Note that the $H^2 \times H^1$ regularity of the Stokes equations for convex polygon is a particularity of the 2D case, the equivalent result for convex polyhedrons (up to our knowledge) is believed to be true, but proven only for some particular cases [66]. Remark however, that for smooth boundaries, the result exists in any dimension [21]. Note that for the a posteriori error analysis below, we do not need the extra regularity $(\mathbf{U}(t), P(t)) \in (H^2(\Omega))^2 \times H^1(\Omega)$ and we shall only use the fact that $(\mathbf{U}(t), P(t))$ satisfies the equations (3.40) in the weak formulation

$$\begin{aligned} \mu\int_\Omega \nabla\mathbf{U}(t) : \nabla\mathbf{v}d\mathbf{x} - \int_\Omega P(t)\operatorname{div}\mathbf{v}d\mathbf{x} = \int_\Omega \left(\mathbf{f}(t) - \rho\frac{\partial \mathbf{u}_h}{\partial t}(t)\right)\cdot\mathbf{v}d\mathbf{x}, \quad \forall\mathbf{v} \in (H_0^1(\Omega))^2, \\ -\int_\Omega q\operatorname{div}\mathbf{U}(t) = 0, \quad \forall q \in L_0^2(\Omega). \end{aligned} \tag{3.41}$$

However, considering the time variable, some smoothness is required and we must be able to differentiate $(\mathbf{U}, P)$ and the equations (3.41) with respect to $t$ (for our demonstrations at least two times). So it is necessary that the force term $\mathbf{f}$ and the numerical solution $\mathbf{u}_h$ (and consequently the pressure $p_h$) are at least of "equivalent" regularity in time. We do not pretend to give an exhaustive analysis of the regularity of the solutions of (3.40), therefore we content ourself to assume from now that $\mathbf{u}, p, \mathbf{u}_h, p_h, \mathbf{U}, P$ are sufficiently smooth to justify the computations. Still, we write below at least necessary conditions such that the a posteriori estimates have a sense. We might assume that

$$\mathbf{u}, \mathbf{u}_h, \mathbf{U} \in C^0\left([0,T]; (H_0^1(\Omega))^2\right), \frac{\partial \mathbf{u}}{\partial t}, \frac{\partial \mathbf{U}}{\partial t} \in C^0\left(0,T; (L^2(\Omega))^2\right) \cap L^2\left(0,T; (H_0^1(\Omega))^2\right),$$

$$\frac{\partial \mathbf{u}_h}{\partial t}, \frac{\partial^2 \mathbf{u}_h}{\partial t^2} \in C^0\left([0,T]; (H^1(\Omega))^2\right), \frac{\partial^3 \mathbf{u}_h}{\partial t^3}, \frac{\partial^2 \mathbf{U}}{\partial t^2}, \in C^0\left(0,T; (L^2(\Omega))^2\right)$$

$$p, P \in C^0\left([0,T]; L_0^2(\Omega)\right), p_h \in C^0\left(0,T; L_0^2(\Omega)\right) \cap H^1\left(0,T; H^1(\Omega)\right)$$

$$\mathbf{f} \in C^2\left([0,T]; (L^2(\Omega))^2\right).$$

**Remark 3.16.**
We write the Stokes reconstruction system in a slightly different way that the one used in [61], where the right hand side of (3.40) is chosen as

$$\mathbf{f} - \mathbf{f}_h - \mu \tilde{\Delta}_h \mathbf{u}_h,$$

where $\mathbf{f}_h$ stands for the $L^2(\Omega)$ projection into the finite elements space and $\tilde{\Delta}_h$ for a proper discrete version of the Laplace operator. Observe that, at least formally and working in a divergence free space to eliminate the pressure, we can consider that

$$\mathbf{f}_h - \mu \tilde{\Delta}_h \mathbf{u}_h = \rho \frac{\partial \mathbf{u}_h}{\partial t} \text{ in } L^2(\Omega).$$

In the next proposition, we show the link between $(\mathbf{U}, P)$ and the numerical solutions $(\mathbf{u}_h, p_h)$. Let us assume that we discretize the equations (3.40) with $\mathbb{P}^1$ finite elements and that for any $t \in [0,T]$ we look for $(\mathbf{U}_h(t), P_h(t)) \in V_h \times Q_h$ the solution of the Petrov-Galerkin method

$$\begin{aligned} &\mu \int_\Omega \nabla \mathbf{U}_h : \nabla \mathbf{v}_h d\mathbf{x} - \int_\Omega P_h \operatorname{div} \mathbf{v}_h d\mathbf{x} = \int_\Omega \mathbf{f} \cdot \mathbf{v}_h d\mathbf{x} - \rho \int_\Omega \frac{\partial \mathbf{u}_h}{\partial t} \cdot \mathbf{v}_h d\mathbf{x}, \quad \forall \mathbf{v}_h \in V_h, \\ &- \int_\Omega q_h \operatorname{div} \mathbf{U}_h d\mathbf{x} + \sum_{K \in \mathcal{T}_h} \alpha_K \int_K \left(\mathbf{f} - \rho \frac{\partial \mathbf{u}_h}{\partial t} + \mu \Delta \mathbf{U}_h - \nabla P_h\right) \cdot \nabla q_h d\mathbf{x} = 0, \quad \forall q_h \in Q_h, \end{aligned} \tag{3.42}$$

where we choose $\alpha_K$ as in (3.28). Then, one can prove the following result

**Proposition 3.17.**
*For all $t \in [0,T]$, $(\mathbf{U}_h(t), P_h(t)) = (\mathbf{u}_h(t), p_h(t))$ where $(\mathbf{U}_h, P_h)$ is the solution of (3.42) and $(\mathbf{u}_h, p_h)$ the solution of (3.27).*

*Proof.* Substracting (3.27) from (3.42), it yields for all $t \in [0,T]$ that (note that we use the fact $\Delta \mathbf{v}_h = 0, \forall \mathbf{v}_h \in V_h$ to eliminate the Laplacian in the stabilization term)

$$\begin{aligned} &\mu \int_\Omega \nabla(\mathbf{U}_h(t) - \mathbf{u}_h(t)) : \nabla \mathbf{v}_h d\mathbf{x} - \int_\Omega (P_h(t) - p_h(t)) \operatorname{div} \mathbf{v}_h d\mathbf{x} = 0, \forall \mathbf{v}_h \in V_h, \\ &- \int q_h \operatorname{div}(\mathbf{U}_h(t) - \mathbf{u}_h(t)) d\mathbf{x} - \sum_{K \in \mathcal{T}_h} \alpha_K \int_K \nabla(P_h(t) - p_h(t)) \cdot \nabla q_h d\mathbf{x} = 0, \forall q_h \in Q_h. \end{aligned}$$

Choosing $\mathbf{v}_h = \mathbf{U}_h(t) - \mathbf{u}_h(t)$ and $q_h = -(P_h(t) - p_h(t))$, we get by summing the two equations

$$\mu \int_\Omega |\nabla(\mathbf{U}_h(t) - \mathbf{u}_h(t))|^2 d\mathbf{x} + \sum_{K \in \mathcal{T}_h} \alpha_K \int_K |\nabla(P_h(t) - p_h(t))|^2 d\mathbf{x} = 0,$$

which implies that $\mathbf{U}_h(t) = \mathbf{u}_h(t)$ and $P_h(t) = p_h(t)$ since both terms are non negative. □

The above proposition tell us that we can think to the Stokes reconstruction as a smooth version of the numerical solution $(\mathbf{u}_h, p_h)$ since we recover it after discretizing the equations (3.40). Moreover, one can prove the following Lemma, that can be interpreted as a Galerkin orthogonality between $(\mathbf{U}, P)$ and $(\mathbf{u}_h, p_h)$ and that we shall use later.

**Lemma 3.18** (Galerkin orthogonality of the Stokes reconstruction)**.**
*Let $(\mathbf{u}_h, p_h)$ be the solution of the semi-discretized equations (3.27) and $(\mathbf{U}, P)$ its the Stokes reconstruction given by (3.41). For all $t \in [0, T]$, the following identities hold*

$$\mu \int_\Omega \nabla(\mathbf{U} - \mathbf{u}_h)(t) : \nabla \mathbf{v}_h d\mathbf{x} - \int_\Omega (P - p_h)(t) \operatorname{div} \mathbf{v}_h d\mathbf{x} = 0, \quad \forall \mathbf{v}_h \in V_h, \tag{3.43}$$

$$-\int_\Omega q_h \operatorname{div}(\mathbf{U} - \mathbf{u}_h)(t) d\mathbf{x} - \sum_{K \in \mathcal{T}_h} \alpha_K \left( \mathbf{f}(t) - \rho \frac{\partial \mathbf{u}_h(t)}{\partial t} + \mu \Delta \mathbf{u}_h(t) - \nabla p_h(t) \right) \cdot \nabla q_h d\mathbf{x} = 0, \quad \forall q_h \in Q_h. \tag{3.44}$$

*Moreover, assuming that $\mathbf{f}, \mathbf{u}_h, p_h, \mathbf{U}, P$ are smooth enough, we have for $k > 0$*

$$\mu \int_\Omega \nabla \frac{\partial^k (\mathbf{U} - \mathbf{u}_h)(t)}{\partial t^k} : \nabla \mathbf{v}_h d\mathbf{x} - \int_\Omega \frac{\partial^k (P - p_h)(t)}{\partial t^k} \operatorname{div} \mathbf{v}_h = 0, \quad \forall \mathbf{v}_h \in V_h, \tag{3.45}$$

$$\begin{aligned} &-\int_\Omega q_h \operatorname{div} \frac{\partial^k (\mathbf{U} - \mathbf{u}_h)(t)}{\partial t^k} \\ &- \sum_{K \in \mathcal{T}_h} \alpha_K \left( \frac{\partial^k \mathbf{f}(t)}{\partial t^k} - \rho \frac{\partial^{k+1} \mathbf{u}_h(t)}{\partial t^{k+1}} + \mu \Delta \frac{\partial^k \mathbf{u}_h(t)}{\partial t^k} - \nabla \frac{\partial^k p_h(t)}{\partial t^k} \right) \cdot \nabla q_h = 0, \quad \forall q_h \in Q_h. \end{aligned} \tag{3.46}$$

*Proof.* The proof of (3.43) and (3.44) are straightforward by taking the difference between (3.41) and (3.27). By assuming enough smoothness, (3.45) and (3.46) follow by differentiating (3.43) and (3.44) with respect to $t$. □

To prove an a posteriori error estimate using the Stokes reconstruction, the idea is the following: we cut the numerical errors $\mathbf{u} - \mathbf{u}_h$ and $p - p_h$ as

$$\mathbf{u} - \mathbf{u}_h = (\mathbf{u} - \mathbf{U}) + (\mathbf{U} - \mathbf{u}_h), \quad p - p_h = (p - P) + (P - p_h)$$

and we prove independently estimates for $\mathbf{u} - \mathbf{U}, p - P$ and $\mathbf{U} - \mathbf{u}_h, P - p_h$.

We now prove upper bounds for the *continuous* errors $\mathbf{u} - \mathbf{U}$ and $p - P$. There are contained in the two next propositions.

**Proposition 3.19** (Continuous error estimate for the veloctiy)**.**
*Let $(\mathbf{u}, p)$ be the solution of the unsteady Stokes equations (3.26), $(\mathbf{u}_h, p_h)$ be the solution of the semi-discretized problem (3.27), and $(\mathbf{U}, P)$ its Stokes reconstruction given by (3.41) The following error estimates hold for all $t \in (0, T]$, where $C_P$ stands for the Poincaré constant of $\Omega$:*

$$\begin{aligned} &\rho \|(\mathbf{u} - \mathbf{U})(t)\|^2_{L^2(\Omega)} + \mu \int_0^t \|\nabla(\mathbf{u} - \mathbf{U})(s)\|^2_{L^2(\Omega)} ds \\ &\qquad \leq \rho \|(\mathbf{u} - \mathbf{U})(0)\|^2_{L^2(\Omega)} + \frac{\rho^2 C_P^2}{\mu} \int_0^t \left\| \frac{\partial \mathbf{u}_h}{\partial t}(s) - \frac{\partial \mathbf{U}}{\partial t}(s) \right\|^2_{L^2(\Omega)} ds. \end{aligned} \tag{3.47}$$

$$\begin{aligned} &\rho \left\| \frac{\partial \mathbf{u}}{\partial t}(t) - \frac{\partial \mathbf{U}}{\partial t}(t) \right\|^2_{L^2(\Omega)} + \mu \int_0^t \left\| \nabla \left( \frac{\partial \mathbf{u}}{\partial t} - \frac{\partial \mathbf{U}}{\partial t} \right)(s) \right\|^2_{L^2(\Omega)} ds \\ &\qquad \leq \rho^2 \left\| \frac{\partial \mathbf{u}}{\partial t}(0) - \frac{\partial \mathbf{U}}{\partial t}(0) \right\|^2_{L^2(\Omega)} + \frac{C_P^2 \rho}{\mu} \int_0^t \left\| \frac{\partial^2 \mathbf{u}_h}{\partial t^2}(s) - \frac{\partial^2 \mathbf{U}}{\partial t^2}(s) \right\|^2_{L^2(\Omega)} ds. \end{aligned} \tag{3.48}$$

$$\rho\int_0^t \left\|\frac{\partial \mathbf{u}}{\partial t}(s)-\frac{\partial \mathbf{U}}{\partial t}(s)\right\|^2_{L^2(\Omega)} ds+\mu\|\nabla(\mathbf{u}-\mathbf{U})(t)\|^2_{L^2(\Omega)}$$
$$\leq \mu\|\nabla(\mathbf{u}-\mathbf{U})(0)\|^2_{L^2(\Omega)}+\rho\int_0^t \left\|\frac{\partial \mathbf{u}_h}{\partial t}(s)-\frac{\partial \mathbf{U}}{\partial t}(s)\right\|^2_{L^2(\Omega)} ds. \quad (3.49)$$

*Proof.* Observe that the momentum equation of (3.40) can also be written as

$$\rho\frac{\partial \mathbf{U}}{\partial t}-\mu\Delta\mathbf{U}+\nabla P=\mathbf{f}-\rho\left(\frac{\partial \mathbf{u}_h}{\partial t}-\frac{\partial \mathbf{U}}{\partial t}\right).$$

Then, taking the difference between (3.25) and (3.40) yields, integrated with respect to a test function in $(H^1_0(\Omega))^2$,

$$\rho\int_\Omega \frac{\partial(\mathbf{u}-\mathbf{U})}{\partial t}\cdot\mathbf{v}d\mathbf{x}+\mu\int_\Omega\nabla(\mathbf{u}-\mathbf{U}):\nabla\mathbf{v}d\mathbf{x}-\int_\Omega(p-P)\,\mathrm{div}\,\mathbf{v}d\mathbf{x}=\int_\Omega\rho\left(\frac{\partial \mathbf{u}_h}{\partial t}-\frac{\partial \mathbf{U}}{\partial t}\right)\cdot\mathbf{v}d\mathbf{x}. \quad (3.50)$$

Taking $\mathbf{v}=\mathbf{u}-\mathbf{U}$ and using Young's, Poincaré and Cauchy-Schwarz inequalities yield (3.47) after integration with respect to the time. To derive, (3.48), we differentiate (3.50) with respect to $t$ and proceed as before taking $\mathbf{v}=\dfrac{\partial \mathbf{u}}{\partial t}-\dfrac{\partial \mathbf{U}}{\partial t}$ instead. Finally, we obtain (3.49) choosing $\mathbf{v}=\dfrac{\partial \mathbf{u}}{\partial t}-\dfrac{\partial \mathbf{U}}{\partial t}$ in (3.50). □

**Remark 3.20.**
One step of the above proof of (3.47) is to choose $\mathbf{v}=\mathbf{u}-\mathbf{U}$ in (3.50) and thanks to Cauchy-Schwarz and Young's inequalities to derive that

$$\frac{\rho}{2}\frac{d}{dt}\|(\mathbf{u}-\mathbf{U})(s)\|^2_{L^2(\Omega)}+\mu\|\nabla(\mathbf{u}-\mathbf{U})(s)\|^2_{L^2(\Omega)}$$
$$\leq\frac{\rho\varepsilon}{2}\left\|\frac{\partial \mathbf{u}_h}{\partial t}(s)-\frac{\partial \mathbf{U}}{\partial t}(s)\right\|^2_{L^2(\Omega)}+\frac{\rho}{2\varepsilon}\|(\mathbf{u}-\mathbf{U})(s)\|^2_{L^2(\Omega)}. \quad (3.51)$$

In the proof of Proposition 3.19, we choose to control the $L^2$ norm $\|(\mathbf{u}-\mathbf{U})(s)\|^2_{L^2(\Omega)}$ in the right hand side thanks to the Poincaré inequality which yields

$$\frac{\rho}{2}\frac{d}{dt}\|(\mathbf{u}-\mathbf{U})(s)\|^2_{L^2(\Omega)}+\mu\|\nabla(\mathbf{u}-\mathbf{U})(s)\|^2_{L^2(\Omega)}$$
$$\leq\frac{\rho\varepsilon}{2}\left\|\frac{\partial \mathbf{u}_h}{\partial t}(s)-\frac{\partial \mathbf{U}}{\partial t}(s)\right\|^2_{L^2(\Omega)}+\frac{\rho C_P^2}{2\varepsilon}\|\nabla(\mathbf{u}-\mathbf{U})(s)\|^2_{L^2(\Omega)}.$$

Choosing $\varepsilon={}^{\rho C_P^2}/_{\mu}$, the last term of the right hand side is absorbed in the $H^1$ semi-norm and integration over the time yields the estimate. Note that in (3.51), we could also use a Gronwall's type argument (see the proof of Theorem A.3 with $N=1$ for instance) with respect to quantity $\rho\|(\mathbf{u}-\mathbf{U})(s)\|^2_{L^2(\Omega)}$ and it yields the final estimate

$$\rho\|(\mathbf{u}-\mathbf{U})(t)\|^2_{L^2(\Omega)}+\mu\int_0^t\|\nabla(\mathbf{u}-\mathbf{U})(s)\|^2_{L^2(\Omega)}ds$$
$$\leq\exp\left(\frac{t}{\varepsilon}\right)\left(\rho\|(\mathbf{u}-\mathbf{U})(0)\|^2_{L^2(\Omega)}+\rho\varepsilon\int_0^t\left\|\frac{\partial \mathbf{u}_h}{\partial t}(s)-\frac{\partial \mathbf{U}}{\partial t}(s)\right\|^2_{L^2(\Omega)}ds\right).$$

Choosing $\varepsilon=t$, we can eliminate the exponential growth of the bound and we obtain finally

$$\rho\|(\mathbf{u}-\mathbf{U})(t)\|^2_{L^2(\Omega)}+\mu\int_0^t\|\nabla(\mathbf{u}-\mathbf{U})(s)\|^2_{L^2(\Omega)}ds$$
$$\leq\exp(1)\left(\rho\|(\mathbf{u}-\mathbf{U})(0)\|^2_{L^2(\Omega)}+\rho t\int_0^t\left\|\frac{\partial \mathbf{u}_h}{\partial t}(s)-\frac{\partial \mathbf{U}}{\partial t}(s)\right\|^2_{L^2(\Omega)}ds\right).$$

Observe that, up to the multiplicative constant $\exp(1)$, we obtain the same estimate as (3.47) with $\rho t$ instead of ${}^{\rho^2 C_P^2}/_{\mu}$. Note that the ratio between ${}^{\rho^2 C_P^2}/_{\mu}$ and $\rho t$ is

$$\frac{\rho C_P}{\mu} \frac{C_P}{t}.$$

Since the Poincaré constant is bounded by the diameter of the domain $L$, this ratio is finally bounded by

$$\frac{\rho L}{\mu} \frac{L}{t}.$$

Finally, writing $V = {}^{L}/_{t}$ as the characteristic velocity and $L$ as the characteristic length of the domain, we obtain that the ration between ${}^{\rho^2 C_P^2}/_{\mu}$ and $\rho T$ is nothing else that the Reynolds number

$$\frac{\rho L V}{\mu}.$$

**Proposition 3.21** (Continuous error estimate for the pressure)**.**
*Let $(\mathbf{u}, p)$ be the solution of the unsteady Stokes equations (3.26), $(\mathbf{u}_h, p_h)$ be the solution of the semi-discretized problem (3.27), and $(\mathbf{U}, P)$ its Stokes reconstruction given by (3.41). Then there exists a constant $C > 0$ depending only on $\Omega$ such that for all $t \in (0, T]$*

$$\begin{aligned}
&\|(p-P)(t)\|^2_{L^2(\Omega)} \\
&\quad \leq C \max(\mu, \rho) \left( \rho \left\| \frac{\partial \mathbf{u}}{\partial t}(0) - \frac{\partial \mathbf{U}}{\partial t}(0) \right\|^2_{L^2(\Omega)} + \frac{\rho^2}{\mu} \int_0^t \left\| \frac{\partial^2 \mathbf{u}_h}{\partial t^2}(s) - \frac{\partial^2 \mathbf{U}}{\partial t^2}(s) \right\|^2_{L^2(\Omega)} ds \right. \\
&\qquad\qquad + \mu \|\nabla(\mathbf{u} - \mathbf{U})(0)\|^2_{L^2(\Omega)} + \rho \int_0^t \left\| \frac{\partial \mathbf{u}_h}{\partial t}(s) - \frac{\partial \mathbf{U}}{\partial t}(s) \right\|^2_{L^2(\Omega)} ds \\
&\qquad\qquad\qquad \left. + \rho \left\| \frac{\partial \mathbf{u}_h}{\partial t}(t) - \frac{\partial \mathbf{U}}{\partial t}(t) \right\|^2_{L^2(\Omega)} \right). \qquad (3.52)
\end{aligned}$$

*Proof.* We denote by $C$ any constant that depends on $\Omega$ but which value may change from line to line. Taking the difference between (3.25) and (3.40), we obtain by the inf-sup condition between $L^2_0(\Omega)$ and $(H^1_0(\Omega))^2$ and the Poincaré inequality that there exists $C > 0$ depending only on $\Omega$ such that

$$\begin{aligned}
\|(p-P)(t)\|_{L^2(\Omega)} &\leq C \sup_{\substack{\mathbf{v} \in (H^1_0(\Omega))^2 \\ \mathbf{v} \neq 0}} \frac{\displaystyle\int_\Omega (p-P)(t) \operatorname{div} \mathbf{v} d\mathbf{x}}{\|\nabla \mathbf{v}\|_{L^2(\Omega)}} \\
&= C \sup_{\substack{\mathbf{v} \in (H^1_0(\Omega))^2 \\ \mathbf{v} \neq 0}} \frac{\displaystyle\rho \int_\Omega \frac{\partial(\mathbf{u} - \mathbf{U})}{\partial t}(t) \mathbf{v} d\mathbf{x} + \mu \int_\Omega \nabla(\mathbf{u} - \mathbf{U})(t) : \nabla \mathbf{v} d\mathbf{x} + \rho \int_\Omega \left( \frac{\partial \mathbf{u}_h}{\partial t}(t) - \frac{\partial \mathbf{U}}{\partial t}(t) \right) \mathbf{v} d\mathbf{x}}{\|\nabla \mathbf{v}\|_{L^2(\Omega)}} \\
&\leq C \left( \rho \left\| \frac{\partial(\mathbf{u} - \mathbf{U})}{\partial t}(t) \right\|_{L^2(\Omega)} + \mu \|\nabla(\mathbf{u} - \mathbf{U})(t)\|_{L^2(\Omega)} + \rho \left\| \frac{\partial \mathbf{u}_h}{\partial t}(t) - \frac{\partial \mathbf{U}}{\partial t}(t) \right\|_{L^2(\Omega)} \right).
\end{aligned}$$

Squaring the last inequality and combining it with the Proposition 3.19 gives the desired estimate. ☐

**Remark 3.22.** (i) To obtain the estimate (3.47) is straightforward, since $\mathbf{u} - \mathbf{U}$ is a free divergence function, which eliminates the pressure when choosing the test function $\mathbf{v} = \mathbf{u} - \mathbf{U}$ in (3.50). This is due to the fact that we build $\mathbf{U}$ itself as a smooth version of the approximated velocity $\mathbf{u}_h$ that satisfies the zero divergence constraint.

(ii) Anticipating the sequel, we will show that all the terms containing

$$\left\| \frac{\partial^k \mathbf{u}_h}{\partial t^k} - \frac{\partial^k \mathbf{U}}{\partial t^k} \right\|_{L^2(\Omega)}, k = 0, 1, 2,$$

are of higher order in space compared to the $H^1-$ semi-norm of the error $\mathbf{u} - \mathbf{u}_h$.

We now prove an upper bound for the *discrete* errors $\mathbf{U} - \mathbf{u}_h$ and $P - p_h$. There are contained in the next proposition

**Proposition 3.23** (Discrete error estimate)**.**
*Let $(\mathbf{u}_h, p_h)$ be the semi-discretized solution of (3.27) and $(\mathbf{U}, P)$ its Stokes reconstruction given by (3.41). Moreover, for any $t \in [0, T]$, let $(\mathbf{w}(t), r(t)) \in (H_0^1(\Omega))^2 \times L_0^2(\Omega)$ the weak solution of the dual problem*

$$\begin{cases} -\mu \Delta \mathbf{w}(t) + \nabla r(t) = 0, & \textit{in } \Omega, \\ \operatorname{div} \mathbf{w}(t) = p_h(t) - P(t), & \textit{in } \Omega, \\ \mathbf{w}(t) = 0, & \textit{on } \partial\Omega. \end{cases} \tag{3.53}$$

*Then, there exists a constant $C$ that depends only on the reference triangle and $\Omega$ such that for every $t \in [0, T]$*

$$\mu \|\nabla(\mathbf{U} - \mathbf{u}_h)(t)\|_{L^2(\Omega)}^2 + \frac{1}{\mu} \|(P - p_h)(t)\|_{L^2(\Omega)}^2 \leq C \sum_{K \in \mathcal{T}_h} (\eta_{K,\mathbf{u}}^A)^2(t) + (\eta_{K,p}^A)^2(t) + (\eta_K^{\text{div}})^2(t), \tag{3.54}$$

*where we define for every $t \in [0, T]$*

$$(\eta_{K,\mathbf{u}}^A)^2(t) = \left( \left\| \mathbf{f}(t) - \rho \frac{\partial \mathbf{u}_h}{\partial t}(t) + \mu \Delta \mathbf{u}_h(t) - \nabla p_h(t) \right\|_{L^2(K)} + \frac{1}{2\sqrt{\lambda_{2,K}}} \|[\mu \nabla \mathbf{u}_h(t) \cdot \mathbf{n}]\|_{L^2(\partial K)} \right) \omega_K \left( (\mathbf{U} - \mathbf{u}_h)(t) \right),$$

$$(\eta_{K,p}^A)^2(t) = \frac{1}{\mu} \left( \left\| \mathbf{f}(t) - \rho \frac{\partial \mathbf{u}_h}{\partial t}(t) + \mu \Delta \mathbf{u}_h(t) - \nabla p_h(t) \right\|_{L^2(K)} + \frac{1}{2\sqrt{\lambda_{2,K}}} \|[\mu \nabla \mathbf{u}_h(t) \cdot \mathbf{n}]\|_{L^2(\partial K)} \right) \omega_K(\mathbf{w}(t)),$$

$$(\eta_K^{\text{div}})^2(t) = \mu \| \operatorname{div} \mathbf{u}_h(t)\|_{L^2(K)}^2.$$

*Proof.* The proof follows the steps of Theorem 3.6 for the steady Navier-Stokes equations. We denote by $C$ any positive constant that may depend on the reference triangle or $\Omega$, by $\hat{C}$ any positive constant that depends only on the reference triangle, and by $\tilde{C}$ any constant that depends on $\Omega$ only. To lighten the notations, we omit to write the explicit dependence on $t$ of the functions. Observe that all the computations presented below holds for any $t \in [0, T]$.

*Step 1. Estimate for the velocity.*

Using the weak formulation of the Stokes reconstruction (3.41) and the numerical method (3.27), we obtain

$$\mu\|\nabla(\mathbf{U}-\mathbf{u}_h)\|^2_{L^2(\Omega)} = \mu\int_\Omega \nabla(\mathbf{U}-\mathbf{u}_h) : \nabla(\mathbf{U}-\mathbf{u}_h)d\mathbf{x}$$

$$= \mu\int_\Omega \nabla(\mathbf{U}-\mathbf{u}_h) : \nabla(\mathbf{U}-\mathbf{u}_h)d\mathbf{x}$$

$$+ \int_\Omega (P-p_h)\operatorname{div}(\mathbf{U}-\mathbf{u}_h)d\mathbf{x} - \int_\Omega (P-p_h)\operatorname{div}(\mathbf{U}-\mathbf{u}_h)d\mathbf{x}$$

$$= \int_\Omega \left(\mathbf{f}-\rho\frac{\partial \mathbf{u}_h}{\partial t}\right)\cdot(\mathbf{U}-\mathbf{u}_h)d\mathbf{x} - \mu\int_\Omega \nabla\mathbf{u}_h : \nabla(\mathbf{U}-\mathbf{u}_h)d\mathbf{x}$$

$$+ \int_\Omega p_h \operatorname{div}(\mathbf{U}-\mathbf{u}_h)d\mathbf{x} + \int (P-p_h)\operatorname{div}\mathbf{u}_h d\mathbf{x}$$

$$= \int_\Omega \left(\mathbf{f}-\rho\frac{\partial \mathbf{u}_h}{\partial t}\right)\cdot(\mathbf{U}-\mathbf{u}_h-\mathbf{v}_h)d\mathbf{x} - \mu\int_\Omega \nabla u_h : \nabla(\mathbf{U}-\mathbf{u}_h-\mathbf{v}_h)$$

$$+ \int_\Omega p_h \operatorname{div}(\mathbf{U}-\mathbf{u}_h-\mathbf{v}_h)d\mathbf{x} + \int (P-p_h)\operatorname{div}\mathbf{u}_h d\mathbf{x}$$

$$= \sum_{K\in\mathcal{T}_h}\int_K \left(\mathbf{f}-\rho\frac{\partial \mathbf{u}_h}{\partial t}+\mu\Delta\mathbf{u}_h-\nabla p_h\right)\cdot(\mathbf{U}-\mathbf{u}_h-\mathbf{v}_h)d\mathbf{x} + \frac{1}{2}\int_{\partial K}[\mu\nabla\mathbf{u}_h\cdot\mathbf{n}]\cdot(\mathbf{U}-\mathbf{u}_h-\mathbf{v}_h)d\mathbf{x}$$

$$+ \int_\Omega (P-p_h)\operatorname{div}\mathbf{u}_h d\mathbf{x},$$

where the last equality is derived by integrating by parts on every triangle. Choosing $\mathbf{v}_h = R_h(\mathbf{U}-\mathbf{u}_h)$ and $q_h = 0$, the Cauchy-Schwarz and Young's inequalities and the interpolation error estimates for the Clément's interpolant yield

$$\mu\|\nabla(\mathbf{U}-\mathbf{u}_h)\|^2_{L^2(\Omega)}$$

$$\le \hat{C}\sum_{K\in\mathcal{T}_h}\left(\left\|\mathbf{f}-\rho\frac{\partial \mathbf{u}_h}{\partial t}+\mu\Delta\mathbf{u}_h-\nabla p_h\right\|_{L^2(K)} + \frac{1}{2\sqrt{\lambda_{2,K}}}\|\mu\nabla\mathbf{u}_h\cdot n\|_{L^2(\partial K)}\right)\omega_K(\mathbf{U}-\mathbf{u}_h)$$

$$+ \frac{1}{2\varepsilon}\|P-p_h\|^2_{L^2(\Omega)} + \frac{\varepsilon}{2}\|\operatorname{div}\mathbf{u}_h\|^2_{L^2(\Omega)}. \quad (3.55)$$

*Step 2. Estimate for the pressure.*

To simplify the notation, let us note as before

$$\nu_K = \left\|\mathbf{f}-\rho\frac{\partial \mathbf{u}_h}{\partial t}+\mu\Delta\mathbf{u}_h-\nabla p_h\right\|_{L^2(K)} + \frac{1}{2\sqrt{\lambda_{2,K}}}\|\mu\nabla\mathbf{u}_h\cdot n\|_{L^2(\partial K)}.$$

Let $\mathbf{w}$ be the solution of the dual problem (3.79). We have using again (3.40) and the numerical method (3.27)

$$\|P-p_h\|^2_{L^2(\Omega)} = -\int_\Omega (P-p_h)\operatorname{div}\mathbf{w}d\mathbf{x} = -\int_\Omega P\operatorname{div}\mathbf{w}d\mathbf{x} + \int_\Omega p_h\operatorname{div}\mathbf{w}d\mathbf{x}$$

$$= \int_\Omega \left(\mathbf{f}-\rho\frac{\partial \mathbf{u}_h}{\partial t}\right)\cdot\mathbf{w}d\mathbf{x} + \mu\int_\Omega \nabla\mathbf{U} : \nabla\mathbf{w}d\mathbf{x} + \int_\Omega p_h\operatorname{div}\mathbf{w}d\mathbf{x}$$

$$= \int_\Omega \left(\mathbf{f}-\rho\frac{\partial \mathbf{u}_h}{\partial t}\right)\cdot\mathbf{w}d\mathbf{x} + \mu\int_\Omega \nabla\mathbf{u}_h : \nabla\mathbf{w}d\mathbf{x} + \int_\Omega p_h\operatorname{div}\mathbf{w}d\mathbf{x}$$

$$+ \mu\int_\Omega \nabla(\mathbf{U}-\mathbf{u}_h) : \nabla\mathbf{w}d\mathbf{x}$$

$$= \int_\Omega \left(\mathbf{f}-\rho\frac{\partial \mathbf{u}_h}{\partial t}\right)\cdot(\mathbf{w}-\mathbf{v}_h)d\mathbf{x} + \mu\int_\Omega \nabla\mathbf{u}_h : \nabla(\mathbf{w}-\mathbf{v}_h)d\mathbf{x} + \int_\Omega p_h\operatorname{div}(\mathbf{w}-\mathbf{v}_h)d\mathbf{x}$$

$$+ \mu\int_\Omega \nabla(\mathbf{U}-\mathbf{u}_h) : \nabla\mathbf{w}d\mathbf{x}.$$

Choosing $\mathbf{v}_h = R_h(\mathbf{w})$, integration by parts, Cauchy-Schwarz, Young's and interpolation error inequalites yield finally

$$\|P - p_h\|^2_{L^2(\Omega)} \leq \hat{C} \sum_{K\in\mathcal{T}_h} \nu_K \omega_K(\mathbf{w}) + \frac{\mu^2\varepsilon}{2}\|\nabla(\mathbf{U} - \mathbf{u}_h)\|^2_{L^2(\Omega)} + \frac{1}{2\varepsilon}\|\nabla\mathbf{w}\|^2_{L^2(\Omega)}.$$

The following a priori estimate is valid for the dual problem (3.79)

$$\|\nabla\mathbf{w}\|_{L^2(\Omega)} + \frac{1}{\mu}\|r\|_{L^2(\Omega)} \leq \tilde{C}\|P - p_h\|_{L^2(\Omega)}.$$

Therefore choosing $\varepsilon = \tilde{C}^2$, where $\tilde{C}$ is the constant given in the estimate above, we finally obtain

$$\|P - p_h\|^2_{L^2(\Omega)} \leq \hat{C} \sum_{K\in\mathcal{T}_h} \nu_K \omega_K(\mathbf{w}) + \mu^2\tilde{C}\|\nabla(\mathbf{U} - \mathbf{u}_h)\|^2_{L^2(\Omega)}. \tag{3.56}$$

*Step 3. Putting all together.*
Plugging (3.56) into (3.55), and choosing $\varepsilon = \mu\tilde{C}$, we obtain for the velocity error

$$\mu\|\nabla(\mathbf{U} - \mathbf{u}_h)\|^2_{L^2(\Omega)} \leq \hat{C} \sum_{K\in\mathcal{T}_h} \nu_K \omega_K(\mathbf{U} - \mathbf{u}_h) + \frac{1}{\mu}\nu_K \omega_K(\mathbf{w}) + \mu\tilde{C}\|\operatorname{div}\mathbf{u}_h\|^2_{L^2(\Omega)},$$

Plugging it back into (3.56) and dividing by $\mu$, we obtain for the pressure error

$$\frac{1}{\mu}\|P - p_h\|^2_{L^2(\Omega)} \leq \hat{C} \sum_{K\in\mathcal{T}_h} \nu_K \omega_K(\mathbf{U} - \mathbf{u}_h) + \frac{1}{\mu}\nu_K \omega_K(\mathbf{w}) + \mu\tilde{C}\|\operatorname{div}\mathbf{u}_h\|^2_{L^2(\Omega)},$$

The result is then obtained by summing together the last two estimates. □

**Remark 3.24.**
We could have obtained a finer estimate for the pressure error $P - p_h$ by use of the Galerkin orthogonality (Lemma 3.18). We keep the same convention for the constant as in the proof of Proposition 3.23. Indeed, observe that using the first equation of the dual problem (3.79), one have that

$$\mu\int_\Omega \nabla\mathbf{w} : \nabla\mathbf{v} d\mathbf{x} - \int_\Omega r \operatorname{div}\mathbf{v} d\mathbf{x} = 0, \quad \forall\mathbf{v} \in (H^1_0(\Omega))^2.$$

Therefore one can write that

$$\begin{aligned}\|P - p_h\|^2_{L^2(\Omega)} &= -\int_\Omega (P - p_h) \operatorname{div}\mathbf{w} d\mathbf{x} \\ &= -\int_\Omega (P - p_h) \operatorname{div}\mathbf{w} d\mathbf{x} + \mu\int_\Omega \nabla\mathbf{w} : \nabla(\mathbf{U} - \mathbf{u}_h) d\mathbf{x} - \int_\Omega r \operatorname{div}(\mathbf{U} - \mathbf{u}_h) d\mathbf{x}.\end{aligned}$$

Now using the Galerkin orthogonality of Lemma 3.18 (instead of the numerical scheme as in the step 2 of the proof above), one can remove any $\mathbf{v}_h$ from the two first terms and we have that

$$\begin{aligned}&\|P - p_h\|^2_{L^2(\Omega)} \\ &= -\int_\Omega (P - p_h) \operatorname{div}(\mathbf{w} - \mathbf{v}_h) d\mathbf{x} + \mu\int_\Omega \nabla(\mathbf{w} - \mathbf{v}_h) : \nabla(\mathbf{U} - \mathbf{u}_h) d\mathbf{x} - \int_\Omega r \operatorname{div}(\mathbf{U} - \mathbf{u}_h) d\mathbf{x}.\end{aligned}$$

From there, we proceed as usual : we choose $\mathbf{v}_h = R_h(\mathbf{w})$, and integration by parts on the triangles, Cauchy-Schwarz and Young's inequalities and interpolation estimates, yields

$$\begin{aligned}
&\|P - p_h\|^2_{L^2(\Omega)} \\
&\leq \hat{C} \sum_{K\in\mathcal{T}_h} \left( \|-\mu(\Delta\mathbf{U} - \Delta\mathbf{u}_h) + \nabla(P - p_h)\|_{L^2(K)} + \frac{1}{2\sqrt{\lambda_{2,K}}} \|[\mu\nabla(\mathbf{U} - \mathbf{u}_h)\cdot\mathbf{n}]\|_{L^2(\partial K)} \right) \omega_K(\mathbf{w}) \\
&\qquad + \frac{1}{2\varepsilon}\|r\|^2_{L^2(\Omega)} + \frac{\varepsilon}{2}\|\operatorname{div}\mathbf{u}_h\|^2_{L^2(\Omega)}.
\end{aligned}$$

We recall that in our particular context we have that $\mathbf{U} \in (H^2(\Omega))^2$ and satisfies in the strong form

$$-\mu\Delta\mathbf{U} + \nabla P = \mathbf{f} - \rho\frac{\partial \mathbf{u}_h}{\partial t}.$$

Moreover, the jump $[\nabla\mathbf{U}\cdot\mathbf{n}] = 0$ since $\mathbf{U}$ is a $H^2$ function. Therefore, using the a priori estimate for the dual problem

$$\|\nabla\mathbf{w}\|_{L^2(\Omega)} + \frac{1}{\mu}\|r\|_{L^2(\Omega)} \leq \tilde{C}\|P - p_h\|_{L^2(\Omega)},$$

and by choosing $\varepsilon = \mu^2\tilde{C}^2$ yields finally that

$$\begin{aligned}
&\|P - p_h\|^2_{L^2(\Omega)} \\
&\leq \hat{C} \sum_{K\in\mathcal{T}_h} \left( \left\|\mathbf{f} - \rho\frac{\partial\mathbf{u}_h}{\partial t} + \mu\Delta\mathbf{u}_h - \nabla p_h\right\|_{L^2(K)} + \frac{1}{2\sqrt{\lambda_{2,K}}} \|[\mu\nabla\mathbf{u}_h\cdot\mathbf{n}]\|_{L^2(\partial K)} \right) \omega_K(\mathbf{w}) \\
&\qquad + \tilde{C}\mu^2\|\operatorname{div}\mathbf{u}_h\|^2_{L^2(\Omega)}.
\end{aligned}$$

In conclusion, we obtain that, using the same notations as in the Proposition 3.23,

$$\frac{1}{\mu}\|P - p_h\|^2_{L^2(\Omega)} \leq C \sum_{K\in\mathcal{T}_h} (\eta^A_{K,p})^2 + (\eta^{\text{div}}_K)^2.$$

Compared to the estimate that yields (3.54) for the pressure error, the upper bound above is derived *independently* of the velocity estimate, what explained why the velocity error indicator $(\eta^A_{K,\mathbf{u}})^2$ is not present. Nevertheless, this approach requires to use the a priori smoothness of $\mathbf{U}$, mainly that $\mathbf{U} \in (H^2(\Omega))^2$ and satisfies the equations in the strong form. This is in general not appropriate for an a posteriori error analysis since we do not necessarily know a priori the regularity of the exact solution (here $\mathbf{U}$). Moreover, we only need in fact that the exact solution satisfies the equations in a weak form to be able to prove an a posteriori error estimate (see for instance the step 1 of Proposition 3.23).

Combining the estimates of Propositions 3.19, 3.21 and 3.23, we easily obtain estimates for $\mathbf{u} - \mathbf{u}_h$ and $p - p_h$ by use of the triangle inequality. It only remains to prove an upper bounds for the terms

$$\left\|\frac{\partial^k\mathbf{u}_h}{\partial t^k} - \frac{\partial^k\mathbf{U}}{\partial t^k}\right\|_{L^2(\Omega)}, \quad k = 0, 1, 2.$$

In the next proposition, we will show that they are of higher order in space, and therefore will be in practice negligible in the final a posteriori error estimates.

**Proposition 3.25** (Dual estimates for the velocity)**.**
*Let* $(\mathbf{u}_h, p_h)$ *be the solution of the semi-discretized problem (3.27) and* $(\mathbf{U}, P)$ *its Stokes*

*reconstruction defined in (3.41). Let $k = 0, 1, 2$. There exists a constant $C > 0$ independent of the mesh size but depending on the mesh aspect ratio and $\Omega$ such that for all $t \in [0, T]$*

$$\left\| \frac{\partial^k \mathbf{u}_h}{\partial t^k}(t) - \frac{\partial^k \mathbf{U}}{\partial t^k}(t) \right\|^2_{L^2(\Omega)} \leq C \sum_{K \in \mathcal{T}_h} (\varepsilon^I_{K,\mathbf{u},k})^2(t), \tag{3.57}$$

*where*

$$\begin{aligned}
&(\varepsilon^I_{K,\mathbf{u},k})^2(t) \\
&= \frac{1}{\mu^2} h_K^4 \left\| \frac{\partial^k \mathbf{f}}{\partial t^k}(t) - \rho \frac{\partial^{k+1} \mathbf{u}_h}{\partial t^{k+1}}(t) + \mu \Delta \frac{\partial^k \mathbf{u}_h}{\partial t^k}(t) - \nabla \frac{\partial^k p_h}{\partial t^k}(t) \right\|^2_{L^2(K)} + \frac{1}{\mu} h_K^3 \left\| \nabla \frac{\partial^k \mathbf{u}_h}{\partial t^k}(t) \cdot \mathbf{n} \right\|^2_{L^2(\partial K)} \\
&\quad + h_K^2 \left\| \operatorname{div} \frac{\partial^k \mathbf{u}_h}{\partial t^k}(t) \right\|^2_{L^2(K)}
\end{aligned}$$

*Proof.* Let $k = 0, 1, 2$. To lighten the notations and when the context is clear, we do not write the explicit dependence in time of the functions since all our computations hold for any $t \in [0, T]$. For this particular proof, we denote by $C$ any constant that is independent of the mesh size but may depend on the aspect ratio and $\Omega$.

We shall use the following dual problem : for any $t \in [0, T]$, find $(\mathbf{w}(t), r(t)) \in (H^1_0(\Omega))^2 \times L^2_0(\Omega)$ the weak solution of

$$\begin{cases} -\mu \Delta \mathbf{w}(t) + \nabla r(t) = \dfrac{\partial^k \mathbf{u}_h}{\partial t^k}(t) - \dfrac{\partial^k \mathbf{U}}{\partial t^k}(t), & \text{in } \Omega, \\ \operatorname{div} \mathbf{w}(t) = 0, & \text{in } \Omega, \\ \mathbf{w}(t) = 0, & \text{on } \partial\Omega. \end{cases} \tag{3.58}$$

Since we are in two dimensions, $\Omega$ is convex and we assume that for any $t \in [0, T]$

$$\frac{\partial^k \mathbf{u}_h}{\partial t^k}(t) - \frac{\partial^k \mathbf{U}}{\partial t^k}(t) \in (L^2(\Omega))^2, \tag{3.59}$$

one can prove that $(\mathbf{w}(t), r(t)) \in (H^2(\Omega))^2 \times H^1(\Omega)$ [62] and that the following a priori estimate holds

$$\mu \|\mathbf{w}(t)\|_{H^2(\Omega)} + \|\nabla r(t)\|_{L^2(\Omega)} \leq \tilde{C} \left\| \frac{\partial^k \mathbf{u}_h}{\partial t^k}(t) - \frac{\partial^k \mathbf{U}}{\partial t^k}(t) \right\|_{L^2(\Omega)}, \tag{3.60}$$

where $\tilde{C}$ depends only on $\Omega$.

We have, using the orthogonality between $(\mathbf{U}, P)$ and $(\mathbf{u}_h, p_h)$ (see Lemma 3.18)

$$\begin{aligned}
\int_\Omega \left( \frac{\partial^k \mathbf{u}_h}{\partial t^k} - \frac{\partial^k \mathbf{U}}{\partial t^k} \right)^2 &= \mu \int_\Omega \nabla \mathbf{w} : \nabla \left( \frac{\partial^k \mathbf{u}_h}{\partial t^k} - \frac{\partial^k \mathbf{U}}{\partial t^k} \right) d\mathbf{x} - \int_\Omega r \operatorname{div} \left( \frac{\partial^k \mathbf{u}_h}{\partial t^k} - \frac{\partial^k \mathbf{U}}{\partial t^k} \right) d\mathbf{x} \\
&\quad - \int_\Omega \operatorname{div} \mathbf{w} \left( \frac{\partial^k p_h}{\partial t^k} - \frac{\partial^k P}{\partial t^k} \right) d\mathbf{x} \\
&= \mu \int_\Omega \nabla (\mathbf{w} - \mathbf{v}_h) : \nabla \left( \frac{\partial^k \mathbf{u}_h}{\partial t^k} - \frac{\partial^k \mathbf{U}}{\partial t^k} \right) d\mathbf{x} - \int_\Omega (r - q_h) \operatorname{div} \left( \frac{\partial^k \mathbf{u}_h}{\partial t^k} - \frac{\partial^k \mathbf{U}}{\partial t^k} \right) d\mathbf{x} \\
&\quad - \int_\Omega \operatorname{div} (\mathbf{w} - \mathbf{v}_h) \left( \frac{\partial^k p_h}{\partial t^k} - \frac{\partial^k P}{\partial t^k} \right) d\mathbf{x} \\
&\quad + \sum_{K \in \mathcal{T}_h} \alpha_K \left( \frac{\partial^k \mathbf{f}}{\partial t^k} - \rho \frac{\partial^{k+1} \mathbf{u}_h}{\partial t^{k+1}} + \mu \Delta \frac{\partial^k \mathbf{u}_h}{\partial t^k} - \nabla \frac{\partial^k p_h}{\partial t^k} \right) \cdot \nabla q_h d\mathbf{x}.
\end{aligned}$$

Note that, assuming enough regularity, one can differentiate with respect to the time the weak formulation (3.41) and we have for $k = 1, 2$.

$$\mu \int_\Omega \nabla \frac{\partial^k \mathbf{U}}{\partial t^k}(t) : \nabla \mathbf{v} d\mathbf{x} - \int_\Omega \frac{\partial^k P}{\partial t^k}(t) \operatorname{div} \mathbf{v} d\mathbf{x}$$
$$= \int_\Omega \left( \frac{\partial^k \mathbf{f}}{\partial t^k}(t) - \rho \frac{\partial^{k+1} \mathbf{u}_h}{\partial t^{k+1}}(t) \right) \cdot \mathbf{v} d\mathbf{x}, \quad \forall \mathbf{v} \in (H_0^1(\Omega))^2,$$
$$- \int_\Omega q \operatorname{div} \frac{\partial^k \mathbf{U}}{\partial t^k}(t) = 0, \quad \forall q \in L_0^2(\Omega). \quad (3.61)$$

Note that for $k = 0$, the equations are trivially satisfy since there are nothing else than the weak formulation (3.41). Therefore for $k = 0, 1, 2$, using (3.61), integrating by parts and applying the Cauchy-Schwarz inequality we have

$$\int_\Omega \left( \frac{\partial^k \mathbf{u}_h}{\partial t^k} - \frac{\partial^k \mathbf{U}}{\partial t^k} \right)^2 d\mathbf{x}$$
$$\leq \sum_{K \in \mathcal{T}_h} \left\| \frac{\partial^k \mathbf{f}}{\partial t^k} - \rho \frac{\partial^{k+1} \mathbf{u}_h}{\partial t^{k+1}} + \mu \Delta \frac{\partial^k \mathbf{u}_h}{\partial t^k} - \nabla \frac{\partial^k p_h}{\partial t^k} \right\|_{L^2(K)} \|\mathbf{w} - \mathbf{v}_h\|_{L^2(K)}$$
$$+ \frac{1}{2} \left\| \left[ \mu \nabla \left( \frac{\partial^k \mathbf{u}_h}{\partial t^k} \right) \cdot n \right] \right\|_{L^2(\partial K)} \|\mathbf{w} - \mathbf{v}_h\|_{L^2(\partial K)}$$
$$+ \|r - q_h\|_{L^2(K)} \left\| \operatorname{div} \frac{\partial^k \mathbf{u}_h}{\partial t^k} \right\|_{L^2(K)} + \alpha_K \left\| \frac{\partial^k \mathbf{f}}{\partial t^k} - \rho \frac{\partial^{k+1} \mathbf{u}_h}{\partial t^{k+1}} + \mu \Delta \frac{\partial^k \mathbf{u}_h}{\partial t^k} - \nabla \frac{\partial^k p_h}{\partial t^k} \right\|_{L^2(K)} \|\nabla q_h\|_{L^2(K)}$$

Choosing $\mathbf{v}_h = r_h(\mathbf{w}), q_h = R_h(r)$, classical interpolation results yield there exists $\bar{C} > 0$ independent of the mesh size but dependent on the mesh aspect ratio such that

$$\int_\Omega \left( \frac{\partial^k \mathbf{u}_h}{\partial t^k} - \frac{\partial^k \mathbf{U}}{\partial t^k} \right)^2 \leq \bar{C} \sum_{K \in \mathcal{T}_h} h_K^2 \left\| \frac{\partial^k \mathbf{f}}{\partial t^k} - \rho \frac{\partial^{k+1} \mathbf{u}_h}{\partial t^{k+1}} + \mu \Delta \frac{\partial^k \mathbf{u}_h}{\partial t^k} - \nabla \frac{\partial^k p_h}{\partial t^k} \right\|_{L^2(K)} \|w\|_{H^2(K)}$$
$$+ \frac{1}{2} h_K^{3/2} \left\| \left[ \mu \nabla \left( \frac{\partial^k \mathbf{u}_h}{\partial t^k} \right) \cdot n \right] \right\|_{L^2(\partial K)} \|w\|_{H^2(K)}$$
$$+ h_K \left\| \operatorname{div} \frac{\partial^k \mathbf{u}_h}{\partial t^k} \right\|_{L^2(K)} \|\nabla r\|_{L^2(\Delta K)} + \alpha_K \left\| \frac{\partial^k \mathbf{f}}{\partial t^k} - \rho \frac{\partial^{k+1} \mathbf{u}_h}{\partial t^{k+1}} + \mu \Delta \frac{\partial^k \mathbf{u}_h}{\partial t^k} - \nabla \frac{\partial^k p_h}{\partial t^k} \right\|_{L^2(K)} \|\nabla r\|_{L^2(\Delta K)}.$$

By using the discrete Cauchy-Schwarz inequality, a priori error estimate (3.60) and Young's inequality, we obtain

$$\left\| \frac{\partial^k \mathbf{u}_h}{\partial t^k}(t) - \frac{\partial^k \mathbf{U}}{\partial t^k}(t) \right\|_{L^2(\Omega)}^2$$
$$\leq \frac{C}{\mu^2} \sum_{K \in \mathcal{T}_h} h_K^4 \left\| \frac{\partial^k \mathbf{f}}{\partial t^k}(t) - \rho \frac{\partial^{k+1} \mathbf{u}_h}{\partial t^{k+1}}(t) + \mu \Delta \frac{\partial^k \mathbf{u}_h}{\partial t^k}(t) - \nabla \frac{\partial^k p_h}{\partial t^k}(t) \right\|_{L^2(K)}^2 + h_K^3 \left\| \mu \nabla \frac{\partial^k \mathbf{u}_h}{\partial t^k}(t) \cdot \mathbf{n} \right\|_{L^2(\partial K)}^2$$
$$+ \mu^2 h_K^2 \left\| \operatorname{div} \frac{\partial^k \mathbf{u}_h}{\partial t^k}(t) \right\|_{L^2(K)}^2 + \mu^2 \alpha_K^2 \left\| \frac{\partial^k \mathbf{f}}{\partial t^k}(t) - \rho \frac{\partial^{k+1} \mathbf{u}_h}{\partial t^{k+1}}(t) + \mu \Delta \frac{\partial^k \mathbf{u}_h}{\partial t^k}(t) - \nabla \frac{\partial^k p_h}{\partial t^k}(t) \right\|_{L^2(K)}^2.$$

Recalling that

$$\alpha_K = \frac{\alpha \lambda_{2,K}^2}{\mu}, \quad \lambda_{2,K} \leq \hat{C} h_K, \forall K \in \mathcal{T}_h,$$

where $\hat{C}$ depends on the reference triangle only, we can absorb the last term of the sum over $K$ into the first one ant it yields finally

$$\left\| \frac{\partial^k \mathbf{u}_h}{\partial t^k}(t) - \frac{\partial^k \mathbf{U}}{\partial t^k}(t) \right\|^2_{L^2(\Omega)}$$
$$\leq \frac{C}{\mu^2} \sum_{K \in \mathcal{T}_h} h_K^4 \left\| \frac{\partial^k \mathbf{f}}{\partial t^k}(t) - \rho \frac{\partial^{k+1} \mathbf{u}_h}{\partial t^{k+1}}(t) + \mu \Delta \frac{\partial^k \mathbf{u}_h}{\partial t^k}(t) - \nabla \frac{\partial^k p_h}{\partial t^k}(t) \right\|^2_{L^2(K)} + h_K^3 \left\| \mu \nabla \frac{\partial^k \mathbf{u}_h}{\partial t^k}(t) \cdot \mathbf{n} \right\|^2_{L^2(\partial K)}$$
$$+ \mu^2 h_K^2 \left\| \operatorname{div} \frac{\partial^k \mathbf{u}_h}{\partial t^k}(t) \right\|^2_{L^2(K)},$$

which is the desired estimate. □

**Remark 3.26.** 1. The fact that $C$ in (3.57) depends on the mesh aspect ratio is not an issue since the error indicator $(\varepsilon^I_{K,\mathbf{u},k})^2 \simeq h^2$ is of higher order in space, compared to the $H^1$ semi-norm

$$\|\nabla(\mathbf{u} - \mathbf{u}_h)\|_{L^2(\Omega)} \simeq h.$$

2. Note the particular form of $(\varepsilon^I_{K,\mathbf{u}})^2$ which is, roughly speaking, the $k-th$ time derivative of the residual of the equations.

3. Observe that in the proof of Proposition 3.25, we strongly use the fact that the dual problem (3.58) has an $(H^2(\Omega))^2 \times H^1(\Omega)$ solution. As already mentioned, this is true in dimension 2 and 3 for smooth domains [21], but is in general only true for convex polytopes in dimension 2 (that is to say convex polygons). For $\mathbb{R}^3$ and convex polyhedrons, the results still holds but some restrictions on the inner angles must be imposed [66]. For our concerns, it is true if the polyhedron is a cube or any rectangular parallelepiped. Therefore, one can extend the Proposition 3.25 to the three dimensional case at least in the above cases. Note that the other results (Propositions 3.19 and 3.21) are independent of the dimension, and up to switch to the 3D anisotropic settings (see Section 1.6 of Chapter 1), Proposition 3.23 can be adapted to the third dimension without any difficulties. So, our a posteriori error analysis as the two theorems that will come below are completely generalizable to $\mathbb{R}^3$.

We are now in position to prove an a posteriori error estimate for the discrete error $\mathbf{u} - \mathbf{u}_h$. By sake of completeness, we also present an a posteriori error estimate for the pressure error $p - p_h$. There are contained in the next two Theorems

**Theorem 3.27** (An a posteriori error estimate for the velocity using the Stokes reconstruction)**.**
*Let $(\mathbf{u}, p)$ be the solution of the unsteady Stokes equation (3.26), $(\mathbf{u}_h, p_h)$ be the approximated solutions of the semi-discretized problem (3.27), and $(\mathbf{U}, P)$ its the Stokes reconstruction defined by (3.41). Then there exists $C_1$ only depending on the reference triangle and $\Omega$ and $C_2 > 0$ independent of the mesh size, but dependent on the mesh aspect ratio and $\Omega$ such that*

$$\rho \|(\mathbf{u} - \mathbf{u}_h)(T)\|^2_{L^2(\Omega)} + \mu \int_0^T \|\nabla(\mathbf{u} - \mathbf{u}_h)(s)\|^2_{L^2(\Omega)} dt$$
$$\leq C_1 \left( \rho \|(\mathbf{u} - \mathbf{u}_h)(0)\|^2_{L^2(\Omega)} + \int_0^T \sum_{K \in \mathcal{T}_h} (\eta^A_{K,\mathbf{u}})^2(s) + (\eta^A_{K,p})^2(s) + (\eta^{\operatorname{div}}_K)^2(s) ds \right)$$
$$+ C_2 \left( \rho \sum_{K \in \mathcal{T}_h} (\varepsilon^I_{K,\mathbf{u},0})^2(0) + (\varepsilon^I_{K,\mathbf{u},0})^2(T) + \frac{\rho^2}{\mu} \int_0^T \sum_{K \in \mathcal{T}_h} (\varepsilon^I_{K,\mathbf{u},1})^2(s) ds \right), \quad (3.62)$$

*where the error indicators* $(\eta^A_{K,\mathbf{u}})^2, (\eta^A_{K,p})^2$ *and* $(\eta^{\mathrm{div}}_K)^2$ *are given by Proposition 3.23 and* $(\varepsilon^I_{K,\mathbf{u},k})^2, k = 0, 1,$ *by Proposition 3.25.*

*Proof.* The proof is direct. By the triangle inequality, we have

$$\begin{aligned}\rho\|(\mathbf{u}-\mathbf{u}_h)(T)\|^2_{L^2(\Omega)} + \mu\int_0^T \|\nabla(\mathbf{u}-\mathbf{u}_h)(s)\|^2_{L^2(\Omega)}\,ds \\ \leq 2\rho\|(\mathbf{u}-\mathbf{U})(T)\|^2_{L^2(\Omega)} + 2\mu\int_0^T \|\nabla(\mathbf{u}-\mathbf{U})(s)\|^2_{L^2(\Omega)}\,ds \\ + 2\rho\|(\mathbf{U}-\mathbf{u}_h)(T)\|^2_{L^2(\Omega)} + 2\mu\int_0^T \|\nabla(\mathbf{U}-\mathbf{u}_h)(s)\|^2_{L^2(\Omega)}\,ds.\end{aligned}$$

Then we use Propositions 3.19, combined with 3.25, and 3.23 to bound every terms.

Finally, the initial error

$$\rho\|(\mathbf{u}-\mathbf{U})(0)\|^2_{L^2(\Omega)}$$

is split as

$$2\rho\|(\mathbf{u}-\mathbf{u}_h)(0)\|^2_{L^2(\Omega)} + 2\rho\|(\mathbf{U}-\mathbf{u}_h)(0)\|^2_{L^2(\Omega)},$$

the second term being estimated through (3.57). □

**Remark 3.28.** (i) For practical purpose with our adaptive algorithms, we are interested to provide an estimate for the numerical error evaluated at the final time $T$. Note that (3.62) holds in fact for any $t \in (0, T]$.

(ii) We recall that the key idea behind the Stokes reconstruction is to split the discrete error $\mathbf{u}-\mathbf{u}_h$ between

$$\mathbf{u}-\mathbf{U} \text{ and } \mathbf{U}-\mathbf{u}_h.$$

We recall moreover that the main issue to derive an a posteriori upper bound for the unsteady Stokes equation is that it is difficult to rely the pressure error to the velocity one. With the splitting presented above, this issue is solved since no information on the pressure is required to estimate $\mathbf{u}-\mathbf{U}$ (see Remark 3.22) and estimating $\mathbf{U}-\mathbf{u}_h$ consists to work with a steady problem for which estimate for the pressure is available (we recall that $\mathbf{u}_h$ can be seen as an approximation of $\mathbf{U}$ see Lemma 3.17).

(iii) We are mainly interested in the $L^2 - H^1_0$ norm

$$e_{L^2(H^1)} = \left(\int_0^T \|\nabla(\mathbf{u}-\mathbf{u}_h)(s)\|^2_{L^2(\Omega)}dt\right)^{1/2},$$

which can be assumed to be $O(h)$. The Theorem 3.27 basically means that, up to some higher order terms that are $O(h^2)$ that is to say

$$\|(\mathbf{u}-\mathbf{u}_h)(0)\|_{L^2(\Omega)} = \rho\|\mathbf{u}(0) - r_h\mathbf{u}(0)\|_{L^2(\Omega)},$$

and

$$\left(\sum_{K\in\mathcal{T}_h}(\varepsilon^I_{K,\mathbf{u},0})^2(0) + (\varepsilon^I_{K,\mathbf{u},0})^2(T) + \frac{\rho^2}{\mu}\int_0^T \sum_{K\in\mathcal{T}_h}(\varepsilon^I_{K,\mathbf{u},1})^2(s)ds\right)^{1/2},$$

the $e_{L^2(H^1)}$ norm of the velocity error can be estimated by

$$\eta^A = \frac{1}{\mu}\left(\int_0^T \sum_{K\in\mathcal{T}_h}(\eta^A_{K,\mathbf{u}})^2(s) + (\eta^A_{K,p})^2(s) + (\eta^{\mathrm{div}}_K)^2(s)ds\right)^{1/2} \simeq O(h).$$

Note that all these higher order terms are coming from the estimate of the continuous error $\mathbf{u} - U$.

An estimate of optimal order is also available through the same arguments for the $L^\infty - L^2$ error

$$e_{L^\infty(L^2)} = \max_{t\in[0,T]} \|(\mathbf{u} - \mathbf{u}_h)(t)\|_{L^2(\Omega)}$$

that we assume to be $O(h^2)$. Indeed, since we can estimate for any $t \in (0, T]$

$$\|(\mathbf{u} - \mathbf{u}_h(t))\|_{L^2(\Omega)} \leq \|(\mathbf{u} - \mathbf{U})(t)\|_{L^2(\Omega)} + \|(\mathbf{U} - \mathbf{u}_h)(t)\|_{L^2(\Omega)},$$

then Propositions 3.19 and 3.25 provide an a posteriori error estimates (up to a constant that may depends on the mesh aspect ratio) that is $O(h^2)$ since it will only contains the higher terms presented above. Providing an optimal a posteriori upper bound for $e_{L^\infty(L^2)}$ was one of the motivation to the introduction of the elliptic/Stokes reconstruction [74, 61].

(iv) The upper bound (3.62) is not fully computable since the continuous reconstruction $\mathbf{U}$ is contained in $(\eta^A_{K,\mathbf{u}})^2$ and that $P$ is implicitly involved in $(\eta^A_{K,p})^2$, the solution of the dual problem (3.79) being unknown. Since we are mainly interested on error indicators for the velocity, we did not investigate the question for $(\eta^A_{K,p})^2$ and we refer to the Section 3.1 for a similar discussion.

To make $(\eta^A_{K,\mathbf{u}})^2$ computable, we propose to use the ZZ post-processing as already presented for other problems. In practice, we replace $\mathbf{U}$ in $(\eta^A_{K,\mathbf{u}})^2$ by $\Pi_h^{ZZ}\mathbf{u}_h$. This can be justify by the following observation. Let us consider the quantity

$$\int_0^T \sum_{K\in\mathcal{T}_h} (\eta^A_{K,\mathbf{u}})^2(s)ds = \int_0^T \sum_{K\in\mathcal{T}_h} \nu_K(s)\omega_K(\mathbf{U}(s) - \mathbf{u}_h(s))ds$$

where use again the notation

$$\nu_K(t) = \left\|\mathbf{f}(t) - \rho\frac{\partial \mathbf{u}_h}{\partial t}(t) + \mu\Delta\mathbf{u}_h(t) - \nabla p_h(t)\right\|_{L^2(K)} + \frac{1}{2\sqrt{\lambda_{2,K}}} \|[\mu\nabla\mathbf{u}_h(t)\cdot\mathbf{n}]\|_{L^2(\partial K)}.$$

First observe that by the triangle inequality

$$\omega_K(\mathbf{U} - \mathbf{u}_h) \leq \omega_K(\mathbf{u} - \mathbf{u}_h) + \omega_K(\mathbf{u} - \mathbf{U})$$

and therefore we have

$$\int_0^T \sum_{K\in\mathcal{T}_h} (\eta^A_{K,\mathbf{u}})^2(s)ds \leq \int_0^T \sum_{K\in\mathcal{T}_h} \nu_K(s)\omega_K(\mathbf{u}(s) - \mathbf{u}_h(s))ds + \int_0^T \sum_{K\in\mathcal{T}_h} \nu_K(s)\omega_K(\mathbf{U}(s) - \mathbf{u}(s))ds.$$

One can show that the second term is of higher order. Indeed, we have

$$\int_0^T \sum_{K\in\mathcal{T}_h} \nu_K(s)\omega_K(\mathbf{U}(s)-\mathbf{u}(s))ds = \int_0^T \sum_{K\in\mathcal{T}_h} \frac{\lambda_{1,K}}{\lambda_{2,K}}\lambda_{2,K}\nu_K(s)\|\nabla(\mathbf{u}-\mathbf{U})(s)\|_{L^2(\Delta K)}ds.$$

Using the discrete Cauchy-Schwarz inequality for the sum over the triangle and the Cauchy-Schwarz inequality for the time integral, we obtain finally that

$$\int_0^T \sum_{K\in\mathcal{T}_h} \nu_K(s)\omega_K(\mathbf{U}(s) - \mathbf{u}(s))ds \leq C\left(\int_0^T \lambda_{2,K}^2\nu_K^2(s)ds\right)^{1/2}\left(\int_0^T \|\nabla(\mathbf{u} - \mathbf{U})(s)\|^2_{L^2(\Omega)}ds\right)^{1/2},$$

where $C$ depends on the aspect ratio $\lambda_{1,K}/\lambda_{2,K}$. We have then that

$$\left(\int_0^T \lambda_{2,K}^2 \nu_K^2(s)ds\right)^{1/2} = O(h)$$

and thanks to Propositions 3.19 and 3.25

$$\left(\int_0^T \|\nabla(\mathbf{u}-\mathbf{U})(s)\|_{L^2(\Omega)}^2 ds\right)^{1/2} = O(h^2),$$

so finally we obtain that

$$\left(\int_0^T \sum_{K\in\mathcal{T}_h} \nu_K(s)\omega_K(\mathbf{U}(s)-\mathbf{u}(s))ds\right)^{1/2} = O(h^{3/2})$$

and therefore of higher order compared to $e_{L^2(H^1)}$ (see *(ii)* above).

Thus, to summarize, we have that, up to some higher order terms,

$$\int_0^T \sum_{K\in\mathcal{T}_h} (\eta_{K,\mathbf{u}}^A)^2(s)ds$$

is bounded by

$$\int_0^T \sum_{K\in\mathcal{T}_h} \nu_K(s)\omega_K(\mathbf{u}(s)-\mathbf{u}_h(s))ds$$

that we can make computable by replacing $\mathbf{u}$ by its ZZ post-processing $\Pi_h^{ZZ}\mathbf{u}_h$.

**Theorem 3.29** (An a posteriori error estimate for the pressure using the Stokes reconstruction)**.**
*Let $(\mathbf{u},p)$ be the solution of the unsteady Stokes equation* (3.26)*, $(\mathbf{u}_h,p_h)$ be the approximated solutions of the semi-discretized problem* (3.27)*, and $(\mathbf{U},P)$ its the Stokes reconstruction defined by* (3.41)*. Then there exists $C_1$ only depending on the reference triangle and $\Omega$ and $C_2>0$ independent of the mesh size, but dependent on the mesh aspect ratio and $\Omega$ such that for every $t\in(0,T]$*

$$\begin{aligned}\|p-p_h(t)\|_{L^2(\Omega)}^2 \le C_1\mu &\sum_{K\in\mathcal{T}_h} (\eta_{K,\mathbf{u}}^A)^2(t)+(\eta_{K,p}^A)^2(t)+(\eta_K^{\mathrm{div}})^2(t)\\
&+C_1\mu\sum_{K\in\mathcal{T}_h} (\eta_{K,\mathbf{u}}^A)^2(0)+(\eta_{K,p}^A)^2(0)+(\eta_K^{\mathrm{div}})^2(0)\\
&+C_2\max(\mu,\rho)\left(\rho\left\|\frac{\partial\mathbf{u}}{\partial t}(0)-\frac{\partial\mathbf{u}_h}{\partial t}(0)\right\|_{L^2(\Omega)}^2+\mu\|\nabla(\mathbf{u}-\mathbf{u}_h)(0)\|_{L^2(\Omega)}^2\right.\\
&+\rho\sum_{K\in\mathcal{T}_h}(\varepsilon_{K,\mathbf{u},1}^I)^2(0)+(\varepsilon_{K,\mathbf{u},1}^I)^2(t)\\
&\left.+\rho\int_0^t\sum_{K\in\mathcal{T}_h}(\varepsilon_{K,\mathbf{u},1}^I)^2(s)ds+\frac{\rho^2}{\mu}\int_0^t\sum_{K\in\mathcal{T}_h}(\varepsilon_{K,\mathbf{u},2}^I)^2(s)ds\right),\end{aligned} \quad (3.63)$$

*where the error indicators $(\eta_{K,\mathbf{u}}^A)^2,(\eta_{K,p}^A)^2$ and $(\eta_K^{\mathrm{div}})^2$ are given by Proposition 3.23 and $(\varepsilon_{K,\mathbf{u},k}^I)^2, k=0,1,2$ by Proposition 3.25.*

*Proof.* The proof follows the same steps as the estimate for the velocity proven in Theorem 3.27 by splitting the numerical error $p-p_h$ into $p-P$ and $P-p_h$ and by using the propositions 3.21, 3.23 and 3.25. □

**Remark 3.30.**
The estimate (3.63) is not fully satisfactory from an anisotropic perspective since terms of low order (such as $\|\nabla(\mathbf{u}-\mathbf{u}_h)(0)\|^2_{L^2(\Omega)}$) appear in the estimate but are multiplied by a constant (here $C_2$) which depends on the mesh aspect ratio. Moreover, no a priori estimate is available for

$$\rho \left\| \frac{\partial \mathbf{u}}{\partial t}(0) - \frac{\partial \mathbf{u}_h}{\partial t}(0) \right\|^2_{L^2(\Omega)}.$$

We summarize the results obtained in this section. The goal of the discussion was to try to correct the drawbacks of Theorem 3.12, for which the way we solved the issue of relating the pressure to the velocity was not satisfactory. The first attempt was the Theorem 3.14, where we used the *Stokes projection*, but non-anisotropic terms were involved in the corresponding a posteriori estimates. We then proposed another approach using the *Stokes reconstruction.* We think that the estimate of Theorem 3.27, where we used the Stokes reconstruction, achieves this goal for the two following reasons:

(1) The terms involving

$$\left\| \operatorname{div} \frac{\partial \mathbf{u}_h}{\partial t} \right\|_{L^2(K)}$$

are of higher order, and even if there are multiplied by a constant depending on the mesh aspect ratio, as already mentioned , it is from our perspective sufficient.

(2) The estimate is written in a fully anisotropic settings by comparison with the estimate (3.37) of Theorem 3.14 where we use the Stokes projection $\Pi^{\text{div}}$. Indeed, in Theorem 3.14, we was not able to bound the part of the estimate containing the factor $\omega_K(\Pi^{\text{div}}(\mathbf{u}-\mathbf{u}_h))$ independently of the mesh aspect ratio. We refer to the discussion coming after the proof of Theorem 3.14 for more details.

Following this two observations, we choose to use the Stokes reconstruction technique (and later on its Navier-Stokes version) to prove our future estimates.

## 3.5 A posteriori error estimates for the unsteady Stokes equations with constant coefficients: spatial and temporal approximation

In this section, we prove an a posteriori error estimate for the unsteady Stokes equations involving the space and the time discretizations. We work with the same framework that the one chosen in the previous section. We denote by $\Omega$ a convex domain of $\mathbb{R}^2$, $T > 0$ the final time, and $\rho, \mu > 0$ the density and the viscosity. The force term $\mathbf{f}$ is chosen in $C^0([0,T];(L^2(\Omega))^2)$, and the initial condition $\mathbf{u}_0 \in (H^1_0(\Omega))^2$ is such that $\operatorname{div} \mathbf{u}_0 = 0$. We recall that we are looking for $(\mathbf{u}, p)$ the solution of the incompressible unsteady Stokes equations (3.25)

$$\begin{cases} \rho \dfrac{\partial \mathbf{u}}{\partial t} - \mu \Delta \mathbf{u} + \nabla p = \mathbf{f}, & \text{in } \Omega \times (0,T), \\ \operatorname{div} \mathbf{u} = 0, & \text{in } \Omega \times (0,T), \\ \mathbf{u} = 0, & \text{on } \partial\Omega \times (0,T), \\ \mathbf{u}(\cdot, 0) = \mathbf{u}_0, & \text{in } \Omega. \end{cases}$$

The weak formulation (3.26) reads: find $(\mathbf{u}, p)$ such that $\mathbf{u}(\cdot, 0) = \mathbf{u}_0$ almost everywhere in $\Omega$ and for almost every $t \in (0, T)$

$$\rho \int_\Omega \frac{\partial \mathbf{u}}{\partial t} \cdot \mathbf{v} d\mathbf{x} + \mu \int_\Omega \nabla \mathbf{u} : \nabla \mathbf{v} d\mathbf{x} - \int_\Omega p \operatorname{div} \mathbf{v} d\mathbf{x} = \int_\Omega \mathbf{f} \cdot \mathbf{v} d\mathbf{x}, \quad \forall \mathbf{v} \in (H_0^1(\Omega))^2,$$
$$- \int_\Omega q \operatorname{div} \mathbf{u} d\mathbf{x} = 0, \quad \forall q \in L_0^2(\Omega).$$

In the previous section, we focused on the spatial approximation of the above equations. We now also consider a finite difference scheme to discretize the evolution in time. We focus on the Backward Euler method. As before, for all $h > 0$, let $\mathcal{T}_h$ be a conformal triangulation of $\Omega$ into triangles $K$ of diameter $h_K \leq h$, $W_h$ the classical finite elements set of all continuous, piecewise linear functions, and $W_{h,0}$ the subset of $W_h$ which elements have zero value on $\partial\Omega$. The discrete velocity space and pressure space are given by $V_h = (W_{h,0})^2$ and $Q_h = W_h \cap L_0^2(\Omega)$ and we consider the partition of $[0, T]$ $0 = t^0 < t^1 < ... < t^N = T$, for an integer $N > 0$. Assuming that $\mathbf{u}_0 \in (H_0^1(\Omega))^2 \cap (H^2(\Omega))^2$, then starting from $\mathbf{u}_h^0 = r_h(\mathbf{u}_0)$, we are looking for every $n = 0, 1, ...N - 1$, for $(\mathbf{u}_h^{n+1}, p_h^{n+1})$ the solutions of

$$\rho \int_\Omega \frac{\mathbf{u}_h^{n+1} - \mathbf{u}_h^n}{\tau^{n+1}} \cdot \mathbf{v}_h d\mathbf{x} + \mu \int_\Omega \nabla \mathbf{u}_h^{n+1} : \nabla \mathbf{v}_h d\mathbf{x} - \int_\Omega p_h^{n+1} \operatorname{div} \mathbf{v}_h d\mathbf{x} = \int_\Omega \mathbf{f}^{n+1} \cdot \mathbf{v}_h d\mathbf{x}, \quad \forall \mathbf{v}_h \in V_h,$$
$$- \int_\Omega q_h \operatorname{div} \mathbf{u}_h^{n+1} d\mathbf{x}$$
$$+ \sum_{K \in \mathcal{T}_h} \alpha_K \int_K \left( \mathbf{f}^{n+1} - \rho \frac{\mathbf{u}_h^{n+1} - \mathbf{u}_h^n}{\tau^{n+1}} + \mu \Delta \mathbf{u}_h^{n+1} - \nabla p_h^{n+1} \right) \cdot \nabla q_h d\mathbf{x} = 0, \quad \forall q_h \in Q_h, \tag{3.64}$$

where we note the time step

$$\tau^{n+1} = t^{n+1} - t^n, \quad n = 0, 1, ..., N - 1,$$

and we denote

$$\mathbf{f}^n = \mathbf{f}(t^n), \quad n = 0, 1, ..., N.$$

The stabilization parameter $\alpha_K$ is defined by (3.28), i.e.,

$$\alpha_K = \frac{\alpha \lambda_{2,K}^2}{\mu}$$

where $\alpha > 0$ is a dimensionless prescribed positive value.

**Remark 3.31.**
As for the semi-discrete approximation in space, it is not necessary give an initial condition for the pressure to solve the discrete problem (3.64). However, we must to give a sense to $p_h^0$ for the need of our future computations. Therefore, one can as previously assume that the exact pressure $p(\cdot, 0) = p_0$ is well defined and smooth enough to define $p_h^0 = r_h(p_0)$ or we can also define $p_h^0 = p_h(0)$ where $p_h(0)$ is the solution at time $t = 0$ of the semi-discrete problem (3.27).

In [68], an a priori error analysis of the numerical method (3.64) is proposed for isotropic finite elements and constant time steps. We are not interested now in extending this discussion to the case of anisotropic finite elements, but we comment some of the conclusions obtained. Observe that the stabilization used in (3.64) is consistent since the whole residue of the momentum equation is added to the divergence equation. With a consistent stabilization, the author demonstrates in [68] that the numerical method is well-posed and that $(\mathbf{u}_h^n, p^n)$ converges to $(\mathbf{u}, p)$ (in the $H^1$ semi-norm) with an order of convergence $O(h+\tau)$, $\tau$ standing for the constant time step. It requires that $\tau > \max_{K\in\mathcal{T}_h} \alpha_K$ where here we choose $\alpha_K$ as in the isotropic settings, that is to say

$$\alpha_K = \frac{\alpha h_K^2}{\mu}.$$

That means that the time steps cannot be chosen too small and it was observed in practice instabilities when it is the case. However, this seems to appear only with very small time steps. In an anisotropic setting and with variable time steps, this condition would read

$$\min_{n=0,1,...,N-1} \tau^{n+1} > \max_{K\in\mathcal{T}_h} \frac{\alpha\lambda_{2,K}^2}{\mu}.$$

From an adaptation point of view, we think that this condition is not issue since we will equidistribute the error between the time and space discretization, and roughly speaking, build of sequence of meshes and time steps such that $h \simeq \tau$. Therefore, the above condition should be satisfied. In any case, the a priori analysis of the numerical method (3.64) is out of the scope of the present work, and we will simply assume its well-posedness. The convergence will be checked numerically.

We will prove an a posteriori error estimate for the numerical method (3.64) that takes in account space and time discretizations. For simplification, we are interested only in an estimate about the velocity error. In [16], such a bound is proven for isotropic finite elements and the Backward Euler method, where the Stokes projection $\Pi^{\text{div}}$ (3.35) is used to deal with the pressure estimate issue. Below, we propose to prove a similar upper bound, but using the Stokes reconstruction (3.40) instead, since it is more convenient with anisotropic finite elements. In [65] a similar study was already done for parabolic problem and isotropic finite elements. Note that in [16] the authors were also able to prove a lower bound. As commented in the previous chapters, such bounds are hardly accessible in the anisotropic framework and therefore we focus on the upper estimate. For every $n = 0, ..., N-1$ we define the discrete Stokes reconstruction $(\mathbf{U}^{n+1}, P^{n+1})$ of $(\mathbf{u}_h^{n+1}, p^{n+1})$ as the unique weak solution in $(H_0^1(\Omega))^2 \times L_0^2(\Omega)$ of

$$\begin{cases} -\mu\Delta\mathbf{U}^{n+1} + \nabla P^{n+1} = \mathbf{f}^{n+1} - \rho\dfrac{\mathbf{u}_h^{n+1} - \mathbf{u}_h^n}{\tau^{n+1}}, & \text{in } \Omega, \\ \operatorname{div} \mathbf{U}^{n+1} = 0, & \text{in } \Omega, \\ \mathbf{U}^{n+1} = 0, & \text{on } \partial\Omega. \end{cases} \tag{3.65}$$

The weak formulation reads: for $n = 0, 1, ..., N-1$, we look for $(\mathbf{U}^{n+1}, P^{n+1}) \in (H_0^1(\Omega))^2 \times L_0^2(\Omega)$ the solution of

$$\mu \int_\Omega \nabla\mathbf{U}^{n+1} : \nabla\mathbf{v} d\mathbf{x} - \int_\Omega P^{n+1} \operatorname{div} \mathbf{v} d\mathbf{x} = \int_\Omega \left(\mathbf{f}^{n+1} - \rho\frac{\mathbf{u}_h^{n+1} - \mathbf{u}_h^n}{\tau^{n+1}}\right) \cdot \mathbf{v} d\mathbf{x}, \quad \forall \mathbf{v} \in (H_0^1(\Omega))^2,$$
$$-\int_\Omega q \operatorname{div} \mathbf{U}^{n+1} = 0, \quad \forall q \in L_0^2(\Omega). \tag{3.66}$$

Observe that the reconstructed sequence $(\mathbf{U}^n, P^n)$ starts with $(\mathbf{U}^1, P^1)$ and for the needs of the demonstrations below, we also have to define $(\mathbf{U}^0, P^0)$. We choose it as the solution of

$$\mu \int_\Omega \nabla\mathbf{U}^0 : \nabla\mathbf{v} d\mathbf{x} - \int_\Omega P^0 \operatorname{div} \mathbf{v} d\mathbf{x} = \int_\Omega \left(\mathbf{f}^0 - \rho\frac{\partial \mathbf{u}_h}{\partial t}(0)\right) \cdot \mathbf{v} d\mathbf{x}, \quad \forall \mathbf{v} \in (H_0^1(\Omega))^2,$$
$$-\int_\Omega q \operatorname{div} \mathbf{U}^0 = 0, \quad \forall q \in L_0^2(\Omega), \tag{3.67}$$

where $\frac{\partial \mathbf{u}_h}{\partial t}(0)$ is the semi-discrete approximation of $\frac{\partial \mathbf{u}}{\partial t}(0)$ obtained by evaluating the finite elements problem (3.27) at $t = 0$. This implies in particular that $(\mathbf{U}^0, P^0) = (\mathbf{U}(0), P(0))$ where $(\mathbf{U}(0), P(0))$ are nothing else than the (semi-discrete) Stokes reconstruction of $(\mathbf{u}_h(0), p_h(0))$ given by (3.41) and $(\mathbf{u}_h(0), p_h(0))$ are the semi-discrete approximation given by (3.27).

We first prove the discrete versions of Proposition 3.17 that shows the link between the numerical solution $(\mathbf{u}_h^{n+1}, p_h^{n+1})$ and its discrete Stokes reconstruction. Let assume that for every $n = 0, 1, ..., N-1$ we discretize the equations (3.66) with a Petrov-Galerkin finite elements methods, that is to say, for every $n = 0, 1, ..., N-1$ we look for the unique solution $(\mathbf{U}_h^{n+1}, P_h^{n+1}) \in V_h \times Q_h$ of

$$\begin{aligned} \mu \int_\Omega \nabla \mathbf{U}_h^{n+1} : \nabla \mathbf{v}_h d\mathbf{x} - \int_\Omega P_h^{n+1} \operatorname{div} \mathbf{v}_h d\mathbf{x} = \int_\Omega \mathbf{f}^{n+1} \cdot \mathbf{v}_h d\mathbf{x} - \rho \int_\Omega \frac{\mathbf{u}_h^{n+1} - \mathbf{u}_h^n}{\tau^{n+1}} \cdot \mathbf{v}_h d\mathbf{x}, \quad \forall \mathbf{v}_h \in V_h, \\ - \int_\Omega q_h \operatorname{div} \mathbf{U}_h^{n+1} d\mathbf{x} \\ + \sum_{K \in \mathcal{T}_h} \alpha_K \int_K \left( \mathbf{f}^{n+1} - \rho \frac{\mathbf{u}_h^{n+1} - \mathbf{u}_h^n}{\tau^{n+1}} + \mu \Delta \mathbf{U}_h^{n+1} - \nabla P_h^{n+1} \right) \cdot \nabla q_h d\mathbf{x} = 0, \quad \forall q_h \in Q_h, \end{aligned} \tag{3.68}$$

where we choose $\alpha_K$ as (3.28).

**Proposition 3.32.**
*For all $n = 0, 1, ..., N-1$, $(\mathbf{U}_h^{n+1}, P_h^{n+1}) = (\mathbf{u}_h^{n+1}, p_h^{n+1})$ where $(\mathbf{U}_h^{n+1}, P_h^{n+1})$ is the solution of (3.68) and $(\mathbf{u}_h^{n+1}, p_h^{n+1})$ the solution of (3.64).*

*Proof.* The proof is formally the same as the one of Proposition 3.17. Subtracting (3.64) from (3.68), it yields for all $0 \le n \le N-1$ that

$$\begin{aligned} \mu \int_\Omega \nabla (\mathbf{U}_h^{n+1} - \mathbf{u}_h^{n+1}) : \nabla \mathbf{v}_h d\mathbf{x} - \int_\Omega (P_h^{n+1} - p_h^{n+1}) \operatorname{div} \mathbf{v}_h d\mathbf{x} = 0, \forall \mathbf{v}_h \in V_h, \\ - \int q_h \operatorname{div}(\mathbf{U}_h^{n+1} - \mathbf{u}_h^{n+1}) d\mathbf{x} - \sum_{K \in \mathcal{T}_h} \alpha_K \int_K \nabla (P_h^{n+1} - p_h^{n+1}) \cdot \nabla q_h d\mathbf{x} = 0, \forall q_h \in Q_h. \end{aligned}$$

Choosing $\mathbf{v}_h = \mathbf{U}_h^{n+1} - \mathbf{u}_h^{n+1}$ and $q_h = -(P_h^{n+1} - p_h^{n+1})$ yields

$$\mu \int_\Omega |\nabla (\mathbf{U}_h^{n+1} - \mathbf{u}_h^{n+1})|^2 d\mathbf{x} + \sum_{K \in \mathcal{T}_h} \alpha_K \int_K |\nabla (P_h^{n+1} - p_h^{n+1})|^2 d\mathbf{x} = 0,$$

which implies that $\mathbf{U}_h^{n+1} = \mathbf{u}_h^{n+1}$ and $P_h^{n+1} = p_h^{n+1}$ since both terms are non negative. □

We now start the a posteriori error analysis. To simplify the computations, we introduce similar notations as those used for the treatment of the transport equation in Chapter 2. We note

$$\partial \mathbf{U}^{n+1} = \frac{\mathbf{U}^{n+1} - \mathbf{U}^n}{\tau^{n+1}}, \partial P^{n+1} = \frac{P^{n+1} - P^n}{\tau^{n+1}}, \partial \mathbf{f}^{n+1} = \frac{\mathbf{f}^{n+1} - \mathbf{f}^n}{\tau^{n+1}} \quad n = 0, 1, ..., N-1, \tag{3.69}$$

and

$$\partial \mathbf{u}_h^{n+1} = \frac{\mathbf{u}_h^{n+1} - \mathbf{u}_h^n}{\tau^{n+1}}, \partial p_h^{n+1} = \frac{p_h^{n+1} - p_h^n}{\tau^{n+1}}, \quad n = 0, 1, ..., N-1, \tag{3.70}$$

$$\partial \mathbf{u}_h^0 = \frac{\partial \mathbf{u}_h}{\partial t}(0), \tag{3.71}$$

$$\partial^2 \mathbf{u}_h^{n+1} = \frac{\frac{\mathbf{u}_h^{n+1} - \mathbf{u}_h^n}{\tau^{n+1}} - \frac{\mathbf{u}_h^n - \mathbf{u}_h^{n-1}}{\tau^n}}{\tau^{n+1} + \tau^n/2}, \quad n = 1, ..., N-1 \tag{3.72}$$

$$\partial^2 \mathbf{u}_h^1 = \frac{\frac{\mathbf{u}_h^1 - \mathbf{u}_h^0}{\tau^1} - \frac{\partial \mathbf{u}_h}{\partial t}(0)}{\tau^1}. \tag{3.73}$$

**Lemma 3.33** (Galerkin orthogonality of the discrete Stokes reconstruction)**.**
*Let* $(\mathbf{u}_h^n, p_h^n)$ *be the solution of the fully discretized equations (3.64) and* $(\mathbf{U}^n, P^n)$ *its discrete Stokes reconstruction given by (3.66). For all* $0 \le n \le N$ *the following identities hold*

$$\mu \int_\Omega \nabla(\mathbf{U}^n - \mathbf{u}_h^n) : \nabla \mathbf{v}_h d\mathbf{x} - \int_\Omega (P^n - p_h^n) \operatorname{div} \mathbf{v}_h d\mathbf{x} = 0, \quad \forall \mathbf{v}_h \in V_h, \tag{3.74}$$

$$-\int_\Omega q_h \operatorname{div}(\mathbf{U}^n - \mathbf{u}_h^n) d\mathbf{x} - \sum_{K \in \mathcal{T}_h} \alpha_K \left(\mathbf{f}^n - \rho \partial \mathbf{u}_h^n + \mu \Delta \mathbf{u}_h^n - \nabla p_h^n\right) \cdot \nabla q_h d\mathbf{x} = 0, \quad \forall q_h \in Q_h. \tag{3.75}$$

*Moreover, we have for all* $0 \le n \le N-1$

$$\mu \int_\Omega \nabla(\partial \mathbf{U}^{n+1} - \partial \mathbf{u}_h^{n+1}) : \nabla \mathbf{v}_h d\mathbf{x} - \int_\Omega (\partial P^{n+1} - \partial p_h^{n+1}) \operatorname{div} \mathbf{v}_h = 0, \quad \forall \mathbf{v}_h \in V_h, \tag{3.76}$$

$$\begin{aligned} &- \int_\Omega q_h \operatorname{div} \left(\partial \mathbf{U}^{n+1} - \partial \mathbf{u}_h^{n+1}\right) d\mathbf{x} \\ &- \sum_{K \in \mathcal{T}_h} \alpha_K \left(\partial \mathbf{f}^{n+1} - \rho \partial^2 \mathbf{u}_h^{n+1} + \mu \Delta \partial \mathbf{u}_h^{n+1} - \nabla \partial p_h^{n+1}\right) \cdot \nabla q_h = 0, \quad \forall q_h \in Q_h. \end{aligned} \tag{3.77}$$

*Proof.* The proof of (3.74) and (3.75) are straightforward by taking the difference between (3.66) and (3.64). The case $n = 0$ is obtained thanks to Lemma 3.18 due the definition of $(U^0, P^0)$ and the fact that $(\mathbf{u}_h^0, p_h^0) = (r_h \mathbf{u}_0, p_h(0)) = (\mathbf{u}_h(0), p_h(0))$ (whatever the choice we do for $p_h(0)$) where $(\mathbf{u}_h(0), p_h(0))$ are the solution of the semi-discretized approximation (3.27).

(3.76) follows by taking the difference between (3.74) at $n$ and $n-1$ and dividing by $\tau^{n+1}$. The same argument implies (3.77). □

To derive an a posteriori error estimate that involves the time discretization, we proceed as we did for the transport equation, and we interpolate the numerical solution $(\mathbf{u}_h^n, p_h^n)$ as its discrete Stokes reconstruction $(\mathbf{U}^n, P^n)$ over $[0, T]$ using a linear Newtonian polynomial. We set the following definition

**Definition 3.34** (Piecewise linear reconstruction)**.**
Let $(\mathbf{u}_h^n, p_h^n)$ be the solution of the fully discretized equations (3.64) and $(\mathbf{U}^n, P^n)$ its discrete Stokes reconstruction given by (3.66). We define $(\mathbf{u}_{h\tau}, p_{h\tau})$ and $(\mathbf{U}_\tau, P_\tau)$ the piecewise linear functions in time given by

$$\begin{aligned} \mathbf{u}_{h\tau}(t) &= \mathbf{u}_h^{n+1} + (t - t^{n+1}) \partial \mathbf{u}_h^{n+1}, \quad t \in [t^n, t^{n+1}], n = 0, 1, ..., N-1, \\ p_{h\tau}(t) &= p_h^{n+1} + (t - t^{n+1}) \partial p_h^{n+1}, \quad t \in [t^n, t^{n+1}], n = 0, 1, ..., N-1, \end{aligned}$$

and

$$\mathbf{U}_\tau(t) = \mathbf{U}^{n+1} + (t - t^{n+1})\partial\mathbf{U}^{n+1}, \quad t \in [t^n, t^{n+1}], n = 0, 1, ..., N-1,$$
$$P_\tau(t) = P^{n+1} + (t - t^{n+1})\partial P^{n+1}, \quad t \in [t^n, t^{n+1}], n = 0, 1, ..., N-1.$$

**Remark 3.35.**
Observing that for any $n = 0, 1, ..., N$

$$(\mathbf{u}_h^n, p_h^n) = (\mathbf{u}_{h\tau}(t^n), p_{h\tau}(t^n)), \quad (\mathbf{U}^n, P^n) = (\mathbf{U}_\tau(t^n), P_\tau(t^n))$$

and for any $n = 0, 1, ..., N-1$ and for any $t \in [t^n, t^{n+1}]$

$$\left(\frac{\partial \mathbf{u}_{h\tau}}{\partial t}(t), \frac{\partial p_{h\tau}}{\partial t}(t)\right) = \left(\partial \mathbf{u}_h^{n+1}, \partial p_h^{n+1}\right), \quad \left(\frac{\partial \mathbf{U}_\tau}{\partial t}(t), \frac{\partial P_\tau}{\partial t}(t)\right) = \left(\partial \mathbf{U}^{n+1}, \partial P^{n+1}\right)$$

then the Lemma 3.33 can be written in the notations $\mathbf{u}_{h\tau}, p_{h\tau}, \mathbf{U}_\tau, P_\tau$.

The strategy of the proof follows the idea of Theorem 3.27 for the semi-discrete approximation and we split the error $\mathbf{u} - \mathbf{u}_{h\tau}$ as

$$\mathbf{u} - \mathbf{U}_\tau \text{ and } \mathbf{U}_\tau - \mathbf{u}_{h\tau}.$$

We first prove Propositions 3.36, 3.38 and 3.39, that provide estimates for each part, and then we prove the final bound for $\mathbf{u} - \mathbf{u}_{h\tau}$ in the Theorem 3.41. Roughly speaking, a time error estimator will by obtained by estimating $\mathbf{u} - \mathbf{U}_\tau$ and its spatial counterpart by bounding $\mathbf{U}_\tau - \mathbf{u}_{h\tau}$. The estimate for $\mathbf{u} - \mathbf{U}_\tau$ is contained in the Proposition

**Proposition 3.36** (Continuous error estimate for the velocity)**.**
*Let $(\mathbf{u}, p)$ be the exact solution of the unsteady Stokes equation (3.26), $(\mathbf{u}_h^n, p^n)_{n=0}^N$ be the numerical solution obtained by solving (3.64) and $(\mathbf{U}^n, P^n)_{n=0}^N$ its discrete Stokes reconstruction given by (3.66) and (3.67). Finally, let $\mathbf{U}_\tau$ be the piecewise linear interpolation of the Stokes reconstructed velocity $(\mathbf{U}^n)_{n=0}^N$ given by Definition 3.34. Then, the following estimate holds, where $C_P$ stands for the Poincaré constant of $\Omega$ and we denote $\mathbf{f}_\rho = \mathbf{f}/\rho$:*

$$\begin{aligned}
\rho\|(\mathbf{u} - \mathbf{U}_\tau)(T)\|^2 &+ \mu \int_0^T \|\nabla(\mathbf{u} - \mathbf{U}_\tau)(t)\|_{L^2(\Omega)}^2 dt \\
&\leq \rho\|(\mathbf{u} - \mathbf{U}_\tau)(0)\|^2 \\
&+ \frac{3\rho^2 C_P^2}{2\mu} \sum_{n=0}^{N-1} \int_{t^n}^{t^{n+1}} \|\mathbf{f}_\rho(t) - \mathbf{f}_\rho^{n+1}\|_{L^2(\Omega)}^2 dt + \frac{3\mu}{2} \sum_{n=0}^{N-1} (\tau^{n+1})^3 \|\nabla \partial \mathbf{u}_h^{n+1}\|_{L^2(\Omega)}^2 dt \\
&+ \frac{3\mu}{2} \sum_{n=0}^{N-1} \tau^{n+1} \|\nabla(\mathbf{U}^{n+1} - \mathbf{u}_h^{n+1})\|_{L^2(\Omega)}^2 + \tau^{n+1} \|\nabla(\mathbf{U}^n - \mathbf{u}_h^n)\|_{L^2(\Omega)}^2 \\
&+ \frac{3\rho^2 C_P^2}{2\mu} \sum_{n=0}^{N-1} \tau^{n+1} \left\|\partial \mathbf{u}_h^{n+1} - \partial \mathbf{U}^{n+1}\right\|_{L^2(\Omega)}^2. \qquad (3.78)
\end{aligned}$$

*Proof.* Let $n = 0, 1, ..., N-1$ and $t \in [t^n, t^{n+1}]$. We have

$$\begin{aligned}
&\frac{\rho}{2}\frac{d}{dt}\|(\mathbf{u} - \mathbf{U}_\tau)(t)\|_{L^2(\Omega)}^2 + \mu\|\nabla(\mathbf{u} - \mathbf{U}_\tau)(t)\|_{L^2(\Omega)}^2 \\
&\quad = \rho \int_\Omega \frac{\partial}{\partial t}(\mathbf{u} - \mathbf{U}_\tau)(t) \cdot (\mathbf{u} - \mathbf{U}_\tau)(t) d\mathbf{x} + \mu \int_\Omega \nabla(\mathbf{u} - \mathbf{U}_\tau)(t) : \nabla(\mathbf{u} - \mathbf{U}_\tau)(t) d\mathbf{x} \\
&\qquad - \int_\Omega (p - P^{n+1}) \operatorname{div}(\mathbf{u} - \mathbf{U}_\tau)(t) d\mathbf{x} \\
&\quad = \rho \int_\Omega \frac{\partial}{\partial t}(\mathbf{u} - \mathbf{U}_\tau)(t) \cdot (\mathbf{u} - \mathbf{U}_\tau)(t) d\mathbf{x} + \mu \int_\Omega \nabla(\mathbf{u}(t) - \mathbf{U}^{n+1}) : \nabla(\mathbf{u} - \mathbf{U}_\tau)(t) d\mathbf{x} \\
&\quad - \int_\Omega (p(t) - P^{n+1}) \operatorname{div}(\mathbf{u} - \mathbf{U}_\tau)(t) d\mathbf{x} + \mu \int_\Omega \nabla(\mathbf{U}^{n+1} - \mathbf{U}_\tau(t)) : \nabla(\mathbf{u} - \mathbf{U}_\tau)(t) d\mathbf{x},
\end{aligned}$$

where we use the fact that $\mathrm{div}(\mathbf{u}-\mathbf{U}_\tau)(t)=0$ to add the term

$$\int_\Omega (p-P^{n+1})\,\mathrm{div}(\mathbf{u}-\mathbf{U}_\tau)(t)d\mathbf{x}.$$

Now using the momentum equation of (3.26) and (3.64), we obtain that

$$\begin{aligned}
&\frac{\rho}{2}\frac{d}{dt}\|(\mathbf{u}-\mathbf{U}_\tau)(t)\|^2_{L^2(\Omega)}+\mu\|\nabla(\mathbf{u}-\mathbf{U}_\tau)(t)\|^2_{L^2(\Omega)}\\
&\quad\le \int_\Omega (\mathbf{f}(t)-\mathbf{f}^{n+1})\cdot(\mathbf{u}-\mathbf{U}_\tau)(t)d\mathbf{x}+\rho\int_\Omega\left(\frac{\partial\mathbf{u}_{h\tau}}{\partial t}(t)-\frac{\partial\mathbf{U}_\tau}{\partial t}(t)\right)\cdot(\mathbf{u}-\mathbf{U}_\tau)(t)d\mathbf{x}\\
&\qquad+\mu\int_\Omega\nabla(\mathbf{U}^{n+1}-\mathbf{U}_\tau(t)):\nabla(\mathbf{u}-\mathbf{U}_\tau)(t)d\mathbf{x}\\
&\quad\le \rho\int_\Omega (\mathbf{f}_\rho(t)-\mathbf{f}_\rho^{n+1})\cdot(\mathbf{u}-\mathbf{U}_\tau)(t)d\mathbf{x}+\rho\int_\Omega\left(\frac{\partial\mathbf{u}_{h\tau}}{\partial t}(t)-\frac{\partial\mathbf{U}_\tau}{\partial t}(t)\right)\cdot(\mathbf{u}-\mathbf{U}_\tau)(t)d\mathbf{x}\\
&\qquad+\mu\int_\Omega\nabla(\mathbf{U}^{n+1}-\mathbf{U}_\tau(t)):\nabla(\mathbf{u}-\mathbf{U}_\tau)(t)d\mathbf{x}.
\end{aligned}$$

Combining Cauchy-Schwarz, Young's and Poincaré inequality, it yields

$$\begin{aligned}
&\rho\frac{d}{dt}\|(\mathbf{u}-\mathbf{U}_\tau)(t)\|^2_{L^2(\Omega)}+\mu\|\nabla(\mathbf{u}-\mathbf{U}_\tau)(t)\|^2_{L^2(\Omega)}\\
&\quad\le\frac{3\rho^2C_P^2}{2\mu}\|\mathbf{f}_\rho(t)-\mathbf{f}_\rho^{n+1}\|^2_{L^2(\Omega)}+\frac{3\rho^2C_P^2}{2\mu}\left\|\frac{\partial\mathbf{u}_{h\tau}}{\partial t}(t)-\frac{\partial\mathbf{U}_\tau}{\partial t}(t)\right\|^2_{L^2(\Omega)}\\
&\qquad+\frac{3\mu}{2}\|\nabla(\mathbf{U}^{n+1}-\mathbf{U}_\tau(t))\|^2_{L^2(\Omega)}.
\end{aligned}$$

Integrating from $t^n$ to $t^{n+1}$ and summing up from $n=0$ to $n=N$, it yields

$$\begin{aligned}
&\rho\|(\mathbf{u}-\mathbf{U}_\tau)(T)\|^2+\mu\int_0^T\|\nabla(\mathbf{u}-\mathbf{U}_\tau)(t)\|^2_{L^2(\Omega)}dt\\
&\quad\le\rho\|(\mathbf{u}-\mathbf{U}_\tau)(0)\|^2+\frac{3\rho^2C_P^2}{2\mu}\sum_{n=0}^{N-1}\int_{t^n}^{t^{n+1}}\|\mathbf{f}_\rho(t)-\mathbf{f}_\rho^{n+1}\|^2_{L^2(\Omega)}dt\\
&+\frac{3\mu}{2}\sum_{n=0}^{N-1}\int_{t^n}^{t^{n+1}}\left(t-t^{n+1}\right)^2\|\nabla\partial\mathbf{U}^{n+1}\|^2_{L^2(\Omega)}dt+\frac{3\rho^2C_P^2}{2\mu}\int_0^T\left\|\frac{\partial\mathbf{u}_{h\tau}}{\partial t}(t)-\frac{\partial\mathbf{U}_\tau}{\partial t}(t)\right\|^2_{L^2(\Omega)}dt.
\end{aligned}$$

Since

$$\partial\mathbf{U}^{n+1}=\frac{\mathbf{U}^{n+1}-\mathbf{U}^n}{\tau^{n+1}}=\frac{\mathbf{U}^{n+1}-\mathbf{u}_h^{n+1}}{\tau^{n+1}}+\frac{\mathbf{u}_h^{n+1}-\mathbf{u}_h^n}{\tau^{n+1}}+\frac{\mathbf{u}_h^n-\mathbf{U}^n}{\tau^{n+1}},$$

and

$$\int_{t^n}^{t^{n+1}}\left(t-t^{n+1}\right)^2dt=\frac{(\tau^{n+1})^3}{3}$$

we derive that

$$\begin{aligned}
&\rho\|(\mathbf{u}-\mathbf{U}_\tau)(T)\|^2+\mu\int_0^T\|\nabla(\mathbf{u}-U_\tau)(t)\|^2_{L^2(\Omega)}dt\\
&\quad\le\rho\|(\mathbf{u}-\mathbf{U}_\tau)(0)\|^2\\
&+\frac{3\rho^2C_P^2}{2\mu}\sum_{n=0}^{N-1}\int_{t^n}^{t^{n+1}}\|\mathbf{f}_\rho(t)-\mathbf{f}_\rho^{n+1}\|^2_{L^2(\Omega)}dt+\frac{3\mu}{2}\sum_{n=0}^{N-1}(\tau^{n+1})^3\|\nabla\partial\mathbf{u}_h^{n+1}\|^2_{L^2(\Omega)}dt\\
&+\frac{3\mu}{2}\sum_{n=0}^{N-1}\tau^{n+1}\|\nabla(\mathbf{U}^{n+1}-\mathbf{u}_h^{n+1})\|^2_{L^2(\Omega)}+\tau^{n+1}\|\nabla(\mathbf{U}^n-\mathbf{u}_h^n)\|^2_{L^2(\Omega)}\\
&+\frac{3\rho^2C_P^2}{2\mu}\int_0^T\left\|\frac{\partial\mathbf{u}_{h\tau}}{\partial t}(t)-\frac{\partial\mathbf{U}_\tau}{\partial t}(t)\right\|^2_{L^2(\Omega)}dt,
\end{aligned}$$

that concludes the proof by using the definition of $\mathbf{u}_{h\tau}$ and $\mathbf{U}_\tau$. □

**Remark 3.37.**
As already commented in the Remark 3.20, using the Gronwall's Lemma (see Theorem A.3) instead of the Poincaré inequality to control the $L^2$ norm $\rho\|\mathbf{u}-\mathbf{U}\|_{L^2(\Omega)}$ yields, up to a multiplicative constant, the same estimate with $\rho T$ replacing the factor ${}^{\rho^2 C_P^2}/_{\mu}$.

Estimate (3.78) already contains a time error indicator given by

$$\frac{\rho^2 C_P^2}{\mu}\sum_{n=0}^{N-1}\int_{t^n}^{t^{n+1}}\|\mathbf{f}_\rho(t)-\mathbf{f}_\rho^{n+1}\|^2_{L^2(\Omega)}dt+\mu\sum_{n=0}^{N-1}(\tau^{n+1})^3\|\nabla\partial\mathbf{u}_h^{n+1}\|^2_{L^2(\Omega)}dt$$

which of order $O(\tau)$ after taking the square root, and so achieves the right order with respect to the time discretization, the Backward Euler method being an order 1 in time advancing scheme. To complete the a posteriori error estimate, we have to bound the terms

$$\|\nabla(\mathbf{U}^{n+1}-\mathbf{u}_h^{n+1})\|^2_{L^2(\Omega)},\forall n,$$

and

$$\left\|\frac{\partial\mathbf{u}_{h\tau}}{\partial t}(t)-\frac{\partial\mathbf{U}_\tau}{\partial t}(t)\right\|^2_{L^2(\Omega)},\forall t\in[t^n,t^{n+1}].$$

There are pointwise estimates for every $n$ that can be obtained by proving similar results to Propositions 3.23 and 3.25 presented in Section 3.4. The proof are formally the same and we write the corresponding propositions without presenting the demonstrations.

**Proposition 3.38** (Discrete error estimate)**.**
*Let $(\mathbf{u}_h^n,p_h^n)_{n=0}^N$ be the fully discretized solution of (3.64) and $(\mathbf{U}^n,P^n)_{n=0}^N$ its discrete Stokes reconstruction given by (3.66) and (3.67. Moreover, for any $0\le n\le N$, let $(\mathbf{w}^n,r^n)\in(H_0^1(\Omega))^2\times L_0^2(\Omega)$ the weak solution of the dual problem*

$$\begin{cases}-\mu\Delta\mathbf{w}^n+\nabla r^n=0, & in\ \Omega,\\ \operatorname{div}\mathbf{w}^n=p_h^n-P^n, & in\ \Omega,\\ \mathbf{w}^n=0, & on\ \partial\Omega.\end{cases}\tag{3.79}$$

*Then, there exists a constant $C$ that depends only on the reference triangle and $\Omega$ such that for every $0\le n\le N$*

$$\mu\|\nabla\mathbf{U}^n-\mathbf{u}_h^n\|^2_{L^2(\Omega)}+\frac{1}{\mu}\|P^n-p_h^n\|^2_{L^2(\Omega)}\le C\sum_{K\in\mathcal{T}_h}(\eta_{K,\mathbf{u}}^{A,n})^2+(\eta_{K,p}^{A,n})^2+(\eta_K^{\mathrm{div},n})^2,\tag{3.80}$$

*where we define for every $n=0,1,...N$*

$$(\eta_{K,\mathbf{u}}^{A,n})^2=\left(\|\mathbf{f}^n-\rho\partial\mathbf{u}_h^n+\mu\Delta\mathbf{u}_h^n-\nabla p_h^n\|_{L^2(K)}+\frac{1}{2\sqrt{\lambda_{2,K}}}\|[\mu\nabla\mathbf{u}_h^n\cdot\mathbf{n}]\|_{L^2(\partial K)}\right)\\ \omega_K\left(\left(\mathbf{U}^n-\mathbf{u}_h^n\right)(t)\right),$$

$$(\eta_{K,p}^{A,n})^2=\frac{1}{\mu}\left(\|\mathbf{f}^n-\rho\partial\mathbf{u}_h^n+\mu\Delta\mathbf{u}_h^n-\nabla p_h^n\|_{L^2(K)}+\frac{1}{2\sqrt{\lambda_{2,K}}}\|[\mu\nabla\mathbf{u}_h^n\cdot\mathbf{n}]\|_{L^2(\partial K)}\right)\\ \omega_K(\mathbf{w}^n),$$

$$(\eta_K^{\mathrm{div},n})^2(t)=\mu\|\operatorname{div}\mathbf{u}_h^n\|^2_{L^2(K)}.$$

**Proposition 3.39** (Dual estimates for the velocity)**.**
*Let* $(\mathbf{u}_h^n, p_h^n)_{n=0}^N$ *be the solution of the fully discretized problem (3.64) and* $(\mathbf{U}^n, P^n)_{n=0}^N$ *its Stokes reconstruction defined in (3.66) and (3.67). Then there exists a constant* $C > 0$ *independent of the mesh size but depending on the mesh aspect ratio and* $\Omega$ *such that for all* $0 \leq n \leq N$

$$\|\mathbf{u}_h^n - \mathbf{U}^n\|_{L^2(\Omega)}^2 \leq C \sum_{K \in \mathcal{T}_h} (\varepsilon_{K,\mathbf{u},0}^{I,n})^2, \tag{3.81}$$

*where*

$$(\varepsilon_{K,\mathbf{u},0}^{I,n})^2 = \frac{1}{\mu^2} h_K^4 \left\|\mathbf{f}^n - \rho \partial \mathbf{u}_h^n + \mu \Delta \mathbf{u}_h^n - \nabla p_h^n\right\|_{L^2(K)}^2 + \frac{1}{\mu} h_K^3 \left\|\nabla \mathbf{u}_h^n \cdot \mathbf{n}\right\|_{L^2(\partial K)}^2 + h_K^2 \left\|\operatorname{div} \mathbf{u}_h^n\right\|_{L^2(K)}^2,$$

*and for all* $0 \leq n \leq N-1$

$$\left\|\partial \mathbf{u}_h^{n+1} - \partial \mathbf{U}^{n+1}\right\|_{L^2(\Omega)}^2 \leq C \sum_{K \in \mathcal{T}_h} (\varepsilon_{K,\mathbf{u},1}^{I,n+1})^2, \tag{3.82}$$

*where*

$$(\varepsilon_{K,\mathbf{u},1}^{I,n+1})^2 = \frac{1}{\mu^2} h_K^4 \left\|\partial \mathbf{f}^{n+1} - \rho \partial^2 \mathbf{u}_h^{n+1} + \mu \Delta \partial \mathbf{u}_h^{n+1} - \nabla \partial p_h^{n+1}\right\|_{L^2(K)}^2 + \frac{1}{\mu} h_K^3 \left\|\nabla \partial \mathbf{u}_h^{n+1} \cdot \mathbf{n}\right\|_{L^2(\partial K)}^2 + h_K^2 \left\|\operatorname{div} \partial \mathbf{u}_h^{n+1}\right\|_{L^2(K)}^2.$$

We are now ready to prove an a posteriori error estimates for the numerical error $\mathbf{u} - \mathbf{u}_{h\tau}$ by combining Propositions 3.36, 3.38 and 3.39. We only need the following technical Lemma, whose proof can be found in [16].

**Lemma 3.40** (Equivalence between continuous and discrete norms)**.**
*Let* $(V^n)_{n=0}^N$, $V^n \in (H^1(\Omega))^{2+2}$, *a family of matrix valued functions, and* $V_\tau$ *defined by*

$$V_\tau(t) = V^n + (t - t^n) \frac{V^{n+1} - V^n}{\tau^{n+1}}, \quad t \in [t^n, t^{n+1}], n = 0, 1, .., N-1.$$

*Then the following inequality holds for all* $0 \leq n \leq N-1$

$$\frac{\tau^{n+1}}{6} \left( \left\|V^{n+1}\right\|_{L^2(\Omega)}^2 + \|V^n\|_{L^2(\Omega)}^2 \right) \leq \int_{t^n}^{t^{n+1}} \|V_\tau\|_{L^2(\Omega)}^2 \, dt \leq \frac{\tau^{n+1}}{2} \left( \left\|V^{n+1}\right\|_{L^2(\Omega)}^2 + \|V^n\|_{L^2(\Omega)}^2 \right).$$

*Moreover, we have for all* $1 \leq m \leq N$

$$\frac{1}{6} \sum_{n=0}^{m-1} \tau^{n+1} \|V^{n+1}\|_{L^2(\Omega)}^2 \leq \int_0^{t^m} \|V_\tau\|_{L^2(\Omega)}^2 dt \leq \frac{1+\sigma}{2} \sum_{n=0}^{m-1} \tau^{n+1} \|V^{n+1}\|_{L^2(\Omega)}^2 + \tau^1 \|V^0\|_{L^2(\Omega)}^2,$$

*where* $\sigma_\tau$ *is the regularization parameter defined by*

$$\sigma_\tau = \max_{0 \leq n \leq N-1} \frac{\tau^{n+1}}{\tau^n}. \tag{3.83}$$

*Proof.* By applying the Simpson rule, we get

$$\int_{t^n}^{t^{n+1}} \|V_\tau\|_{L^2(\Omega)}^2 \, dt = \frac{\tau^{n+1}}{3} \left( \left\|V^{n+1}\right\|_{L^2(\Omega)}^2 + \|V^n\|_{L^2(\Omega)}^2 + \int_\Omega V^{n+1} : V^n \right) d\mathbf{x}.$$

Using the inequalities $ab \leq \frac{1}{2}a^2 + \frac{1}{2}b^2$ and $ab \geq -\frac{1}{2}a^2 - \frac{1}{2}b^2$ yields

$$\frac{\tau^{n+1}}{6} \left( \left\|V^{n+1}\right\|_{L^2(\Omega)}^2 + \|V^n\|_{L^2(\Omega)}^2 \right) \leq \int_{t^n}^{t^{n+1}} \|V_\tau\|_{L^2(\Omega)}^2 \, dt \leq \frac{\tau^{n+1}}{2} \left( \left\|V^{n+1}\right\|_{L^2(\Omega)}^2 + \|V^n\|_{L^2(\Omega)}^2 \right).$$

Using the definition of $\sigma_\tau$ and summing over $n$ yield the second inequality. □

The a posteriori error estimate is contained in

**Theorem 3.41** (Fully discretized a posteriori error estimate for the the unsteady Stokes equations)**.**
*Let* $(\mathbf{u}, p)$ *be the solution of the unsteady Stokes equation* (3.26), $((\mathbf{u}_h^n, p_h^n))_{n=0}^N$ *be numerical solutions of the fully discretized problem* (3.64), *and* $((\mathbf{U}^n, P^n))_{n=0}^N$ *its the discrete Stokes reconstruction defined by (3.66) and (3.67). Finally let* $\mathbf{u}_{h\tau}$ *be the piecewise linear numerical reconstruction given by Definition 3.34. Then there exists* $C_0$ *that depends only on* $\Omega$, $C_1$ *only depending on the reference triangle and* $\Omega$ *and* $C_2 > 0$ *independent of the mesh size, but dependent on the mesh aspect ratio and* $\Omega$ *such that*

$$\begin{aligned}
&\rho\|(\mathbf{u}-\mathbf{u}_{h\tau})(T)\|_{L^2(\Omega)}^2 + \mu\int_0^T \|\nabla(\mathbf{u}-\mathbf{u}_{h\tau})(t)\|_{L^2(\Omega)}^2 dt \\
&\leq C_0\left(\rho\|\mathbf{u}_0-\mathbf{u}_h^0\|_{L^2(\Omega)}^2 + \frac{1}{\mu}\sum_{n=0}^{N-1}\int_{t^n}^{t^{n+1}} \|\mathbf{f}(t)-\mathbf{f}^{n+1}\|_{L^2(\Omega)}^2 dt + \mu\sum_{n=0}^{N-1}(\tau^{n+1})^3\|\nabla\partial\mathbf{u}_h^{n+1}\|_{L^2(\Omega)}^2 dt\right) \\
&\qquad + C_1\left(\sum_{K\in\mathcal{T}_h}\tau^1\left((\eta_{K,\mathbf{u}}^{A,0})^2 + (\eta_{K,p}^{A,0})^2 + (\eta_K^{\mathrm{div},0})^2\right)\right. \\
&\qquad \left. + \frac{1+\sigma_\tau}{2}\sum_{n=0}^{N-1}\sum_{K\in\mathcal{T}_h}\tau^{n+1}\left((\eta_{K,\mathbf{u}}^{A,n+1})^2 + (\eta_{K,p}^{A,n+1})^2 + (\eta_K^{\mathrm{div},n+1})^2\right)\right) \\
&\qquad C_2\left(\rho\sum_{K\in\mathcal{T}_h}(\varepsilon_{K,\mathbf{u},0}^{I,0})^2 + (\varepsilon_{K,\mathbf{u},0}^{I,N})^2 + \frac{\rho^2}{\mu}\sum_{n=0}^{N-1}\sum_{K\in\mathcal{T}_h}\tau^{n+1}(\varepsilon_{K,\mathbf{u},1}^{I,n+1})^2\right), \qquad (3.84)
\end{aligned}$$

*where* $\eta_{K,\mathbf{u}}^{A,n}, \eta_{K,p}^{A,n}, \eta_K^{\mathrm{div},n}$ *are given by Proposition 3.38,* $\varepsilon_{K,\mathbf{u},k}^{I,n}, k = 0, 1$, *is given by by Proposition 3.39 and we recall that the regularization parameter is defined by*

$$\sigma_\tau = \max_{0\leq n\leq N-1}\frac{\tau^{n+1}}{\tau^n}.$$

*Proof.* To simplify the writing, we denote by $c$ any positive constant, that is a pure numeric quantity (that is to say a given number, independent of any data, solutions, discretization parameters etc...) and whose value can change from line to line. Thanks to the triangle inequality, one can write

$$\begin{aligned}
&\rho\|(\mathbf{u}-\mathbf{u}_{h\tau})(T)\|_{L^2(\Omega)}^2 + \mu\int_0^T \|\nabla(\mathbf{u}-\mathbf{u}_{h\tau})(t)\|_{L^2(\Omega)}^2 dt \\
&\qquad \leq c\left(\rho\|(\mathbf{u}-\mathbf{U}_\tau)(T)\|_{L^2(\Omega)}^2 + \mu\int_0^T \|\nabla(\mathbf{u}-\mathbf{U}_\tau)(t)\|_{L^2(\Omega)}^2 dt\right. \\
&\qquad\qquad \left.\rho\|(\mathbf{U}_\tau-\mathbf{u}_{h\tau})(T)\|_{L^2(\Omega)}^2 + \mu\int_0^T \|\nabla(\mathbf{U}_\tau-\mathbf{u}_{h\tau})(t)\|_{L^2(\Omega)}^2 dt\right).
\end{aligned}$$

Thanks to Proposition 3.36, one can estimate the two first terms :

$$
\begin{aligned}
&\rho\|(\mathbf{u}-\mathbf{u}_{h\tau})(T)\|^2_{L^2(\Omega)} + \mu\int_0^T \|\nabla(\mathbf{u}-\mathbf{u}_{h\tau})(t)\|^2_{L^2(\Omega)}dt \\
&\quad \leq c\Bigg(\rho\|(\mathbf{u}-\mathbf{U}_\tau)(0)\|^2_{L^2(\Omega)} + \frac{\rho^2C_P^2}{\mu}\sum_{n=0}^{N-1}\int_{t^n}^{t^{n+1}} \|\mathbf{f}_\rho(t)-\mathbf{f}_\rho^{n+1}\|^2_{L^2(\Omega)}dt \\
&\qquad + \mu\sum_{n=0}^{N-1}(\tau^{n+1})^3\|\nabla\partial\mathbf{u}_h^{n+1}\|^2_{L^2(\Omega)}dt \\
&\qquad + \mu\sum_{n=0}^{N-1}\tau^{n+1}\|\nabla(\mathbf{U}^{n+1}-\mathbf{u}_h^{n+1})\|^2_{L^2(\Omega)} + \tau^{n+1}\|\nabla(\mathbf{U}^{n}-\mathbf{u}_h^{n})\|^2_{L^2(\Omega)} \\
&\qquad + \frac{\rho^2C_P^2}{\mu}\sum_{n=0}^{N-1}\tau^{n+1}\left\|\partial\mathbf{u}_h^{n+1}-\partial\mathbf{U}^{n+1}\right\|^2_{L^2(\Omega)} \\
&\qquad + \rho\|(\mathbf{U}_\tau-\mathbf{u}_{h\tau})(T)\|^2_{L^2(\Omega)} + \mu\int_0^T \|\nabla(\mathbf{U}_\tau-\mathbf{u}_{h\tau})(t)\|^2_{L^2(\Omega)}dt\Bigg).
\end{aligned}
$$

Thanks to Lemma 3.40, the third line of the right hand side and its last term can be put together, and splitting the initial error $\mathbf{u}(0)-\mathbf{U}_\tau(0) = \mathbf{u}(0)-\mathbf{U}^0 = \mathbf{u}(0)-\mathbf{u}_h^0+\mathbf{u}_h^0-\mathbf{U}^0$, it yields

$$
\begin{aligned}
&\rho\|(\mathbf{u}-\mathbf{u}_{h\tau})(T)\|^2_{L^2(\Omega)} + \mu\int_0^T \|\nabla(\mathbf{u}-\mathbf{u}_{h\tau})(t)\|^2_{L^2(\Omega)}dt \\
&\quad \leq c\Bigg(\rho\|\mathbf{u}(0)-\mathbf{u}_h^0\|^2_{L^2(\Omega)} + \frac{\rho^2C_P^2}{\mu}\sum_{n=0}^{N-1}\int_{t^n}^{t^{n+1}} \|\mathbf{f}_\rho(t)-\mathbf{f}_\rho^{n+1}\|^2_{L^2(\Omega)}dt \\
&\qquad + \mu\sum_{n=0}^{N-1}(\tau^{n+1})^3\|\nabla\partial\mathbf{u}_h^{n+1}\|^2_{L^2(\Omega)}dt + \mu\int_0^T \|\nabla(\mathbf{U}_\tau-\mathbf{u}_{h\tau})(t)\|^2_{L^2(\Omega)}dt \\
&\qquad + \frac{\rho^2C_P^2}{\mu}\sum_{n=0}^{N-1}\tau^{n+1}\left\|\partial\mathbf{u}_h^{n+1}-\partial\mathbf{U}^{n+1}\right\|^2_{L^2(\Omega)} \\
&\qquad + \rho\|\mathbf{U}^0-\mathbf{u}_h^0\|^2_{L^2(\Omega)} + \rho\|(\mathbf{U}^N-\mathbf{u}_h^N)\|^2_{L^2(\Omega)}\Bigg).
\end{aligned}
$$

Finally, using again the Lemma 3.40 on

$$
\mu\int_0^T \|\nabla(\mathbf{U}_\tau-\mathbf{u}_{h\tau})(t)\|^2_{L^2(\Omega)}dt,
$$

we obtain

$$
\begin{aligned}
&\rho\|(\mathbf{u}-\mathbf{u}_{h\tau})(T)\|^2_{L^2(\Omega)} + \mu\int_0^T \|\nabla(\mathbf{u}-\mathbf{u}_{h\tau})(t)\|^2_{L^2(\Omega)}dt \\
&\quad \leq c\Bigg(\rho\|\mathbf{u}(0)-\mathbf{u}_h^0\|^2_{L^2(\Omega)} + \frac{\rho^2C_P^2}{\mu}\sum_{n=0}^{N-1}\int_{t^n}^{t^{n+1}} \|\mathbf{f}_\rho(t)-\mathbf{f}_\rho^{n+1}\|^2_{L^2(\Omega)}dt \\
&+ \mu\sum_{n=0}^{N-1}(\tau^{n+1})^3\|\nabla\partial\mathbf{u}_h^{n+1}\|^2_{L^2(\Omega)}dt + \frac{(1+\sigma_\tau)}{2}\sum_{n=0}^{N-1}\tau^{n+1}\mu\|\nabla(\mathbf{U}^{n+1}-\mathbf{u}_h^{n+1})\|^2_{L^2(\Omega)} + \tau^1\mu\|\nabla(\mathbf{U}^0-\mathbf{u}_h^0)\|^2_{L^2(\Omega)} \\
&\qquad + \frac{\rho^2C_P^2}{\mu}\sum_{n=0}^{N-1}\tau^{n+1}\left\|\partial\mathbf{u}_h^{n+1}-\partial\mathbf{U}^{n+1}\right\|^2_{L^2(\Omega)} \\
&\qquad + \rho\|\mathbf{U}^0-\mathbf{u}_h^0\|^2_{L^2(\Omega)} + \rho\|(\mathbf{U}^N-\mathbf{u}_h^N)\|^2_{L^2(\Omega)}\Bigg).
\end{aligned}
$$

We conclude by using Proposition 3.38 and 3.39. □

We finish this section with some comments on the upper bound (3.84):

(1) As already commented for the semi-discrete case in Remark 3.28, the upper bound presented above is not fully computable since the Stokes reconstruction $(\mathbf{U}^n, P^n)$ is contained in the error indicators $\eta_{K,\mathbf{u}}^{A,n}$ and $\eta_{K,p}^{A,n}$. From a practical point of view, we do not take in consideration the error indicator for the pressure $\eta_{K,p}^{A,n}$ since it requires to solve the dual problem (3.79) and that for our purpose an error indicator for the velocity is judged sufficient. Then to make the error indicator $\eta_{K,\mathbf{u}}^{A,n}$ computable, we have to replace $\omega_K(\mathbf{U}^n - \mathbf{u}_h^n)$ by a good approximation, and as advocated in Remark 3.28, we replace $\mathbf{U}^n$ by the ZZ post-processing of $\mathbf{u}_h^n$ that is to say $\Pi_h^{ZZ}\mathbf{u}_h^n$. This choice will be also justified through the numerical experiments.

(2) Observe that the terms involving $\varepsilon_{K,\mathbf{u},k}^{I,n}$ for $k = 0, 1$, are of higher order (namely $O(h^2)$) compared to rest of the estimate. Since we are interesting to have a good indicator for the error norm $\left(\int_0^T \mu \|\nabla(\mathbf{u} - \mathbf{u}_{h\tau})\|_{L^2(\Omega)}^2 dt\right)^{1/2}$ that we check numerically to behave as $O(h + \tau)$, these terms can be neglected in practice.

(3) Note the presence of the regularization parameter $\sigma_\tau$, that is also present in the bounds derived in [16]. This size of $\sigma_\tau$ can be easily control in practice with an adaptive algorithm.

(4) Note finally the presence of the initial quantities

$$\|\mathbf{u}_0 - \mathbf{u}_h^0\|_{L^2(\Omega)}^2 \text{ and } \sum_{K \in \mathcal{T}_h} \tau^1 \left((\eta_{K,\mathbf{u}}^{A,0})^2 + (\eta_{K,p}^{A,0})^2 + (\eta_K^{\text{div},0})^2\right).$$

Since we assume $\mathbf{u}_0 \in (H^2(\Omega))^2$ and $\mathbf{u}_h^0 = r_h(\mathbf{u}_0)$ thanks to the Lagrange interpolation error estimate, the first quantity is of higher order (namely $O(h^2)$). For the second one, we can either heuristically not consider it, or in a adaptive algorithm, start with an initial grid and an initial time step that are fine enough to make it small.

## 3.6 A posteriori error estimates for the incompressible time dependent Navier-Stokes equations with constant coefficients: spatial approximation

In this section, we apply to the Navier-Stokes equations the techniques used to derive a posteriori error estimates for the Stokes equations, that is to say we reproduce the results that we obtain in the linear case for the nonlinear case. Before presenting the numerical methods, we state the exact equations we are interested to solve.

The problem is the following: let $\Omega$ be an open, connected, bounded, Lipschitz domain of $\mathbb{R}^d, d = 2, 3$, $0 < T \leq +\infty$ the final time, $\rho, \mu > 0$ standing respectively for the density and the viscosity, the force term $\mathbf{f} \in L^2(0, T; (L^2(\Omega))^2)$, and an initial condition $\mathbf{u}_0 \in (H_0^1(\Omega))^2$ such that $\operatorname{div} \mathbf{u}_0 = 0$. We are looking for $(\mathbf{u}, p) : \Omega \times (0, T] \to \mathbb{R}^d \times R$ the solution of the incompressible unsteady Navier-Stokes equations

$$\begin{cases} \rho \dfrac{\partial \mathbf{u}}{\partial t} + \rho(\mathbf{u} \cdot \nabla)\mathbf{u} - \mu \Delta \mathbf{u} + \nabla p = \mathbf{f}, & \text{in } \Omega \times (0, T), \\ \operatorname{div} \mathbf{u} = 0, & \text{in } \Omega \times (0, T), \\ \mathbf{u} = 0, & \text{on } \partial\Omega \times (0, T), \\ \mathbf{u}(\cdot, 0) = \mathbf{u}_0, & \text{in } \Omega. \end{cases} \tag{3.85}$$

The existence and the regularity of the solutions to the above equations is one of the most studied question in mathematics. We do not pretend to give here an exhaustive presentation of all the known results, but we briefly summarize those that are meaningful for our concerns. Existence of weak solutions to problem (3.85) was proven by J. Leray [21, 58, 99] in both dimensions 2 and 3. Moreover, theses solutions are global in time. In particular that means that if $T = +\infty$, then the solution are defined for any $t \geq 0$. In our settings, it reads: there exists a pair $(\mathbf{u}, p) \in L^\infty(0,T;(L^2(\Omega))^d) \cap L^2(0,T;(H_0^1(\Omega))^d) \times W^{-1,\infty}(0,T;L_0^2(\Omega))$ such that for almost every $t \in (0,T)$

$$\left(\rho\frac{\partial \mathbf{u}}{\partial t}, \mathbf{v}\right) + \rho\int_\Omega((\mathbf{u}\cdot\nabla)\mathbf{u})\cdot\mathbf{v}d\mathbf{x} + \mu\int_\Omega \nabla\mathbf{u} : \nabla\mathbf{v}d\mathbf{x}$$
$$-\int_\Omega p \operatorname{div}\mathbf{v}d\mathbf{x} = \int_\Omega \mathbf{f}\cdot\mathbf{v}d\mathbf{x}, \quad \forall \mathbf{v} \in (H_0^1(\Omega))^2,$$
$$-\int_\Omega q \operatorname{div}\mathbf{u}d\mathbf{x} = 0, \quad \forall q \in L_0^2(\Omega),$$

where $(\cdot,\cdot)$ stands for the duality pairing between $(H^{-1}(\Omega))^d$ and $(H_0^1(\Omega))^d$.

For the case $d = 2$, one can prove the uniqueness of the weak solution and the continuity with respect to the time of the velocity field, that is to say

$$\mathbf{u} \in C^0([0,T];(L^2(\Omega))^2).$$

Moreover, in the case $\Omega$ is a smooth or convex domain, one can even prove this well-known and spectacular result that the weak solution is in fact a "strong" solution. Indeed, one can prove the additional regularity

$$\mathbf{u} \in C^0([0,T];(H_0^1(\Omega))^2) \cap L^2(0,T;(H^2(\Omega))^2), \quad \frac{\partial \mathbf{u}}{\partial t} \in L^2(0,T;(L^2(\Omega))^2),$$
$$p \in L^2(0,T;H^1(\Omega)).$$

We have also that the time derivative satisfies the boundary conditions and the divergence equation for almost every $t \in (0,T)$, that is to say

$$\frac{\partial \mathbf{u}}{\partial t} = 0 \text{ on } \partial\Omega, \text{ and } \operatorname{div}\frac{\partial \mathbf{u}}{\partial t} = 0.$$

Moreover, the solutions are uniformly bounded in time, i.e. there exists a constant $C_{NS} > 0$ such that

$$\sup_{t\in(0,T)} \|\nabla\mathbf{u}(t)\|_{L^2(\Omega)} \leq C_{NS}. \tag{3.86}$$

We refer to [58] for more details on theses questions. Note that they are still results that hold globally in time, that is to say even in the case $T = +\infty$.

For $d = 3$, the situation is still an open problem. In general, weak solutions are not unique, and more regular solutions (that can be shown to be unique) are not global in time, unless if we assume that the force term $\mathbf{f}$ and the initial condition $\mathbf{u}_0$ are small enough. For more details, we refer to [21], [99] and [69]. To avoid problem of well-posedness for the three dimensional case, one can assume that the bound (3.86) holds *a priori*. This makes strong solutions exist globally, without requiring any conditions on the data [58].

The previous considerations are only a quick and non-exhaustive overview of the existing results about the regularity of the solutions to the Navier-Stokes equations. To simplify, and since we are mainly interested in their numerical approximation, we will always assume that these solutions are smooth enough for our needs. In particular, we require that

$$\frac{\partial \mathbf{u}}{\partial t} \in L^2(0,T;(L^2(\Omega))^2)$$

so that the duality pairing between $(H^{-1}(\Omega))^d$ and $(H_0^1(\Omega))^d$ can be written as the $L^2$ scalar product and the following weak formulation is valid:

$$\rho \int_\Omega \frac{\partial \mathbf{u}}{\partial t} \cdot \mathbf{v} dx + \rho \int_\Omega ((\mathbf{u} \cdot \nabla)\mathbf{u}) \cdot \mathbf{v} d\mathbf{x} + \mu \int_\Omega \nabla \mathbf{u} : \nabla \mathbf{v} d\mathbf{x}$$
$$- \int_\Omega p \operatorname{div} \mathbf{v} d\mathbf{x} = \int_\Omega \mathbf{f} \cdot \mathbf{v} d\mathbf{x}, \quad \forall \mathbf{v} \in (H_0^1(\Omega))^2,$$
$$- \int_\Omega q \operatorname{div} \mathbf{u} d\mathbf{x} = 0, \quad \forall q \in L_0^2(\Omega). \quad (3.87)$$

We first focus on the spatial approximation to the equations (3.87). By analogy with the numerical methods proposed in Section 3.1 for the steady Navier-Stokes equations and in the Section 3.4 for the unsteady Stokes equations, we approximate the equations with continuous, piecewise linear finite elements. From now we assume that $\Omega$ is a convex polygon in $\mathbb{R}^2$ and $\mathbf{f} \in C^0([0,T],(L^2(\Omega))^2)$. Our results are straightforwardly generalizable to $\mathbb{R}^3$ and the small modifications that occurs will be let in comments. Let $h > 0$ and $\mathcal{T}_h$ be a conformal triangulation of $\Omega$ with triangles $K$ of diameter $h_K \leq h$. Assuming now that $\mathbf{u}_0 \in (H^2(\Omega))^2$, we are looking for $(\mathbf{u}, p_h) : \Omega \times [0,T] \to \mathbb{R}^2 \times \mathbb{R}$ such that $(\mathbf{u}_h(t), p_h(t)) \in V_h \times Q_h$ for all $t \in [0,T]$, where $V_h$ and $Q_h$ are the functional spaces introduced in Section 3.1, $\mathbf{u}_h(0) = r_h(u_0)$ and for all $t \in [0,T]$

$$\rho \int_\Omega \frac{\partial \mathbf{u}_h}{\partial t} \cdot \mathbf{v}_h d\mathbf{x} + \rho \int_\Omega (\mathbf{u}_h \cdot \nabla)\mathbf{u}_h \cdot \mathbf{v}_h d\mathbf{x} + \mu \int_\Omega \nabla \mathbf{u}_h \cdot \nabla \mathbf{v}_h d\mathbf{x} - \int_\Omega p_h \operatorname{div} \mathbf{v}_h d\mathbf{x}$$
$$+ \sum_{K \in \mathcal{T}_h} \alpha_K \int_K \left( \mathbf{f} - \rho \frac{\partial \mathbf{u}_h}{\partial t} - \rho(\mathbf{u}_h \cdot \nabla)\mathbf{u}_h + \mu \Delta \mathbf{u}_h - \nabla p_h \right) \cdot \left( \rho(\mathbf{u}_h \cdot \nabla)\mathbf{v}_h - \mu \Delta \mathbf{v}_h \right) d\mathbf{x}$$
$$= \int_\Omega \mathbf{f} \cdot \mathbf{v}_h d\mathbf{x}, \quad \forall \mathbf{v}_h \in V_h,$$
$$- \int_\Omega q_h \operatorname{div} \mathbf{u}_h d\mathbf{x}$$
$$+ \sum_{K \in \mathcal{T}_h} \alpha_K \int_K \left( \mathbf{f} - \rho \frac{\partial \mathbf{u}_h}{\partial t} - \rho(\mathbf{u}_h \cdot \nabla)\mathbf{u}_h + \mu \Delta \mathbf{u}_h - \nabla p_h \right) \cdot \nabla q_h d\mathbf{x} = 0, \quad \forall q_h \in Q_h,$$
$$(3.88)$$

where $\alpha_K$ is given by

$$\alpha_K = \frac{\alpha \lambda_{2,K}^2}{\mu \xi(Re_K)}$$

with $\alpha > 0$ and

$$\xi(Re_K) = \begin{cases} 1 & \text{if } Re_K \leq 1, \\ Re_K & \text{if } Re_K \geq 1, \end{cases}$$

where we define the local anisotropic Reynolds number $Re_K$ by

$$Re_K = \frac{\rho \|\mathbf{u}_h\|_{L^\infty(K)} \lambda_{2,K}}{\mu}.$$

The numerical method reads the same if $\Omega \in \mathbb{R}^3$, the only change being that we write $\lambda_{3,K}$ in the definitions of $\alpha_K$ and $Re_K$ instead of $\lambda_{2,K}$. Note that here, and for future needs, we directly ask that the approximated equations (3.88) holds also at $t = 0$. The a priori error analysis of the numerical method (3.88) is not obvious task and we will assume, as we did for the linear case, that the numerical solution $(\mathbf{u}_h, p_h)$ converges to $(\mathbf{u}, p)$ as $h$ goes to 0. Moreover we assume that all the quantities of interests, that is to say the force term $\mathbf{f}$, the exact solution $(\mathbf{u}, p)$ and the numerical solution $(\mathbf{u}_h, p_h)$ are smooth enough to justify the future computations.

To prove an a posteriori error estimate for the semi-discrete numerical method (3.88), we proceed as we did for the unsteady Stokes equations and we define a suitable reconstruction $(\mathbf{U}, P)$ of the numerical approximation $(\mathbf{u}_h, p_h)$. Then, we estimate the error $\mathbf{u} - \mathbf{u}_h$ by splitting it between the continuous error $\mathbf{u} - \mathbf{U}$ and the discrete error $\mathbf{U} - \mathbf{u}_h$. By simplification, and since we are not interested in it, we do not treat the pressure errors. One choice to define the reconstruction $(\mathbf{U}, P)$ appears naturally. By analogy with the Stokes case, we define it for all $t$ as the solution of the steady Navier-Stokes equations

$$\begin{cases} \rho(\mathbf{U}(t) \cdot \nabla)\mathbf{U}(t) - \mu\Delta\mathbf{U}(t) + \nabla P(t) = \mathbf{f}(t) - \rho\dfrac{\partial \mathbf{u}_h}{\partial t}(t), & \text{in } \Omega, \\ \operatorname{div} \mathbf{U}(t) = 0, & \text{in } \Omega, \\ \mathbf{U}(t) = 0, & \text{on } \partial\Omega. \end{cases} \tag{3.89}$$

Note that the fact that the problem (3.89) is itself non linear implies that, for estimating the errors $\mathbf{u} - \mathbf{U}$ and $\mathbf{U} - \mathbf{u}_h$, we will have to bound in particular the differences of the non-linear terms.

$$(\mathbf{u} \cdot \nabla)\mathbf{u} - (\mathbf{U} \cdot \nabla)\mathbf{U}, \quad (\mathbf{U} \cdot \nabla)\mathbf{U} - (\mathbf{u}_h \cdot \nabla)\mathbf{u}_h.$$

Therefore, to simplify the treatment of the non-linear terms, one may use another choice for defining $(\mathbf{U}, P)$ and choose instead a linearized version of the reconstruction (3.89). This approach was first used in [107] (written in a sightly different way that the one proposed below), where they derived a posteriori error estimates for $\mathbb{P}^2 - \mathbb{P}^1$ isotropic finite elements. We apply the same techniques to the (anisotropic) stabilized numerical method (3.88). Observe that an other a posteriori error analysis for the time dependent Navier-Stokes equations was already performed in [106] using other techniques, in particular by mean of the Inverse Function Theorem.

For all $t \in [0, T]$, we define the linearized Navier-Stokes reconstruction of $(\mathbf{u}_h(t), p_h(t))$ as the unique weak solution $(\mathbf{U}(t), P(t))$ of the linear equations

$$\begin{cases} \rho(\mathbf{U}(t) \cdot \nabla)\mathbf{u}_h(t) + \rho(\mathbf{u}(t) \cdot \nabla)(\mathbf{U}(t) - \mathbf{u}_h(t)) - \mu\Delta\mathbf{U}(t) + \nabla P(t) \\ \qquad = \mathbf{f}(t) - \rho\dfrac{\partial \mathbf{u}_h}{\partial t}(t), & \text{in } \Omega, \\ \operatorname{div} \mathbf{U}(t) = 0, & \text{in } \Omega, \\ \mathbf{U}(t) = 0, & \text{on } \partial\Omega. \end{cases} \tag{3.90}$$

Note that the first terms of the momentum equation can also be written alternatively as

$$-\rho((\mathbf{u} - \mathbf{U}) \cdot \nabla)\mathbf{u}_h + \rho(\mathbf{u} \cdot \nabla)\mathbf{U}.$$

As anticipated, the motivation for the introduction of the linearized Navier-Stokes reconstruction (3.90) is that it yields a natural splitting for the treatment of the non-linearity due to the convection term. Indeed observe that

$$\begin{aligned} (\mathbf{u} \cdot \nabla)\mathbf{u} - (\mathbf{u}_h \cdot \nabla)\mathbf{u}_h &= (\mathbf{u} \cdot \nabla)\mathbf{u} - [(\mathbf{u} \cdot \nabla)\mathbf{U} - ((\mathbf{u} - \mathbf{U}) \cdot \nabla)\mathbf{u}_h] \\ &\quad + [(\mathbf{U} \cdot \nabla)\mathbf{u}_h + (\mathbf{u} \cdot \nabla)(\mathbf{U} - \mathbf{u}_h)] - (\mathbf{u}_h \cdot \nabla)\mathbf{u}_h \\ &= (\mathbf{u} \cdot \nabla)(\mathbf{u} - \mathbf{U}) + ((\mathbf{u} - \mathbf{U}) \cdot \nabla)\mathbf{u}_h \\ &\quad + ((\mathbf{U} - \mathbf{u}_h) \cdot \nabla)\mathbf{u}_h + (\mathbf{u} \cdot \nabla)(\mathbf{U} - \mathbf{u}_h). \end{aligned}$$

Thus, the error in the non-linear terms can be directly related to the errors $\mathbf{u} - \mathbf{U}$ and $\mathbf{U} - \mathbf{u}_h$ that will be estimated independently. This is the main technical advantage of (3.90) compared to (3.89).

Beyond these technicalities, we think important to make the following comment: in both cases, the fact that $(\mathbf{U}, P)$ is well-defined is linked to the well-posedness of problems (3.89) or (3.90). In particular, for (3.89), since we have to solve a steady Navier-Stokes equation, the uniqueness of the solutions requires that the terms in the right hand side, here $\mathbf{f}$ and $\dfrac{\partial \mathbf{u}_h}{\partial t}$, are "small" (see Proposition 3.3 in the Section 3.1). Imposing that $\mathbf{f}$ is small appears to be an important drawback of the reconstruction (3.89) since it's not necessar in the 2D situation to have a global and strong solutions to the Navier-Stokes equation (3.85). Therefore, we would have to work in a weaker framework that the one obtained in the theory. Unfortunately, for the moment, even with the linearized version (3.90), we cannot prove the existence of a well-defined pair $(\mathbf{U}, P)$ unless some restrictions on the size of the data or the solutions are made, as we show in the next proposition.

Let us write (3.90) under a weak formulation. It reads:

$$\begin{aligned}
&\rho \int_\Omega ((\mathbf{U}(t)\cdot\nabla)\mathbf{u}_h(t))\cdot\mathbf{v}d\mathbf{x} + \rho\int_\Omega ((\mathbf{u}(t)\cdot\nabla)(\mathbf{U}(t)-\mathbf{u}_h(t)))\cdot\mathbf{v}d\mathbf{x}\\
&+\mu\int_\Omega \nabla\mathbf{U}(t):\nabla\mathbf{v}d\mathbf{x} - \int_\Omega P(t)\operatorname{div}\mathbf{v}d\mathbf{x} = \int_\Omega\left(\mathbf{f}(t)-\rho\frac{\partial\mathbf{u}_h}{\partial t}(t)\right)\cdot\mathbf{v}d\mathbf{x},\quad \forall\mathbf{v}\in(H_0^1(\Omega))^2,\\
&-\int_\Omega q\operatorname{div}\mathbf{U}(t) = 0,\quad \forall q\in L_0^2(\Omega).
\end{aligned}\tag{3.91}$$

Then, under some restrictions on the mesh size and the size of the exact velocity field $\mathbf{u}$, one can ensures that, for all $t\in[0,T]$, there exists a unique weak solution $(\mathbf{U}(t), P(t)) \in (H_0^1(\Omega))^2\times L_0^2(\Omega)$ to the problem (3.87).

**Proposition 3.42.**
*Let $C_{SOB}$ be the constant in Proposition A.8 of the Appendix A.2. We assume that there exists $h_0>0$ and $0<\gamma<1$ such that for all $h\le h_0$*

$$\sup_{t\in(0,T)}\|\nabla\mathbf{u}_h(t)\|_{L^2(\Omega)} \le \frac{\gamma\mu}{\rho C_{SOB}}.\tag{3.92}$$

*Then for all $h\le h_0$ and for all $t\in[0,T]$, there exists a unique solution $(\mathbf{U}(t), P(t)) \in (H_0^1(\Omega))^2\times L_0^2(\Omega)$ to the problem (3.87).*

*Proof.* Let $h\le h_0$ and let us write the problem (3.91) in a more abstract form: for all $t\in[0,T]$ find $(\mathbf{U}(t), P(t))$ the solution of

$$\begin{cases} a(\mathbf{U}(t),\mathbf{v}) + b(\mathbf{v},P(t)) = F_t(\mathbf{v}), \forall\mathbf{v}\in(H_0^1(\Omega))^2,\\ b(\mathbf{U}(t),q)=0, \forall q\in L_0^2(\Omega),\end{cases}\tag{3.93}$$

where

$$a(\mathbf{U},\mathbf{v}) = \rho\int_\Omega((\mathbf{U}(t)\cdot\nabla)\mathbf{u}_h(t))\cdot\mathbf{v}d\mathbf{x} + \rho\int_\Omega((\mathbf{u}(t)\cdot\nabla)\mathbf{U}(t))\cdot\mathbf{v}d\mathbf{x} + \mu\int_\Omega\nabla\mathbf{U}(t):\nabla\mathbf{v}d\mathbf{x},$$

$$F_t(v) = \int_\Omega\left(\mathbf{f}(t) - \rho\frac{\partial\mathbf{u}_h}{\partial t}(t) + \rho(\mathbf{u}(t)\cdot\nabla)\mathbf{u}_h(t)\right)\cdot\mathbf{v}d\mathbf{x},$$

$$b(\mathbf{v},P(t)) = -\int_\Omega P(t)\operatorname{div}\mathbf{v}dx,\quad b(\mathbf{U}(t),q) = -\int_\Omega q\operatorname{div}\mathbf{U}(t).$$

Let us denote

$$V=\left\{\mathbf{v}\in(H_0^1(\Omega))^2 : \operatorname{div}\mathbf{v}=0\right\}$$

the subspace of $(H_0^1(\Omega))^2$ containing the free divergence vector fields. Note that $V$ is a close subspace of $(H_0^1(\Omega))^2$ and therefore is an Hilbert space. The idea of the proof is classical for this kind of problem and consists to take the test functions in $V$ rather than in $(H^1_0(\Omega))^2$ to eliminate the pressure from the first equation of (3.93) and after to recover it thanks to the inf-sup condition.

Observe indeed that if there exists $\mathbf{U}(t) \in V$ that is a solution to

$$a(\mathbf{U}(t), \mathbf{v}) = F_t(\mathbf{v}), \forall \mathbf{v} \in V, \tag{3.94}$$

then $b(\mathbf{U}(t), q) = 0, \forall q \in L^2_0(\Omega)$ is trivially satisfied and moreover by the inf-sup condition (3.2), there exists a unique $P(t) \in L^2_0(\Omega)$ that satisfies

$$b(P(t), \mathbf{v}) = F_t(\mathbf{v}) - a(\mathbf{U}(t), \mathbf{v}), \forall \mathbf{v} \in (H^1_0(\Omega))^2.$$

Therefore it is sufficient to show that (3.94) is uniquely solvable in $V$, that is the case thanks to the Lax-Milgram Lemma. Indeed, we immediately have that $F_t : V \to \mathbb{R}$ is linear and continuous and that $a : V \times V \to \mathbb{R}$ is bilinear and continuous. We only have to check the coercivity of $a$ to conclude the proof. This is done by observing first that the term

$$\rho \int_\Omega ((\mathbf{u}(t) \cdot \nabla)\mathbf{v}) \cdot \mathbf{v} d\mathbf{x} = 0, \forall \mathbf{v} \in V,$$

thanks to the divergence theorem and the fact that $\mathbf{u}$ is divergence free. It remains to prove that there exists $\alpha > 0$ such that

$$\mu \|\nabla \mathbf{U}\|^2_{L^2(\Omega)} + \rho \int_\Omega ((\mathbf{U} \cdot \nabla)\mathbf{u}_h(t)) \cdot \mathbf{U} d\mathbf{x} \geq \alpha \|\nabla \mathbf{U}\|^2_{L^2(\Omega)}.$$

Observe the easily fact that for any integrable function $f$, one have that

$$\int_\Omega f d\mathbf{x} \geq -\int_\Omega |f| d\mathbf{x}.$$

Therefore,

$$\rho \int_\Omega ((\mathbf{U} \cdot \nabla)\mathbf{u}_h(t)) \cdot \mathbf{U} d\mathbf{x} \geq -\rho \int_\Omega |((\mathbf{U} \cdot \nabla)\mathbf{u}_h(t)) \cdot \mathbf{U}| d\mathbf{x}.$$

Now, applying the Cauchy-Schwarz inequality in $\mathbb{R}^2$, the Proposition A.8 and the hypothesis (3.92) , one have that

$$-\rho \int_\Omega |((\mathbf{U} \cdot \nabla)\mathbf{u}_h(t)) \cdot \mathbf{U}| d\mathbf{x} \geq -\rho C_{SOB} \|\nabla \mathbf{u}_h(t)\|_{L^2(\Omega)} \|\nabla \mathbf{U}\|^2_{L^2(\Omega)} \geq -\gamma\mu \|\nabla \mathbf{U}(t)\|^2_{L^2(\Omega)}.$$

therefore,

$$\mu \|\nabla \mathbf{U}\|^2_{L^2(\Omega)} + \rho \int_\Omega ((\mathbf{U} \cdot \nabla)\mathbf{u}_h(t)) \cdot \mathbf{U} d\mathbf{x} \geq (\mu - \gamma\mu) \|\nabla \mathbf{U}\|^2_{L^2(\Omega)}.$$

Since $0 < \gamma < 1$ one have $\alpha = (1-\gamma)\mu > 0$. Then, all the assumptions to apply the Lax-Milgram Lemma are satisfied, and therefore there exists a unique $\mathbf{U}(t) \in V$ that is a solution to (3.93), that concludes the proof. □

**Remark 3.43.** (i) The above proposition is independent of the dimension and holds in general in $\mathbb{R}^d$ for $d = 2$ as $d = 3$.

(ii) The hypothesis (3.86) is valid if we assume the stronger convergence (that we think reasonable at least for smooth solution)

$$\sup_{t \in (0,T)} \|\nabla(\mathbf{u}(t) - \mathbf{u}_h(t))\|_{L^2(\Omega)} \to 0 \text{ as } h \to 0,$$

and the fact that the exact solution satisfies itself

$$\sup_{t \in (0,T)} \|\nabla \mathbf{u}(t)\|_{L^2(\Omega)} \leq \frac{\gamma' \mu}{\rho C_{SOB}},$$

for $0 < \gamma' < 1$, (that we think being also a reasonable assumption if we ask either that $\mathbf{f}$ and $\mathbf{u}_0$ are sufficiently "small" or that the final time $T$ is not too large.) Indeed, we have by triangle inequality that

$$\sup_{t\in(0,T)} \|\nabla \mathbf{u}_h(t)\|_{L^2(\Omega)} \leq \sup_{t\in(0,T)} \|\nabla(\mathbf{u}(t) - \mathbf{u}_h(t))\|_{L^2(\Omega)} + \sup_{t\in(0,T)} \|\nabla \mathbf{u}(t)\|_{L^2(\Omega)}$$
$$\leq \sup_{t\in(0,T)} \|\nabla(\mathbf{u}(t) - \mathbf{u}_h(t))\|_{L^2(\Omega)} + \frac{\gamma'\mu}{\rho C_{SOB}}.$$

Now, since $\nabla \mathbf{u}_h(t)$ converges to $\nabla \mathbf{u}(t)$ uniformly with respect to $t$, one can find $h_0 > 0$ small enough, such that for all $h \leq h_0$ one have

$$\sup_{t\in(0,T)} \|\nabla(\mathbf{u}(t) - \mathbf{u}_h(t))\|_{L^2(\Omega)} \leq \frac{\gamma''\mu}{C_{SOB}\rho},$$

where $0 < \gamma'' < 1 - \gamma'$ and therefore the hypothesis (3.86) is satisfied with

$$\gamma = \gamma'' + \gamma'.$$

(iii) We give more details about the second point above. In particular, assuming that

$$\sup_{t\in(0,T)} \|\nabla \mathbf{u}(t)\|_{L^2(\Omega)} \leq \frac{\gamma'\mu}{\rho C_{SOB}},$$

roughly speaking means that, up to constants, we ask that

$$\sup_{t\in(0,T)} \|\nabla \mathbf{u}(t)\|_{L^2(\Omega)} \leq \frac{1}{Re},$$

where $Re$ stands for the Reynolds numbers. This means that for high Reynolds number, we are able to prove the well-posedness of (3.91) only for very "small" solution of the Navier-Stokes equations (3.85).

We now successively prove an upper bound for the continuous error $\mathbf{u} - \mathbf{U}$ and for the discrete error $\mathbf{U} - \mathbf{u}_h$, where we choose $\mathbf{U}$ as the linearized reconstruction of $\mathbf{u}_h$ given by (3.91). To estimate these two quantities is rather a technical story, very close to the previous computations performed for the Stokes equations in the previous sections, the only differences being to bound the non-linearity. In a first reading, the discussion below can be skipped and we may go directly to the Theorem 3.49 that contains the final estimate for $\mathbf{u} - \mathbf{u}_h$

From this point, we make the two following assumptions:

(1) To keep the discussion in a simple framework, the exact solution $(\mathbf{u}, p)$ as its numerical approximation $(\mathbf{u}_h, p_h)$ and the linearized Navier-Stokes reconstruction $(\mathbf{U}(t), P(t))$ given by (3.91) are assumed to be smooth enough to justify the computations below and the existence of the estimates. For more details about the necessary regularity, we refer to the Section 3.4 where this question is briefly commented for the case of the Stokes equations.

(2) $\mathbf{u}_h$ is assumed to satisfy the "small size" hypothesis (3.92), since it is anyway necessary to the existence of the solutions of (3.91).

In particular from now, we assume that the mesh size $h$ is small enough to satisfy $h \leq h_0$, where $h_0$ is given in (3.92). Following the previous remark, we therefore prove all our estimates under the hypothesis of a small mesh size and a small exact solution (that is in fact equivalent to impose small data). Under this hypothesis, roughly speaking, proving estimate for the Navier-Stokes equations, is in fact only a matter of knowing how to prove the similar estimate for the linear Stokes equations of Section 3.4, since all the non-linear terms of the form

$$\rho \int_\Omega ((\mathbf{v} \cdot \nabla)\mathbf{u}_h)\mathbf{v} d\mathbf{x}$$

will be controlled by

$$\gamma\mu \|\nabla \mathbf{v}\|^2_{L^2(\Omega)},$$

that can be absorb in the $H^1$ semi-norm in the left hand side since $0 < \gamma < 1$. This is somewhere a "moral" of non-linear problem: to prove estimate, we must know how to do it for the linear equation and assume that the solution of the non-linear problem is "small" such that, roughly speaking, it stays close the solution of the linear problem.

The first estimate is contained in the Proposition 3.44 where we estimate the error $\mathbf{u} - \mathbf{U}$.

**Proposition 3.44** (Continuous error estimate)**.**
*Let $(\mathbf{u}, p)$ be the solution of (3.87), $(\mathbf{u}_h, p_h)$ the solution of the finite element scheme (3.88) and $(\mathbf{U}, P)$ the solution of the linearized reconstruction. We assume that the hypothesis of Proposition 3.42 are satisfied. Then, for any $h \leq h_0$ and any $t \in (0, T]$,*

$$\rho \|\mathbf{u} - \mathbf{U}(t)\|^2_{L^2(\Omega)} + \mu \int_0^t \|\nabla(\mathbf{u} - \mathbf{U})(s)\|^2_{L^2(\Omega)} ds \\ \leq \rho \|\mathbf{u} - \mathbf{U}(0)\|^2_{L^2(\Omega)} + \frac{\rho^2 C_P^2}{\mu(1-\gamma)^2} \int_0^t \left\| \frac{\partial(\mathbf{u}_h - \mathbf{U})}{\partial t}(s) \right\|^2_{L^2(\Omega)} ds, \quad (3.95)$$

*where $C_P$ is the Poincaré constant of $\Omega$.*

*Proof.* Taking the difference between (3.87) and (3.91) yields

$$\rho \int_\Omega \frac{\partial(\mathbf{u} - \mathbf{U})}{\partial t} \cdot \mathbf{v} d\mathbf{x} + \rho \int_\Omega ((\mathbf{u} \cdot \nabla)(\mathbf{u} - \mathbf{U})) \cdot \mathbf{v} d\mathbf{x} + \rho \int_\Omega ((\mathbf{u} - \mathbf{U}) \cdot \nabla \mathbf{u}_h) \cdot \mathbf{v} d\mathbf{x} \\ + \mu \int_\Omega \nabla(\mathbf{u} - \mathbf{U}) : \nabla \mathbf{v} d\mathbf{x} + \int_\Omega (p - P) \operatorname{div} \mathbf{v} d\mathbf{x} = \rho \int_\Omega \frac{\partial(\mathbf{u}_h - \mathbf{U})}{\partial t} \cdot \mathbf{v} d\mathbf{x}.$$

Choosing $\mathbf{v} = \mathbf{u} - \mathbf{U}$ and using the fact that $\operatorname{div} u = \operatorname{div} \mathbf{U} = 0$ the pressure term disappears and as computed several time before, we have

$$\int_\Omega ((\mathbf{u} \cdot \nabla)(\mathbf{u} - \mathbf{U})) \cdot \mathbf{v} d\mathbf{x} = 0$$

thanks to the boundary conditions. Therefore, it remains

$$\frac{\rho}{2} \frac{d}{dt} \|\mathbf{u} - \mathbf{U}(t)\|^2_{L^2(\Omega)} + \mu \|\nabla(\mathbf{u} - \mathbf{U})(t)\|^2_{L^2(\Omega)} \\ = \rho \int_\Omega \frac{\partial(\mathbf{u}_h - \mathbf{U})}{\partial t} \cdot (\mathbf{u} - \mathbf{U}) d\mathbf{x} - \rho \int_\Omega ((\mathbf{u} - \mathbf{U}) \cdot \nabla \mathbf{u}_h) \cdot (\mathbf{u} - \mathbf{U}) d\mathbf{x}.$$

Using Cauchy-Schwarz, Young's and Poincaré inequalities, and the Sobolev estimates of Proposition A.8, we obtain

$$\frac{\rho}{2} \frac{d}{dt} \|\mathbf{u} - \mathbf{U}(t)\|^2_{L^2(\Omega)} + \mu \|\nabla(\mathbf{u} - \mathbf{U})(t)\|^2_{L^2(\Omega)} \leq \frac{\rho C_P^2}{2(1-\gamma)\mu} \left\| \frac{\partial(\mathbf{u}_h - \mathbf{U})}{\partial t}(t) \right\|^2_{L^2(\Omega)} \\ + \frac{1-\gamma}{2} \mu \|\nabla(\mathbf{u} - \mathbf{U})(t)\|^2_{L^2(\Omega)} + \rho C_{SOB} \|\nabla \mathbf{u}_h(t)\|_{L^2(\Omega)} \|\nabla(\mathbf{u} - \mathbf{U})(t)\|^2_{L^2(\Omega)}.$$

Using the hypothesis on $\nabla \mathbf{u}_h$, one can pass all the gradient term to the left hand side, and we get

$$\frac{\rho}{2}\frac{d}{dt}\|\mathbf{u}-\mathbf{U}(t)\|_{L^2(\Omega)}^2+\frac{1-\gamma}{2}\mu\|\nabla(\mathbf{u}-\mathbf{U})(t)\|_{L^2(\Omega)}^2 \le \frac{\rho^2 C_P^2}{2(1-\gamma)\mu}\left\|\frac{\partial(\mathbf{u}_h-\mathbf{U})}{\partial t}(t)\right\|_{L^2(\Omega)}^2.$$

Since $1-\gamma<1$, one can write the last inequality as

$$\frac{\rho(1-\gamma)}{2}\frac{d}{dt}\|\mathbf{u}-\mathbf{U}(t)\|_{L^2(\Omega)}^2+\frac{1-\gamma}{2}\mu\|\nabla(\mathbf{u}-\mathbf{U})(t)\|_{L^2(\Omega)}^2 \le \frac{\rho^2 C_P^2}{2(1-\gamma)\mu}\left\|\frac{\partial(\mathbf{u}_h-\mathbf{U})}{\partial t}(t)\right\|_{L^2(\Omega)}^2.$$

We then conclude the proof by multiplying $\frac{2}{1-\gamma}$ and integrating from 0 to $t$. □

**Remark 3.45.**
It is possible to prove an estimate for $\mathbf{u}-\mathbf{U}$ without requiring that $\sup_{t\in(0,T)}\|\nabla \mathbf{u}_h(t)\|_{L^2(\Omega)}$ is small (note that in this case we have to assume the well-posedness of the linearized reconstruction (3.91)). Indeed, one have in fact that by Proposition A.8, in the Appendix

$$\begin{aligned}
&\frac{\rho}{2}\frac{d}{dt}\|\mathbf{u}-\mathbf{U}(t)\|_{L^2(\Omega)}^2+\mu\|\nabla(\mathbf{u}-\mathbf{U})(t)\|_{L^2(\Omega)}^2\\
&\qquad=\rho\int_\Omega \frac{\partial(\mathbf{u}-\mathbf{U})}{\partial t}\cdot(\mathbf{u}-\mathbf{U})d\mathbf{x}-\rho\int_\Omega((\mathbf{u}-\mathbf{U})\cdot\nabla\mathbf{u}_h)\cdot(\mathbf{u}-\mathbf{U})d\mathbf{x}\\
&\qquad\le \frac{\rho^2C_P^2}{\mu}\left\|\frac{\partial(\mathbf{u}_h-\mathbf{U})}{\partial t}\right\|_{L^2(\Omega)}^2+\frac{\mu}{4}\|\nabla(\mathbf{u}-\mathbf{U})\|^2\\
&\qquad\quad+\frac{C_{SOB}\rho^2\|\nabla\mathbf{u}_h\|_{L^2(\Omega)}^2}{\mu}\|\mathbf{u}-\mathbf{U}\|_{L^2(\Omega)}^2+\frac{\mu}{4}\|\nabla(\mathbf{u}-\mathbf{U})|_{L^2(\Omega)}^2.
\end{aligned}$$

Therefore it is possible to obtain a bound by a Gronwall's type argument applied to $\|\mathbf{u}-\mathbf{U}\|_{L^2(\Omega)}^2$ and we get

$$\begin{aligned}
&\rho\|\mathbf{u}-\mathbf{U}(t)\|_{L^2(\Omega)}^2+\mu\int_0^t\|\nabla(\mathbf{u}-\mathbf{U})(s)\|_{L^2(\Omega)}^2ds\\
&\le \exp\left(C_{SOB}\frac{\rho^2}{\mu}\int_0^t\|\nabla\mathbf{u}_h(s)\|_{L^2(\Omega)}^2ds\right)\left(\rho\|\mathbf{u}-\mathbf{U}(0)\|_{L^2(\Omega)}^2+\frac{\rho^2C_P^2}{\mu}\int_0^t\left\|\frac{\partial(\mathbf{u}_h-\mathbf{U})}{\partial t}(s)\right\|_{L^2(\Omega)}^2ds\right).
\end{aligned}$$

The quantity

$$\int_0^t\|\nabla\mathbf{u}_h(s)\|_{L^2(\Omega)}^2ds$$

should be estimated through a stability analysis of the method (3.88) that we do not pretend to perform. However, assuming the convergence of the numerical method, one can estimate it as

$$\int_0^t\|\nabla\mathbf{u}_h(s)\|_{L^2(\Omega)}^2ds\le 2\int_0^t\|\nabla\mathbf{u}(s)\|_{L^2(\Omega)}^2ds+2\int_0^t\|\nabla(\mathbf{u}-\mathbf{u}_h)(s)\|_{L^2(\Omega)}^2ds.$$

The convergence assumption implies that there exists $h_0$ such that for all $h\le h_0$

$$\int_0^t\|\nabla(\mathbf{u}-\mathbf{u}_h)(s)\|_{L^2(\Omega)}^2ds\le\int_0^t\|\nabla\mathbf{u}(s)\|_{L^2(\Omega)}^2ds$$

that yields

$$\int_0^t\|\nabla\mathbf{u}_h(s)\|_{L^2(\Omega)}^2ds\le 4\int_0^t\|\nabla\mathbf{u}(s)\|_{L^2(\Omega)}^2ds.$$

Now, as we did for the Stokes equations, we estimate the error between $\mathbf{U}$ and $\mathbf{u}_h$. The bound is contained in the next proposition.

**Proposition 3.46** (Discrete error estimate)**.**
*Let* $(\mathbf{u}, p)$ *be the solution of (3.87),* $(\mathbf{u}_h, p_h)$ *the solution of the finite element scheme (3.88) and* $(\mathbf{U}, P)$ *the solution of the linearized reconstruction. We assume that the hypothesis of Proposition 3.42 are satisfied. In particular, we assume that there exists* $0 < \gamma < 1$

$$\sup_{t\in(0,T)} \|\nabla \mathbf{u}(t)\|_{L^2(\Omega)} \leq \frac{\gamma\mu}{\rho C_{SOB}},$$

*and that there exists* $h_0 > 0$ *such that for all* $h \leq h_0$

$$\sup_{t\in(0,T)} \|\nabla \mathbf{u}_h(t)\|_{L^2(\Omega)} \leq \frac{\gamma\mu}{\rho C_{SOB}},$$

*where* $C_{SOB}$ *is the Sobolev constant of Proposition A.8 of the Appendix A.2. Finally, let* $(\mathbf{w}, r) \in (H^1_0(\Omega))^2 \times L^2_0(\Omega)$ *the weak solution of the dual problem*

$$\begin{cases} -\mu\Delta\mathbf{w} + \nabla r = 0, & \text{in } \Omega, \\ \operatorname{div}\mathbf{w} = p_h - P, & \text{in } \Omega, \\ \mathbf{w} = 0, & \text{on } \partial\Omega. \end{cases} \tag{3.96}$$

*Then, there exists a constant* $C > 0$ *depending only on* $\Omega$ *and the reference triangle such that for any* $h \leq h_0$ *and any* $t \in [0, T]$

$$\mu\|\nabla(\mathbf{U}-\mathbf{u}_h)(t)\|^2_{L^2(\Omega)} + \frac{1}{\mu}\|P - p_h(t)\|^2_{L^2(\Omega)} \leq \frac{C}{(1-\gamma)^2} \sum_{K\in\mathcal{T}_h} (\eta^A_{K,\mathbf{u}})^2(t) + (\eta^A_{K,p})^2(t) + (\eta^{\text{div}}_K)(t)^2, \tag{3.97}$$

*where*

$$(\eta^A_{K,\mathbf{u}})^2 = \left(\left\|\mathbf{f} - \rho\frac{\partial \mathbf{u}_h}{\partial t} - \rho(\mathbf{u}_h\cdot\nabla)\mathbf{u}_h + \mu\Delta\mathbf{u}_h - \nabla p_h\right\|_{L^2(K)} + \frac{1}{2\sqrt{\lambda_{2,K}}}\|[\mu\nabla\mathbf{u}_h\cdot\mathbf{n}]\|_{L^2(\partial K)}\right)\omega_K(\mathbf{u}-\mathbf{u}_h),$$

$$(\eta^A_{K,p})^2 = \frac{1}{\mu}\left(\left\|\mathbf{f} - \rho\frac{\partial \mathbf{u}_h}{\partial t} - \rho(\mathbf{u}_h\cdot\nabla)\mathbf{u}_h + \mu\Delta\mathbf{u}_h - \nabla p_h\right\|_{L^2(K)} + \frac{1}{2\sqrt{\lambda_{2,K}}}\|[\mu\nabla\mathbf{u}_h\cdot\mathbf{n}]\|_{L^2(\partial K)}\right)\omega_K(\mathbf{w}),$$

$$(\eta^{\text{div}}_K)^2(t) = \mu\|\operatorname{div}\mathbf{u}_h(t)\|^2_{L^2(K)}.$$

*Proof.* To lighten the notations, we do not write the explicit dependence on $t$ of the function,since every quantity is evaluated at the same time. In what follows, we denote by $C$ or $\tilde{C}$ any positive constant that may depends only on the reference triangle or $\Omega$ and which values can change from line to line. We proceed as in Theorem 3.6 and first provide an estimate for the velocity

*Step 1. Estimate for* $\mathbf{U} - \mathbf{u}_h$.

$$
\begin{aligned}
\mu\|\nabla(\mathbf{U}-\mathbf{u}_h)\|^2_{L^2(\Omega)} &= \int_\Omega \mu\nabla(\mathbf{U}-\mathbf{u}_h):\nabla(\mathbf{U}-\mathbf{u}_h)d\mathbf{x} \\
&+ \int_\Omega (P-p_h)\operatorname{div}(\mathbf{U}-\mathbf{u}_h)d\mathbf{x} - \int_\Omega (P-p_h)\operatorname{div}(\mathbf{U}-\mathbf{u}_h)d\mathbf{x} \\
&+ \rho\int_\Omega ((\mathbf{U}\cdot\nabla)\mathbf{u}_h)\cdot(\mathbf{U}-\mathbf{u}_h)d\mathbf{x} - \rho\int_\Omega ((\mathbf{U}\cdot\nabla)\mathbf{u}_h)\cdot(\mathbf{U}-\mathbf{u}_h)d\mathbf{x} \\
&+ \rho\int_\Omega ((\mathbf{u}\cdot\nabla)(\mathbf{U}-\mathbf{u}_h)\cdot(\mathbf{U}-\mathbf{u}_h)d\mathbf{x} \\
&+ \rho\int_\Omega ((\mathbf{u}_h\cdot\nabla)\mathbf{u}_h)\cdot(\mathbf{U}-\mathbf{u}_h)d\mathbf{x} - \rho\int_\Omega ((\mathbf{u}_h\cdot\nabla)\mathbf{u}_h)\cdot(\mathbf{U}-\mathbf{u}_h)d\mathbf{x}.
\end{aligned}
$$

Note that in the the fourth line of the above equality, the term

$$
\rho\int_\Omega ((\mathbf{u}\cdot\nabla)(\mathbf{U}-\mathbf{u}_h))\cdot(\mathbf{U}-\mathbf{u}_h)d\mathbf{x} = 0
$$

thanks to boundary conditions and the fact that $\mathbf{u}$ is divergence free. Therefore, we do not have to add it and subtract it as we did for the other terms. Using the fact that $(\mathbf{U}, P)$ is the solution of the problem (3.91), it yields

$$
\begin{aligned}
\mu\|\nabla(\mathbf{U}-\mathbf{u}_h)\|^2_{L^2(\Omega)} &= \int_\Omega \left(\mathbf{f}-\rho\frac{\partial \mathbf{u}_h}{\partial t}\right)\cdot(\mathbf{U}-\mathbf{u}_h)d\mathbf{x} - \rho\int_\Omega ((\mathbf{u}_h\cdot\nabla)\mathbf{u}_h)\cdot(\mathbf{U}-\mathbf{u}_h)d\mathbf{x} \\
&- \mu\int_\Omega \nabla\mathbf{u}_h:\nabla(\mathbf{U}-\mathbf{u}_h)d\mathbf{x} + \int_\Omega p_h\operatorname{div}(\mathbf{U}-\mathbf{u}_h) \\
&+ \int_\Omega (P-p_h)\operatorname{div}\mathbf{u}_h d\mathbf{x} - \rho\int_\Omega ((\mathbf{U}-\mathbf{u}_h)\cdot\nabla)\mathbf{u}_h)\cdot(\mathbf{U}-\mathbf{u}_h)d\mathbf{x}.
\end{aligned}
$$

Thanks to the numerical method (3.88), one can remove any test functions $(\mathbf{v}_h, q_h)$, and integrating by parts it yields

$$
\begin{aligned}
\mu\|\nabla(\mathbf{U}-\mathbf{u}_h)\|^2_{L^2(\Omega)} &= \sum_{K\in\mathcal{T}_h}\int_K \left(\mathbf{f}-\rho\frac{\partial \mathbf{u}_h}{\partial t}-\rho(\mathbf{u}_h\cdot)\nabla\mathbf{u}_h+\mu\Delta\mathbf{u}_h-\nabla p_h\right)\cdot(\mathbf{U}-\mathbf{u}_h-\mathbf{v}_h)d\mathbf{x} \\
&+ \frac{1}{2}\sum_{K\in\mathcal{T}_h}\int_{\partial K}[\mu\nabla\mathbf{u}_h\cdot\mathbf{n}]\cdot(\mathbf{U}-\mathbf{u}_h-\mathbf{v}_h)d\mathbf{x} \\
+ \sum_{K\in\mathcal{T}_h}\alpha_K\int_K &\left(\mathbf{f}-\rho\frac{\partial \mathbf{u}_h}{\partial t}-\rho(\mathbf{u}_h\cdot)\nabla\mathbf{u}_h+\mu\Delta\mathbf{u}_h-\nabla p_h\right)\cdot(\rho(\mathbf{u}_h\cdot)\nabla\mathbf{v}_h-\mu\Delta\mathbf{v}_h+\nabla q_h)d\mathbf{x} \\
&+ \int_\Omega (P-p_h-q_h)\operatorname{div}\mathbf{u}_h d\mathbf{x} - \rho\int_\Omega ((\mathbf{U}-\mathbf{u}_h)\cdot\nabla)\mathbf{u}_h)\cdot(\mathbf{U}-\mathbf{u}_h)d\mathbf{x}.
\end{aligned}
$$

Choosing $\mathbf{v}_h = R_h(\mathbf{U}-\mathbf{u}_h)$ and $q_h = 0$, Cauchy-Schwarz inequality ad interpolation error estimates yield that there exist $C > 0$ depending only on the reference triangle such that

$$
\begin{aligned}
\mu\|\nabla(\mathbf{U}-\mathbf{u}_h)\|^2_{L^2(\Omega)} \le C\sum_{K\in\mathcal{T}_h}\nu_K\omega_K(\mathbf{U}-\mathbf{u}_h) + \|P-p_h\|_{L^2(\Omega)}\|\operatorname{div}\mathbf{u}_h\|_{L^2(\Omega)} \\
+ \rho\|\nabla\mathbf{u}_h\|_{L^2(\Omega)}\|\mathbf{U}-\mathbf{u}_h\|^2_{L^2(\Omega)},
\end{aligned}
$$

where we note

$$
\nu_K = \left\|\mathbf{f}-\rho\frac{\partial \mathbf{u}_h}{\partial t}-\rho(\mathbf{u}_h\cdot\nabla)\mathbf{u}_h+\mu\Delta\mathbf{u}_h-\nabla p_h\right\|_{L^2(\Omega)} + \frac{1}{2\sqrt{\lambda_{2,K}}}\|[\mu\nabla\mathbf{u}_h\cdot\mathbf{n}]\|_{L^2(\partial K)}\cdot
$$

Observe that, as we did in Theorem 3.4, the stabilization terms are put into the residual term $\nu_K\omega_K(\mathbf{U}-\mathbf{u}_h)$ thanks to our choice for $\alpha_K$. Finally, thanks to the hypothesis on

$\|\nabla \mathbf{u}_h\|_{L^2(\Omega)}$ one can pass the last term of the right hand side into the left one and we obtain that

$$\mu\|\nabla(\mathbf{U}-\mathbf{u}_h)\|^2_{L^2(\Omega)} \leq \frac{C}{1-\gamma}\sum_{K\in\mathcal{T}_h}\nu_K\omega_K(\mathbf{U}-\mathbf{u}_h)+\frac{1}{1-\gamma}\|P-p_h\|_{L^2(\Omega)}\|\operatorname{div}\mathbf{u}_h\|_{L^2(\Omega)}. \tag{3.98}$$

*Step 2. Estimate for $P-p_h$.* We now consider the dual problem (3.96) to recover an estimate for the pressure error. We have

$$\begin{aligned}
\int_\Omega (P-p_h)^2 d\mathbf{x} &= -\int_\Omega (P-p_h)\operatorname{div}\mathbf{w}d\mathbf{x} = -\int_\Omega P\operatorname{div}\mathbf{w}d\mathbf{x} + \int_\Omega p_h \operatorname{div}\mathbf{w}d\mathbf{x}\\
&= \int_\Omega \left(\mathbf{f}-\rho\frac{\partial \mathbf{u}_h}{\partial t}\right)\cdot\mathbf{w}d\mathbf{x} - \rho\int_\Omega ((\mathbf{U}\cdot\nabla)\mathbf{u}_h)\cdot\mathbf{w}d\mathbf{x} - \rho\int_\Omega (\mathbf{u}\cdot\nabla(\mathbf{U}-\mathbf{u}_h))\cdot\mathbf{w}d\mathbf{x}\\
&\quad -\mu\int_\Omega \nabla\mathbf{U}:\nabla\mathbf{w}d\mathbf{x} + \int_\Omega p_h\operatorname{div}\mathbf{w}d\mathbf{x}\\
&= \int_\Omega \left(\mathbf{f}-\rho\frac{\partial \mathbf{u}_h}{\partial t}\right)\cdot\mathbf{w}d\mathbf{x} - \rho\int_\Omega ((\mathbf{u}_h\cdot\nabla)\mathbf{u}_h)\cdot\mathbf{w}d\mathbf{x} - \mu\int_\Omega \nabla\mathbf{u}_h:\nabla\mathbf{w}d\mathbf{x} + \int_\Omega p_h\operatorname{div}\mathbf{w}d\mathbf{x}\\
&\quad +\rho\int_\Omega ((\mathbf{u}_h\cdot\nabla)\mathbf{u}_h - (\mathbf{U}\cdot\nabla)\mathbf{u}_h - (\mathbf{u}\cdot\nabla)(\mathbf{U}-\mathbf{u}_h))\cdot\mathbf{w}d\mathbf{x} - \mu\int_\Omega \nabla(\mathbf{U}-\mathbf{u}_h):\nabla\mathbf{w}d\mathbf{x}\\
&= \int_\Omega \left(\mathbf{f}-\rho\frac{\partial \mathbf{u}_h}{\partial t}\right)\cdot\mathbf{w}d\mathbf{x} - \rho\int_\Omega ((\mathbf{u}_h\cdot\nabla)\mathbf{u}_h)\cdot\mathbf{w}d\mathbf{x} - \mu\int_\Omega \nabla\mathbf{u}_h:\nabla\mathbf{w}d\mathbf{x} + \int_\Omega p_h\operatorname{div}\mathbf{w}d\mathbf{x}\\
&\quad -\rho\int_\Omega (((\mathbf{U}-\mathbf{u}_h)\cdot\nabla)\mathbf{u}_h + (\mathbf{u}\cdot\nabla)(\mathbf{U}-\mathbf{u}_h))\cdot\mathbf{w}d\mathbf{x} - \mu\int_\Omega \nabla(\mathbf{U}-\mathbf{u}_h):\nabla\mathbf{w}d\mathbf{x}.
\end{aligned}$$

Removing the test function $\mathbf{v}_h = R_h(\mathbf{w})$, integrating by part, using Cauchy-Swchwarz, Sobolev and interpolation inequalities, and absorbing the stabilization terms, we obtain finally that

$$\begin{aligned}
\|P-p_h\|^2_{L^2(\Omega)} &\leq C\sum_{K\in\mathcal{T}_h}\nu_K\omega_K(\mathbf{w}) + \mu\|\nabla(\mathbf{U}-\mathbf{u}_h)\|_{L^2(\Omega)}\|\nabla\mathbf{w}\|_{L^2(\Omega)}\\
&\quad + \rho C_{SOB}(\|\nabla\mathbf{u}_h\|_{L^2(\Omega)} + \|\nabla\mathbf{u}\|_{L^2(\Omega)})\|\nabla(\mathbf{U}-\mathbf{u}_h)\|_{L^2(\Omega)}\|\nabla\mathbf{w}\|_{L^2(\Omega)}.
\end{aligned}$$

Since by hypothesis, both $\mathbf{u}_h$ and $\mathbf{u}$ satisfy

$$\sup_{t\in(0,T)}\|\nabla\mathbf{u}(t)\|_{L^2(\Omega)},\ \sup_{t\in(0,T)}\|\nabla\mathbf{u}_h(t)\|_{L^2(\Omega)} \leq \frac{\mu}{\rho C_{SOB}},$$

we finally obtain that

$$\|P-p_h\|^2_{L^2(\Omega)} \leq C\sum_{K\in\mathcal{T}_h}\nu_K\omega_K(\mathbf{w}) + 3\mu\|\nabla(\mathbf{U}-\mathbf{u}_h)\|_{L^2(\Omega)}\|\nabla\mathbf{w}\|_{L^2(\Omega)}.$$

We recall that the following a priori estimate is valid for the dual problem (3.96):

$$\|\nabla\mathbf{w}\|_{L^2(\Omega)} \leq C\|P-p_h\|_{L^2(\Omega)}.$$

Then Young's inequality implies

$$\|P-p_h\| \leq \tilde{C}\left(\sum_{K\in\mathcal{T}_h}\nu_K\omega_K(\mathbf{w}) + \mu^2\|\nabla(\mathbf{U}-\mathbf{u}_h)\|^2_{L^2(\Omega)}\right)^{1/2}. \tag{3.99}$$

*Step 3. Putting all together* Plugging (3.99) into (3.98) yields

$$\mu\|\nabla(\mathbf{U}-\mathbf{u}_h)\|^2_{L^2(\Omega)} \le \frac{C}{1-\gamma}\sum_{K\in\mathcal{T}_h}\nu_K\omega_K(\mathbf{U}-\mathbf{u}_h)$$
$$+\frac{\tilde{C}}{1-\gamma}\left(\sum_{K\in\mathcal{T}_h}\nu_K\omega_K(\mathbf{w})+\mu^2\|\nabla(\mathbf{U}-\mathbf{u}_h)\|^2_{L^2(\Omega)}\right)^{1/2}\|\operatorname{div}\mathbf{u}_h\|_{L^2(\Omega)}.$$

Young's inequality implies

$$\mu\|\nabla(\mathbf{U}-\mathbf{u}_h)\|^2_{L^2(\Omega)} \le \frac{C}{1-\gamma}\sum_{K\in\mathcal{T}_h}\nu_K\omega_K(\mathbf{U}-\mathbf{u}_h)$$
$$+\frac{\tilde{C}}{2\varepsilon(1-\gamma)}\sum_{K\in\mathcal{T}_h}\nu_K\omega_K(\mathbf{w})++\frac{\tilde{C}}{2\varepsilon(1-\gamma)}\mu^2\|\nabla(\mathbf{U}-\mathbf{u}_h)\|^2_{L^2(\Omega)}+\frac{\tilde{C}\varepsilon}{2(1-\gamma)}\|\operatorname{div}\mathbf{u}_h\|^2_{L^2(\Omega)}.$$

Choosing $\varepsilon=\dfrac{\tilde{C}\mu}{1-\gamma}$, passing the gradient term to the left hand side and using the fact that $\dfrac{1}{1-\gamma}\le\dfrac{1}{(1-\gamma)^2}$ yields

$$\mu\|\nabla(\mathbf{U}-\mathbf{u}_h)\|^2_{L^2(\Omega)} \le \frac{C}{(1-\gamma)^2}\sum_{K\in\mathcal{T}_h}\nu_K\omega_K(\mathbf{U}-\mathbf{u}_h)+\frac{1}{\mu}\nu_K\omega_K(\mathbf{w})+\mu\|\operatorname{div}\mathbf{u}_h\|^2_{L^2(K)}.$$

Plugging back the last estimate into (3.99) yields the result. □

To provide the final a posteriori error estimate for the velocity error $\mathbf{u}-\mathbf{u}_h$, it remains to prove estimates for the $L^2$ norms

$$\|\mathbf{U}-\mathbf{u}_h\|_{L^2(\Omega)},\quad \left\|\frac{\partial\mathbf{u}_h}{\partial t}-\frac{\partial\mathbf{U}}{\partial t}\right\|_{L^2(\Omega)},$$

since they are contained in (3.95) (the $L^2$ norm $\mathbf{U}-\mathbf{u}_h$ is hidden in $\mathbf{u}(0)-\mathbf{U}(0)$ that has to be split into $\mathbf{u}(0)-\mathbf{u}_h(0)$ and $\mathbf{u}_h(0)-\mathbf{U}(0)$). This is done through a dual argument and the use of the orthogonility between $\mathbf{U}$ and $\mathbf{u}_h$ as we did for the Stokes equations. The only difference here is that we have to tackle the issue coming from the non-linearity when differentiating the weak forms with respect to the time variable. The result is contained in the next proposition for which we need use the following dual problem to derive the estimates: for any $\mathbf{g}\in(L^2(\Omega))^2$, and for all $t\in[0,T]$, let $(\mathbf{w}(t),r(t))\in(H^1_0(\Omega))^2\times L^2_0(\Omega)$ the weak solution of

$$\rho\int_\Omega((\mathbf{u}(t)\cdot\nabla)\mathbf{v})\cdot\mathbf{w}(t)d\mathbf{x}+\rho\int_\Omega((\mathbf{v}\cdot\nabla)\mathbf{u}_h(t))\cdot\mathbf{w}(t)d\mathbf{x}+\mu\int_\Omega\nabla\mathbf{w}(t):\nabla\mathbf{v}d\mathbf{x}$$
$$-\int_\Omega r(t)\operatorname{div}\mathbf{v}d\mathbf{x}=\int_\Omega\mathbf{g}\cdot\mathbf{v}d\mathbf{x},\forall\mathbf{v}\in(H^1_0(\Omega))^2,$$
$$\int_\Omega q\operatorname{div}\mathbf{w}(t)d\mathbf{x}=0,\forall q\in L^2_0(\Omega).\quad(3.100)$$

By hypothesis on $\mathbf{u}$ and $\mathbf{u}_h$, the same argument that the one advanced in the proof of Proposition 3.42 ensures that the problem (3.100) is well-posed and that the following a priori estimate holds for any $t$

$$\mu\|\nabla\mathbf{w}(t)\|_{L^2(\Omega)}+\|r(t)\|_{L^2(\Omega)}\le\frac{C}{1-\gamma}\|\mathbf{g}\|_{L^2(\Omega)},$$

where $C$ depends only on $\Omega$. Moreover, we can show that $(\mathbf{w}, r) \in (H^2(\Omega))^2 \times H^1(\Omega)$. Indeed, observe that $(\mathbf{w}, r)$ satisfies the (weak) Stokes problem

$$\mu \int_\Omega \nabla \mathbf{w}(t) : \nabla \mathbf{v} d\mathbf{x} - \int_\Omega r(t) \operatorname{div} \mathbf{v} d\mathbf{x} = \int_\Omega \mathbf{g} \cdot \mathbf{v} d\mathbf{x}$$
$$- \rho \int_\Omega ((\mathbf{u}(t) \cdot \nabla)\mathbf{v}) \cdot \mathbf{w}(t) d\mathbf{x} - \rho \int_\Omega ((\mathbf{v} \cdot \nabla)\mathbf{u}_h(t)) \cdot \mathbf{w}(t) d\mathbf{x}, \forall \mathbf{v} \in (H_0^1(\Omega))^2,$$
$$\int_\Omega q \operatorname{div} \mathbf{w}(t) d\mathbf{x} = 0, \forall q \in L_0^2(\Omega).$$

Integrating by parts the right hand side, it can be written as

$$\mu \int_\Omega \nabla \mathbf{w}(t) : \nabla \mathbf{v} d\mathbf{x} - \int_\Omega r(t) \operatorname{div} \mathbf{v} d\mathbf{x} = \int_\Omega \tilde{g} \cdot \mathbf{v} d\mathbf{x}, \forall \mathbf{v} \in (H_0^1(\Omega))^2,$$
$$\int_\Omega q \operatorname{div} \mathbf{w}(t) d\mathbf{x} = 0, \forall q \in L_0^2(\Omega),$$

where

$$\tilde{g} = \mathbf{g} + \rho(\mathbf{u} \cdot \nabla)\mathbf{w} - \rho \nabla \mathbf{u}_h^T \cdot \mathbf{w}.$$

Since $\Omega$ is a convex polygon and $\tilde{g}$ is easily shown to be in $(L^2(\Omega))^2$, we know that $(\mathbf{w}, r) \in (H^2(\Omega))^2 \times H^1(\Omega)$ [21],[62] (see [99],[58] [107] for smooth domains).

Here we are mainly interested in exhibiting the a priori estimate that holds in the $H^2 - H^1$ norms. For understanding, let us integrate (3.100) by parts to write (3.100) in the strong form

$$-\rho(\mathbf{u} \cdot \nabla)\mathbf{w} + \rho \nabla \mathbf{u}_h^T \cdot \mathbf{w} - \mu \Delta \mathbf{w} + \nabla r = \mathbf{g}. \tag{3.101}$$

which corresponds as seen before to the Stokes problem

$$-\mu \Delta \mathbf{w} + \nabla r = \mathbf{g} + \rho(\mathbf{u} \cdot \nabla)\mathbf{w} - \rho \nabla \mathbf{u}_h^T \cdot \mathbf{w}.$$

Using the $H^2 - H^1$ a priori estimate for the Stokes equations (see for instance again [21] or the proof of Proposition 3.25), we can prove that there exists $C > 0$ only depending on $\Omega$ such that for all $t$

$$\mu \|\mathbf{w}(t)\|_{H^2(\Omega)} + \|r(t)\|_{H^1(\Omega)} \leq \frac{C}{1-\gamma} \|\mathbf{g}\|_{L^2(\Omega)}. \tag{3.102}$$

We will also need the same estimates for the time derivatives of $\mathbf{w}(t)$ and $r(t)$. Assuming moreover that

$$\sup_{t \in (0,T)} \left\| \nabla \frac{\partial \mathbf{u}}{\partial t}(t) \right\|_{L^2(\Omega)} \leq \frac{\tilde{C}\mu(1-\gamma)}{\rho}$$

and that for all $h \leq h_0$ (up to take $h_0$ smaller)

$$\sup_{t \in (0,T)} \left\| \nabla \frac{\partial \mathbf{u}_h}{\partial t}(t) \right\|_{L^2(\Omega)} \leq \frac{\tilde{C}\mu(1-\gamma)}{\rho},$$

where $\tilde{C}$ may depends only on $\Omega$, by differentiating the weak formulation (3.100) with respect to the time it is possible to prove that for all $t$

$$\mu \left\| \nabla \frac{\partial \mathbf{w}}{\partial t}(t) \right\|_{L^2(\Omega)} + \left\| \frac{\partial r}{\partial t}(t) \right\|_{L^2(\Omega)} \leq \frac{C}{1-\gamma} \|\mathbf{g}\|_{L^2(\Omega)}.$$

Under the same hypothesis and differentiating this time the strong form (3.101), one may prove by the same manipulations that for all $t$

$$\mu \left\| \frac{\partial \mathbf{w}}{\partial t}(t) \right\|_{H^2(\Omega)} + \left\| \frac{\partial r}{\partial t}(t) \right\|_{H^1(\Omega)} \leq \frac{C}{1-\gamma} \|\mathbf{g}\|_{L^2(\Omega)}. \tag{3.103}$$

In the two estimates above, the constants $C$ depends only $\Omega$.

**Proposition 3.47** (Dual estimates for the velocity)**.**
*Let* $(\mathbf{u}, p)$ *be the solution of (3.87),* $(\mathbf{u}_h, p_h)$ *the solution of the finite element scheme (3.88) and* $(\mathbf{U}, P)$ *the solution of the linearized reconstruction. Moreover, we assume that there exists* $0 < \gamma < 1$

$$\sup_{t\in(0,T)} \|\nabla \mathbf{u}(t)\|_{L^2(\Omega)} \leq \frac{\gamma\mu}{\rho C_{SOB}}, \quad \sup_{t\in(0,T)} \left\|\nabla \frac{\partial \mathbf{u}}{\partial t}(t)\right\|_{L^2(\Omega)} \leq \frac{\tilde{C}\mu(1-\gamma)}{\rho}$$

*and that there exists* $h_0 > 0$ *such that for all* $h \leq h_0$

$$\sup_{t\in(0,T)} \|\nabla \mathbf{u}_h(t)\|_{L^2(\Omega)} \leq \frac{\gamma\mu}{\rho C_{SOB}}, \quad \sup_{t\in(0,T)} \left\|\nabla \frac{\partial \mathbf{u}_h}{\partial t}(t)\right\|_{L^2(\Omega)} \leq \frac{\tilde{C}\mu(1-\gamma)}{\rho}$$

*where* $C_{SOB}$ *is the Sobolev constant of Proposition A.8 of the Appendix A.2 and* $\tilde{C}$ *depends only on* $\Omega$*. Then, there exists a constant* $C > 0$ *independent of the mesh size, but that depends on the mesh aspect ratio and* $\Omega$ *such that for any* $h \leq h_0$ *and any* $t \in [0, T]$,

$$\|\mathbf{U} - \mathbf{u}_h(t)\|^2_{L^2(\Omega)} \leq \frac{C}{(1-\gamma^2)} \sum_{K\in\mathcal{T}_h} (\varepsilon^I_{K,\mathbf{u},0})^2(t), \tag{3.104}$$

$$\left\|\frac{\partial \mathbf{U}}{\partial t} - \frac{\partial \mathbf{u}_h}{\partial t}(t)\right\|^2_{L^2(\Omega)} \leq \frac{C}{(1-\gamma^2)} \sum_{K\in\mathcal{T}_h} (\varepsilon^I_{K,\mathbf{u},0})^2(t) + (\varepsilon^I_{K,\mathbf{u},1})^2(t), \tag{3.105}$$

*where*

$$\begin{aligned}(\varepsilon^I_{K,\mathbf{u},0})^2(t) = \frac{1}{\mu^2} h_K^4 &\left\|\mathbf{f}(t) - \rho\frac{\partial \mathbf{u}_h}{\partial t}(t) - \rho(\mathbf{u}_h(t)\cdot\nabla)\mathbf{u}_h(t) + \mu\Delta\mathbf{u}_h(t) - \nabla p_h(t)\right\|^2_{L^2(K)} \\ &+ \frac{1}{\mu} h_K^3 \|[\nabla \mathbf{u}_h(t)\cdot \mathbf{n}]\|^2_{L^2(\partial K)} + h_K^2 \|\operatorname{div} \mathbf{u}_h(t)\|^2_{L^2(K)} \\ + \frac{\alpha_K^2}{\mu^2}\Big(\rho\|\mathbf{u}_h(t)\|_{L^\infty(K)} + \mu\Big)^2 &\left\|\mathbf{f}(t) - \rho\frac{\partial \mathbf{u}_h}{\partial t}(t) - \rho(\mathbf{u}_h(t)\cdot\nabla)\mathbf{u}_h(t) + \mu\Delta\mathbf{u}_h(t) - \nabla p_h(t)\right\|^2_{L^2(K)},\end{aligned}$$

*and*

$$\begin{aligned}&(\varepsilon^I_{K,\mathbf{u},1})^2(t) \\ &= \frac{1}{\mu^2} h_K^4 \left\|\frac{\partial \mathbf{f}}{\partial t}(t) - \rho\frac{\partial^2 \mathbf{u}_h}{\partial t^2}(t) - \rho\left(\frac{\partial \mathbf{u}_h}{\partial t}(t)\cdot\nabla\right)\mathbf{u}_h(t) - \rho(\mathbf{u}_h(t)\cdot\nabla)\frac{\partial \mathbf{u}_h}{\partial t}(t)\right. \\ &\qquad \left. + \mu\Delta\frac{\partial \mathbf{u}_h}{\partial t}(t) - \nabla\frac{\partial p_h}{\partial t}(t)\right\|^2_{L^2(K)} \\ &\quad + \frac{1}{\mu} h_K^3 \left\|\left[\nabla\frac{\partial \mathbf{u}_h}{\partial t}(t)\cdot\mathbf{n}\right]\right\|^2_{L^2(\partial K)} + h_K^2 \left\|\operatorname{div}\frac{\partial \mathbf{u}_h}{\partial t}(t)\right\|^2_{L^2(K)} \\ &\quad + \frac{\alpha_K^2}{\mu^2}\Big(\rho\|\mathbf{u}_h(t)\|_{L^\infty(K)} + \mu\Big)^2 \\ &\left\|\frac{\partial \mathbf{f}}{\partial t}(t) - \rho\frac{\partial^2 \mathbf{u}_h}{\partial t^2}(t) - \rho\left(\frac{\partial \mathbf{u}_h}{\partial t}(t)\cdot\nabla\right)\mathbf{u}_h(t) - \rho(\mathbf{u}_h(t)\cdot\nabla)\frac{\partial \mathbf{u}_h}{\partial t}(t) + \mu\Delta\frac{\partial \mathbf{u}_h}{\partial t}(t) - \nabla\frac{\partial p_h}{\partial t}(t)\right\|^2_{L^2(K)} \\ &\quad + \frac{\rho^2}{\mu^2}\left(\alpha_K^2\left\|\frac{\partial \mathbf{u}_h}{\partial t}(t)\right\|^2_{L^\infty(K)} + \left(\frac{d\alpha_K}{dt}\right)^2 \|\mathbf{u}_h(t)\|^2_{L^\infty(K)}\right) \\ &\qquad \left\|\mathbf{f}(t) - \rho\frac{\partial \mathbf{u}_h}{\partial t}(t) - \rho(\mathbf{u}_h(t)\cdot\nabla)\mathbf{u}_h(t) + \mu\Delta\mathbf{u}_h(t) - \nabla p_h(t)\right\|^2_{L^2(K)}.\end{aligned}$$

*Proof.* Let $t \in [0, T]$ be fixed. As in the previous proposition, we dont write the explicit dependence on $t$ of the functions, since every quantity is evaluated at the same time. For this proof, we denote by $C$ any positive constant that is independent of the mesh size, but may depends on the mesh aspect ratio and by $\tilde{C}$ any positive constant depending only on $\Omega$. The value of these constants can change from line to line.

*Part 1. Proof of (3.104)* We proceed as in [107]. It is known that

$$\|\mathbf{U} - \mathbf{u}_h\|_{L^2(\Omega)} = \sup_{\substack{\mathbf{g} \in L^2(\Omega) \\ \mathbf{g} \neq 0}} \frac{(\mathbf{U} - \mathbf{u}_h, \mathbf{g})}{\|\mathbf{g}\|_{L^2(\Omega)}},$$

where $(\cdot, \cdot)$ stands for the usual inner product given by

$$(\mathbf{f}, \mathbf{g}) = \int_\Omega \mathbf{f} \cdot \mathbf{g} d\mathbf{x}.$$

Now let $\mathbf{g}$ be any vector valued function in $(L^2(\Omega))^2$ and let us consider the dual problem (3.100) with this particular $\mathbf{g}$ as right hand side. By taking $\mathbf{v} = \mathbf{U} - \mathbf{u}_h$ and $q = P - p_h$ in (3.100), we have

$$\begin{aligned}\int_\Omega (\mathbf{U} - \mathbf{u}_h) \cdot \mathbf{g} d\mathbf{x} &= \rho \int_\Omega ((\mathbf{u} \cdot \nabla)(\mathbf{U} - \mathbf{u}_h)) \cdot \mathbf{w} d\mathbf{x} + \rho \int_\Omega ((\mathbf{U} - \mathbf{u}_h) \cdot \mathbf{u}_h) \cdot \mathbf{w} d\mathbf{x} \\ &+ \mu \int_\Omega \nabla \mathbf{w} : \nabla(\mathbf{U} - \mathbf{u}_h) d\mathbf{x} - \int_\Omega r \operatorname{div}(\mathbf{U} - \mathbf{u}_h) d\mathbf{x} - \int_\Omega \operatorname{div} \mathbf{w} (P - p_h) d\mathbf{x}.\end{aligned}$$

Since $(\mathbf{U}, P)$ is the solution of (3.91), one obtains

$$\begin{aligned}\int_\Omega (\mathbf{U} - \mathbf{u}_h) \cdot \mathbf{g} d\mathbf{x} = \int_\Omega \left(\mathbf{f} - \rho \frac{\partial \mathbf{u}_h}{\partial t}\right) \cdot \mathbf{w} d\mathbf{x} - \rho \int_\Omega ((\mathbf{u}_h \cdot \nabla)\mathbf{u}_h) \cdot \mathbf{w} d\mathbf{x} - \mu \int_\Omega \nabla \mathbf{u}_h : \nabla \mathbf{w} d\mathbf{x} \\ + \int_\Omega r \operatorname{div} \mathbf{u}_h d\mathbf{x} + \int_\Omega p_h \operatorname{div} \mathbf{w} d\mathbf{x}.\end{aligned}$$

Now using the numerical method (3.88), we can remove any test function $(\mathbf{v}_h, q_h)$ and we get

$$\begin{aligned}\int_\Omega (\mathbf{U} - \mathbf{u}_h) \cdot \mathbf{g} d\mathbf{x} &= \int_\Omega \left(\mathbf{f} - \rho \frac{\partial \mathbf{u}_h}{\partial t}\right) \cdot (\mathbf{w} - \mathbf{v}_h) d\mathbf{x} \\ &- \rho \int_\Omega ((\mathbf{u}_h \cdot \nabla)\mathbf{u}_h) \cdot (\mathbf{w} - \mathbf{v}_h) d\mathbf{x} - \mu \int_\Omega \nabla \mathbf{u}_h : \nabla(\mathbf{w} - \mathbf{v}_h) d\mathbf{x} \\ &+ \int_\Omega (r - q_h) \operatorname{div} \mathbf{u}_h d\mathbf{x} + \int_\Omega p_h (\operatorname{div} \mathbf{w} - v_h) d\mathbf{x} \\ + \sum_{K \in \mathcal{T}_h} \int_K \alpha_K &\left(\mathbf{f} - \rho \frac{\partial \mathbf{u}_h}{\partial t} - \rho(\mathbf{u}_h \cdot \nabla)\mathbf{u}_h + \mu \Delta \mathbf{u}_h - \nabla p_h\right) \cdot (\rho(\mathbf{u}_h \cdot \nabla)\mathbf{v}_h - \mu \Delta \mathbf{v}_h + \nabla q_h) d\mathbf{x} = 0.\end{aligned}$$

Integration by parts over each triangle yields

$$\begin{aligned}\int_\Omega (\mathbf{U} - \mathbf{u}_h) \cdot \mathbf{g} d\mathbf{x} &= \sum_{K \in \mathcal{T}_h} \int_K \left(\mathbf{f} - \rho \frac{\partial \mathbf{u}_h}{\partial t} - \rho(\mathbf{u}_h \cdot \nabla)\mathbf{u}_h + \mu \Delta \mathbf{u}_h - \nabla p_h\right) \cdot (\mathbf{w} - \mathbf{v}_h) d\mathbf{x} \\ &\frac{1}{2} \sum_{K \in \mathcal{T}_h} \int_{\partial K} [\mu \nabla \mathbf{u}_h \cdot \mathbf{n}] \cdot (\mathbf{w} - \mathbf{v}_h) d\mathbf{x} + \sum_{K \in \mathcal{T}_h} \int_K (r - q_h) \operatorname{div} \mathbf{u}_h d\mathbf{x} \\ + \sum_{K \in \mathcal{T}_h} \int_K \alpha_K &\left(\mathbf{f} - \rho \frac{\partial \mathbf{u}_h}{\partial t} - \rho(\mathbf{u}_h \cdot \nabla)\mathbf{u}_h + \mu \Delta \mathbf{u}_h - \nabla p_h\right) \cdot (\rho(\mathbf{u}_h \cdot \nabla)\mathbf{v}_h - \mu \Delta \mathbf{v}_h + \nabla q_h) d\mathbf{x}.\end{aligned} \tag{3.106}$$

We now choose $\mathbf{v}_h = r_h(\mathbf{w})$ and $q_h = R_h(r)$ and the Cauchy-Schwarz inequality and classical isotropic interpolation estimates imply

$$\int_\Omega (\mathbf{U} - \mathbf{u}_h) \cdot \mathbf{g} d\mathbf{x}$$
$$\leq C \sum_{K \in \mathcal{T}_h} \left( h_K^2 \left\| \mathbf{f} - \rho \frac{\partial \mathbf{u}_h}{\partial t} - \rho(\mathbf{u}_h \cdot \nabla)\mathbf{u}_h + \mu \Delta \mathbf{u}_h - \nabla p_h \right\|_{L^2(K)} + \frac{1}{2} h_K^{3/2} \|[\mu \nabla \mathbf{u}_h \cdot \mathbf{n}]\|_{L^2(\partial K)} \right) \|\mathbf{w}\|_{H^2(K)}$$
$$+ C \sum_{K \in \mathcal{T}_h} \mu h_K \| \operatorname{div} \mathbf{u}_h \|_{L^2(K)} \frac{1}{\mu} \|\nabla r\|_{L^2(\Delta K)}$$
$$+ \sum_{K \in \mathcal{T}_h} \alpha_K \left( \rho \|\mathbf{u}_h\|_{L^\infty(K)} + \mu \right) \left\| \mathbf{f} - \rho \frac{\partial \mathbf{u}_h}{\partial t} - \rho(\mathbf{u}_h \cdot \nabla)\mathbf{u}_h + \mu \Delta \mathbf{u}_h - \nabla p_h \right\|_{L^2(K)} \left( \|\mathbf{w}\|_{H^2(K)} + \frac{1}{\mu} \|\nabla r\|_{L^2(\Delta K)} \right).$$

The discrete Cauchy-Schwarz inequality and the a priori estimate (3.102) on $(\mathbf{w}, r)$ imply finally

$$\int_\Omega (\mathbf{U} - \mathbf{u}_h) \cdot \mathbf{g} d\mathbf{x}$$
$$\leq \frac{C}{\mu(1-\gamma)} \left( \sum_{K \in \mathcal{T}_h} h_K^4 \left\| \mathbf{f} - \rho \frac{\partial \mathbf{u}_h}{\partial t} - \rho(\mathbf{u}_h \cdot \nabla)\mathbf{u}_h + \mu \Delta \mathbf{u}_h - \nabla p_h \right\|_{L^2(K)}^2 + \frac{1}{4} h_K^3 \|[\mu \nabla \mathbf{u}_h \cdot \mathbf{n}]\|_{L^2(\partial K)}^2 + \mu^2 h_K^2 \| \operatorname{div} \mathbf{u}_h \|_{L^2(K)}^2 \right.$$
$$\left. + \alpha_K^2 \left( \rho \|\mathbf{u}_h\|_{L^\infty(K)} + \mu \right)^2 \left\| \mathbf{f} - \rho \frac{\partial \mathbf{u}_h}{\partial t} - \rho(\mathbf{u}_h \cdot \nabla)\mathbf{u}_h + \mu \Delta \mathbf{u}_h - \nabla p_h \right\|_{L^2(K)}^2 \right)^{1/2} \|\mathbf{g}\|_{L^2(\Omega)}.$$

Dividing by $\|\mathbf{g}\|_{L^2(\Omega)}$ and taking the supremum on all the $\mathbf{g} \in (L^2(\Omega))^2$ yields the bound (3.104).

*Part 2. Proof of (3.105)*

We start from (3.100). We choose $v_h = r_h(\mathbf{w})$ and $q_h = R_h(r)$, and by differentiating both side of the equations with respect to the time variable and using the fact that $\frac{\partial}{\partial t}$

commutes with $r_h$ and $R_h$, we obtain

$$\int_\Omega \left(\frac{\partial \mathbf{U}}{\partial t} - \frac{\partial \mathbf{u}_h}{\partial t}\right) \cdot \mathbf{g} d\mathbf{x}$$

$$\sum_{K\in\mathcal{T}_h} \int_K \left(\mathbf{f} - \rho\frac{\partial \mathbf{u}_h}{\partial t} - \rho(\mathbf{u}_h\cdot\nabla)\mathbf{u}_h + \mu\Delta\mathbf{u}_h - \nabla p_h\right) \cdot \left(\frac{\partial \mathbf{w}}{\partial t} - r_h\left(\frac{\partial \mathbf{w}}{\partial t}\right)\right) d\mathbf{x}$$

$$\frac{1}{2}\sum_{K\in\mathcal{T}_h} \int_{\partial K} [\mu\nabla\mathbf{u}_h\cdot\mathbf{n}] \cdot \left(\frac{\partial \mathbf{w}}{\partial t} - r_h\left(\frac{\partial \mathbf{w}}{\partial t}\right)\right) d\mathbf{x} + \sum_{K\in\mathcal{T}_h} \int_K \left(\frac{\partial r}{\partial t} - R_h\left(\frac{\partial r}{\partial t}\right)\right) \operatorname{div}\mathbf{u}_h d\mathbf{x}$$

$$+ \sum_{K\in\mathcal{T}_h} \int_K \alpha_K \left(\mathbf{f} - \rho\frac{\partial \mathbf{u}_h}{\partial t} - \rho(\mathbf{u}_h\cdot\nabla)\mathbf{u}_h + \mu\Delta\mathbf{u}_h - \nabla p_h\right)$$

$$\cdot \left(\rho(\mathbf{u}_h\cdot\nabla)r_h\left(\frac{\partial \mathbf{w}}{\partial t}\right) - \mu\Delta r_h\left(\frac{\partial \mathbf{w}}{\partial t}\right) + \nabla R_h\left(\frac{\partial r}{\partial t}\right)\right) d\mathbf{x}$$

$$+\sum_{K\in\mathcal{T}_h} \int_K \left(\frac{\partial \mathbf{f}}{\partial t} - \rho\frac{\partial^2 \mathbf{u}_h}{\partial t^2} - \rho\left(\frac{\partial \mathbf{u}_h}{\partial t}\cdot\nabla\right)\mathbf{u}_h - \rho(\mathbf{u}_h\cdot\nabla)\frac{\partial \mathbf{u}_h}{\partial t} + \mu\Delta\frac{\partial \mathbf{u}_h}{\partial t} - \nabla\frac{\partial p_h}{\partial t}\right) \cdot (\mathbf{w} - r_h(\mathbf{w})) d\mathbf{x}$$

$$\frac{1}{2}\sum_{K\in\mathcal{T}_h} \int_{\partial K} \left[\mu\nabla\frac{\partial \mathbf{u}_h}{\partial t}\cdot\mathbf{n}\right] \cdot (\mathbf{w} - r_h(\mathbf{w})) d\mathbf{x} + \sum_{K\in\mathcal{T}_h} \int_K (r - R_h(r)) \operatorname{div}\frac{\partial \mathbf{u}_h}{\partial t} d\mathbf{x}$$

$$+ \sum_{K\in\mathcal{T}_h} \int_K \alpha_K \left(\frac{\partial \mathbf{f}}{\partial t} - \rho\frac{\partial^2 \mathbf{u}_h}{\partial t^2} - \rho\left(\frac{\partial \mathbf{u}_h}{\partial t}\cdot\nabla\right)\mathbf{u}_h - \rho(\mathbf{u}_h\cdot\nabla)\frac{\partial \mathbf{u}_h}{\partial t} + \mu\Delta\frac{\partial \mathbf{u}_h}{\partial t} - \nabla\frac{\partial p_h}{\partial t}\right)$$

$$\cdot (\rho(\mathbf{u}_h\cdot\nabla)r_h(\mathbf{w}) - \mu\Delta r_h(\mathbf{w}) + \nabla R_h(r)) d\mathbf{x}$$

$$+ \sum_{K\in\mathcal{T}_h} \int_K \alpha_K \left(\mathbf{f} - \rho\frac{\partial \mathbf{u}_h}{\partial t} - \rho(\mathbf{u}_h\cdot\nabla)\mathbf{u}_h + \mu\Delta\mathbf{u}_h - \nabla p_h\right) \cdot \rho\left(\frac{\partial \mathbf{u}_h}{\partial t}\cdot\nabla\right) r_h(\mathbf{w}) d\mathbf{x}$$

$$+ \sum_{K\in\mathcal{T}_h} \int_K \frac{d\alpha_K}{dt} \left(\mathbf{f} - \rho\frac{\partial \mathbf{u}_h}{\partial t} - \rho(\mathbf{u}_h\cdot\nabla)\mathbf{u}_h + \mu\Delta\mathbf{u}_h - \nabla p_h\right) \cdot \rho(\mathbf{u}_h\cdot\nabla) r_h(\mathbf{w}) d\mathbf{x}.$$

The rest of the proof is similar to the Part 1. We use the standard interpolation estimates and conclude by using the a priori estimates (3.102) and (3.103). □

**Remark 3.48.**
Note here that, contrary to what we did before (see Proposition 3.25 for the Stokes equations for instance), it is not possible to absorb all the terms due to the stabilization into the residual part. This is due to the fact that we have to stabilize the convection. Only the terms that involve the factor $\alpha_K^2\mu^2$ can be bounded by the suitable power of $h_K$, that is to say $h_K^4$ (note that we can always bound $\alpha_K$, up to a constant, by $\frac{h_k^2}{\mu}$ since $\xi(Re_K)^{-1} \leq 1$ and $\lambda_{2,K} \leq ch_K$.) We could try a finer estimate for the other terms, but we think that for our purpose, it is enough to observe (the computations will be done here below) that

$$\alpha_K^2 \simeq h_K^4, \left(\frac{d\alpha_K}{dt}\right)^2 \simeq h_K^6$$

and that therefore, up to factor that may depends on $\mathbf{u}_h, \dfrac{\partial \mathbf{u}_h}{\partial t}, \rho, \mu$ all the terms in estimates (3.104) and (3.105) involving $\alpha_K$ are of higher order.

We conclude this remark by providing a proper estimate for $\alpha_K$ and its derivative with respect to $t$. We recall that

$$\alpha_K = \frac{\alpha\lambda_{2,K}^2}{\mu\xi(Re_K)}$$

Since $\xi(x) \geq 1$, and we have that $\lambda_{2,K} \leq ch_K$ with $c$ depending only on the reference triangle, we immediately conclude that

$$\alpha_K \leq \frac{\alpha c}{\mu} h_K^2$$

implying that $\alpha_K^2 \simeq h_K^4$. Moreover we have that

$$\frac{d\alpha_K}{dt} = \frac{\alpha\lambda_{2,K}^2}{\mu}\frac{-\xi'(Re_K)\frac{dRe_K}{dt}}{\xi^2(Re_K)} \leq \frac{\alpha\lambda_{2,K}^2}{\mu}\frac{\left|-\xi'(Re_K)\frac{dRe_K}{dt}\right|}{\xi^2(Re_K)} \leq \frac{\alpha\lambda_{2,K}^2}{\mu}\frac{\lambda_{2,K}\rho\left|\frac{d\|\mathbf{u}_h\|_{L^\infty(K)}}{dt}\right|}{\mu},$$

where we $\xi' \leq 1$. As before we use that $\lambda_{2,K} \leq ch_K$ and we obtain finally

$$\left(\frac{d\alpha_K}{dt}\right)^2 \simeq h_K^6.$$

We are now able to prove an a posteriori error estimate for the semi-discrete error $\mathbf{u}-\mathbf{u}_h$. It is summarized in the Theorem

**Theorem 3.49** (An anisotropic a posteriori error estimate for the unsteady Navier-Stokes with constant coefficients)**.**
*Let* $(\mathbf{u}, p)$ *be the solution of (3.87),* $(\mathbf{u}_h, p_h)$ *the solution of the finite element scheme (3.88) and* $(\mathbf{U}, P)$ *the solution of the linearized reconstruction. We assume that the hypothesis of Propositions 3.44, 3.46 and 3.47 hold. Finally, let* $(\mathbf{w}, r) \in (H_0^1(\Omega))^2 \times L_0^2(\Omega)$ *the weak solution of the dual problem* (3.96)*.*

*Then, there exists a constant* $C_1 > 0$ *depending only on the the reference triangle and* $\Omega$ *and a constant* $C_2 > 0$ *independent of the mesh size, but that depends on the mesh aspect ratio and* $\Omega$ *such that for any* $h \leq h_0$ *and any* $t \in (0, T]$

$$\begin{aligned}
&\rho\|\mathbf{u}-\mathbf{u}_h(t)\|_{L^2(\Omega)}^2 + \mu\int_0^t \|\nabla(\mathbf{u}-\mathbf{u}_h)(s)\|_{L^2(\Omega)}^2 ds \\
&\quad \leq C_1\rho\|\mathbf{u}-\mathbf{u}_h(0)\|_{L^2(\Omega)}^2 + \frac{C_1}{(1-\gamma)^2}\int_0^t \sum_{K\in\mathcal{T}_h} (\eta_{K,\mathbf{u}}^A)^2(s) + (\eta_{K,p}^A)^2(s) + (\eta_K^{\text{div}})(s)^2 ds \\
&\quad + \frac{C_2\rho}{(1-\gamma)^2}\sum_{K\in\mathcal{T}_h}(\varepsilon_{K,\mathbf{u},0}^I)^2(0) + (\varepsilon_{K,\mathbf{u},0}^I)^2(t) + \frac{C_2\rho^2}{\mu(1-\gamma)^4}\int_0^t \sum_{K\in\mathcal{T}_h}(\varepsilon_{K,\mathbf{u},1}^I)^2(s)ds, \quad (3.107)
\end{aligned}$$

*where* $\eta_{K,\mathbf{u}}^A, \eta_{K,p}^A$ *and* $\eta_K^{\text{div}}$ *are given by Proposition 3.46 and* $\varepsilon_{K,\mathbf{u},0}^I$ *and* $\varepsilon_{K,\mathbf{u},1}^I$ *by Proposition 3.47.*

*Proof.* The proof is straightforward by splitting the error $\mathbf{u}-\mathbf{u}_h = \mathbf{u}-\mathbf{U}+\mathbf{U}-\mathbf{u}_h$ and by applying Propositions 3.44, 3.46 and 3.47. □

**Remark 3.50.**
As in general for this type of anisotropic error estimate, the a posteriori error upper bound (3.107) is not standard since it involves the linear reconstruction $\mathbf{U}$ in $\eta_{K,\mathbf{u}}^A$ and requires the solution $\mathbf{w}$ of the dual problem for the pressure reconstruction (3.96). In practice, see Remark 3.28, we replace $\mathbf{U}$ by the ZZ post-processing of $\mathbf{u}_h$ and we do not use the error estimator $\eta_{K,p}^A$ in our adaptive algorithms.

Finally, note that the a posteriori error estimate (3.107) is easily adapted to $\mathbb{R}^3$ by using the corresponding anisotropic framework, among others one replaces $\omega_K$ by its 3D definition. The only issue is to obtain the dual estimates (3.102) and (3.103) in order to prove Proposition 3.47 for $\Omega \in \mathbb{R}^3$. Indeed, as already mentioned for the Stokes equations (see Remark 3.26), the $H^2 - H^1$ regularity of the dual problem (3.100) holds in 3D only for smooth domains or particular convex polygons.

## 3.7 A posteriori error estimates for the incompressible time dependent Navier-Stokes equations with constant coefficients: time approximation

In this section, we present a semi-discrete approximation in time discretization of the Navier-Stokes equations. We focus on the Backward Differentiation Formula type methods (BDF), namely BDF1 (that is to say the Backward Euler method) and the BDF2 method, that is a second order scheme frequently used in the framework of Navier-Stokes equations. Previous works are already dedicated to a posteriori error estimates for the (Navier)-Stokes equations and BDF methods. We point out again [107] where the Navier-Stokes equations are discretized with the Euler method and [23] where the BDF2 method is used to solve the Stokes equations. Note that in [107], they also consider the spatial approximation using Taylor-Hood finite elements. We point out also the reference [106] where both spatial and temporal approximations are taken in account. An a posteriori error estimates in time for the $\theta$-scheme (in particular the case $\theta = 1/2$ that corresponds to the Crank-Nicolson method) are proven, but it is observed to be suboptimal for second order methods.

Before studying the case of the Navier-Stokes equations, we present the method on a simple ODE toy problem and we show the techniques to prove an a posteriori error estimate. We refer to [2] for more details on a posteriori error estimates in the case of abstract parabolic problems. Note that here the authors only consider constant time steps, we propose to extend the result to the case of variable time steps for adaptive purposes.

### 3.7.1 An a posteriori error indicator for the BDF 2: a toy problem

Let $\rho, \mu > 0$ be two positive numbers and let us consider the following Cauchy problem : find $u$ the solution of the ODE

$$\begin{cases} \rho \dfrac{du}{dt}(t) + \mu u(t) = f(t), t \in (0, T], \\ \\ \qquad\qquad u(0) = u_0, \end{cases} \tag{3.108}$$

where $T > 0$ is the final time and $u_0 \in \mathbb{R}$ is the initial condition. The BDF$k$ methods, $k = 1, 2$, reads : let $0 = t^0 < t^1 < t^2 < ...t^N = T$ be a partition of $[0, T]$ and $\tau^{n+1} = t^{n+1} - t^n$ be the time step. Starting from $u^0 = u_0$, find for every $n = 0, 1, 2, ..N - 1$, $u^{n+1}$ the solution of

$$\rho \left( \partial u^{n+1} + \frac{\beta_k^{n+1} \tau^{n+1}}{2} \partial^2 u^{n+1} \right) + \mu u^{n+1} = f^{n+1}, \tag{3.109}$$

where we use the notations

$$\partial u^{n+1} = \frac{u^{n+1} - u^n}{\tau^{n+1}}, \quad \partial^2 u^{n+1} = \frac{\frac{u^{n+1} - u^n}{\tau^{n+1}} - \frac{u^n - u^{n-1}}{\tau^n}}{\frac{\tau^{n+1} + \tau^n}{2}}, \quad f^{n+1} = f(t^{n+1}),$$

and $\beta_k^{n+1}$ is given by

$$\beta_1^{n+1} = 0, n = 0, 1, ..., N - 1, \quad \beta_2^{n+1} = 0, n = 0, \beta_2^{n+1} = 1, n > 0.$$

Note the BDF2 method (that is to say $k = 2$) is a multistep method, requiring $u^n$ but also $u^{n-1}$ to compute $u^{n+1}$. Therefore, when $k = 2$, we initialize the method by solving the first iteration with the Backward Euler method. Another choice would be to use for instance the Crank-Nicolson scheme. In both cases, the choice for the first iteration does not alter the order of convergence of the BDF2 method.

We know quickly present the techniques to obtain an error indicator in the case of the BDFk methods. As we already did in Chapter 2, we introduce a piecewise reconstruction of the numerical solution. We define $\mathbf{u}_{\tau,k}, k = 1, 2$, by

$$u_{\tau,1} = u^{n+1} + (t - t^{n+1})\partial u^{n+1}, t \in [t^n, t^{n+1}], n = 0, 1, 2, ..., N - 1,$$

and

$$u_{\tau,2} = u^{n+1} + (t - t^{n+1})\partial u^{n+1} + \frac{1}{2}(t - t^n)(t - t^{n+1})\partial^2 u^{n+1}, t \in [t^n, t^{n+1}], n = 1, 2, ..., N - 1.$$

Then, the error indicators for the BDF1 and BDF2 methods are contained in the next two Lemmas.

**Lemma 3.51** (An error indicator for the BDF1 method)**.**
*Let* $(u^n)_{n=0}^N$ *the numerical solution of the BDF method (3.109) with* $k = 1$*. Then, for any* $t \in (0, T]$*, it holds*

$$\rho \frac{d}{dt} u_{\tau,1} + \mu u_{\tau,1} = f + \theta_1,$$

*where* $\theta_1$ *is defined by*

$$\theta_1(t) = f^{n+1} - f(t) + (t - t^{n+1})\mu\partial u^{n+1}, t \in [t^n, t^{n+1}], n = 0, 1, 2, ..., N - 1.$$

*Proof.* The proof is a direct computation and is not presented. □

**Lemma 3.52** (An error indicator for the BDF2 method)**.**
*Let* $(u^n)_{n=0}^N$ *the numerical solution of the BDF method (3.109) with* $k = 2$*. Finally, we consider the piecewise reconstruction* $u_\tau$ *defined by*

$$u_\tau(t) = u_{\tau,1}(t), t \in [t^0, t^1], \quad u_\tau(t) = u_{\tau,2}(t), t \in [t^1, T].$$

*Then, for any* $t \in (0, T]$*, it holds*

$$\rho \frac{d}{dt} u_\tau + \mu u_\tau = f + \theta_2,$$

*where* $\theta_2$ *is defined by*

$$\theta_2(t) = f^{n+1} + (t - t^{n+1})\partial f^{n+1} - f(t) - \frac{\tau^n}{2}(t - t^{n+1})\rho\frac{\partial^2 u^{n+1} - \partial^2 u^n}{\tau^{n+1}} + \frac{1}{2}(t - t^n)(t - t^{n+1})\mu\partial^2 u^{n+1}, \quad t \in [t^n, t^{n+1}], n = 2, 3, ..., N - 2,$$

*and*

$$\theta_2(t) = f^2 + (t - t^2)\partial^2 f^2 - f(t) - \frac{\tau^1}{2}\rho\partial^2 u^2 + \frac{1}{2}(t - t^1)(t - t^2)\mu\partial^2 u^2, \quad t \in [t^1, t^2],$$

$$\theta_2(t) = f^1 - f(t) + (t - t^1)\mu\partial f^1, \quad t \in [t^0, t^1],$$

*where we note*

$$\partial f^{n+1} = \frac{f^{n+1} - f^n}{\tau^{n+1}}, n = 0, 1, 2, ..., N - 1.$$

*Proof.* We consider $t \in [t^n, t^{n+1}]$. We separate the proof into three parts.

*Part 1.* $n \geq 2$

We compute

$$\begin{aligned}\rho\frac{d}{dt}u_\tau + \mu u_\tau &= \rho\partial u^{n+1} + (t-t^{n+1/2})\rho\partial^2 u^{n+1} + \mu u^{n+1} + (t-t^{n+1})\mu\partial u^{n+1}\\ &\quad + \frac{1}{2}(t-t^n)(t-t^{n+1})\mu\partial^2 u^{n+1}\\ &= \rho\partial u^{n+1} + \frac{\tau^{n+1}}{2}\rho\partial^2 u^{n+1}\mu u^{n+1} + \left(t - t^{n+1/2} - \frac{\tau^{n+1}}{2}\right)\rho\partial^2 u^{n+1}\\ &\quad + (t-t^{n+1})\mu\partial u^{n+1} + \frac{1}{2}(t-t^n)(t-t^{n+1})\mu\partial^2 u^{n+1}.\end{aligned}$$

Using the numerical scheme (3.109) with $k=2$ (note that here $\beta_2^{n+1}=1$) and the fact that $t^{n+1/2} - \dfrac{\tau^{n+1}}{2} = t^{n+1}$, we obtain

$$\rho\frac{d}{dt}u_\tau + \mu u_\tau = f^{n+1} + (t-t^{n+1})\left(\rho\partial^2 u^{n+1} + \mu\partial u^{n+1}\right) + \frac{1}{2}(t-t^n)(t-t^{n+1})\mu\partial^2 u^{n+1}. \quad (3.110)$$

Now, computing the difference between two consecutive steps of (3.109) and dividing by $\tau^{n+1}$, one can write

$$\rho\left(\frac{\partial u^{n+1} - \partial u^n}{\tau^{n+1}} + \frac{1}{2}\partial^2 u^{n+1} - \frac{\tau^n}{2\tau^{n+1}}\partial^2 u^n\right) + \mu\partial u^{n+1} = \partial f^{n+1}.$$

Observe that the term inside the parenthesis in the left hand side can be written as

$$\begin{aligned}\frac{\partial u^{n+1} - \partial u^n}{\tau^{n+1}} + \frac{1}{2}\partial^2 u^{n+1} - \frac{\tau^n}{2\tau^{n+1}}\partial^2 u^n &= \partial^2 u^{n+1}\frac{\tau^{n+1}+\tau^n}{2\tau^{n+1}} + \frac{1}{2}\partial^2 u^{n+1} - \frac{\tau^n}{2\tau^{n+1}}\partial^2 u^n\\ &= \partial^2 u^{n+1} + \frac{\tau^n}{2}\frac{\partial^2 u^{n+1} - \partial^2 u^n}{\tau^{n+1}}.\end{aligned}$$

Thus, we have

$$\rho\left(\partial^2 u^{n+1} + \frac{\tau^n}{2}\frac{\partial^2 u^{n+1} - \partial^2 u^n}{\tau^{n+1}}\right) + \mu\partial u^{n+1} = \partial f^{n+1},$$

which yields that

$$\rho\partial^2 u^{n+1} + \mu\partial u^{n+1} = \partial f^{n+1} - \rho\,\frac{\tau^n}{2}\frac{\partial^2 u^{n+1} - \partial^2 u^n}{\tau^{n+1}}.$$

Plugging it back into (3.110), we then obtain

$$\begin{aligned}\rho\frac{d}{dt}u_\tau + \mu u_\tau = f^{n+1} + (t-t^{n+1})\partial f^{n+1} - \frac{\tau^n}{2}(t-t^{n+1})\rho\frac{\partial^2 u^{n+1} - \partial^2 u^n}{\tau^{n+1}}&\\ + \frac{1}{2}(t-t^n)(t-t^{n+1})\mu\partial^2 u^{n+1},&\end{aligned}$$

which yields the desired result by adding and substracting $f(t)$.

*Part 2.* $n = 1$

The computation is the same as in the previous part yielding to

$$\rho\frac{d}{dt}u_\tau + \mu u_\tau = f^2 + (t-t^2)\left(\rho\partial^2 u^2 + \mu\partial u^2\right) + \frac{1}{2}(t-t^1)(t-t^2)\mu\partial^2 u^2.$$

Taking the difference between the scheme for $n = 1$ and $n = 0$ (note that here the step $n = 0$ is a BDF1 step), we can deduce that

$$\rho\partial^2 u^2 + \mu\partial u^2 = \partial f^2 - \frac{\tau^1}{2}\rho\partial^2 u^2,$$

which yields that

$$\rho\frac{d}{dt}u_\tau + \mu u_\tau = f^2 + (t - t^2)\partial f^2 - -\frac{\tau^1}{2}(t - t^2)\rho\partial^2 u^2 + \frac{1}{2}(t - t^1)(t - t^2)\mu\partial^2 u^2.$$

*Part 3.* $n = 0$

This last case is a direct consequence of the Lemma 3.51 by using the fact that $u_\tau = u_{\tau,1}$ for $t \in [t^0, t^1]$. □

From Lemmas 3.51 and 3.52, we could derive a posteriori error estimates following the procedure presented in Theorems 2.1 or 2.5 of Chapter 2. We do not present them, by sake of conciseness, and we focus on the application to the Navier-Stokes equations.

### 3.7.2 A posteriori error estimates for the incompressible Navier-Stokes equations with constant coefficients and the BDF methods

We now consider a time discretization of the Navier-Stokes equations (3.87) (written in a weak formulation). We use either the BDF1 or the BDF2 methods do not consider the spatial approximation. The problem now reads : given $N$ a positive integer and $0 = t^0 < t^1 < t^2 < ... < t^N = T$ a partition of $[0, T]$ into intervals of length $\tau^{n+1} = t^{n+1} - t^n$, starting from $\mathbf{u}^0 = \mathbf{u}_0$, find for every $n = 0, 1, ..., N-1$, $(\mathbf{u}^{n+1}, p^{n+1}) \in (H_0^1(\Omega))^2 \times L_0^2(\Omega)$ the solution of

$$\begin{aligned}\rho\int_\Omega \left(\partial\mathbf{u}^{n+1} + \frac{\beta_k^{n+1}\tau^{n+1}}{2}\partial^2\mathbf{u}^{n+1}\right)\cdot\mathbf{v}d\mathbf{x} + \rho\int_\Omega((\mathbf{u}^{n+1}\cdot\nabla)\mathbf{u}^{n+1})\cdot\mathbf{v}d\mathbf{x}&\\ + \mu\int_\Omega \nabla\mathbf{u}^{n+1} : \nabla\mathbf{v}d\mathbf{x} - \int_\Omega p^{n+1}\operatorname{div}\mathbf{v}d\mathbf{x} = \int_\Omega \mathbf{f}^{n+1}\cdot\mathbf{v}d\mathbf{x}, \quad \forall\mathbf{v} \in (H_0^1(\Omega))^2,&\\ -\int_\Omega q\operatorname{div}\mathbf{u}^{n+1}d\mathbf{x} = 0, \quad \forall q \in L_0^2(\Omega),&\end{aligned} \quad (3.111)$$

where we use the same type of notations as before

$$\partial\mathbf{u}^{n+1} = \frac{\mathbf{u}^{n+1} - \mathbf{u}^n}{\tau^{n+1}}, \quad \partial^2\mathbf{u}^{n+1} = \frac{\frac{\mathbf{u}^{n+1}-\mathbf{u}^n}{\tau^{n+1}} - \frac{\mathbf{u}^n-\mathbf{u}^{n-1}}{\tau^n}}{\tau^{n+1}+\tau^n/2}, \quad \mathbf{f}^{n+1} = \mathbf{f}(t^{n+1}),$$

and $\beta_k^{n+1}, k = 1, 2$ is given by

$$\beta_1^{n+1} = 0, \forall n = 0, 1, ..., N-1, \quad \beta_2^{n+1} = 0, n = 0, \beta_2^{n+1} = 1, n > 0.$$

As usual we denote the maximal time step by $\tau = \max_{n=1,...,N}\tau^n$.

We assume that the above numerical method is well-posed and converges as $\tau \to 0$. We focus on the a posteriori error analysis. We first prove an a posteriori error estimate for the case of the BDF1 method. We need the following proposition that contains the error indicator we will use. Observe that we only consider the velocity field. The derivation follows the same ideas presenting in Chapter 2 for the transport equation, we first build an appropriate piecewise reconstruction of the numerical solution, and we look at the remainder when we plug it into the PDE.

**Lemma 3.53** (An error indicator for the BDF1 method applied to the Navier-Stokes equations)**.**
*Let* $(\mathbf{u}^n)_{n=0}^N, (p^n)_{n=1}^N$ *be the approximated solutions to (3.87) obtained by solving the numerical method (3.111) with* $k = 1$*. Let us define the piecewise linear reconstruction of the velocity* $\mathbf{u}_\tau$ *by*

$$\mathbf{u}_\tau(t) = \mathbf{u}^{n+1} + (t - t^{n+1})\partial \mathbf{u}^{n+1}, \quad t \in [t^n, t^{n+1}], n = 0, 1, 2, ..., N-1. \tag{3.112}$$

*Moreover, let us define the piecewise constant reconstruction of the pressure* $p_\tau$

$$p_\tau(t) = p^{n+1}, \quad t \in [t^n, t^{n+1}], n = 0, 1, 2, ..., N-1. \tag{3.113}$$

*Then, it holds for any* $t \in (t^n, t^{n+1}), n = 0, 1, ..., N-1$ *and all* $\mathbf{v} \in (H_0^1(\Omega))^2$

$$\rho \int_\Omega \frac{\partial \mathbf{u}_\tau}{\partial t} \cdot \mathbf{v} d\mathbf{x} + \rho \int_\Omega ((\mathbf{u}_\tau \cdot \nabla)\mathbf{u}_\tau) \cdot \mathbf{v} d\mathbf{x} + \mu \int_\Omega \nabla \mathbf{u}_\tau : \nabla \mathbf{v} d\mathbf{x} - \int_\Omega p_\tau \operatorname{div} \mathbf{v} d\mathbf{x} = \int_\Omega \mathbf{f}^{n+1} \cdot \mathbf{v} d\mathbf{x}$$
$$+ (t - t^{n+1})\rho \int_\Omega \left((\mathbf{u}^{n+1} \cdot \nabla)\partial \mathbf{u}^{n+1} + (\partial \mathbf{u}^{n+1} \cdot \nabla)\mathbf{u}^{n+1}\right) \cdot \mathbf{v} d\mathbf{x} + (t - t^{n+1})\mu \int_\Omega \nabla \partial \mathbf{u}^{n+1} : \nabla \mathbf{v} d\mathbf{x}$$
$$+ (t - t^{n+1})^2 \rho \int_\Omega \left((\partial \mathbf{u}^{n+1} \cdot \nabla)\partial \mathbf{u}^{n+1}\right) \cdot \mathbf{v} d\mathbf{x}.$$

*Proof.* The proof is a direct computation and is not presented. □

We now prove a semi-discrete a posteriori error estimate involving only the time discretization when the Navier-Stokes equations are approximated with BDF1 method.

**Theorem 3.54** (A semi-discrete a posteriori error estimate for the Navier-Stokes equations and the BDF1 method)**.**
*Let* $(\mathbf{u}, p)$ *be the solution of the Navier-Stokes equations (3.87),* $(\mathbf{u}^n)_{n=0}^N, (p^n)_{n=1}^N$ *be the approximated solutions to (3.87) obtained by solving the numerical method (3.111) with* $k = 1$*. Let us define the piecewise linear reconstruction of the velocity* $\mathbf{u}_\tau$ *by* (3.112) *and the piecewise constant reconstruction of the pressure* $p_\tau$ *by* (3.113)*. Finally, assume that there exists* $\tau_0$ *and* $0 < \gamma < 1$ *such that for all* $\tau < \tau_0$

$$\sup_{t \in (0,T)} \|\nabla \mathbf{u}_\tau(t)\|_{L^2(\Omega)} \leq \frac{\gamma \mu}{C_{SOB}\rho}, \tag{3.114}$$

*where* $C_{SOB}$ *is the Sobolev constant in Proposition A.8 of the Appendix A.2. Then, for all* $\tau < \tau_0$ *there exists a constant* $C$ *depending only on* $\Omega$ *such that*

$$\rho \|\mathbf{u} - \mathbf{u}_\tau(T)\|_{L^2(\Omega)}^2 + \mu \int_0^T \|\nabla(\mathbf{u} - \mathbf{u}_\tau)(t)\|_{L^2(\Omega)}^2 dt$$
$$\leq \frac{C}{(1-\gamma)^2} \left( \rho \|\mathbf{u} - \mathbf{u}_\tau(0)\|_{L^2(\Omega)}^2 + \frac{\rho}{\mu} \sum_{n=0}^{N-1} (\eta_{\mathbf{f},n}^T)^2 + (\eta_{\rho,n}^T)^2 + (\epsilon_n^T)^2 + \sum_{n=0}^{N-1} (\eta_{\mu,n}^T)^2 \right), \tag{3.115}$$

*where*

$$(\eta_{\mathbf{f},n}^T)^2 = \rho^{-1} \int_{t^n}^{t^{n+1}} \|\mathbf{f}(t) - \mathbf{f}^{n+1}\|_{L^2(\Omega)}^2 dt,$$
$$(\eta_{\rho,n}^T)^2 = \frac{(\tau^{n+1})^3}{3} \rho \|((\mathbf{u}^{n+1} \cdot \nabla)\partial \mathbf{u}^{n+1} + (\partial \mathbf{u}^{n+1} \cdot \nabla)\mathbf{u}^{n+1})\|_{L^2(\Omega)}^2,$$
$$(\epsilon_n^T)^2 = \frac{(\tau^{n+1})^5}{5} \rho \|(\partial \mathbf{u}^{n+1} \cdot \nabla)\partial \mathbf{u}^{n+1}\|_{L^2(\Omega)}^2,$$

*and*

$$(\eta_{\mu,n}^T)^2 = \frac{(\tau^{n+1})^3}{3} \mu \|\nabla \partial \mathbf{u}^{n+1}\|_{L^2(\Omega)}^2.$$

*Proof.* Let $n \geq 0$ and $t \in (t^n, t^{n+1})$. To lighten the notations, we don't write the explicit dependence on the time of the functions. We have

$$\begin{aligned}
\frac{\rho}{2}\frac{d}{dt}\|\mathbf{u}-\mathbf{u}_\tau\|^2_{L^2(\Omega)} + \mu\|\nabla(\mathbf{u}-\mathbf{u}_\tau)\|^2_{L^2(\Omega)} &= \rho\int_\Omega \frac{\partial}{\partial t}(\mathbf{u}-\mathbf{u}_\tau)\cdot(\mathbf{u}-\mathbf{u}_\tau)d\mathbf{x} \\
&+ \mu\int_\Omega \nabla(\mathbf{u}-\mathbf{u}_\tau) : \nabla(\mathbf{u}-\mathbf{u}_\tau)d\mathbf{x} \\
&= \rho\int_\Omega \frac{\partial}{\partial t}(\mathbf{u}-\mathbf{u}_\tau)\cdot(\mathbf{u}-\mathbf{u}_\tau)d\mathbf{x} \\
&+ \mu\int_\Omega \nabla(\mathbf{u}-\mathbf{u}_\tau) : \nabla(\mathbf{u}-\mathbf{u}_\tau)d\mathbf{x} \\
&+ \rho\int_\Omega ((\mathbf{u}\cdot\nabla)\mathbf{u} - (\mathbf{u}_\tau\cdot\nabla)\mathbf{u}_\tau)(\mathbf{u}-\mathbf{u}_\tau)d\mathbf{x} \\
&- \int_\Omega (p-p_\tau)\operatorname{div}(\mathbf{u}-\mathbf{u}_\tau) \\
&- \rho\int_\Omega ((\mathbf{u}\cdot\nabla)\mathbf{u} - (\mathbf{u}_\tau\cdot\nabla)\mathbf{u}_\tau)(\mathbf{u}-\mathbf{u}_\tau)d\mathbf{x}.
\end{aligned}$$

Note that $\operatorname{div}(\mathbf{u}) = \operatorname{div}(\mathbf{u}_\tau) = 0$ so we can add the pressure term for free. Using the fact $(\mathbf{u}, p)$ is the exact solution and rearranging the non-linear terms, we obtain that

$$\begin{aligned}
\frac{\rho}{2}\frac{d}{dt}\|\mathbf{u}-\mathbf{u}_\tau\|^2_{L^2(\Omega)} + \mu\|\nabla(\mathbf{u}-\mathbf{u}_\tau)\|^2_{L^2(\Omega)} &= \int_\Omega \mathbf{f}\cdot(\mathbf{u}-\mathbf{u}_\tau)d\mathbf{x} - \rho\int \frac{\partial \mathbf{u}_\tau}{\partial t}\cdot(\mathbf{u}-\mathbf{u}_\tau)d\mathbf{x} \\
&- \mu\int_\Omega \nabla\mathbf{u}_\tau : \nabla(\mathbf{u}-\mathbf{u}_\tau)d\mathbf{x} \\
&- \rho\int_\Omega (\mathbf{u}_\tau\cdot\nabla)\mathbf{u}_\tau)(\mathbf{u}-\mathbf{u}_\tau)d\mathbf{x} + \int_\Omega p_\tau \operatorname{div}(\mathbf{u}-\mathbf{u}_\tau) \\
&- \rho\int_\Omega ((\mathbf{u}\cdot\nabla)(\mathbf{u}-\mathbf{u}_\tau))\cdot(\mathbf{u}-\mathbf{u}_\tau)d\mathbf{x} \\
&- \rho\int_\Omega ((\mathbf{u}-\mathbf{u}_\tau)\cdot\nabla)\mathbf{u}_\tau)\cdot(\mathbf{u}-\mathbf{u}_\tau)d\mathbf{x}.
\end{aligned}$$

Since $\mathbf{u}$ is divergence free, the term

$$\rho\int_\Omega ((\mathbf{u}\cdot\nabla)(\mathbf{u}-\mathbf{u}_\tau))\cdot(\mathbf{u}-\mathbf{u}_\tau)d\mathbf{x}$$

is null thanks to divergence theorem and the boundary conditions. Using then the Lemma 3.53, Cauchy-Schwarz and Sobolev inequalities, we obtain

$$\begin{aligned}
\frac{\rho}{2}\frac{d}{dt}\|\mathbf{u}-\mathbf{u}_\tau\|^2_{L^2(\Omega)} + \mu\|\nabla(\mathbf{u}-\mathbf{u}_\tau)\|^2_{L^2(\Omega)} &\leq \|\mathbf{f}-\mathbf{f}^{n+1}\|_{L^2(\Omega)}\|\mathbf{u}-\mathbf{u}_\tau\|_{L^2(\Omega)} \\
+ |t-t^{n+1}|\rho\|(\mathbf{u}^{n+1}\cdot\nabla)\partial\mathbf{u}^{n+1} &+ (\partial\mathbf{u}^{n+1}\cdot\nabla)\mathbf{u}^{n+1}\|_{L^2(\Omega)}\|\mathbf{u}-\mathbf{u}_\tau\|_{L^2(\Omega)} \\
&+ |t-t^{n+1}|\mu\|\nabla\partial\mathbf{u}^{n+1}\|_{L^2(\Omega)}\|\nabla(\mathbf{u}-\mathbf{u}_\tau)\|_{L^2(\Omega)} \\
+|t-t^{n+1}|^2\rho\|(\partial\mathbf{u}^{n+1}\cdot\nabla)\partial\mathbf{u}^{n+1}\|_{L^2(\Omega)}&\|\mathbf{u}-\mathbf{u}_\tau\|_{L^2(\Omega)} + C_{SOB}\rho\|\nabla\mathbf{u}_\tau\|_{L^2(\Omega)}\|\nabla(\mathbf{u}-\mathbf{u}_\tau)\|^2_{L^2(\Omega)}.
\end{aligned}$$

Using the Poincaré and the Young's inequalities, and the hypothesis on $\|\nabla\mathbf{u}_\tau\|_{L^2(\Omega)}$, we have

$$\begin{aligned}
\frac{\rho}{2}\frac{d}{dt}\|\mathbf{u}-\mathbf{u}_\tau\|^2_{L^2(\Omega)} + \frac{1-\gamma}{2}\mu\|\nabla(\mathbf{u}-\mathbf{u}_\tau)\|^2_{L^2(\Omega)} &\leq \frac{2C_P^2\rho}{\mu(1-\gamma)}\Big(\rho^{-1}\|\mathbf{f}-\mathbf{f}^{n+1}\|^2_{L^2(\Omega)} \\
+|t-t^{n+1}|^2\rho\left\|(\mathbf{u}^{n+1}\cdot\nabla)\partial\mathbf{u}^{n+1} + (\partial\mathbf{u}^{n+1}\cdot\nabla)\mathbf{u}^{n+1}\right\|^2_{L^2(\Omega)}\Big) \\
+ |t-t^{n+1}|^2\mu\|\nabla\partial\mathbf{u}^{n+1}\|^2_{L^2(\Omega)} \\
+ \frac{2C_P^2\rho}{\mu(1-\gamma)}|t-t^{n+1}|^4\rho\|(\partial\mathbf{u}^{n+1}\cdot\nabla)\partial\mathbf{u}^{n+1}\|^2_{L^2(\Omega)},
\end{aligned}$$

where $C_P$ stands for the Poincaré constant of $\Omega$. Then integrating from $t^n$ to $t^{n+1}$ and summing up over $n$ yields the final result. $\square$

**Remark 3.55.** (i) As already commented in Remark 3.20, it is possible to replace (thanks to Gronwall's Lemma) the factor $\rho/\mu$ in front of the first sum of (3.115) by $T$.

(ii) Note that the error indicator $\epsilon_n^T$ will yield to an higher order contribution (namely $O(\tau^2)$), while the BDF1 method is of order 1.

(iii) The terms $\eta_{\rho,n}^T$ and $\eta_{\mu,n}^T$ go like

$$\tau\frac{\partial}{\partial t}\left((\mathbf{u}_\tau\cdot\nabla)\mathbf{u}_\tau\right),\quad \tau\frac{\partial}{\partial t}\nabla\mathbf{u}_\tau.$$

(iv) The hypothesis (3.114) is valid that the solution satisfies itself the same condition for a certain $\gamma'$ and that

$$\sup_{t\in(0,T)}\|\nabla(\mathbf{u}-\mathbf{u}_\tau)(t)\|_{L^2(\Omega)}\to 0,\quad \tau\to 0.$$

Indeed the triangle inequality implies

$$\|\nabla\mathbf{u}_\tau(t)\|_{L^2(\Omega)}\leq\|\nabla(\mathbf{u}-\mathbf{u}_\tau)(t)\|_{L^2(\Omega)}+\|\nabla\mathbf{u}(t)\|_{L^2(\Omega)}.$$

We now prove equivalent results for the BDF2 method. For the need of the proof, we also build a piecewise linear reconstruction of the pressure, for which we keep the same notations as the one introduced for the velocity. In particular, we note

$$\partial p^{n+1}=\frac{p^{n+1}-p^n}{\tau^{n+1}}.$$

The error indicator for the BDF2 method is then contained in the Lemma

**Lemma 3.56** (An error indicator for the BDF2 method applied to the Navier-Stokes equations)**.**
*Let $(\mathbf{u}^n)_{n=0}^N, (p^n)_{n=0}^N$ be the approximated solutions to (3.87) obtained by solving the numerical method (3.111) with $k=2$. Let us define the piecewise reconstruction of the velocity $\mathbf{u}_\tau$ by*

$$\mathbf{u}_\tau(t)=\mathbf{u}^1+(t-t^1)\partial\mathbf{u}^1,\quad t\in[t^0,t^1],\tag{3.116}$$

*and*

$$\mathbf{u}_\tau(t)=\mathbf{u}^{n+1}+(t-t^{n+1})\partial\mathbf{u}^{n+1}+\frac{1}{2}(t-t^n)(t-t^{n+1})\partial^2\mathbf{u}^{n+1},\quad t\in[t^n,t^{n+1}], n=1,2,...N-1.\tag{3.117}$$

*Moreover, let us define the piecewise reconstruction of the pressure $p_\tau$*

$$p_\tau(t)=p^1,\quad t\in[t^0,t^1],\tag{3.118}$$

*and*

$$p_\tau(t)=p^{n+1}+(t-t^{n+1})\partial p^{n+1},\quad t\in[t^n,t^{n+1}], n=1,2,...,N-1.\tag{3.119}$$

*Then, it holds for any $t \in (t^n, t^{n+1}), n = 1, 2, ..., N-1$ and all $\mathbf{v} \in (H_0^1(\Omega))^2$*

$$\rho \int_\Omega \frac{\partial \mathbf{u}_\tau}{\partial t} \cdot \mathbf{v} d\mathbf{x} + \rho \int_\Omega ((\mathbf{u}_\tau \cdot \nabla)\mathbf{u}_\tau) \cdot \mathbf{v} d\mathbf{x} + \mu \int_\Omega \nabla \mathbf{u}_\tau : \nabla \mathbf{v} d\mathbf{x} - \int_\Omega p_\tau \operatorname{div} \mathbf{v} d\mathbf{x}$$
$$= \int_\Omega \Big(\mathbf{f}^{n+1} + (t - t^{n+1})\partial \mathbf{f}^{n+1}\Big) \cdot \mathbf{v} d\mathbf{x} - \frac{\tau^n}{2}(t - t^{n+1})\rho \int_\Omega \tilde{\partial} \mathbf{u}^{n+1} \cdot \mathbf{v} d\mathbf{x}$$
$$+\rho(t-t^n)(t-t^{n+1}) \int_\Omega \Big(\frac{1}{2}(\mathbf{u}^{n+1} \cdot \nabla)\partial^2 \mathbf{u}^{n+1} + (\partial \mathbf{u}^{n+1} \cdot \nabla)\partial \mathbf{u}^{n+1} + \frac{1}{2}(\partial^2 \mathbf{u}^{n+1} \cdot \nabla)\mathbf{u}^{n+1}\Big) \cdot \mathbf{v} d\mathbf{x}$$
$$+ \frac{\mu}{2}(t - t^n)(t - t^{n+1}) \int_\Omega \nabla \partial^2 \mathbf{u}^{n+1} : \nabla \mathbf{v} d\mathbf{x}$$
$$+ \frac{\rho}{2}(t - t^n)(t - t^{n+1})^2 \int_\Omega \Big((\partial^2 \mathbf{u}^{n+1} \cdot \nabla)\partial \mathbf{u}^{n+1} + (\partial \mathbf{u}^{n+1} \cdot \nabla)\partial^2 \mathbf{u}^{n+1}\Big) \cdot \mathbf{v} d\mathbf{x}$$
$$+ \frac{\rho}{4}(t - t^n)^2(t - t^{n+1})^2 \int_\Omega \Big((\partial^2 \mathbf{u}^{n+1} \cdot \nabla)\partial^2 \mathbf{u}^{n+1}\Big) \cdot \mathbf{v} d\mathbf{x}, \quad (3.120)$$

*where we note*

$$\tilde{\partial} \mathbf{u}^{n+1} = \frac{\partial^2 \mathbf{u}^{n+1} - \partial^2 \mathbf{u}^n}{\tau^{n+1}}, n = 2, 3, ..., N-1, \quad \tilde{\partial} \mathbf{u}^2 = \partial^2 \mathbf{u}^2.$$

*Moreover, for any $t \in (t^0, t^1)$ and all $\mathbf{v} \in (H_0^1(\Omega))^2$*

$$\rho \int_\Omega \frac{\partial \mathbf{u}_\tau}{\partial t} \cdot \mathbf{v} d\mathbf{x} + \rho \int_\Omega ((\mathbf{u}_\tau \cdot \nabla)\mathbf{u}_\tau) \cdot \mathbf{v} d\mathbf{x} + \mu \int_\Omega \nabla \mathbf{u}_\tau : \nabla \mathbf{v} d\mathbf{x} - \int_\Omega p_\tau \operatorname{div} \mathbf{v} d\mathbf{x} = \int_\Omega \mathbf{f}^1 \cdot \mathbf{v} d\mathbf{x}$$
$$+ (t - t^1)\rho \int_\Omega \Big((\mathbf{u}^1 \cdot \nabla)\partial \mathbf{u}^1 + (\partial \mathbf{u}^1 \cdot \nabla)\mathbf{u}^1\Big) \cdot \mathbf{v} d\mathbf{x} + (t - t^1)\mu \int_\Omega \nabla \partial \mathbf{u}^1 : \nabla \mathbf{v} d\mathbf{x}$$
$$+ (t - t^1)^2 \rho \int_\Omega \Big((\partial \mathbf{u}^1 \cdot \nabla)\partial \mathbf{u}^1\Big) \cdot \mathbf{v} d\mathbf{x}. \quad (3.121)$$

*Proof.* Let $t \in (t^n, t^{n+1})$. Observe that the case $n = 0$ is a application of the Lemma 3.53 since the first step in the BDF2 method is an Euler step. Therefore, we consider the case where $n \geq 1$. We recall that $\mathbf{u}_\tau$ is then given by

$$\mathbf{u}_\tau(t) = \mathbf{u}^{n+1} + (t - t^{n+1})\partial \mathbf{u}^{n+1} + \frac{1}{2}(t - t^n)(t - t^{n+1})\partial^2 \mathbf{u}^{n+1}$$

and a direct computation yields

$$\rho \int_\Omega \frac{\partial \mathbf{u}_\tau}{\partial t} \cdot \mathbf{v} d\mathbf{x} + \rho \int_\Omega ((\mathbf{u}_\tau \cdot \nabla)\mathbf{u}_\tau) \cdot \mathbf{v} d\mathbf{x} + \mu \int_\Omega \nabla \mathbf{u}_\tau : \nabla \mathbf{v} d\mathbf{x} - \int_\Omega p_\tau \operatorname{div} \mathbf{v} d\mathbf{x} = I_1 + I_2 + I_3 + I_4,$$

where

$$I_1 = \rho \int_\Omega \partial \mathbf{u}^{n+1} \cdot \mathbf{v} d\mathbf{x} + \frac{\tau^{n+1}}{2}\rho \int_\Omega \partial^2 \mathbf{u}^{n+1} \cdot \mathbf{v} d\mathbf{x} + \rho \int_\Omega ((\mathbf{u}^{n+1} \cdot \nabla)\mathbf{u}^{n+1}) \cdot v d\mathbf{x}$$
$$+ \mu \int_\Omega \nabla \mathbf{u}^{n+1} : \nabla \mathbf{v} d\mathbf{x} - \int_\Omega p^{n+1} \operatorname{div} \mathbf{v} d\mathbf{x},$$

$$I_2 = (t - t^{n+1}) \Big(\rho \int_\Omega \partial^2 \mathbf{u}^{n+1} \cdot \mathbf{v} d\mathbf{x} + \rho \int_\Omega \Big((\mathbf{u}^{n+1} \cdot \nabla)\partial \mathbf{u}^{n+1} + (\partial \mathbf{u}^{n+1} \cdot \nabla)\mathbf{u}^{n+1}\Big) \cdot \mathbf{v} d\mathbf{x}$$
$$+\mu \int_\Omega \nabla \partial \mathbf{u}^{n+1} : \nabla \mathbf{v} d\mathbf{x} - \int_\Omega \partial p^{n+1} \operatorname{div} \mathbf{v} d\mathbf{x}\Big)$$

$$I_3 = \frac{\rho}{2}(t - t^n)(t - t^{n+1}) \int_\Omega \Big((\mathbf{u}^{n+1} \cdot \nabla)\partial^2 \mathbf{u}^{n+1} + (\partial^2 \mathbf{u}^{n+1} \cdot \nabla)\mathbf{u}^{n+1}\Big) \cdot \mathbf{v} d\mathbf{x}$$
$$+ \rho(t - t^{n+1})^2 \int_\Omega \Big(\partial \mathbf{u}^{n+1} \cdot \nabla)\partial \mathbf{u}^{n+1}\Big) \cdot \mathbf{v} d\mathbf{x} + \frac{\mu}{2}(t - t^n)(t - t^{n+1}) \int_\Omega \nabla \partial^2 \mathbf{u}^{n+1} : \nabla \mathbf{v} d\mathbf{x},$$

$$I_4 = \frac{\rho}{2}(t-t^n)(t-t^{n+1})^2 \int_\Omega \Big( (\partial^2 \mathbf{u}^{n+1}\cdot\nabla)\partial\mathbf{u}^{n+1} + (\partial\mathbf{u}^{n+1}\cdot\nabla)\partial^2\mathbf{u}^{n+1}\Big)\cdot \mathbf{v}d\mathbf{x}$$
$$+ \frac{\rho}{4}(t-t^n)^2(t-t^{n+1})^2 \int_\Omega \Big( (\partial^2 \mathbf{u}^{n+1}\cdot\nabla)\partial^2\mathbf{u}^{n+1}\Big)\cdot \mathbf{v}d\mathbf{x}.$$

The numerical method (3.111) implies that $I_1 = \mathbf{f}^{n+1}$. Observe that $I_4$ is already the correct quantity and $I_3$ is of second order, we only have to treat $I_2$ that is a low order quantity, namely order 1.

Taking the difference between (3.111) at two consecutive steps, following the computations performed in Lemma 3.52, one derive that

$$\rho\int_\Omega \partial^2\mathbf{u}^{n+1}\cdot\mathbf{v}d\mathbf{x} + \rho\int_\Omega \Big( (\mathbf{u}^{n+1}\cdot\nabla)\partial\mathbf{u}^{n+1} + (\partial\mathbf{u}^{n+1}\cdot\nabla)\mathbf{u}^{n+1}\Big)\cdot\mathbf{v}d\mathbf{x}$$
$$+\mu\int_\Omega \nabla\partial\mathbf{u}^{n+1} : \nabla\mathbf{v}d\mathbf{x} - \int_\Omega \partial p^{n+1}\operatorname{div}\mathbf{v}d\mathbf{x}$$
$$= \int_\Omega \partial\mathbf{f}^{n+1}\cdot\mathbf{v}d\mathbf{x} - \rho\frac{\tau^n}{2}\int_\Omega \tilde{\partial}\mathbf{u}^{n+1}\cdot\mathbf{v}d\mathbf{x} + \tau^{n+1}\rho\int_\Omega \Big(\partial\mathbf{u}^{n+1}\cdot\nabla)\partial\mathbf{u}^{n+1}\Big)\cdot\mathbf{v}d\mathbf{x}.$$

Then

$$I_2 = (t-t^{n+1})\int_\Omega \partial\mathbf{f}^{n+1}\cdot\mathbf{v}d\mathbf{x} - \rho\frac{\tau^n}{2}(t-t^{n+1})\int_\Omega \tilde{\partial}\mathbf{u}^{n+1}\cdot\mathbf{v}d\mathbf{x}$$
$$+\tau^{n+1}(t-t^{n+1})\rho\int_\Omega \Big(\partial\mathbf{u}^{n+1}\cdot\nabla)\partial\mathbf{u}^{n+1}\Big)\cdot\mathbf{v}d\mathbf{x}.$$

Combining the expression for $I_1, I_2, I_3$ and $I_4$ yields the result. □

The a posteriori error estimates for the BDF2 method is then contained in the Theorem

**Theorem 3.57** (A semi-discrete a posteriori error estimate for the Navier-Stokes equations and the BDF2 method**).**
*Let $(\mathbf{u}, p)$ be the solution of the Navier-Stokes equations (3.87), $(\mathbf{u}^n)_{n=0}^N, (p^n)_{n=1}^N$ be the approximated solutions to (3.87) obtained by solving the numerical method (3.111) with $k = 2$. Let us define the piecewise reconstruction of the velocity $\mathbf{u}_\tau$ by* (3.116), (3.117) *and the piecewise reconstruction of the pressure $p_\tau$ by* (3.118), (3.119). *Finally, assume that there exists $\tau_0$ and $0 < \gamma < 1$ such that for all $\tau < \tau_0$, where $\tau = \max_{n=1,\dots,N}\tau^n$*

$$\sup_{t\in(0,T)} \|\nabla\mathbf{u}_\tau(t)\|_{L^2(\Omega)} \leq \frac{\gamma\mu}{C_{SOB}\rho}, \tag{3.122}$$

*where $C_{SOB}$ is the Sobolev constant in Proposition A.8 of the Appendix A.2. Then, for all $\tau < \tau_0$ there exists a constant $C$ depending only on $\Omega$ such that*

$$\rho\|\mathbf{u}-\mathbf{u}_\tau(T)\|^2_{L^2(\Omega)} + \mu\int_{t^1}^T \|\nabla(\mathbf{u}-\mathbf{u}_\tau)(t)\|^2_{L^2(\Omega)}dt$$
$$\leq \frac{C}{(1-\gamma)^2}\left(\rho\|\mathbf{u}-\mathbf{u}_\tau(t^1)\|^2_{L^2(\Omega)} + \frac{\rho}{\mu}\sum_{n=1}^{N-1}(\eta^T_{\mathbf{f},n})^2 + (\eta^T_{\frac{\partial}{\partial t},n})^2 + (\eta^T_{\rho,n})^2 + (\epsilon^T_n)^2 + \sum_{n=1}^{N-1}(\eta^T_{\mu,n})^2\right), \tag{3.123}$$

*where*

$$(\eta^T_{\mathbf{f},n})^2 = \rho^{-1}\int_{t^n}^{t^{n+1}} \|\mathbf{f}(t) - \mathbf{f}^{n+1} - (t-t^{n+1})\partial\mathbf{f}^{n+1}\|^2_{L^2(\Omega)}dt,$$

$$(\eta^T_{\frac{\partial}{\partial t},n})^2 = \frac{(\tau^n)^2(\tau^{n+1})^3}{12}\rho\|\tilde{\partial}\mathbf{u}^{n+1}\|^2_{L^2(\Omega)},$$

*with*

$$\tilde{\partial}\mathbf{u}^{n+1} = \frac{\partial^2\mathbf{u}^{n+1} - \partial^2\mathbf{u}^n}{\tau^{n+1}}, n = 2, 3, ..., N-1, \quad \tilde{\partial}\mathbf{u}^2 = \partial^2\mathbf{u}^2.$$

$$(\eta_{\rho,n}^T)^2 = \frac{(\tau^{n+1})^5}{120}\rho\|(\mathbf{u}^{n+1}\cdot\nabla)\partial^2\mathbf{u}^{n+1} + (\partial\mathbf{u}^{n+1}\cdot\nabla)\partial\mathbf{u}^{n+1} + (\partial^2\mathbf{u}^{n+1}\cdot\nabla)\mathbf{u}^{n+1}\|^2_{L^2(\Omega)},$$

$$(\epsilon_n^T)^2 = \frac{(\tau^{n+1})^7}{420}\rho\|(\partial^2\mathbf{u}^{n+1}\cdot\nabla)\partial\mathbf{u}^{n+1} + (\partial\mathbf{u}^{n+1}\cdot\nabla)\partial^2\mathbf{u}^{n+1}\|^2_{L^2(\Omega)} + \frac{(\tau^{n+1})^9}{10080}\rho\|(\partial^2\mathbf{u}^{n+1}\cdot\nabla)\partial^2\mathbf{u}^{n+1}\|^2_{L^2(\Omega)},$$

*and*

$$(\eta_{\mu,n}^T)^2 = \frac{(\tau^{n+1})^5}{120}\mu\|\nabla\partial^2\mathbf{u}^{n+1}\|^2_{L^2(\Omega)}.$$

*Moreover, we have*

$$\rho\|\mathbf{u}-\mathbf{u}_\tau(t^1)\|^2_{L^2(\Omega)} + \mu\int_0^{t^1}\|\nabla(\mathbf{u}-\mathbf{u}_\tau)(t)\|^2_{L^2(\Omega)}dt$$
$$\leq \frac{C}{(1-\gamma)^2}\left(\rho\|\mathbf{u}-\mathbf{u}_\tau(0)\|^2_{L^2(\Omega)} + \frac{\rho}{\mu}(\eta_{\mathbf{f},0}^T)^2 + (\eta_{\rho,0}^T)^2 + (\epsilon_0^T)^2 + (\eta_{\mu,0}^T)^2\right), \quad (3.124)$$

*where*

$$(\eta_{\mathbf{f},0}^T)^2 = \rho^{-1}\int_{t^0}^{t^1}\|\mathbf{f}(t)-\mathbf{f}^1\|^2_{L^2(\Omega)}dt,$$

$$(\eta_{\rho,0}^T)^2 = \frac{(\tau^1)^3}{3}\rho\|((\mathbf{u}^1\cdot\nabla)\partial\mathbf{u}^1 + (\partial\mathbf{u}^1\cdot\nabla)\mathbf{u}^1)\|^2_{L^2(\Omega)},$$

$$(\epsilon_0^T)^2 = \frac{(\tau^1)^5}{5}\rho\|(\partial\mathbf{u}^1\cdot\nabla)\partial\mathbf{u}^1\|^2_{L^2(\Omega)},$$

*and*

$$(\eta_{\mu,0}^T)^2 = \frac{(\tau^1)^3}{3}\mu\|\nabla\partial\mathbf{u}^1\|^2_{L^2(\Omega)}.$$

*Proof.* To prove (3.124), we directly apply Theorem 3.54 between $t^0$ and $t^1$.

Now to prove (3.123), we choose $t \in [t^n, t^{n+1}]$ for $n \geq 1$ and we proceed in the same way as in Theorem 3.57. Following the same arguments, we deduce that

$$\begin{aligned}\frac{\rho}{2}\frac{d}{dt}\|\mathbf{u}-\mathbf{u}_\tau\|^2_{L^2(\Omega)} + \mu\|\nabla(\mathbf{u}-\mathbf{u}_\tau)\|^2_{L^2(\Omega)} &= \int_\Omega \mathbf{f}\cdot(\mathbf{u}-\mathbf{u}_\tau)d\mathbf{x} - \rho\int\frac{\partial\mathbf{u}_\tau}{\partial t}\cdot(\mathbf{u}-\mathbf{u}_\tau)d\mathbf{x}\\ &- \mu\int_\Omega\nabla\mathbf{u}_\tau : \nabla(\mathbf{u}-\mathbf{u}_\tau)d\mathbf{x}\\ &- \rho\int_\Omega(\mathbf{u}_\tau\cdot\nabla)\mathbf{u}_\tau)(\mathbf{u}-\mathbf{u}_\tau)d\mathbf{x} + \int_\Omega p_\tau\,\mathrm{div}(\mathbf{u}-\mathbf{u}_\tau)\\ &- \rho\int_\Omega((\mathbf{u}-\mathbf{u}_\tau)\cdot\nabla)\mathbf{u}_\tau)\cdot(\mathbf{u}-\mathbf{u}_\tau)d\mathbf{x}.\end{aligned}$$

We conclude by using Lemma 3.56, (3.120), instead of Lemma 3.53, and we follow the end of the proof of Theorem 3.54, the only difference being that we sum every contribution from $n = 1$ to $N-1$. □

**Remark 3.58.** (i) By analogy with the BDF1 method, observe that the error indicator contained in the a posteriori error estimate (3.123) is roughly speaking

$$\tau^2\frac{d^2}{dt^2}(\mathbf{u}_\tau\cdot\nabla)\mathbf{u}_\tau + \tau^2\frac{d^2}{dt^2}\nabla\mathbf{u}_\tau.$$

(ii) As for the BDF1 method, the hypothesis (3.122) is valid if we assume the convergence of the method and that the exact solution satifies the same condition.

(iii) Both Theorems 3.54 and 3.57 are independent of the dimension and holds in $\mathbb{R}^d$ for $d = 2$ or $d = 3$.

## 3.8 Error indicators for the incompressible Navier-Stokes equations with constant coefficients: spatial and temporal approximation

In this section, we define an error indicator for the unsteady incompressible Navier-Stokes equations (3.85), involving the space and the time discretization. The choice of the indicators are motivated by the spatial semi-discrete a posteriori error estimate ( Theorem 3.49) and the two temporal semi-discrete a posteriori error estimates (Theorems 3.54 and 3.57).

We now briefly expose the fully discretized method we used in our numerical experiments. The framework is the same as the one presented in previous section: let $\Omega$ be a convex domain of $\mathbb{R}^2$, $T > 0$ the final time and $\rho, \mu$ the constant density and viscosity of the fluid. We choose to discretize the time by applying the BDF1 or BDF2 methods to the semi-discrete stabilized finite element scheme (3.88). As before, for all $h > 0$, let $\mathcal{T}_h$ be a conformal triangulation of $\Omega$ into triangles of diameter $h_K \leq h$ and let $0 = t^0 < t^1 < ... < t^N = T$ a partition of $[0, T]$ for $N > 0$ an integer. As before we note the time step $\tau^{n+1} = t^{n+1} - t^n$. Finally let us note $\beta_k^{n+1} \in \{0, 1\}$ given by

$$\beta_1^{n+1} = 0, n = 0, 1, ..., N-1, \quad \beta_2^{n+1} = 0, n = 0, \beta_2^{n+1} = 1, n > 0.$$

Then assuming that $\mathbf{u}_0 \in (H_0^1(\Omega))^2 \times (H^2(\Omega))^2$ and starting from $\mathbf{u}_h^0 = r_h(\mathbf{u}_0)$, we are looking for every $n = 0, 1, ..., N-1$ for $(\mathbf{u}_h^{n+1}, p_h^{n+1}) \in V_h \times Q_h$ the solutions of

$$\begin{aligned}
\rho \int_\Omega \left( \partial \mathbf{u}_h^{n+1} + \frac{\beta_k^{n+1}\tau^{n+1}}{2} \partial^2 \mathbf{u}_h^{n+1} \right) \cdot \mathbf{v}_h d\mathbf{x} + \rho \int_\Omega (\mathbf{u}_h^{n+1} \cdot \nabla) \mathbf{u}_h^{n+1} \cdot \mathbf{v}_h d\mathbf{x} \\
+ \mu \int_\Omega \nabla \mathbf{u}_h^{n+1} : \nabla \mathbf{v}_h d\mathbf{x} - \int_\Omega p_h^{n+1} \operatorname{div} \mathbf{v}_h d\mathbf{x} \\
+ \sum_{K \in \mathcal{T}_h} \alpha_K \int_K R_{h,n+1}^{NS} \cdot \left( \rho(\mathbf{u}_h^{n+1} \cdot \nabla) \mathbf{v}_h - \mu \Delta \mathbf{v}_h \right) d\mathbf{x} = \int_\Omega \mathbf{f}^{n+1} \cdot \mathbf{v}_h d\mathbf{x}, \quad \forall \mathbf{v}_h \in V_h, \\
- \int_\Omega q_h \operatorname{div} \mathbf{u}_h^{n+1} d\mathbf{x} + \sum_{K \in \mathcal{T}_h} \alpha_K \int_K R_{h,n+1}^{NS} \cdot \nabla q_h d\mathbf{x} = 0, \quad \forall q_h \in Q_h, \quad (3.125)
\end{aligned}$$

where we note the residue

$$R_{h,n+1}^{NS} = \mathbf{f}^{n+1} - \rho \left( \partial \mathbf{u}_h^{n+1} + \frac{\beta^n \tau^{n+1}}{2} \partial^2 \mathbf{u}_h^{n+1} \right) - \rho (\mathbf{u}_h^{n+1} \cdot \nabla) \mathbf{u}_h^{n+1} + \mu \Delta \mathbf{u}_h^{n+1} - \nabla p_h^{n+1}$$

and where $\alpha_K$ is given by

$$\alpha_K = \frac{\alpha \lambda_{2,K}^2}{\mu \xi(Re_K)}$$

with $\alpha > 0$ and

$$\xi(Re_K) = \begin{cases} 1 & \text{if } Re_K \leq 1, \\ Re_K & \text{if } Re_K \geq 1, \end{cases}$$

where we define the local anisotropic Reynolds number $Re_K$ by

$$Re_K = \frac{\rho \|\mathbf{u}_h^{n+1}\|_{L^\infty(K)} \lambda_{2,K}}{\mu}.$$

We recall that we note

$$\partial \mathbf{u}_h^{n+1} = \frac{\mathbf{u}_h^{n+1} - \mathbf{u}_h^n}{\tau^{n+1}}, \partial^2 \mathbf{u}_h^{n+1} = \frac{\frac{\mathbf{u}_h^{n+1} - \mathbf{u}_h^n}{\tau^{n+1}} - \frac{\mathbf{u}_h^n - \mathbf{u}_h^{n-1}}{\tau^n}}{\tau^{n+1} + \tau^n / 2}.$$

To lighten the notations, we introduce

$$\partial_\beta \mathbf{u}_h^{n+1} = \partial \mathbf{u}_h^{n+1} + \frac{\beta_k^{n+1}\tau^{n+1}}{2}\partial^2 \mathbf{u}_h^{n+1}, \quad n = 0,1,2,...,N-1. \tag{3.126}$$

**Remark 3.59** (Practical implementation)**.**
Since the equation is non-linear, we decide to solve the discrete problem (3.125) by performing one step of a Newton method at every time iteration. To simplify, lets us consider only the time discretization. We shall solve

$$\rho\left(\frac{\mathbf{u}^{n+1}-\mathbf{u}^n}{\tau^{n+1}} + \frac{\beta_k^{n+1}\tau^{n+1}}{2}\partial^2\mathbf{u}^{n+1}\right) + \rho\Big((\mathbf{u}^*\cdot\nabla)\mathbf{u}^{n+1} + (\mathbf{u}^{n+1}\cdot\nabla)\mathbf{u}^*\Big)$$
$$-\mu\Delta\mathbf{u}^{n+1} + \nabla p^{n+1} = \mathbf{f}^{n+1} + \rho(\mathbf{u}^*\cdot\nabla)\mathbf{u}^*,$$

where we choose $\mathbf{u}^*$ such that the order of the method is conserved.

For instance in the case of the BDF2 method (i.e $k=2$), for $n=0$, since the method reduces to the Backward Euler scheme, we choose $\mathbf{u}^* = \mathbf{u}^0$. Then, for $n \geq 1$, to conserve the second order of convergence, we choose $\mathbf{u}^*$ as the extrapolated solution

$$\mathbf{u}^* = 2\mathbf{u}^n - \mathbf{u}^{n-1}.$$

Otherwise, if we would like to solve the equations with the Backward Euler method at every time iteration, it suffices to set $\mathbf{u}^* = \mathbf{u}^n$ for every $n \geq 0$.

We now define space and time error indicators for the numerical method (3.125). As for the steady case, we only consider error indicators for the velocity. Based on the a posteriori error estimate proven for the semi-discrete approximation, we define the space error indicator $\eta^A$ by

$$\eta^A = \left(\sum_{n=0}^{N-1}\sum_{K\in\mathcal{T}_h}(\eta_{K,n}^A)^2\right)^{1/2}, \tag{3.127}$$

where

$$(\eta_{K,n}^A)^2 = \tau^{n+1}\Bigg(\left\|\mathbf{f}^{n+1} - \rho\partial_\beta\mathbf{u}_h^{n+1} - \rho(\mathbf{u}_h^{n+1}\cdot\nabla)\mathbf{u}_h^{n+1} + \mu\Delta\mathbf{u}_h^{n+1} - \nabla p_h^{n+1}\right\|_{L^2(K)}$$
$$+\frac{1}{2\sqrt{\lambda_{2,K}}}\left\|\left[\mu\nabla\mathbf{u}_h^{n+1}\cdot\mathbf{n}\right]\right\|_{L^2(\partial K)}\Bigg)\tilde{\omega}_K\left(\Pi_h^{ZZ}\mathbf{u}_h^{n+1} - \mathbf{u}_h^{n+1}\right),$$

where $\Pi_h^{ZZ}$ stands for the ZZ post-processing and $\tilde{\omega}_K$ for the simplified anisotropic form given by (1.18).

For the time error indicators, we adapt the results of Theorems 3.54 and 3.57. When using the BDFk method, we advocated the following error indicator $\eta_{BDFk}^T$ defined by

$$\eta_{BDFk}^T = \left(\sum_{n=0}^{N-1}\sum_{K\in\mathcal{T}_h}(\eta_{K,n}^{T,k})^2\right)^{1/2}, \quad k=1,2 \tag{3.128}$$

where, for $k=1$,

$$(\eta_{K,n}^{T,1})^2 = (\tau^{n+1})^3\rho\left\|(\mathbf{u}_h^{n+1}\cdot\nabla)\partial\mathbf{u}_h^{n+1} + (\partial\mathbf{u}_h^{n+1}\cdot\nabla)\mathbf{u}_h^{n+1}\right\|_{L^2(K)}^2 + (\tau^{n+1})^3\mu\left\|\nabla\partial\mathbf{u}_h^{n+1}\right\|_{L^2(K)}^2.$$

and for $k=2$

$$(\eta_{K,n}^{T,2})^2 = (\tau^{n+1})^5\rho\left\|(\mathbf{u}_h^{n+1}\cdot\nabla)\partial^2\mathbf{u}_h^{n+1} + (\partial\mathbf{u}_h^{n+1}\cdot\nabla)\partial\mathbf{u}_h^{n+1} + (\partial^2\mathbf{u}_h^{n+1}\cdot\nabla)\mathbf{u}_h^{n+1}\right\|_{L^2(K)}^2$$
$$+(\tau^{n+1})^5\mu\left\|\nabla\partial^2\mathbf{u}_h^{n+1}\right\|_{L^2(K)}^2.$$

The total error indicator is defined by

$$\eta_k = \left((\eta^A)^2 + (\eta^T_{BDFk})^2\right)^{1/2}, \quad k = 1, 2.$$

To check its sharpness we define the effectivity indices

$$ei_k = \frac{\eta_k}{e_{\mu,H^1}}, k = 1, 2, \quad ei^{ZZ} = \frac{\eta^{ZZ}}{e_{H^1}},$$

where we note

$$e_{\mu,H^1} = \left(\mu \int_{t^{k-1}}^T \|\nabla(\mathbf{u} - \mathbf{u}_{h\tau})\|^2_{L^2(\Omega)} dt\right)^{1/2}, \quad k = 1, 2,$$

$$e_{H^1} = \left(\int_0^T \|\nabla(\mathbf{u} - \mathbf{u}_{h\tau})\|^2_{L^2(\Omega)} dt\right)^{1/2},$$

and

$$\eta^{ZZ} = \left(\int_0^T \|\nabla(\Pi_h^{ZZ}\mathbf{u}_{h\tau} - \mathbf{u}_{h\tau})\|^2_{L^2(\Omega)} dt\right)^{1/2}.$$

Here $\mathbf{u}_{h\tau}$ is either a piecewise linear or quadratic numerical reconstruction (depending if we use the BDF1 or the BDF2 methods to advance in time). Finally, to check the convergence in the pressure, we note

$$e_p = \left(\int_0^T \|p - p_{h\tau}\|^2_{L^2(\Omega)} dt\right)^{1/2}.$$

**Remark 3.60** (Comments on the choices of the time error indicators). (i) We could define an heuristic error indicators by exploiting the previous knowledges obtained for instance in Chapter 2 for the transport equations, or in Section 3.5 for the Stokes equations, or in Theorems 3.54 and 3.57 for the Navier-Stokes ones. Formally speaking, we know that if we apply a finite difference scheme to solve the ODE

$$\frac{du(t)}{dt} + A(t)u(t) = 0, \tag{3.129}$$

where $A$ is seen as a general operator between functional spaces, then an error indicator for the time discretization is given by

$$\tau^k \frac{d^k}{dt^k}(A(t)u_\tau(t)),$$

where $k$ is the order of convergence of the method and $u_\tau$ is a suitable piecewise reconstruction of the numerical solution (linear for first order scheme, quadratic for second order scheme, etc...) See also [72], [82], [3], [2] for parabolic problems, [73] and [41] for hyperbolic problems or [16], [23], and [107] for (Navier-)Stokes equations. Then, heuristically, we can define the local error indicators as

$$\eta_n^T = (\tau^{n+1})^k \left|\frac{d^k}{dt^k}(A(t^{n+1})u_\tau(t^{n+1}))\right|, \tag{3.130}$$

and observe that all our estimators are of this type. Differentiating the equation (3.129), we also know that

$$\frac{d^k}{dt^k}(A(t)u(t)) = -\frac{d^{k+1}}{dt^{k+1}}u(t),$$

and moreover we know that the numerical error will *a priori* goes as

$$\tau^k \left| \frac{d^{k+1}}{dt^{k+1}} u(t) \right| = \tau^k \left| \frac{d^k}{dt^k} (A(t)u(t)) \right|.$$

We emphasize again that these last observations motivate the definition (3.130) since the error indicator imitates the a priori estimate.

Another choice could be to directly use a finite difference to approximate $\frac{d^{k+1}}{dt^{k+1}} u(t)$, and define an other error indicator that reads, here written for instance for a second order method,

$$\eta_n^T = (\tau^{n+1})^2 \frac{\partial^2 u^{n+1} - \partial^2 u^n}{\tau^{n+1}},$$

compared with the a priori error that behaves as

$$\tau^2 \frac{d^3 u}{dt^3}.$$

A future work would be to compare this last error indicator, given by the heuristic, to the one that will be given by a proper proof.

(ii) Note that it is possible to give a quick and formal justification to the definition of (3.130). Let us consider the simpler case where $k = 1$, for instance by approximating (3.129) with the Backward Euler method. It reads

$$\frac{u^{n+1} - u^n}{\tau^{n+1}} + A(t^{n+1})u^{n+1} = 0. \tag{3.131}$$

Now, choosing a linear reconstruction

$$u_\tau(t) = u^{n+1} + (t - t^{n+1}) \frac{u^{n+1} - u^n}{\tau^{n+1}}$$

we easily compute, by using a Taylor expansion at $t^{n+1}$ of $A(t)u_\tau(t)$, that

$$\begin{aligned}
&\frac{du_\tau(t)}{dt} + A(t)u_\tau(t) \\
&= \frac{u^{n+1} - u^n}{\tau^{n+1}} + A(t^{n+1})u_\tau(t^{n+1}) + (t - t^{n+1}) \frac{d}{dt} \left( A(t^{n+1})u_\tau(t^{n+1}) \right) + O\left( |t - t^{n+1}|^2 \right) \\
&= \underbrace{\frac{u^{n+1} - u^n}{\tau^{n+1}} + A(t^{n+1})u^{n+1}}_{=0} + (t - t^{n+1}) \frac{d}{dt} \left( A(t^{n+1})u_\tau(t^{n+1}) \right) + O\left( |t - t^{n+1}|^2 \right) \\
&= (t - t^{n+1}) \frac{d}{dt} \left( A(t^{n+1})u_\tau(t^{n+1}) \right) + O\left( |t - t^{n+1}|^2 \right).
\end{aligned}$$

## 3.9 Numerical experiments with non-adapted meshes and non-adapted time steps

In this section, we perform numerical experiments with non-adapted meshes and constant time steps to check the convergence of the numerical methods and analyse the accuracy of the error indicators. We consider the classical test of Poiseuille flow, but where the inflow depends on the time.

**Example 3.61** (A Poiseuille experiment with a time-varying inflow).
We set $\Omega$ as the rectangle $(0, 0.15) \times (0, 0.03)$ and $T = 1$. We compute $\mathbf{f}$ such that the exact solution is a Poiseuille flow given by

$$\mathbf{u}(x_1, x_2, t) = \begin{pmatrix} 2.25e^{-4}x_2(0.03 - x_2)\sin(2\pi\omega t + 0.5) \\ 0 \end{pmatrix},$$

$$p(x_1, x_2, t) = \mu 2.25e^{-4}(0.3 - 2x_1)\sin(2\pi\omega t + 0.5).$$

where $\omega > 0$ controls the frequency of the inflow oscillations. We impose Dirichlet boundary conditions on the left, top and bottom side of $\Omega$ and Neumann boundary condition on the right side, thus we do not have to impose the pressure. As in Example 3.9 for the steady Navier-Stokes equations, the Reynolds number is given by $Re = \frac{\rho 0.03}{\mu}$. We fix $\rho = 1$ so that the Reynolds number is only controlled by the viscosity. As mentioned several times, we would like to observe the following:

- The error indicator must preserve the order of the method. In particular, $\eta^A$ must be $O(h)$ and $\eta^T_{BDFk}$ must behaves as $O(\tau^k)$.

- $ei_k, k = 1, 2$ stays close to a constant and is independent of the Reynolds number, the solution and the discretization parameter, in particular the mesh aspect ratio.

- $ei^{ZZ}$ must be asymptotically 1.

We first investigate the values of $ei_1$ and $ei_2$ when the error is mainly due to spatial approximation. In Tables 3.4 and 3.5, we present the convergence results when $\omega = 1$. Both the velocity and the pressure errors are $O(h)$ that is consistent with the use of linear finite elements. The effectivity index stays close to a value of 3, independently of the choice of the time discretization method, the solution, the Reynolds number or the mesh aspect ratio. In any case, the ZZ post-processing is asymptotically exact. To check that the value of $ei_i$ does not depends on the solution, we run the same experiments with $\omega = 10$. The results when using the BDF2 method are reported in the Table 3.6. The same conclusions can be made with the BDF1 method.

| $h_1 - h_2$ | $\tau$ | $e_{\mu,H^1}$ | $e_p$ | $ei_1$ | $ei^{ZZ}$ |
|---|---|---|---|---|---|
| 0.05 - 0.005 | 0.001 | 0.086 | 0.024 | 2.72 | 1.00 |
| 0.025 - 0.0025 | 0.00025 | 0.041 | 0.0064 | 2.73 | 1.00 |
| 0.0125 - 0.00125 | 0.0000625 | 0.021 | 0.0016 | 2.75 | 1.00 |
| 0.05 - 0.001 | 0.001 | 0.018 | 0.0053 | 2.86 | 1.00 |
| 0.025 - 0.0005 | 0.00025 | 0.0085 | 0.0014 | 2.92 | 1.00 |
| 0.0125 - 0.00025 | 0.0000625 | 0.0043 | 0.00068 | 2.81 | 1.00 |
| 0.05 - 0.001 | 0.001 | 0.0087 | 0.00077 | 2.82 | 1.00 |
| 0.025 - 0.0005 | 0.00025 | 0.0041 | 0.00031 | 2.74 | 1.00 |
| 0.0125 - 0.00025 | 0.0000625 | 0.0021 | 0.00013 | 2.72 | 0.99 |
| 0.05 - 0.001 | 0.001 | 0.0017 | 0.000074 | 2.87 | 1.00 |
| 0.025 - 0.0005 | 0.00025 | 0.00085 | 0.000019 | 2.92 | 1.00 |
| 0.0125 - 0.00025 | 0.0000625 | 0.00043 | 0.000011 | 2.81 | 1.00 |

Table 3.4: Convergence results for Example 3.61 with $\omega = 1$, when $\tau = O(h^2)$. The time advancing scheme is chosen as BDF1. Aspect ratio 10 (rows 1-3 and 7-9) and 50 (rows 4-6 and 10-12). $Re = 1$ (row 1-6), $Re = 100$ (rows 7-12).

| $h_1 - h_2$ | $\tau$ | $e_{\mu,H^1}$ | $e_p$ | $ei_1$ | $ei^{ZZ}$ |
|---|---|---|---|---|---|
| 0.05 - 0.005 | 0.001 | 0.086 | 0.024 | 2.72 | 1.00 |
| 0.025 - 0.0025 | 0.00025 | 0.041 | 0.0064 | 2.73 | 1.00 |
| 0.0125 - 0.00125 | 0.0000625 | 0.021 | 0.0016 | 2.75 | 1.00 |
| 0.05 - 0.001 | 0.001 | 0.018 | 0.0053 | 2.86 | 1.00 |
| 0.025 - 0.0005 | 0.00025 | 0.0085 | 0.0014 | 2.92 | 1.00 |
| 0.0125 - 0.00025 | 0.0000625 | 0.0043 | 0.00068 | 2.81 | 1.00 |
| 0.05 - 0.005 | 0.001 | 0.0087 | 0.00077 | 2.82 | 1.00 |
| 0.025 - 0.0025 | 0.00025 | 0.0041 | 0.00031 | 2.74 | 1.00 |
| 0.0125 - 0.00125 | 0.0000625 | 0.0021 | 0.00013 | 2.72 | 0.99 |
| 0.05 - 0.001 | 0.001 | 0.0017 | 0.000074 | 2.87 | 1.00 |
| 0.025 - 0.0005 | 0.00025 | 0.00085 | 0.000019 | 2.92 | 1.00 |
| 0.0125 - 0.00025 | 0.0000625 | 0.00043 | 0.000011 | 2.81 | 1.00 |

Table 3.5: Convergence results for Example 3.61 with $\omega = 1$, when $\tau = O(h^2)$. The time advancing scheme is chosen as BDF2. Aspect ratio 10 (rows 1-3 and 7-9) and 50 (rows 4-6 and 10-12). $Re = 1$ (row 1-6), $Re = 100$ (rows 7-12).

| $h_1 - h_2$ | $\tau$ | $e_{\mu,H^1}$ | $e_p$ | $ei_2$ | $ei^{ZZ}$ |
|---|---|---|---|---|---|
| 0.0125 - 0.00125 | 0.0000625 | 0.021 | 0.0015 | 2.75 | 1.00 |
| 0.0125 - 0.00025 | 0.0000625 | 0.0043 | 0.00068 | 2.83 | 1.00 |
| 0.0125 - 0.00125 | 0.0000625 | 0.0021 | 0.00052 | 2.74 | 1.00 |
| 0.0125 - 0.00025 | 0.0000625 | 0.00045 | 0.00037 | 2.77 | 0.97 |

Table 3.6: Convergence results for Example 3.61 with $\omega = 10$.The time advancing scheme is chosen as BDF2. Aspect ratio 10 (rows 1 and 3) and 50 (rows 2 and 4). $Re = 1$ (rows 1-2), $Re = 100$ (rows 3-4).

**Example 3.62** (A solution with a small dependence in the space variable)**.**
To evaluate the effectivity indices when the error due to the time discretization is dominating, we consider another problem when the velocity is a linear function, so that the error due to the space discretization is negligible. The solution is given by

$$\mathbf{u}(x_1, x_2, t) = \begin{pmatrix} \frac{1}{0.015}(0.03 - x_2)\sin(2\pi\omega t + 0.5) \\ 0 \end{pmatrix},$$

$$p(x_1, x_2, t) = \frac{\mu}{0.015}(0.3 - 2x_1)\sin(2\pi\omega t + 0.5).$$

All the computations are performed on a grid of mesh size $0.0125 - 0.00125$ and $0.0125 - 0.00025$. In Table 3.7 and 3.8, we check the convergence for the BDF1 method and the BDF2 method for $\omega = 25$ and $Re = 1$. The time error indicators $\eta^T_{BDFk}$ are of optimal order, being $O(\tau^k)$ and the effectivity indices stays close to a value of 7 for the BDF1 method and 2 for the BDF2 method. Note that, as already observed with the transport equation, $ei^{ZZ}$ is far from 1, but this is not an issue since the error due the spatial approximation is smaller than the error due to the time discretization. To check that the effectivity index does not depend on the solution or the Reynolds number, we perform the same experiments with $\omega = 2.5$ and $Re = 10$. The results are reported in Table 3.9

| $h_1 - h_2$ | $\tau$ | $e_{\mu,H^1}$ | $e_p$ | $\eta^T_{BDF1}$ | $ei_2$ | $ei^{ZZ}$ |
|---|---|---|---|---|---|---|
| 0.0125 - 0.00125 | 0.01 | 0.061 | 0.47 | 0.45 | 7.37 | 0.11 |
| 0.0125 - 0.00125 | 0.005 | 0.033 | 0.25 | 0.24 | 7.32 | 0.14 |
| 0.0125 - 0.00125 | 0.0025 | 0.017 | 0.13 | 0.12 | 7.22 | 0.14 |
| 0.0125 - 0.00025 | 0.01 | 0.059 | 0.47 | 0.45 | 7.61 | 0.13 |
| 0.0125 - 0.00025 | 0.005 | 0.032 | 0.25 | 0.24 | 7.58 | 0.17 |
| 0.0125 - 0.00025 | 0.0025 | 0.017 | 0.13 | 0.12 | 7.49 | 0.18 |

Table 3.7: Convergence results for Example 3.62 with $Re = 1$ and $\omega = 25$. The time advancing scheme is chosen as BDF1. Aspect ratio 10 (rows 1-3), 50 (rows 4-6).

| $h_1 - h_2$ | $\tau$ | $e_{\mu,H^1}$ | $e_p$ | $\eta^T_{BDF2}$ | $ei_2$ | $ei^{ZZ}$ |
|---|---|---|---|---|---|---|
| 0.0125 - 0.00125 | 0.01 | 0.057 | 0.45 | 0.11 | 1.91 | 0.11 |
| 0.0125 - 0.00125 | 0.005 | 0.017 | 0.12 | 0.029 | 1.78 | 0.13 |
| 0.0125 - 0.00125 | 0.0025 | 0.0045 | 0.033 | 0.0076 | 1.78 | 0.14 |
| 0.0125 - 0.00025 | 0.01 | 0.056 | 0.45 | 0.11 | 1.97 | 0.13 |
| 0.0125 - 0.00025 | 0.005 | 0.017 | 0.13 | 0.029 | 1.94 | 0.17 |
| 0.0125 - 0.00025 | 0.0025 | 0.0044 | 0.034 | 0.0076 | 1.95 | 0.18 |

Table 3.8: Convergence results for Example 3.62 with $Re = 1$ and $\omega = 25$. The time advancing scheme is chosen as BDF2. Aspect ratio 10 (rows 1-3), 50 (rows 4-6).

| $h_1 - h_2$ | $\tau$ | $e_{\mu,H^1}$ | $e_p$ | $\eta^T_{BDF1}$ | $ei_2$ | $ei^{ZZ}$ |
|---|---|---|---|---|---|---|
| 0.0125 - 0.00125 | 0.02 | 0.0043 | 0.0108 | 0.031 | 7.16 | 0.14 |
| 0.0125 - 0.00125 | 0.01 | 0.0022 | 0.0051 | 0.016 | 7.14 | 0.14 |
| 0.0125 - 0.00125 | 0.005 | 0.0011 | 0.0025 | 0.0078 | 7.13 | 0.14 |
| $h_1 - h_2$ | $\tau$ | $e_{\mu,H^1}$ | $e_p$ | $\eta^T_{BDF2}$ | $ei_2$ | $ei^{ZZ}$ |
| 0.0125 - 0.00125 | 0.02 | 0.00098 | 0.0024 | 0.0016 | 1.68 | 0.18 |
| 0.0125 - 0.00125 | 0.01 | 0.00025 | 0.00066 | 0.00038 | 1.78 | 0.14 |
| 0.0125 - 0.00125 | 0.005 | 0.000068 | 0.0.00018 | 0.000097 | 1.53 | 0.14 |

Table 3.9: Convergence results for Example 3.62 with $\omega = 2.5$ and $Re = 10$. The time advancing scheme is chosen as BDF1 (rows 1-3) and BDF2 (rows 4-6).

## 3.10 A space-time adaptive algorithm for the Navier-Stokes equations with constant viscosity and density

The purpose of this section is to adapt the space-time adaptive algorithm 2.15 proposed to solve the transport equation to the case of the incompressible Navier-Stokes equations.

Let us prescribe two tolerances $TOL_S$ that will control the spatial error and $TOL_T$ that will rule the temporal error. The main goal is to build a sequence of meshes and time steps such that

$$0.75TOL \leq \frac{\eta_k}{\left(\mu \int_0^T \|\nabla \mathbf{u}_{h\tau}(t)\|^2_{L^2(\Omega)} dt\right)^{1/2}} \leq 1.25TOL, \tag{3.132}$$

where $\eta_k, k = 1, 2$ is the velocity error indicator defined in Section 3.8 and we note

$$TOL = (TOL_S^2 + TOL_T^2)^{1/2}.$$

We recall that, according to (3.127) and (3.128)

$$\eta_k^2 = (\eta^A)^2 + (\eta^T_{BDFk})^2, k = 1, 2,$$

depending if we use the Backward Euler (BDF1) method or the BDF2 method to advance in time. Sufficient conditions so that (3.132) holds are

$$0.75^2 TOL_S^2 \mu \int_0^T \|\nabla \mathbf{u}_{h\tau}(t)\|^2_{L^2(\Omega)} dt \leq (\eta^A)^2 \leq 1.25^2 TOL_S^2 \mu \int_0^T \|\nabla \mathbf{u}_{h\tau}(t)\|^2_{L^2(\Omega)} dt,$$

and

$$0.75^2 TOL_T^2 \mu \int_0^T \|\nabla \mathbf{u}_{h\tau}(t)\|^2_{L^2(\Omega)} dt \leq (\eta^T_{BDFk})^2 \leq 1.25^2 TOL_T^2 \mu \int_0^T \|\nabla \mathbf{u}_{h\tau}(t)\|^2_{L^2(\Omega)} dt.$$

Therefore, we ask that for any $n = 0, 1, ..., N-1$, it holds

$$0.75^2 TOL_S^2 \mu \int_{t^n}^{t^{n+1}} \|\nabla \mathbf{u}_{h\tau}(t)\|^2_{L^2(\Omega)} dt \leq \sum_{K \in \mathcal{T}_h} (\eta^A_{K,n})^2 \leq 1.25^2 TOL_S^2 \mu \int_{t^n}^{t^{n+1}} \|\nabla \mathbf{u}_{h\tau}(t)\|^2_{L^2(\Omega)} dt, \quad (3.133)$$

and

$$0.75^2 TOL_T^2 \mu \int_{t^n}^{t^{n+1}} \|\nabla \mathbf{u}_{h\tau}(t)\|^2_{L^2(\Omega)} dt \leq \sum_{K \in \mathcal{T}_h} (\eta^{T,k}_{K,n})^2 \leq 1.25^2 TOL_T^2 \mu \int_{t^n}^{t^{n+1}} \|\nabla \mathbf{u}_{h\tau}(t)\|^2_{L^2(\Omega)} dt. \quad (3.134)$$

Finally, we equidistribute the stopping criterion (3.133) in each direction of anisotropy be defining the local anisotropic error indicator in direction $i = 1, 2$

$$(\eta^A_{i,K,n})^2 = \tau^{n+1} \left( \left\| \mathbf{f}^{n+1} - \rho \partial_{\beta^n} \mathbf{u}_h^{n+1} - \rho(\mathbf{u}_h^{n+1} \cdot \nabla)\mathbf{u}_h^{n+1} + \mu \Delta \mathbf{u}_h^{n+1} - \nabla p_h^{n+1} \right\|_{L^2(K)} + \frac{1}{2\sqrt{\lambda_{2,K}}} \left\| \left[ \mu \nabla \mathbf{u}_h^{n+1} \cdot \mathbf{n} \right] \right\|_{L^2(\partial K)} \right) \tilde{\omega}_{i,K} \left( \Pi_h^{ZZ} \mathbf{u}_h^{n+1} - \mathbf{u}_h^{n+1} \right),$$

Then, for any $P \in \mathcal{T}_h$, we define

$$(\eta^A_{P,n})^2 = \sum_{\substack{K \in \mathcal{T}_h \\ P \in K}} (\eta^A_{K,n})^2, \quad (\eta^A_{i,P,n})^2 = \sum_{\substack{K \in \mathcal{T}_h \\ P \in K}} (\eta^A_{i,K,n})^2, i = 1, 2.$$

As before, we have that $\sum_{P \in \mathcal{T}_h} (\eta^A_{P,n})^2 = 3 \sum_{K \in \mathcal{T}_h} (\eta^A_{K,n})^2$ therefore sufficient conditions to satisfy (3.133) are that for any $P \in \mathcal{T}_h$, we have for $i = 1, 2$,

$$\frac{3\sigma_{P,n} 0.75^2 TOL_S^2}{2N_P} \mu \int_{t^n}^{t^{n+1}} \|\nabla \mathbf{u}_{h\tau}(t)\|^2_{L^2(\Omega)} dt \leq (\eta^A_{i,P,n})^2 \leq \frac{3\sigma_{P,n} 1.25^2 TOL_S^2}{2N_P} \mu \int_{t^n}^{t^{n+1}} \|\nabla \mathbf{u}_{h\tau}(t)\|^2_{L^2(\Omega)} dt,$$

where the equidisitribution factor $\sigma_P$ is defined by

$$\sigma_{P,n} \frac{(\eta^A_{1,P,n})^2 + (\eta^A_{2,P,n})^2}{(\eta^A_{P,n})^2}.$$

The algorithm follows those of Section 1.4 of Chapter 1 and Section 2.4 of Chapter 2. Since we deal with a time dependent equation, every time the mesh is changed, we must interpolate previous values of the solutions. We choose to use the conservative algorithm [5] and we refer to Section 2.5 for more details on interpolation between meshes.

We now check the efficiency of the algorithm on several examples. We recall in Table 3.10 the notations already used.

| | |
|---|---|
| $N_v$ : | Number of vertices of the mesh at final time |
| $N_\tau$ : | Number of time steps |
| $N_m$ : | Number of remeshings |
| $N_c$ : | Number of time step changes |
| $ar$ : | Maximum aspect ratio at final time |
| $\overline{ar}$ : | Average aspect ratio at final time |

Table 3.10: Additional notations for the analysis of the adaptive algorithm.

**Example 3.63** (A Poiseuille experiment with a time-varying inflow)**.**
We first test our adaptive algorithm on the Example 3.61. We fix $Re = \omega = 1$ and we use the second order BDF method to advance in time. The initial grid is an anisotropic mesh of aspect ratio 50. This choice is made in order to improve a bit the remeshings procedure, knowing a priori that the initial condition is itself depending only on the $x_2$ variable. The initial time step is chosen as $\tau^1 = 0.01$ and we do not adapt the time step for the first iteration. Note that to obtain effectivity indices close to 1, we divide the space error indicator and the time error indicator by the corresponding weights obtained in the previous section. Therefore, we run the adaptive algorithm with

$$\eta_2 = \left( \frac{(\eta^A)^2}{9} + \frac{(\eta BDF2^T)^2}{4} \right)^{1/2}.$$

For this example, we set a tolerance $TOL$ and we choose $TOL_S = TOL_T = TOL/\sqrt{2}$ so that the errors between the space and time discretizations are equidistributed. Thus we built meshes and time steps such half of the error is due to spatial approximation and half is due to time approximation. We report the results in Table 3.11. Both the velocity and the pressure error are $O(TOL)$. The number of time steps is multiplied by $\sqrt{2}$ when the tolerance is divided by two, expressing the second order in time of the method. In Figure 3.11, we represent the meshes and the solutions at final time for $TOL = 0.0125$.

| $TOL$ | $e_{\mu,H^1}$ | $e_p$ | $ei_2$ | $ei^{ZZ}$ | $\eta^A$ | $\eta^T_{BDF2}$ | $ar$ | $\bar{ar}$ | $N_v$ | $N_\tau$ | $N_m$ | $N_c$ |
|---|---|---|---|---|---|---|---|---|---|---|---|---|
| 0.0125 | 0.0061 | 0.0071 | 1.31 | 0.96 | 0.0055 | 0.0058 | 917 | 224 | 215 | 13 | 8 | 31 |
| 0.00625 | 0.0031 | 0.0053 | 1.28 | 0.95 | 0.0027 | 0.0028 | 1960 | 409 | 689 | 18 | 13 | 35 |
| 0.00315 | 0.0015 | 0.0021 | 1.28 | 0.98 | 0.0014 | 0.0014 | 1926 | 330 | 1901 | 26 | 8 | 27 |

Table 3.11: Example 3.61 with $Re = \omega = 1$. Convergence results with the BDF2 method.

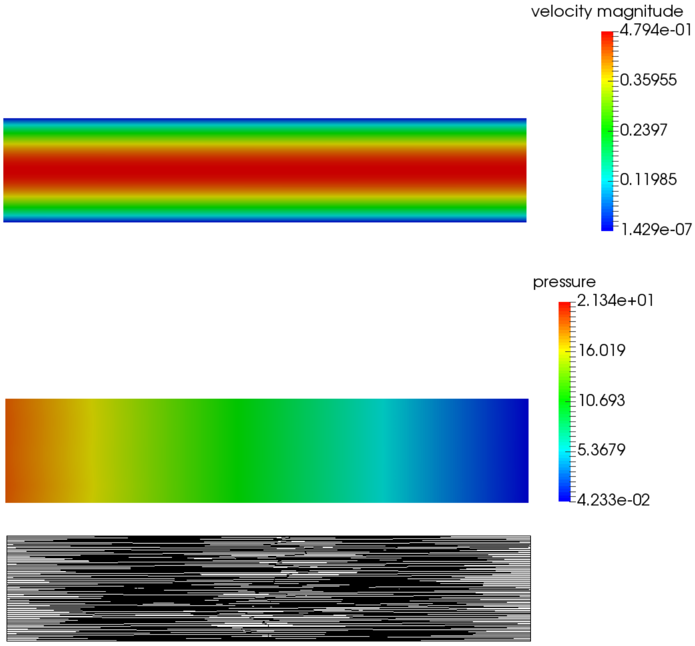


Figure 3.11: Example 3.61. Mesh and solutions at final time with $TOL = 0.0125$.

**Example 3.64** (An other Poiseuille experiment with a time-varying inflow)**.**
We present below a slight modification of the Example 3.61 where we consider now a time dependent frequency $\omega = \omega(t)$ given by

$$\omega(t) = 1 + 9H_\varepsilon(t - 0.5) \tag{3.135}$$

where we recall that $H_\varepsilon$ is the smoothing of the Heavyside graph given by (1.25). Then the frequency is mainly 1 or 10, except in a small layer of size $\varepsilon$ around the time $t = 0.5$. For the numerical experiment, we choose $\varepsilon = 0.03$. We then compute the right hand side $\mathbf{f}$ so that the solutions are given by

$$\mathbf{u}(x_1, x_2, t) = \begin{pmatrix} 2.25e^{-4}x_2(0.03 - x_2)\sin(2\pi\omega(t)t + 0.5) \\ 0 \end{pmatrix},$$

$$p(x_1, x_2, t) = \mu 2.25e^{-4}(0.3 - 2x_1)\sin(2\pi\omega(t)t + 0.5)$$

and we fix $\mu = 0.03$ so that the Reynolds number is 1. The goal of this example is to check if our time error indicator is able to capture the change in the oscillations of the solution. We run numerical tests for several choices of tolerances, starting from an anisotropic initial mesh of aspect ratio 10 and an initial time step $\tau^1 = 0.01$. We consider again the adaptive algorithm with the error indicator $\eta_2$ given by

$$\eta_2 = \left( \frac{(\eta^A)^2}{9} + \frac{(\eta BDF2^T)^2}{4} \right)^{1/2}$$

and we do not adapt the time step for the first iteration. Finally, here we make the choice $TOL_T = TOL_S/10$ to have time steps small enough to ensure a good convergence of the numerical method.

The numerical results are presented in the Table 3.12. The correct orders of the method in both the space and time variables are observed since the number of vertices is multiplied by 2 as the space tolerance is divided by 2, and in the same manner the number of time steps is multiplied by $\sqrt{2}$ as the time tolerance is divided by 2. In Figure 3.12, we compare the size of the time steps during the simulation with the norm of the solution. It is observed that the adaptive algorithm captures the changes in the period length, taking smaller time steps, when the frequency is larger. In particular, when the frequency is 10 times larger, the time steps are chosen 10 times smaller. In the boundary layer around $t = 0.5$, the algorithm takes even smaller time steps due to the high oscillatory nature of the solution.

| $TOL_S$ | $TOL_T$ | $e_{\mu,H^1}$ | $ei_2$ | $ei^{ZZ}$ | $\eta^A$ | $\eta^T_{BDF2}$ | $ar$ | $\bar{ar}$ | $N_v$ | $N_\tau$ | $N_m$ | $N_c$ |
|---|---|---|---|---|---|---|---|---|---|---|---|---|
| 0.1 | 0.01 | 0.048 | 0.88 | 0.94 | 0.042 | 0.0064 | 113 | 27 | 33 | 125 | 104 | 230 |
| 0.05 | 0.005 | 0.024 | 0.92 | 0.97 | 0.022 | 0.0031 | 244 | 48 | 76 | 180 | 103 | 281 |
| 0.025 | 0.0025 | 0.013 | 0.93 | 0.98 | 0.012 | 0.0016 | 449 | 86 | 162 | 258 | 64 | 264 |
| 0.0125 | 0.00125 | 0.0067 | 0.94 | 0.99 | 0.0062 | 0.00078 | 886 | 177 | 378 | 366 | 75 | 298 |

Table 3.12: Example 3.61 with a time dependent frequency $\omega$ given by (3.135). Convergence results with the BDF2 method.

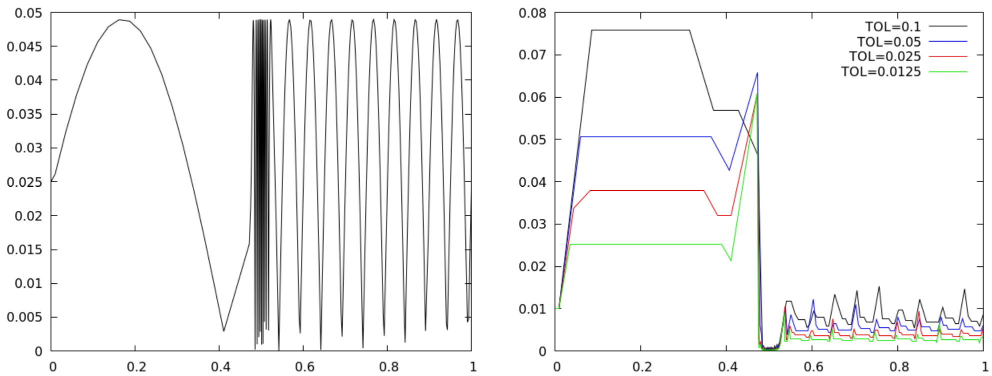


Figure 3.12: Example 3.61 with a time dependent frequency $\omega$ given by (3.135). Comparison between the evolution of the norm of the velocity $\|\mathbf{u}(t)\|_{L^2(\Omega)}$ (left) and the evolution of the time steps (right) for several values of the tolerances (here we note $TOL = TOL_S$ and we recall that $TOL_T = TOL_S/10$).

**Example 3.65** (Two-walls driven square cavity flow: periodic solutions)**.**
We now come back to the Example 3.10 and the two-walls driven cavity experiments. The Reynolds number is now set to 5000 and we solve the complete evolutiv problem

$$\begin{cases} \rho\dfrac{\partial \mathbf{u}}{\partial t} + \rho(\mathbf{u}\cdot\nabla)\mathbf{u} - \mu\Delta\mathbf{u} + \nabla p = 0, & \text{in } \Omega\times(0,+\infty), \\ \operatorname{div}\mathbf{u} = 0, & \text{in } \Omega\times(0,+\infty), \end{cases} \tag{3.136}$$

where we impose the following boundary conditions

$$\begin{cases} \mathbf{u}(x_1,1,t) = (1,0), & 0\le x_1\le 1, t\in(0,+\infty) \\ \mathbf{u}(0,x_2,t) = (0,-1), & 0\le x_2\le 1, t\in(0,+\infty) \\ \mathbf{u}(x_1,x_2,t) = 0, & \text{otherwise}\ . \end{cases} \tag{3.137}$$

in $\Omega = (0,1)\times(0,1)$.

The initial condition is chosen as the steady solution obtained for $Re = 4000$. The initial mesh is the final mesh generated when solving the steady case with $TOL = 0.125$. We run the adaptive algorithm with $TOL_S = 0.1$ and $TOL_T = 0.001$.

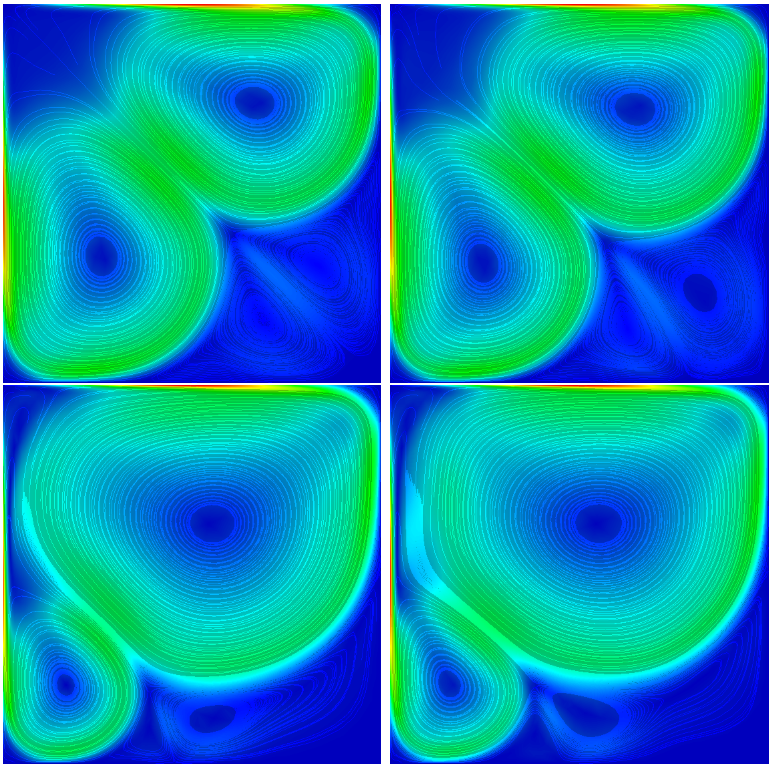

Figure 3.13: Example 3.10. Evolution of the streamlines when the adaptive algorithm is used with $TOL_S = 0.1$ and $TOL_T = 0.001$. $t = 0$ (top left), $t = 100$ (top right), $t = 750$ (bottom left), and $t = 1000$ (bottom right).

As presented in [50], a bifurcation occurs after $t = 100$ seconds and the solution is not symmetric anymore and reach a periodic (in time) pattern after $t = 750$ seconds. The length of the period is approximatively 3 seconds. In Figure 3.13, we present the evolution of the velocity fields obtained when applying the adaptive algorithm with the BDF2 method to advance in time and $TOL_S = 0.1$ and $TOL_T = 0.001$ and in Figure 3.15, we represent the initial and the final meshes. In Figure 3.14, we present the evolution of the velocity during one period (after $t = 900$ sec). In Figures 3.16 and 3.17, we present the history of the norms of the velocity $\|\nabla \mathbf{u}_{h\tau}(t)\|_{L^2(\Omega)}$ and $\|\mathbf{u}_{h\tau}(t)\|_{L^2(\Omega)}$.

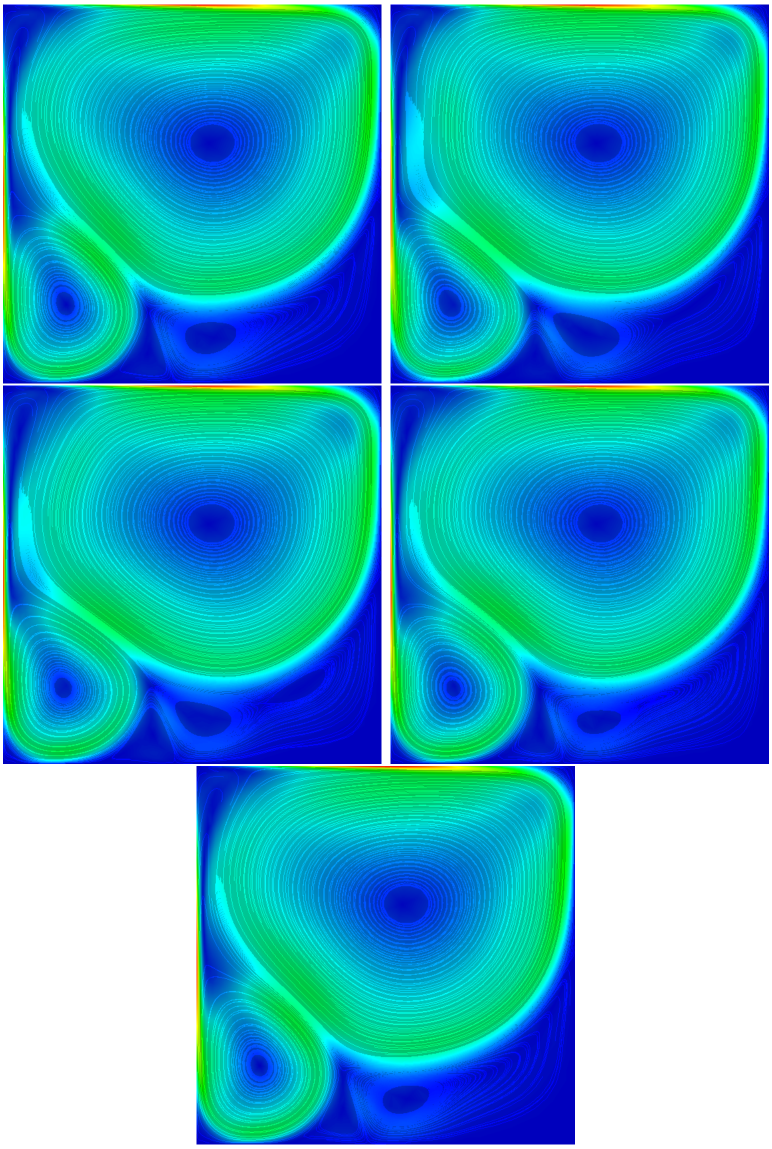

Figure 3.14: Example 3.10. Evolution of the streamlines during one period. The adaptive aglorithm is run with $TOL_S = 0.1$ and $TOL_T = 0.001$.

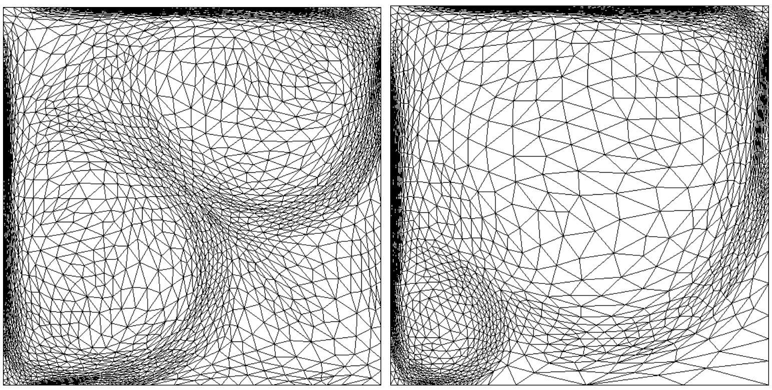

Figure 3.15: Example 3.10. Initial mesh (left) and final mesh (right).

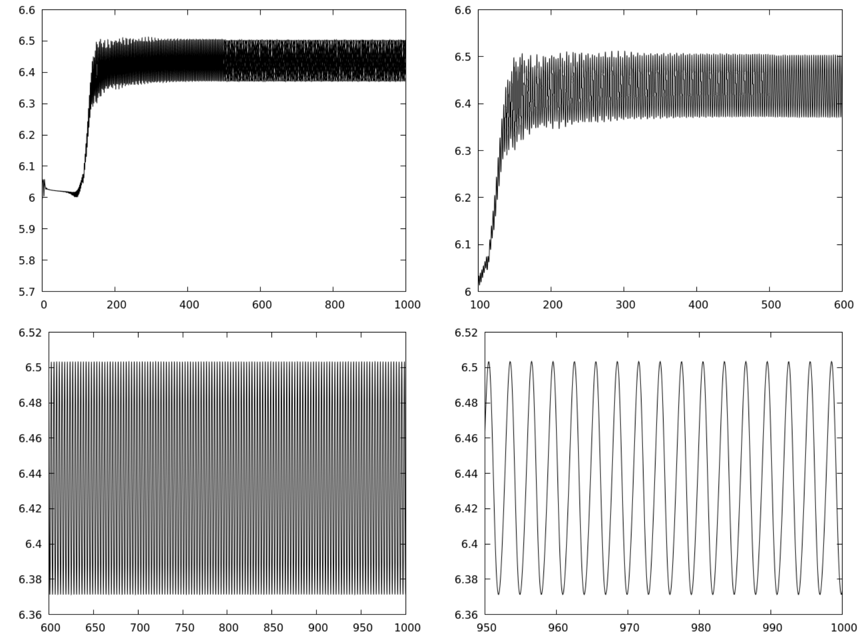


Figure 3.16: Example 3.10. Evolution of $\|\nabla \mathbf{u}_{h\tau}(t)\|_{L^2(\Omega)}$.

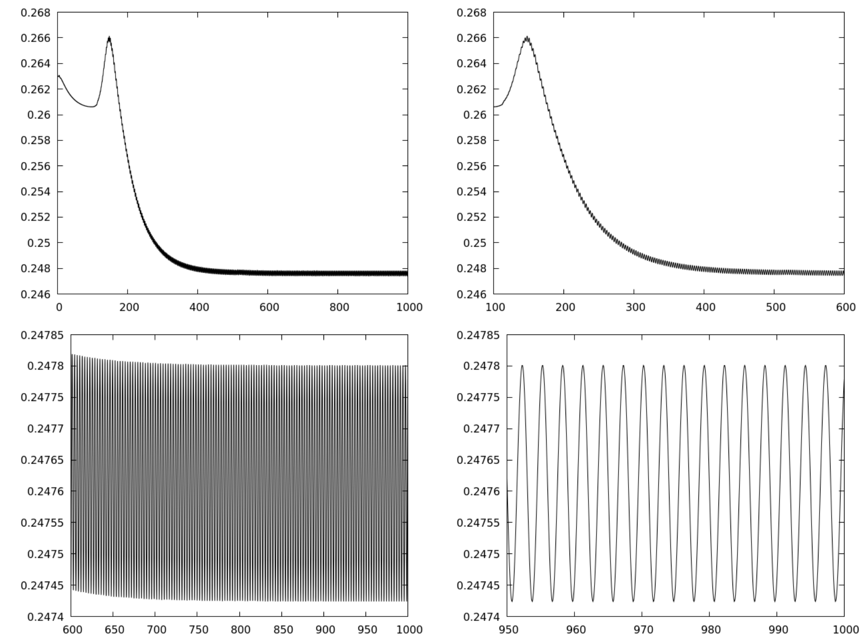


Figure 3.17: Example 3.10. Evolution of $\|\mathbf{u}_{h\tau}(t)\|_{L^2(\Omega)}$.

# Chapter 4

# A posteriori error estimates and adaptive algorithms for the incompressible Navier-Stokes equations with variable viscosity and density

In this last chapter, we focus on the analysis of a special case of the incompressible Navier-Stokes equations for non-homogeneous fluids. We are interested in approximating and solving with an adaptive strategy the equations of motion of two fluids, separated by a free surface.

We briefly summarize the main problem to approximate, that was presented at the beginning of the thesis, in the introduction. We consider a cavity $\Omega \in \mathbb{R}^d$, $d = 2, 3$, filled with two incompressible, immiscible fluids, separated by a free surface. At any time, the domain can be split into two subdomains $\Omega_1, \Omega_2$ that are separated by the free surface $\Sigma$. In each subdomain, the fluid motion is governed by the Navier-Stokes equations

$$\rho_i \frac{\partial}{\partial t}\mathbf{u}_i + \rho_i(\mathbf{u}_i \cdot \nabla)\mathbf{u}_i - \mu_i \Delta \mathbf{u}_i + \nabla p_i = \rho_i \mathbf{f}, \quad \operatorname{div} \mathbf{u}_i = 0.$$

where $\rho_i, \mu_i, \mathbf{u}_i$ and $p_i$ stand respectively for the density, the viscosity, the velocity and the pressure in the domain $\Omega_i$. If we define the global quantities

$$\mathbf{u}, p, \rho, \mu = \begin{cases} \mathbf{u}_1, p_1, \rho_1, \mu_1 \text{ in } \Omega_1, \\ \mathbf{u}_2, p_2, \rho_2, \mu_2 \text{ in } \Omega_2, \end{cases}$$

then the equations in the whole domain $\Omega$ reads:

$$\rho \frac{\partial}{\partial t}\mathbf{u} + \rho(\mathbf{u} \cdot \nabla)\mathbf{u} - \operatorname{div}(2\mu D(\mathbf{u})) + \nabla p = \rho \mathbf{f}, \quad \operatorname{div} \mathbf{u} = 0.$$

To describe the evolution of the interface $\Sigma$, we use the piecewise constant function $\varphi$ that is defined by

$$\varphi = \begin{cases} 1, & \text{in } \Omega_1, \\ 0, & \text{in } \Omega_2. \end{cases}$$

Thus $\Sigma$ is identified at any time by the set of points where $\varphi$ is discontinuous. Finally, we ask that $\varphi$ is transported by the velocity field and satisfies the conservation equation

$$\frac{\partial \varphi}{\partial t} + \mathbf{u} \cdot \nabla \varphi = 0.$$

The complete model reads: find $(\mathbf{u}, p, \varphi)$ the solutions of

$$\begin{cases} \rho \dfrac{\partial \mathbf{u}}{\partial t} + \rho(\mathbf{u} \cdot \nabla)\mathbf{u} - \operatorname{div}(2\mu D(\mathbf{u})) + \nabla p = \rho \mathbf{f}, \\ \operatorname{div} \mathbf{u} = 0, \\ \dfrac{\partial \varphi}{\partial t} + \mathbf{u} \cdot \nabla \varphi = 0, \\ \rho = \rho_1 \varphi + \rho_2 (1 - \varphi), \\ \mu = \mu_1 \varphi + \mu_2 (1 - \varphi). \end{cases} \tag{4.1}$$

This chapter is separated in two parts. In Part 1, we present a numerical method to solve the two fluids problem (4.1) and we study its a posteriori error analysis. In Part 2, we focus on a limit case of this model, where one of the fluid as a huge viscosity, approximating thus the motion of rigid body. For both parts, error indicators for space and time discretizations are advocated based on semi-discrete a posteriori error estimates and an adaptive algorithm is then proposed.

The main objectives of Part 1 are:

- Present a space-time discretization of the equations (4.1) based on anisotropic, continuous, piecewise linear finite elements and a combination of the BDF2 methods, resp. the Crank-Nicolson scheme to approximate in time the Navier-Stokes equations, resp. the transport of the density and viscosity. In practice, the interface function $\varphi$ is regularized and approximated by a smooth map, that takes the values 0 or 1, except in a small region.
- Prove semi-discrete (for both spatial and time discretizations) a posteriori error estimates and introduce an error indicator that takes in account both the time and the space approximations and control the numerical errors of the velocity and the transported quantities.
- Introduce and study an adaptive algorithm to solve some real physical situations, namely hydrodynamic instabilities.

The outline of the Part 1 is the following: in Section 4.1, we briefly present and comment some general and theoretical results for the solutions of the Navier-Stokes equations for a non-homogeneous fluid, where the density and the viscosity are variable. In Section 4.2, we present a anisotropic finite elements methods to discretize (in space) the equations and we prove a corresponding a posteriori error estimate. In Section 4.3, we present the time discretization of the same equations, and we derive an a posteriori error estimate that is of optimal order, namely of order 2, since the BDF2 method and the Crank-Nicolson scheme will be used. In Section 4.4, we present a fully discrete method to approximate the equations (4.1) and in Section 4.5, we introduce the adaptive strategy. Finally, in Section 4.6, the convergence of the numerical method and the adaptive algorithm is investigated and in Section 4.7, we apply the algorithm to some particular physical situations, as Rayleigh-Taylor or Kelvin-Helmoltz instabilities occurring at the demarcation between two fluids in motion. The main theoretical results are the Theorem 4.14 that contains the spatial a posteriori error estimate and the Theorem 4.21 that shows the temporal counterpart.

The objectives of Part 2 are:

– Present the particular situation we are interested in, namely the fall of a rigid disk (sphere) into a cavity filled with a viscous, incompressible fluid. We introduce a particular model and its numerical approximation.

– Prove semi-discrete (for both spatial and time discretizations) a posteriori error estimates and introduce an error indicator that takes in account both the time and the space approximations.

– Introduce an adaptive algorithm to capture the motion of the disk when it reaches the bottom of the cavity. It is theoretically expected that no collision occurs, and we motivate the use of an adaptive strategy to check this paradoxal behavior.

The outline of the Part 2 is as follows: in Section 4.8, we present the continuous equations and the numerical method to approximate them. In Section 4.9, we prove semi-discrete a posteriori error estimates for a simplified problem. Finally, in Section 4.10, we introduce error indicators and we simulate the motion of the disk in Section 4.11 with fixed grids and constant time steps and in Section 4.12 where the adaptive algorithm is used. The main theorems are Theorem 4.29 where we prove the semi-discrete in time a posteriori error estimate and the Theorem 4.31 that demonstrates the spatial estimation.

# Part 1. A space-time adaptive algorithm for a two fluids flow separated by a free surface

## 4.1 Non-homogeneous Navier-Stokes equations: problem statement and theoretical framework

In this section, we briefly present the theoretical framework of non-homogeneous Navier-Stokes equations. We state the results for a more general situation than the one we are interested in (namely two fluids flows), and then we come back to our particular problem.

We consider $\Omega \in \mathbb{R}^d$ a cavity filled with a fluid of variable density $\rho$ and viscosity $\mu$ that are assumed to be smooth and non-negative functions. In particular, we ask that $\rho \geq 0$ and we reduce to the the case where $\mu$ is a function of $\rho$, that is to say $\mu = \mu(\rho)$ where for $x \in \mathbb{R}, \mu(x)$ is a $C^1$ function satisfying

$$\mu_{\min} \leq \mu(x) \leq \mu_{\max}, \quad \mu_{\max} \geq \mu_{\min} > 0, \quad \mu' \text{ is bounded.}$$

Then, for a given final time $T > 0$, we are looking for the solution of the non-homogeneous incompressible Navier-Stokes

$$\begin{cases} \rho \dfrac{\partial \mathbf{u}}{\partial t} + \rho \mathbf{u} \cdot \nabla \mathbf{u} - \operatorname{div}(2\mu D(\mathbf{u})) + \nabla p = \rho \mathbf{f}, \quad \text{in } \Omega \times (0,T], \\ \operatorname{div} \mathbf{u} = 0, \quad \text{in } \Omega \times (0,T], \end{cases} \tag{4.2}$$

where we impose the Dirichlet condition $\mathbf{u} = \mathbf{u}_D$ on the boundary of $\Omega$ and the initial condition $\mathbf{u}(\mathbf{x}, 0) = \mathbf{u}_0(\mathbf{x})$. Observe that here, contrary to what we did before the Navier-Stokes equations with constant coefficients, we write the force term as a density of force since $\rho$ is also a unknown of the problem.

An additional equation for the density is needed. We couple the momentum equation with the conservation of the mass and we consider the (transport) equation

$$\frac{\partial \rho}{\partial t} + \mathbf{u} \cdot \nabla \rho = 0, \text{ in } \Omega \times (0,T], \tag{4.3}$$

where we impose that $\rho = \rho^{in}$ on the inflow boundary

$$\Gamma^-(t) = \{\mathbf{x} \in \partial\Omega : \mathbf{u}(t) \cdot \mathbf{n} < 0\}$$

and at $t = 0$ the initial condition $\rho(\mathbf{x}, 0) = \rho_0(\mathbf{x})$. Observe that, due to the fact that it is a function of the density, we also have that $\mu$ is transported by the velocity field and satisfies the conservation equation

$$\frac{\partial \mu}{\partial t} + \mathbf{u} \cdot \nabla \mu = 0, \text{ in } \Omega \times (0, T]. \tag{4.4}$$

The well-posedness of the complete problem given by equations (4.2)-(4.3) with the respective boundary and initial conditions is still an open problem in the general case. We do not pretend to give an exhaustive overview of the known results on these questions, but we present those that are significant for our numerical purpose and give some references for more details. For instance, it was proven (see [69] and [21]) that if $\Omega$ is Lipschitz and

$$\begin{gathered} \rho^{in}, \rho_0 \geq 0, \\ \rho_0 \in L^\infty(\Omega), \rho^{in} \in L^\infty((0,T) \times \partial\Omega), \\ \mathbf{f} \in L^1(0, T; (L^2(\Omega))^d), \\ \mathbf{u}_D \in (H^1(\Omega))^2, \operatorname{div} \mathbf{u}_D = 0 \\ \mathbf{u}_0 \in (H^1_0(\Omega))^d, \operatorname{div} \mathbf{u}_0 = 0, \mathbf{u}_0 = \mathbf{u}_D \text{ on } \partial\Omega. \end{gathered}$$

then there exists at least one weak solution satisfying

$$\begin{gathered} \mathbf{u} \in \mathbf{u}_D + L^2(0, T; (H^1_0(\Omega))^d), \\ p \in W^{-1,\infty}(0, T; L^2_0(\Omega)), \\ \rho \in C^0([0, T]; L^2(\Omega)), \\ \rho_{\min} \leq \rho(\mathbf{x}, t) \leq \rho_{\max} \text{ for a.e } (\mathbf{x}, t) \in \Omega \times (0, T), \end{gathered}$$

where

$$\rho_{\min} = \min(\inf \rho_0, \inf \rho^{in}), \quad \rho_{\max} = \max(\sup \rho_0, \sup \rho^{in}).$$

The uniqueness and the regularity of the solutions are still open problems, even in 2D. However [69], when $d = 2$, $\mu$ is a constant and $\rho_0, \rho^{in} > 0$, one can establish for instance strong regularity (and therefore uniqueness) of the velocity. In particular, we have that

$$\mathbf{u} \in L^2(0, T; (H^2(\Omega))^2) \cap C^0([0, T], (H^1(\Omega))^2), \frac{\partial \mathbf{u}}{\partial t} \in L^2(0, T; (L^2(\Omega))^2).$$

In a more general situation, we can prove that if $\rho_0, \rho^{in}$ does not vanish, then a strong solution exists at least up to a small time $T^*$, and that any weak solutions coincide with the strong one on the time interval $[0, T^*]$.

Concerning the numerical approximation of the Navier-Stokes equations with variable density and viscosity, we cite as an example the work presented in [70] where the analysis of the convergence of the discontinuous Galerkin method is performed.

As stated in the introduction, in this work, we focus on a particular case of the equations (4.2)-(4.3) where the density and the viscosity are given by

$$\rho(\mathbf{x}, t) = \rho_1 \varphi_\varepsilon(\mathbf{x}, t) + \rho_2(1 - \varphi_\varepsilon(\mathbf{x}, t)), \mu(\mathbf{x}, t) = \mu_1 \varphi_\varepsilon(\mathbf{x}, t) + \mu_2(1 - \varphi_\varepsilon(\mathbf{x}, t)),$$

with $\rho_1, \rho_2 \geq 0, \rho_1 \neq \rho_2, \mu_1, \mu_2 > 0$ and where $\varphi_\varepsilon$ is a smooth function taking values between 0 and 1, except in a small region of width controlled by $\varepsilon$ (in the next sections, we will omit to mention the index $\varepsilon$ to lighten the notation). First observe that we satisfy the density dependence of the viscosity since $\mu$ is in fact given by

$$\mu(\mathbf{x}, t) = \mu_2 + \frac{\mu_1 - \mu_2}{\rho_1 - \rho_2}(\rho(\mathbf{x}, t) - \rho_2) = \mu(\rho(\mathbf{x}, t)).$$

Moreover, due to the particular form of $\rho$ and $\mu$, both equations (4.3) and (4.4) reduce to solve in fact

$$\begin{cases} \dfrac{\partial \varphi_\varepsilon}{\partial t} + \mathbf{u} \cdot \nabla \varphi_\varepsilon = 0, & \text{in } \Omega \times (0,T], \\ \varphi_\varepsilon = \varphi^{in}, & \text{on } \Gamma^-(t) \times (0,T], \\ \varphi_\varepsilon(\mathbf{x},0) = \varphi_0(\mathbf{x}), & \text{in } \Omega, \end{cases} \tag{4.5}$$

that is to say the transport of the smooth function $\varphi_\varepsilon$.

This model can be used to approximate the flow of two immiscible fluids that are separated by a free surface. Indeed, for a two fluids flow, the domain $\Omega$ is split into two parts $\Omega_1(t)$ and $\Omega_2(t)$ such that $\Omega = \Omega_1(t) \cup \Omega_2(t)$ and that are separated by a free surface localized by $\Sigma(t)$. Then in each phase, the density and the viscosity are constant and given by

$$\rho(\mathbf{x},t) = \begin{cases} \rho_1, & \mathbf{x} \in \Omega_1(t), \\ \rho_2, & \mathbf{x} \in \Omega_2(t), \end{cases}$$

and

$$\mu(\mathbf{x},t) = \begin{cases} \mu_1, & \mathbf{x} \in \Omega_1(t), \\ \mu_2, & \mathbf{x} \in \Omega_2(t). \end{cases}$$

In other words, one may write

$$\rho = \rho_1 \chi_{\Omega_1(t)} + \rho_2 \chi_{\Omega_2(t)}, \mu = \mu_1 \chi_{\Omega_1(t)} + \mu_2 \chi_{\Omega_2(t)},$$

and since $\Omega_1, \Omega_2$ form a partition of $\Omega$ at any $t$ we have in fact that

$$\rho = \rho_1 \chi_{\Omega_1(t)} + \rho_2(1 - \chi_{\Omega_1(t)}), \mu = \mu_1 \chi_{\Omega_1(t)} + \mu_2(1 - \chi_{\Omega_1(t)}).$$

Now, if we regularize the characteristic function of $\Omega_1(t)$ with a smooth function $\varphi_\varepsilon(\mathbf{x},t)$, where $\varepsilon$ controls the width of the boundary layer capturing the free surface $\Sigma(t)$, then we obtain an approximated density and viscosity $\rho_\varepsilon, \mu_\varepsilon$ given by

$$\rho_\varepsilon = \rho_1 \varphi_\varepsilon + \rho_2(1 - \varphi_\varepsilon), \mu_\varepsilon = \mu_1 \varphi_\varepsilon + \mu_2(1 - \varphi_\varepsilon).$$

**Remark 4.1.** (i) Note that this approach is very close to the level set interface model, see for instance [32], where the free surface $\Sigma(t)$ is seen as the zero level set of a smooth function $\phi$ that is such that

$$\phi(\mathbf{x},t) > 0, \mathbf{x} \in \Omega_1(t), \quad \phi(\mathbf{x},t) < 0, \mathbf{x} \in \Omega_2(t), \quad \phi(\mathbf{x},t) = 0, \mathbf{x} \in \Sigma(t).$$

Then the density and the viscosity are simply given by

$$\rho = \rho_1 H(\phi) + \rho_2(1 - H(\phi)), \quad \mu = \mu_1 H(\phi) + \mu_2(1 - H(\phi)),$$

where $H$ is the Heavyside graph. In practice, the Heavyside graph will be replaced by its smooth version $H_\varepsilon$ (1.25) and we finally obtain

$$\rho = \rho_1 H_\varepsilon(\phi) + \rho_2(1 - H_\varepsilon(\phi)), \quad \mu = \mu_1 H_\varepsilon(\phi) + \mu_2(1 - H_\varepsilon(\phi)),$$

where the composition $H_\varepsilon \circ \phi$ is smooth. The difference between the two approaches is that in the level set method, we transport the function $\phi$ through the equation

$$\frac{\partial \phi}{\partial t} + \mathbf{u} \cdot \nabla \phi = 0,$$

while in our approach we transport in fact $H_\varepsilon(\phi)$.

(ii) Our method (as the level set method) is a so-called *front capturing method* [31, 91], where the two phases are seen as one fluid with variable density and viscosity, moving in a fix domain, where we identify the free surface as the boundary layer of the smooth function $\varphi_\varepsilon$. The other family of methods to solve a free surface problem are the so-called *front tracking methods* [91], where the free surface is seen as the boundary of two moving subdomains. These methods requires to build a mesh that fits the interface between the fluids at any time, that is not the case in the front capturing approach where the free surface can cross the elements of the grid.

## 4.2 A posteriori error estimate for the spatial approximation

In this section, we present a semi-discrete approximation (in space) of the two fluids flow model described in the previous section. We recall briefly the problem we are considering. Let $\Omega \in \mathbb{R}^d, d = 2, 3$ be an open, connected and bounded subset and $T > 0$ a given final time. Given a source term $\mathbf{f}$, two densities $\rho_1, \rho_2$ and two viscosities $\mu_1, \mu_2$, we are looking in $\Omega \times (0, T]$ for $(\mathbf{u}, p), \varphi$ the solutions of the coupled Navier-Stokes/transport equations

$$\begin{cases} \rho \dfrac{\partial \mathbf{u}}{\partial t} + \rho \mathbf{u} \cdot \nabla \mathbf{u} - \operatorname{div}(2\mu D(\mathbf{u})) + \nabla p = \rho \mathbf{f}, \\ \operatorname{div} \mathbf{u} = 0, \\ \dfrac{\partial \varphi}{\partial t} + \mathbf{u} \cdot \nabla \varphi = 0, \\ \rho = \rho_1 \varphi + (1 - \varphi)\rho_2, \\ \mu = \mu_1 \varphi + (1 - \varphi)\mu_2, \\ \rho_1, \rho_2 \geq 0, \mu_1, \mu_2 > 0, \end{cases} \tag{4.6}$$

with the initial/boundary conditions

$$\begin{aligned} \mathbf{u} &= 0, \quad \text{on } \partial\Omega \times (0, T], \\ \mathbf{u}(\cdot, 0) &= \mathbf{u}_0 \quad \text{in } \Omega, \\ \varphi(\cdot, 0) &= \varphi_0, \quad \text{in } \Omega. \end{aligned} \tag{4.7}$$

Here we assume that $\mathbf{u}_0 \in (H_0^1(\Omega))^2, \operatorname{div} \mathbf{u}_0 = 0$, and the stronger assumption (for future needs in the proofs below) that $\mathbf{f} \in L^\infty(\Omega \times (0, T))$.

The initial interface function $\varphi_0$ is a smooth function, taking values between 0 and 1 except in a small region of size $\varepsilon$. Since the equations (4.6)-(4.7) approximates a two fluids flow, $\varphi_0$ describes in fact the initial state inside the cavity, and the location of each fluid.

Here, to simplify the theoretical analysis, we assume $\mathbf{u} = 0$ on the whole boundary of $\Omega$, implying also that we do not have to impose any inflow boundary condition for $\varphi$. Note that the situation is the same if for instance we impose only $\mathbf{u} \cdot \mathbf{n} = 0$ on some parts of $\partial\Omega$. Observe finally that, under our assumptions and following the results presented in Section 4.1, there exists at least a weak solution to the equations (4.6)-(4.7). Moreover we have

$$\rho_{\min} \leq \rho(\mathbf{x}, t) \leq \rho_{\max}, \quad \mu_{\min} \leq \mu(\mathbf{x}, t) \leq \mu_{\max}, \quad \text{for a.e. } (\mathbf{x}, t) \in \Omega \times (0, T),$$

where we note

$$\rho_{\min} = \min(\rho_1, \rho_2), \rho_{\max} = \max(\rho_1, \rho_2), \quad \mu_{\min} = \min(\mu_1, \mu_2), \mu_{\max} = \max(\mu_1, \mu_2).$$

To approximate (in space) the equations (4.6)-(4.7), we use anisotropic, continuous, piecewise linear finite elements that are stabilized with the methods introduced in Chapter 2 (for the transport of $\varphi$) and in Chapter 3 (for the momentum and mass equations). From now, we assume that $\Omega$ is a convex polygon in $\mathbb{R}^2$. The numerical methods reads as follows. For all $h > 0$, let $\mathcal{T}_h$ be a conformal triangle of $\Omega$ into triangles $K$ of diameter $h_K \le h$ and let $V_h, Q_h$ the piecewise linear functions spaces for the velocity and the pressure introduced in Chapter 3. We also consider $\Psi_h$ the set of all piecewise linear functions on $\mathcal{T}_h$. Then assuming that $\mathbf{u}_0 \in (H^2(\Omega))^2, \varphi_0 \in H^2(\Omega)$, starting from $\mathbf{u}_h(0) = r_h(\mathbf{u}_0)$ and $\varphi_h(0) = r_h(\varphi_0)$, we are looking for any $t \in (0, T]$ for $(\mathbf{u}_h(t), p_h(t)) \in V_h \times Q_h$ and $\varphi_h(t) \in \Psi_h$, the solution of

$$\begin{aligned}\int_\Omega \rho_h \frac{\partial \mathbf{u}_h}{\partial t} \cdot \mathbf{v}_h d\mathbf{x} + \int_\Omega \rho_h (\mathbf{u}_h \cdot \nabla)\mathbf{u}_h \cdot \mathbf{v}_h d\mathbf{x} + \int_\Omega 2\mu_h D(\mathbf{u}_h) : D(\mathbf{v}_h) d\mathbf{x} \\ - \int_\Omega p_h \operatorname{div} \mathbf{v}_h d\mathbf{x} \\ + \sum_{K\in\mathcal{T}_h} \alpha_K \int_K R_h^{NS} \cdot (\rho_h (\mathbf{u}_h \cdot \nabla)\mathbf{v}_h)\, d\mathbf{x} = \int_\Omega \rho_h \mathbf{f} \cdot \mathbf{v}_h d\mathbf{x}, \forall \mathbf{v}_h \in V_h, \end{aligned} \quad (4.8)$$

$$- \int_\Omega q_h \operatorname{div} \mathbf{u}_h d\mathbf{x} + \sum_{K\in\mathcal{T}_h} \alpha_K \int_K R_h^{NS} \cdot \nabla q_h d\mathbf{x} = 0, \forall q_h \in Q_h, \quad (4.9)$$

$$\int_\Omega \left( \frac{\partial \varphi_h}{\partial t} + \mathbf{u}_h \cdot \nabla \varphi_h \right) \psi_h d\mathbf{x} + \sum_{K\in\mathcal{T}_h} \delta_K \int_K R_h^{transport} \cdot \nabla \psi_h d\mathbf{x} = 0, \forall \psi_h \in \Psi_h, \quad (4.10)$$

$$\rho_h = \rho_1 \varphi_h + \rho_2(1 - \varphi_h), \mu_h = \mu_1 \varphi_h + \mu_2(1 - \varphi_h), \quad (4.11)$$

where we note the residuals of the equations.

$$R_h^{NS} = \rho_h \mathbf{f} - \rho_h \frac{\partial \mathbf{u}_h}{\partial t} - \rho_h (\mathbf{u}_h \cdot \nabla)\mathbf{u}_h + \operatorname{div}(2\mu_h D(\mathbf{u}_h)) - \nabla p_h, \quad (4.12)$$

and

$$R_h^{transport} = \frac{\partial \varphi_h}{\partial t} + \mathbf{u}_h \cdot \nabla \varphi_h. \quad (4.13)$$

$\alpha_K$ and $\delta_K$ are respectively the Navier-Stokes equations and the transport equation stabilization parameters that we choose as follows. By analogy with the methods presented in Chapter 2 and 3, we define

$$\alpha_K = \frac{\alpha \lambda_{2,K}^2}{\mu_K \xi(Re_K)}, \alpha > 0,$$

where

$$\xi(Re_K) = \begin{cases} 1 & \text{if } Re_K \le 1, \\ Re_K & \text{if } Re_K \ge 1, \end{cases}$$

and the local anisotropic Reynolds number is given by

$$Re_K = \frac{\|\rho_h \mathbf{u}_h\|_{L^\infty(K)} \lambda_{2,K}}{\mu_K},$$

where $\mu_K$ the minimal viscosity in the triangle $K$. For the transport stabilization, we choose

$$\delta_K = \frac{\delta \lambda_{2,K}}{\|\mathbf{u}_h\|_{L^\infty(K)}}, \delta > 0$$

and we set $\delta_K = 0$ in case $\mathbf{u}_h$ is zero in $K$. In practice, we choose $\alpha = 0.01$ and $\delta = 0.5$. Observe that the methods is easily adapted to $\mathbb{R}^3$ by replacing $\lambda_{2,K}$ by $\lambda_{3,K}$ in the definition of the stabilization parameters.

The a priori analysis of the above numerical approximation is not obvious and we will focus on a posteriori error estimates. The convergence of the methods will be checked in the numerical experiments. From now, we will assume that the problems (4.6) and (4.8)-(4.9)-(4.10)-(4.11) are well-posed (their solutions exist and are unique) and that the method converges. Moreover, the data, the exact and numerical solutions will be assumed to be smooth enough to justify our future computations. The goal of the next pages is to prove an a posteriori error estimate for the velocity and for the density/viscosity errors. We thus have to combine the techniques used for the transport equations in Chapter 2 with those used for the Navier-Stokes equations with constant coefficients in Chapter 3. The proofs are very similar to those presented in the previous chapters, the two main differences to consider are the following:

1. In Chapter 2, the transport velocity field $\mathbf{u}$ is a given data, while here it is an unknown and therefore the errors $\rho - \rho_h$ and $\mu - \mu_h$ will depend on the velocity error $\mathbf{u} - \mathbf{u}_h$.

2. Conversely, in Chapter 3, the density and the viscosity are constant and given quantities, while here there are unknowns (and thus variable) quantities. The numerical error $\mathbf{u} - \mathbf{u}_h$ will depend on $\rho - \rho_h$ and $\mu - \mu_h$.

Then, the strategy to prove an a posteriori error estimate for the sum of the errors $\mathbf{u} - \mathbf{u}_h$ and $\rho - \rho_h, \mu - \mu_h$ is:

(i) To prove estimates for $\rho - \rho_h$ and $\mu - \mu_h$ by reproducing what we did in Chapter 2 for the transport equation (Proposition 4.2).

(ii) To prove an estimate for $\mathbf{u} - \mathbf{u}_h$ by following the steps of Chapter 3, that is to say we split the error into $\mathbf{u} - \mathbf{U}$ and $\mathbf{U} - \mathbf{u}_h$ where $\mathbf{U}$ is a "good" reconstruction and we derive:

   (a) an estimate for $\mathbf{u} - \mathbf{U}$ (Proposition 4.7),
   (b) an estimate for $\mathbf{U} - \mathbf{u}_h$ (Proposition 4.8),
   (c) an estimate for the remaining higher order terms (Proposition 4.10),
   (d) an estimate for $\mathbf{u} - \mathbf{u}_h$ by combining the three previous results (Proposition 4.12).

(iii) To derive the desired a posteriori error bound by summing the estimates for $\rho - \rho_h, \mu - \mu_h$ and $\mathbf{u} - \mathbf{u}_h$ (Theorem 4.14).

All the proofs of these results are presented in the next pages. The arguments are mostly technical and the reader can first skip them and focus on the different estimates are combined all together.

**A posteriori error estimates for $\rho - \rho_h$ and $\mu - \mu_h$**

The first proposition gives a preliminary a posteriori upper bound for the density error $\rho - \rho_h$ and by extension for the viscosity error $\mu - \mu_h$. The proof is an adaptation of the one of Theorem 2.55.

**Proposition 4.2** (A posteriori upper bound for the transport of the density and the viscosity)**.**
*There exists a constant $C > 0$ that depends only the reference triangle such that for any $t \in (0, T]$ one have*

$$\|(\rho-\rho_h)(t)\|^2_{L^2(\Omega)} \le \|(\rho-\rho_h)(0)\|^2_{L^2(\Omega)} + C\int_0^t \sum_{K\in\mathcal{T}_h} (\eta^A_{K,\rho})^2(s)ds$$
$$+ 2\|\nabla\rho_h\|_{L^\infty(\Omega\times(0,T))}\int_0^t \|(\mathbf{u}-\mathbf{u}_h)(s)\|_{L^2(\Omega)}\|(\rho-\rho_h)(s)\|_{L^2(\Omega)}ds, \quad (4.14)$$

$$\|(\mu-\mu_h)(t)\|^2_{L^2(\Omega)} \le \|(\mu-\mu_h)(0)\|^2_{L^2(\Omega)} + C\int_0^t \sum_{K\in\mathcal{T}_h} (\eta^A_{K,\mu})^2(s)ds$$
$$+ 2\|\nabla\mu_h\|_{L^\infty(\Omega\times(0,T))}\int_0^t \|(\mathbf{u}-\mathbf{u}_h)(s)\|_{L^2(\Omega)}\|(\mu-\mu_h)(s)\|_{L^2(\Omega)}ds, \quad (4.15)$$

*where*

$$(\eta^A_{K,\rho})^2(t) = \left\|\frac{\partial\rho_h}{\partial t}(t) + \mathbf{u}_h(t)\cdot\nabla\rho_h(t)\right\|_{L^2(K)} \omega_K((\rho-\rho_h)(t)),$$
$$(\eta^A_{K,\mu})^2(t) = \left\|\frac{\partial\mu_h}{\partial t}(t) + \mathbf{u}_h(t)\cdot\nabla\mu_h(t)\right\|_{L^2(K)} \omega_K((\mu-\mu_h)(t)).$$

*Proof.* We prove only (4.14), (4.15) can be obtained either by reproducing the same proof, or directly by using the fact that in our case we explicitly know the viscosity and its finite elements approximation through the relation $\mu = \mu(\rho)$ and $\mu_h = \mu(\rho_h)$ where

$$\mu(x) = \mu_2 + \frac{\mu_1-\mu_2}{\rho_1-\rho_2}(x-\rho_2), x \in \mathbb{R}.$$

Let $e = \rho - \rho_h$. We denote by $C$ any constant that depends only on the reference triangle, but which value can change from line to line.

We reproduce the same arguments as those of Theorem 2.55 in Chapter 2, when we study the transport equation. Since $\mathbf{u}$ is divergence free and has zero boundary values, we have that

$$\int_\Omega (\mathbf{u}\cdot\nabla\psi)\psi d\mathbf{x} = 0, \quad \forall\psi \in H^1(\Omega),$$

therefore one has

$$\frac{1}{2}\frac{d}{dt}\|e\|^2_{L^2(\Omega)} = \int_\Omega \frac{\partial e}{\partial t} e d\mathbf{x} + \int_\Omega (\mathbf{u}\cdot\nabla e)e d\mathbf{x}$$
$$= -\int_\Omega \frac{\partial\rho_h}{\partial t} e d\mathbf{x} - \int_\Omega (\mathbf{u}\cdot\nabla\rho_h)e d\mathbf{x} = -\int_\Omega \frac{\partial\rho_h}{\partial t} e d\mathbf{x} - \int_\Omega (\mathbf{u}_h\cdot\nabla\rho_h)e d\mathbf{x} + \int_\Omega ((\mathbf{u}_h-\mathbf{u})\cdot\nabla\rho_h)e d\mathbf{x},$$

thanks to the fact that $\rho$ satisfies (4.3). Using the finite elements approximations (4.10) (observe that $\rho_h$ satisfies necessarily the same scheme as $\varphi_h$), we can remove any test function $\psi_h$ and we obtain

$$\frac{d}{dt}\frac{1}{2}\|e\|^2_{L^2(\Omega)}$$
$$= -\int_\Omega \left(\frac{\partial\rho_h}{\partial t} + \mathbf{u}_h\cdot\nabla\rho_h\right)(e - \psi_h - \delta_h\mathbf{u}_h\cdot\nabla\psi_h) - \int_\Omega ((\mathbf{u}-\mathbf{u}_h)\cdot\nabla\rho_h)e d\mathbf{x},$$

where we denote by $\delta_h$ the piecewise constant function that the value $\delta_K$ in each triangle $K$. Choosing $\psi_h = R_h e$ and using Cauchy-Schwarz inequality and the anisotropic Clément interpolation error estimate, we finally obtain that there exists a constant $C > 0$ that depends only the reference triangle such that

$$\frac{d}{dt}\frac{1}{2}\|e\|^2_{L^2(\Omega)} \leq C \sum_{K\in\mathcal{T}_h} \left\| \frac{\partial \rho_h}{\partial t} + \mathbf{u}_h \cdot \nabla\rho_h \right\|_{L^2(K)} \Big(\omega_K(e) + \|\delta_h \mathbf{u}_h \cdot \nabla R_h e\|_{L^2(K)}\Big) + \|\nabla\rho_h\|_{L^\infty(\Omega\times(0,T))}\|\mathbf{u}-\mathbf{u}_h\|_{L^2(\Omega)}\|e\|_{L^2(\Omega)}. \quad (4.16)$$

Using the definition of $\delta_h$ and $\delta_K$ one can estimate

$$\|\delta_h \mathbf{u}_h \cdot \nabla R_h e\|_{L^2(K)} \leq \delta_K \|\mathbf{u}_h\|_{L^2(K)}\|\nabla R_h e\|_{L^2(K)} \leq \delta\lambda_{2,K}\|\nabla R_h e\|_{L^2(K)}.$$

Finally, as we did in Theorem 2.55, we derive that there exists a constant $C > 0$ depending only the reference triangle such that

$$\lambda_{2,K}\|\nabla R_h e\|_{L^2(K)} \leq C\omega_K(e)$$

yielding that

$$\|\delta_h \mathbf{u}_h \cdot \nabla R_h e\|_{L^2(K)} \leq C\omega_K(e).$$

Plugging it into (4.16) and integrating over the time yields the desired result. □

**Remark 4.3.** (i) Note that we only use the fact that $\rho$, respectively $\rho_h$, is the solution to the transport equation, respectively its spatial approximation. We never use their particular formulation that are

$$\rho = \rho_1\varphi + \rho_2(1-\varphi), \quad \rho_h = \rho_1\varphi_h + \rho_2(1-\varphi_h).$$

Therefore the proof and the resulting estimates are valid for more general cases of non-homogeneous Navier-Stokes equations.

(ii) The term

$$\|\nabla\rho_h\|_{L^\infty(\Omega\times(0,T))}\int_0^t \|(\mathbf{u}-\mathbf{u}_h)(s)\|_{L^2(\Omega)}\|(\rho-\rho_h)(s)\|_{L^2(\Omega)}ds$$

can be controlled by

$$\|\nabla\rho_h\|^2_{L^\infty(\Omega\times(0,T))}\int_0^t \|(\rho-\rho_h)(s)\|^2_{L^2(\Omega)}ds + \int_0^t \|(\mathbf{u}-\mathbf{u}_h)(s)\|^2_{L^2(\Omega)}ds.$$

The $L^2$ norm of $\mathbf{u}-\mathbf{u}_h$ will be absorbed in the estimate coming from the error analysis of the momentum equation and the term

$$\|\nabla\rho_h\|^2_{L^\infty(\Omega\times(0,T))}\|\rho-\rho_h\|^2_{L^2(\Omega)}$$

will be controlled with Gronwall's Lemma.

(iii) From Chapter 2, it is expected that

$$\|\rho-\rho_h\|^2_{L^2(\Omega)} = O(h^3).$$

It is also reasonable to expect that for all $t$

$$\|(\mathbf{u}-\mathbf{u}_h)(t)\|_{L^2(\Omega)} = O(h^2).$$

Then $(\eta^A_{K,\rho})^2$ can be used as an error indicator for $\|\rho - \rho_h\|_{L^2(\Omega)}$. Indeed, starting from (4.14), and using the Young's inequality, one derives that

$$\|(\rho - \rho_h)(t)\|^2_{L^2(\Omega)} \le \|(\rho - \rho_h)(0)\|^2_{L^2(\Omega)} + C\int_0^t \sum_{K\in\mathcal{T}_h} (\eta^A_{K,\rho})^2(s)ds$$
$$+ \frac{1}{T}\int_0^t \|(\rho - \rho_h)(s)\|^2_{L^2(\Omega)}ds + T\|\nabla\rho_h\|^2_{L^\infty(\Omega\times(0,T))}\int_0^t \|(\mathbf{u} - \mathbf{u}_h)(s)\|^2_{L^2(\Omega)}ds.$$

which yields (after using the Gronwall's Lemma)

$$\|(\rho - \rho_h)(t)\|^2_{L^2(\Omega)}$$
$$\le \exp(1)\left(\|(\rho - \rho_h)(0)\|^2_{L^2(\Omega)} + C\int_0^t \sum_{K\in\mathcal{T}_h} (\eta^A_{K,\rho})^2(s)ds\right.$$
$$\left. T\|\nabla\rho_h\|^2_{L^\infty(\Omega\times(0,T))}\int_0^t \|(\mathbf{u} - \mathbf{u}_h)(s)\|^2_{L^2(\Omega)}ds\right). \quad (4.17)$$

Moreover, it will be confirmed by the numerical experiments at the end of this chapter that

$$\int_0^t \sum_{K\in\mathcal{T}_h} (\eta^A_{K,\rho})^2(s)ds = O(h^3).$$

Thus (4.17) is an optimal a posteriori error estimate, up to some higher order terms that are

$$\|(\rho - \rho_h)(0)\|^2_{L^2(\Omega)} = \|(\rho - r_h(\rho))(0)\|^2_{L^2(\Omega)} = O(h^4), \quad \int_0^t \|(\mathbf{u} - \mathbf{u}_h)(s)\|^2_{L^2(\Omega)}ds = O(h^4).$$

**A posteriori error estimates for $\mathbf{u} - \mathbf{u}_h$**

The largest part of the a posteriori error analysis is to derive a velocity error estimate. As in Chapter 3, we will introduce a suitable reconstruction of the approximated velocity $\mathbf{u}_h(t)$ and the approximated pressure $p_h(t)$. The proofs that will be presented below are very similar to those presented in Chapter 3 for the unsteady Navier-Stokes equations with constant coefficients, except that the terms of the form

$$\int_\Omega \rho(\mathbf{u}\cdot\nabla)\mathbf{v}\cdot\mathbf{v}d\mathbf{x}$$

are not zero, since $\rho$ is non constant in general. Indeed, it is in general not possible to write something as

$$\int_\Omega \rho(\mathbf{u}\cdot\nabla)\mathbf{v}\cdot\mathbf{v}d\mathbf{x} = \frac{1}{2}\int_\Omega \operatorname{div}\left(\rho\mathbf{u}|\mathbf{v}|^2\right)d\mathbf{x}$$

and conclude by using divergence theorem and boundary conditions. This is due to the fact that $\operatorname{div}(\rho\mathbf{u}) \neq 0$ since $\rho$ varies.

We state the main definition below.

**Definition 4.4** (Linearized Navier-Stokes reconstruction for variable density and viscosity)**.**
Let $(\mathbf{u}, p)$, $\rho$ and $\mu$ be the solutions of (4.6)-(4.7) and $\mathbf{u}_h, p_h$ the finite elements approximations given by (4.8)-(4.11). For any $t \in [0, T]$, we define $(\mathbf{U}(t), P(t)) \in (H^1_0(\Omega))^2 \times L^2_0(\Omega)$

the linearized Navier-Stokes reconstruction of $(\mathbf{u}_h(t), p_h(t))$ as the weak solutions of

$$\int_\Omega \rho((\mathbf{U}(t)\cdot\nabla)\mathbf{u}_h(t))\cdot\mathbf{v}d\mathbf{x} + \int_\Omega \rho((\mathbf{u}(t)\cdot\nabla)(\mathbf{U}(t)-\mathbf{u}_h(t)))\cdot\mathbf{v}d\mathbf{x}$$
$$+\int_\Omega 2\mu D(\mathbf{U}(t)) : D(\mathbf{v})d\mathbf{x} - \int_\Omega P(t)\operatorname{div}\mathbf{v}d\mathbf{x} = \int_\Omega \rho\left(\mathbf{f}(t) - \frac{\partial \mathbf{u}_h}{\partial t}(t)\right)\cdot\mathbf{v}d\mathbf{x}, \quad \forall \mathbf{v}\in (H_0^1(\Omega))^2,$$
$$-\int_\Omega q\operatorname{div}\mathbf{U}(t) = 0, \quad \forall q\in L_0^2(\Omega). \quad (4.18)$$

In the next proposition, we prove that(4.18) is well-posed. The demonstration is an adaptation of that of Proposition 3.42, taking in account the fact $\rho$ and $\mu$ are functions, rather than scalars.

**Proposition 4.5.**
*Let $C_{SOB}$ be the constant in Proposition A.8 of Appendix A.2. We assume that there exists $h_0 > 0$ and $0 < \gamma < 1$ such that for all $h \le h_0$*

$$\sup_{t\in(0,T)} \left(\|\nabla \mathbf{u}_h(t)\|_{L^2(\Omega)} + \|\nabla \mathbf{u}(t)\|_{L^2(\Omega)}\right) \le \frac{\gamma\mu_{\min}}{\rho_{\max} C_{SOB}}. \quad (4.19)$$

*Then for all $h \le h_0$ and for all $t\in[0,T]$, there exists a unique solution $(\mathbf{U}(t), P(t))$ of (4.18).*

*Proof.* Let $h \le h_0$. We follow the proof of Proposition 3.42 Let $h \le h_0$. We write the problem (4.18) in a abstract form: for all $t\in[0,T]$ we look for $(\mathbf{U}(t), P(t))$ the solution of

$$\begin{cases} a(\mathbf{U}(t),\mathbf{v}) + b(\mathbf{v}, P(t)) = F(\mathbf{v}), \forall \mathbf{v}\in (H_0^1(\Omega))^2, \\ b(\mathbf{U}(t), q) = 0, \forall q\in L_0^2(\Omega), \end{cases} \quad (4.20)$$

where

$$a(\mathbf{U},\mathbf{v}) = \int_\Omega \rho((\mathbf{U}(t)\cdot\nabla)\mathbf{u}_h(t))\cdot\mathbf{v}d\mathbf{x} + \int_\Omega \rho((\mathbf{u}(t)\cdot\nabla)\mathbf{U}(t))\cdot\mathbf{v}d\mathbf{x} + \mu\int_\Omega \nabla\mathbf{U}(t) : \nabla\mathbf{v}d\mathbf{x},$$

$$F(v) = \int_\Omega \rho\left(\mathbf{f}(t) - \frac{\partial \mathbf{u}_h}{\partial t}(t) + (\mathbf{u}(t)\cdot\nabla)\mathbf{u}_h(t)\right)\cdot\mathbf{v}d\mathbf{x},$$

$$b(\mathbf{v}, P(t)) = -\int_\Omega P(t)\operatorname{div}\mathbf{v}dx, \quad b(\mathbf{U}(t), q) = -\int_\Omega q\operatorname{div}\mathbf{U}(t).$$

Let

$$V = \left\{\mathbf{v}\in (H_0^1(\Omega))^2 : \operatorname{div}\mathbf{v} = 0\right\}$$

the subspace of $(H_0^1(\Omega))^2$ containing the free divergence vector fields. As in Proposition 3.42, it sufficient to find $\mathbf{U}(t)\in V$ solution of

$$a(\mathbf{U}(t),\mathbf{v}) = F(\mathbf{v}), \forall\mathbf{v}\in V, \quad (4.21)$$

to conclude since $P(t)$ will be obtain trough the inf-sup condition.

The continuity of the bilinear form $a$ and the linear functional $F$ are a direct consequence since $\rho$, respectively $\mu$ are bounded. In order to apply the Lax-Milgram Lemma to (4.21), the only issue is to check the coercivity of $a$. Since $\mu \ge \mu_{\min} > 0$, we immediately have that

$$\int_\Omega 2\mu D(\mathbf{U}) : D(\mathbf{U})d\mathbf{x} \ge \mu_{\min}\|\nabla\mathbf{U}\|^2_{L^2(\Omega)},$$

where we use the Korn's inequality that reads for any $\mathbf{v}\in(H_0^1(\Omega))^2$

$$2\|D(\mathbf{v})\|^2_{L^2(\Omega)} \ge \|\nabla\mathbf{v}\|^2_{L^2(\Omega)}.$$

Therefore, it remains to control the terms

$$\int_\Omega \rho((\mathbf{U}\cdot\nabla)\mathbf{u}_h(t))\cdot\mathbf{U}d\mathbf{x}, \int_\Omega \rho((\mathbf{u}(t)\cdot\nabla)\mathbf{U})\cdot\mathbf{U}d\mathbf{x}.$$

Observe as we did before that

$$\int_\Omega \rho((\mathbf{U}\cdot\nabla)\mathbf{u}_h(t))\cdot\mathbf{U}d\mathbf{x} \geq -\int_\Omega |\rho((\mathbf{U}\cdot\nabla)\mathbf{u}_h(t))\cdot\mathbf{U}|d\mathbf{x}.$$

Applying the Cauchy-Schwarz inequality and the Proposition A.8, one has that

$$-\int_\Omega |\rho((\mathbf{U}\cdot\nabla)\mathbf{u}_h(t))\cdot\mathbf{U}|d\mathbf{x} \geq -\rho_{\max}C_{SOB}\|\nabla\mathbf{u}_h(t)\|_{L^2(\Omega)}\|\nabla\mathbf{U}\|^2_{L^2(\Omega)},$$

therefore

$$\int_\Omega \rho((\mathbf{U}\cdot\nabla)\mathbf{u}_h(t))\cdot\mathbf{U}d\mathbf{x} \geq -\rho_{\max}C_{SOB}\|\nabla\mathbf{u}_h(t)\|_{L^2(\Omega)}\|\nabla\mathbf{U}\|^2_{L^2(\Omega)}.$$

By the same argument, we prove that

$$\int_\Omega \rho((\mathbf{u}(t)\cdot\nabla)\mathbf{U})\cdot\mathbf{U}(t)d\mathbf{x} \geq -\rho_{\max}C_{SOB}\|\nabla\mathbf{u}(t)\|_{L^2(\Omega)}\|\nabla\mathbf{U}\|^2_{L^2(\Omega)}.$$

Thus, using the hypothesis (4.27), we have

$$\begin{aligned} a(\mathbf{U},\mathbf{U}) \geq \mu_{\min}\|\nabla\mathbf{U}\|^2_{L^2(\Omega)} - \rho_{\max}C_{SOB}\left(\|\nabla\mathbf{u}_h(t)\|_{L^2(\Omega)} + \|\nabla\mathbf{u}(t)\|_{L^2(\Omega)}\right)\|\nabla\mathbf{U}\|^2_{L^2(\Omega)} \\ \geq (1-\gamma)\mu_{\min}\|\nabla\mathbf{U}\|^2_{L^2(\Omega)}, \end{aligned}$$

which proves the coercivity of $a$ since $0<\gamma<1$. □

**Remark 4.6.** (i) As in Chapter 3, the hypothesis (4.27) holds if we assume that

(1) There exists $0<\gamma'<1$ such that

$$\sup_{t\in(0,T)} \|\nabla\mathbf{u}(t)\|_{L^2(\Omega)} \leq \frac{\gamma'\mu_{\min}}{\rho_{\max}C_{SOB}},$$

that is to say the velocity field $\mathbf{u}$ is *small*. This is a reasonable assumption if we assume the data $\mathbf{f}$,$\mathbf{u}_0$,$T$ and the difference $\rho_{\max}-\rho_{\min}, \mu_{\max}-\mu_{\min}$ are small enough.

(2) Strong convergence holds:

$$\sup_{t\in(0,T)} \|\nabla(\mathbf{u}(t)-\mathbf{u}_h(t))\|_{L^2(\Omega)} \to 0 \text{ as } h\to 0.$$

(ii) Observe that the following orthogonality relations hold between $(\mathbf{U},P)$ and $(\mathbf{u}_h,p_h)$ holds:

$$\begin{aligned} \int_\Omega \rho((\mathbf{u}\cdot\nabla)(\mathbf{U}-\mathbf{u}_h))\cdot\mathbf{v}_h d\mathbf{x} + \int_\Omega \rho(((\mathbf{U}-\mathbf{u}_h)\cdot\nabla)\mathbf{u}_h))\cdot\mathbf{v}_h d\mathbf{x} + \int_\Omega 2\mu D(\mathbf{U}-\mathbf{u}_h) : D(\mathbf{v}_h)d\mathbf{x} \\ -\int_\Omega (P-p_h)\operatorname{div}\mathbf{v}_h = \sum_K \alpha_K \int_K R_h^{NS}\cdot(\rho_h(\mathbf{u}_h\cdot\nabla)\mathbf{v}_h)d\mathbf{x} \\ +\int_\Omega (\rho-\rho_h)\mathbf{f}\cdot\mathbf{v}_h d\mathbf{x} - \int_\Omega (\rho-\rho_h)\frac{\partial\mathbf{u}_h}{\partial t}\cdot\mathbf{v}_h d\mathbf{x} - \int_\Omega (\rho-\rho_h)((\mathbf{u}_h\cdot\nabla)\mathbf{u}_h)\cdot\mathbf{v}_h d\mathbf{x} \\ -\int_\Omega (\mu-\mu_h)D(\mathbf{u}_h) : D(\mathbf{v}_h)d\mathbf{x}, \quad \forall\mathbf{v}_h\in V_h, \quad (4.22) \end{aligned}$$

and

$$\int_\Omega q_h \operatorname{div}(\mathbf{U}-\mathbf{u}_h)d\mathbf{x} = \sum_{K\in\mathcal{T}_h} \alpha_K \int_K R_h^{NS}\cdot\nabla q_h d\mathbf{x}, \quad \forall q_h \in Q_h. \tag{4.23}$$

Morally, this orthogonality means (as we proved it for the linear Stokes equations) that if we discretize (4.18) and we consider its finite elements approximations $(\mathbf{U}_h, P_h)$ (computed with the same method as $\mathbf{u}_h, p_h$ and we use $\rho_h, \mu_h$ as approximation of $\rho, \mu$), then we will have $\mathbf{U}_h = \mathbf{u}_h$ and $P_h = p_h$)

Now, as for the Navier-Stokes equations with constant density and viscosity, we split the error $\mathbf{u}-\mathbf{u}_h$ into two parts, namely a continuous estimate $\mathbf{u}-\mathbf{U}$ and a discrete estimate $\mathbf{U}-\mathbf{u}_h$. Since we work with a variable density, the following well-known identity is needed: for any $\mathbf{v}\in H^1(0,T;(H^1(\Omega))^2)$, we have that

$$\frac{1}{2}\frac{d}{dt}\int_\Omega \rho\mathbf{v}^2 d\mathbf{x} = \int_\Omega \rho\frac{\partial \mathbf{v}}{\partial t}\cdot\mathbf{v}d\mathbf{x} + \int_\Omega \rho((\mathbf{u}\cdot\nabla)\mathbf{v})\cdot\mathbf{v}d\mathbf{x}. \tag{4.24}$$

We give a quick proof of (4.24). Since

$$\frac{\partial\rho}{\partial t} + \mathbf{u}\cdot\nabla\rho = 0$$

we have

$$\begin{aligned}
\frac{1}{2}\frac{d}{dt}\int_\Omega \rho\mathbf{v}^2 d\mathbf{x} &= \int_\Omega \rho\frac{\partial \mathbf{v}}{\partial t}\cdot\mathbf{v}d\mathbf{x} + \frac{1}{2}\int_\Omega \frac{\partial\rho}{\partial t}\mathbf{v}^2 d\mathbf{x}\\
&= \int_\Omega \rho\frac{\partial \mathbf{v}}{\partial t}\cdot\mathbf{v}d\mathbf{x} - \frac{1}{2}\int_\Omega (\mathbf{u}\cdot\nabla\rho)\mathbf{v}^2 d\mathbf{x}\\
&= \int_\Omega \rho\frac{\partial \mathbf{v}}{\partial t}\cdot\mathbf{v}d\mathbf{x} - \frac{1}{2}\int_\Omega \operatorname{div}(\rho\mathbf{u})\mathbf{v}^2 d\mathbf{x}\\
&= \int_\Omega \rho\frac{\partial \mathbf{v}}{\partial t}\cdot\mathbf{v}d\mathbf{x} - \frac{1}{2}\int_{\partial\Omega} \rho\underbrace{\mathbf{u}}_{=0}\cdot\mathbf{n}\mathbf{v}^2 d\mathbf{x} + \int_\Omega \rho((\mathbf{u}\cdot\nabla)\mathbf{v})\mathbf{v}d\mathbf{x}\\
&= \int_\Omega \rho\frac{\partial \mathbf{v}}{\partial t}\cdot\mathbf{v}d\mathbf{x} + \int_\Omega \rho((\mathbf{u}\cdot\nabla)\mathbf{v})\cdot\mathbf{v}d\mathbf{x}.
\end{aligned}$$

**Proposition 4.7** (Continuous error estimate)**.**
*Let $(\mathbf{u}, p)$ be the exact velocity and pressure fields, and $(\mathbf{U}, P)$ the reconstruction given by (4.18) of the numerical solution $(\mathbf{u}_h, p_h)$ obtained by solving (4.8)-(4.11). Moreover, we assume that there exists $h_0 > 0$ and $0 < \gamma < 1$ such that for all $h \le h_0$*

$$\sup_{t\in(0,T)}\Big(\|\nabla\mathbf{u}_h(t)\|_{L^2(\Omega)} + \|\nabla\mathbf{u}(t)\|_{L^2(\Omega)}\Big) \le \frac{\gamma\mu_{\min}}{\rho_{\max}C_{SOB}}. \tag{4.25}$$

*Then for all $h \le h_0$ and for all $t \in (0,T]$, it holds*

$$\begin{aligned}
&\rho_{\min}\|(\mathbf{u}-\mathbf{U})(t)\|^2 + (1-\gamma)\mu_{\min}\int_0^t \|\nabla(\mathbf{u}-\mathbf{U})(s)\|^2_{L^2(\Omega)}ds\\
&\qquad\le \rho_{\max}\|(\mathbf{u}-\mathbf{U})(0)\|^2 + \frac{2C_P^2\rho_{\max}^2}{(1-\gamma)\mu_{\min}}\int_0^t \left\|\frac{\partial\mathbf{U}}{\partial t}(s) - \frac{\partial\mathbf{u}_h}{\partial t}(s)\right\|^2_{L^2(\Omega)} ds,
\end{aligned}$$

*where $C_P$ stands for the Poincaré constant of $\Omega$.*

*Proof.* We apply identity (4.24) to $\mathbf{u}-\mathbf{U}$.

$$\frac{1}{2}\frac{d}{dt}\int_\Omega \rho|\mathbf{u}-\mathbf{U}|^2 d\mathbf{x} + \int_\Omega 2\mu D(\mathbf{u}-\mathbf{U}) : D(\mathbf{u}-\mathbf{U})d\mathbf{x}$$
$$= \int_\Omega \rho\frac{\partial(\mathbf{u}-\mathbf{U})}{\partial t}\cdot(\mathbf{u}-\mathbf{U})d\mathbf{x} + \int_\Omega \rho\left((\mathbf{u}\cdot\nabla)(\mathbf{u}-\mathbf{U})\right)\cdot(\mathbf{u}-\mathbf{U})d\mathbf{x} + \int_\Omega 2\mu D(\mathbf{u}-\mathbf{U}) : D(\mathbf{u}-\mathbf{U})d\mathbf{x}$$
$$= \int_\Omega \rho\frac{\partial(\mathbf{u}-\mathbf{U})}{\partial t}\cdot(\mathbf{u}-\mathbf{U})d\mathbf{x} + \int_\Omega \rho\left((\mathbf{u}\cdot\nabla)(\mathbf{u}-\mathbf{U})\right)\cdot(\mathbf{u}-\mathbf{U})d\mathbf{x} + \int_\Omega \rho\left(((\mathbf{u}-\mathbf{U})\cdot\nabla)\mathbf{u}_h\right)\cdot(\mathbf{u}-\mathbf{U})d\mathbf{x}$$
$$\int_\Omega 2\mu D(\mathbf{u}-\mathbf{U}) : D(\mathbf{u}-\mathbf{U})d\mathbf{x} - \int_\Omega \rho\left(((\mathbf{u}-\mathbf{U})\cdot\nabla)\mathbf{u}_h\right)\cdot(\mathbf{u}-\mathbf{U})d\mathbf{x}$$
$$= \int_\Omega \rho\frac{\partial(\mathbf{u}-\mathbf{U})}{\partial t}\cdot(\mathbf{u}-\mathbf{U})d\mathbf{x} + \int_\Omega \rho\left((\mathbf{u}\cdot\nabla)(\mathbf{u}-\mathbf{U})\right)\cdot(\mathbf{u}-\mathbf{U})d\mathbf{x} + \int_\Omega \rho\left(((\mathbf{u}-\mathbf{U})\cdot\nabla)\mathbf{u}_h\right)\cdot(\mathbf{u}-\mathbf{U})d\mathbf{x}$$
$$\int_\Omega 2\mu D(\mathbf{u}-\mathbf{U}) : D(\mathbf{u}-\mathbf{U})d\mathbf{x} - \int_\Omega (p-P)\operatorname{div}(\mathbf{u}-\mathbf{U}) - \int_\Omega \rho\left(((\mathbf{u}-\mathbf{U})\cdot\nabla)\mathbf{u}_h\right)\cdot(\mathbf{u}-\mathbf{U})d\mathbf{x}$$

where we add the pressure term for free since $\mathbf{u}-\mathbf{U}$ is divergence free. Now taking the difference between (4.6) (written in a weak form) and (4.18), one has

$$\frac{1}{2}\frac{d}{dt}\int_\Omega \rho|\mathbf{u}-\mathbf{U}|^2 d\mathbf{x} + \int_\Omega 2\mu D(\mathbf{u}-\mathbf{U}) : D(\mathbf{u}-\mathbf{U})d\mathbf{x}$$
$$= -\int_\Omega \rho\left(\frac{\partial \mathbf{U}}{\partial t} - \frac{\partial \mathbf{u}_h}{\partial t}\right)\cdot(\mathbf{u}-\mathbf{U})d\mathbf{x}$$
$$- \int_\Omega \rho\left(((\mathbf{u}-\mathbf{U})\cdot\nabla)\mathbf{u}_h\right)\cdot(\mathbf{u}-\mathbf{U})d\mathbf{x}.$$

Cauchy-Schwarz, Poincaré, Young's and Korn's inequality and the hypothesis on $\nabla\mathbf{u}_h$ imply then

$$\frac{1}{2}\frac{d}{dt}\int_\Omega \rho|\mathbf{u}-\mathbf{U}|^2 d\mathbf{x} + \mu_{\min}\|\nabla(\mathbf{u}-\mathbf{U})\|^2_{L^2(\Omega)}$$
$$\leq \frac{C_P^2\rho_{\max}^2}{(1-\gamma)\mu_{\min}}\left\|\frac{\partial \mathbf{U}}{\partial t} - \frac{\partial \mathbf{u}_h}{\partial t}\right\|^2_{L^2(\Omega)} + \frac{1+\gamma}{2}\mu_{\min}\|\nabla(\mathbf{u}-\mathbf{U})\|^2_{L^2(\Omega)},$$

which yields the result by passing the gradient term to the left hand side and integrating over the time. □

We now focus on the discrete estimate $\mathbf{U}-\mathbf{u}_h$. We first prove an a posteriori upper bounds for $\|\nabla(\mathbf{U}-\mathbf{u}_h)\|_{L^2(\Omega)}$ and $\|P-p_h\|_{L^2(\Omega)}$. The proof is very similar to the proof of Proposition 3.46, we only have to adapt it, taking in account that now the density and the viscosity are variable and unknowns of the problem too. We will use the following dual problem to recover the pressure error estimate $P-p_h$ (note that it is a $\mu$-variable version of the dual problem used in Chapter 3) :

$$\begin{cases} -\operatorname{div}(2\mu D(\mathbf{w}(t))) + \nabla r(t) = 0, & \text{in } \Omega,\\ \operatorname{div}\mathbf{w} = p_h - P(t), & \text{in } \Omega,\\ \mathbf{w} = 0, & \text{on } \partial\Omega. \end{cases} \tag{4.26}$$

Since $\mu > 0$ and is bounded above and below, observe that the problem is well-posed and admits for any $t$ a unique weak solution $(\mathbf{w}(t), r(t)) \in (H_0^1(\Omega))^2 \times L_0^2(\Omega)$. Moreover the following a priori estimate (see Theorem B.4 in the Appendix) holds: there exists a constant $C > 0$ depending only on $\Omega$ such that for any $t \in [0,T]$

$$\frac{\mu_{\min}}{\mu_{\max}}\|\nabla\mathbf{w}(t)\|_{L^2(\Omega)} + \frac{\mu_{\min}}{\mu_{\max}^2}\|r(t)\|_{L^2(\Omega)} \leq C\|P-p_h(t)\|_{L^2(\Omega)}.$$

**Proposition 4.8** (Discrete error estimates)**.**
*Let $(\mathbf{U}, P)$ be the Navier-Stokes reconstruction of the approximated velocity and pressure $(\mathbf{u}_h, p_h)$. Let $(\mathbf{w}, r)$ be the weak dual solutions obtained of (4.26). Assume that there exists $h_0 > 0$ and $0 < \gamma < 1$ such that for all $h \leq h_0$*

$$\sup_{t\in(0,T)} \left(\|\nabla \mathbf{u}_h(t)\|_{L^2(\Omega)} + \|\nabla \mathbf{u}(t)\|_{L^2(\Omega)}\right) \leq \frac{\gamma \mu_{\min}}{\rho_{\max} C_{SOB}}, \tag{4.27}$$

*where $C_{SOB}$ is the constant in Proposition A.8 of the Appendix A.2. Then there exists $C_1 > 0$ that depends only on the reference triangle et $C_2$ that depends only on $\Omega$ such that for all $h \leq h_0$ and for all $t \in [0, T]$, we have*

$$\begin{aligned}
\mu_{\min}\|\nabla(\mathbf{U} - \mathbf{u}_h)(t)\|^2_{L^2(\Omega)} &+ \frac{\mu^3_{\min}}{\mu^4_{\max}}\|(P - p_h)(t)\|^2_{L^2(\Omega)} \\
&\leq \frac{C_1}{(1-\gamma)^2} \sum_{K\in\mathcal{T}_h} (\eta^A_{K,\mathbf{u}})^2(t) + (\eta^A_{K,p})^2(t) + (\eta^{\text{div}}_K)^2(t) \\
&+ \frac{C_2}{(1-\gamma)^2} \frac{\mu^2_{\max}}{\mu^3_{\min}} L^2_\infty \left(\|(\rho - \rho_h)(t)\|^2_{L^2(\Omega)} + \|(\mu - \mu_h)(t)\|^2_{L^2(\Omega)}\right),
\end{aligned} \tag{4.28}$$

*where*

$$\begin{aligned}
(\eta^A_{K,\mathbf{u}})^2 = \Bigg(&\left\|\rho_h \mathbf{f} - \rho_h \frac{\partial \mathbf{u}_h}{\partial t} - \rho_h(\mathbf{u}_h \cdot \nabla)\mathbf{u}_h + \operatorname{div}(2\mu_h D(\mathbf{u}_h)) - \nabla p_h\right\|_{L^2(K)} \\
&+ \frac{1}{2\sqrt{\lambda_{2,K}}} \|[2\mu_h D(\mathbf{u}_h)\cdot \mathbf{n}]\|_{L^2(\partial K)}\Bigg) \omega_K(\mathbf{U} - \mathbf{u}_h),
\end{aligned}$$

$$\begin{aligned}
(\eta^A_{K,p})^2 = \frac{\mu^3_{\min}}{\mu^4_{\max}} \Bigg(&\left\|\rho_h \mathbf{f} - \rho_h \frac{\partial \mathbf{u}_h}{\partial t} - \rho_h(\mathbf{u}_h \cdot \nabla)\mathbf{u}_h + \operatorname{div}(2\mu_h D(\mathbf{u}_h)) - \nabla p_h\right\|_{L^2(K)} \\
&+ \frac{1}{2\sqrt{\lambda_{2,K}}} \|[2\mu_h D(\mathbf{u}_h)\cdot \mathbf{n}]\|_{L^2(\partial K)}\Bigg) \omega_K(\mathbf{w}),
\end{aligned}$$

$$(\eta^{\text{div}}_K)^2 = \frac{\mu^4_{\max}}{\mu^3_{\min}} \|\operatorname{div} \mathbf{u}_h\|^2_{L^2(\Omega)},$$

$$L(\mathbf{u}_h) = \left(\left\|\mathbf{f} - \frac{\partial \mathbf{u}_h}{\partial t} - (\mathbf{u}_h \cdot \nabla)\mathbf{u}_h\right\|^2_{L^\infty(\Omega\times(0,T))} + \|D(\mathbf{u}_h)\|^2_{L^\infty(\Omega\times(0,T))}\right).$$

**Remark 4.9.**
Observe that this upper bound is consistent with the previous results obtained in Chapter 3 for the Navier-Stokes equations with constant coefficients. Indeed, if we assume that the viscosity and the density are constant then $\rho = \rho_h = \rho_{\min} = \rho_{\max}$ and $\mu = \mu_{\min} = \mu_{\max}$, and Proposition 4.8 reduces to Proposition 3.46.

*Proof.* To lighten the notations, we do not write the explicit dependence on $t$ of the function, since every quantity is evaluated at the same time. In what follows, we denote by $C$ or $\tilde{C}$ any positive constant that may depend only on the reference triangle or $\Omega$ and which values can change from line to line.

*Part 1. Estimate for the velocity.*

$$\int_\Omega 2\mu D(\mathbf{U}-\mathbf{u}_h):D(\mathbf{U}-\mathbf{u}_h)d\mathbf{x} = \int_\Omega 2\mu D(\mathbf{U}-\mathbf{u}_h):D(\mathbf{U}-\mathbf{u}_h)d\mathbf{x}$$
$$+\int_\Omega (P-p_h)\operatorname{div}(\mathbf{U}-\mathbf{u}_h)d\mathbf{x} - \int_\Omega (P-p_h)\operatorname{div}(\mathbf{U}-\mathbf{u}_h)d\mathbf{x}$$
$$+\int_\Omega \rho((\mathbf{U}\cdot\nabla)\mathbf{u}_h)\cdot(\mathbf{U}-\mathbf{u}_h)d\mathbf{x} - \int_\Omega \rho((\mathbf{U}\cdot\nabla)\mathbf{u}_h)\cdot(\mathbf{U}-\mathbf{u}_h)d\mathbf{x}$$
$$+\int_\Omega \rho((\mathbf{u}\cdot\nabla)(\mathbf{U}-\mathbf{u}_h)\cdot(\mathbf{U}-\mathbf{u}_h)d\mathbf{x} - \int_\Omega \rho((\mathbf{u}\cdot\nabla)(\mathbf{U}-\mathbf{u}_h)\cdot(\mathbf{U}-\mathbf{u}_h)d\mathbf{x}$$
$$+\int_\Omega \rho((\mathbf{u}_h\cdot\nabla)\mathbf{u}_h)\cdot(\mathbf{U}-\mathbf{u}_h)d\mathbf{x} - \int_\Omega \rho((\mathbf{u}_h\cdot\nabla)\mathbf{u}_h)\cdot(\mathbf{U}-\mathbf{u}_h)d\mathbf{x}.$$

Using that $(\mathbf{U}, P)$ are solution of the weak equations (4.18), we have thus

$$\int_\Omega 2\mu D(\mathbf{U}-\mathbf{u}_h):D(\mathbf{U}-\mathbf{u}_h)d\mathbf{x} = \int_\Omega \left(\rho\mathbf{f}-\rho\frac{\partial \mathbf{u}_h}{\partial t}\right)\cdot(\mathbf{U}-\mathbf{u}_h)d\mathbf{x}$$
$$-\int_\Omega \rho((\mathbf{u}_h\cdot\nabla)\mathbf{u}_h)\cdot(\mathbf{U}-\mathbf{u}_h)d\mathbf{x} - \int_\Omega 2\mu D(\mathbf{u}_h):D(\mathbf{U}-\mathbf{u}_h)d\mathbf{x} + \int_\Omega p_h\operatorname{div}(\mathbf{U}-\mathbf{u}_h)d\mathbf{x}$$
$$+\int_\Omega (P-p_h)\operatorname{div}(\mathbf{U}-\mathbf{u}_h)d\mathbf{x} - \int_\Omega \rho((\mathbf{U}\cdot\nabla)\mathbf{u}_h)\cdot(\mathbf{U}-\mathbf{u}_h)d\mathbf{x}$$
$$-\int_\Omega \rho((\mathbf{u}\cdot\nabla)(\mathbf{U}-\mathbf{u}_h)\cdot(\mathbf{U}-\mathbf{u}_h)d\mathbf{x} + \int_\Omega \rho((\mathbf{u}_h\cdot\nabla)\mathbf{u}_h)\cdot(\mathbf{U}-\mathbf{u}_h)d\mathbf{x}.$$

This yields

$$\int_\Omega 2\mu D(\mathbf{U}-\mathbf{u}_h):D(\mathbf{U}-\mathbf{u}_h)d\mathbf{x} = \int_\Omega \left(\rho_h\mathbf{f}-\rho_h\frac{\partial \mathbf{u}_h}{\partial t}\right)\cdot(\mathbf{U}-\mathbf{u}_h)d\mathbf{x}$$
$$-\int_\Omega \rho_h((\mathbf{u}_h\cdot\nabla)\mathbf{u}_h)\cdot(\mathbf{U}-\mathbf{u}_h)d\mathbf{x} - \int_\Omega 2\mu_h D(\mathbf{u}_h):D(\mathbf{U}-\mathbf{u}_h)d\mathbf{x} + \int_\Omega p_h\operatorname{div}(\mathbf{U}-\mathbf{u}_h)d\mathbf{x}$$
$$+\int_\Omega (P-p_h)\operatorname{div}(\mathbf{U}-\mathbf{u}_h)d\mathbf{x} - \int_\Omega \rho\left(((\mathbf{U}-\mathbf{u}_h)\cdot\nabla)\mathbf{u}_h + (\mathbf{u}\cdot\nabla)(\mathbf{U}-\mathbf{u}_h)\right)\cdot(\mathbf{U}-\mathbf{u}_h)d\mathbf{x}$$
$$+\int_\Omega (\rho-\rho_h)\left(\mathbf{f}-\frac{\partial \mathbf{u}_h}{\partial t}\right)\cdot(\mathbf{U}-\mathbf{u}_h)d\mathbf{x} - \int_\Omega 2(\mu-\mu_h)D(\mathbf{u}_h):D(\mathbf{U}-\mathbf{u}_h)d\mathbf{x}$$
$$-\int_\Omega (\rho-\rho_h)((\mathbf{u}_h\cdot\nabla)\mathbf{u}_h)\cdot(\mathbf{U}-\mathbf{u}_h)d\mathbf{x}.$$

Using the finite elements approximation of the momentum equation, we can remove any test function $\mathbf{v}_h$ and we obtain after an integration by parts

$$\int_\Omega 2\mu D(\mathbf{U}-\mathbf{u}_h):D(\mathbf{U}-\mathbf{u}_h)d\mathbf{x}$$
$$=\sum_{K\in\mathcal{T}_h}\int_K R_h^{NS}\cdot(\mathbf{U}-\mathbf{u}_h-\mathbf{v}_h)dx + \frac{1}{2}\int_{\partial K} R_{h,j}^{NS}\cdot(\mathbf{U}-\mathbf{u}_h-\mathbf{v}_h)d\mathbf{x} + \sum_{K\in\mathcal{T}_h}\alpha_K\int_K R_h^{NS}\cdot(\rho_h(\mathbf{u}_h\cdot\nabla)\mathbf{v}_h)d\mathbf{x}$$
$$+\int_\Omega (P-p_h)\operatorname{div}(\mathbf{U}-\mathbf{u}_h)d\mathbf{x} - \int_\Omega \rho\left(((\mathbf{U}-\mathbf{u}_h)\cdot\nabla)\mathbf{u}_h + (\mathbf{u}\cdot\nabla)(\mathbf{U}-\mathbf{u}_h)\right)\cdot(\mathbf{U}-\mathbf{u}_h)d\mathbf{x}$$
$$+\int_\Omega (\rho-\rho_h)\left(\mathbf{f}-\frac{\partial \mathbf{u}_h}{\partial t}\right)\cdot(\mathbf{U}-\mathbf{u}_h)d\mathbf{x} - \int_\Omega 2(\mu-\mu_h)D(\mathbf{u}_h):D(\mathbf{U}-\mathbf{u}_h)d\mathbf{x}$$
$$-\int_\Omega (\rho-\rho_h)((\mathbf{u}_h\cdot\nabla)\mathbf{u}_h)\cdot(\mathbf{U}-\mathbf{u}_h)d\mathbf{x},$$

where we recall that

$$R_h^{NS} = \rho_h\mathbf{f} - \rho_h\frac{\partial \mathbf{u}_h}{\partial t} - \rho_h(\mathbf{u}_h\cdot\nabla)\mathbf{u}_h + \operatorname{div}(2\mu_h D(\mathbf{u}_h)) - \nabla p_h,$$

and we note the jump terms over the edges

$$R_{h,j}^{NS} = [2\mu_h D(\mathbf{u}_h) \cdot \mathbf{n}] .$$

We now choose $\mathbf{v}_h$ as the Clément's interpolant $R_h(\mathbf{U} - \mathbf{u}_h)$ and we get by using Cauchy-Schwarz, Korn's, Poincaré and Sobolev inequalities and the anisotropic interpolation error estimates that

$$\begin{aligned}
&\mu_{\min}\|\nabla(\mathbf{U}-\mathbf{u}_h)\|^2_{L^2(\Omega)} \leq C \sum_{K\in\mathcal{T}_h} \left( \|R_h^{NS}\|_{L^2(K)} + \frac{1}{2\sqrt{\lambda_{2,K}}}\|R_{h,j}^{NS}\|_{L^2(\partial K)} \right) \omega_K(\mathbf{U}-\mathbf{u}_h) \\
&+ \sum_{K\in\mathcal{T}_h} \|R_h^{NS}\|_{L^2(K)}\alpha_K\|\rho_h\mathbf{u}_h\|_{L^\infty(K)}\|\nabla(R_h(\mathbf{U}-\mathbf{u}_h))\|_{L^2(K)} + \|P-p_h\|_{L^2(\Omega)}\|\operatorname{div}(\mathbf{U}-\mathbf{u}_h)\|_{L^2(\Omega)} \\
&\qquad + \rho_{\max} C_{SOB} \sup_{t\in(0,T)} \left( \|\nabla\mathbf{u}_h(t)\|_{L^2(\Omega)} + \|\nabla\mathbf{u}(t)\|_{L^2(\Omega)} \right) \|\nabla(\mathbf{U}-\mathbf{u}_h)\|^2_{L^2(\Omega)} \\
&\qquad + C_P\|\rho-\rho_h\|_{L^2(\Omega)} \left\| \mathbf{f} - \frac{\partial\mathbf{u}_h}{\partial t} - (\mathbf{u}_h\cdot\nabla)\mathbf{u}_h \right\|_{L^\infty(\Omega\times(0,T))} \|\nabla(\mathbf{U}-\mathbf{u}_h)\|_{L^2(\Omega)} \\
&\qquad\qquad + 2\|\mu-\mu_h\|_{L^2(\Omega)}\|D(\mathbf{u}_h)\|_{L^\infty(\Omega\times(0,T))}\|\nabla(\mathbf{U}-\mathbf{u}_h)\|_{L^2(\Omega)},
\end{aligned}$$

where $C_P$ stands for the Poincaré constant of $\Omega$. Thanks to the definition of $\alpha_K$ we have that

$$\alpha_K\|\rho_h\mathbf{u}_h\|_{L^\infty(K)}\|\nabla(R_h(\mathbf{U}-\mathbf{u}_h))\|_{L^2(K)} \leq \alpha\lambda_{2,K}\|\nabla(R_h(\mathbf{U}-\mathbf{u}_h))\|_{L^2(K)} \leq C\omega_K(\mathbf{U}-\mathbf{u}_h).$$

Thus the stabilization terms can be absorbed into the residual ones. Now using the hypothesis on $\nabla\mathbf{u}$ and $\nabla\mathbf{u}_h$ and the Young's inequality, one can state

$$\begin{aligned}
&\frac{1-\gamma}{2}\mu_{\min}\|\nabla(\mathbf{U}-\mathbf{u}_h)\|^2_{L^2(\Omega)} \leq C \sum_{K\in\mathcal{T}_h} \left( \|R_h^{NS}\|_{L^2(K)} + \frac{1}{2\sqrt{\lambda_{2,K}}}\|R_{h,j}^{NS}\|_{L^2(\partial K)} \right) \omega_K(\mathbf{U}-\mathbf{u}_h) \\
&+\|P-p_h\|_{L^2(\Omega)}\|\operatorname{div}(\mathbf{U}-\mathbf{u}_h)\|_{L^2(\Omega)} + \frac{C}{(1-\gamma)\mu_{\min}} L(\mathbf{u}_h) \left( \|\rho-\rho_h\|^2_{L^2(\Omega)} + \|\mu-\mu_h\|^2_{L^2(\Omega)} \right).
\end{aligned} \tag{4.29}$$

*Part 2. Estimate for the pressure.* We now use the dual problem (4.26). We have

$$\begin{aligned}
\|P-p_h\|^2_{L^2(\Omega)} &= -\int_\Omega (P-p_h)\operatorname{div}\mathbf{w}d\mathbf{x} = \int_\Omega \left(\rho\mathbf{f} - \rho\frac{\partial\mathbf{u}_h}{\partial t}\right)\cdot\mathbf{w}d\mathbf{x} - \int_\Omega 2\mu D(\mathbf{u}) : D(\mathbf{w})d\mathbf{x} \\
&- \int_\Omega \rho((\mathbf{U}\cdot\nabla)\mathbf{u}_h)\cdot\mathbf{w}d\mathbf{x} - \int_\Omega \rho((\mathbf{u}\cdot\nabla)(\mathbf{U}-\mathbf{u}_h))\cdot\mathbf{w}d\mathbf{x} + \int_\Omega p_h\operatorname{div}\mathbf{w}d\mathbf{x} \\
&= \int_\Omega \left(\rho_h\mathbf{f} - \rho_h\frac{\partial\mathbf{u}_h}{\partial t} - \rho_h(\mathbf{u}_h\cdot\nabla)\mathbf{u}_h\right)\cdot\mathbf{w}d\mathbf{x} - \int_\Omega 2\mu_h D(\mathbf{u}_h) : D(\mathbf{w})d\mathbf{x} \\
&+ \int_\Omega p_h\operatorname{div}\mathbf{w}d\mathbf{x} - \int_\Omega \rho(((\mathbf{U}-\mathbf{u}_h)\cdot\nabla)\mathbf{u}_h + (\mathbf{u}\cdot\nabla)(\mathbf{U}-\mathbf{u}_h))\cdot\mathbf{w}d\mathbf{x} \\
&+ \int_\Omega (\rho-\rho_h)\left(\mathbf{f} - \frac{\partial\mathbf{u}_h}{\partial t} - (\mathbf{u}_h\cdot\nabla)\mathbf{u}_h\right)\cdot\mathbf{w}d\mathbf{x} \\
&- \int_\Omega 2(\mu-\mu_h)D(\mathbf{u}_h) : D(\mathbf{w})d\mathbf{x} - \int_\Omega 2\mu D(\mathbf{u}-\mathbf{u}_h) : D(\mathbf{w})d\mathbf{x}.
\end{aligned}$$

Finally, removing any test function $\mathbf{v}_h$, one have

$$\begin{aligned}\|P-p_h\|^2_{L^2(\Omega)} = \int_\Omega \left(\rho_h \mathbf{f} - \rho_h \frac{\partial \mathbf{u}_h}{\partial t} - \rho_h(\mathbf{u}_h\cdot\nabla)\mathbf{u}_h\right)\cdot(\mathbf{w}-\mathbf{v}_h)d\mathbf{x} - \int_\Omega 2\mu_h D(\mathbf{u}_h) : D(\mathbf{w}-\mathbf{v}_h)d\mathbf{x} \\ + \int_\Omega p_h \operatorname{div}(\mathbf{w}-\mathbf{v}_h)d\mathbf{x} + \sum_{K\in\mathcal{T}_h} \alpha_K \int_K R_h^{NS}\cdot(\rho_h(\mathbf{u}_h\cdot\nabla)\mathbf{v}_h)d\mathbf{x} \\ - \int_\Omega \rho(((\mathbf{U}-\mathbf{u}_h)\cdot\nabla)\mathbf{u}_h + (\mathbf{u}\cdot\nabla)(\mathbf{U}-\mathbf{u}_h))\cdot\mathbf{w}d\mathbf{x} + \int_\Omega (\rho-\rho_h)\left(\mathbf{f} - \frac{\partial \mathbf{u}_h}{\partial t} - (\mathbf{u}_h\cdot\nabla)\mathbf{u}_h\right)\cdot\mathbf{w}d\mathbf{x} \\ - \int_\Omega 2(\mu-\mu_h)D(\mathbf{u}_h) : D(\mathbf{w})d\mathbf{x} - \int_\Omega 2\mu D(\mathbf{u}-\mathbf{u}_h) : D(\mathbf{w})d\mathbf{x}.\end{aligned}$$

We now proceed as in the end of Part 2. of Proposition 3.46. We choose $\mathbf{v}_h$ as the Clément's interpolant $R_h(\mathbf{w})$, and we use the a priori estimate that holds for the dual problem

$$\|\nabla \mathbf{w}\|_{L^2(\Omega)} \leq C\frac{\mu_{\max}}{\mu_{\min}}\|P-p_h\|_{L^2(\Omega)}.$$

We obtain finally that

$$\begin{aligned}\|P-p_h\|_{L^2(\Omega)} \leq \\ \tilde{C}\left(\sum_{K\in\mathcal{T}_h}\left(\|R_h^{NS}\|_{L^2(K)} + \frac{1}{2\sqrt{\lambda_{2,K}}}\|R_{h,j}^{NS}\|_{L^2(\partial K)}\right)\omega_K(\mathbf{w}) + \frac{\mu^4_{\max}}{\mu^2_{\min}}\|\nabla(\mathbf{U}-\mathbf{u}_h)\|^2_{L^2(\Omega)}\right. \\ \left. + \frac{\mu^2_{\max}}{\mu^2_{\min}} L(\mathbf{u}_h)\left(\|\rho-\rho_h\|^2_{L^2(\Omega)} + \|\mu-\mu_h\|^2_{L^2(\Omega)}\right)\right)^{1/2}. \quad (4.30)\end{aligned}$$

*Part 3. Putting all together.* We now combine estimate (4.29) and (4.30) to conclude. From (4.29) we have

$$\begin{aligned}\frac{1-\gamma}{2}\mu_{\min}\|\nabla(\mathbf{U}-\mathbf{u}_h)\|_{L^2(\Omega)} \leq C\sum_{K\in\mathcal{T}_h}\left(\|R_h^{NS}\|_{L^2(K)} + \frac{1}{2\sqrt{\lambda_{2,K}}}\|R_{h,j}^{NS}\|_{L^2(\partial K)}\right)\omega_K(\mathbf{U}-\mathbf{u}_h) \\ + \frac{C}{(1-\gamma)\mu_{\min}} L(\mathbf{u}_h)\left(\|\rho-\rho_h\|^2_{L^2(\Omega)} + \|\mu-\mu_h\|^2_{L^2(\Omega)}\right) \\ + \frac{\varepsilon}{2}\|P-p_h\|^2_{L^2(\Omega)} + \frac{1}{2\varepsilon}\|\operatorname{div}(\mathbf{u}_h)\|^2_{L^2(\Omega)}.\end{aligned}$$

Using (4.30), we therefore obtain

$$\begin{aligned}\frac{1-\gamma}{2}\mu_{\min}\|\nabla(\mathbf{U}-\mathbf{u}_h)\|^2_{L^2(\Omega)} \leq C\sum_{K\in\mathcal{T}_h}\left(\|R_h^{NS}\|_{L^2(K)} + \frac{1}{2\sqrt{\lambda_{2,K}}}\|R_{h,j}^{NS}\|_{L^2(\partial K)}\right)\omega_K(\mathbf{U}-\mathbf{u}_h) \\ + \frac{C}{(1-\gamma)\mu_{\min}} L(\mathbf{u}_h)\left(\|\rho-\rho_h\|^2_{L^2(\Omega)} + \|\mu-\mu_h\|^2_{L^2(\Omega)}\right) \\ + \frac{\varepsilon}{2}\tilde{C}\sum_{K\in\mathcal{T}_h}\left(\|R_h^{NS}\|_{L^2(K)} + \frac{1}{2\sqrt{\lambda_{2,K}}}\|R_{h,j}^{NS}\|_{L^2(\partial K)}\right)\omega_K(\mathbf{w}) \\ + \frac{\varepsilon}{2}\tilde{C}\frac{\mu^4_{\max}}{\mu^2_{\min}}\|\nabla(\mathbf{U}-\mathbf{u}_h)\|^2_{L^2(\Omega)} \\ + \frac{\varepsilon}{2}\tilde{C}\frac{\mu^2_{\max}}{\mu^2_{\min}} L(\mathbf{u}_h)\left(\|\rho-\rho_h\|^2_{L^2(\Omega)} + \|\mu-\mu_h\|^2_{L^2(\Omega)}\right) + \frac{1}{2\varepsilon}\|\operatorname{div}(\mathbf{u}_h)\|^2_{L^2(\Omega)}.\end{aligned}$$

Choosing

$$\varepsilon = \frac{1-\gamma}{2\tilde{C}}\frac{\mu^3_{\min}}{\mu^4_{\max}},$$

we obtain

$$\frac{1-\gamma}{4}\mu_{\min}\|\nabla(\mathbf{U}-\mathbf{u}_h)\|^2_{L^2(\Omega)} \leq C\sum_{K\in\mathcal{T}_h}\left(\|R_h^{NS}\|_{L^2(K)} + \frac{1}{2\sqrt{\lambda_{2,K}}}\|R_{h,j}^{NS}\|_{L^2(\partial K)}\right)\omega_K(\mathbf{U}-\mathbf{u}_h)$$
$$+\frac{C}{(1-\gamma)\mu_{\min}}L(\mathbf{u}_h)\left(\|\rho-\rho_h\|^2_{L^2(\Omega)} + \|\mu-\mu_h\|^2_{L^2(\Omega)}\right)$$
$$+\frac{1-\gamma}{4}\frac{\mu_{\min}^3}{\mu_{\max}^4}\sum_{K\in\mathcal{T}_h}\left(\|R_h^{NS}\|_{L^2(K)} + \frac{1}{2\sqrt{\lambda_{2,K}}}\|R_{h,j}^{NS}\|_{L^2(\partial K)}\right)\omega_K(\mathbf{w})$$
$$+\frac{1-\gamma}{4}\frac{\mu_{\min}}{\mu_{\max}^2}L(\mathbf{u}_h)\left(\|\rho-\rho_h\|^2_{L^2(\Omega)} + \|\mu-\mu_h\|^2_{L^2(\Omega)}\right)$$
$$+\frac{\tilde{C}}{1-\gamma}\frac{\mu_{\max}^4}{\mu_{\min}^3}\|\operatorname{div}(\mathbf{u}_h)\|^2_{L^2(\Omega)}.$$

So finally, dividing by $1-\gamma$ and putting in factor the biggest constant, we obtain for the velocity error

$$\mu_{\min}\|\nabla(\mathbf{U}-\mathbf{u}_h)\|^2_{L^2(\Omega)}$$
$$\leq \frac{C}{(1-\gamma)^2}\left(\sum_{K\in\mathcal{T}_h}\left(\|R_h^{NS}\|_{L^2(K)} + \frac{1}{2\sqrt{\lambda_{2,K}}}\|R_{h,j}^{NS}\|_{L^2(\partial K)}\right)\omega_K(\mathbf{U}-\mathbf{u}_h)\right.$$
$$\left.+\frac{\mu_{\min}^3}{\mu_{\max}^4}\sum_{K\in\mathcal{T}_h}\left(\|R_h^{NS}\|_{L^2(K)} + \frac{1}{2\sqrt{\lambda_{2,K}}}\|R_{h,j}^{NS}\|_{L^2(\partial K)}\right)\omega_K(\mathbf{w}) + \frac{\mu_{\max}^4}{\mu_{\min}^3}\|\operatorname{div}(\mathbf{u}_h)\|^2_{L^2(\Omega)}\right)$$
$$+\frac{C}{\mu_{\min}(1-\gamma)^2}L(\mathbf{u}_h)\left(\|\rho-\rho_h\|^2_{L^2(\Omega)} + \|\mu-\mu_h\|^2_{L^2(\Omega)}\right), \quad (4.31)$$

and we use the fact that

$$\frac{1}{\mu_{\max}} \leq \frac{1}{\mu_{\min}}$$

to write the terms involving the $L^\infty(\Omega\times(0,T))$ norm in compact form. Finally, plugging (4.31) into (4.30) yields finally that

$$\|P-p_h\|^2_{L^2(\Omega)} \leq \frac{C}{(1-\gamma)^2}\left(\sum_{K\in\mathcal{T}_h}\left(\|R_h^{NS}\|_{L^2(K)} + \frac{1}{2\sqrt{\lambda_{2,K}}}\|R_{h,j}^{NS}\|_{L^2(\partial K)}\right)\omega_K(\mathbf{w})\right.$$
$$+\frac{\mu_{\max}^4}{\mu_{\min}^3}\sum_{K\in\mathcal{T}_h}\left(\|R_h^{NS}\|_{L^2(K)} + \frac{1}{2\sqrt{\lambda_{2,K}}}\|R_{h,j}^{NS}\|_{L^2(\partial K)}\right)\omega_K(\mathbf{U}-\mathbf{u}_h)$$
$$\left.+\left(\frac{\mu_{\max}^4}{\mu_{\min}^3}\right)^2\|\operatorname{div}(\mathbf{u}_h)\|^2_{L^2(\Omega)}\right) + \frac{C}{(1-\gamma)^2}\frac{\mu_{\max}^6}{\mu_{\min}^6}L(\mathbf{u}_h)\left(\|\rho-\rho_h\|^2_{L^2(\Omega)} + \|\mu-\mu_h\|^2_{L^2(\Omega)}\right).$$

Dividing the pressure estimate by $\mu_{\max}^4/\mu_{\min}^3$ and summing it with (4.31), we obtain the desired estimate. $\square$

The last part consists to provide an estimate for the $L^2$ norms

$$\|\mathbf{U}-\mathbf{u}_h\|_{L^2(\Omega)} \quad \text{and} \quad \left\|\frac{\partial\mathbf{U}}{\partial t} - \frac{\partial\mathbf{u}_h}{\partial t}\right\|_{L^2(\Omega)}.$$

We will use a duality argument. Let $\mathbf{u}$ be the exact velocity field, $\rho, \mu$ the exact density and viscosity and $\mathbf{u}_h$ the finite elements approximation of $\mathbf{u}$. For any $t\in[0,T]$ and any

$\mathbf{g} \in (L^2(\Omega))^2$, we consider $(\mathbf{w}, r)$ the solution of the dual problem (that we write in a weak formulation)

$$\int_\Omega \rho(t)((\mathbf{u}(t)\cdot\nabla)\mathbf{v})\cdot\mathbf{w}(t)d\mathbf{x} + \int_\Omega \rho(t)((\mathbf{v}\cdot\nabla)\mathbf{u}_h(t))\cdot\mathbf{w}(t)d\mathbf{x} + \int_\Omega 2\mu(t)D(\mathbf{w}(t)) : D(\mathbf{v})d\mathbf{x}$$
$$- \int_\Omega r(t)\,\mathrm{div}\,\mathbf{v}d\mathbf{x} = \int_\Omega \mathbf{g}\cdot\mathbf{v}d\mathbf{x}, \quad \forall \mathbf{v} \in (H_0^1(\Omega))^2,$$
$$\int_\Omega q\,\mathrm{div}\,\mathbf{w}(t) = 0, \quad \forall q \in L_0^2(\Omega). \quad (4.32)$$

For understanding, we can write the previous problem in a strong form, thanks to an integration by parts :

$$\begin{cases} -\rho(\mathbf{u}\cdot\nabla)\mathbf{w} - (\mathbf{u}\cdot\nabla\rho)\mathbf{w} + \rho\nabla\mathbf{u}_h^T\cdot\mathbf{w} - \mathrm{div}(2\mu D(\mathbf{w})) + \nabla r = \mathbf{g}, & \text{in } \Omega \\ \mathrm{div}\,\mathbf{w} = 0, & \text{in } \Omega \\ \mathbf{w} = 0. & \text{on } \partial\Omega \end{cases}$$

Under the hypothesis (4.27), one can show that the weak problem (4.32) is well-posed in $(H_0^1(\Omega))^2 \times L_0^2(\Omega)$ and that the following a priori estimate holds for any $t \in [0,T]$

$$\mu_{\min}\|\nabla\mathbf{w}(t)\|_{L^2(\Omega)} + \frac{\mu_{\min}}{\mu_{\max}}\|r\|_{L^2(\Omega)} \leq \frac{C}{1-\gamma}\|\mathbf{g}\|_{L^2(\Omega)},$$

where $C > 0$ depends only on $\Omega$.

Moreover, noting that we can write the later equations as a Stokes problem

$$\begin{cases} -\mathrm{div}(2\mu D(\mathbf{w})) + \nabla r = \mathbf{g} + \rho(\mathbf{u}\cdot\nabla)\mathbf{w} + (\mathbf{u}\cdot\nabla\rho)\mathbf{w} - \rho\nabla\mathbf{u}_h^T\cdot\mathbf{w}, & \text{in } \Omega \\ \mathrm{div}\,\mathbf{w} = 0, & \text{in } \Omega \\ \mathbf{w} = 0. & \text{on } \partial\Omega \end{cases}$$

one can show that in fact $(\mathbf{w}(t), r(t)) \in (H^2(\Omega))^2 \times H^1(\Omega)$ for any $t \in [0,T]$ (we point out again the references [21, 62] for convex polygonal domains and [58, 99, 107] for smooth ones, see also the discussion for the case of constant $\mu$ and $\rho$ in Chapter 3, Proposition 3.47 and Theorem B.8 in the Appendix).

Moreover, if we assume that there exists a constant $C' > 0$ that may depend only on $\Omega$ such that

$$\frac{\|\nabla\mu\|_{L^\infty(\Omega\times(0,T))}}{\mu_{min}}, \frac{\|\nabla\rho\|_{L^\infty(\Omega\times(0,T))}}{\rho_{max}} \leq C' \quad (4.33)$$

then one can show the following $H^2 - H^1$ a priori estimate

$$\mu_{\min}\|\mathbf{w}(t)\|_{H^2(\Omega)} + \frac{\mu_{\min}}{\mu_{\max}}\|r(t)\|_{H^1(\Omega)} \leq \frac{C}{1-\gamma}\frac{\mu_{\max}}{\mu_{\min}}\|\mathbf{g}\|_{L^2(\Omega)},$$

where $C$ depends only on $\Omega$.

We will need also estimates for $\frac{\partial \mathbf{w}}{\partial t}, \frac{\partial r}{\partial t}$. Differentiating the weak formulation (4.32), and assuming moreover that there exists $h_0$ small enough such that for all $h \leq h_0$ (if necessary we reduce the $h_0$ of (4.27))

$$\frac{\left\|\frac{\partial\mu}{\partial t}\right\|_{L^\infty(\Omega\times(0,T))}}{\mu_{\min}} + \frac{\left\|\frac{\partial\rho}{\partial t}\right\|_{L^\infty(\Omega\times(0,T))}}{\rho_{\max}}$$
$$+ \frac{\rho_{\max}}{\mu_{\min}}\left(\sup_{t\in(0,T)}\left\|\nabla\frac{\partial\mathbf{u}}{\partial t}(t)\right\|_{L^2(\Omega)} + \sup_{t\in(0,T)}\left\|\nabla\frac{\partial\mathbf{u}_h}{\partial t}(t)\right\|_{L^2(\Omega)}\right) \leq C''(1-\gamma), \quad (4.34)$$

where $C''$ depends only on $\Omega$, one can prove that

$$\mu_{\min}\left\|\nabla\frac{\partial \mathbf{w}}{\partial t}(t)\right\|_{L^2(\Omega)}+\frac{\mu_{\min}}{\mu_{\max}}\left\|\frac{\partial r}{\partial t}(t)\right\|_{L^2(\Omega)}\leq\frac{C}{1-\gamma}\|\mathbf{g}\|_{L^2(\Omega)},$$

where $C>0$ depends only on $\Omega$.

Differentiating the strong form with respect to the time (let us assume that we satisfy all the necessary regularity requirements), we obtain that $\dfrac{\partial \mathbf{w}}{\partial t},\dfrac{\partial r}{\partial t}$ are solution of

$$\begin{aligned}
-\rho(\mathbf{u}\cdot\nabla)\frac{\partial \mathbf{w}}{\partial t}-(\mathbf{u}\cdot\nabla\rho)\frac{\partial \mathbf{w}}{\partial t}+\rho\nabla\mathbf{u}_h^T\cdot\frac{\partial \mathbf{w}}{\partial t}-\operatorname{div}\left(2\mu D\left(\frac{\partial \mathbf{w}}{\partial t}\right)\right)+\nabla\frac{\partial r}{\partial t}=\mathbf{g}\\
+\frac{\partial \rho}{\partial t}(\mathbf{u}\cdot\nabla)\mathbf{w}+\rho\left(\frac{\partial \mathbf{u}}{\partial t}\cdot\nabla\right)\mathbf{w}+\left(\frac{\partial \mathbf{u}}{\partial t}\cdot\nabla\rho\right)+\left(\mathbf{u}\cdot\nabla\frac{\partial \rho}{\partial t}\right)\mathbf{w}\\
-\frac{\partial \rho}{\partial t}\nabla\mathbf{u}_h^T\cdot\mathbf{w}-\rho\nabla\frac{\partial \mathbf{u}_h}{\partial t}^T\cdot\mathbf{w}+\operatorname{div}\left(2\frac{\partial \mu}{\partial t}D\left(\mathbf{w}\right)\right),
\end{aligned}$$

and $\dfrac{\partial \mathbf{w}}{\partial t}$ satisfies the free divergence constrain and the zero value boundary conditions. Finally if we assume

$$\frac{\left\|\nabla\frac{\partial \mu}{\partial t}\right\|_{L^\infty(\Omega\times(0,T))}}{\mu_{min}},\frac{\left\|\nabla\frac{\partial \rho}{\partial t}\right\|_{L^\infty(\Omega\times(0,T))}}{\rho_{max}}\leq C''' \tag{4.35}$$

where $C'''>0$ may depend only on $\Omega$, we also have the a priori estimate

$$\mu_{\min}\left\|\frac{\partial \mathbf{w}}{\partial t}(t)\right\|_{H^2(\Omega)}+\frac{\mu_{\min}}{\mu_{\max}}\left\|\frac{\partial r}{\partial t}(t)\right\|_{H^1(\Omega)}\leq\frac{C}{1-\gamma}\frac{\mu_{\max}}{\mu_{\min}}\|\mathbf{g}\|_{L^2(\Omega)},$$

where $C$ depends only on $\Omega$. For our needs, we will summarize all the a priori estimates as follows:

(i) Under the hypothesis (4.27) and (4.34), it holds

$$\begin{aligned}
\mu_{\min}\|\nabla\mathbf{w}(t)\|_{L^2(\Omega)}+\mu_{\min}\left\|\nabla\frac{\partial \mathbf{w}}{\partial t}(t)\right\|_{L^2(\Omega)}+\frac{\mu_{\min}}{\mu_{\max}}\|r(t)\|_{L^2(\Omega)}+\frac{\mu_{\min}}{\mu_{\max}}\left\|\frac{\partial r}{\partial t}(t)\right\|_{L^2(\Omega)}\\
\leq\frac{C}{1-\gamma}\frac{\mu_{\max}}{\mu_{\min}}\|\mathbf{g}\|_{L^2(\Omega)}.
\end{aligned} \tag{4.36}$$

(ii) Under the hypothesis (4.27), (4.33), (4.34) and (4.35), it holds

$$\begin{aligned}
\mu_{\min}\|\mathbf{w}(t)\|_{H^2(\Omega)}+\mu_{\min}\left\|\frac{\partial \mathbf{w}}{\partial t}(t)\right\|_{H^2(\Omega)}+\frac{\mu_{\min}}{\mu_{\max}}\|r(t)\|_{H^1(\Omega)}+\frac{\mu_{\min}}{\mu_{\max}}\left\|\frac{\partial r}{\partial t}(t)\right\|_{H^1(\Omega)}\\
\leq\frac{C}{1-\gamma}\frac{\mu_{\max}}{\mu_{\min}}\|\mathbf{g}\|_{L^2(\Omega)},
\end{aligned} \tag{4.37}$$

where $C>0$ depends on only $\Omega$.

We recall for the next proposition the notation we introduced before, namely where we use the same notation as before for the jump term across the edges

$$R_h^{NS}=\rho_h\mathbf{f}-\rho_h\frac{\partial \mathbf{u}_h}{\partial t}-\rho_h(\mathbf{u}_h\cdot\nabla)\mathbf{u}_h+\operatorname{div}(2\mu_h D(\mathbf{u}_h))-\nabla p_h$$

and

$$R_{h,j}^{NS}=\left[2\mu_h D(\mathbf{u}_h)\cdot\mathbf{n}\right].$$

**Proposition 4.10** (Higher order estimates for $\mathbf{U}-\mathbf{u}_h$).
*Under the hypothesis (4.27), (4.33), (4.34) and (4.35), there exists $C_1>0$ that is independent of the mesh size, but that may depend on the aspect ratio and $\Omega$ and $C_2>0$ that depends only on $\Omega$ such that for all $h\le h_0$ and all $t\in[0,T]$, we have*

$$\|(\mathbf{U}-\mathbf{u}_h)(t)\|^2_{L^2(\Omega)} \le \frac{C_1}{(1-\gamma)2}\sum_{K\in\mathcal{T}_h}(\epsilon^I_{K,1})^2(t) + \frac{C_2}{\mu^2_{\min}(1-\gamma)^2}L(\mathbf{u}_h)\left(\|(\rho-\rho_h)(t)\|^2_{L^2(\Omega)}+\|(\mu-\mu_h)(t)\|^2_{L^2(\Omega)}\right), \quad (4.38)$$

*where*

$$(\epsilon^I_{K,1})^2=\frac{\mu^2_{\max}}{\mu^4_{\min}}\left(h^4_K\|R^{NS}_h\|^2_{L^2(K)}+h^3_K\|R^{NS}_{h,j}\|^2_{L^2(\partial K)}+\mu^2_{\max}h^2_K\|\operatorname{div}\mathbf{u}_h\|^2_{L^2(K)}\right).$$

*and*

$$L(\mathbf{u}_h)=\left\|\mathbf{f}-\frac{\partial\mathbf{u}_h}{\partial t}-(\mathbf{u}_h\cdot\nabla)\mathbf{u}_h\right\|^2_{L^\infty(\Omega\times(0,T))}+\|D(\mathbf{u}_h)\|^2_{L^\infty(\Omega\times(0,T))}.$$

*Moreover, we also have*

$$\left\|\frac{\partial\mathbf{U}}{\partial t}(t)-\frac{\partial\mathbf{u}_h}{\partial t}(t)\right\|^2_{L^2(\Omega)}\le\frac{C_1}{(1-\gamma^2)}\sum_{K\in\mathcal{T}_h}(\epsilon^I_{K,1})^2(t)+(\epsilon^I_{K,2})^2(t) + \frac{C_2}{\mu^2_{\min}(1-\gamma)^2}\left(L(\mathbf{u}_h)+L\left(\frac{\partial\mathbf{u}_h}{\partial t}\right)\right)\left(\|(\rho-\rho_h)(t)\|^2_{L^2(\Omega)}+\|(\mu-\mu_h)(t)\|^2_{L^2(\Omega)}\right) + \frac{C_2}{\mu^2_{\min}(1-\gamma)^2}L^2_\infty((\nu^I_\rho)^2(t)+(\nu^I_\mu)^2(t)). \quad (4.39)$$

*where*

$$(\epsilon^I_{K,2})^2=\frac{\mu^2_{\max}}{\mu^4_{\min}}\left(h^4_K\left\|\frac{\partial}{\partial t}R^{NS}_h\right\|^2_{L^2(K)}+h^3_K\left\|\frac{\partial}{\partial t}R^{NS}_{h,j}\right\|^2_{L^2(\partial K)}+\mu^2_{\max}h^2_K\left\|\operatorname{div}\frac{\partial}{\partial t}\mathbf{u}_h\right\|^2_{L^2(K)} + \left(\alpha^2_K+\left(\frac{d\alpha_K}{dt}\right)^2\right)\left(\left\|R^{NS}_h\right\|^2_{L^2(K)}+\left\|\frac{\partial}{\partial t}R^{NS}_h\right\|^2_{L^2(K)}\right)\left(\|\rho_h\mathbf{u}_h\|^2_{L^\infty(K)}+\left\|\frac{\partial\rho_h\mathbf{u}_h}{\partial t}\right\|^2_{L^\infty(K)}+\mu^2_{\max}\right)\right),$$

$$L\left(\frac{\partial\mathbf{u}_h}{\partial t}\right)=\left\|\frac{\partial\mathbf{f}}{\partial t}-\frac{\partial^2\mathbf{u}_h}{\partial t^2}-\left(\frac{\partial\mathbf{u}_h}{\partial t}\cdot\nabla\right)\mathbf{u}_h-(\mathbf{u}_h\cdot\nabla)\frac{\partial\mathbf{u}_h}{\partial t}\right\|^2_{L^\infty(\Omega\times(0,T))}+\left\|D\left(\frac{\partial\mathbf{u}_h}{\partial t}\right)\right\|^2_{L^\infty(\Omega\times(0,T))}.$$

*and*

$$(\nu^I_\rho)^2=\left\|\frac{\partial\rho}{\partial t}-\frac{\partial\rho}{\partial t}\right\|^2_{L^2(\Omega)},\quad(\nu^I_\mu)^2=\left\|\frac{\partial\mu}{\partial t}-\frac{\partial\mu_h}{\partial t}\right\|^2_{L^2(\Omega)}.$$

**Remark 4.11.**
It will be checked numerically that

$$\left\|\frac{\partial\rho}{\partial t}-\frac{\partial\rho_h}{\partial t}\right\|^2_{L^2(\Omega)}\text{ and }\left\|\frac{\partial\mu}{\partial t}-\frac{\partial\mu_h}{\partial t}\right\|^2_{L^2(\Omega)},$$

are higher order terms (compared to $\|\nabla(\mathbf{u}-\mathbf{u}_h)\|^2_{L^2(\Omega)}$), namely being $O(h^3)$.

From a theoretical point of view, we were only able to bound them as follows:

$$\begin{aligned}\left\|\frac{\partial\rho}{\partial t}-\frac{\partial\rho_h}{\partial t}\right\|_{L^2(\Omega)}&=\left\|-\mathbf{u}\cdot\nabla\rho-\frac{\partial\rho_h}{\partial t}\right\|_{L^2(\Omega)}\le\left\|\frac{\partial\rho_h}{\partial t}+\mathbf{u}_h\cdot\nabla\rho_h\right\|_{L^2(\Omega)}+\|\mathbf{u}\cdot\nabla\rho-\mathbf{u}_h\cdot\nabla\rho_h\|_{L^2(\Omega)}\\&\le\left\|\frac{\partial\rho_h}{\partial t}+\mathbf{u}_h\cdot\nabla\rho_h\right\|_{L^2(\Omega)}+\|\nabla\rho_h\|_{L^\infty(\Omega)}\|\mathbf{u}-\mathbf{u}_h\|_{L^2(\Omega)}\\&\quad+\|\mathbf{u}_h\|_{L^\infty(\Omega)}\|\nabla(\rho-\rho_h)\|_{L^2(\Omega)}+\|\mathbf{u}-\mathbf{u}_h\|_{L^\infty(\Omega)}\|\nabla(\rho-\rho_h)\|_{L^2(\Omega)},\end{aligned}$$

and

$$\left\|\frac{\partial \mu}{\partial t}-\frac{\partial \mu_h}{\partial t}\right\|_{L^2(\Omega)} \\ \leq \left\|\frac{\partial \mu_h}{\partial t}+\mathbf{u}_h\cdot\nabla\mu_h\right\|_{L^2(\Omega)}+\|\nabla\mu_h\|_{L^\infty(\Omega)}\|\mathbf{u}-\mathbf{u}_h\|_{L^2(\Omega)} \\ +\|\mathbf{u}_h\|_{L^\infty(\Omega)}\|\nabla(\mu-\mu_h)\|_{L^2(\Omega)}+\|\mathbf{u}-\mathbf{u}_h\|_{L^\infty(\Omega)}\|\nabla(\mu-\mu_h)\|_{L^2(\Omega)}.$$

The last estimates are quite pessimistic since the two residuals (that will be checked in the numerical experiments)

$$\left\|\frac{\partial \rho_h}{\partial t}+\mathbf{u}_h\cdot\nabla\rho_h\right\|_{L^2(\Omega)},\quad \left\|\frac{\partial \mu_h}{\partial t}+\mathbf{u}_h\cdot\nabla\mu_h\right\|_{L^2(\Omega)}$$

and the gradient norms (that we should post-process to make them computable)

$$\|\nabla(\rho-\rho_h)\|_{L^2(\Omega)},\quad \|\nabla(\mu-\mu_h)\|_{L^2(\Omega)},$$

are only $O(h)$. At least, it guarantees that the final estimate for $\|\nabla(\mathbf{u}-\mathbf{u}_h)\|_{L^2(\Omega)}$ is $O(h)$, with no constant depending of the mesh aspect ratio multiplying the low order terms.

*Proof of Proposition 4.10.* In the lines below, we do not write the explicit dependence on the time of the function, in order to lighten the notation. Moreover, we denote by $C$ any constant that is independent of the mesh size, but may depends on the mesh aspect ratio or $\Omega$ and by $\tilde{C}$ constants that may depend only on $\Omega$.

*Part 1. Estimate for* $\|\mathbf{U}-\mathbf{u}_h\|_{L^2(\Omega)}$.

Let $t\in[0,T]$ and $\mathbf{g}$ be any $(L^2(\Omega))^2$ function. Let us consider $(\mathbf{w}(t), r(t)$ be the solution obtained by solving the dual problem (4.32) with $\mathbf{g}$ as right hand side. Taking the test function $\mathbf{v}=\mathbf{U}-\mathbf{u}_h$,$q=P-p_h$ we have therefore

$$\int_\Omega \mathbf{g}\cdot(\mathbf{U}-\mathbf{u}_h)d\mathbf{x}=\int_\Omega \rho((\mathbf{u}\cdot\nabla)(\mathbf{U}-\mathbf{u}_h))\cdot\mathbf{w}d\mathbf{x}+\int_\Omega\rho(((\mathbf{U}-\mathbf{u}_h)\cdot\nabla)\mathbf{u}_h)\cdot\mathbf{w}d\mathbf{x} \\ +\int_\Omega 2\mu D(\mathbf{w}):D(\mathbf{U}-\mathbf{u}_h)d\mathbf{x}-\int_\Omega r\operatorname{div}(\mathbf{U}-\mathbf{u}_h)d\mathbf{x}-\int_\Omega \operatorname{div}\mathbf{w}(P-p_h)d\mathbf{x}.$$

We now use the orthogonality (4.22) and (4.23) and we remove any test function $(\mathbf{v}_h, q_h)$. We get

$$\int_\Omega \mathbf{g}\cdot(\mathbf{U}-\mathbf{u}_h)d\mathbf{x}=\int_\Omega \rho((\mathbf{u}\cdot\nabla)(\mathbf{U}-\mathbf{u}_h))\cdot(\mathbf{w}-\mathbf{v}_h)d\mathbf{x}+\int_\Omega\rho(((\mathbf{U}-\mathbf{u}_h)\cdot\nabla)\mathbf{u}_h)\cdot(\mathbf{w}-\mathbf{v}_h)d\mathbf{x} \\ +\int_\Omega 2\mu D(\mathbf{w}-\mathbf{v}_h):D(\mathbf{U}-\mathbf{u}_h)d\mathbf{x}-\int_\Omega (r-q_h)\operatorname{div}(\mathbf{U}-\mathbf{u}_h)d\mathbf{x}-\int_\Omega \operatorname{div}(\mathbf{w}-\mathbf{v}_h)(P-p_h)d\mathbf{x} \\ +\int_\Omega(\rho-\rho_h)\mathbf{f}\cdot\mathbf{v}_h d\mathbf{x}-\int_\Omega(\rho-\rho_h)\frac{\partial\mathbf{u}_h}{\partial t}\cdot\mathbf{v}_h d\mathbf{x}-\int_\Omega(\rho-\rho_h)((\mathbf{u}_h\cdot\nabla)\mathbf{u}_h)\cdot\mathbf{v}_h d\mathbf{x} \\ -2\int_\Omega(\mu-\mu_h)D(\mathbf{u}_h):D(\mathbf{v}_h)d\mathbf{x}+\sum_K\alpha_K\int_K R_h^{NS}\cdot(\rho_h(\mathbf{u}_h\cdot\nabla)\mathbf{v}_h)d\mathbf{x} \\ +\sum_{K\in\mathcal{T}_h}\alpha_K\int_K R_h^{NS}\cdot\nabla q_h d\mathbf{x}.$$

Using the fact that $(\mathbf{U}, P)$ are the solutions of (4.18), we can write

$$\int_\Omega \mathbf{g}\cdot(\mathbf{U}-\mathbf{u}_h)d\mathbf{x} = \int_\Omega \rho\left(\mathbf{f}-\frac{\partial \mathbf{u}_h}{\partial t}\right)\cdot(\mathbf{w}-\mathbf{v}_h)d\mathbf{x} - \int_\Omega \rho((\mathbf{u}_h\cdot\nabla)\mathbf{u}_h)\cdot(\mathbf{w}-\mathbf{v}_h)d\mathbf{x}$$
$$- \int_\Omega 2\mu D(\mathbf{w}-\mathbf{v}_h) : D(\mathbf{u}_h)d\mathbf{x}$$
$$+ \int_\Omega (r-q_h)\operatorname{div}\mathbf{u}_h d\mathbf{x} + \int_\Omega \operatorname{div}(\mathbf{w}-\mathbf{v}_h)p_h d\mathbf{x} + \int_\Omega (\rho-\rho_h)\mathbf{f}\cdot\mathbf{v}_h d\mathbf{x}$$
$$- \int_\Omega (\rho-\rho_h)\frac{\partial \mathbf{u}_h}{\partial t}\cdot\mathbf{v}_h d\mathbf{x} - \int_\Omega (\rho-\rho_h)((\mathbf{u}_h\cdot\nabla)\mathbf{u}_h)\cdot\mathbf{v}_h d\mathbf{x} - 2\int_\Omega (\mu-\mu_h)D(\mathbf{u}_h) : D(\mathbf{v}_h)d\mathbf{x}$$
$$+ \sum_K \alpha_K \int_K R_h^{NS}\cdot(\rho_h(\mathbf{u}_h\cdot\nabla)\mathbf{v}_h)d\mathbf{x} + \sum_{K\in\mathcal{T}_h} \alpha_K \int_K R_h^{NS}\cdot\nabla q_h d\mathbf{x}.$$

Adding and subtracting the terms

$$\int_\Omega \rho_h\left(\mathbf{f}-\frac{\partial \mathbf{u}_h}{\partial t}\right)\cdot(\mathbf{w}-\mathbf{v}_h)d\mathbf{x}, \int_\Omega \rho_h((\mathbf{u}_h\cdot\nabla)\mathbf{u}_h)\cdot(\mathbf{w}-\mathbf{v}_h)d\mathbf{x}, \int_\Omega 2\mu_h D(\mathbf{w}-\mathbf{v}_h) : D(\mathbf{u}_h)d\mathbf{x},$$

one can finally write

$$\int_\Omega \mathbf{g}\cdot(\mathbf{U}-\mathbf{u}_h)d\mathbf{x} = \int_\Omega \rho_h\left(\mathbf{f}-\frac{\partial \mathbf{u}_h}{\partial t}\right)\cdot(\mathbf{w}-\mathbf{v}_h)d\mathbf{x} - \int_\Omega \rho_h((\mathbf{u}_h\cdot\nabla)\mathbf{u}_h)\cdot(\mathbf{w}-\mathbf{v}_h)d\mathbf{x}$$
$$- \int_\Omega 2\mu_h D(\mathbf{w}-\mathbf{v}_h) : D(\mathbf{u}_h)d\mathbf{x}$$
$$+ \int_\Omega (r-q_h)\operatorname{div}\mathbf{u}_h d\mathbf{x} + \int_\Omega \operatorname{div}(\mathbf{w}-\mathbf{v}_h)p_h d\mathbf{x} + \int_\Omega (\rho-\rho_h)\mathbf{f}\cdot\mathbf{w} d\mathbf{x}$$
$$- \int_\Omega (\rho-\rho_h)\frac{\partial \mathbf{u}_h}{\partial t}\cdot\mathbf{w} d\mathbf{x} - \int_\Omega (\rho-\rho_h)((\mathbf{u}_h\cdot\nabla)\mathbf{u}_h)\cdot\mathbf{w} d\mathbf{x} - 2\int_\Omega (\mu-\mu_h)D(\mathbf{u}_h) : D(\mathbf{w})d\mathbf{x}$$
$$+ \sum_K \alpha_K \int_K R_h^{NS}\cdot(\rho_h(\mathbf{u}_h\cdot\nabla)\mathbf{v}_h)d\mathbf{x} + \sum_{K\in\mathcal{T}_h} \alpha_K \int_K R_h^{NS}\cdot\nabla q_h d\mathbf{x}.$$

Integrating by parts on every triangles, we obtain

$$\int_\Omega \mathbf{g}\cdot(\mathbf{U}-\mathbf{u}_h)d\mathbf{x} = \sum_{K\in\mathcal{T}_h}\int_K R_h^{NS}\cdot(\mathbf{w}-\mathbf{v}_h)d\mathbf{x} + \frac{1}{2}\int_{\partial K} R_{h,j}^{NS}\cdot(\mathbf{w}-\mathbf{v}_h)d\mathbf{x} + \sum_{K\in\mathcal{T}_h}\int_K (r-q_h)\operatorname{div}\mathbf{u}_h d\mathbf{x}$$
$$+ \int_\Omega (\rho-\rho_h)\mathbf{f}\cdot\mathbf{w} d\mathbf{x} - \int_\Omega (\rho-\rho_h)\frac{\partial \mathbf{u}_h}{\partial t}\cdot\mathbf{w} d\mathbf{x} - \int_\Omega (\rho-\rho_h)((\mathbf{u}_h\cdot\nabla)\mathbf{u}_h)\cdot\mathbf{w} d\mathbf{x}$$
$$- 2\int_\Omega (\mu-\mu_h)D(\mathbf{u}_h) : D(\mathbf{w})d\mathbf{x}$$
$$+ \sum_K \alpha_K \int_K R_h^{NS}\cdot(\rho_h(\mathbf{u}_h\cdot\nabla)\mathbf{v}_h + \nabla q_h)d\mathbf{x}. \quad (4.40)$$

Now choosing $\mathbf{v}_h = r_h(\mathbf{w})$ and $q_h = R_h(r)$, using the Cauchy-Schwarz inequality, the classical isotropic interpolation error estimates and absorbing as before the stabilization terms into the residual part, we obtain

$$\begin{aligned}
&\int_\Omega \mathbf{g}\cdot(\mathbf{U}-\mathbf{u}_h)d\mathbf{x}\\
&\quad\le C\left(\sum_{K\in\mathcal{T}_h} h_K^4\|R_h^{NS}\|^2_{L^2(K)} + h_K^3\|R_{h,j}^{NS}\|^2_{L^2(\partial K)} + \mu_{\max}^2 h_K^2\|\operatorname{div}\mathbf{u}_h\|^2_{L^2(K)}\right)^{1/2}\\
&\qquad\qquad\left(\|\mathbf{w}\|_{H^2(\Omega)} + \frac{1}{\mu_{\max}}\|r\|_{H^1(\Omega)}\right)\\
&\quad + \tilde{C}\left(\left\|\mathbf{f}-\frac{\partial \mathbf{u}_h}{\partial t} - (\mathbf{u}_h\cdot\nabla)\mathbf{u}_h\right\|^2_{L^\infty(\Omega\times(0,T))} + \|D(\mathbf{u}_h)\|^2_{L^\infty(\Omega\times(0,T))}\right)^{1/2}\\
&\qquad\qquad\left(\|\rho-\rho_h\|^2_{L^2(\Omega)} + \|\mu-\mu_h\|^2_{L^2(\Omega)}\right)^{1/2}\|\nabla\mathbf{w}\|_{L^2(\Omega)}.
\end{aligned}$$

Finally using the a priori estimates (4.36) and (4.37), we obtain

$$\begin{aligned}
&\int_\Omega \mathbf{g}\cdot(\mathbf{U}-\mathbf{u}_h)d\mathbf{x}\\
&\le \frac{C}{1-\gamma}\left(\sum_{K\in\mathcal{T}_h} h_K^4\|R_h^{NS}\|^2_{L^2(K)} + h_K^3\|R_{h,j}^{NS}\|^2_{L^2(\partial K)} + h_K^2\|\operatorname{div}\mathbf{u}_h\|^2_{L^2(K)}\right)^{1/2}\frac{\mu_{\max}}{\mu_{\min}^2}\|\mathbf{g}\|_{L^2(\Omega)}\\
&\quad + \frac{\tilde{C}}{\mu_{\min}(1-\gamma)}\left(\left\|\mathbf{f}-\frac{\partial \mathbf{u}_h}{\partial t} - (\mathbf{u}_h\cdot\nabla)\mathbf{u}_h\right\|^2_{L^\infty(\Omega\times(0,T))} + \|D(\mathbf{u}_h)\|^2_{L^\infty(\Omega\times(0,T))}\right)^{1/2}\\
&\qquad\qquad\left(\|\rho-\rho_h\|^2_{L^2(\Omega)} + \|\mu-\mu_h\|^2_{L^2(\Omega)}\right)^{1/2}\|\mathbf{g}\|_{L^2(\Omega)}.
\end{aligned}$$

Dividing on both side by $\|\mathbf{g}\|_{L^2(\Omega)}$ and taking the supremum over all the non zero $L^2$ functions, we get

$$\begin{aligned}
&\|\mathbf{U}-\mathbf{u}_h\|_{L^2(\Omega)} = \sup\frac{\int_\Omega(\mathbf{U}-\mathbf{u}_h)\cdot\mathbf{g}d\mathbf{x}}{\|\mathbf{g}\|_{L^2(\Omega)}}\\
&\le \frac{C}{1-\gamma}\frac{\mu_{\max}}{\mu_{\min}^2}\left(\sum_{K\in\mathcal{T}_h} h_K^4\|R_h^{NS}\|^2_{L^2(K)} + h_K^3\|R_{h,j}^{NS}\|^2_{L^2(\partial K)} + \mu_{\max}^2 h_K^2\|\operatorname{div}\mathbf{u}_h\|^2_{L^2(K)}\right)^{1/2}\\
&\quad + \frac{\tilde{C}}{\mu_{\min}(1-\gamma)}\left(\left\|\mathbf{f}-\frac{\partial \mathbf{u}_h}{\partial t} - (\mathbf{u}_h\cdot\nabla)\mathbf{u}_h\right\|^2_{L^\infty(\Omega\times(0,T))} + \|D(\mathbf{u}_h)\|^2_{L^\infty(\Omega\times(0,T))}\right)^{1/2}\\
&\qquad\qquad\left(\|\rho-\rho_h\|^2_{L^2(\Omega)} + \|\mu-\mu_h\|^2_{L^2(\Omega)}\right)^{1/2}.
\end{aligned}$$

*Part 2. Estimate for* $\left\|\frac{\partial \mathbf{U}}{\partial t} - \frac{\partial \mathbf{u}_h}{\partial t}\right\|_{L^2(\Omega)}$.

Let $t\in[0,T]$ and $\mathbf{g}$ be any $(L^2(\Omega))^2$ function. We start from (4.40) and we choose $\mathbf{v}_h = r_h(\mathbf{w})$ and $q_h = R_h(r)$

$$\begin{aligned}
\int_\Omega \mathbf{g}\cdot(\mathbf{U}-\mathbf{u}_h)d\mathbf{x} &= \sum_{K\in\mathcal{T}_h}\int_K R_h^{NS}\cdot(\mathbf{w}-r_h(\mathbf{w}))d\mathbf{x} + \frac{1}{2}\int_{\partial K} R_{h,j}^{NS}\cdot(\mathbf{w}-r_h(\mathbf{w}))d\mathbf{x}\\
&\quad + \sum_{K\in\mathcal{T}_h}\int_K (r-R_h(r))\operatorname{div}\mathbf{u}_h d\mathbf{x}\\
&+ \int_\Omega(\rho-\rho_h)\mathbf{f}\cdot\mathbf{w}d\mathbf{x} - \int_\Omega(\rho-\rho_h)\frac{\partial\mathbf{u}_h}{\partial t}\cdot\mathbf{w}d\mathbf{x} - \int_\Omega(\rho-\rho_h)((\mathbf{u}_h\cdot\nabla)\mathbf{u}_h)\cdot\mathbf{w}d\mathbf{x}\\
&- 2\int_\Omega(\mu-\mu_h)D(\mathbf{u}_h):D(\mathbf{w})d\mathbf{x} + \sum_K\alpha_K\int_K R_h^{NS}\cdot(\rho_h(\mathbf{u}_h\cdot\nabla)r_h(\mathbf{w}) + \nabla R_h(r))d\mathbf{x}.
\end{aligned}$$

We now differentiate with respect to $t$ both side of the equation and using the fact the time derivative commutes with the interpolation operators, we obtain

$$
\begin{aligned}
&\int_\Omega \mathbf{g}\cdot \left(\frac{\partial \mathbf{U}}{\partial t} - \frac{\partial \mathbf{u}_h}{\partial t}\right) d\mathbf{x} \\
&\quad = \sum_{K\in\mathcal{T}_h} \int_K \frac{\partial}{\partial t} R_h^{NS} \cdot (\mathbf{w} - r_h(\mathbf{w})) d\mathbf{x} + \frac{1}{2}\int_{\partial K} \frac{\partial}{\partial t} R_{h,j}^{NS} \cdot (\mathbf{w} - r_h(\mathbf{w})) d\mathbf{x} \\
&\quad + \sum_{K\in\mathcal{T}_h} \int_K \operatorname{div} \frac{\partial \mathbf{u}_h}{\partial t} (r - R_h(r)) d\mathbf{x} \\
&\quad + \sum_{K\in\mathcal{T}_h} \int_K R_h^{NS} \cdot \left(\frac{\partial \mathbf{w}}{\partial t} - r_h\left(\frac{\partial \mathbf{w}}{\partial t}\right)\right) d\mathbf{x} + \frac{1}{2}\int_{\partial K} R_{h,j}^{NS} \cdot \left(\frac{\partial \mathbf{w}}{\partial t} - r_h\left(\frac{\partial \mathbf{w}}{\partial t}\right)\right) d\mathbf{x} \\
&\quad + \sum_{K\in\mathcal{T}_h} \int_K \operatorname{div} \mathbf{u}_h \left(\frac{\partial r}{\partial t} - R_h\left(\frac{\partial r}{\partial t}\right)\right) d\mathbf{x} \\
&\quad + \int_\Omega (\rho - \rho_h) \left(\frac{\partial \mathbf{f}}{\partial t} - \frac{\partial^2 \mathbf{u}_h}{\partial t^2} - \left(\frac{\partial \mathbf{u}_h}{\partial t}\cdot\nabla\right)\mathbf{u}_h - (\mathbf{u}_h\cdot\nabla)\frac{\partial \mathbf{u}_h}{\partial t}\right)\cdot \mathbf{w} d\mathbf{x} \\
&\quad + \int_\Omega (\rho - \rho_h) \left(\mathbf{f} - \frac{\partial \mathbf{u}_h}{\partial t} - (\mathbf{u}_h\cdot\nabla)\mathbf{u}_h\right)\cdot \frac{\partial \mathbf{w}}{\partial t} d\mathbf{x} \\
&\quad - 2\int_\Omega (\mu - \mu_h) D\left(\frac{\partial \mathbf{u}_h}{\partial t}\right) : D(\mathbf{w}) d\mathbf{x} - 2\int_\Omega (\mu - \mu_h) D(\mathbf{u}_h) : D\left(\frac{\partial \mathbf{w}}{\partial t}\right) d\mathbf{x} \\
&\quad + \int_\Omega \left(\frac{\partial \rho}{\partial t} - \frac{\partial \rho_h}{\partial t}\right)\left(\mathbf{f} - \frac{\partial \mathbf{u}_h}{\partial t} - (\mathbf{u}_h\cdot\nabla)\mathbf{u}_h\right)\cdot \mathbf{w} d\mathbf{x} - 2\int_\Omega \left(\frac{\partial \mu}{\partial t} - \frac{\partial \mu_h}{\partial t}\right) D(\mathbf{u}_h) : D(\mathbf{w}) d\mathbf{x} \\
&\quad + \sum_{K\in\mathcal{T}_h} \frac{d\alpha_K}{dt} \int_K R_h^{NS} \cdot ((\rho_h \mathbf{u}_h\cdot\nabla) r_h(\mathbf{w}) + \nabla R_h(r)) d\mathbf{x} \\
&\quad + \sum_{K\in\mathcal{T}_h} \alpha_K \int_K \frac{\partial}{\partial t} R_h^{NS} \cdot ((\rho_h \mathbf{u}_h\cdot\nabla) r_h(\mathbf{w}) + \nabla R_h(r)) d\mathbf{x} \\
&\quad + \sum_{K\in\mathcal{T}_h} \alpha_K \int_K R_h^{NS} \cdot \left(\left(\frac{\partial \rho_h \mathbf{u}_h}{\partial t}\right)\cdot\nabla) r_h(\mathbf{w}) + (\rho_h \mathbf{u}_h\cdot\nabla) r_h\left(\frac{\partial \mathbf{w}}{\partial t}\right) + \nabla R_h\left(\frac{\partial r}{\partial t}\right)\right) d\mathbf{x}.
\end{aligned}
$$

Using the Cauchy-Schwarz inequality and the isotropic interpolation error estimates yields

$$
\begin{aligned}
&\int_\Omega \mathbf{g}\cdot\left(\frac{\partial \mathbf{U}}{\partial t}-\frac{\partial \mathbf{u}_h}{\partial t}\right)d\mathbf{x}\\
&\leq C\left(\sum_{K\in\mathcal{T}_h} h_K^4\left\|R_h^{NS}\right\|_{L^2(K)}^2 + h_K^4\left\|\frac{\partial}{\partial t}R_h^{NS}\right\|_{L^2(K)}^2 + h_K^3\left\|R_{h,j}^{NS}\right\|_{L^2(\partial K)}^2 + h_K^3\left\|\frac{\partial}{\partial t}R_{h,j}^{NS}\right\|_{L^2(\partial K)}^2\right.\\
&\quad\left. +\mu_{\max}^2 h_K^2\|\operatorname{div}\mathbf{u}_h\|_{L^2(K)}^2 + \mu_{\max}^2 h_K^2\left\|\operatorname{div}\frac{\partial}{\partial t}\mathbf{u}_h\right\|_{L^2(K)}^2\right)^{1/2}\\
&\quad\left(\|\mathbf{w}\|_{H^2(\Omega)} + \left\|\frac{\partial \mathbf{w}}{\partial t}\right\|_{H^2(\Omega)} + \frac{1}{\mu_{\max}}\|r\|_{H^1(\Omega)} + \frac{1}{\mu_{\max}}\left\|\frac{\partial r}{\partial t}\right\|_{H^1(\Omega)}\right)\\
&+C\left(\sum_{K\in\mathcal{T}_h}\left(\alpha_K^2+\left(\frac{d\alpha_K}{dt}\right)^2\right)\left(\left\|R_h^{NS}\right\|_{L^2(K)}^2 + \left\|\frac{\partial}{\partial t}R_h^{NS}\right\|_{L^2(K)}^2\right)\right.\\
&\quad\left.\left(\|\rho_h\mathbf{u}_h\|_{L^\infty(K)}^2 + \left\|\frac{\partial \rho_h\mathbf{u}_h}{\partial t}\right\|_{L^\infty(K)}^2 + \mu_{\max}^2\right)\right)^{1/2}\\
&\quad\left(\|\mathbf{w}\|_{H^2(\Omega)} + \left\|\frac{\partial \mathbf{w}}{\partial t}\right\|_{H^2(\Omega)} + \frac{1}{\mu_{\max}}\|r\|_{H^1(\Omega)} + \frac{1}{\mu_{\max}}\left\|\frac{\partial r}{\partial t}\right\|_{H^1(\Omega)}\right)\\
&+\tilde{C}\left(L(\mathbf{u}_h)+L\left(\frac{\partial \mathbf{u}_h}{\partial t}\right)\right)^{1/2}\\
&\quad\left(\|\rho-\rho_h\|_{L^2(\Omega)}^2 + \|\mu-\mu_h\|_{L^2(\Omega)}^2\right)^{1/2}\left(\|\nabla\mathbf{w}\|_{L^2(\Omega)} + \left\|\nabla\frac{\partial \mathbf{w}}{\partial t}\right\|_{L^2(\Omega)}\right)\\
&+\tilde{C}L(\mathbf{u}_h)^{1/2}\\
&\quad\left(\left\|\frac{\partial \rho}{\partial t}-\frac{\partial \rho_h}{\partial t}\right\|_{L^2(\Omega)}^2 + \left\|\frac{\partial \mu}{\partial t}-\frac{\partial \mu_h}{\partial t}\right\|_{L^2(\Omega)}^2\right)^{1/2}\|\nabla\mathbf{w}\|_{L^2(\Omega)}.
\end{aligned}
$$

We then conclude as in Part 1 by using the a priori estimates (4.36) and (4.37). □

We are now in position to prove a final estimate for the velocity error $\|\nabla(\mathbf{u}-\mathbf{u}_h)\|_{L^2(\Omega)}$.

**Proposition 4.12** (A posteriori error estimate for $\nabla(\mathbf{u}-\mathbf{u}_h)$)**.**
*Under the same assumption as Proposition 4.10, there exists a constant $C_1 > 0$ that depends only on $\Omega$ and the reference triangle, a constant $C_2 > 0$ that depends only on $\Omega$ and a constant $C_3 > 0$ that is independent of the mesh size, but may depend on the mesh*

*aspect ratio and $\Omega$ such that for all $h \leq h_0$ and all $t \in (0,T]$ we have*

$$
\begin{aligned}
\rho_{\min}\|(\mathbf{u}-\mathbf{u}_h)(t)\|^2_{L^2(\Omega)} &+ \mu_{\min}\int_0^t \|\nabla(\mathbf{u}-\mathbf{u}_h)(s)\|^2_{L^2(\Omega)}ds \\
&\leq \frac{C_1}{(1-\gamma)^2}\int_0^t \sum_{K\in\mathcal{T}_h} (\eta^A_{K,\mathbf{u}})^2(s) + (\eta^A_{K,p})^2(s) + (\eta^{\mathrm{div}}_K)^2(s)ds \\
&\quad + \frac{C_2\rho^2_{\max}L(\mathbf{u}_h)}{\mu^2_{\min}(1-\gamma)^4}\int_0^t (\nu^I_\rho)^2(s) + (\nu^I_\mu)^2(s)ds \\
&+ \frac{C_2L(\mathbf{u}_h)}{\mu^2_{\min}(1-\gamma)^2}\left(\|(\rho-\rho_h)(t)\|^2_{L^2(\Omega)} + \|(\mu-\mu_h)(t)\|^2_{L^2(\Omega)}\right) \\
+ C_2\frac{\mu^2_{\max}+\rho^2_{\max}}{\mu^3_{\min}(1-\gamma)^4}&\left(L(\mathbf{u}_h) + L\left(\frac{\partial \mathbf{u}_h}{\partial t}\right)\right)\int_0^t \|(\rho-\rho_h)(s)\|^2_{L^2(\Omega)} + \|(\mu-\mu_h)(s)\|^2_{L^2(\Omega)}ds \\
&+ \frac{C_2\rho_{\max}L(\mathbf{u}_h)}{\mu^2_{\min}(1-\gamma)^4}\left(\|(\rho-\rho_h)(0)\|^2_{L^2(\Omega)} + \|(\mu-\mu_h)(0)\|^2_{L^2(\Omega)}\right) \\
&+ \frac{\rho_{\max}}{(1-\gamma)^4}\|(\mathbf{u}-\mathbf{u}_h)(0)\|^2_{L^2(\Omega)} + \frac{C_3\rho_{\max}}{(1-\gamma)^4}\sum_{K\in\mathcal{T}_h}(\epsilon^I_{K,1})^2(0) + (\epsilon^I_{K,1})^2(t) \\
&\qquad + \frac{C_3\rho^2_{\max}}{\mu_{\min}(1-\gamma)^4}\int_0^t \sum_{K\in\mathcal{T}_h}(\epsilon^I_{K,1})^2(s) + (\epsilon^I_{K,2})^2(s)ds. \quad (4.41)
\end{aligned}
$$

*The error indicators $\eta^A_{K,\mathbf{u}}, \eta^2_{K,p}, \eta^{\mathrm{div}}_K$ are given by Proposition 4.8 and the quantities $L(\mathbf{u}_h)$, $L\left(\frac{\partial \mathbf{u}_h}{\partial t}\right)$ and $\nu^I_\rho, \nu^I_\mu, \epsilon^I_{K,1}$ and $\epsilon^I_{K,2}$ by Proposition 4.10.*

*Proof.* The proof is straightforward by splitting the error $\mathbf{u}-\mathbf{u}_h$ into $\mathbf{u}-\mathbf{U}$ and $\mathbf{U}-\mathbf{u}_h$ and using Propositions 4.7, 4.8 and 4.10. □

**Remark 4.13.** (i) Up to some higher order terms that are composed by the last five lines of the right hand side of (4.41) the a posteriori estimate above is optimal, namely giving an $O(h)$ a posteriori error estimate of the error $\int_0^t \|\nabla(\mathbf{u}-\mathbf{u}_h)(s)\|^2_{L^2(\Omega)}ds$, that is the result we were expected since we use linear finite elements. We recall that (see Propositon 4.20) that for the errors $\|\rho-\rho_h(t)\|_{L^2(\Omega)}$ and $\|\mu-\mu_h(t)\|_{L^2(\Omega)}$, we were able to prove $O(h^{3/2})$ a posteriori error estimates.

(ii) We prove everything under the three assumptions (4.33), (4.34) and (4.35) that come from Proposition 4.10. In fact, we could have proven an estimate without these assumptions, but additional constants that may depend on the exact and approximated solutions (in particular derivatives of $\rho$ and $\mu$) will appear in the estimation. Since they will only multiply higher order terms, this is not an issue in itself, but we work under the above assumptions to be able to write the a posteriori bound in a more "compact" form.

**Final a posteriori error estimate**

In the next Theorem, we summarize and combine the two a posteriori error estimates of Proposition 4.20 for the transport equations and of Proposition 4.12 for the momentum equations.

**Theorem 4.14** (A posteriori error estimate for the complete Navier-Stokes/transport problem)**.**

*Let $C_\infty$ be given by*

$$C_\infty = L(\mathbf{u}_h) + L\left(\frac{\partial \mathbf{u}_h}{\partial t}\right) + L(\rho_h) + L(\mu_h),$$

*where*

$$L(\mathbf{u}_h) = \left\| \mathbf{f} - \frac{\partial \mathbf{u}_h}{\partial t} - (\mathbf{u}_h \cdot \nabla)\mathbf{u}_h \right\|^2_{L^\infty(\Omega\times(0,T))} + \|D(\mathbf{u}_h)\|^2_{L^\infty(\Omega\times(0,T))},$$

$$L\left(\frac{\partial \mathbf{u}_h}{\partial t}\right) = \left\| \frac{\partial \mathbf{f}}{\partial t} - \frac{\partial^2 \mathbf{u}_h}{\partial t^2} - \left(\frac{\partial \mathbf{u}_h}{\partial t} \cdot \nabla\right)\mathbf{u}_h - (\mathbf{u}_h \cdot \nabla)\frac{\partial \mathbf{u}_h}{\partial t} \right\|^2_{L^\infty(\Omega\times(0,T))} + \left\| D\left(\frac{\partial \mathbf{u}_h}{\partial t}\right)\right\|^2_{L^\infty(\Omega\times(0,T))},$$

*and*

$$L(\rho_h) = \|\nabla \rho_h\|^2_{L^\infty(\Omega\times(0,T))}, \quad L(\mu_h) = \|\nabla \mu_h\|^2_{L^\infty(\Omega\times(0,T))}.$$

*Under the hypothesis (4.27), (4.33), (4.34) and (4.35), there exists three constant $C_1, C_2$ and $C_3$ such that for all $h \leq h_0$ and all $t \in (0,T]$*

$$\begin{aligned}
&\rho_{\min}\|(\mathbf{u}-\mathbf{u}_h)(t)\|^2_{L^2(\Omega)} + \mu_{\min}\int_0^t \|\nabla(\mathbf{u}-\mathbf{u}_h)(s)\|^2_{L^2(\Omega)}ds \\
&\qquad + \|(\rho-\rho_h)(t)\|^2_{L^2(\Omega)} + \|(\mu-\mu_h)(t)\|^2_{L^2(\Omega)} \\
&\leq C_1\left(\int_0^t \sum_{K\in\mathcal{T}_h} (\eta^A_{K,\mathbf{u}})^2(s) + (\eta^A_{K,p})^2(s) + (\eta^{\mathrm{div}}_K)^2(s) + (\eta^A_{K,\rho})^2(s) + (\eta^A_{K,\mu})^2(s)ds\right) \\
&\qquad + C_2\int_0^t (\nu^I_\rho)^2(s) + (\nu^I_\mu)^2(s)ds \\
&\quad + C_3\Big(\|(\mathbf{u}-\mathbf{u}_h)(0)\|^2_{L^2(\Omega)} + \|(\rho-\rho_h)(0)\|^2_{L^2(\Omega)} + \|(\mu-\mu_h)(0)\|^2_{L^2(\Omega)} \\
&\qquad + \sum_{K\in\mathcal{T}_h}(\epsilon^I_{K,1})^2(0) + (\epsilon^I_{K,1})^2(t) + \int_0^t \sum_{K\in\mathcal{T}_h}(\epsilon^I_{K,1})^2(s) + (\epsilon^I_{K,2})^2(s)ds\Big). \qquad (4.42)
\end{aligned}$$

*The constant $C_1$ depends only on the reference triangle, $\Omega, T$, $\mu_{\max}, \mu_{\min}, \rho_{\max}, (1-\gamma)^{-1}$ and the constant $C_\infty$. The constant $C_2$ is independent of the mesh size or aspect ratio, but may depend on $\Omega, T, \rho_{\max}, \mu_{\max}, \mu_{\min}, (1-\gamma)^{-1}$ and the constant $C_\infty$. Finally the constant $C_3$ is independent of the mesh size but may depend on the aspect ratio and depends $\Omega, T, \rho_{\max}, \mu_{\max}, \mu_{\min}, (1-\gamma)^{-1}$ and the constant $C_\infty$.*

*The error indicators $\eta^A_{K,\mathbf{u}}, \eta^2_{K,p}, \eta^{\mathrm{div}}_K$ are given by Proposition 4.8, the higher order quantities $\nu^I_\rho, \nu^I_\mu, \epsilon^I_{K,1}$ and $\epsilon^I_{K,2}$ by Proposition 4.10. The error indicators $\eta^A_{K,\rho}$ and $\eta^2_{K,\mu}$ are given by Proposition 4.2.*

*Proof.* The proof is straightforward and consists to sum up the estimates of Proposition 4.2 and 4.12, and then use the Gronwall's Lemma (in its integral form) to conclude. □

**Remark 4.15.** (i) Up to change for the 3D anisotropic framework, the a posteriori error estimate (4.42) can be derived for $\Omega \in \mathbb{R}^3$. As for the case of the Navier-Stokes equations with constant viscosity and density, the main change is to prove the dual estimates (4.36) and (4.37) for $\Omega \in \mathbb{R}^3$, that hold only in smooth domains or for particular convex polygons.

(ii) As already commented several times, this type of a posteriori error estimate is not standard since it involves, in particular, the exact solutions $\mathbf{u}, \rho$ and $\mu$ in the error indicators $\eta^A_{K,\mathbf{u}}, \eta^A_{K,\rho}, \eta^A_{K,\mu}, \nu^I_\rho, \nu^I_\mu$ and the solution of the dual problem (4.26) in $\eta^A_{K,p}$. In practice, we do not consider $\eta^A_{K,p}$ and we use the ZZ post-processing to make $\eta^A_{K,\mathbf{u}}, \eta^A_{K,\rho}, \eta^A_{K,\mu}$ computable.

## 4.3 A posteriori error estimate for the time discretization

We now present the time discretization of the system of equations (4.6)-(4.7). The numerical method is a combination of the schemes we use to solve independently the transport and the Navier-Stokes equations, namely the Crank-Nicolson method and the multistep BDF2 method.

Let $N$ be an integer and $0 = t^0 < t^1 < t^2 < ... < t^N = T$ a partition of the interval $[0,T]$. We still denote by $\tau^{n+1} = t^{n+1} - t^n$ the current time step and by $\tau = \max_{n=0,1,...,N-1} \tau^{n+1}$ the maximal time step. The numerical approximation reads : starting from $\varphi^0 = \varphi_0$ and $\mathbf{u}^0 = \mathbf{u}_0$, we are looking for every $n = 0, 1, 2, .., N-1$ for $(\mathbf{u}^{n+1}, p^{n+1}) \in (H_0^1(\Omega))^2 \times L_0^2(\Omega)$ and $\varphi^{n+1} \in H^1(\Omega)$ the solution of

$$\int_\Omega \rho^{n+1} \left( \frac{\mathbf{u}^{n+1} - \mathbf{u}^n}{\tau^{n+1}} + \frac{\beta^{n+1}\tau^{n+1}}{2} \partial^2 \mathbf{u}^{n+1} \right) \cdot \mathbf{v} d\mathbf{x} + \int_\Omega \rho^{n+1}((\mathbf{u}^{n+1} \cdot \nabla)\mathbf{u}^{n+1}) \cdot \mathbf{v} d\mathbf{x}$$
$$+ \int_\Omega 2\mu^{n+1} D(\mathbf{u}^{n+1}) : D(\mathbf{v}) d\mathbf{x} - \int_\Omega p^{n+1} \operatorname{div} \mathbf{v} d\mathbf{x} = \int_\Omega \rho^{n+1} \mathbf{f}^{n+1} \cdot \mathbf{v} d\mathbf{x}, \quad \forall \mathbf{v} \in (H_0^1(\Omega))^2,$$
$$- \int_\Omega q \operatorname{div} \mathbf{u}^{n+1} d\mathbf{x} = 0, \quad \forall q \in L_0^2(\Omega), \quad (4.43)$$

$$\int_\Omega \left( \frac{\varphi^{n+1} - \varphi^n}{\tau^{n+1}} + \mathbf{u}^{n+1/2} \cdot \nabla \varphi^{n+1/2} \right) \psi = 0, \forall \psi \in L^2(\Omega), \quad (4.44)$$

where for every $n = 0, 1, 2, ...N$

$$\rho^n = \rho_1 \varphi^n + (1 - \varphi^n)\rho_2, \quad \mu^n = \mu_1 \varphi^n + (1 - \varphi^n)\mu_2. \quad (4.45)$$

We recall that for every $n = 0, 1, 2, ...N - 1$

$$\partial^2 \mathbf{u}^{n+1} = \frac{\frac{\mathbf{u}^{n+1} - \mathbf{u}^n}{\tau^{n+1}} - \frac{\mathbf{u}^n - \mathbf{u}^{n-1}}{\tau^n}}{\tau^{n+1} + \tau^n/2}, \quad \mathbf{f}^{n+1} = \mathbf{f}(t^{n+1}),$$

and $\beta^{n+1}$ is given by

$$\beta^{n+1} = 1, n > 0, \quad \beta^1 = 0.$$

The goal is now to reproduce what we did in Chapter 2 and 3, and prove an a posteriori error estimates of order 2 for the errors

$$\int_0^t \|\nabla(\mathbf{u} - \mathbf{u}_\tau)(s)\|^2_{L^2(\Omega)} ds, \|(\rho - \rho_\tau)(t)\|^2_{L^2(\Omega)}, \|(\mu - \mu_\tau)(t)\|^2_{L^2(\Omega)},$$

where $\mathbf{u}_\tau, \rho_\tau, \mu_\tau$ will be appropriate piecewise reconstruction of the numerical solutions. The strategy to derive a temporal a posteriori error estimate is still the same and is summarized below:

(i) We define piecewise reconstructions of the discrete solutions (here piecewise quadratic in order to achieve the order 2).

(ii) We plug these reconstructions into the corresponding PDEs and we derive local time error indicators (Propositions 4.16 and 4.17 for the velocity and Proposition 4.18 for the density and viscosity).

(iii) Since we want an error bound for the sum of the numerical errors, we first prove preliminary upper bounds for each error individually (Proposition 4.19 for the velocity and Proposition 4.20 for the transported quantities).

(iv) We combine the last two propositions to obtain the final a posteriori error estimate (Theorem 4.21).

We recall here the notations and the piecewise numerical reconstruction we use. For any (scalar or vector value) discrete quantity $(v^n)_{n=0}^N$, we note

$$v^{n+1/2} = \frac{v^{n+1} + v^n}{2}, \partial v^{n+1} = \frac{v^{n+1} - v^n}{\tau^{n+1}}, n \geq 0, \quad \partial^2 v^{n+1} = \frac{\partial v^{n+1} - \partial v^n}{\tau^{n+1} + \tau^n / 2}, \geq 1$$

and

$$\tilde{\partial}^3 v^{n+1} = \frac{\partial^2 v^{n+1} - \partial^2 v^n}{\tau^{n+1}}, n \geq 2, \quad \tilde{\partial}^3 v^1 = \partial^2 v^1.$$

The piecewise *constant* reconstruction $v_{\tau,0}$ of the sets $(v^n)_{n=0}^N$ reads

$$v_{\tau,0}(t) = v^{n+1}, t \in [t^n, t^{n+1}], n = 0, 1, 2, ..., N-1.$$

The piecewise *linear* reconstruction $v_{\tau,1}$ is given by

$$v_{\tau,1}(t) = v^{n+1} + (t - t^{n+1})\partial v^{n+1}, t \in [t^n, t^{n+1}], n = 0, 1, 2, ..., N-1.$$

Note that we will use also the following *midpoint formulation* of $v_\tau$ (that is completely equal to the previous one)

$$v_{\tau,1}(t) = v^{n+1/2} + (t - t^{n+1/2})\partial v^{n+1}.$$

In case of a piecewise *quadratic* reconstruction, $v_{\tau,2}$ is given by

$$v_{\tau,2}(t) = v^{n+1} + (t - t^{n+1})\partial v^{n+1} + \frac{1}{2}(t - t^n)(t - t^{n+1})\partial^2 v^{n+1}, t \in [t^n, t^{n+1}], n = 1, 2, ..., N-1.$$

Observe that the linear part of the previous reconstruction can also be written with respect to the middle of $[t^n, t^{n+1}]$ yielding to the following definition of the quadratic reconstruction

$$v_{\tau,2}(t) = v^{n+1/2} + (t - t^{n+1/2})\partial v^{n+1} + \frac{1}{2}(t - t^n)(t - t^{n+1})\partial^2 v^{n+1}.$$

We now derive the local time error indicators by plugging the numerical reconstructions into the equations. This is done in the next three propositions. The proofs are technically painful, and we encourage the reader to come back to the computations later on and to focus first on the derivation of the error estimates presented in Propositions 4.19 and 4.20, and their associations in Theorem 4.21.

Since the first step of the numerical method (4.43) consists to solve an Euler step for the Navier-Stokes equations, we prove here below the generic error indicator corresponding to Backward Euler discretization of the momentum equation. Then for our particular method, this indicator will be used for $n = 0$ only.

**Proposition 4.16** (Time error indicator for the momentum equation and the BDF1 method)**.**
*Let us consider the Backward Euler discretization of the momentum equation: for any* $n = 0, 1, 2, 3, ..., N-1$*, starting from* $\mathbf{u}^0 = \mathbf{u}_0$*, we look for* $(\mathbf{u}^{n+1}, p^{n+1})$ *the solution of*

$$\begin{aligned} \rho^{n+1}\partial\mathbf{u}^{n+1} + \rho^{n+1}(\mathbf{u}^{n+1} \cdot \nabla)\mathbf{u}^{n+1} + 2\mu^{n+1}D(\mathbf{u}^{n+1}) - p^{n+1} = \rho^{n+1}\mathbf{f}^{n+1}, \\ \operatorname{div} \mathbf{u}^{n+1} = 0. \end{aligned} \tag{4.46}$$

*Let* $\mathbf{u}_\tau, \rho_\tau, \mu_\tau$ *and* $p_\tau$ *be the piecewise reconstruction given by, for* $t \in [t^n, t^{n+1}], n = 0, 1, 2, ..., N-1$

$$\begin{gathered} \mathbf{u}_\tau = \mathbf{u}_{\tau,1} = \mathbf{u}^{n+1} + (t - t^{n+1})\partial\mathbf{u}^{n+1}, \quad p_\tau = p_{\tau,0} = p^{n+1}, \\ \rho_\tau = \rho_{\tau,1} = \rho^{n+1} + (t - t^{n+1})\partial\rho^{n+1}, \quad \mu_\tau = \mu_{\tau,1} = \mu^{n+1} + (t - t^{n+1})\partial\mu^{n+1}. \end{gathered}$$

*Then, for every $n = 0, 1, 2, ..., N-1$ and any $t \in (t^n, t^{n+1})$, we have*

$$\int_\Omega \rho_\tau \frac{\partial \mathbf{u}_\tau}{\partial t} \cdot \mathbf{v} d\mathbf{x} + \int_\Omega \rho_\tau ((\mathbf{u}_\tau \cdot \nabla)\mathbf{u}_\tau) \cdot \mathbf{v} d\mathbf{x}$$
$$+ \int_\Omega 2\mu_\tau D(\mathbf{u}_\tau) : D(\mathbf{v}) d\mathbf{x} - \int_\Omega p_\tau \operatorname{div}(\mathbf{v})$$
$$= \int_\Omega \rho_\tau \mathbf{f} \cdot \mathbf{v} d\mathbf{x} + \int_\Omega \theta_{\mathbf{u},1}^{n+1} \cdot \mathbf{v} d\mathbf{x} + \int_\Omega \theta_{\mathbf{u},2}^{n+1} : D(\mathbf{v}) d\mathbf{x} + \int_\Omega \epsilon_{\mathbf{u},1}^{n+1} \cdot \mathbf{v} d\mathbf{x} + \int_\Omega \epsilon_{\mathbf{u},2}^{n+1} : D(\mathbf{v}) d\mathbf{x}, \forall \mathbf{v} \in (H_0^1(\Omega))^2,$$

*where*

$$\theta_{\mathbf{u},1}^{n+1} = (t - t^{n+1}) \left( \partial\rho^{n+1} (\mathbf{u}^{n+1} \cdot \nabla) \mathbf{u}^{n+1} + \rho^{n+1} (\partial \mathbf{u}^{n+1} \cdot \nabla) \mathbf{u}^{n+1} + \rho^{n+1} (\mathbf{u}^{n+1} \cdot \nabla) \partial \mathbf{u}^{n+1} \right)$$
$$- \rho_\tau (\mathbf{f} - \mathbf{f}^{n+1}) - (\rho_\tau - \rho^{n+1}) \mathbf{f}^{n+1} + (t - t^{n+1}) \partial \rho^{n+1} \partial \mathbf{u}^{n+1},$$
$$\theta_{\mathbf{u},2}^{n+1} = 2(t - t^{n+1}) \left( \partial \mu^{n+1} D(\mathbf{u}^{n+1}) + \mu^{n+1} D(\partial \mathbf{u}^{n+1}) \right),$$

$$\epsilon_{\mathbf{u},1}^{n+1} = (t - t^{n+1})^2 \left( \partial\rho^{n+1} \partial \mathbf{u}^{n+1} \cdot \nabla) \mathbf{u}^{n+1} + \partial \rho^{n+1} (\mathbf{u}^{n+1} \cdot \nabla) \partial \mathbf{u}^{n+1} + \rho^{n+1} (\partial \mathbf{u}^{n+1} \cdot \nabla) \partial \mathbf{u}^{n+1} \right)$$
$$+ (t - t^{n+1})^3 \left( \partial \rho^{n+1} (\partial \mathbf{u}^{n+1} \cdot \nabla) \partial \mathbf{u}^{n+1} \right),$$
$$\epsilon_{\mathbf{u},2}^{n+1} = 2(t - t^{n+1})^2 \left( \partial \mu^{n+1} D(\partial \mathbf{u}^{n+1}) \right).$$

*Proof.* For the time being and to lighten the notations, we opt for the following convention: all the equations being linear with respect to the test functions, which are moreover time independent, we choose to not write them. We set the following convention, that we will use in the next propositions too.

**Convention 1.** (i) For any quantity involving the velocity or the right hand side, we write:

(1) $F(\mathbf{u})$ instead of $\int_\Omega F(\mathbf{u}) \cdot \mathbf{v} d\mathbf{x}$,

(2) $G(D(\mathbf{u}))$ instead of $\int_\Omega G(D(\mathbf{u})) : D(\mathbf{v}) d\mathbf{x}$,

(3) $F(\mathbf{f})$ instead of $\int_\Omega F(\mathbf{f}) \cdot \mathbf{v} d\mathbf{x}$

(ii) For any quantity involving the pressure, we write: $H(p)$ instead of $\int_\Omega H(p) \operatorname{div} \mathbf{v} d\mathbf{x}$.

(iii) For any quantity involving $\rho$ or $\mu$, we write:

(1) $H(\rho)$ instead of $\int_\Omega H(\rho) \psi d\mathbf{x}$,

(2) $H(\mu)$ instead of $\int_\Omega H(\mu) \psi d\mathbf{x}$.

Now $n = 0, 1, 2, 3, ..., N-1$ and $t \in (t^n, t^{n+1})$. We compute

$$\rho_\tau \frac{\partial \mathbf{u}_\tau}{\partial t} + \rho_\tau (\mathbf{u}_\tau \cdot \nabla) \mathbf{u}_\tau + 2\mu_\tau D(\mathbf{u}_\tau) - p_\tau$$
$$= \rho^{n+1} \partial \mathbf{u}^{n+1} + \rho^{n+1} (\mathbf{u}^{n+1} \cdot \nabla) \mathbf{u}^{n+1} + 2\mu^{n+1} D(\mathbf{u}^{n+1}) - p^{n+1} + (t - t^{n+1}) \partial \rho^{n+1} \partial \mathbf{u}^{n+1}$$
$$+ (t - t^{n+1}) \left( \partial \rho^{n+1} (\mathbf{u}^{n+1} \cdot \nabla) \mathbf{u}^{n+1} + \rho^{n+1} (\partial \mathbf{u}^{n+1} \cdot \nabla) \mathbf{u}^{n+1} + \rho^{n+1} (\mathbf{u}^{n+1} \cdot \nabla) \partial \mathbf{u}^{n+1} \right)$$
$$+ (t - t^{n+1})^2 \left( \partial \rho^{n+1} \partial \mathbf{u}^{n+1} \cdot \nabla) \mathbf{u}^{n+1} + \partial \rho^{n+1} (\mathbf{u}^{n+1} \cdot \nabla) \partial \mathbf{u}^{n+1} + \rho^{n+1} (\partial \mathbf{u}^{n+1} \cdot \nabla) \partial \mathbf{u}^{n+1} \right)$$
$$+ (t - t^{n+1})^3 \left( \partial \rho^{n+1} (\partial \mathbf{u}^{n+1} \cdot \nabla) \partial \mathbf{u}^{n+1} \right)$$
$$+ 2(t - t^{n+1}) \left( \partial \mu^{n+1} D(\mathbf{u}^{n+1}) + \mu^{n+1} D(\partial \mathbf{u}^{n+1}) \right) + 2(t - t^{n+1})^2 \left( \partial \mu^{n+1} D(\partial \mathbf{u}^{n+1}) \right)$$

Using the fact that $\mathbf{u}^{n+1}, p^{n+1}\rho^{n+1}$ and $\mu^{n+1}$ solve the Euler step (4.46) it yields finally

$$\rho_\tau \frac{\partial \mathbf{u}_\tau}{\partial t} + \rho_\tau(\mathbf{u}_\tau \cdot \nabla)\mathbf{u}_\tau + 2\mu_\tau D(\mathbf{u}_\tau) - p_\tau = \rho^{n+1}\mathbf{f}^{n+1} + (t-t^{n+1})\partial\rho^{n+1}\partial\mathbf{u}^{n+1}$$
$$+ (t-t^{n+1})\left(\partial\rho^{n+1}(\mathbf{u}^{n+1}\cdot\nabla)\mathbf{u}^{n+1} + \rho^{n+1}(\partial\mathbf{u}^{n+1}\cdot\nabla)\mathbf{u}^{n+1} + \rho^{n+1}(\mathbf{u}^{n+1}\cdot\nabla)\partial\mathbf{u}^{n+1}\right)$$
$$+ (t-t^{n+1})^2\left(\partial\rho^{n+1}\partial\mathbf{u}^{n+1}\cdot\nabla)\mathbf{u}^{n+1} + \partial\rho^{n+1}(\mathbf{u}^{n+1}\cdot\nabla)\partial\mathbf{u}^{n+1} + \rho^{n+1}(\partial\mathbf{u}^{n+1}\cdot\nabla)\partial\mathbf{u}^{n+1}\right)$$
$$+ (t-t^{n+1})^3\left(\partial\rho^{n+1}(\partial\mathbf{u}^{n+1}\cdot\nabla)\partial\mathbf{u}^{n+1}\right)$$
$$+ 2(t-t^{n+1})\left(\partial\mu^{n+1}D(\mathbf{u}^{n+1}) + \mu^{n+1}D(\partial\mathbf{u}^{n+1})\right) + 2(t-t^{n+1})^2\left(\partial\mu^{n+1}D(\partial\mathbf{u}^{n+1})\right).$$

We then conclude by rewriting the force term as

$$\rho^{n+1}\mathbf{f}^{n+1} = \rho_\tau\mathbf{f}^{n+1} - (\rho_\tau - \rho^{n+1})\mathbf{f}^{n+1} = \rho_\tau\mathbf{f} - \rho_\tau(\mathbf{f}-\mathbf{f}^{n+1}) - (\rho_\tau - \rho^{n+1})\mathbf{f}^{n+1}.$$

□

We now prove a similar results when we consider a BDF2 step to solve the momentum equations. We need to assume that either the pressure is well-defined at $t=0$ or that the initial pressure $p_0$ is given and we define $p^0 = p_0$.

**Proposition 4.17** (Time error indicator for the momentum equation and the BDF2 method)**.**
*Let $(\mathbf{u}^n, p^n)_{n=0}^N, (\rho^n, \mu^n)_{n=0}^N$ be the solutions of (4.43)-(4.45). Let $\mathbf{u}_\tau, p_\tau, \rho_\tau, \mu_\tau$ the piecewise reconstruction of the numerical solutions given by*

$$\mathbf{u}_\tau(t) = \mathbf{u}_{\tau,1}(t) = \mathbf{u}^1 + (t-t^1)\partial\mathbf{u}^1, p_\tau(t) = p_{\tau,0}(t) = p^1, t\in[t^0,t^1],$$
$$\rho_\tau(t) = \rho_{\tau,1}(t) = \rho^1 + (t-t^1)\partial\rho^1, \mu_\tau(t) = \mu_{\tau,1}(t) = \mu^1 + (t-t^1)\partial\mu^1, t\in[t^0,t^1],$$

*and for all $n = 1,2,...,N-1$ and all $t\in[t^n,t^{n+1}]$ by*

$$\mathbf{u}_\tau(t) = \mathbf{u}_{\tau,2}(t) = \mathbf{u}^{n+1} + (t-t^{n+1})\partial\mathbf{u}^{n+1} + \frac{1}{2}(t-t^n)(t-t^{n+1})\partial^2\mathbf{u}^{n+1},$$
$$p_\tau(t) = p_{\tau,1}(t) = p^{n+1} + (t-t^{n+1})\partial p^{n+1},$$
$$\rho_\tau(t) = \rho_{\tau,2}(t) = \rho^{n+1} + (t-t^{n+1})\partial\rho^{n+1} + \frac{1}{2}(t-t^n)(t-t^{n+1})\partial^2\rho^{n+1},$$
$$\mu_\tau(t) = \mu_{\tau,2}(t) = \mu^{n+1} + (t-t^{n+1})\partial\mu^{n+1} + \frac{1}{2}(t-t^n)(t-t^{n+1})\partial^2\mu^{n+1}.$$

*Then, for every $n = 0,1,2,...,N-1$ and any $t\in(t^n,t^{n+1})$ it holds*

$$\int_\Omega \rho_\tau\frac{\partial\mathbf{u}_\tau}{\partial t}\cdot\mathbf{v}d\mathbf{x} + \int_\Omega \rho_\tau((\mathbf{u}_\tau\cdot\nabla)\mathbf{u}_\tau)\cdot\mathbf{v}d\mathbf{x}$$
$$+ \int_\Omega 2\mu_\tau D(\mathbf{u}_\tau) : D(\mathbf{v})d\mathbf{x} - \int_\Omega p_\tau\,\mathrm{div}(\mathbf{v})$$
$$= \int_\Omega \rho_\tau\mathbf{f}\cdot\mathbf{v}d\mathbf{x} + \int_\Omega \theta_{\mathbf{u},1}^{n+1}\cdot\mathbf{v}d\mathbf{x} + \int_\Omega \theta_{\mathbf{u},2}^{n+1} : D(\mathbf{v})d\mathbf{x} + \int_\Omega \epsilon_{\mathbf{u},1}^{n+1}\cdot\mathbf{v}d\mathbf{x} + \int_\Omega \epsilon_{\mathbf{u},2}^{n+1} : D(\mathbf{v})d\mathbf{x}, \forall\mathbf{v}\in(H_0^1(\Omega))^2,$$

*where for $n\geq 1$*

$$\theta_{\mathbf{u},1}^{n+1} = (t-t^n)(t-t^{n+1})\rho^{n+1}\left(\frac{1}{2}(\partial^2\mathbf{u}^{n+1}\cdot\nabla)\mathbf{u}^{n+1} + (\partial\mathbf{u}^{n+1}\cdot\nabla)\partial\mathbf{u}^{n+1} + \frac{1}{2}(\mathbf{u}^{n+1}\cdot\nabla)\partial^2\mathbf{u}^{n+1}\right)$$
$$+ (t-t^n)(t-t^{n+1})\partial\rho^{n+1}\left(\partial\mathbf{u}^{n+1}\cdot\nabla)\mathbf{u}^{n+1} + (\mathbf{u}^{n+1}\cdot\nabla)\partial\mathbf{u}^{n+1}\right)$$
$$+ \frac{1}{2}(t-t^n)(t-t^{n+1})\partial^2\rho^{n+1}(\partial\mathbf{u}^{n+1} + (\mathbf{u}^{n+1}\cdot\nabla)\mathbf{u}^{n+1}) + (t-s^n)(t-t^{n+1})\partial\rho^{n+1}\partial^2\mathbf{u}^{n+1}$$
$$- \frac{\tau^n}{2}(t-t^{n+1})\rho^{n+1}\tilde{\partial}^3\mathbf{u}^{n+1}$$
$$+ \rho_\tau\left(\mathbf{f}^{n+1} + (t-t^{n+1})\partial\mathbf{f}^{n+1} - \mathbf{f}\right) - \frac{1}{2}(t-t^n)(t-t^{n+1})\left(\partial^2\rho^{n+1}\mathbf{f}^{n+1} + \partial\rho^{n+1}\partial\mathbf{f}^{n+1}\right),$$

*where* $s^n = t^n, n \geq 2, s^1 = \frac{t^1}{2}$,

$$\theta_{\mathbf{u},2}^{n+1} = (t-t^n)(t-t^{n+1})\left(\frac{1}{2}\partial^2\mu^{n+1}D(\mathbf{u}^{n+1} + \partial\mu^{n+1}D(\partial\mathbf{u}^{n+1}) + \frac{1}{2}\mu^{n+1}D(\partial^2\mathbf{u}^{n+1})\right),$$

$$\begin{aligned}
\epsilon_{\mathbf{u},1}^{n+1} = &\frac{1}{2}(t-t^n)(t-t^{n+1})^2\rho^{n+1}\left((\partial\mathbf{u}^{n+1}\cdot\nabla)\partial^2\mathbf{u}^{n+1} + (\partial^2\mathbf{u}^{n+1}\cdot\nabla)\partial\mathbf{u}^{n+1}\right) \\
&+ \left((t-t^{n+1})^3 + (\tau^{n+1})^2(t-t^{n+1})^2\right)\partial\rho^{n+1}(\partial\mathbf{u}^{n+1}\cdot\nabla)\partial\mathbf{u}^{n+1} \\
&+ \frac{1}{2}(t-t^n)(t-t^{n+1})^2\partial\rho^{n+1}\left((\mathbf{u}^{n+1}\cdot\nabla)\partial^2\mathbf{u}^{n+1} + (\partial^2\mathbf{u}^{n+1}\cdot\nabla)\mathbf{u}^{n+1}\right) \\
&\frac{1}{2}(t-t^n)(t-t^{n+1})^2\partial^2\rho^{n+1}\left((\mathbf{u}^{n+1}\cdot\nabla)\partial\mathbf{u}^{n+1} + (\partial\mathbf{u}^{n+1}\cdot\nabla)\mathbf{u}^{n+1}\right) \\
&+ \frac{1}{4}(t-t^n)^2(t-t^{n+1})^2\rho^{n+1}(\partial^2\mathbf{u}^{n+1}\cdot\nabla)\partial^2\mathbf{u}^{n+1} \\
&+ \frac{1}{2}(t-t^n)(t-t^{n+1})^3\partial\rho^{n+1}\left((\partial\mathbf{u}^{n+1}\cdot\nabla)\partial^2\mathbf{u}^{n+1} + (\partial^2\mathbf{u}^{n+1}\cdot\nabla)\partial\mathbf{u}^{n+1}\right) \\
&+ \frac{1}{2}(t-t^n)(t-t^{n+1})^3\partial^2\rho^{n+1}(\partial\mathbf{u}^{n+1}\cdot\nabla)\partial\mathbf{u}^{n+1} \\
&+ \frac{1}{4}(t-t^n)^2(t-t^{n+1})^2\partial^2\rho^{n+1}\left((\mathbf{u}^{n+1}\cdot\nabla)\partial^2\mathbf{u}^{n+1} + (\partial^2\mathbf{u}^{n+1}\cdot\nabla)\mathbf{u}^{n+1}\right) \\
&+ \frac{1}{4}(t-t^n)^2(t-t^{n+1})^3\partial\rho^{n+1}(\partial^2\mathbf{u}^{n+1}\cdot\nabla)\partial^2\mathbf{u}^{n+1} \\
&+ \frac{1}{4}(t-t^n)^2(t-t^{n+1})^3\partial^2\rho^{n+1}\left((\partial\mathbf{u}^{n+1}\cdot\nabla)\partial^2\mathbf{u}^{n+1} + (\partial^2\mathbf{u}^{n+1}\cdot\nabla)\partial\mathbf{u}^{n+1}\right) \\
&+ \frac{1}{8}(t-t^n)^3(t-t^{n+1})^3\partial^2\rho^{n+1}(\partial^2\mathbf{u}^{n+1}\cdot\nabla)\partial^2\mathbf{u}^{n+1} \\
&+ \gamma_n(t-t^{n+1})\frac{\tau^n\tau^{n+1}}{2}\partial\rho^{n+1}\tilde{\partial}^3\mathbf{u}^{n+1} \\
&\frac{1}{2}(t-t^n)(t-t^{n+1})(t-t^{n+1/2})\partial^2\rho^{n+1}\partial^2\mathbf{u}^{n+1} \\
&- \frac{1}{2}(t-t^n)(t-t^{n+1})^2\partial^2\rho^{n+1}\partial\mathbf{u}^{n+1} - \frac{1}{2}(t-t^n)(t-t^{n+1})^2\partial^2\rho^{n+1}\partial\mathbf{f}^{n+1},
\end{aligned}$$

*where* $\gamma_n = 1, n \geq 2, \gamma_1 = 0$,

$$\begin{aligned}
\epsilon_{\mathbf{u},2}^{n+1} = &\frac{1}{2}(t-t^n)(t-t^{n+1})^2\left(\partial^2\mu^{n+1}D(\partial\mathbf{u}^{n+1}) + \partial\mu^{n+1}D(\partial^2\mathbf{u}^{n+1})\right) \\
&+ \frac{1}{4}(t-t^n)^2(t-t^{n+1})^2\left(\partial^2\mu^{n+1}D(\partial^2\mathbf{u}^{n+1})\right).
\end{aligned}$$

*and (at* $n = 0$*) we define,*

$$\begin{aligned}
\theta_{\mathbf{u},1}^1 = &(t-t^1)\left(\partial\rho^1(\mathbf{u}^1\cdot\nabla)\mathbf{u}^1 + \rho^1(\partial\mathbf{u}^1\cdot\nabla)\mathbf{u}^1 + \rho^1(\mathbf{u}^1\cdot\nabla)\partial\mathbf{u}^1\right) \\
&- \rho_\tau(\mathbf{f}-\mathbf{f}^1) - (\rho_\tau - \rho^1)\mathbf{f}^1 + (t-t^1)\partial\rho^1\partial\mathbf{u}^1,
\end{aligned}$$

$$\theta_{\mathbf{u},2}^1 = 2(t-t^1)\left(\partial\mu^1 D(\mathbf{u}^1) + \mu^1 D(\partial\mathbf{u}^1)\right),$$

$$\begin{aligned}
\epsilon_{\mathbf{u},1}^1 = &(t-t^1)^2\left(\partial\rho^1\partial\mathbf{u}^1\cdot\nabla)\mathbf{u}^1 + \partial\rho^1(\mathbf{u}^1\cdot\nabla)\partial\mathbf{u}^1 + \rho^1(\partial\mathbf{u}^1\cdot\nabla)\partial\mathbf{u}^1\right) \\
&+ (t-t^1)^3\left(\partial\rho^1(\partial\mathbf{u}^1\cdot\nabla)\partial\mathbf{u}^1\right),
\end{aligned}$$

$$\epsilon_{\mathbf{u},2}^1 = 2(t-t^1)^2\left(\partial\mu^1 D(\partial\mathbf{u}^1)\right).$$

*Proof.* The step $n = 0$ is a direct consequence of Proposition 4.16. We now consider $n \geq 1$ and $t \in (t^n, t^{n+1})$. We treat in one shot the cases $n \geq 2$ and $n = 1$ by indicating in the proof the minor modification that appears. We write everything with respect to the Convention 1, presented at the beginning of the proof Proposition 4.16, in order to lighten the notations.

We recall that the discretization of the momentum equation (for $n \geq 1$) reads:

$$\partial \mathbf{u}^{n+1} + \frac{\tau^{n+1}}{2}\partial^2 \mathbf{u}^{n+1} + \rho^{n+1}(\mathbf{u}^{n+1}\cdot\nabla)\mathbf{u}^{n+1} + 2\mu^{n+1}D(\mathbf{u}^{n+1}) - p^{n+1} = \rho^{n+1}\mathbf{f}^{n+1}. \quad (4.47)$$

The recipe is still the same (and we are largely inspired by the computations we did in the case of constant density and viscosity)

1. Compute straightforwardly the quantity
$$\rho_\tau \frac{\partial \mathbf{u}_\tau}{\partial t} + \rho_\tau(\mathbf{u}_\tau\cdot\nabla)\mathbf{u}_\tau + 2\mu_\tau D(\mathbf{u}_\tau) - p_\tau.$$
2. Gather all the terms that give the left hand side of (4.47) and can be eliminated through it.
3. Gather all the terms that are already of the right order (here two).
4. Gather all the terms that are of higher order.
5. Gather all the terms that are of lower order (here one) and differentiate the numerical method (4.47) to obtain an expression of them that are of the correct order.
6. Use as much as needed the $a - a = 0$ trick to make appear all the quantities of interest.

We compute

$$\begin{aligned}
\rho_\tau \frac{\partial \mathbf{u}_\tau}{\partial t} &+ \rho_\tau(\mathbf{u}_\tau\cdot\nabla)\mathbf{u}_\tau + 2\mu_\tau D(\mathbf{u}_\tau) - p_\tau \\
&= \partial \mathbf{u}^{n+1} + \frac{\tau^{n+1}}{2}\partial^2 \mathbf{u}^{n+1} + \rho^{n+1}(\mathbf{u}^{n+1}\cdot\nabla)\mathbf{u}^{n+1} + 2\mu^{n+1}D(\mathbf{u}^{n+1}) - p^{n+1}
\end{aligned}$$

$$\begin{aligned}
+(t-t^{n+1})\Big(\rho^{n+1}\partial^2\mathbf{u}^{n+1} &+ \partial\rho^{n+1}\partial\mathbf{u}^{n+1} \\
&+\rho^{n+1}\left((\partial\mathbf{u}^{n+1}\cdot\nabla)\mathbf{u}^{n+1} + (\mathbf{u}^{n+1}\cdot\nabla)\partial\mathbf{u}^{n+1}\right) \\
&\qquad +2\mu^{n+1}D(\partial\mathbf{u}^{n+1}) + 2\partial\mu^{n+1}D(\mathbf{u}^{n+1}) - \partial p^{n+1}\Big)
\end{aligned}$$

$$\begin{aligned}
&+(t-t^{n+1})(t-t^{n+1/2})\partial\rho^{n+1}\partial^2\mathbf{u}^{n+1} + \frac{1}{2}(t-t^n)(t-t^{n+1})\partial^2\rho^{n+1}\partial\mathbf{u}^{n+1} \\
&+(t-t^{n+1})^2\rho^{n+1}(\partial\mathbf{u}^{n+1}\cdot\nabla)\partial\mathbf{u}^{n+1} + \frac{1}{2}(t-t^n)(t-t^{n+1})\rho^{n+1}\left((\partial^2\mathbf{u}^{n+1}\cdot\nabla)\mathbf{u}^{n+1} + (\mathbf{u}^{n+1}\cdot\nabla)\partial^2\mathbf{u}^{n+1}\right) \\
&\qquad +(t-t^{n+1})^2\partial\rho^{n+1}\left((\partial\mathbf{u}^{n+1}\cdot\nabla)\mathbf{u}^{n+1} + (\mathbf{u}^{n+1}\cdot\nabla)\partial\mathbf{u}^{n+1}\right) \\
&\qquad\quad +\frac{1}{2}(t-t^n)(t-t^{n+1})\partial^2\rho^{n+1}(\mathbf{u}^{n+1}\cdot\nabla)\mathbf{u}^{n+1} \\
&+(t-t^{n+1})^2 2\partial\mu^{n+1}D(\partial\mathbf{u}^{n+1}) + \frac{1}{2}(t-t^n)(t-t^{n+1})\left(\partial^2\mu^{n+1}D(\mathbf{u}^{n+1}) + \mu^{n+1}D(\partial^2\mathbf{u}^{n+1})\right)
\end{aligned}$$

$$
\begin{aligned}
&+\frac{1}{2}(t-t^n)(t-t^{n+1})^2\rho^{n+1}\left((\partial\mathbf{u}^{n+1}\cdot\nabla)\partial^2\mathbf{u}^{n+1}+(\partial^2\mathbf{u}^{n+1}\cdot\nabla)\partial\mathbf{u}^{n+1}\right)\\
&\qquad+(t-t^{n+1})^3\partial\rho^{n+1}(\partial\mathbf{u}^{n+1}\cdot\nabla)\partial\mathbf{u}^{n+1}\\
&\quad+\frac{1}{2}(t-t^n)(t-t^{n+1})^2\partial\rho^{n+1}\left((\mathbf{u}^{n+1}\cdot\nabla)\partial^2\mathbf{u}^{n+1}+(\partial^2\mathbf{u}^{n+1}\cdot\nabla)\mathbf{u}^{n+1}\right)\\
&\quad\frac{1}{2}(t-t^n)(t-t^{n+1})^2\partial^2\rho^{n+1}\left((\mathbf{u}^{n+1}\cdot\nabla)\partial\mathbf{u}^{n+1}+(\partial\mathbf{u}^{n+1}\cdot\nabla)\mathbf{u}^{n+1}\right)\\
&\qquad+\frac{1}{4}(t-t^n)^2(t-t^{n+1})^2\rho^{n+1}(\partial^2\mathbf{u}^{n+1}\cdot\nabla)\partial^2\mathbf{u}^{n+1}\\
&\quad+\frac{1}{2}(t-t^n)(t-t^{n+1})^3\partial\rho^{n+1}\left((\partial\mathbf{u}^{n+1}\cdot\nabla)\partial^2\mathbf{u}^{n+1}+(\partial^2\mathbf{u}^{n+1}\cdot\nabla)\partial\mathbf{u}^{n+1}\right)\\
&\qquad+\frac{1}{2}(t-t^n)(t-t^{n+1})^3\partial^2\rho^{n+1}(\partial\mathbf{u}^{n+1}\cdot\nabla)\partial\mathbf{u}^{n+1}\\
&\quad+\frac{1}{4}(t-t^n)^2(t-t^{n+1})^2\partial^2\rho^{n+1}\left((\mathbf{u}^{n+1}\cdot\nabla)\partial^2\mathbf{u}^{n+1}+(\partial^2\mathbf{u}^{n+1}\cdot\nabla)\mathbf{u}^{n+1}\right)\\
&\qquad+\frac{1}{4}(t-t^n)^2(t-t^{n+1})^3\partial\rho^{n+1}(\partial^2\mathbf{u}^{n+1}\cdot\nabla)\partial^2\mathbf{u}^{n+1}\\
&\quad+\frac{1}{4}(t-t^n)^2(t-t^{n+1})^3\partial^2\rho^{n+1}\left((\partial\mathbf{u}^{n+1}\cdot\nabla)\partial^2\mathbf{u}^{n+1}+(\partial^2\mathbf{u}^{n+1}\cdot\nabla)\partial\mathbf{u}^{n+1}\right)\\
&\qquad+\frac{1}{8}(t-t^n)^3(t-t^{n+1})^3\partial^2\rho^{n+1}(\partial^2\mathbf{u}^{n+1}\cdot\nabla)\partial^2\mathbf{u}^{n+1}\\
&\qquad\frac{1}{2}(t-t^n)(t-t^{n+1})(t-t^{n+1/2})\partial^2\rho^{n+1}\partial^2\mathbf{u}^{n+1}\\
&\qquad-\frac{1}{2}(t-t^n)(t-t^{n+1})^2\partial^2\rho^{n+1}\partial\mathbf{u}^{n+1}\\
&\quad\frac{1}{2}(t-t^n)(t-t^{n+1})^2\left(\partial^2\mu^{n+1}D(\partial\mathbf{u}^{n+1})+\partial\mu^{n+1}D(\partial^2\mathbf{u}^{n+1})\right)\\
&\qquad+\frac{1}{4}(t-t^n)^2(t-t^{n+1})^2\left(\partial^2\mu^{n+1}D(\partial^2\mathbf{u}^{n+1})\right)
\end{aligned}
$$

The red terms are all of order 2 and therefore we will not modify them and put it immediately in $\theta_{\mathbf{u},1}^{n+1}$ and $\theta_{\mathbf{u},2}^{n+1}$. The orange term are equal to $\rho^{n+1}\mathbf{f}^{n+1}$ that we keep aside for the moment . The black terms are of higher order and will contribute to $\epsilon_{\mathbf{u},1}^{n+1}$ and $\epsilon_{\mathbf{u},2}^{n+1}$.

Now we treat the blue terms. Taking the difference between (4.47) at two consecutive steps and dividing by $\tau^{n+1}$, we can prove that

$$
\begin{aligned}
&\rho^{n+1}\partial^2\mathbf{u}^{n+1}+(t-t^{n+1})\partial\rho^{n+1}\partial\mathbf{u}^{n+1}\\
&\qquad\rho^{n+1}\left((\partial\mathbf{u}^{n+1}\cdot\nabla)\mathbf{u}^{n+1}+(\mathbf{u}^{n+1}\cdot\nabla)\partial\mathbf{u}^{n+1}\right)\\
&\qquad+2\mu^{n+1}D(\partial\mathbf{u}^{n+1})+2\partial\mu^{n+1}D(\mathbf{u}^{n+1})-\partial p^{n+1}\\
&\qquad=\rho^{n+1}\partial\mathbf{f}^{n+1}+\partial\rho^{n+1}\mathbf{f}^{n+1}\\
&+\tau^{n+1}\rho^{n+1}(\partial\mathbf{u}^{n+1}\cdot\nabla)\partial\mathbf{u}^{n+1}+\tau^{n+1}\partial\rho^{n+1}\left(\mathbf{u}^{n+1}\cdot\nabla)\partial\mathbf{u}^{n+1}+(\partial\mathbf{u}^{n+1}\cdot\nabla)\mathbf{u}^{n+1}\right)\\
&\qquad-(\tau^{n+1})^2\partial\rho^{n+1}(\partial\mathbf{u}^{n+1}\cdot\nabla)\partial\mathbf{u}^{n+1}+\tau^{n+1}2\partial\mu^{n+1}D(\partial\mathbf{u}^{n+1})\\
&\qquad-\frac{\tau^n}{2}\rho^{n+1}\tilde\partial^3\mathbf{u}^{n+1}+\frac{\tau^{n+1}}{2}\partial\rho^{n+1}\partial^2\mathbf{u}^{n+1}+\frac{\tau^n\tau^{n+1}}{2}\partial\rho^{n+1}\tilde\partial^3\mathbf{u}^{n+1}.
\end{aligned}
$$

Note that if $n=1$, then the last two terms do not appear and are replaced by

$$\frac{\tau^{n+1}+\tau^n}{2}\partial\rho^{n+1}\partial\rho^{n+1}\partial^2\mathbf{u}^{n+1}.$$

This is due to the fact that we make the difference between the BDF2 method and the first step, that is only the BDF1 method.

Now multiplying by $(t-t^{n+1})$, we get an expression for the blue terms an we put the corresponding parts into $\theta_{\mathbf{u},1}^{n+1}, \theta_{\mathbf{u},2}^{n+1}, \epsilon_{\mathbf{u},1}^{n+1}$ and $\epsilon_{\mathbf{u},2}^{n+1}$.

Finally, it remains to gather the terms involving the force term that are

$$\rho^{n+1}\mathbf{f}^{n+1} + (t-t^{n+1})\rho^{n+1}\partial\mathbf{f}^{n+1} + (t-t^{n+1})\partial\rho^{n+1}\mathbf{f}^{n}$$

that we rewrite as

$$\rho_\tau\mathbf{f} + \rho_\tau\left(\mathbf{f}^{n+1} + (t-t^{n+1})\partial\mathbf{f}^{n+1} - \mathbf{f}\right) \\ - \frac{1}{2}(t-t^n)(t-t^{n+1})\rho_\tau\left(\partial^2\rho^{n+1}\mathbf{f}^{n+1} + \partial\rho^{n+1}\partial\mathbf{f}^{n+1}\right) \\ - \frac{1}{2}(t-t^n)(t-t^{n+1})^2\partial^2\rho^{n+1}\partial\mathbf{f}^{n+1}.$$

We put all the terms of order 2 into $\theta_{\mathbf{u},1}^{n+1}$ and the last one into $\epsilon_{\mathbf{u},1}^{n+1}$. This conclude the proof. □

We now prove a similar result for the transport problem and the Crank-Nicolson method. The computations are very close to those performed in the Proposition 2.53 of Chapter 2, where the transport velocity field depends on the time. Here below, we will use the midpoint formulation of the piecewise reconstructions, so that the computations will be more direct.

**Proposition 4.18** (Time error indicator for the transport equation and the Crank-Nicolson method)**.**
*Let $(\mathbf{u}^n)_{n=0}^N, (\rho^n, \mu^n)_{n=0}^N$ be the solutions of (4.43)-(4.45). Let $\mathbf{u}_\tau, p_\tau, \rho_\tau, \mu_\tau$ the piecewise reconstruction of the numerical solutions given by*

$$\mathbf{u}_\tau(t) = \mathbf{u}_{\tau,1}(t) = \mathbf{u}^{1/2} + (t-t^{1/2})\partial\mathbf{u}^1, t \in [t^0, t^1],$$

$$\rho_\tau(t) = \rho_{\tau,1}(t) = \rho^{1/2} + (t-t^{1/2})\partial\rho^1, \mu_\tau(t) = \mu_{\tau,1}(t) = \mu^{1/2} + (t-t^{1/2})\partial\mu^1, t \in [t^0, t^1],$$

*and for all $n = 1, 2, ..., N-1$ and all $t \in [t^n, t^{n+1}]$ by*

$$\mathbf{u}_\tau(t) = \mathbf{u}_{\tau,2}(t) = \mathbf{u}^{n+1/2} + (t-t^{n+1/2})\partial\mathbf{u}^{n+1} + \frac{1}{2}(t-t^n)(t-t^{n+1})\partial^2\mathbf{u}^{n+1},$$

$$\rho_\tau(t) = \rho_{\tau,2}(t) = \rho^{n+1/2} + (t-t^{n+1/2})\partial\rho^{n+1} + \frac{1}{2}(t-t^n)(t-t^{n+1})\partial^2\rho^{n+1},$$

$$\mu_\tau(t) = \mu_{\tau,2}(t) = \mu^{n+1/2} + (t-t^{n+1/2})\partial\mu^{n+1} + \frac{1}{2}(t-t^n)(t-t^{n+1})\partial^2\mu^{n+1}.$$

*Then, for every $n = 0, 1, 2, ..., N-1$ and any $t \in (t^n, t^{n+1})$ it holds*

$$\int_\Omega \left(\frac{\partial\rho_\tau}{\partial t} + \mathbf{u}_\tau \cdot \nabla\rho_\tau\right)\psi d\mathbf{x} = \int_\Omega \theta_\rho^{n+1}\psi d\mathbf{x} + \int_\Omega \epsilon_\rho^{n+1}\psi d\mathbf{x}, \forall\psi \in L^2(\Omega),$$

*where for $n \geq 1$*

$$\theta_\rho^{n+1} = \left(\frac{1}{2}(t-t^n)(t-t^{n+1}) + \frac{\tau^n}{2}(t-t^{n+1/2})\right)\left(\partial^2\mathbf{u}^{n+1}\nabla\rho^{n+1/2} + \mathbf{u}^{n+1/2}\cdot\nabla\partial^2\rho^{n+1}\right) \\ + \left((t-t^{n+1/2})^2 + (\tau^{n+1}+\tau^n)(t-t^{n+1/2})\right)\partial\mathbf{u}^{n+1}\cdot\nabla\partial\rho^{n+1},$$

$$\epsilon_\rho^{n+1} = \left(\frac{1}{2}(t-t^n)(t-t^{n+1})^2 - (\tau^{n+1}+\tau^n)\frac{\tau^n}{2}(t-t^{n+1/2})\right)\left(\partial\mathbf{u}^{n+1}\cdot\nabla\partial^2\rho^{n+1} + \partial^2\mathbf{u}^{n+1}\cdot\nabla\partial\rho^{n+1}\right) \\ + \left(\frac{1}{4}(t-t^n)^2(t-t^{n+1})^2 - (\tau^{n+1}+\tau^n)\frac{(\tau^n)^2}{4}(t-t^{n+1/2})\right)\partial^2\mathbf{u}^{n+1}\cdot\nabla\partial^2\rho^{n+1},$$

*and (at $n=0$)*

$$\theta_\rho^1 = (t - t^{1/2})\left(\mathbf{u}^{1/2}\cdot\nabla\partial\rho^1 + \partial\mathbf{u}^1\cdot\nabla\rho^{1/2}\right),$$

$$\epsilon_\rho^1 = (t-t^{1/2})^2\partial\mathbf{u}^1\cdot\nabla\partial\rho^1.$$

*For the viscosity, the same results holds, and we have for every $n = 0,1,2,...,N-1$ and any $t \in (t^n, t^{n+1})$*

$$\int_\Omega \left(\frac{\partial\mu_\tau}{\partial t} + \mathbf{u}_\tau\cdot\nabla\mu_\tau\right)\psi d\mathbf{x} = \int_\Omega \theta_\mu^{n+1}\psi d\mathbf{x} + \int_\Omega \epsilon_\mu^{n+1}\psi d\mathbf{x},$$

*where for $n \geq 1$*

$$\theta_\mu^{n+1} = \left(\frac{1}{2}(t-t^n)(t-t^{n+1}) + \frac{\tau^n}{2}(t-t^{n+1/2})\right)\left(\partial^2\mathbf{u}^{n+1}\nabla\mu^{n+1/2} + \mathbf{u}^{n+1/2}\cdot\nabla\partial^2\mu^{n+1}\right)$$
$$+\left((t-t^{n+1/2})^2 + (\tau^{n+1}+\tau^n)(t-t^{n+1/2})\right)\partial\mathbf{u}^{n+1}\cdot\nabla\partial\mu^{n+1},$$

$$\epsilon_\mu^{n+1} = \left(\frac{1}{2}(t-t^n)(t-t^{n+1})^2 - (\tau^{n+1}+\tau^n)\frac{\tau^n}{2}(t-t^{n+1/2})\right)\left(\partial\mathbf{u}^{n+1}\cdot\nabla\partial^2\mu^{n+1} + \partial^2\mathbf{u}^{n+1}\cdot\nabla\partial\mu^{n+1}\right)$$
$$+\left(\frac{1}{4}(t-t^n)^2(t-t^{n+1})^2 - (\tau^{n+1}+\tau^n)\frac{(\tau^n)^2}{4}(t-t^{n+1/2})\right)\partial^2\mathbf{u}^{n+1}\cdot\nabla\partial^2\mu^{n+1},$$

*and (at $n=0$)*

$$\theta_\mu^1 = (t - t^{1/2})\left(\mathbf{u}^{1/2}\cdot\nabla\partial\mu^1 + \partial\mathbf{u}^1\cdot\nabla\mu^{1/2}\right),$$

$$\epsilon_\mu^1 = (t-t^{1/2})^2\partial\mathbf{u}^1\cdot\nabla\partial\mu^1.$$

*Proof.* We only prove the corresponding result for $\rho$, the one for $\mu$ being exactly the same computation. Moreover, as we did previously in Propositions 4.16 and 4.17, we simplify all the weak formulations by using the Convention 1.

The case $n = 0$ is straightforward by plugging the definition of $\rho_\tau$ on $(t^0, t^1)$. Let $n \geq 1$ and $t \in (t^n, t^{n+1})$. We proceed as previously and we gather together the terms of same orders. We have

$$\frac{\partial\rho_\tau}{\partial t} + \mathbf{u}_\tau\cdot\nabla\rho_\tau = \partial\rho^{n+1} + \mathbf{u}^{n+1/2}\cdot\nabla\rho^{n+1/2}$$
$$+ (t-t^{n+1/2})\left(\partial^2\rho^{n+1} + \partial\mathbf{u}^{n+1}\cdot\nabla\rho^{n+1/2} + \mathbf{u}^{n+1/2}\cdot\nabla\partial\rho^{n+1}\right)$$
$$+ (t-t^{n+1/2})^2\partial\mathbf{u}^{n+1}\cdot\nabla\rho^{n+1} + \frac{1}{2}(t-t^n)(t-t^{n+1})\left(\partial^2\mathbf{u}^{n+1}\nabla\rho^{n+1/2} + \mathbf{u}^{n+1/2}\cdot\nabla\partial^2\rho^{n+1}\right)$$
$$\frac{1}{2}(t-t^n)(t-t^{n+1})^2\left(\partial\mathbf{u}^{n+1}\cdot\nabla\partial^2\rho^{n+1} + \partial^2\mathbf{u}^{n+1}\cdot\nabla\partial\rho^{n+1}\right)$$
$$+\frac{1}{4}(t-t^n)^2(t-t^{n+1})^2\partial^2\mathbf{u}^{n+1}\cdot\nabla\partial^2\rho^{n+1}.$$

The orange terms are eliminated using the numerical method (4.44). The red terms are already of order 2 and the black terms of higher order. To express the blue terms as a quantity of order 2, we consider the difference

$$\partial\rho^{n+1} + \mathbf{u}^{n+1/2}\cdot\rho^{n+1/2} - \partial\rho^n - \mathbf{u}^{n-1/2}\cdot\nabla\rho^{n-1/2}$$

and we divide by $\tau^{n+1}+\tau^n/2$. This yields to

$$\partial^2\rho^{n+1} + \frac{\mathbf{u}^{n+1}-\mathbf{u}^{n-1}}{\tau^{n+1}+\tau^n}\cdot\nabla\rho^{n+1/2} + \mathbf{u}^{n-1/2}\cdot\nabla\frac{\rho^{n+1}-\rho^{n-1}}{\tau^{n+1}+\tau^n} = 0,$$

that we rewrite

$$\partial^2\rho^{n+1} + \frac{\mathbf{u}^{n+1}-\mathbf{u}^{n-1}}{\tau^{n+1}+\tau^n}\cdot\nabla\rho^{n+1/2} + \mathbf{u}^{n+1/2}\cdot\nabla\frac{\rho^{n+1}-\rho^{n-1}}{\tau^{n+1}+\tau^n} - (\tau^{n+1}+\tau)\frac{\mathbf{u}^{n+1}-\mathbf{u}^{n-1}}{\tau^{n+1}+\tau^n}\cdot\nabla\frac{\rho^{n+1}-\rho^{n-1}}{\tau^{n+1}+\tau^n} = 0$$

Using the identity

$$\frac{v^{n+1}-v^n}{\tau^{n+1}+\tau^n} = \frac{v^{n+1}-v^n}{\tau^{n+1}} - \frac{\tau^n}{2}\partial^2 v^{n+1}$$

we finally arrive to

$$\partial^2\rho^{n+1} + \partial\mathbf{u}^{n+1}\cdot\nabla\rho^{n+1/2} + \mathbf{u}^{n+1/2}\cdot\nabla\partial\rho^{n+1} = \frac{\tau^n}{2}\left(\partial^2\mathbf{u}^{n+1}\cdot\nabla\rho^{n+1/2} + \mathbf{u}^{n+1/2}\cdot\nabla\partial^2\rho^{n+1}\right)$$
$$+ (\tau^{n+1}+\tau^n)\partial\mathbf{u}^{n+1}\cdot\nabla\partial\rho^{n+1} - (\tau^{n+1}+\tau^n)\frac{\tau^n}{2}\left(\partial^2\mathbf{u}^{n+1}\cdot\nabla\partial\rho^{n+1} + \partial\mathbf{u}^{n+1}\cdot\nabla\partial^2\rho^{n+1}\right)$$
$$+ (\tau^{n+1}+\tau^n)\frac{(\tau^n)^2}{4}\partial^2\mathbf{u}^{n+1}\cdot\nabla\partial^2\rho^{n+1}.$$

Multiplying by $(t - t^{n+1/2})$ we obtain an expression for the blue terms, which concludes the proof by gathering all the terms of same orders. □

In the next two propositions, we state preliminary upper bounds that we will use to prove an a posteriori error estimate for the numerical method (4.43)-(4.45).

**Proposition 4.19** (Estimate for the velocity)**.**
*Let $(\mathbf{u}, p)$ be the exact velocity and pressure fields and $\rho, \mu$ the exact density and viscosity that are solutions of (4.6)-(4.7).Let $(\mathbf{u}^n, p^n)_{n=0}^N, (\rho^n, \mu^n)_{n=0}^N$ be the solutions of (4.43)-(4.45). Let $\mathbf{u}_\tau, p_\tau, \rho_\tau, \mu_\tau$ the piecewise reconstruction of the numerical solutions given by*

$$\mathbf{u}_\tau(t) = \mathbf{u}_{\tau,1}(t) = \mathbf{u}^1 + (t-t^1)\partial\mathbf{u}^1, p_\tau(t) = p_{\tau,0}(t) = p^1, t\in[t^0,t^1],$$
$$\rho_\tau(t) = \rho_{\tau,1}(t) = \rho^1 + (t-t^1)\partial\rho^1, \mu_\tau(t) = \mu_{\tau,1}(t) = \mu^1 + (t-t^1)\partial\mu^1, t\in[t^0,t^1],$$

*and for all $n = 1, 2, ..., N-1$ and all $t \in [t^n, t^{n+1}]$ by*

$$\mathbf{u}_\tau(t) = \mathbf{u}_{\tau,2}(t) = \mathbf{u}^{n+1} + (t-t^{n+1})\partial\mathbf{u}^{n+1} + \frac{1}{2}(t-t^n)(t-t^{n+1})\partial^2\mathbf{u}^{n+1},$$
$$p_\tau(t) = p_{\tau,1}(t) = p^{n+1} + (t-t^{n+1})\partial p^{n+1},$$
$$\rho_\tau(t) = \rho_{\tau,2}(t) = \rho^{n+1} + (t-t^{n+1})\partial\rho^{n+1} + \frac{1}{2}(t-t^n)(t-t^{n+1})\partial^2\rho^{n+1},$$
$$\mu_\tau(t) = \mu_{\tau,2}(t) = \mu^{n+1} + (t-t^{n+1})\partial\mu^{n+1} + \frac{1}{2}(t-t^n)(t-t^{n+1})\partial^2\mu^{n+1}.$$

*Let assume finally that there exists $0 < \gamma < 1$ and $\tau_0$ small enough such that for all $\tau \le \tau_0$ we have*

$$\sup_{t\in(0,T)} \|\nabla\mathbf{u}_\tau(t)\|_{L^2(\Omega)} \le \frac{\gamma\mu_{\min}}{C_{SOB}\rho_{\max}}, \tag{4.48}$$

*where $C_{SOB}$ is the Sobolev constant of Proposition A.8 in Appendix. Then, there exists a constant $C > 0$ that depends only on $\Omega$ such that for all $\tau \le \tau_0$, it holds for all $n = 0, 1, 2, ..., N-1$ and all $t \in (t^n, t^{n+1})$*

$$\frac{d}{dt}\int_\Omega \rho(\mathbf{u}-\mathbf{u}_\tau)^2(t)d\mathbf{x} + \mu_{\min}\|\nabla(\mathbf{u}-\mathbf{u}_\tau)(t)\|^2_{L^2(\Omega)}$$
$$\le \frac{C}{\mu_{\min}(1-\gamma)^2}\left(\|\theta^{n+1}_{\mathbf{u},1}(t)\|^2_{L^2(\Omega)} + \|\theta^{n+1}_{\mathbf{u},2}(t)\|^2_{L^2(\Omega)} + \|\epsilon^{n+1}_{\mathbf{u},1}(t)\|^2_{L^2(\Omega)} + \|\epsilon^{n+1}_{\mathbf{u},2}(t)\|^2_{L^2(\Omega)}\right)$$
$$+ \frac{CL(\mathbf{u}_\tau)}{\mu_{\min}(1-\gamma)^2}\left((\|(\rho-\rho_\tau)(t)\|^2_{L^2(\Omega)} + \|(\mu-\mu_\tau)(t)\|^2_{L^2(\Omega)}\right), \tag{4.49}$$

*where*

$$L(\mathbf{u}_\tau) = \left\| \mathbf{f} - \frac{\partial \mathbf{u}_\tau}{\partial t} - (\mathbf{u}_\tau \cdot \nabla)\mathbf{u}_\tau \right\|^2_{L^\infty(\Omega\times(0,T))} + \|D(\mathbf{u}_\tau)\|^2_{L^\infty(\Omega\times(0,T))},$$

*and* $\theta^{n+1}_{\mathbf{u},1}, \theta^{n+1}_{\mathbf{u},2}, \epsilon^{n+1}_{\mathbf{u},1}$ *and* $\epsilon^{n+1}_{\mathbf{u},2}$ *are given by Proposition 4.17.*

*Proof.* Let $n = 0, 1, 2, .., N-1$ and $t \in (t^n, t^{n+1})$. We use the identity (4.24) and the fact that $\operatorname{div}(\mathbf{u} - \mathbf{u}_\tau) = 0$. We have

$$\begin{aligned}
&\frac{1}{2}\frac{d}{dt}\int_\Omega \rho(\mathbf{u}-\mathbf{u}_\tau)^2 d\mathbf{x} + 2\int_\Omega \mu|D(\mathbf{u}-\mathbf{u}_\tau)|^2 d\mathbf{x} = \\
&\quad \int_\Omega \rho\frac{\partial}{\partial t}(\mathbf{u}-\mathbf{u}_\tau)\cdot(\mathbf{u}-\mathbf{u}_\tau)d\mathbf{x} + \int_\Omega \rho(((\mathbf{u}-\mathbf{u}_\tau)\cdot\nabla)(\mathbf{u}-\mathbf{u}_\tau))\cdot(\mathbf{u}-\mathbf{u}_\tau)d\mathbf{x} \\
&\qquad + 2\int_\Omega \mu D(\mathbf{u}-\mathbf{u}_\tau) : D(\mathbf{u}-\mathbf{u}_\tau)d\mathbf{x} - \int_\Omega (p-p_\tau)\operatorname{div}(\mathbf{u}-\mathbf{u}_\tau)d\mathbf{x}.
\end{aligned}$$

Using the fact that $\mathbf{u}, p, \rho, \mu$ are the exact solution and rewriting the other terms, we have

$$\begin{aligned}
&\frac{1}{2}\frac{d}{dt}\int_\Omega \rho(\mathbf{u}-\mathbf{u}_\tau)^2 d\mathbf{x} + 2\int_\Omega \mu|D(\mathbf{u}-\mathbf{u}_\tau)|^2 d\mathbf{x} = \\
&\quad \int_\Omega \rho\mathbf{f}\cdot(\mathbf{u}-\mathbf{u}_\tau)d\mathbf{x} - \int_\Omega \rho_\tau\frac{\partial \mathbf{u}_\tau}{\partial t}\cdot(\mathbf{u}-\mathbf{u}_\tau)d\mathbf{x} - \int_\Omega \rho_\tau((\mathbf{u}_\tau\cdot\nabla)\mathbf{u}_\tau)\cdot(\mathbf{u}-\mathbf{u}_\tau)d\mathbf{x} \\
&\qquad - 2\int_\Omega \mu_\tau D(\mathbf{u}_\tau) : D(\mathbf{u}-\mathbf{u}_\tau)d\mathbf{x} + \int_\Omega p_\tau \operatorname{div}(\mathbf{u}-\mathbf{u}_\tau)d\mathbf{x} \\
&\qquad - \int_\Omega (\rho-\rho_\tau)\frac{\partial \mathbf{u}_\tau}{\partial t}\cdot(\mathbf{u}-\mathbf{u}_\tau)d\mathbf{x} - \int_\Omega (\rho-\rho_\tau)(\mathbf{u}_\tau\cdot\nabla)\mathbf{u}_\tau)\cdot(\mathbf{u}-\mathbf{u}_\tau)d\mathbf{x} \\
&\qquad - 2\int_\Omega (\mu-\mu_\tau)D(\mathbf{u}_\tau) : D(\mathbf{u}-\mathbf{u}_\tau)d\mathbf{x} - \int_\Omega \rho(((\mathbf{u}-\mathbf{u}_\tau)\cdot\nabla)\mathbf{u}_\tau)\cdot(\mathbf{u}-\mathbf{u}_\tau)d\mathbf{x}.
\end{aligned}$$

Using Proposition 4.17, we finally have

$$\begin{aligned}
&\frac{1}{2}\frac{d}{dt}\int_\Omega \rho(\mathbf{u}-\mathbf{u}_\tau)^2 d\mathbf{x} + 2\int_\Omega \mu|D(\mathbf{u}-\mathbf{u}_\tau)|^2 d\mathbf{x} = \\
&\quad - \int_\Omega (\theta^{n+1}_{\mathbf{u},1} + \epsilon^{n+1}_{\mathbf{u},1})\cdot(\mathbf{u}-\mathbf{u}_\tau)d\mathbf{x} - \int_\Omega (\theta^{n+1}_{\mathbf{u},2} + \epsilon^{n+1}_{\mathbf{u},2}) : D(\mathbf{u}-\mathbf{u}_\tau)d\mathbf{x} \\
&\qquad - \int_\Omega (\rho-\rho_\tau)\left(\mathbf{f} - \frac{\partial \mathbf{u}_\tau}{\partial t} - (\mathbf{u}_\tau\cdot\nabla)\mathbf{u}_\tau\right)\cdot(\mathbf{u}-\mathbf{u}_\tau)d\mathbf{x} \\
&\qquad - 2\int_\Omega (\mu-\mu_\tau)D(\mathbf{u}_\tau) : D(\mathbf{u}-\mathbf{u}_\tau)d\mathbf{x} - \int_\Omega \rho(((\mathbf{u}-\mathbf{u}_\tau)\cdot\nabla)\mathbf{u}_\tau)\cdot(\mathbf{u}-\mathbf{u}_\tau)d\mathbf{x}.
\end{aligned}$$

We now conclude by using Hölder, Poincaré and Young's inequality, and the hypothesis (4.52) to pass to the left hand side the quantity

$$\int_\Omega \rho(((\mathbf{u}-\mathbf{u}_\tau)\cdot\nabla)\mathbf{u}_\tau)\cdot(\mathbf{u}-\mathbf{u}_\tau)d\mathbf{x}.$$

Korn's inequality yield the final result. □

**Proposition 4.20** (Estimate for the density and the viscosity).
*Let* $\mathbf{u}$ *be the exact velocity field and* $\rho, \mu$ *the exact density and viscosity that are solutions of (4.6)-(4.7). Let* $(\mathbf{u}^n)_{n=0}^N, (\rho^n, \mu^n)_{n=0}^N$ *be the solutions of (4.43)-(4.45). Let* $\mathbf{u}_\tau, p_\tau, \rho_\tau, \mu_\tau$ *the piecewise reconstructions of the numerical solutions given by*

$$\mathbf{u}_\tau(t) = \mathbf{u}_{\tau,1}(t) = \mathbf{u}^{1/2} + (t - t^{1/2})\partial\mathbf{u}^1, t \in [t^0, t^1],$$

$$\rho_\tau(t) = \rho_{\tau,1}(t) = \rho^{1/2} + (t - t^{1/2})\partial\rho^1, \mu_\tau(t) = \mu_{\tau,1}(t) = \mu^{1/2} + (t - t^{1/2})\partial\mu^1, t \in [t^0, t^1],$$

*and for all $n = 1, 2, ..., N-1$ and all $t \in [t^n, t^{n+1}]$ by*

$$\mathbf{u}_\tau(t) = \mathbf{u}_{\tau,2}(t) = \mathbf{u}^{n+1/2} + (t - t^{n+1/2})\partial\mathbf{u}^{n+1} + \frac{1}{2}(t-t^n)(t-t^{n+1})\partial^2\mathbf{u}^{n+1},$$

$$\rho_\tau(t) = \rho_{\tau,2}(t) = \rho^{n+1/2} + (t - t^{n+1/2})\partial\rho^{n+1} + \frac{1}{2}(t-t^n)(t-t^{n+1})\partial^2\rho^{n+1},$$

$$\mu_\tau(t) = \mu_{\tau,2}(t) = \mu^{n+1/2} + (t - t^{n+1/2})\partial\mu^{n+1} + \frac{1}{2}(t-t^n)(t-t^{n+1})\partial^2\mu^{n+1}.$$

*Then, for every $n = 0, 1, 2, ..., N-1$ and any $t \in (t^n, t^{n+1})$, it holds*

$$\begin{aligned}\frac{d}{dt}\|(\rho-\rho_\tau)(t)\|^2_{L^2(\Omega)} &\le 2c_n\left(\|\theta^{n+1}_\rho(t)\|^2_{L^2(\Omega)} + \|\epsilon^{n+1}_\rho(t)\|^2_{L^2(\Omega)}\right)\\ &+\left(c_n^{-1} + \|\nabla\rho_\tau\|^2_{L^\infty(\Omega\times(0,T))}\frac{2C_P^2}{\mu_{\min}}\right)\|(\rho-\rho_\tau)(t)\|^2_{L^2(\Omega)} + \frac{\mu_{\min}}{2}\|\nabla(\mathbf{u}-\mathbf{u}_\tau)(t)\|^2_{L^2(\Omega)},\end{aligned} \tag{4.50}$$

*where $C_P$ stands for the Poincaré constant of $\Omega$ and $\theta^{n+1}_\rho$ and $\epsilon^{n+1}_\rho$ are given by Proposition 4.18 and*

$$c_n = \begin{cases} T, n \ge 1,\\ \tau^1, n = 0.\end{cases}$$

*Likewise for the viscosity, it holds*

$$\begin{aligned}\frac{d}{dt}\|(\mu-\mu_\tau)(t)\|^2_{L^2(\Omega)} &\le 2c_n\left(\|\theta^{n+1}_\mu(t)\|^2_{L^2(\Omega)} + \|\epsilon^{n+1}_\mu(t)\|^2_{L^2(\Omega)}\right)\\ &+\left(c_n^{-1} + \|\nabla\mu_\tau\|^2_{L^\infty(\Omega\times(0,T))}\frac{2C_P^2}{\mu_{\min}}\right)\|(\mu-\mu_\tau)(t)\|^2_{L^2(\Omega)} + \frac{\mu_{\min}}{2}\|\nabla(\mathbf{u}-\mathbf{u}_\tau)(t)\|^2_{L^2(\Omega)},\end{aligned} \tag{4.51}$$

*where $\theta^{n+1}_\mu$ and $\epsilon^{n+1}_\mu$ are given by Proposition 4.18.*

*Proof.* We only prove the result for the density, the same computations yield to the conclusion for the viscosity. Let $n = 0, 1, 2, .., N-1$ and $t \in [t^n, t^{n+1}]$. Using the fact that $\mathbf{u}$ is divergence free and that $\rho$ satisfies the mass equation, we have

$$\begin{aligned}\frac{d}{dt}\frac{1}{2}\|\rho-\rho_\tau\|^2_{L^2(\Omega)} &= \int_\Omega \frac{\partial}{\partial t}(\rho-\rho_\tau)(\rho-\rho_\tau)d\mathbf{x} + \int_\Omega \left(\mathbf{u}\cdot\nabla(\rho-\rho_\tau)\right)(\rho-\rho_\tau)d\mathbf{x}\\ &= -\int_\Omega \frac{\partial\rho_\tau}{\partial t}(\rho-\rho_\tau)d\mathbf{x} - \int_\Omega \left(\mathbf{u}\cdot\nabla\rho_\tau\right)(\rho-\rho_\tau)d\mathbf{x}\\ &= -\int_\Omega \frac{\partial\rho_\tau}{\partial t}(\rho-\rho_\tau)d\mathbf{x} - \int_\Omega \left(\mathbf{u}_\tau\cdot\nabla\rho_\tau\right)(\rho-\rho_\tau)d\mathbf{x} - \int_\Omega \left((\mathbf{u}-\mathbf{u}_\tau)\cdot\nabla\rho_\tau\right)(\rho-\rho_\tau)d\mathbf{x}.\end{aligned}$$

By the Proposition 4.18, we then have

$$\frac{1}{2}\frac{d}{dt}\|\rho-\rho_\tau\|^2_{L^2(\Omega)} = -\int_\Omega(\theta^{n+1}_\rho + \epsilon^{n+1}_\rho)(\rho-\rho_\tau)d\mathbf{x} - \int_\Omega \left((\mathbf{u}-\mathbf{u}_\tau)\cdot\nabla\rho_\tau\right)(\rho-\rho_\tau)d\mathbf{x}.$$

We then conclude by using the Cauchy-Schwarz, Young's and Poincaré inequalities, and integrating over the time and we obtain

$$\begin{aligned}\frac{d}{dt}\|\rho-\rho_\tau\|^2_{L^2(\Omega)} &\le \frac{2}{\varepsilon}\left(\|\theta^{n+1}_\rho(t)\|^2_{L^2(\Omega)} + \|\epsilon^{n+1}_\rho(t)\|^2_{L^2(\Omega)}\right)\\ &\quad + (\varepsilon + \|\nabla\rho_\tau\|^2_{L^\infty(\Omega\times(0,T))}\varepsilon')\|(\rho-\rho_\tau)(t)\|^2_{L^2(\Omega)}ds + \frac{C_P^2}{\varepsilon'}\|\nabla(\mathbf{u}-\mathbf{u}_\tau)(t)\|^2_{L^2(\Omega)}.\end{aligned}$$

Anticipating the next proofs, we choose $\varepsilon = c_n^{-1}$ and $\varepsilon' = \frac{2C_P^2}{\mu_{\min}}$. ☐

We now have all the ingredients to derive an a posteriori error estimate for the time discretization (4.43)-(4.45). Observe that, contrary to what we were able to do in the previous section for the spatial approximation, it is not possible to obtain a "close" estimate for the velocity error independently of the viscosity/density errors, and inversely. This is due to the fact that all the quantities have a priori the same order of convergence (namely 2), while in the case of the spatial approximation, the $L^2$ norm $\|\mathbf{u}-\mathbf{u}_h\|_{L^2(\Omega)}$ converge faster than $\|\rho-\rho_h\|_{L^2(\Omega)} + \|\mu-\mu_h\|_{L^2(\Omega)}$, that converges in turn faster than $\|\nabla(\mathbf{u}-\mathbf{u}_h)\|_{L^2(\Omega)}$. Therefore all the "bad" terms involving one unknown when trying to estimate the error for another could be put in the higher order terms. For the time discretization, the estimate must be done in "a one shot". Our final a posteriori error estimate is then contained in the next Theorem

**Theorem 4.21** (A posteriori error estimate in time for the Navier-Stokes equations with variable density and viscosity)**.**
*Let* $(\mathbf{u}, p)$ *be the exact velocity and pressure fields and* $\rho, \mu$ *the exact density and viscosity that are solutions of (4.6)-(4.7).Let* $(\mathbf{u}^n, p^n)_{n=0}^N, (\rho^n, \mu^n)_{n=0}^N$ *be the solutions of (4.43)-(4.45). Let* $\mathbf{u}_\tau, p_\tau, \rho_\tau, \mu_\tau$ *the piecewise reconstructions of the numerical solutions given by*

$$\mathbf{u}_\tau(t) = \mathbf{u}_{\tau,1}(t) = \mathbf{u}^1 + (t-t^1)\partial\mathbf{u}^1, p_\tau(t) = p_{\tau,0}(t) = p^1, t \in [t^0, t^1],$$

$$\rho_\tau(t) = \rho_{\tau,1}(t) = \rho^1 + (t-t^1)\partial\rho^1, \mu_\tau(t) = \mu_{\tau,1}(t) = \mu^1 + (t-t^1)\partial\mu^1, t \in [t^0, t^1],$$

*and for all* $n = 1, 2, ..., N-1$ *and all* $t \in [t^n, t^{n+1}]$ *by*

$$\mathbf{u}_\tau(t) = \mathbf{u}_{\tau,2}(t) = \mathbf{u}^{n+1} + (t-t^{n+1})\partial\mathbf{u}^{n+1} + \frac{1}{2}(t-t^n)(t-t^{n+1})\partial^2\mathbf{u}^{n+1},$$

$$p_\tau(t) = p_{\tau,1}(t) = p^{n+1} + (t-t^{n+1})\partial p^{n+1},$$

$$\rho_\tau(t) = \rho_{\tau,2}(t) = \rho^{n+1} + (t-t^{n+1})\partial\rho^{n+1} + \frac{1}{2}(t-t^n)(t-t^{n+1})\partial^2\rho^{n+1},$$

$$\mu_\tau(t) = \mu_{\tau,2}(t) = \mu^{n+1} + (t-t^{n+1})\partial\mu^{n+1} + \frac{1}{2}(t-t^n)(t-t^{n+1})\partial^2\mu^{n+1}.$$

*Let assume finally that there exists* $0 < \gamma < 1$ *and* $\tau_0$ *small enough such that for all* $\tau \leq \tau_0$ *we have*

$$\sup_{t\in(0,T)} \|\nabla\mathbf{u}_\tau(t)\|_{L^2(\Omega)} \leq \frac{\gamma\mu_{\min}}{C_{SOB}\rho_{\max}}, \tag{4.52}$$

*where* $C_{SOB}$ *is the Sobolev constant of Proposition A.8 in Appendix. Then, there exists a constant* $C > 0$ *that depends only on* $\Omega$ *such that for all* $\tau \leq \tau_0$

$$\begin{aligned}
&\rho_{\min}\|(\mathbf{u}-\mathbf{u}_\tau)(T)\|^2_{L^2(\Omega)} + \mu_{\min}\int_0^T \|\nabla(\mathbf{u}-\mathbf{u}_\tau)(s)\|^2_{L^2(\Omega)}ds + \|(\rho-\rho_\tau)(T)\|^2_{L^2(\Omega)} + \|(\mu-\mu_\tau)(T)\|^2_{L^2(\Omega)} \\
&\leq C\exp(C_\infty T)\sum_{n=0}^{N-1}\int_{t^n}^{t^{n+1}} c_n\|\theta_\rho^{n+1}(t)\|^2_{L^2(\Omega)} + \|\epsilon_\rho^{n+1}(t)\|^2_{L^2(\Omega)} + \|\theta_\mu^{n+1}(t)\|^2_{L^2(\Omega)} + \|\epsilon_\mu^{n+1}(t)\|^2_{L^2(\Omega)}dt \\
&+ \frac{C}{\mu_{\min}(1-\gamma)^2}\exp(C_\infty T)\sum_{n=0}^{N-1}\int_{t^n}^{t^{n+1}} \|\theta_{\mathbf{u},1}^{n+1}(t)\|^2_{L^2(\Omega)} + \|\theta_{\mathbf{u},2}^{n+1}(t)\|^2_{L^2(\Omega)} + \|\epsilon_{\mathbf{u},1}^{n+1}(t)\|^2_{L^2(\Omega)} + \|\epsilon_{\mathbf{u},2}^{n+1}(t)\|^2_{L^2(\Omega)}dt,
\end{aligned} \tag{4.53}$$

*where*

$$C_\infty = \frac{Cc_n^{-1}T + L(\mathbf{u}_\tau, \rho_\tau, \mu_\tau)T}{\mu_{\min}(1-\gamma)^2},$$

$$L(\mathbf{u}_\tau, \rho_\tau, \mu_\tau) = \left\| \mathbf{f} - \frac{\partial \mathbf{u}_\tau}{\partial t} - (\mathbf{u}_\tau \cdot \nabla)\mathbf{u}_\tau \right\|^2_{L^\infty(\Omega\times(0,T))} + \|D(\mathbf{u}_\tau)\|^2_{L^\infty(\Omega\times(0,T))} + \|\nabla \rho_\tau\|^2_{L^\infty(\Omega\times(0,T))} + \|\nabla \mu_\tau\|^2_{L^\infty(\Omega\times(0,T))},$$

*and*

$$c_n = \begin{cases} T, n \geq 1, \\ \tau^1, n = 0. \end{cases}$$

*The error indicators $\theta_\rho^{n+1}, \theta_\mu^{n+1}, \theta_{\mathbf{u},1}^{n+1}, \theta_{\mathbf{u},2}^{n+1}, \epsilon_\rho^{n+1}, \epsilon_\mu^{n+1}, \epsilon_{\mathbf{u},1}^{n+1}, \epsilon_{\mathbf{u},2}^{n+1}$ are given by Propositions 4.17 and 4.18.*

*Proof.* The proof is straightforward by summing the three estimates (4.50),(4.51) and (4.49) and then use the Gronwall's Lemma. Note that the initial errors

$$\|(\rho - \rho_\tau)(0)\|_{L^2(\Omega)}, \|(\mu - \mu_\tau)(0)\|_{L^2(\Omega)}, \|(\mathbf{u} - \mathbf{u}_\tau)(0)\|_{L^2(\Omega)}$$

are zero, and then disappear from the estimate, since

$$\rho_\tau(0) = \rho^0 = \rho_0 = \rho(0)$$

and similarly for $\mu$ and $\mathbf{u}$. □

**Remark 4.22** (Final remarks for the derivation of a posteriori error estimates for the Navier-Stokes equations with variable density and/or viscosity)**.**
Here, as we already pointed out for the results of Section 4.2 where we consider only the spatial approximation of the equations, we never use in fact the particular form of the density or the viscosity, namely that

$$\rho = \rho_1\varphi + \rho_2(1-\varphi), \quad \mu = \mu_1\varphi + \mu_2(1-\varphi).$$

In fact we only use the fact that both the density and the viscosity satisfies the transport equation and are bounded. Therefore, our results stay valid for more general cases of non-homogeneous Navier-Stokes equations, with more general coefficients.

Observe finally that all the results presented in this section are independent of the dimension and hold in $\mathbb{R}^d$, for $d = 2$ ou $d = 3$.

## 4.4 A numerical method to solve a free surface problem with stabilized anisotropic finite elements and order two time advancing schemes

In this section, we present a fully discretized method to approximate the solution of (4.6)-(4.7). We will use the methods introduced in the previous Chapters, namely stabilized anisotropic finite elements for the spatial approximation and the BDF2/Crank-Nicolson method to advance in time. The BDF2 method is chosen to solve the Navier-Stokes equations and the Crank-Nicolson scheme for the transport equation. For the spatial discretization, the Petrov-Galerkin method introduced in Chapter 3 is used to solve the momentum equations, and the SUPG method described in Chapter 2 is used to solve the transport of the density and the velocity. The numerical method reads as follows. For all $h > 0$, let $\mathcal{T}_h$ be a conformal triangle of $\Omega$ into triangles $K$ of diameter $h_K \leq h$. We choose $V_h, Q_h$ the discrete functional spaces introduced in Chapter 3 to approximate the velocity and the pressure. For the transport of the phase, we shall use $\Psi_h$ that is simply the set of piecewise linear functions on $\mathcal{T}_h$. Let also $N$ be a positive integer and $0 = t^0 < t^1 < ... < t^N = T$ be a partition of $[0,T]$. Then starting from $\mathbf{u}_h^0 = r_h(u_0)$

and $\varphi_h^0 = r_h(\varphi_0)$, where $\mathbf{u}_0, \varphi_0$ are the initial velocity and phase, we are looking for any $n = 0, 1, ..N-1$ for $(\mathbf{u}_h^{n+1}, p_h^{n+1}) \in V_h \times Q_h$ and $\varphi_h^{n+1} \in \Psi_h$, the solutions of

$$\int_\Omega \rho_h^{n+1}\left(\partial \mathbf{u}_h^{n+1} + \frac{\beta^{n+1}\tau^{n+1}}{2}\partial^2 \mathbf{u}_h^{n+1}\right)\cdot \mathbf{v}_h d\mathbf{x} + \int_\Omega \rho_h^{n+1}(\mathbf{u}_h^{n+1}\cdot\nabla)\mathbf{u}_h^{n+1}\cdot\mathbf{v}_h d\mathbf{x}$$
$$+ \int_\Omega 2\mu_h^{n+1} D(\mathbf{u}_h^{n+1}) : D(\mathbf{v}_h) d\mathbf{x} - \int_\Omega p_h^{n+1}\operatorname{div}\mathbf{v}_h d\mathbf{x}$$
$$+ \sum_{K\in\mathcal{T}_h}\alpha_K^{n+1}\int_K R_{h,n+1}^{NS}\cdot\left(\rho_h^{n+1}(\mathbf{u}_h^{n+1}\cdot\nabla)\mathbf{v}_h\right)d\mathbf{x} = \int_\Omega \rho_h^{n+1}\mathbf{f}^{n+1}\cdot\mathbf{v}_h d\mathbf{x}, \forall \mathbf{v}_h \in V_h, \quad (4.54)$$

$$-\int_\Omega q_h \operatorname{div}\mathbf{u}_h^{n+1} d\mathbf{x} + \sum_{K\in\mathcal{T}_h}\alpha_K\int_K R_{h,n+1}^{NS}\cdot\nabla q_h d\mathbf{x} = 0, \forall q_h \in Q_h, \quad (4.55)$$

$$\int_\Omega\left(\frac{\varphi_h^{n+1}-\varphi_h^n}{\tau^{n+1}} + \mathbf{u}_h^{n+1/2}\cdot\nabla\left(\frac{\varphi_h^{n+1}+\varphi_h^n}{2}\right)\right)\psi_h d\mathbf{x}$$
$$+ \sum_{K\in\mathcal{T}_h}\delta_K^{n+1}\int_K R_{h,n+1}^{transport}\left(\mathbf{u}_h^{n+1/2}\cdot\nabla\psi_h\right)d\mathbf{x} = 0, \forall\psi_h\in\Psi_h, \quad (4.56)$$

$$\rho_h^{n+1} = \rho_1\varphi_h^{n+1} + \rho_2(1-\varphi_h^{n+1}), \mu_h^{n+1} = \mu_1\varphi_h^{n+1} + \mu_2(1-\varphi_h^{n+1}), \quad (4.57)$$

where we note $\mathbf{f}^{n+1} = \mathbf{f}(t^{n+1})$, $\beta^{n+1} = 1, n > 0, \beta^1 = 0$ and the residuals of the equations.

$$R_{h,n+1}^{NS} = \rho_h^{n+1}\mathbf{f}^{n+1} - \rho_h^{n+1}\left(\partial\mathbf{u}_h^{n+1} + \frac{\beta^{n+1}\tau^{n+1}}{2}\partial^2\mathbf{u}_h^{n+1}\right) - \rho_h^{n+1}(\mathbf{u}_h^{n+1}\cdot\nabla)\mathbf{u}_h^{n+1}$$
$$+ \operatorname{div}(2\mu_h^{n+1}D(\mathbf{u}_h^{n+1})) - \nabla p_h^{n+1}, \quad (4.58)$$

and

$$R_{h,n+1}^{transport} = \frac{\varphi_h^{n+1}-\varphi_h^n}{\tau^{n+1}} + \mathbf{u}_h^{n+1/2}\cdot\nabla\left(\frac{\varphi_h^{n+1}+\varphi_h^n}{2}\right). \quad (4.59)$$

$\alpha_K^{n+1}$ and $\delta_K^{n+1}$ are respectively the Navier-Stokes equations and the transport equation stabilization parameter that we choose as follows. We define

$$\alpha_K^{n+1} = \frac{\alpha\lambda_{2,K}^2}{\mu_K^{n+1}\xi(Re_K^{n+1})}, \alpha > 0,$$

where

$$\xi(Re_K^{n+1}) = \begin{cases} 1 & \text{if } Re_K^{n+1} \le 1, \\ Re_K & \text{if } Re_K^{n+1} \ge 1, \end{cases}$$

$$Re_K^{n+1} = \frac{\|\rho_h^{n+1}\mathbf{u}_h^{n+1}\|_{L^\infty(K)}\lambda_{2,K}}{\mu_K^{n+1}},$$

and $\mu_K^{n+1}$ denotes the minimal viscosity in the triangle $K$ at the iteration $n+1$. For the transport, we choose

$$\delta_K^{n+1} = \frac{\delta\lambda_{2,K}}{\|\mathbf{u}_h^{n+1}\|_{L^\infty(K)}}, \delta > 0,$$

and we set $\delta_K = 0$ in case $\mathbf{u}_h^{n+1}$ is null in $K$. In practice, we choose $\alpha = 0.01$ and $\delta = 0.5$.

**Remark 4.23** (Computational aspect).
In practice, the problem (4.54)-(4.57) is decoupled in the implementation. For simplification, let us consider only the time discretization. Then given the solutions at step $n$, we compute the solutions at step $n+1$ by solving first the transport problem

$$\frac{\varphi^{n+1}-\varphi^n}{\tau^{n+1}} + \frac{\mathbf{u}^*+\mathbf{u}^n}{2}\cdot\nabla\left(\frac{\varphi_h^{n+1}+\varphi_h^n}{2}\right) = 0,$$

and then by solving one step of the Newton method applied to the momentum equation

$$\rho^{n+1}\left(\frac{\mathbf{u}^{n+1}-\mathbf{u}^n}{\tau^{n+1}} + \frac{\beta^{n+1}\tau^{n+1}}{2}\partial^2\mathbf{u}^{n+1}\right) + \rho^{n+1}\left((\mathbf{u}^*\cdot\nabla)\mathbf{u}_h^{n+1} + (\mathbf{u}_h^{n+1}\cdot\nabla)\mathbf{u}^*\right)$$
$$- \operatorname{div}(2\mu^{n+1}D(\mathbf{u}^{n+1})) + \nabla p^{n+1} = \rho^{n+1}\mathbf{f}^{n+1} + \rho^{n+1}(\mathbf{u}^*\cdot\nabla)\mathbf{u}^*,$$

where we choose $\mathbf{u}^*$ as the extrapolated velocity of $\mathbf{u}^{n+1}$ obtained through

$$\mathbf{u}^* = 2\mathbf{u}^n - \mathbf{u}^{n-1}.$$

Since we need $\mathbf{u}^1$, to initialize the method, we solve at the first step the momentum equation with an Euler method, using $\rho^0$ and $\mu^0$, and then we solve the transport equation with the Crank-Nicolson method using $\mathbf{u}^{1/2}$ as transport velocity to obtain $\rho^1, \mu^1$. Finally, we start the splitting presented above from $n=1$.

## 4.5 Error indicators and adaptive algorithm for two fluids flows separated by a free surface

In this section, we first introduce the error indicators for the numerical method presented in Section 4.4 that we will use later on in our adaptive algorithm. The choice of the error indicators are motivated by the semi-discrete a posteriori error estimates obtained in the previous sections, namely Theorems 4.14 and 4.21. We first define the spatial error indicators $\eta_{\mathbf{u}}^A$ and $\eta_\rho^A$, $\eta_\mu^A$ that stand respectively for the anisotropic spatial velocity error indicator and the density/viscosity anisotropic spatial error indicators.

We choose to not put all the terms of the a posteriori error estimates in our error indicators, and rather to choose those that are "natural" for us, based on the previous results obtained when solving each equations separately. This is obviously an arbitrary choice, and a more careful numerical analysis of the complete error estimators should be performed to determine which parts are the dominant ones. However, in practice, we obtain significant results with our choices, the most important is to choose quantities that contained informations about the spatial and temporal discretizations for all the unknowns.

For the velocity, we set

$$\eta_{\mathbf{u}}^A = \left(\sum_{n=0}^{N-1}\sum_{K\in\mathcal{T}_h}(\eta_{K,n,\mathbf{u}}^A)^2\right)^{1/2}, \tag{4.60}$$

where

$$(\eta_{K,n,\mathbf{u}}^A)^2$$
$$= \tau^{n+1}\left(\left\|\rho_h^{n+1}\mathbf{f} - \rho_h^{n+1}\left(\partial_{\beta^{n+1}}\mathbf{u}_h^{n+1}\right) - \rho_h^{n+1}(\mathbf{u}_h^{n+1}\cdot\nabla)\mathbf{u}_h^{n+1} + \operatorname{div}(2\mu_h^{n+1}D(\mathbf{u}_h^{n+1})) - \nabla p_h^{n+1}\right\|_{L^2(K)}\right.$$
$$\left. + \frac{1}{2\sqrt{\lambda_{2,K}}}\left\|\left[\mu_h^{n+1}D(\mathbf{u}_h^{n+1})\cdot\mathbf{n}\right]\right\|_{L^2(\partial K)}\right)\tilde{\omega}_K\left(\Pi_h^{ZZ}\mathbf{u}_h^{n+1} - \mathbf{u}_h^{n+1}\right),$$

where $\Pi_h^{ZZ}$ stands for the ZZ post-processing and $\tilde{\omega}_K$ for the simplified anisotropic form given by (1.18). Here $\partial_{\beta^{n+1}}$ stands for

$$\partial \mathbf{u}_h^{n+1} + \frac{\beta^{n+1}\tau^{n+1}}{2}\partial^2 \mathbf{u}_h^{n+1}$$

where $\beta^{n+1} = 0$ if we solve an Euler step ($n = 0$) and 1 otherwise ($n > 0$).

The spatial error indicator for the density and the viscosity are given by

$$\eta_\rho^A = \left(\sum_{n=0}^{N-1}\sum_{K\in\mathcal{T}_h}(\eta_{K,n,\rho}^A)^2\right)^{1/2}, \eta_\mu^A = \left(\sum_{n=0}^{N-1}\sum_{K\in\mathcal{T}_h}(\eta_{K,n,\mu}^A)^2\right)^{1/2}, \tag{4.61}$$

where

$$(\eta_{K,n,\rho}^A)^2 = \tau^{n+1}\left\|\partial\rho_h^{n+1} + \mathbf{u}_h^{n+1}\cdot\nabla\rho_h^{n+1}\right\|_{L^2(K)}\tilde{\omega}_K(\Pi_h^{ZZ}\rho_h^{n+1} - \rho_h^{n+1}),$$

and

$$(\eta_{K,n,\mu}^A)^2 = \tau^{n+1}\left\|\partial\mu_h^{n+1} + \mathbf{u}_h^{n+1}\cdot\nabla\mu_h^{n+1}\right\|_{L^2(K)}\tilde{\omega}_K(\Pi_h^{ZZ}\mu_h^{n+1} - \mu_h^{n+1}).$$

By anticipating what follows, we define also the local error indicators in the direction $x_i, i = 1, 2$, that are given by

$$\begin{aligned}
&(\eta_{i,K,n,\mathbf{u}}^A)^2 \\
&= \tau^{n+1}\left(\left\|\rho_h^{n+1}\mathbf{f} - \rho_h^{n+1}\left(\partial_{\beta^{n+1}}\mathbf{u}_h^{n+1}\right) - \rho_h^{n+1}(\mathbf{u}_h^{n+1}\cdot\nabla)\mathbf{u}_h^{n+1} + \operatorname{div}(2\mu_h^{n+1}D(\mathbf{u}_h^{n+1})) - \nabla p_h^{n+1}\right\|_{L^2(K)}\right. \\
&\qquad \left. + \frac{1}{2\sqrt{\lambda_{2,K}}}\left\|\left[\mu_h^{n+1}D(\mathbf{u}_h^{n+1})\cdot\mathbf{n}\right]\right\|_{L^2(\partial K)}\right)\tilde{\omega}_{i,K}\left(\Pi_h^{ZZ}\mathbf{u}_h^{n+1} - \mathbf{u}_h^{n+1}\right),
\end{aligned}$$

and

$$(\eta_{i,K,n,\rho}^A)^2 = \tau^{n+1}\left\|\partial\rho_h^{n+1} + \mathbf{u}_h^{n+1}\cdot\nabla\rho_h^{n+1}\right\|_{L^2(K)}\tilde{\omega}_{i,K}(\Pi_h^{ZZ}\rho_h^{n+1} - \rho_h^{n+1}),$$

$$(\eta_{i,K,n,\mu}^A)^2 = \tau^{n+1}\left\|\partial\mu_h^{n+1} + \mathbf{u}_h^{n+1}\cdot\nabla\mu_h^{n+1}\right\|_{L^2(K)}\tilde{\omega}_{i,K}(\Pi_h^{ZZ}\mu_h^{n+1} - \mu_h^{n+1}).$$

For the time error indicators, we define for the velocity one

$$\eta_{\mathbf{u}}^T = \left(\sum_{n=0}^{N-1}\sum_{K\in\mathcal{T}_h}(\eta_{K,n,\mathbf{u}}^T)^2\right)^{1/2}, \tag{4.62}$$

where

$$(\eta_{K,0,\mathbf{u}}^T)^2 = (\tau^1)^3\left\|\rho_h^1\left((\mathbf{u}_h^1\cdot\nabla)\partial\mathbf{u}_h^1 + (\partial\mathbf{u}_h^1\cdot\nabla)\mathbf{u}_h^1\right)\right\|_{L^2(K)}^2 + (\tau^1)^3\left\|2\mu_h^1 D(\partial\mathbf{u}_h^1)\right\|_{L^2(K)}^2.$$

and for $n \geq 1$

$$\begin{aligned}
(\eta_{K,n,\mathbf{u}}^T)^2 = (\tau^{n+1})^5\left\|\rho_h^{n+1}\left((\mathbf{u}_h^{n+1}\cdot\nabla)\partial^2\mathbf{u}_h^{n+1} + (\partial\mathbf{u}_h^{n+1}\cdot\nabla)\partial\mathbf{u}_h^{n+1} + (\partial^2\mathbf{u}_h^{n+1}\cdot\nabla)\mathbf{u}_h^{n+1}\right)\right\|_{L^2(K)}^2 \\
+ (\tau^{n+1})^5\left\|2\mu_h^{n+1}D(\partial^2\mathbf{u}_h^{n+1})\right\|_{L^2(K)}^2.
\end{aligned}$$

Finally, for the density/viscosity error indicators, we choose

$$\eta_\rho^T = \left(\sum_{n=0}^{N-1}\sum_{K\in\mathcal{T}_h}(\eta_{K,n,\rho}^T)^2\right)^{1/2}, \eta_\mu^T = \left(\sum_{n=0}^{N-1}\sum_{K\in\mathcal{T}_h}(\eta_{K,n,\mu}^T)^2\right)^{1/2}, \tag{4.63}$$

where

$$(\eta^T_{K,0,\rho})^2 = (\tau^1)^4 \left\| \mathbf{u}_h^{1/2} \cdot \nabla \partial \rho_h^1 \right\|^2_{L^2(K)}, (\eta^T_{K,0,\mu})^2 = (\tau^1)^4 \left\| \mathbf{u}_h^{1/2} \cdot \nabla \partial \mu_h^1 \right\|^2_{L^2(K)},$$

and for $n \geq 1$

$$(\eta^T_{K,n,\rho})^2 = T(\tau^{n+1})^5 \left\| \mathbf{u}_h^{n+1/2} \cdot \nabla \partial^2 \rho_h^{n+1} \right\|^2_{L^2(K)}, (\eta^T_{K,n,\mu})^2 = T(\tau^{n+1})^5 \left\| \mathbf{u}_h^{n+1/2} \cdot \nabla \partial^2 \mu_h^{n+1} \right\|^2_{L^2(K)}.$$

We now define the complete spatial and temporal error indicators by

$$\eta^A = \left( \sum_{n=0}^{N-1} \sum_{K \in \mathcal{T}_h} (\eta^A_{K,n})^2 \right)^{1/2},$$

where

$$(\eta^A_{K,n})^2 = (\eta^A_{K,n,\mathbf{u}})^2 + (\eta^A_{K,n,\rho})^2 + (\eta^A_{K,n,\mu})^2$$

and

$$\eta^T = \left( \sum_{n=0}^{N-1} \sum_{K \in \mathcal{T}_h} (\eta^T_{K,n})^2 \right)^{1/2},$$

where

$$(\eta^T_{K,n})^2 = (\eta^T_{K,n,\mathbf{u}})^2 + (\eta^T_{K,n,\rho})^2 + (\eta^T_{K,n,\mu})^2.$$

Finally, the complete spatial error indicator in direction $x_i, i = 1, 2$ is defined by

$$\eta i^A = \left( \sum_{n=0}^{N-1} \sum_{K \in \mathcal{T}_h} (\eta^A_{i,K,n})^2 \right)^{1/2},$$

where

$$(\eta^A_{i,K,n})^2 = (\eta^A_{i,K,n,\mathbf{u}})^2 + (\eta^A_{i,K,n,\rho})^2 + (\eta^A_{i,K,n,\mu})^2$$

The goal of the adaptive algorithm is then, for a prescribed tolerance, to build a sequence of meshes and time step such that the estimated relative error satisfies

$$(1 - \alpha_{dist}) TOL \leq \left( \frac{(\eta^A)^2 + (\eta^T)^2}{\int_0^T \|\|\mathbf{u}_{h\tau}, \rho_{h\tau}, \mu_{h\tau}\|\|^2_{L^2(\Omega)} dt} \right)^{1/2} \leq (1 + \alpha_{dist}) TOL, \tag{4.64}$$

where

$$\|\|\mathbf{u}_{h\tau}, \rho_{h\tau}, \mu_{h\tau}\|\|^2_{L^2(\Omega)} = \|\sqrt{2\mu_{h,\tau}} D(\mathbf{u}_{h,\tau})\|^2_{L^2(\Omega)} + \|\rho_{h,\tau}\|^2_{L^2(\Omega)} + \|\mu_{h,\tau}\|^2_{L^2(\Omega)},$$

and $\mathbf{u}_{h,\tau}, \rho_{h,\tau}, \mu_{h,\tau}$ are continuous (linear or quadratic) piecewise reconstructions of the numerical approximations. The parameter $\alpha_{dist}$ will be set to 0.25 or 0.125 in the numerical experiments, and controls how close is the estimator from the tolerance. In practice, the smaller is $\alpha_{dist}$ the larger is the number of remeshings/changes of the time steps necessary to reach (4.64). To satisfy (4.64), we write $TOL$ as

$$TOL = \sqrt{TOL_S^2 + TOL_T^2}$$

where $TOL_S$ is the tolerance for the spatial error and $TOL_T$ the tolerance for the temporal error and we impose that for any $n$

$$(1 - \alpha_{dist})^2 TOL_S^2 \int_{t^n}^{t^{n+1}} \|\|\mathbf{u}_{h\tau}, \rho_{h\tau}, \mu_{h\tau}\|\|^2_{L^2(\Omega)} dt \leq \sum_{K \in \mathcal{T}_h} (\eta^A_{K,n})^2$$
$$\leq (1 + \alpha_{dist})^2 TOL_S^2 \int_{t^n}^{t^{n+1}} \|\|\mathbf{u}_{h\tau}, \rho_{h\tau}, \mu_{h\tau}\|\|^2_{L^2(\Omega)} dt, \tag{4.65}$$

and

$$(1-\alpha_{dist})^2 TOL_T^2 \int_{t^n}^{t^{n+1}} |||\mathbf{u}_{h\tau},\rho_{h\tau},\mu_{h\tau}|||^2_{L^2(\Omega)} dt \leq \sum_{K\in\mathcal{T}_h} (\eta^T_{K,n})^2$$
$$\leq (1+\alpha_{dist})^2 TOL_T^2 \int_{t^n}^{t^{n+1}} |||\mathbf{u}_{h\tau},\rho_{h\tau},\mu_{h\tau}|||^2_{L^2(\Omega)} dt. \quad (4.66)$$

Finally, as we did in Chapter 1,2 and 3, to equidistribute the spatial error indicator in the two directions of anisotropy, we define for every $P \in \mathcal{T}_h$ the pointwise error estimators

$$(\eta^A_{P,n})^2 = \sum_{\substack{K\in\mathcal{T}_h\\ P\in K}} (\eta^A_{K,n})^2, (\eta^A_{i,P,n})^2 = \sum_{\substack{K\in\mathcal{T}_h\\ P\in K}} (\eta^A_{i,K,n})^2, i=1,2.$$

Then, sufficient conditions to obtain (4.67) is that for all $P \in \mathcal{T}_h$ and for $i = 1, 2$,

$$3\frac{(1-\alpha_{dist})^2 TOL_S^2 \sigma_{P,n}}{2N_P} \int_{t^n}^{t^{n+1}} |||\mathbf{u}_{h\tau},\rho_{h\tau},\mu_{h\tau}|||^2_{L^2(\Omega)} dt \leq (\eta^A_{i,P,n})^2$$
$$\leq 3\frac{(1+\alpha_{dist})^2 TOL_S^2 \sigma_{P,n}}{2N_P} \int_{t^n}^{t^{n+1}} |||\mathbf{u}_{h\tau},\rho_{h\tau},\mu_{h\tau}|||^2_{L^2(\Omega)} dt, \quad (4.67)$$

where the equidistribution factor $\sigma_{P,n}$ is given by

$$\sigma_{P,n} \frac{(\eta^A_{1,P,n})^2 + (\eta^A_{2,P,n})^2}{(\eta^A_{P,n})^2}.$$

The adaptive algorithm, including the resmeshing and the interpolation between meshes, follows the procedure described in Chapter 1,2 and 3. Concerning the interpolation of the old solutions on the new generated meshes, we use the conservative algorithm of [5].

## 4.6 A first and academic numerical experiment

We now perform numerical experiments for an example with a known exact solution in order to check the convergence of the method (4.54)-(4.57).

We consider the continuous equations (4.6) in a cavity $\Omega = ]0,1[^2$. The viscosity is kept constant to a value of 1 and we compute the force term $\mathbf{f}$ such that the exact solutions are given by

$$\mathbf{u}(\mathbf{x},t) = \begin{pmatrix} t(1+4x_2(1-x_2))+1 \\ 0 \end{pmatrix}, \quad p(\mathbf{x},t) = 1 - x_1,$$

and

$$\rho(\mathbf{x},t) = 1 + \varphi(\mathbf{x},t), \quad \varphi(\mathbf{x},t) = H_\varepsilon\left(x_1 - 0.25 - \int_0^t \mathbf{u}_1(\mathbf{x},t)dt\right).$$

$\rho$ varies smoothly from 1 to 2 and is almost constant except in a boundary layer (initially situated at $x_1 = 0.25$) that is controlled by $\varepsilon$. Here we recall that $H_\varepsilon$ is the smoothing of the Heavyside graph (1.25), that we used several times already. This experiment can be seen as a modified Poiseuille flow. For the momentum equations, we apply Dirichlet boundary conditions on the left, bottom and top side of $\Omega$ and Neumann boundary conditions on the right side, so we do not have to impose a pressure. For the transport of $\varphi$, we impose a inflow boundary condition on the left side of the domain. Finally, the equations are solved until $T = 0.45$.

To check the convergence of the method, we introduce the following quantities :

$$e_{\mathbf{u}} = \left(\int_0^T \|\nabla(\mathbf{u} - \mathbf{u}_{h\tau})(t)\|^2_{L^2(\Omega)} dt\right)^{1/2},$$
$$e_p = \left(\int_0^T \|(p - p_{h\tau})(t)\|^2_{L^2(\Omega)} dt\right)^{1/2},$$
$$e_\rho = \|(\rho - \rho_{h\tau})(T)\|_{L^2(\Omega)},$$

where $\mathbf{u}_{h\tau}, p_{h\tau}, \rho_{h\tau}$ a continuous piecewise reconstruction of the numerical approximations $\mathbf{u}_h^n, p_h^n, \rho_h^n$.

To check the efficiency of our error indicators, we first compute $ei_{\mathbf{u}}^{ZZ}$ that stands for the effectivity index of the ZZ post-processing of the gradient of the velocity and $ei_\rho^{ZZ}$ that stands for the effectivity index of the ZZ post-processing of the gradient of the density. Both are expected to be close to 1. We also compute the effectivity index

$$ei = \left(\frac{(\eta^A)^2 + (\eta^T)^2}{e_{\mathbf{u}}^2 + e_\rho^2}\right)^{1/2}.$$

Note that to check the second order accuracy of $\eta^T$, we do not add the velocity contribution $\sum_{K\in\mathcal{T}_h}(\eta^T_{K,0,\mathbf{u}})^2$ at the first time step (this error indicator being only of order 3/2 due to the Euler step.)

Finally, to ensure that the semi-discrete a posteriori error estimate (4.41) yields an upper bound of optimal order (in particular to determine the order of $\nu_\rho^I$), we also compute $L^2$ error of the time derivative of the density

$$e_{\partial_t\rho} = \left\|\left(\frac{\partial\rho}{\partial t} - \frac{\partial\rho_{h\tau}}{\partial t}\right)(T)\right\|_{L^2(\Omega)},$$

that is expected to behave as $O(h^{3/2})$.

We first run a couple of experiments with constant time steps and fixed meshes. We choose $\varepsilon = 0.25$.

The convergence results are reported in Table 4.1 where the mesh size and the time step are chosen so that the error is mainly due to the space discretization. As expected $e_{\mathbf{u}}$ and $e_p$ are $O(h)$ while $e_\rho$ and $e_{\partial_t\rho}$ are $\simeq O(h^{1.8})$. All the errors indicators demonstrate the expected behavior, namely $\eta^A_{\mathbf{u}} = O(h)$ and $\eta^A_\rho = O(h^{3/2})$. The ZZ post-processing of the velocity is asymptotically exact and the global effectivity index $ei$ stays close to a value of 3. To test that the space error indicators are independent of the mesh aspect ratio, we perform the same experiments with meshes of aspect ratio 10. The results are reported in the Table 4.2.

| $e_{\mathbf{u}}$ | $e_p$ | $e_\rho$ | $e_{\partial_t\rho}$ | $\eta^A_{\mathbf{u}}$ | $\eta^A_\rho$ | $\eta^T_{\mathbf{u}}$ | $\eta^T_\rho$ | $ei^{ZZ}_{\mathbf{u}}$ | $ei^{ZZ}_\rho$ | $ei$ |
|---|---|---|---|---|---|---|---|---|---|---|
| 0.018 | 0.0067 | 0.0047 | 0.104 | 0.046 | 0.035 | 3.46e-6 | 0.0027 | 0.99 | 0.97 | 3.19 |
| 0.0089 | 0.0031 | 0.0012 | 0.025 | 0.023 | 0.013 | 1.28e-7 | 0.00018 | 1.00 | 0.95 | 3.00 |
| 0.0044 | 0.0013 | 0.00034 | 0.0062 | 0.012 | 0.0046 | 5.04e-9 | 1.16e-5 | 1.00 | 0.91 | 2.84 |

Table 4.1: Two fluids flows with a known solution. The aspect ratio is 1 and the first grid has typical mesh size $0.05 - 0.05$ and the initial time step $\tau = 0.01$. Then the grid is refined in every direction by 2 and we choose $\tau = O(h^2)$.

| $e_{\mathbf{u}}$ | $e_p$ | $e_\rho$ | $e_{\partial_t \rho}$ | $\eta^A_{\mathbf{u}}$ | $\eta^A_\rho$ | $\eta^T_{\mathbf{u}}$ | $\eta^T_\rho$ | $ei^{ZZ}_{\mathbf{u}}$ | $ei^{ZZ}_\rho$ | $ei$ |
|---|---|---|---|---|---|---|---|---|---|---|
| 0.15 | 0.23 | 0.0064 | 0.099 | 0.48 | 0.016 | 5.42e-5 | 0.0029 | 0.98 | 0.92 | 3.23 |
| 0.077 | 0.088 | 0.0022 | 0.024 | 0.24 | 0.0053 | 1.73e-6 | 0.00019 | 0.98 | 0.92 | 3.15 |
| 0.0403 | 0.043 | 0.00076 | 0.0061 | 0.12 | 0.0018 | 1.35e-7 | 1.18e-5 | 0.99 | 0.88 | 3.04 |

Table 4.2: Two fluids flows with a known solution. The aspect ratio is 10 and the first grid has typical mesh size $0.01 - 0.1$ and the initial time step $\tau = 0.01$. Then the grid is refined in every direction by 2 and we choose $\tau = O(h^2)$.

The second experiment consists to make the error due the space approximation negligible to check the second order accuracy in time of the method and the time error indicators. The results are reported in the Table 4.3. It is shown that the errors and the time error indicators are $O(\tau^2)$. As previously observed for other time dependent equations, the ZZ post-processing is less good (in this case for the transport problem), but this can be attributed to the fact that the error due to the time discretization is dominating.

| $e_{\mathbf{u}}$ | $e_p$ | $e_\rho$ | $\eta^A_{\mathbf{u}}$ | $\eta^A_\rho$ | $\eta^T_{\mathbf{u}}$ | $\eta^T_\rho$ | $ei^{ZZ}_{\mathbf{u}}$ | $ei^{ZZ}_\rho$ | $ei$ |
|---|---|---|---|---|---|---|---|---|---|
| 0.018 | 0.012 | 0.032 | 0.047 | 0.033 | 8.97e-5 | 0.055 | 0.99 | 0.56 | 2.28 |
| 0.0045 | 0.0035 | 0.0087 | 0.012 | 0.0045 | 1.5e-5 | 0.017 | 0.99 | 0.49 | 2.18 |
| 0.0014 | 0.0013 | 0.0022 | 0.0029 | 0.00057 | 4.01e-6 | 0.0045 | 0.78 | 0.44 | 2.06 |

Table 4.3: Two fluids flows with a known solution. The aspect ratio is 1 and the first grid has the mesh size $0.05 - 0.05$ and the initial time step $\tau = 0.05$. Then the time step is divide by 2 and we choose $h = O(\tau^2)$.

We now check the efficiency of our adaptive algorithm. We consider again the case $\varepsilon = 0.25$. We recall the notations we use here below. We note:

- $N_v$ : number of vertices of the mesh at final time.
- $N_\tau$ : number of time steps .
- $N_m$ : number of remeshings.
- $N_c$ : number of time step changes .
- $ar$ : maximum aspect ratio at final time, the aspect ratio on an element $K$ being $\lambda_{1,K}/\lambda_{2,K}$.
- $\overline{ar}$ : Average aspect ratio at final time

We also denote by $e = \left(e^2_{\mathbf{u}} + e^2_\rho\right)^{1/2}$ the total error. We run the adaptive algorithm with $TOL_S = TOL_T = TOL$. The distribution parameter $\alpha_{dist}$ is set to 0.25. The initial grid is an isotropic grid of mesh size $h = 0.1$ and the initial time step $\tau = 0.01$. The convergence results are reported in the Table 4.4. It can been observed that the error, as the indicators, are $O(TOL)$. The number of time steps is multiplied by $\sqrt{2}$ as the tolerance is divided by 2, showing that the method is of order 2 in time, even with moving meshes. The number of vertices is approximatively multiplied by 3 when the tolerance is divided by 2, so we are almost in an isotropic case. This can be explained by the fact that we must refine the mesh with respect to both the velocity and the transport of the interface, that are "orthogonal". The effectivity index of the ZZ post-processing of the velocity is still close to 1, but the one of the density seems to stay constant around 0.5. To try to detect the reasons of this behavior, we run the adaptive algorithm without adapting the time step by setting $TOL = TOL_S$ and $TOL_T = 0$. Instead we choose small time steps in such way $\tau = O(TOL^2)$. The convergence result are reported in the Table 4.5. The effectivity index corresponding to the transport problem is closer to 1 (around 0.8). Therefore, one part of the explanation is that we must force the adaptive to choose small time steps to guarantee a good convergence of the post-processing for the transport equation (for instance by choosing $TOL_T \ll TOL_S$.) In Table 4.6, we report the result obtained when $TOL_T = TOL_S/10$.

| $TOL$ | $e$ | $\eta^A$ | $\eta^T$ | $ei$ | $ei_{\mathbf{u}}^{ZZ}$ | $ei_{\rho}^{ZZ}$ | $ar$ | $\overline{ar}$ | $N_v$ | $N_m$ | $N_\tau$ | $N_c$ |
|---|---|---|---|---|---|---|---|---|---|---|---|---|
| 0.125 | 0.085 | 0.13 | 0.12 | 2.09 | 0.85 | 0.26 | 10.37 | 2.58 | 512 | 11 | 4 | 13 |
| 0.0625 | 0.043 | 0.069 | 0.061 | 2.14 | 0.94 | 0.43 | 6.77 | 2.20 | 1361 | 6 | 7 | 12 |
| 0.03125 | 0.022 | 0.036 | 0.032 | 2.22 | 0.95 | 0.43 | 8.74 | 2.32 | 3545 | 6 | 11 | 8 |
| 0.015625 | 0.011 | 0.017 | 0.017 | 2.17 | 0.90 | 0.44 | 20.05 | 2.41 | 14932 | 10 | 17 | 18 |

Table 4.4: Two fluids flows with a known solution. Convergence results when the adaptive algorithm is applied with $TOL_S = TOL_T = TOL$. The boundary layer is set to $\varepsilon = 0.25$.

| $TOL$ | $\tau$ | $e$ | $\eta^A$ | $\eta^T$ | $ei$ | $ei_{\mathbf{u}}^{ZZ}$ | $ei_{\rho}^{ZZ}$ | $ar$ | $\overline{ar}$ | $N_v$ | $N_m$ |
|---|---|---|---|---|---|---|---|---|---|---|---|
| 0.0625 | 1e-3 | 0.025 | 0.071 | 2.6e-4 | 2.86 | 0.96 | 0.79 | 6.41 | 2.17 | 972 | 9 |
| 0.03125 | 2.5e-4 | 0.013 | 0.036 | 8.31e-5 | 2.78 | 0.98 | 0.78 | 10.61 | 2.26 | 4011 | 20 |

Table 4.5: Two fluids flows with a known solution. Convergence results when the adaptive algorithm is applied with $TOL_S = TOL$ and $TOL_T = 0$ The time step is chosen as $\tau = O(TOL^2)$. The boundary layer is set to $\varepsilon = 0.25$.

| $TOL_S$ | $TOL_T$ | $\eta^A$ | $\eta^T$ | $ei$ | $ei_{\mathbf{u}}^{ZZ}$ | $ei_{\rho}^{ZZ}$ | $ar$ | $\overline{ar}$ | $N_v$ | $N_m$ | $N_\tau$ | $N_c$ |
|---|---|---|---|---|---|---|---|---|---|---|---|---|
| 0.125 | 0.0125 | 0.14 | 0.013 | 2.78 | 0.95 | 0.68 | 10.64 | 2.45 | 380 | 17 | 20 | 15 |
| 0.0625 | 0.00625 | 0.073 | 0.0064 | 2.92 | 0.97 | 0.79 | 8.82 | 2.26 | 1173 | 8 | 28 | 30 |
| 0.03125 | 0.003125 | 0.036 | 0.0032 | 2.89 | 0.98 | 0.83 | 10.49 | 2.41 | 3738 | 7 | 45 | 40 |

Table 4.6: Two fluids flows with a known solution. Convergence results when the adaptive algorithm is applied with $TOL_T = TOL_S/10$. The boundary layer is set to $\varepsilon = 0.25$.

We change $\varepsilon$ and we compute the solution to the same problem but where the boundary layer is $\varepsilon = 0.01$. The convergence results are reported in the Table 4.7. The meshes and the solution are represented in Figure 4.1 and Figures 4.2 and 4.3 for $TOL_S = 0.03125$ and $TOL_T = 0.003125$. Several conclusions can be made:

(i) The number of remeshings seems to depend on the tolerance.

(ii) The number of time steps increases drastically when the tolerance is divided by 2.

(iii) The post-processing of the density is clearly suboptimal, $ei_{\rho}^{ZZ}$ being close to 0.2.

We do not have any clear explanations for these bad results. This could be attributed to the interpolation errors, that we cannot estimate, or simply to the fact that we are approximating a really "stiff" problem, $\varepsilon$ being small relatively to the complexity of the present equations. Also the splitting between the two equations (momentum equation and transport of the interface) could be a source of errors. In fact, we can observe in the numerical experiments that $ei_{\rho}^{ZZ}$ starts close to 1, and decreases during the simulation. A deeper numerical analysis should be performed to identify the sources of all theses errors. We think that it could be interested to study

- The impact of the interpolation procedure between meshes.

- The impact of the splitting.

- The impact of the amplitude and the non-divergence free nature of the approximated velocity.

All these impacts are directly related to a bad conservation of the density during the simulation. Nevertheless, Figure 4.1 indicates at least that the algorithm converges and that the solution "looks" good. However, if we look carefully at the interface at final time, we observe two things. First some oscillations occurs, secondly the mesh does not fit very well to the interface and is, at first sight, too isotropic, see Figure 4.3 when we perform a zoom on the final mesh, and Figure 4.4 where we represent the density along the $x_1$ axes at final time.

| $TOL_S$ | $TOL_T$ | $\eta^A$ | $\eta^T$ | $ei$ | $ei_{\mathbf{u}}^{ZZ}$ | $ei_{\rho}^{ZZ}$ | $ar$ | $\overline{ar}$ | $N_v$ | $N_m$ | $N_\tau$ | $N_c$ |
|---|---|---|---|---|---|---|---|---|---|---|---|---|
| 0.125 | 0.0125 | 0.13 | 0.012 | 2.39 | 0.96 | 0.17 | 29 | 4.01 | 737 | 49 | 344 | 272 |
| 0.0625 | 0.00625 | 0.068 | 0.0061 | 2.64 | 0.97 | 0.22 | 78 | 6.99 | 1694 | 105 | 997 | 644 |
| 0.03125 | 0.003125 | 0.033 | 0.0031 | 3.15 | 0.88 | 0.32 | 145 | 8.5 | 5922 | 203 | 2240 | 1697 |

Table 4.7: Two fluids flows with a known solution. Convergence results when the adaptive algorithm is applied with $TOL_T = TOL_S/10$. The boundary layer is set to $\varepsilon = 0.01$.

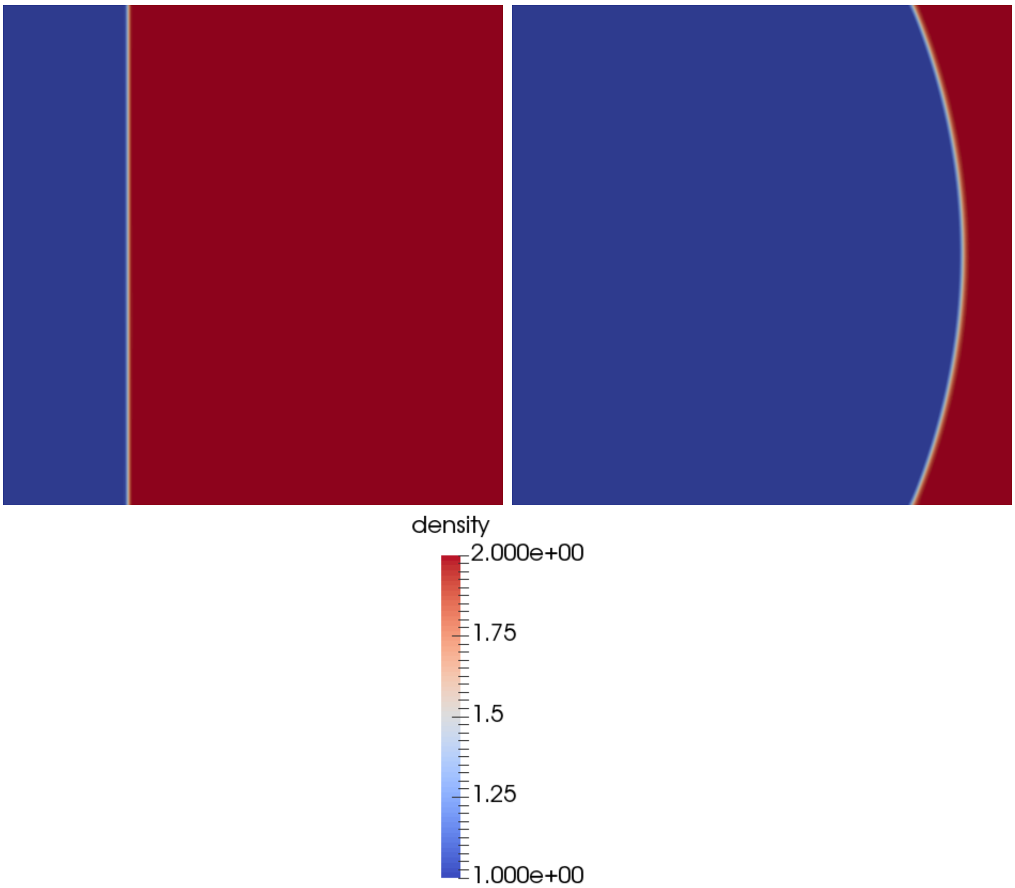


Figure 4.1: Approximated density obtained when using the adaptive algorithm with $TOL_S = 0.03125$ and $TOL_T = 0.003125$. The boundary layer is $\varepsilon = 0.01$. $t = 0$ (left), $t = 0.45$ (right).

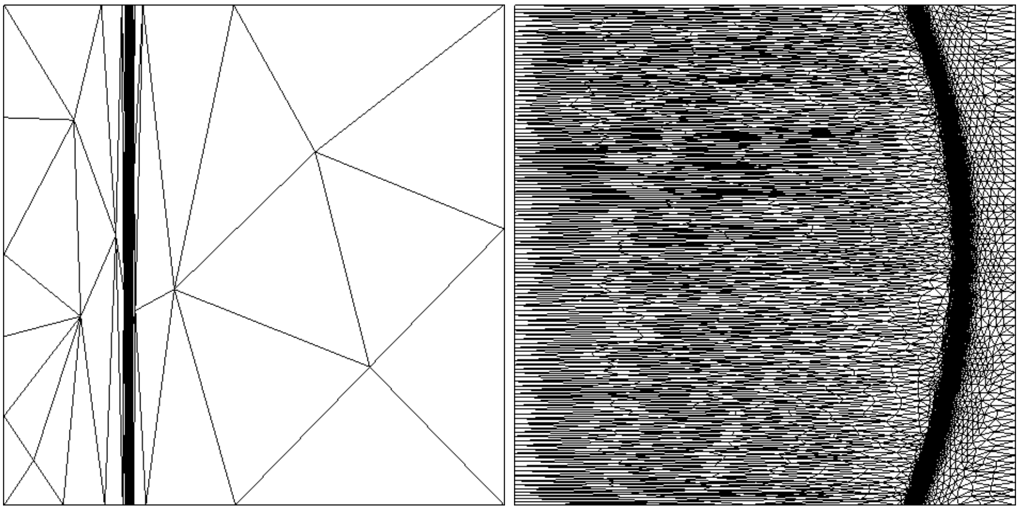

Figure 4.2: Adapted meshes obtained when using the adaptive algorithm with $TOL_S = 0.03125$ and $TOL_T = 0.003125$. The boundary layer is $\varepsilon = 0.01$. $t = 0$ (left), $t = 0.45$ (right).

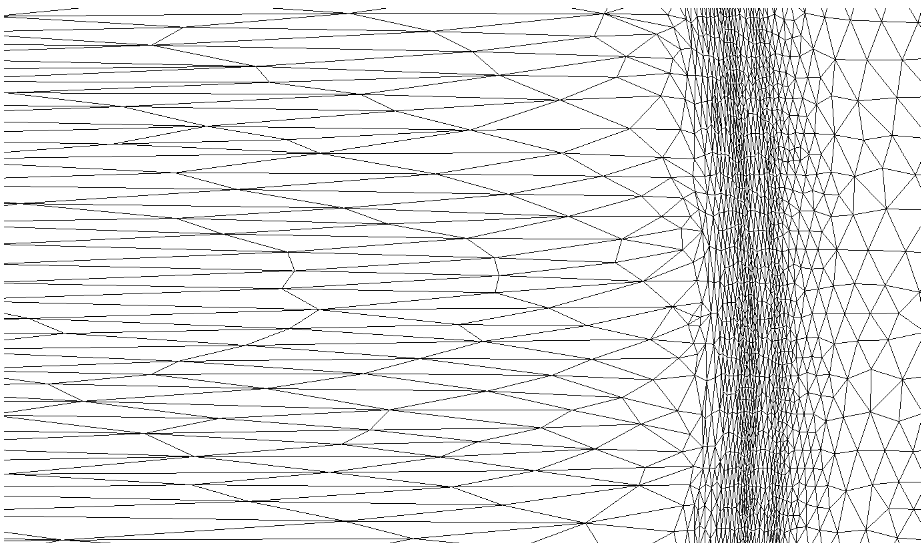

Figure 4.3: Zoom on the final obtained when using the adaptive algorithm with $TOL_S = 0.03125$ and $TOL_T = 0.003125$. The boundary layer is $\varepsilon = 0.01$.

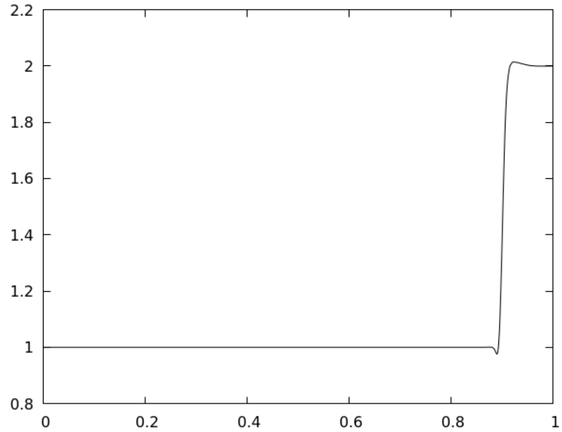


Figure 4.4: Plot of the density at final time along the $x$-axe. The adaptive algorithm was runned with $TOL_S = 0.03125$ and $TOL_T = 0.003125$. The boudary layer is $\varepsilon = 0.01$.

To counter these drawbacks, we can heuristically force the algorithm to mesh several times in a row when a grid is accepted before going to the next time iteration. This procedure produces meshes that are less "left behind" the solution. We also observe that in this case, the oscillations around the interface are not present anymore, see Figures 4.5, 4.6 and Figure 4.7. This choice is obviously costly, since it implies to recompute several times the solutions, but improves the quality of the solution and the mesh, that is more anisotropic and has less points (here 3 times less for the present experiment). In the present example, we only force one additional remeshing, and the resulting mesh is already considerably better.

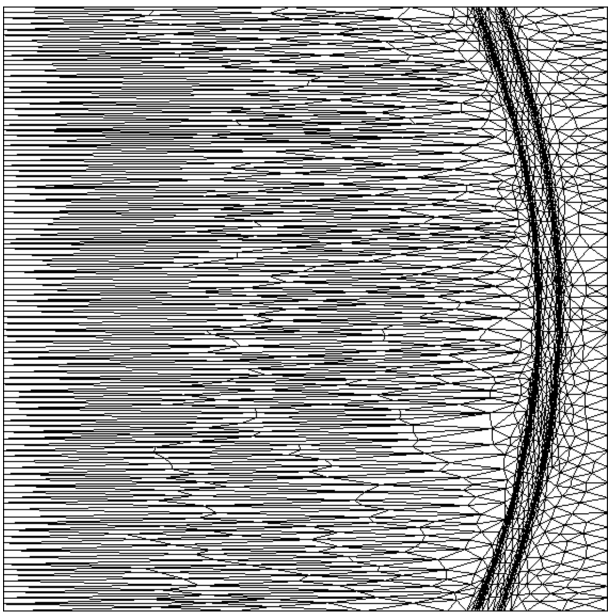

Figure 4.5: Final mesh obtained when using the adaptive algorithm with $TOL_S = 0.03125$ and $TOL_T = 0.003125$. The boundary layer is $\varepsilon = 0.01$. We force the algorithm to remesh one more time when a mesh is accepted.

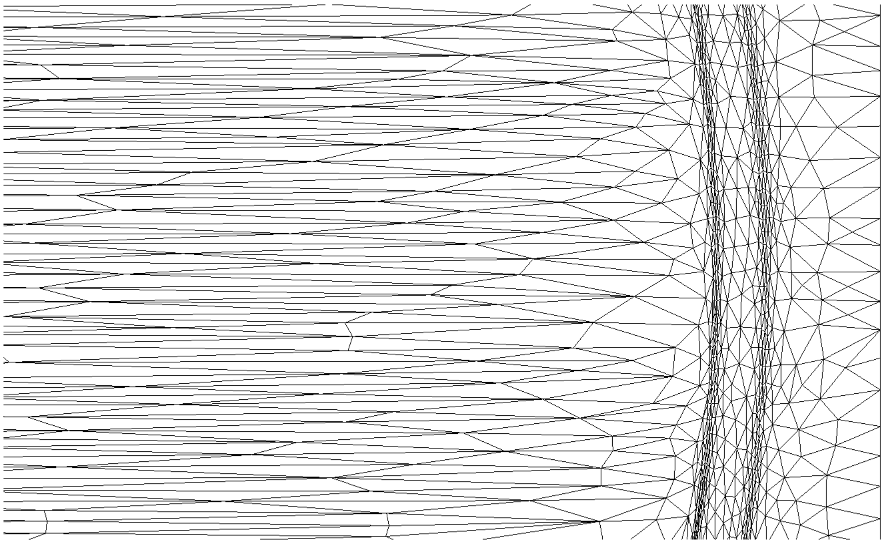

Figure 4.6: Zoom on the final obtained when using the adaptive algorithm with $TOL_S = 0.03125$ and $TOL_T = 0.003125$. We force the algorithm to remesh one more time when a mesh is accepted. The boundary layer is $\varepsilon = 0.01$.

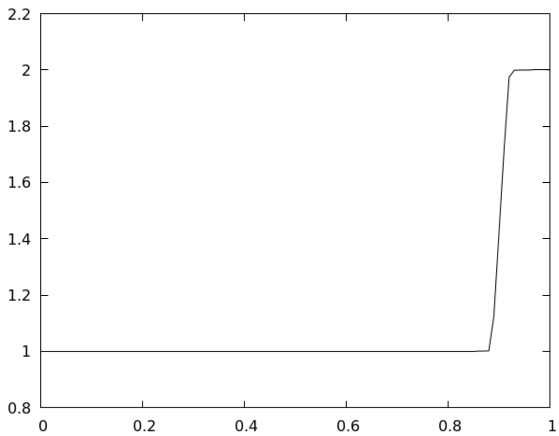


Figure 4.7: Plot of the density at final time along the $x_1$-axe. The adaptive algorithm was runned with $TOL_S = 0.03125$ and $TOL_T = 0.003125$. We force the algorithm to remesh one more time when a mesh is accepted. The boundary layer is $\varepsilon = 0.01$.

## 4.7 Application of the adaptive algorithm to the solutions of some physical instabilities phenomena

In this section, we apply the adaptive strategy presented in Sections 4.5 and 4.6 to more interesting situations. In every example, the flow is at rest at the beginning and the initial interface function $\varphi_0$ is of the type

$$\varphi_0(\mathbf{x}) = H_\varepsilon(\phi(\mathbf{x}))$$

where $H_\varepsilon$ is the smoothing of the Heavyside graph (1.25). All the dynamical system evolves only under the action of the gravitational force $\mathbf{g}$. The two situations we will consider are the following:

(i) The growth of Rayleigh-Taylor and Kelvin-Helmoltz instabilities that appear between fluids of different densities and viscosities

(ii) The motion of rigid body into an incompressible fluid, that can be seen as a limit problem when one of the two fluids has a "infinite" viscosity

We do not pretend to perform neither a deep physical analysis or numerical analysis of this phenomena, we only consider them as an illustration for the performance of our adaptive strategy. Some references will be mentioned, that treat these problems in a more complete approach. The second situation will receive a special attention since it will constitute the second part of this chapter.

**Example 4.24** (Rayleigh-Taylor and Kelvin-Helmoltz instabilities)**.**
Rayleigh-Taylor instabilities develop when an heavy fluid lies above a lighter one and starts to move under the effect of the gravitation. We consider two layers of fluid with different densities $\rho_1, \rho_2$ and equal viscosity $\mu = \mu_1 = \mu_2$. The problem is solved in a rectangular box $\Omega = (0, d) \times (0, 4d)$ where we apply the natural boundary conditions $\mathbf{u} = 0$ on the top and bottom side and $\mathbf{u} \cdot \mathbf{n} = 0$ on the left and right wall.

Initially, the two layers are at rest, and the free surface separated the two fluids is slightly perturbed, choosing as initial condition for the phase function $\varphi$

$$\varphi_0(x_1, x_2) = H_\varepsilon\left(x_2 - 2d - 0.1d\cos\left(\frac{2\pi x_1}{d}\right)\right), \tag{4.68}$$

Therefore, the initial distribution of density in $\Omega$ is a smooth function given by

$$\rho_0 = \rho_1\varphi_0 + \rho_2(1 - \varphi_0). \tag{4.69}$$

The dynamic of the problem is mainly governed by the Atwood number and the Reynolds number. They are defined in the following way : let $\rho_{\max} = \max(\rho_1, \rho_2), \rho_{\min} = \min(\rho_1, \rho_2)$, then we define the Atwood number

$$A_t = \frac{\rho_{\max} - \rho_{\min}}{\rho_{\max} + \rho_{\min}} \tag{4.70}$$

and the Reynolds number (we take the same definition as the one used in [53])

$$Re = \frac{\rho_{\min} g^{1/2} d^{3/2}}{\mu}, \tag{4.71}$$

where $g$ is the intensity of the gravity field $\mathbf{g}$. For the numerical experiments that follows, we set $d = 1$ and we choose $A_t = 0.2$ that corresponds to a density ratio $\rho_{\max}/\rho_{\min} = 1.5$ or $A_t = 0.5$ that gives a ratio of 3. The Reynolds numbers is set to 100 or 1000.

When $\rho_1 > \rho_2$, that is to say with our choice for $\varphi_0$ when the upper fluid is the heavier one, it is well know that the situation is unstable and that the heavy fluid falls into the light one, developing "mushroom" shapes (see Figure 4.8). The Atwood number controls the length of the mushroom trunk and the Reynolds number the appearance of roll-ups. A large amount of works is dedicated to the physical and mathematical studiers of the Rayleigh-Taylor instabilities, we cite, among others, the classical references [30] and [40] for the mathematical/physical approaches. From the numerical approximation perspectives, the development of theses instabilities were carefully documented by Tryggvason [100] and is still studied since this time [53].

For our experiments, we would like to capture the interface with accuracy, therefore we choose the next parameters as follows :

1. To have a thin boundary layer, we set $\varepsilon = 0.001$.

2. To capture the interface with accuracy, we force the error indicators to stay close to the prescribed tolerance by setting $\alpha_{dist} = 0.125$.

3. Finally, as commented in the the previous section, to capture with accuracy the interface, it is important to force the algorithm to mesh several times in a row when a mesh is accepted. Therefore, we set the number of additional remeshings to 3.

4. Small time steps are necessary for avoiding oscillations and numerical instabilities around the interface, therefore we choose $TOL_T \leq TOL_S$.

We first check the convergence of the adaptive algorithm by comparing the evolution of the interface and the meshes obtained with several choices for $TOL_S$ and $TOL_T$ for $A_t = 0.2$ and $Re = 100$. The initial grid is an isotropic grid of mesh size $h = 0.025$ and the initial time step is chosen as $\tau = 0.001$. The results are reported in the Figures 4.8 and 4.9. For "large" tolerances, the symmetry of the solutions is not preserved and a lot of diffusion can be observed around the boundary layer. In Figures 4.10 and 4.11, we zoom at the meshes obtained with the finest tolerances. In Figure 4.12, we present the solution for $A_t = 0.5$ (Above fluid is 3 times heavier than the bottom fluid) and $Re = 100$. Finally, in Figure 4.13, we present the evolution of the solution when $A_t = 0.2$ and $Re = 1000$.

To conclude this example, we present two last experiments, one is the growth of the Kelvin-Helmoltz instabilities, that appear along the interface when a shear of velocity is present, the second is close to the shallow water experiment, where we observe the evolution of waves at the surface of a water region. For the Kelvin-Helmoltz instability, we start from a situation close what we did before, and we consider the evolution of two fluids in a box $\Omega = (0, d) \times (0, 4d)$ where we fix $d = 0.1$. The heavier fluid is put above and has a density $\rho_1 = 1000$ and viscosity $\mu_1 = 1e-3$ while for the lighter fluid we choose $\rho_2 = 780$ and $\mu_2 = 1.5e-3$. This corresponds to respectively water and ethanol. The Atwood number is then 0.12 and the Reynolds number 5000. The initial interface function is given by

$$\varphi_0(\mathbf{x}) = H_{0.001}\left(x_2 - 2d - 0.01d\cos\left(\frac{8\pi x_1}{d}\right)\right).$$

The solution and the meshes are presented in Figure 4.14 at different times when the adaptive algorithm is run where we choose as parameters $TOL_S = TOL_T = 0.00125$ and $\alpha_{dist} = 0.25$. We still remesh 3 times in a row when a mesh is accepted by the algorithm.

The last experiment is inspired by the shallow water test case. We consider a small cavity $\Omega = ]-0.04, 0.04[\times]-0.005, 0.005[$ filled with water and air. At time $t = 0$, a "bump" of water starts to move under the action of the gravity and waves appear, that rebound on the walls of the cavity until the two fluids are at rest. We solve this problem using the adaptive algorithm, where we set $TOL_S = TOL_T = 0.025$ and $\alpha_{dist} = 0.25$. The size of the boundary layer is $\varepsilon = 0.001$ at the beginning. 3 additional remeshings are performed at each step. In Figure 4.15, we represent the evolution of the free surface at several time steps. In Figure 4.16, the corresponding meshes are presented.

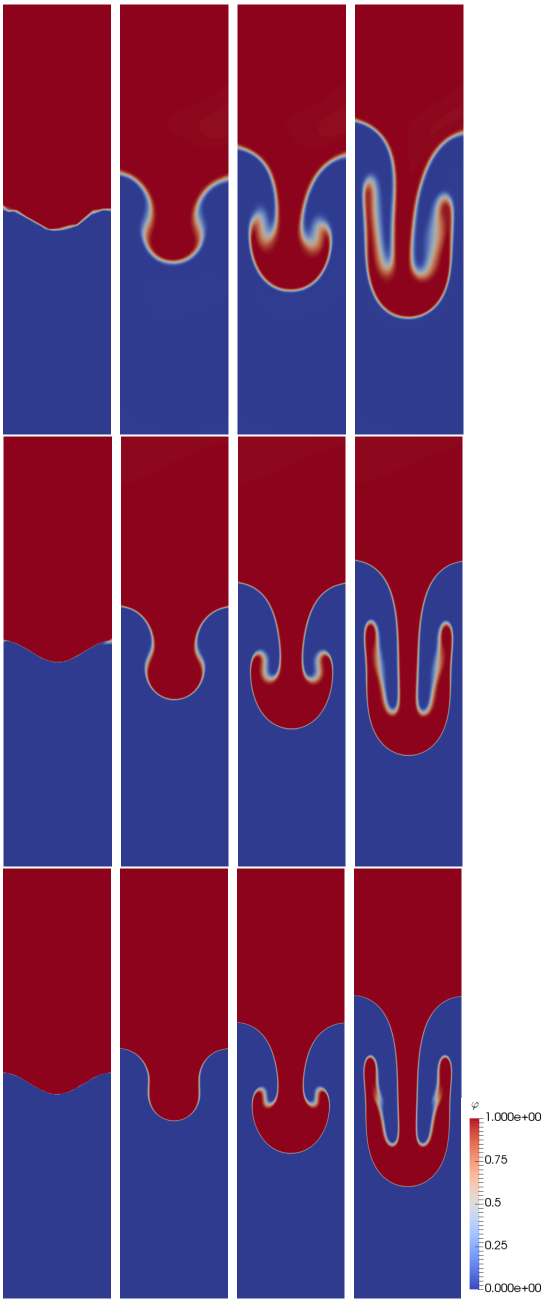


Figure 4.8: Evolution of the approximated interface function $\varphi_h^n$ obtained when using the adaptive algorithm. The red phase is 1.5 heavier than the blue phase ($A_t = 0.2$) and the Reynolds number is 100. Solution is presented at time $t = 0$, $t = 1$, $t = 1.5$, $t = 2$ (from left to right). Tolerances are set to $TOL_S = 0.125, TOL_T = 0.0125$ (top), $TOL_S = 0.0625, TOL_T = 0.00625$ (middle), $TOL_S = 0.03125, TOL_T = 0.003125$ (bottom).

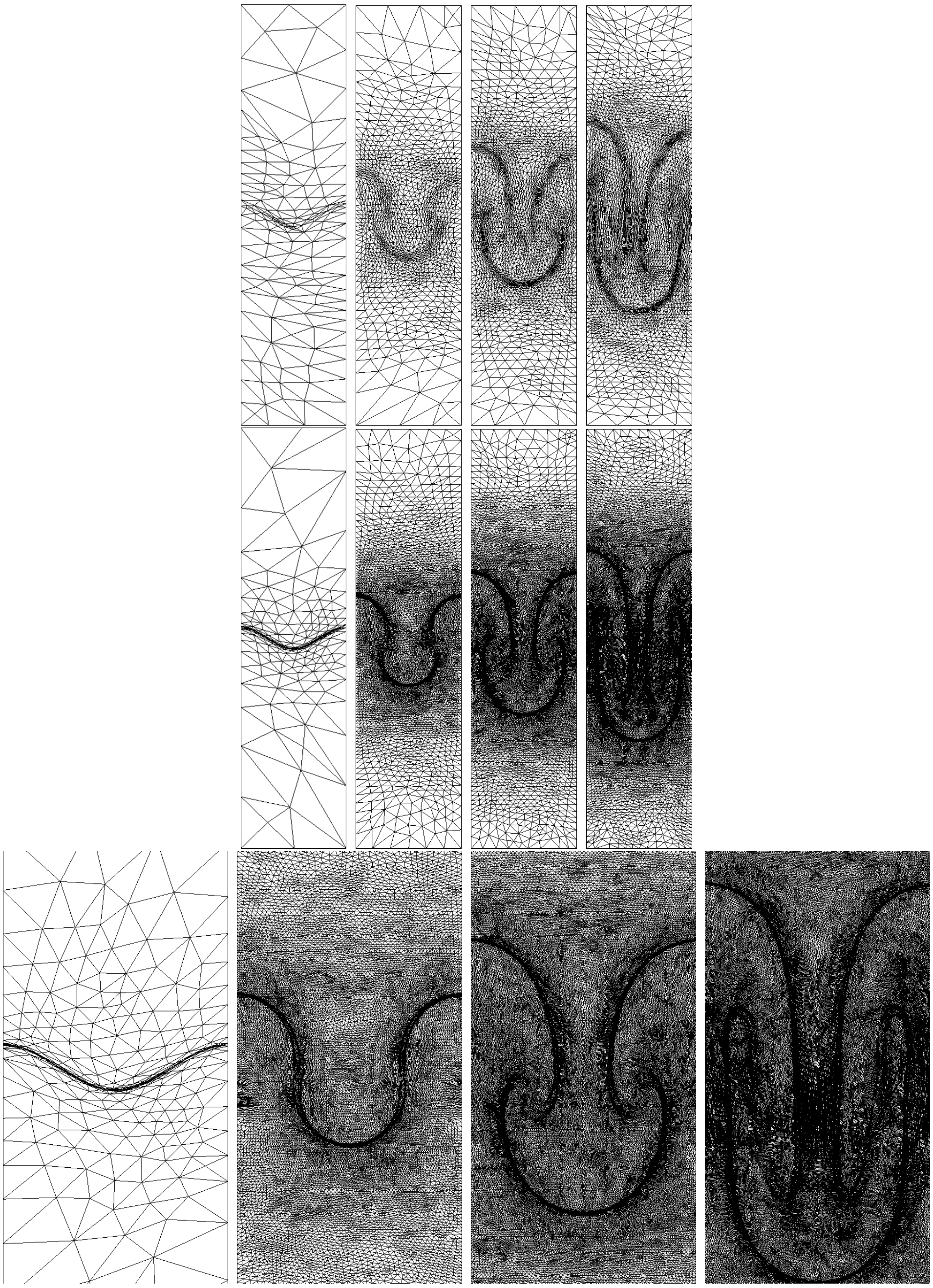

Figure 4.9: Evolution of the meshes generated when using the adaptive algorithm with $A_t = 0.2$ and $Re = 100$. Solution is presented at time $t = 0$, $t = 1$, $t = 1.5$, $t = 2$ (from left to right). Tolerances are set to $TOL_S = 0.125, TOL_T = 0.0125$ (top), $TOL_S = 0.0625, TOL_T = 0.00625$ (middle), $TOL_S = 0.03125, TOL_T = 0.003125$ (bottom).

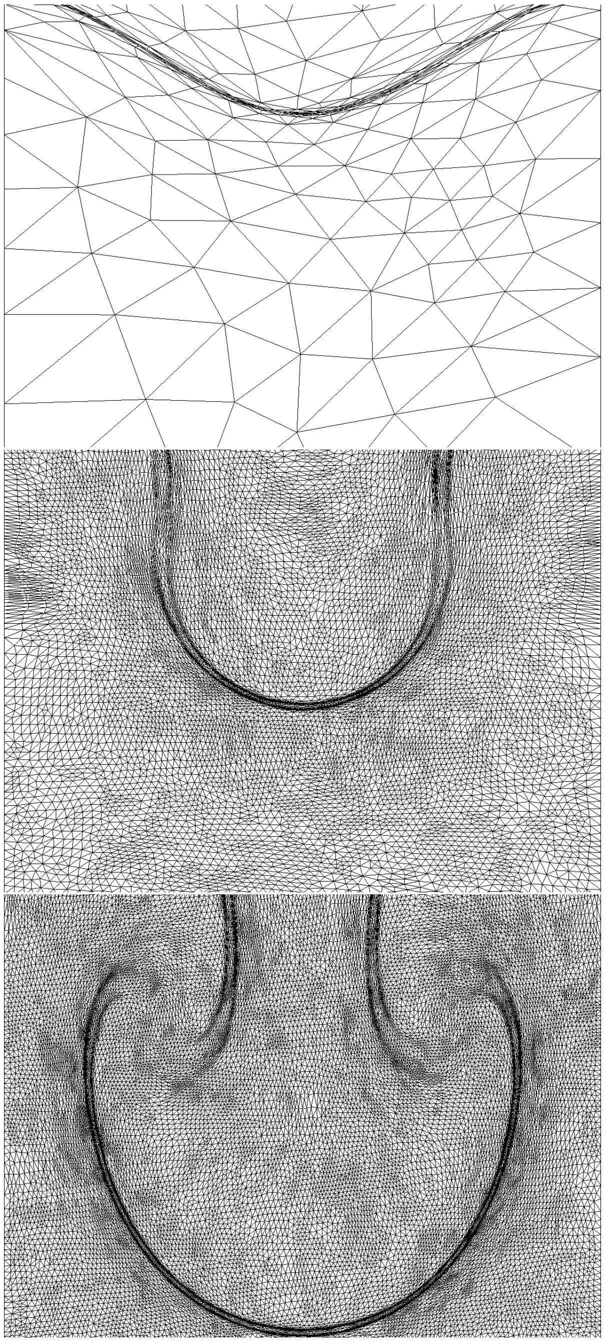

Figure 4.10: Zoom at the meshes generated when using the adaptive algorithm with $TOL_S = 0.03125$ and $TOL_T = 0.003125$. The Atwood number is 0.2 and the Reynolds number 100. Meshes are presented at time $t = 0$ (top), $t = 1$ (middle), $t = 1.5$ (bottom).

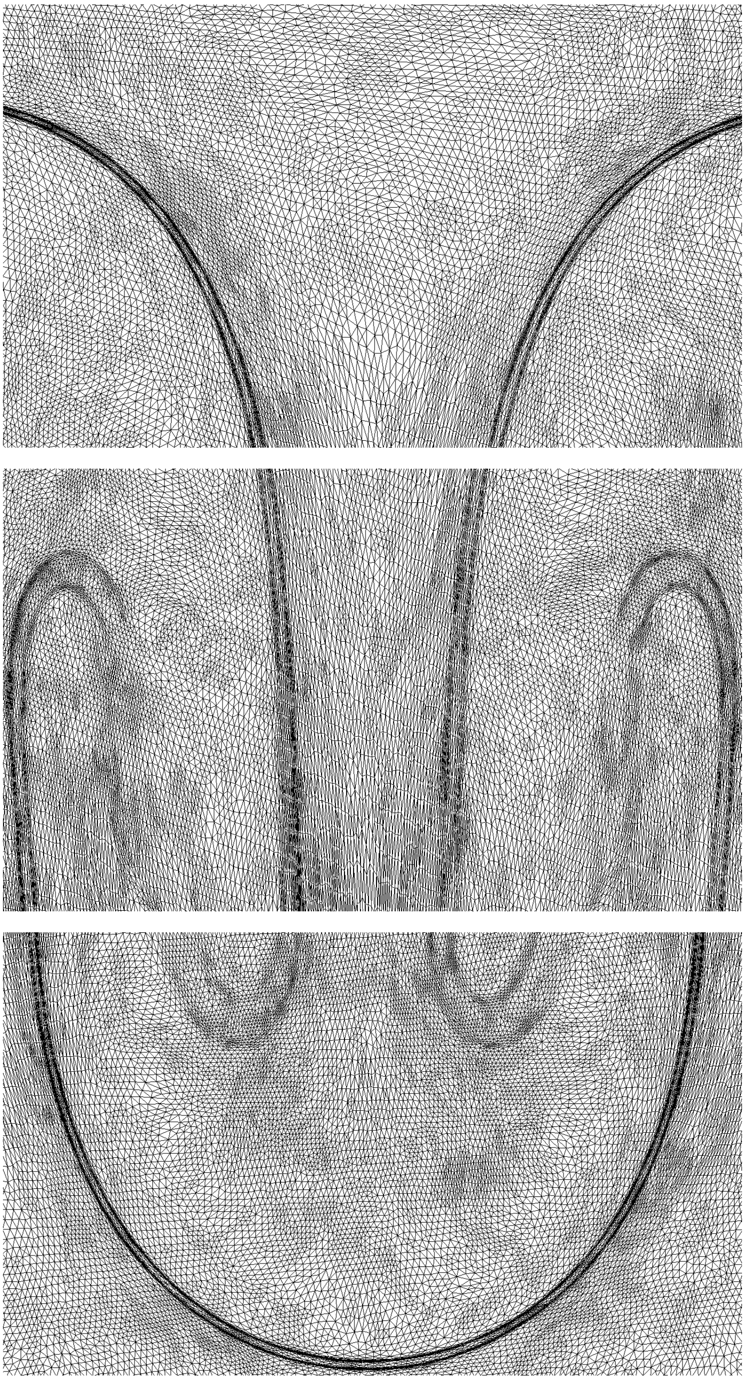

Figure 4.11: Zoom at the mesh at $t = 2$ generated when using the adaptive algorithm with $TOL_S = 0.03125$ and $TOL_T = 0.003125$. The Atwood number is 0.2 and the Reynolds number 100.

**Example 4.25** (Motion of a rigid body in a incompressible fluid)**.**
One method to simulate the motion of a rigid body into a incompressible fluid consists to use a penalization approach [57]. More precisely, rather than simulate the interaction between a viscous fluid and a solid body, we consider the latter as a fluid of viscosity $1/\delta$ with $\delta \ll 1$. The evolution of a two fluids flow is then solved, and we can use the numerical method presented above to approximate the solutions.

The data of the experiments are the following : we consider a square box $\Omega = ]0, 0.1[^2$ in which a solid disk is falling. The disk has a radius $r = 0.01$ $[m]$ for a density of $10'000$

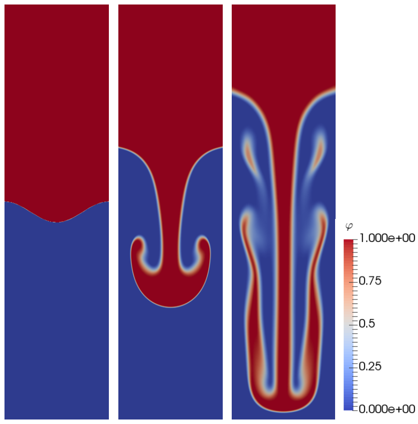


Figure 4.12: Evolution of the approximated interface function $\varphi_h^n$ obtained when using the adaptive algorithm. The red phase is 3 heavier than the blue phase ($A_t = 0.5$) and the Reynolds number is 100. Solution is presented at time $t = 0$, $t = 1$, $t = 2$ (from left to right). Tolerances are set to $TOL_S = 0.03125$ and $TOL_T = 0.003125$ .

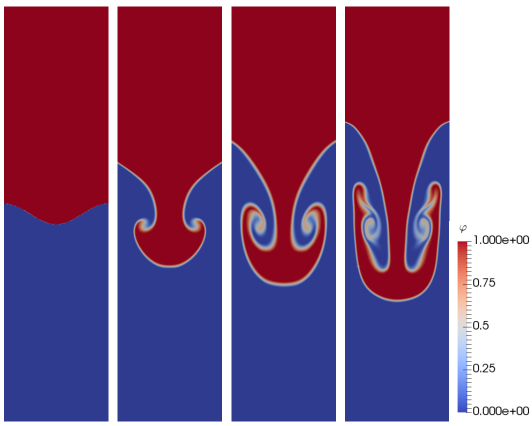


Figure 4.13: Evolution of the approximated interface function $\varphi_h^n$ obtained when using the adaptive algorithm. The red phase is 1.5 heavier than the blue phase ($A_t = 0.2$) and the Reynolds number is 1000. Solution is presented at time $t = 0$, $t = 1$, $t = 1.35$, $t = 1.65$ (from left to right). Tolerances are set to $TOL_S = 0.03125$ and $TOL_T = 0.003125$ .

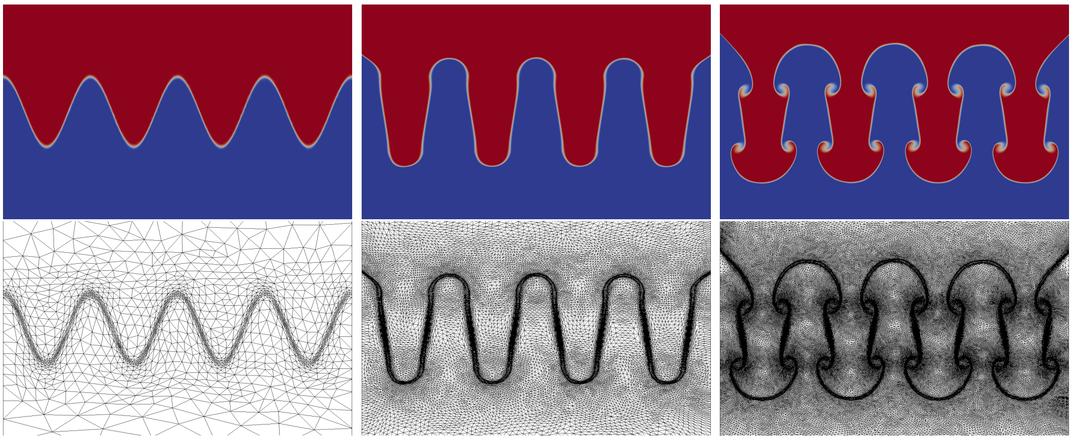

Figure 4.14: Evolution of the solution and meshes when the adaptive algorithm is used to simulate the fall of water into ethanol. Solution are presented at times $t = 0$, $t = 1$ and $t = 1.8$ (from left to right). Kelvin-Helmoltz instabilies manifest in small waves appearing along the interface.

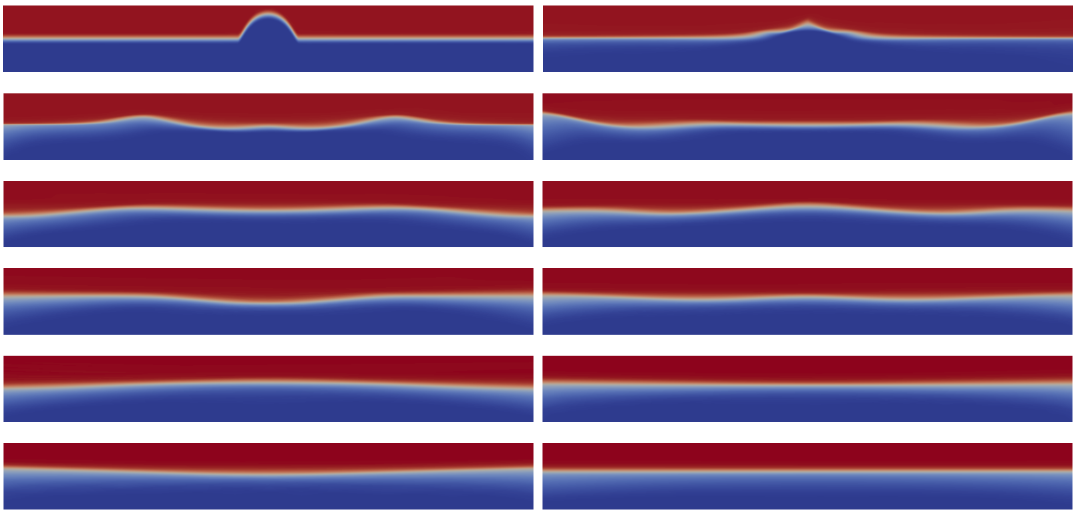

Figure 4.15: Evolution of waves at the surface of water. The solution is presented at time $t = 0, 0.025, 0.1, 0.2, 0.3, 0.4, 0.5, 0.6, 0.7, 0.8, 0.9$ and $1$ $[s]$ (from left to right, top to bottom).

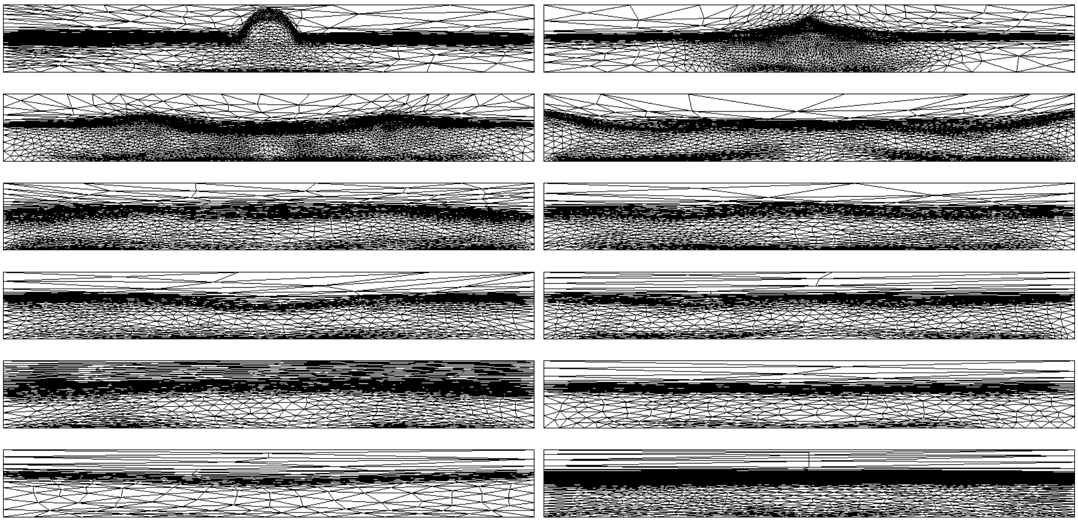

Figure 4.16: Adapted meshes corresponding to the evolution of waves at the surface of water. The solution is presented at time $t = 0, 0.025, 0.1, 0.2, 0.3, 0.4, 0.5, 0.6, 0.7, 0.8, 0.9$ and 1 $[s]$ (from left to right, top to bottom).

$[kg/m^3]$ and the surrounding fluid has a density of 1000 $[kg/m^3]$ for a viscosity of 1 $[Pa]$, that corresponds to glycerin. To model the disk, we penalize the fluid phase represented it and set its viscosity to $10'000$ $[Pa]$. At the beginning, the disk is at rest, centered at the point $(0.05, 0.05)$. The initial situation is represented through the initial interface function that is given by

$$\varphi_0(\mathbf{x}) = H_{0.001}\left(0.01 - \sqrt{(x_1 - 0.05)^2 + (x_2 - 0.05)^2}\right).$$

A remarkable result is proven in [56]: the disk will never touch the boundary of the domain in a finite time. This is due to the fact that the pressure becomes infinite at the bottom of the cavity, which prevents the disk to reach the bottom. To validate this result numerically, we use our adaptive algorithm. In Figure 4.17, we represent the mesh, the pressure and the velocity field that are computed at $t = 0.14$ $[s]$ when the peak of pressure is the highest. The adaptive algorithm was run with $TOL_S = 0.0025$ and $TOL_T = 1$. Note that the time discretization is larger than the spatial one.

Our numerical simulation show indeed that the the disk does not collide with the boundary of $\Omega$. In the second part of this chapter, we will focus on this particular experiment and present numerical results, obtained with another model, that also verify the non-collision property.

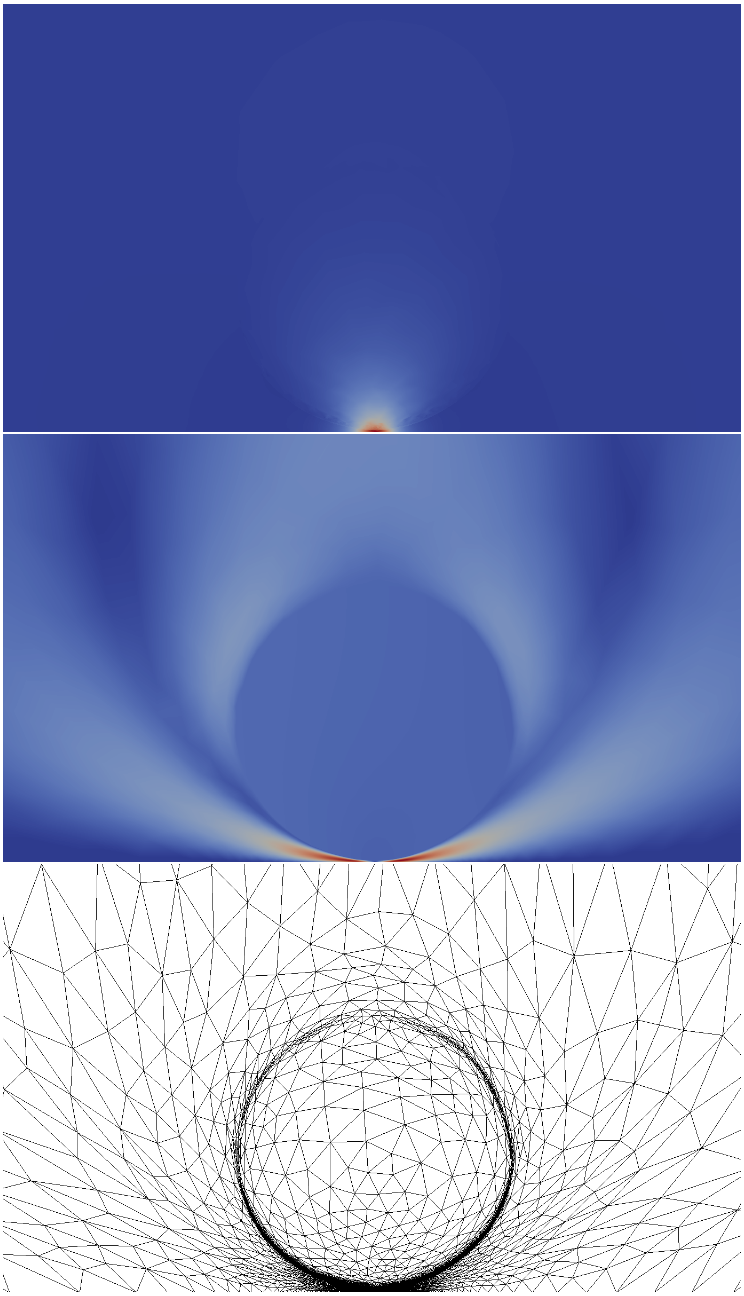

Figure 4.17: Falling disk into a viscous flow: zoom at the bottom of the cavity. Top : pressure peak at time $t = 0.14$ ; the pressure is around $10^5$ $[Pa]$ under the disk. Middle : amplitude of the velocity field at time $t = 0.14$ ; the disk is almost stopped and the fluid under the disk is evacuated at a velocity around 1 $[m/s]$. Bottom : adapted mesh.

## Part 2. Application to the motion of a rigid body in a cavity filled with an incompressible fluid

### 4.8 Problem statement and numerical method

In this part, we study the motion of a rigid disk of radius $R$ inside a bounded, convex cavity $\Omega \subset \mathbb{R}^2$ filled with a fluid of constant viscosity and density. By sake of simplicity, we choose $\Omega$ as a squared cavity. The fluid is governed by the incompressible Navier-Stokes equations while the dynamic of the rigid disk is ruled by the Newton law. Given a final time $T \in (0, +\infty]$, we denote by $\mathcal{B}(\mathbf{X}(t))$ the disk centered at $\mathbf{X}(t)$ where $t \in [0, T]$. The equations of motions reads [56]: find $(\mathbf{X}, \mathbf{u}, p, \mathbf{V}, \omega)$ the solutions of

$$\begin{cases} \rho_{\mathcal{F}} \dfrac{\partial \mathbf{u}}{\partial t} + \rho_{\mathcal{F}} \mathbf{u} \cdot \nabla \mathbf{u} - \mu_{\mathcal{F}} \Delta \mathbf{u} + \nabla p = \rho_{\mathcal{F}} \mathbf{g}, \quad (\mathbf{x}, t) \in \Omega \setminus \overline{\mathcal{B}(\mathbf{X}(t))} \times (0, T], \\ \operatorname{div} \mathbf{u} = 0, \quad (\mathbf{x}, t) \in \Omega \setminus \overline{\mathcal{B}(\mathbf{X}(t)} \times (0, T], \\ \mathbf{u} = 0, \quad (\mathbf{x}, t) \in \partial\Omega \times (0, T], \\ \mathbf{u} = \mathbf{V} + \omega (x - \mathbf{X}(t))^{\perp}, \quad (\mathbf{x}, t) \in \partial\mathcal{B}(\mathbf{X}(t)) \times (0, T], \end{cases} \tag{4.72}$$

and

$$\begin{cases} -\displaystyle\int_{\partial\mathcal{B}(\mathbf{X}(t))} (2\mu_{\mathcal{F}} D(\mathbf{u}) - pI) \mathbf{n} d\sigma = m\dot{\mathbf{V}}, \quad t \in (0, T], \\ -\displaystyle\int_{\partial\mathcal{B}(\mathbf{X}(t))} (2\mu_{\mathcal{F}} D(\mathbf{u}) - pI)(x - \mathbf{X}(t))^{\perp} \cdot \mathbf{n} d\sigma = J\dot{\omega}, \quad t \in (0, T], \end{cases} \tag{4.73}$$

where $\mathbf{g}$ is gravitational acceleration, $\mu_{\mathcal{F}}$ and $\rho_{\mathcal{F}}$ denote the viscosity and the density of the fluid, $m$ and $J$ are the mass and the inertia of the disk. In the above system, $(\mathbf{u}, p)$ are the velocity and pressure fields of the fluid and $(\mathbf{V}, \omega)$ the translational and rotational speeds of $\mathcal{B}(\mathbf{X}(t))$. In [56], it is shown that the disk will never touch the boundary of $\Omega$ in a finite time. This is a really strange and unexpected behavior, and the goal of this second part of Chapter 4 is too developed a numerical approach to verify it.

In [57], a penalization of the viscous stress tensor is introduced in order to model fluid-rigid body interaction. We briefly explain the main idea. One may first observe that to find a weak solution of (4.72) consists in particular to look at any $t$ for $\mathbf{u}(t) \in H_{\mathcal{B}(\mathbf{X}(t))}$ where

$$H_{\mathcal{B}(\mathbf{X}(t))} = \left\{ \mathbf{v} \in (H_0^1(\Omega))^2 : \exists (\mathbf{V}, \omega) \in \mathbb{R}^2 \times \mathbb{R} : \mathbf{v} = \mathbf{V} + \omega (x - \mathbf{X}(t))^{\perp} \text{ a.e. in } \mathcal{B}(\mathbf{X}(t)) \right\}$$

is the space of rigid motion inside $\mathcal{B}(\mathbf{X}(t))$. It can be shown (see for instance [96]) that the space of rigid motion can be written as

$$H_{\mathcal{B}(\mathbf{X}(t))} = \left\{ \mathbf{v} \in (H_0^1(\Omega))^2 : D(\mathbf{v}) = 0 \text{ a.e. in } \mathcal{B}(\mathbf{X}(t)) \right\}.$$

Moreover, it is shown (see for instance [77]) that constrains of the type $D(\mathbf{u}(t)) = 0$ in $\mathcal{B}(\mathbf{X}(t))$ can be well approximated by penalizing the momentum equation, which, roughly speaking , consists to extend the velocity field inside the disk and considering the differential operator

$$\operatorname{div}(2\mu_{\mathbf{X}(t)} D(\mathbf{u}(t))), \quad \mu_{\mathbf{X}(t)} = \frac{1}{\varepsilon} \chi_{\mathcal{B}(\mathbf{X}(t))} + \mu_{\mathcal{F}} (1 - \chi_{\mathcal{B}(\mathbf{X}(t))}), 0 < \varepsilon \ll 1,$$

rather the laplacian term $\mu_{\mathcal{F}}\Delta\mathbf{u}(t)$. This means, physically, that the rigid body is modeled as a fluid of "huge" viscosity.

The equations of motion (4.72), (4.73) can be then approximated by the following two fluids flow system [57]. Starting from initial conditions $(\mathbf{X}_0, \mathbf{u}_0)$, we are looking for $(\mathbf{X}(t), \mathbf{u}(t), p(t))$ the solution of

$$\begin{cases} \rho_{\mathbf{X}(t)}\dfrac{\partial \mathbf{u}}{\partial t} + \rho_{\mathbf{X}(t)}(\mathbf{u}(t)\cdot\nabla)\mathbf{u}(t) & \\ -\operatorname{div}(2\mu_{\mathbf{X}(t)}D(\mathbf{u}(t))) + \nabla p(t) = \rho_{\mathbf{X}(t)}\mathbf{g}, & \text{in } \Omega\times(0,T], \\ \operatorname{div}\mathbf{u}(t) = 0, & \text{in } \Omega\times(0,T], \\ \mathbf{u} = 0, & \text{on } \partial\Omega\times(0,T], \\ \rho_{\mathbf{X}(t)} = \rho_{\mathcal{B}}\chi_{\mathcal{B}(\mathbf{X}(t))} + \rho_{\mathcal{F}}(1-\chi_{\mathcal{B}(\mathbf{X}(t))}), & \text{in } \Omega\times(0,T], \\ \mu_{\mathbf{X}(t)} = \dfrac{1}{\varepsilon}\chi_{\mathcal{B}(\mathbf{X}(t))} + \mu_{\mathcal{F}}(1-\chi_{\mathcal{B}(\mathbf{X}(t))}), & \text{in } \Omega\times(0,T], \\ \dot{\mathbf{X}}(t) = \dfrac{1}{\pi R^2}\displaystyle\int_{\mathcal{B}(\mathbf{X}(t))}\mathbf{u}(t)dx, & t\in(0,T]. \end{cases} \tag{4.74}$$

where $0 < \varepsilon \ll 1$ is a penality parameter and $\rho_{\mathcal{B}}$ denotes the density of the disk. The last equation in (4.74) is the Newton law for the conservation of the linear momentum. Observe that we do not write any equation for the conservation of the angular momentum, assuming that the disk falls without spinning. Moreover, observe that the formulation (4.74) is exactly the one we were considering on the part 1 of the this chapter, the only differences being that the transport equation is replaced by the evolution law of $\mathbf{X}(t)$.

Convergence of the solutions of (4.74) as $\varepsilon$ goes to 0 was studied in [57, 77]. Note that such a penalization method was also used to prove global existence of weak solutions to the motion of rigid bodies in a viscous incompressible fluid [76].

Solutions of (4.74) are approximated using the backward Euler method and stabilized anisotropic finite elements. The discretization of the Navier-Stokes equations are done as it was proposed in Chapter 3 and the part 1 of Chapter 4 and we briefly recall it below. Let $T < \infty$ be the final time. Let $h > 0$ and $\mathcal{T}_h$ be a conformal triangulation of $\Omega$ into triangles $K$ of diameter $h_K \leq h$. We consider the finite spaces $V_h$ and $Q_h$ that are respectively the linear finite elements space for velocity and the linear finite elements space for pressure. The discretization of the Navier-Stokes equations reads: given a integer $N > 0$ and $0 = t^0 < t^1 < .... < t^N = T$ a partition of $[0, T]$, starting from $\mathbf{X}_h^0 = \mathbf{X}_0, \mathbf{u}_h^0 = r_h(\mathbf{u}_0)$, where $r_h$ stands for the Lagrange interpolant on $V_h$, for every $n = 0, 1, 2, ..., N-1$, we are looking for $(\mathbf{u}_h^{n+1}, p_h^{n+1}) \in V_h \times Q_h$ the solution of

$$\begin{aligned} &\int_\Omega \rho_{\mathbf{X}_h^{n+1}}\left(\frac{\mathbf{u}_h^{n+1}-\mathbf{u}_h^n}{\tau^{n+1}} + (\mathbf{u}_h^{n+1}\cdot\nabla)\mathbf{u}_h^{n+1}\right)\cdot\mathbf{v}_h dx + \int_\Omega \mu_{\mathbf{X}_h^{n+1}}D(\mathbf{u}_h^{n+1}):D(\mathbf{v}_h)dx \\ &\qquad - \int_\Omega p_h^{n+1}\operatorname{div}\mathbf{v}_h dx - \int_\Omega q_h \operatorname{div}\mathbf{u}_h^{n+1}dx \\ &+ \sum_{K\in\mathcal{T}_h}\frac{\alpha\lambda_{2,K}^2}{\mu_{\mathcal{F}}\xi(Re_K)}\int_K \left(\rho_{\mathbf{X}_h^{n+1}}\mathbf{g} - \rho_{\mathbf{X}_h^{n+1}}(\mathbf{u}_h^{n+1}\cdot\nabla)\mathbf{u}_h^{n+1} - \nabla p_h^{n+1}\right)\cdot\left(\rho_{\mathbf{X}_h^{n+1}}(\mathbf{u}_h^{n+1}\cdot\nabla)\mathbf{v}_h + \nabla q_h\right)dx \\ &\qquad = \int_\Omega \rho_{\mathbf{X}_h^{n+1}}\mathbf{g}\cdot\mathbf{v}_h, \quad \forall(\mathbf{v}_h, q_h)\in V_h\times Q_h, \end{aligned} \tag{4.75}$$

where we note $\tau^{n+1} = t^{n+1} - t^n$, the time step, $\alpha > 0$ a positive dimensionless constant and

$$\xi(Re_K) = \begin{cases} 1 & \text{if } Re_K \leq 1, \\ Re_K & \text{if } Re_K \geq 1, \end{cases} \tag{4.76}$$

where we define the local anisotropic Reynolds number $Re_K$ by

$$Re_K = \frac{\rho_B \|\mathbf{u}_h^{n+1}\|_{L^\infty(K)} \lambda_{2,K}}{\mu_F}, . \tag{4.77}$$

The position of the disk is advanced solving

$$\frac{\mathbf{X}_h^{n+1} - \mathbf{X}_h^n}{\tau^{n+1}} = \frac{1}{\pi R^2} \int_{\mathcal{B}(\mathbf{X}_h^{n+1})} \mathbf{u}_h^{n+1} dx. \tag{4.78}$$

In the numerical experiments presented below, $\alpha$ is set to 0.1.

**Remark 4.26** (Practical implementation)**.**
In practice, equations (4.75) and (4.78) are decoupled by using a semi-implicit approximation. We first solve (4.75) with explicit coefficients $\rho_{\mathbf{X}_h^n}, \mu_{\mathbf{X}_h^n}$ instead of $\rho_{\mathbf{X}_h^{n+1}}, \mu_{\mathbf{X}_h^{n+1}}$, and then advance the disk center with

$$\frac{\mathbf{X}_h^{n+1} - \mathbf{X}_h^n}{\tau^{n+1}} = \frac{1}{\pi R^2} \int_{\mathcal{B}(\mathbf{X}_h^n)} \mathbf{u}_h^{n+1} dx.$$

The nonlinearity due the convective terms in (4.75) is handled at every iteration by solving one step of a Newton method. Finally, $\rho_{\mathbf{X}_h^n}$ and $\mu_{\mathbf{X}_h^n}$ are regularized using the approximation (1.25) of the Heavyside graph: given $\varepsilon' > 0$, we approximate the characteristic function $\chi_{\mathcal{B}(\mathbf{X}_h^n)}$ by the smooth function

$$\chi_{\varepsilon'}^n(\mathbf{x}) = H_{\varepsilon'}\left(R - |\mathbf{x} - \mathbf{X}_h^n|\right).$$

**Remark 4.27** (Fall of a sphere in 3D)**.**
We focus on the 2D situation, but the "non-collision" results of [56] also holds in 3D when considering the fall of a sphere inside a cubic cavity $\Omega$ and a similar numerical approximation can be used to verify it. Indeed, the model (4.74) can be written for $\Omega \in \mathbb{R}^3$, in particular one may only have to change the equation for the motion of $\mathbf{X}(t)$ by

$$\dot{\mathbf{X}}(t) = \frac{3}{4\pi R^3} \int_{\mathcal{B}(\mathbf{X}(t))} \mathbf{u}(t) dx.$$

The numerical method (4.75)-(4.78) reads then the same for the 3D case, we mainly have to replace $\lambda_{2,K}$ by $\lambda_{3,K}$ in the stabilization parameter. In the following pages, a derivation of error indicators will be done; these latter, and the computations presented to derive them, are also generalizable to $\mathbb{R}^3$.

## 4.9 Error estimates

In this section, we prove a posteriori error estimates for the time and the space discretization of a simplified model. Namely, we consider the steady Stokes version of equations (4.74), that is to say, starting from the initial position $\mathbf{X}_0$, we are looking for the solution

$(\mathbf{X}(t), \mathbf{u}_{\mathbf{X}(t)}, p_{\mathbf{X}(t)})$ of

$$\begin{cases} -\operatorname{div}(2\mu_{\mathbf{X}(t)} D(\mathbf{u}_{\mathbf{X}(t)})) + \nabla p_{\mathbf{X}(t)} = \rho_{\mathbf{X}(t)}\mathbf{g}, \quad \text{in } \Omega \times [0,T], \\ \operatorname{div} \mathbf{u}_{\mathbf{X}(t)} = 0, \quad \text{in } \Omega \times [0,T], \\ \mathbf{u}_{\mathbf{X}(t)} = 0, \quad \text{on } \partial\Omega \times [0,T], \\ \rho_{\mathbf{X}(t)} = \rho_{\mathcal{B}}\chi_{\mathcal{B}(\mathbf{X}(t))} + \rho_{\mathcal{F}}(1-\chi_{\mathcal{B}(\mathbf{X}(t))}), \quad \text{in } \Omega \times [0,T], \\ \mu_{\mathbf{X}(t)} = \frac{1}{\varepsilon}\chi_{\mathcal{B}(\mathbf{X}(t))} + \mu_{\mathcal{F}}(1-\chi_{\mathcal{B}(\mathbf{X}(t))}), \quad \text{in } \Omega \times [0,T], \\ \dot{\mathbf{X}}(t) = \frac{1}{\pi R^2}\int_{\mathcal{B}(\mathbf{X}(t))} \mathbf{u}_{\mathbf{X}(t)} dx, t > 0, \\ \mathbf{X}(0) = \mathbf{X}_0. \end{cases} \tag{4.79}$$

Note that here, and to simplify, we do not impose $\mathbf{u}_{\mathbf{X}(0)}$, but we assume that it is given by solving the Stokes equations at $t = 0$. The solutions to (4.79) are then completely determined by the initial position $\mathbf{X}_0$. To avoid trivial solutions, we assume that $\mathbf{X}_0$ is far enough from the boundary of $\Omega$, that is to say $d(\mathcal{B}(\mathbf{X}_0), \partial\Omega) > 0$.

The above simplified model can be understood as a rather good approximation of the full model (4.74) since we work with quite highly viscous fluid and the "non-collision" result is also true for the steady Stokes equations [56].

### 4.9.1 Semi-discrete error estimate for the time discretization

We now prove a semi-discrete a posteriori error estimate for the time discretization of the simplified problem (4.79). We choose the forward Euler method. Given a integer $N > 0$ and $0 = t^0 < t^1 < .... < t^N = T$, starting from $\mathbf{X}_0$, for every $n = 0, 1, 2, ..., N-1$, we approximate the exact position of the center $\mathbf{X}(t^{n+1})$ by $\mathbf{X}^{n+1}$, and for every $n = 0, 1, 2, ...N$, the exact Stokes solutions $(\mathbf{u}_{\mathbf{X}(t^n)}, p_{\mathbf{X}(t^n)})$ by the approximated solutions $(\mathbf{u}_{\mathbf{X}^n}, p_{\mathbf{X}^n})$, obtained by solving

$$\begin{cases} -\operatorname{div}(2\mu_{\mathbf{X}^n} D(\mathbf{u}_{\mathbf{X}^n})) + \nabla p_{\mathbf{X}^n} = \rho_{\mathbf{X}^n}\mathbf{g}, \quad \text{in } \Omega, \\ \operatorname{div} \mathbf{u}_{\mathbf{X}^n} = 0, \quad \text{in } \Omega, \\ \mathbf{u}_{\mathbf{X}^n} = 0, \quad \text{on } \partial\Omega, \\ \rho_{\mathbf{X}^n} = \rho_{\mathcal{B}}\chi_{\mathcal{B}(\mathbf{X}^n)} + \rho_{\mathcal{F}}(1-\chi_{\mathcal{B}(\mathbf{X}^n)}), \quad \text{in } \Omega, \\ \mu_{\mathbf{X}^n} = \frac{1}{\varepsilon}\chi_{\mathcal{B}(\mathbf{X}^n)} + \mu_{\mathcal{F}}(1-\chi_{\mathcal{B}(\mathbf{X}^n)}), \quad \text{in } \Omega, \\ \frac{\mathbf{X}^{n+1}-\mathbf{X}^n}{\tau^{n+1}} = \frac{1}{\pi R^2}\int_{\mathcal{B}(\mathbf{X}^n)} \mathbf{u}_{\mathbf{X}^n} dx, \\ \mathbf{X}^0 = \mathbf{X}_0 \end{cases} \tag{4.80}$$

We do not claim anything on the well-posedness of problems (4.79) and (4.80), neither on the a priori error analysis of the numerical method. So far, we will assume that there exists a unique solution $(\mathbf{u}_{\mathbf{X}(t)}, p_{\mathbf{X}(t)}) \in C([0,T]; (H_0^1(\Omega))^2) \times L^2((0,T); L_0^2(\Omega))$ associated with a unique solution $\mathbf{X}(t) \in C^1[0,T]$ to problem (4.79). Moreover, we assume that $\varepsilon$ is small enough such that $d(\mathcal{B}(\mathbf{X}(t);\partial\Omega) > 0$ for all $t \in [0,T]$. This is a reasonable assumption since we can expect that the solutions of the penalized problem (4.79) converges to the "non colliding" solution of [56].

We now prove a semi-discrete a posteriori error estimate for the problem (4.79) and its numerical approximation (4.80). We make a few comments before presenting the main proofs. Observe that problem (4.79) reads in fact: starting from $\mathbf{X}(0) = \mathbf{X}_0$ find $\mathbf{X}(t)$, for $t > 0$, such that

$$\dot{\mathbf{X}}(t) = \mathbf{F}(\mathbf{X}(t)),$$

where, for any $\mathbf{x} \in \mathbb{R}^2$ such that $\mathcal{B}(\mathbf{x})$ is compactly supported in $\Omega$, $\mathbf{F}(\mathbf{x})$ is given by

$$\mathbf{F}(\mathbf{x}) = \frac{1}{\pi R^2}\int_{\mathcal{B}(\mathbf{x})} \mathbf{u}_{\mathbf{x}} dx \tag{4.81}$$

with $\mathbf{u}_{\mathbf{x}}$ being the unique solution to the Stokes problem

$$\begin{cases} -\operatorname{div}(2\mu_{\mathbf{x}} D(\mathbf{u}_{\mathbf{x}}) + \nabla p_{\mathbf{x}} = \rho_{\mathbf{x}}\mathbf{g}, \quad \text{in } \Omega, \\ \operatorname{div}\mathbf{u}_{\mathbf{x}} = 0, \quad \text{in } \Omega, \\ \mathbf{u}_{\mathbf{x}} = 0, \quad \text{on } \partial\Omega, \\ \rho_{\mathbf{X}(t)} = \rho_{\mathcal{B}}\chi_{\mathcal{B}(\mathbf{x})} + \rho_{\mathcal{F}}(1-\chi_{\mathcal{B}(\mathbf{x})}), \quad \text{in } \Omega, \\ \mu_{\mathbf{X}(t)} = \dfrac{1}{\varepsilon}\chi_{\mathcal{B}(\mathbf{x})} + \mu_{\mathcal{F}}(1-\chi_{\mathcal{B}(\mathbf{x})}), \quad \text{in } \Omega. \end{cases}$$

From this point of view, deriving a temporal a posteriori error estimate for the equations (4.79) and their numerical approximations (4.80) reduces to know how prove an a posteriori error estimate for the forward Euler approximation of the autonomous ODE $y' = f(y)$. This can be done provided $f$ is Lipschitz continuous. Coming back to our particular problem, the main work will consist then to prove that $\mathbf{F}$ given by (4.81) is Lipschitz. This is achieved in the Theorem B.10 in the Appendix. In the next proposition, we show the main consequence of this result, that will be used to prove the a posteriori error bound. We work under the assumption that the numerical method (4.80) converges.

**Proposition 4.28.**
*Let* $(\mathbf{X}(t), \mathbf{u}_{\mathbf{X}(t)}), t \in [t^n, t^{n+1}]$ *be the solution of* (4.79) *and* $(\mathbf{X}^n, \mathbf{u}_{\mathbf{X}^n}), n = 0, 1..., N$ *the solution of* (4.80)*. Let* $\tau = \max_{n=0,1,2,...,N-1} t^{n+1} - t^n$ *be the maximal time step size and let us assume that for all* $n = 1, 2, 3, ...N$, $\mathbf{X}^n$ *converges to* $\mathbf{X}(t^n)$ *as* $\tau$ *goes to* $0$*. Then, if* $\tau$ *is small enough, there exists* $C > 0$ *depending only on* $\Omega$ *such that for all* $t \in [t^n, t^{n+1}]$

$$\left| \frac{1}{\pi R^2}\int_{\mathcal{B}(\mathbf{X}(t))} \mathbf{u}_{\mathbf{X}(t)} dx - \frac{1}{\pi R^2}\int_{\mathcal{B}(\mathbf{X}^n)} \mathbf{u}_{\mathbf{X}^n} dx \right| \le C \frac{\rho_{\mathcal{B}}|g|}{R\mu_{\mathcal{F}}^2\varepsilon} \frac{|\mathbf{X}(t) - \mathbf{X}^n|}{d(\mathcal{B}(\mathbf{X}(t));\partial\Omega)}, \tag{4.82}$$

*Proof.* The proof of (4.82) is a direct consequence of Theorem B.10 in the Appendix applied to problems (4.79) and (4.80). We only have to check that the ratio

$$\frac{|\mathbf{X}(t) - \mathbf{X}^n|}{d(\mathcal{B}(\mathbf{X}(t));\partial\Omega)}$$

is small enough and that

$$d(\mathcal{B}(\mathbf{X}^n);\partial\Omega) > 0,$$

which is true since $d(\mathcal{B}(\mathbf{X}(t);\partial\Omega) > 0$ and that the numerical method converges. □

We now introduce the piecewise linear reconstruction $\mathbf{X}_\tau$ defined by

$$\mathbf{X}_\tau(t) = \mathbf{X}^n + (t - t^n)\frac{\mathbf{X}^{n+1} - \mathbf{X}^n}{\tau^{n+1}}, \quad t \in [t^n, t^{n+1}], n = 0, 1, 2, ..., N-1. \tag{4.83}$$

The main result of this section is semi-discrete a posteriori error estimate contained in the theorem

**Theorem 4.29** (A semi-discrete a posteriori error estimate for the time approximation of the motion of a rigid disk into an incompressible fluid)**.**
*Let $e(t) = \mathbf{X}(t) - \mathbf{X}_\tau(t)$. Under the assumptions of Proposition 4.28, there exists a constant $C > 0$ depending only on $\Omega$, such that*

$$|\mathbf{e}(T)| \leq CL\sum_{n=0}^{N-1}\int_{t^n}^{t^{n+1}} \frac{1}{d(\mathcal{B}(\mathbf{X}(t);\partial\Omega))}(t-t^n)\left|\frac{\mathbf{X}^{n+1} - \mathbf{X}^n}{\tau^{n+1}}\right| \exp\left(\int_t^T \frac{CL}{d(\mathcal{B}(\mathbf{X}(s));\partial\Omega)}ds\right) dt \tag{4.84}$$

*where* $L = \dfrac{\rho_{\mathcal{B}}|g|}{R\mu_{\mathcal{F}}^2\varepsilon}$.

*Proof.* Let $n \geq 0$ and $t \in (t^n, t^{n+1})$. Using (4.79) and (4.80), we have

$$\dot{\mathbf{e}}(t) = \frac{1}{\pi R^2}\int_{\mathcal{B}(\mathbf{X}(t))} \mathbf{u}_{\mathbf{X}(t)}dx - \frac{1}{\pi R^2}\int_{\mathcal{B}(\mathbf{X}^n)} \mathbf{u}_{\mathbf{X}^n}dx.$$

Taking the scalar product of the last equation with $\mathbf{e}(t)$, using the Cauchy-Schwarz inequality and the Proposition 4.28 yields

$$\frac{1}{2}\frac{d}{dt}|\mathbf{e}(t)|^2 \leq C\frac{L}{d(\mathcal{B}(\mathbf{X}(t));\partial\Omega)}|\mathbf{X}(t) - \mathbf{X}^n||\mathbf{e}(t)|.$$

Without loss of generality, we assume that $\mathbf{e}(t) \neq 0, t \in (t^n, t^{n+1})$. Therefore, dividing by $|\mathbf{e}(t)|$ we get

$$\frac{d}{dt}|\mathbf{e}(t)| = \frac{\frac{d}{dt}|\mathbf{e}(t)|^2}{2|\mathbf{e}(t)|} \leq C\frac{L}{d(\mathcal{B}(\mathbf{X}(t));\partial\Omega)}|\mathbf{X}(t) - \mathbf{X}^n|,$$

where we use that $|\mathbf{e}(t)| = \sqrt{|\mathbf{e}(t)|^2}$. Applying the triangle inequality, we obtain

$$\frac{d}{dt}|\mathbf{e}(t)| \leq C\frac{L}{d(\mathcal{B}(\mathbf{X}(t));\partial\Omega)}|\mathbf{X}_\tau - \mathbf{X}^n| + C\frac{L}{d(\mathcal{B}(\mathbf{X}(t));\partial\Omega)}|\mathbf{e}(t)|,$$

Multiplying the last inequality by $\exp\left(-\int_0^t \frac{CL}{d(\mathcal{B}(\mathbf{X}(s));\partial\Omega)}ds\right)$, and integrating from $t^n$ to $t^{n+1}$

$$\begin{aligned}|\mathbf{e}(t^{n+1})| \exp\left(-\int_0^{t^{n+1}} \frac{CL}{d(\mathcal{B}(\mathbf{X}(t));\partial\Omega)}dt\right) - |\mathbf{e}(t^n)| \exp\left(-\int_0^{t^n} \frac{CL}{d(\mathcal{B}(\mathbf{X}(t));\partial\Omega)}dt\right)\\ \leq CL\int_{t^n}^{t^{n+1}}\left(\frac{|\mathbf{X}_\tau(t) - \mathbf{X}^n|}{d(\mathcal{B}(\mathbf{X}(t);\partial\Omega))}\right)\exp\left(-\int_0^t \frac{CL}{d(\mathcal{B}(\mathbf{X}(s));\partial\Omega)}ds\right)dt,\end{aligned}$$

Summing up over $n$ leads to

$$|\mathbf{e}(T)| \leq CL\sum_{n=0}^{N-1}\int_{t^n}^{t^{n+1}} \frac{|\mathbf{X}_\tau(t) - \mathbf{X}^n|}{d(\mathcal{B}(\mathbf{X}(t);\partial\Omega))}\exp\left(\int_t^T \frac{CL}{d(\mathcal{B}(\mathbf{X}(s));\partial\Omega)}ds\right)dt,$$

where we use that $e(0) = 0$ to get rid of the error at $t = 0$. The desired estimate is then obtained by using the definition of $\mathbf{X}_\tau$. □

**Remark 4.30.**
The bound (4.84) is not a standard a posteriori error estimate since it involves the exact solution $\mathbf{X}(t)$. In practice, and to obtain a computable error indicator, we will replace $d(\mathcal{B}(\mathbf{X}(s));\partial\Omega)$ by $d(\mathcal{B}(\mathbf{X}_\tau(s));\partial\Omega)$

### 4.9.2 Semi-discrete error estimate for the space approximation

In the section, we prove a (anisotropic) semi-discrete a posteriori error estimate for the finite elements approximation of the simplified problem that are the Stokes equations (4.79). We will assume that the exact trajectory $\mathbf{X}(t)$ is a priori known and we will focus on the approximation at each $t \in [0, T]$ of the Stokes equations

$$\begin{cases} -\operatorname{div}(2\mu_{\mathbf{X}(t)} D(\mathbf{u}_{\mathbf{X}(t)})) + \nabla p_{\mathbf{X}(t)} = \rho_{\mathbf{X}(t)} \mathbf{g}, \quad \text{in } \Omega, \\ \operatorname{div} \mathbf{u}_{\mathbf{X}(t)} = 0, \quad \text{in } \Omega, \\ \mathbf{u}_{\mathbf{X}(t)} = 0, \quad \text{on } \partial\Omega, \\ \rho_{\mathbf{X}(t)} = \rho_{\mathcal{B}} \chi_{\mathcal{B}(\mathbf{X}(t))} + \rho_{\mathcal{F}}(1 - \chi_{\mathcal{B}(\mathbf{X}(t))}), \quad \text{in } \Omega, \\ \mu_{\mathbf{X}(t)} = \frac{1}{\varepsilon} \chi_{\mathcal{B}(\mathbf{X}(t))} + \mu_{\mathcal{F}}(1 - \chi_{\mathcal{B}(\mathbf{X}(t))}), \quad \text{in } \Omega, \end{cases} \tag{4.85}$$

The equations (4.85) will be approximated by anisotropic, stabilized, piecewise continuous finite elements. To stay in the framework of the previous chapters, we will do a last simplification and regularize the characteristic function $\chi_{\mathcal{B}(\mathbf{X}(t))}$ by using as approximation

$$\chi_{\varepsilon'}(\mathbf{x}, t) = H_{\varepsilon'}\left(R - |\mathbf{x} - \mathbf{X}(t)|\right),$$

see Example 4.25.

Defining the smooth functions

$$\rho(\mathbf{x}, t) = \rho_{\mathcal{B}} \chi_{\varepsilon'}(\mathbf{x}, t) + \rho_{\mathcal{F}}(1 - \chi_{\varepsilon'}(\mathbf{x}, t)), \mu(\mathbf{x}, t) = \frac{1}{\varepsilon} \varphi_{\varepsilon'}(\mathbf{x}, t) + \mu_{\mathcal{F}}(1 - \varphi_{\varepsilon'}(\mathbf{x}, t)),$$

then instead of (4.85), we consider for each $t \in [0, T]$ the steady Stokes equations with smooth coefficients

$$\begin{cases} -\operatorname{div}(2\mu(t) D(\mathbf{u}(t))) + \nabla p(t) = \rho(t) \mathbf{g}, \quad \text{in } \Omega, \\ \operatorname{div} \mathbf{u}(t) = 0, \quad \text{in } \Omega, \\ \mathbf{u}(t) = 0, \quad \text{on } \partial\Omega, \end{cases} \tag{4.86}$$

The variational formulation of the previous equations reads: for each $t \in [0, T]$ find $(\mathbf{u}(t), p(t)) \in (H_0^1(\Omega))^2 \times L_0^2(\Omega)$

$$\begin{aligned} \int_\Omega 2\mu(t) D(\mathbf{u}(t)) : D(\mathbf{v}) d\mathbf{x} - \int_\Omega p(t) \operatorname{div} \mathbf{v} d\mathbf{x} = \int_\Omega \rho(t) \mathbf{g} \cdot \mathbf{v} d\mathbf{x}, \forall \mathbf{v} \in (H_0^1(\Omega))^2, \\ -\int_\Omega q \operatorname{div} \mathbf{u}(t) d\mathbf{x} = 0, \forall q \in L_0^2(\Omega). \end{aligned} \tag{4.87}$$

The well-posedness of (4.87) is guaranteed by the smoothness of $\rho$ and $\mu$, see for instance [21] or Theorem B.4. Observe that both $\mu$ and $\rho$ are bounded by construction. In particular, one have

$$\mu_{\min} \leq \mu(\mathbf{x}, t) \leq \mu_{\max}, \forall (\mathbf{x}, t), \quad \mu_{\min} = \min(\mu_{\mathcal{F}}, 1/\varepsilon), \mu_{\max} = \max(\mu_{\mathcal{F}}, 1/\varepsilon).$$

Now, the equations (4.87) are discretized as follows: for all $h > 0$, let $\mathcal{T}_h$ be a conformal triangulation of $\Omega$ with triangles of diameter $h_K \leq h$. For any $t \in [0, T]$, we look for $(\mathbf{u}_h(t), p_h(t)) \in V_h \times Q_h$ the solution of

$$\begin{aligned}&\int_\Omega 2\mu(t)D(\mathbf{u}_h(t)) : D(\mathbf{v}_h)d\mathbf{x} - \int_\Omega p_h(t)\operatorname{div}\mathbf{v}_h d\mathbf{x} = \int_\Omega \rho(t)\mathbf{g}\cdot\mathbf{v}_h d\mathbf{x}, \forall \mathbf{v}_h \in V_h,\\ &-\int_\Omega q_h \operatorname{div}\mathbf{u}_h(t)d\mathbf{x} + \sum_{K\in\mathcal{T}_h}\frac{\alpha\lambda_{2,K}^2}{\mu_{\mathcal{F}}}\int_K(\rho(t)\mathbf{g} - \nabla p_h(t))\cdot\nabla q_h d\mathbf{x} = 0, \forall q_h \in Q_h.\end{aligned} \quad (4.88)$$

We now prove an a posteriori error estimate for the numerical error $\|\nabla(\mathbf{u} - \mathbf{u}_h)\|_{L^2(\Omega)}$. The proof follows mainly the proof of Theorem 3.6 for the steady Navier-Stokes equations, taking in account the variation of the coefficient as in Proposition 4.8. Here the situation is simpler since we only consider the (linear) Stokes equations. Therefore, we will be quite concise since the main arguments of the proof were already presented. Note also that the proof is presented for the case of the particular problem (4.86), but works also for more general Stokes equations with smooth variable coefficients.

As for the case of the steady Navier-Stokes equations, the pressure estimate is recovered through a dual problem. For any $t \in [0, T]$, we look for $(\mathbf{w}(t), r(t)) \in (H_0^1(\Omega))^2 \times L_0^2(\Omega)$ the weak solution of

$$\begin{cases} -\operatorname{div}(2\mu(t)D(\mathbf{w}(t))) + \nabla r(t) = 0, & \text{in } \Omega,\\ \operatorname{div}\mathbf{w}(t) = p_h(t) - p(t), & \text{in } \Omega,\\ \mathbf{w}(t) = 0, & \text{on } \partial\Omega.\end{cases} \quad (4.89)$$

By the Theorem B.4 in the Appendix, the following a priori estimate holds

$$\frac{\mu_{\min}}{\mu_{\max}}\|\nabla\mathbf{w}(t)\|_{L^2(\Omega)} + \frac{\mu_{\min}}{\mu_{\max}^2}\|r(t)\|_{L^2(\Omega)} \leq C\|P - p_h(t)\|_{L^2(\Omega)},$$

where $C$ depends only on $\Omega$. The a posteriori error estimate is contained in the Theorem

**Theorem 4.31** (A semi-discrete a posteriori error estimate for the space approximation of the Stokes equations with variable viscosity)**.**
*Let $(\mathbf{u}(t), p(t))$ be the solution of (4.87), $(\mathbf{u}_h(t), p_h(t))$ the solution of the finite elements approximation (4.88) and $(\mathbf{w}(t), r(t))$ the solution of the dual problem (4.89). Then there exists a constant $C > 0$ that depends only on the reference triangle, in particular independent of the mesh aspect ratio, such that for any $t \in [0, T]$*

$$\begin{aligned}\mu_{\min}\|\nabla(\mathbf{u} - \mathbf{u}_h)(t)\|^2 L^2(\Omega) + \frac{\mu_{\min}^3}{\mu_{\max}^4}\|p(t) - p_h(t)\|_{L^2(\Omega)}^2&\\ \leq C\sum_{K\in\mathcal{T}_h}(\eta_{K,\mathbf{u}}^A)^2(t) + (\eta_{K,p}^A)^2(t) + (\eta_K^{\text{div}})^2(t),&\end{aligned} \quad (4.90)$$

*where*

$$(\eta_{K,\mathbf{u}}^A)^2 = \left(\|\rho\mathbf{g} + \operatorname{div}(2\mu D(\mathbf{u}_h)) - \nabla p_h\|_{L^2(K)} + \frac{1}{2\sqrt{\lambda_{2,K}}}\|[2\mu D(\mathbf{u}_h)\cdot\mathbf{n}]\|_{L^2(\partial K)}\right)\omega_K(\mathbf{u}-\mathbf{u}_h),$$

$$(\eta_{K,p}^A)^2 = \frac{\mu_{\min}^3}{\mu_{\max}^4}\left(\|\rho\mathbf{g} + \operatorname{div}(2\mu D(\mathbf{u}_h)) - \nabla p_h\|_{L^2(K)} + \frac{1}{2\sqrt{\lambda_{2,K}}}\|[2\mu D(\mathbf{u}_h)\cdot\mathbf{n}]\|_{L^2(\partial K)}\right)\omega_K(\mathbf{w}),$$

$$(\eta_K^{\text{div}})^2 = \frac{\mu_{\max}^4}{\mu_{\min}^3}\|\operatorname{div}\mathbf{u}_h\|_{L^2(\Omega)}^2.$$

*Proof.* We note by $C$ any positive constant that may depend only on the reference triangle or the domain, which value can change from line to line. To simplify the notations, we also do not write the dependence on $t$. Following the first step of the proof of Proposition 4.8, we can prove that

$$\mu_{\min}\|\nabla(\mathbf{U}-\mathbf{u}_h)\|^2_{L^2(\Omega)} \leq C\sum_{K\in\mathcal{T}_h}\left(\|R_h^S\|_{L^2(K)} + \frac{1}{2\sqrt{\lambda_{2,K}}}\|R^S_{h,j}\|_{L^2(\partial K)}\right)\omega_K(\mathbf{u}-\mathbf{u}_h) \tag{4.91}$$

$$+\|p-p_h\|_{L^2(\Omega)}\|\operatorname{div}(\mathbf{u}-\mathbf{u}_h)\|_{L^2(\Omega)}, \tag{4.92}$$

where

$$R_h^S = \rho\mathbf{g} + \operatorname{div}(2\mu D(\mathbf{u}_h)) - \nabla p_h, R^S_{h,j} = [2\mu D(\mathbf{u}_h)\cdot\mathbf{n}].$$

Now, following the second part of the proof of Proposition 4.8, by using the dual problem (4.89) one can establish for the pressure

$$\|p-p_h\|_{L^2(\Omega)} \leq C\left(\sum_{K\in\mathcal{T}_h}\left(\|R_h^S\|_{L^2(K)} + \frac{1}{2\sqrt{\lambda_{2,K}}}\|R^S_{h,j}\|_{L^2(\partial K)}\right)\omega_K(\mathbf{w}) + \frac{\mu^4_{\max}}{\mu^2_{\min}}\|\nabla(\mathbf{u}-\mathbf{u}_h)\|^2_{L^2(\Omega)}\right) \tag{4.93}$$

Combining estimates (4.91) and (4.93)as in the last part of the proof of Proposition 4.8 yields the result. □

## 4.10 Error indicators and adaptive algorithm

We now briefly introduce the error indicators we use in the numerical experiments. Let $(\mathbf{u}_h^n)_{n=0}^N, (\mathbf{X}_h^n)_{n=0}^N$ be the approximated velocity fields and the approximated position of the center of mass obtained with the numerical method (4.75)-(4.78). We introduce the piecewise linear reconstructions $\mathbf{u}_{h\tau}$ and $\mathbf{X}_{h\tau}$ defined by

$$\mathbf{u}_{h\tau}(t) = \mathbf{u}_h^n + (t-t^n)\frac{\mathbf{u}_h^{n+1}-\mathbf{u}_h^n}{\tau^{n+1}}, \tag{4.94}$$

$$\mathbf{X}_{h\tau}(t) = \mathbf{X}_h^n + (t-t^n)\frac{\mathbf{X}_h^{n+1}-\mathbf{X}_h^n}{\tau^{n+1}}, \tag{4.95}$$

for $t\in[t^n,t^{n+1}], n=0,1,2,...,N-1$. Moreover, we introduce the smooth version of the density and the viscosity given by

$$\rho_{h\tau} = \rho_{\mathcal{B}}\chi_{h\tau} + \rho_{\mathcal{F}}(1-\chi_{h\tau}), \mu_{h\tau} = \frac{1}{\varepsilon}\chi_{h\tau} + \mu_{\mathcal{F}}(1-\chi_{h\tau}),$$

where the smooth characteristic function $\chi_{h\tau}$ is given by

$$\chi_{h\tau}(\mathbf{x},t) = H_{\varepsilon'}\left(R - |\mathbf{x}-\mathbf{X}_{h\tau}(t)|\right).$$

Based on (4.84), we choose $\eta^T$ defined by

$$\eta^T = \sum_{n=0}^{N-1}\eta_n^T, \quad \eta_n^T = \frac{1}{d(\mathcal{B}(\mathbf{X}_h^{n+1});\partial\Omega)}\frac{(t^{n+1}-t^n)^2}{2}\left|\frac{\mathbf{X}_h^{n+1}-\mathbf{X}_h^n}{\tau^{n+1}}\right|, \tag{4.96}$$

as the time error indicator for the error $|\mathbf{X}(T)-\mathbf{X}_{h\tau}(T)|$.

To adapt the mesh, we use the following space error indicator for $\|\nabla(\mathbf{u}-\mathbf{u}_{h\tau})\|_{L^2(0,T;L^2(\Omega))}$ that is motivated by the estimate (4.90). We introduce the anisotropic error indicator $\eta$ given by

$$\eta^A = \left( \sum_{K \in \mathcal{T}_h} (\eta^A_{K,n})^2 \right)^{1/2}, \tag{4.97}$$

where

$$(\eta^A_{K,n})^2 = \int_{t^n}^{t^{n+1}} \Big( \|\rho_{h\tau}(t)\mathbf{g} + \operatorname{div}(2\mu_{h\tau}(t)D(\mathbf{u}_{h\tau}(t))) - \nabla p_{h\tau}\|_{L^2(K)} + \frac{1}{2\sqrt{\lambda_{2,K}}} \|2[\mu_{h\tau}(t)D(\mathbf{u}_{h\tau}(t)) \cdot \mathbf{n}]\|_{L^2(\partial K)} \Big) \omega_K(\Pi_h \mathbf{u}_{h\tau}(t) - \mathbf{u}_{h\tau}(t))dt.$$

where $\Pi_h^{ZZ}$ stands for the Zienkiewicz-Zhu (ZZ) post-processing.

Given a prescribed tolerance, the goal of the adaptive algorithm is to ensure that

$$0.875TOL \leq \frac{\eta^A}{\left(\int_0^T \|\sqrt{2\mu_{h\tau}} D(\mathbf{u}_{h\tau}(t))\|^2_{L^2(\Omega)} dt\right)^{1/2}} + \frac{\eta^T}{T} \leq 1.125TOL. \tag{4.98}$$

A sufficient condition is to ensure that for every $n = 0, 1, 2, ...$

$$0.875^2 \beta^2 TOL^2 \int_{t^n}^{t^{n+1}} \|\sqrt{2\mu_{h\tau}} D(\mathbf{u}_{h\tau}(t))\|^2_{L^2(\Omega)} dt \leq (\eta^A_{K,n})^2 \leq 1.125^2 \beta^2 TOL^2 \int_{t^n}^{t^{n+1}} \|\sqrt{2\mu_{h\tau}} D(\mathbf{u}_{h\tau}(t))\|^2_{L^2(\Omega)} dt, \tag{4.99}$$

and

$$0.75(1-\beta)TOL\tau^{n+1} \leq \eta^T_n \leq 1.25(1-\beta)TOL\tau^{n+1}. \tag{4.100}$$

If (4.99) is not satisfied, then the mesh is adapted following the anisotropic procedure described in the previous chapters. If (4.100) does not hold, the time step is changed. Here $\beta > 0$ is a parameter to be set, and used to distribute the error between time and space. In practice, best results were obtained where $\beta = 0.5$, which means that the error is equidistributed between time and space.

To build a new mesh from (4.99), we follow the procedure described in Chapter 3 for the Navier-Stokes equations. The interpolation of computed values between meshes are performed using the conservative algorithm described in [5].

## 4.11 Numerical results with non-adapted time steps and non-adapted meshes

We now perform numerical experiments to verify the "non-collision" result of [56]. The physical parameters chosen for our simulations are summarized in the Table 4.8. This corresponds approximatively to the fall of a lead disk into glycerine. In order to check if our numerical solutions exhibit the right behavior, we compare them to a reference solution, computed through lubrication theory [94]. We briefly present how this reference solution was computed. Let us denote by $h(t)$ the height of the disk at time $t$. The velocity fall of the disk is then given by $\dot{h}(t)$. The reference solution is obtained by solving the Newton equation

$$\begin{cases} m\ddot{h}\mathbf{e}_2 = m\mathbf{g} - \rho_{\mathcal{F}}\pi R^2\mathbf{g} + \mathbf{F} + \gamma\dot{h}\mathbf{e}_2, \quad t \in (0,T], \\ h(0) = 0.05, \dot{h} = 0, \end{cases} \tag{4.101}$$

where $\gamma > 0$. In the above equation, $m\mathbf{g}$ is the gravitational force acting on the disk ($m$ standing for its mass), $\rho_{\mathcal{F}}\pi R^2\mathbf{g}$ the Archimède force and $\gamma\dot{h}$ takes in account the velocity of the disk when approaching $\partial\Omega$. The value of $\gamma$ is 41.2 and was obtained by fitting the solution of (4.101) with the numerical results obtained with non-adapted meshes and constant time steps.

$\mathbf{F}$ is the repulsive force generated by the pressure under the disk and is computed by scaling the equations (4.72) with respect to $h$. Its explicit expression can be found in [94]. One can observe that the amplitude $|\mathbf{F}|$ goes like $\frac{\dot{h}}{h}$. Observe that this quantity corresponds to $\frac{1}{d(\mathcal{B}(\mathbf{X}_h^{n+1});\partial\Omega)}\left|\frac{\mathbf{X}_h^{n+1}-\mathbf{X}_h^n}{\tau^{n+1}}\right|$ in (4.96).

We plot in Figure 4.18 the approximated evolution of the height of the ball obtained with the reference solution and in Figure 4.19 the evolution of the pressure. We observe that a peak of pressure appears around $t = 0.1245$ slowing down the disk and preventing the collision.

| | | |
|---|---|---|
| side lenght of $\Omega$ | $a$ | $0.1\ m$ |
| radius of the disk | $R$ | $0.01\ m$ |
| density of the disk | $\rho_{\mathcal{B}}$ | $10^4\ {}^{kg}/_{m^3}$ |
| density of the fluid | $\rho_{\mathcal{F}}$ | $10^3\ {}^{kg}/_{m^3}$ |
| viscosity of the fluid | $\mu_{\mathcal{F}}$ | $1\ {}^{kg}/_{m\cdot s}$ |
| initial position of the disk | $\mathbf{X}_0$ | $(0.05, 0.05)$ |
| final time | $T$ | $0.14$ |

Table 4.8: Physical parameters for numerical simulations.

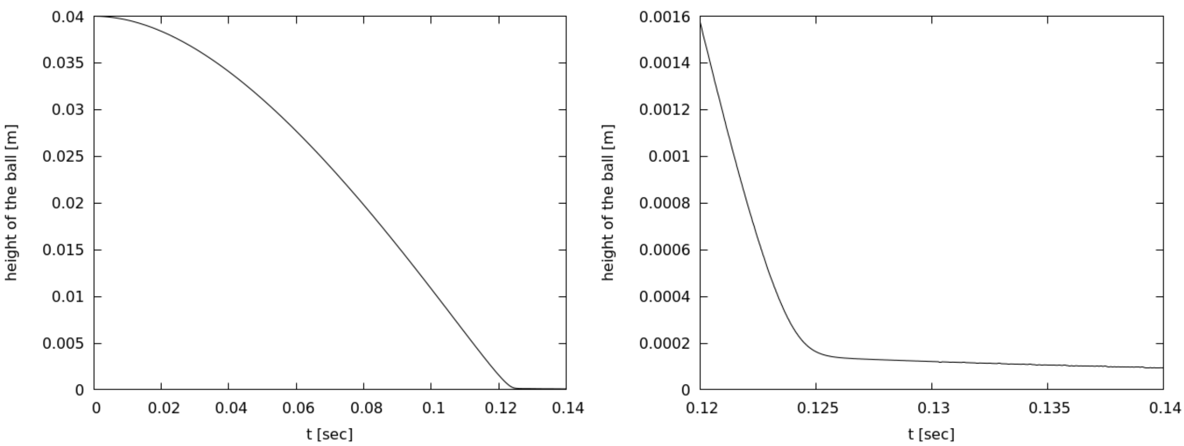


Figure 4.18: Evolution of the height of the disk given by the reference solution (4.101) (left). Zoom (right)

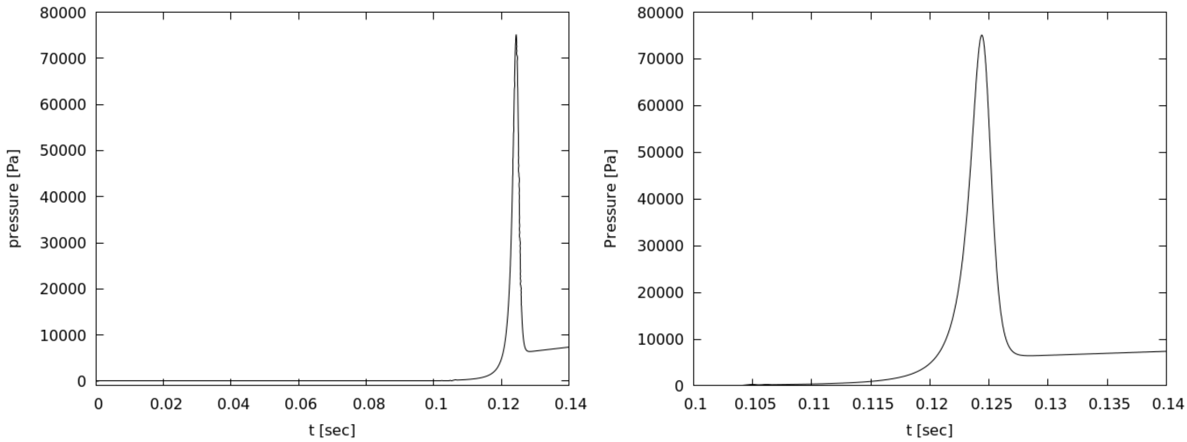


Figure 4.19: Evolution of the reference pressure under the disk(left). Zoom (right)

We first run some numerical tests without adapting the mesh or the time step in order to check if our numerical methods can capture the behavior of the reference solution. To do so, we fix a constant time step and build a "by-hand" adapted grid where the mesh size is small in the region close the bottom of $\Omega$. The time step is chosen as $\tau = 10^{-3}$ and the penalty parameter is set as $\varepsilon = 10^{-5}$. Since we expect a priori that the disk falls vertically, we improve the numerical method (4.78), keeping the first component of $\mathbf{X}_h^n$ constant, and updating only the second with (4.78). The regularization parameter $\varepsilon'$ is set to $10^{-4}$.

The numerical results are reported in Figure 4.20 where we plot the evolution of the distance of the disk to $\partial\Omega$, and in Figure 4.21 the peak of pressure. The mesh and the solutions are represented in Figures 4.22. The numerical tests indicate a pressure appears around $t = 0.12$. The amplitude of the peak is twice bigger than the one predicted by (4.101).

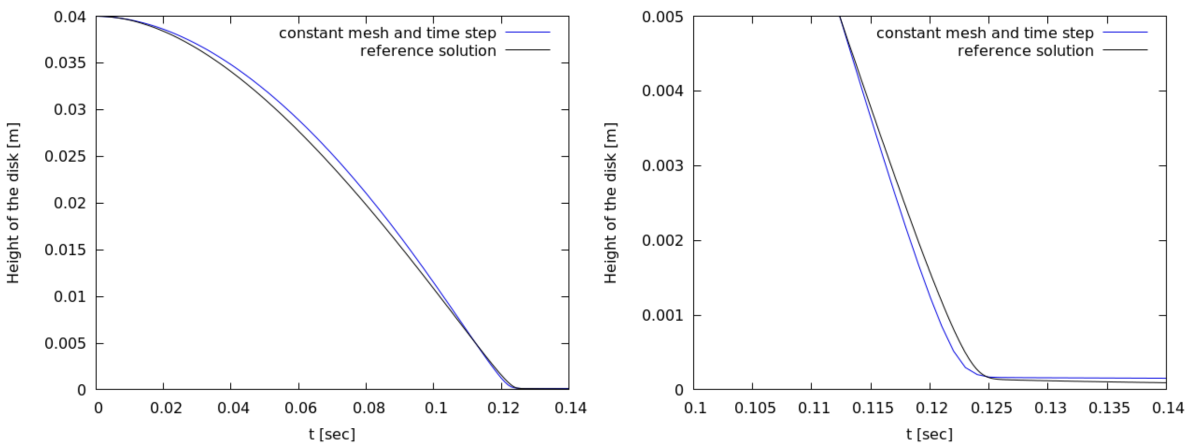


Figure 4.20: Height of the disk computed through numerical method (4.75), (4.80) with a constant mesh and a constant time step.

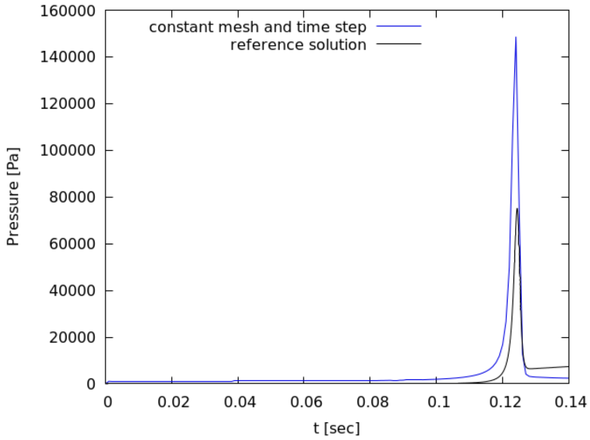


Figure 4.21: Evolution of the pressure under the disk computed through numerical method (4.75), (4.80) with a constant mesh and a constant time step.

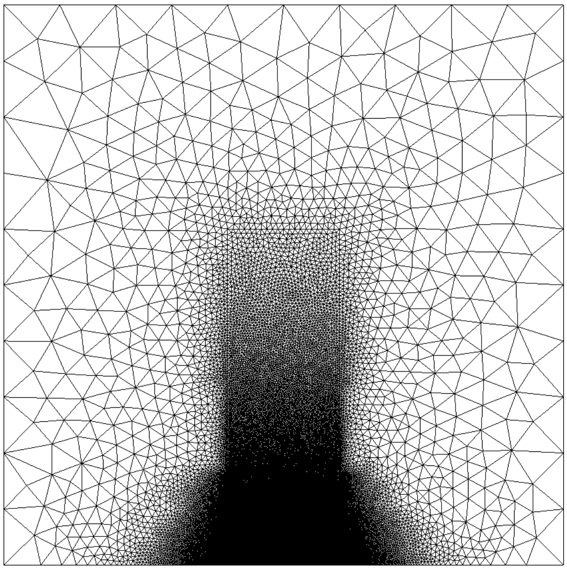

Figure 4.22: Constant mesh used for numerical experiments without adaptive algorithm. Typical mesh size is $h = 0.01$ in the corner, $h = 0.001$ in the middle of the cavity and $h = 0.0001$ near the bottom.

## 4.12 Numerical results with adapted time steps and adapted meshes

We now solve (4.75)-(4.78) with the adaptive algorithm presented in Section 4.10. The initial grid is an isotropic grid of mesh size $h = 0.0025$ and we still fix $\varepsilon = 10^{-5}$.

We first wait until $t = 0.02$ before starting to adapt the mesh, in order to initiate the velocity field. Moreover, the numerical experiments performed on constant meshes with constant time steps indicates that the time error indicator $\eta^T$ (4.96) is relatively small before the peak of pressure. Therefore, we choose to adapt the time steps only after $t = 0.11$. Before $t = 0.11$, the time step is kept constant and chosen proportional to $TOL$ and we only check (4.99) with $\beta = 1$. After $t = 0.11$, we change both grid and time step when needed checking both (4.99) and (4.100) with $\beta = 0.5$, which corresponds to an equidistribution of the error between time and space.

Finally, it was observed that the regularization parameter $\varepsilon'$ may have some importance. Indeed, if it is chosen too "huge", then the disk stops before reaching the distance to the boundary obtained with the reference solution. If it chosen too "small", then the adaptive algorithm has difficulty to converge when the prescribed tolerance $TOL$ is large. Therefore, we decide to choose $\varepsilon'$ going as $O(TOL)$. In Table 4.9, we summarize our choices for the numerical parameters.

| $TOL$ | $\tau$ | $\varepsilon'$ |
|---|---|---|
| 0.25 | 5e-3 | 1e-4 |
| 0.1875 | 3.75e-3 | 7.5e-5 |
| 0.125 | 2.5e-3 | 5e-5 |
| 0.0625 | 1.25e-3 | 2.5e-5 |
| 0.03125 | 6.25e-4 | 1.25e-5 |

Table 4.9: Numerical parameters for the adaptive algorithm. The initial time step and the regularization parameter are chosen as $O(TOL)$.

We plot for several values of $TOL$ the evolution of the height of the ball in Figure 4.23 and evolution of the pressure and the time step in Figure 4.24. We can observe that smaller time steps are chosen by the algorithm when the pressure peak is at its maximum. Meshes and solutions are represented in Figures 4.25, 4.26 and 4.27 for $TOL = 0.03125$. Zoom at time $t = 0.12$ is presented in Figures 4.28 and 4.29. All the numerical results indicate that the disk does not touch the boundary of the domain.

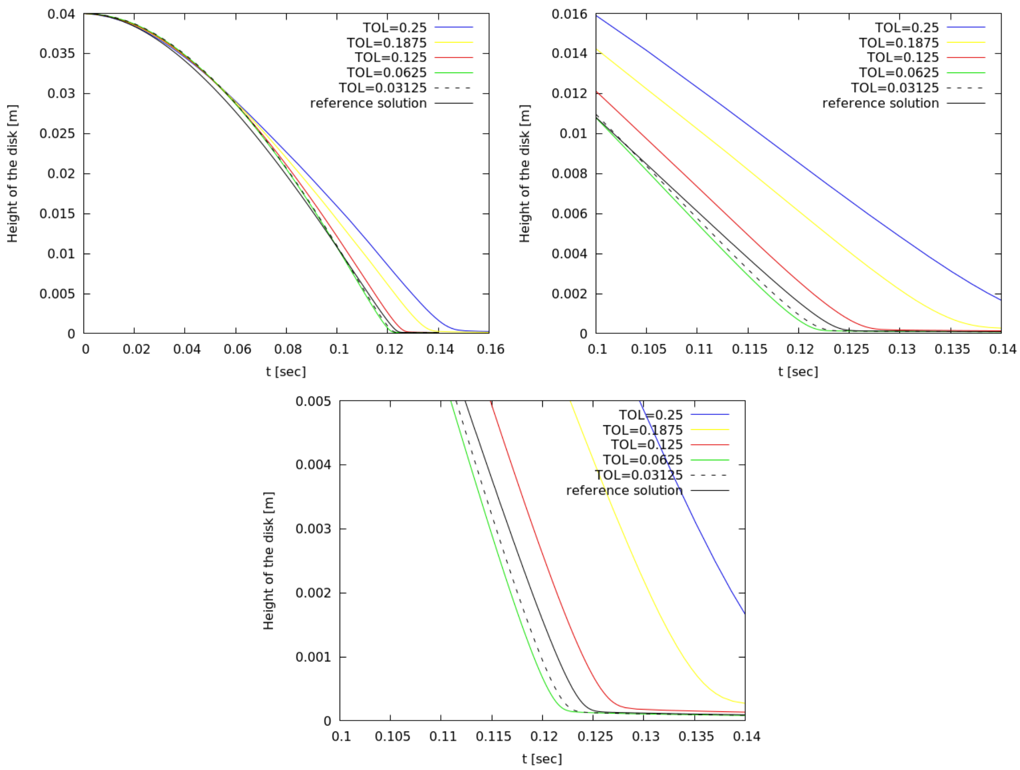


Figure 4.23: Height of the disk computed through numerical method (4.75), (4.80) with adapted time steps and adapted meshes (top left). Zoom (top right and bottom).

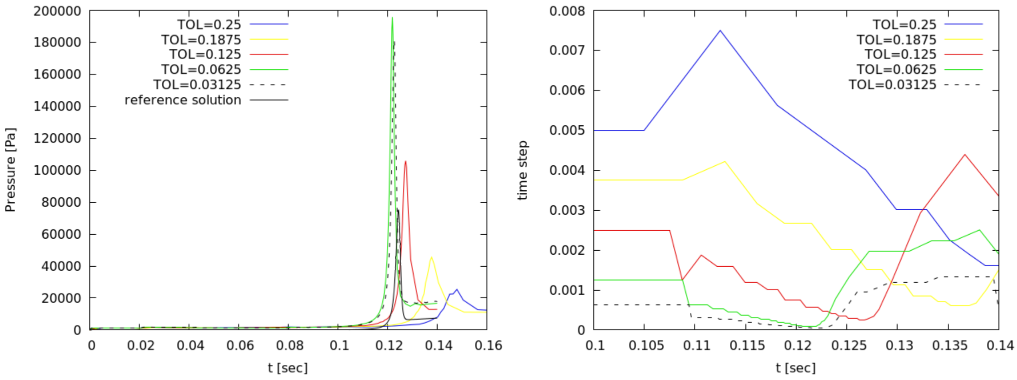


Figure 4.24: Pressure under the disk computed through numerical method (4.75), (4.80) with adapted time steps and adapted meshes (left). Evolution of the time step (right).

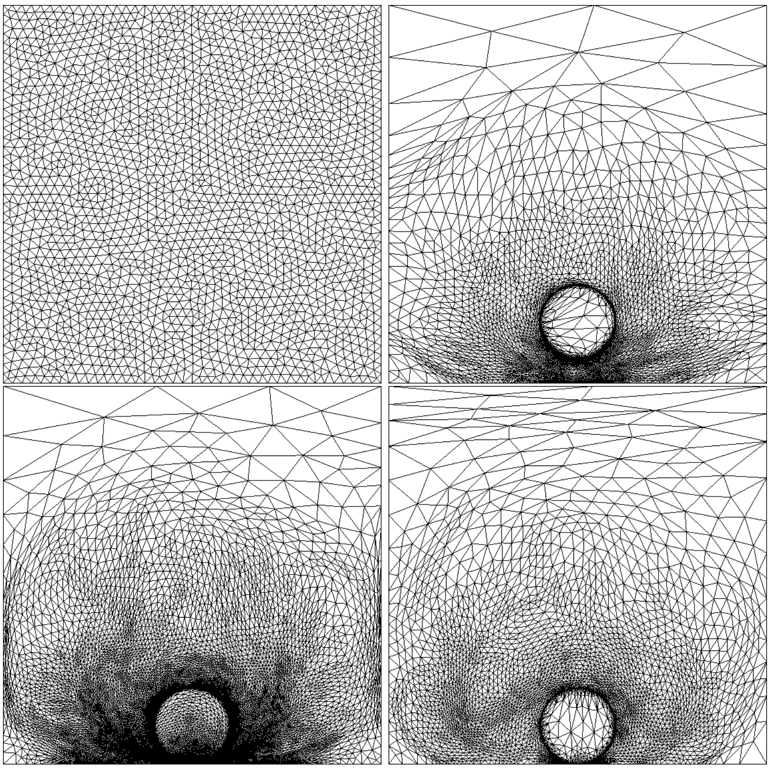

Figure 4.25: Adapted meshes generated with $TOL = 0.03125$ at time $t = 6.25e - 4$ (top left), $t = 0.11$ (top right), $t = 0.12$ (bottom left), $t = 0.14$ (bottom right).

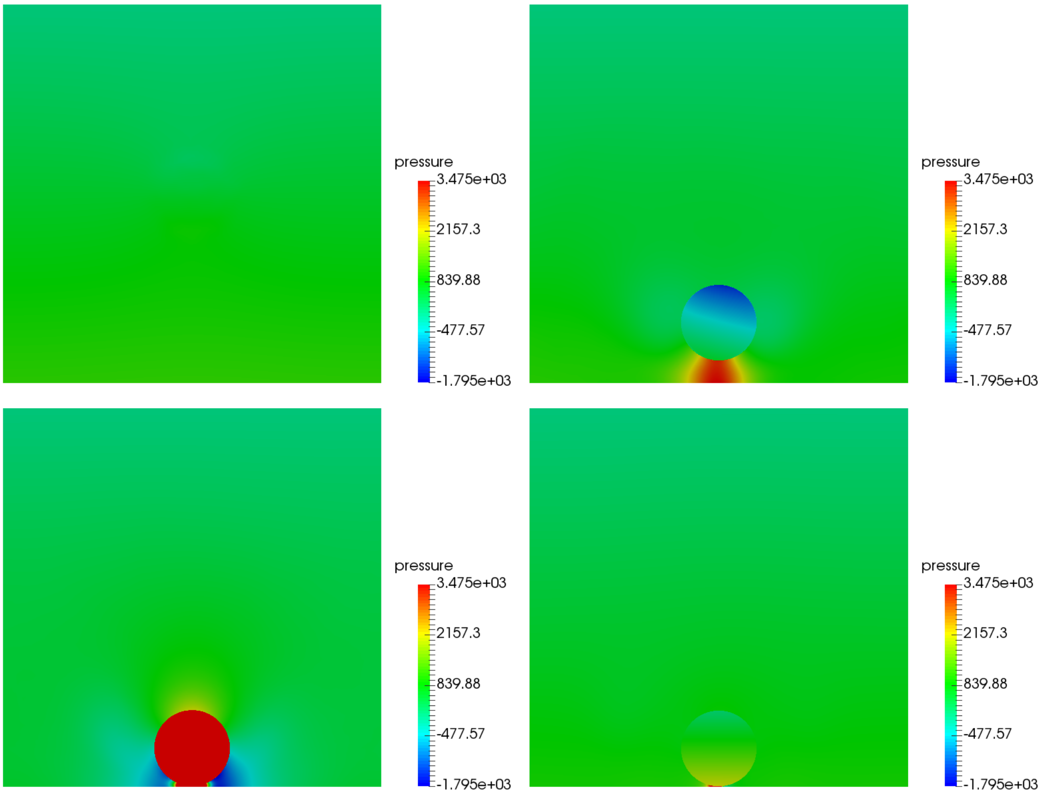


Figure 4.26: Pressure field computed with $TOL = 0.03125$ at time $t = 6.25e-4$ (top left), $t = 0.11$ (top right), $t = 0.12$ (bottom left), $t = 0.14$ (bottom right).

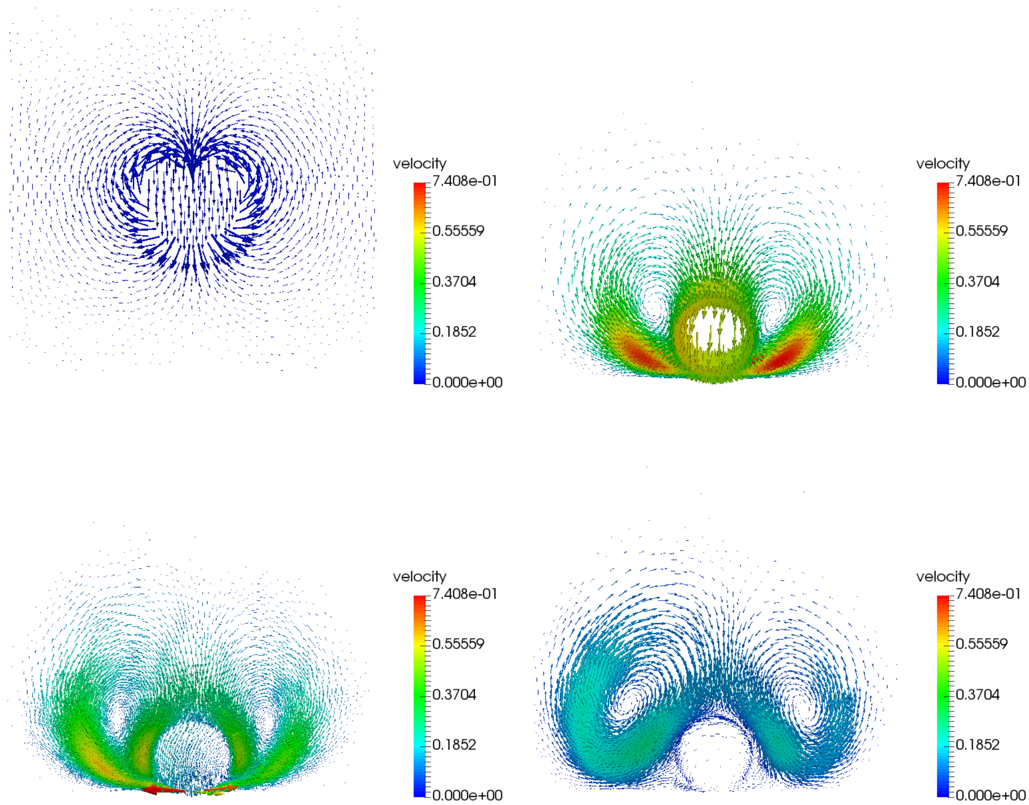


Figure 4.27: Velocity field computed with $TOL = 0.03125$ at time $t = 6.25e-4$ (top left), $t = 0.11$ (top right), $t = 0.12$ (bottom left), $t = 0.14$ (bottom right).

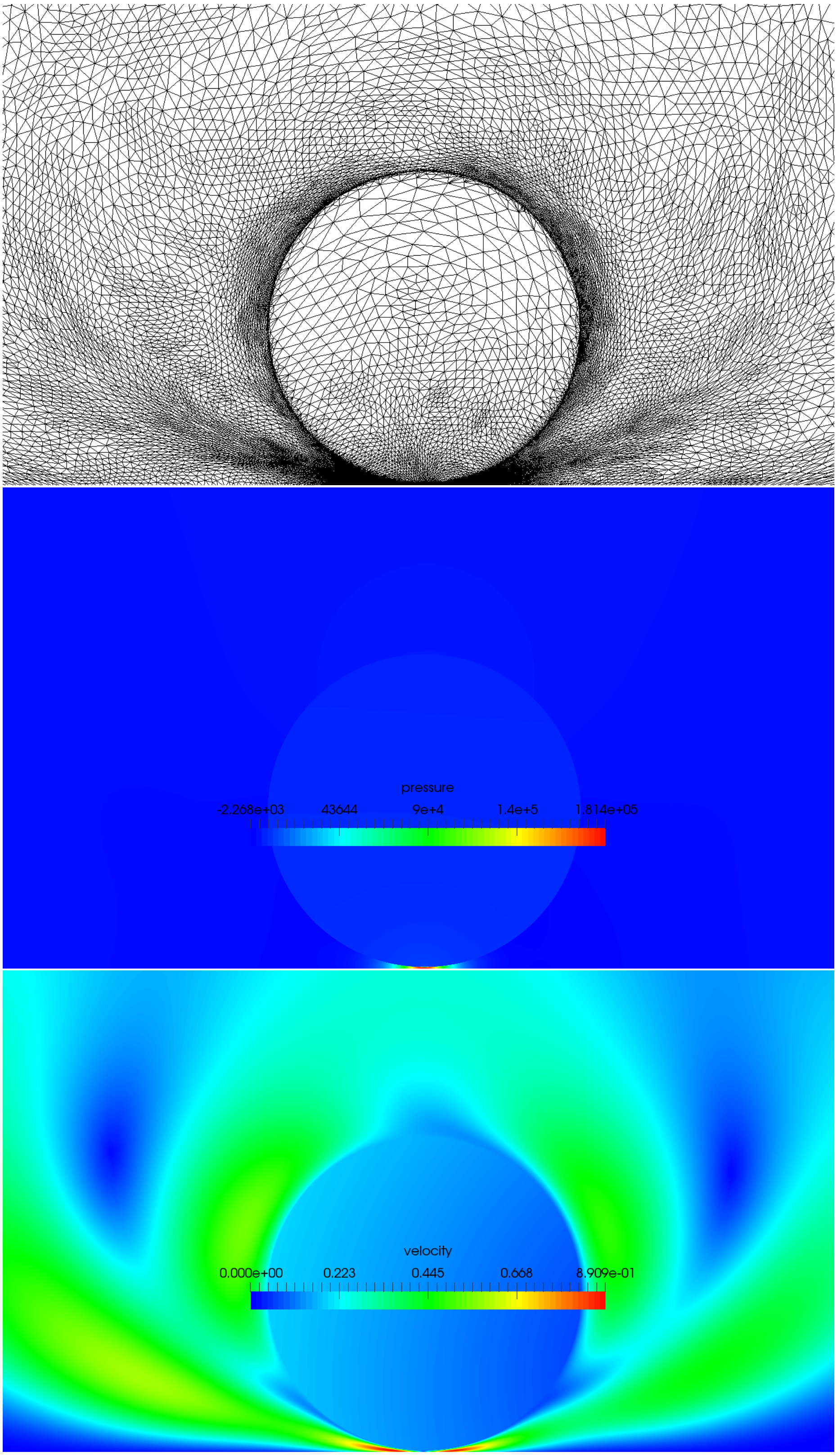


Figure 4.28: Zooms at the adapted mesh (top), pressure (middle) and velocity field (bottom) with $TOL = 0.03125$ at time $t = 0.12$.

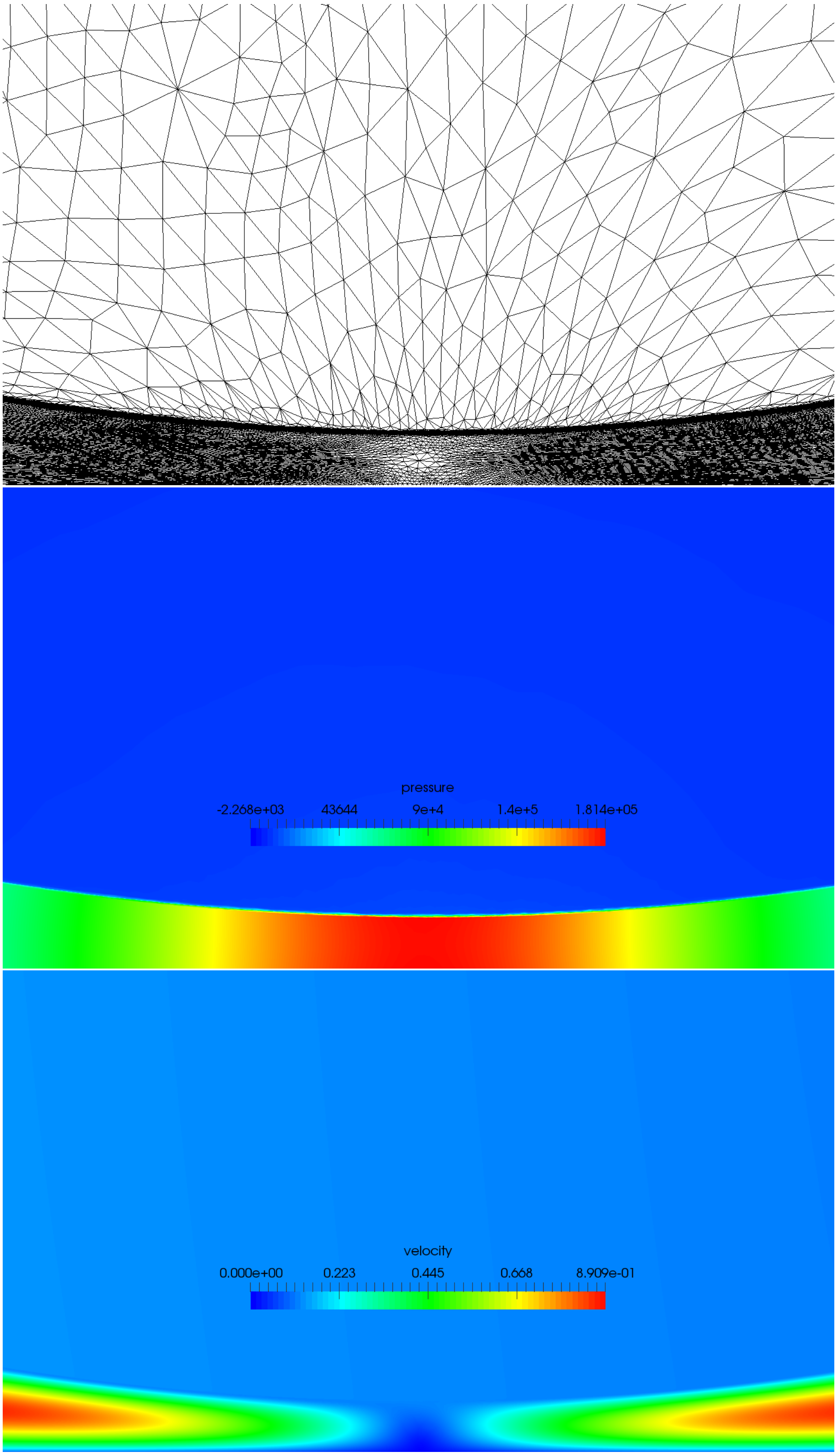


Figure 4.29: Zooms at the adapted mesh (top), pressure (middle) and velocity field (bottom) with $TOL = 0.03125$ at time $t = 0.12$.

# Conclusion and perspectives

In this thesis, a numerical method to solve a two fluids flow separated by a free surface has been presented. We focused on the a posteriori error analysis, in order to derive accurate error indicators. Based on these latter, we proposed a space-time adaptive algorithm. To reduce the computational costs, and in the same time to solve the problem with accuracy, it has been proposed to work with anisotropic finite elements and second order methods to advance in time.

The complete systems of equations is a combination of the non-homogeneous Navier-Stokes equations and the transport of the interface. For the derivations of the error indicators and the proofs of the a posteriori error estimates, we decided to split the technical difficulties into four chapters. In the first chapter, we presented the anisotropic framework and solved Poisson equations with variable coefficients. We proved error estimates that are valid for anisotropic meshes and we presented the procedure to build adapted meshes.

In the second chapter, we focused on the transport equation. We introduced a stabilized finite elements method and we used the Crank-Nicolson method to approximate the equation in time. We proved both a priori and a posteriori error estimates, and then we studied a space-time adaptive algorithm.

In the third chapter, we first presented several ways to derive a posteriori error estimates when using anisotropic finite elements to discretize the Stokes and the Navier-Stokes equations. Then, we focused on BDF methods to advance in time, and we proved the corresponding error estimates. A space-time adaptive algorithm is presented.

In the last chapter, we finally study the two fluids flows problem and we proved semi-discrete error estimates. The chapter has been separated into two parts. In the first one, we proposed an adaptive algorithm to solve fluids instabilities, and in the second part, we applied it to a limit case, used to approximate the motion of a rigid body into an incompressible fluid.

Several questions are still open. We list three topics among others that we think could be interesting perspectives for future works.

1. Only semi-discrete error estimates have been proven for the Navier-Stokes equations and the two fluids flows equations. An a posteriori upper bound involving the space and the time discretizations should be provided. Combining error estimates for stabilized anisotropic finite elements with error estimates coming from second order in time methods is not obvious. We presented it for the transport equation and the Stokes equations (but only for the Backward Euler method). We know however how to extend the proof for the Stokes equations and second order methods and it might be done in a future publication. Then the result should be first adapted to the Navier-Stokes equations, and finally to the two fluids flows problem.

2. Concerning the adaptive procedure, it has been observed that the numerical errors coming from the meshes interpolation can have important consequences. Interpolation of solutions between meshes should be investigated deeper, from both the theoretical and the practical points of view. In particular, we only prove a posteriori error estimates for the simpler case where the mesh is fixed and does not change

during the simulation. We should derive estimates that take in account moving meshes.

3. The error indicator proposed for the two fluids flows problem contains four quantities: one involving the space discretization of the velocity, one its time discretization, another one the space approximation of the interface and finally a last part involving the time approximation of the transport problem. The ratio between these four quantities should be studied in order to improve the efficiency of the adaptive algorithm.

# Appendix A

# Some useful estimates

## A.1 Gronwall's type inequalities

Throughout all this document, we often use the Gronwall's Lemma, or more precisely *a* Gronwall's lemma to conclude the estimates. We present below some of the different (continuous and discrete) versions we use.

We first state a very general Gronwall's Lemma in integral form. The proof can be found in [34] or [21].

**Theorem A.1** (A general Gronwall's Lemma)**.**
*Let $t_0 \geq 0$ and $f, g, G, h$ nonnegative functions and a constant $H \geq 0$ such that*

*(i)* $f, G \in L^\infty(t_0, \infty)$

*(ii)* $g, h \in L^1(t_0, \infty)$

*(iii) for all $t \geq t_0$ we have*

$$f(t) + G(t) \leq H + \int_{t^0}^t h(s)ds + \int_{t^0}^t g(s)f(s)ds.$$

*Then, for all $t \geq t_0$,*

$$f(t) + G(t) \leq \exp\left(\int_{t^0}^t g(s)ds\right)\left(H + \int_{t^0}^t h(s)ds\right).$$

We also write the same result in a differential form, that is a direct consequence of the previous theorem.

**Theorem A.2** (A general Gronwall's Lemma in differential form)**.**
*Let $t_0 \geq 0$ and $f, g, G, h$ nonnegative functions and a constant $H \geq 0$ such that*

*(i)* $g, H, h \in L^\infty(t_0, \infty)$

*(ii)* $f \in W^{1,\infty}(t_0, \infty)$

*(iii) for all $t \geq t_0$ we have*

$$\frac{d}{dt}f(t) + G(t) \leq H + h(t) + g(t)f(t).$$

*Then, for all $t \geq t_0$,*

$$f(t) + \int_0^t G(s)ds \leq \exp\left(\int_{t^0}^t g(s)ds\right)\left(f(0) + Ht + \int_{t^0}^t h(s)ds\right).$$

We prove that, in some particular situations, it is possible to obtain an estimate that does not depend exponentially on $t$.

**Theorem A.3** (A Gronwall's lemma type inequality with no exponential bound)**.**
*Let $0 \leq t_0 < T$ and $t_0 = t^0 < t^1 < t^2 < ... < t^N = T$ a partition of the interval $[t^0, T]$. Let $f, g, h, H$ four real functions such that*

*(i)* $f \in C^0[t_0, T]$,

*(ii)* $f \in C^1[t^n, t^{n+1}], \quad 0 \leq n \leq N-1$,

*(iii)* $g, h, H \in C^0[t^n, t^{n+1}] \quad 0 \leq n \leq N-1$,

*(iv)* $H \geq 0$,

*(v) for all* $0 \leq n \leq N-1$ *and for all* $t \in [t^n, t^{n+1}]$*, we have* $\frac{1}{2}\frac{d}{dt}f^2(t) + H(t) \leq f(t)g(t) + h(t)$.

*Then the following inequality holds*

$$f^2(T) + \sum_{n=0}^{N-1} \int_{t^n}^{t^{n+1}} H(t)dt \leq \exp(1)\left( f^2(t_0) + (T - t_0) \sum_{n=0}^{N-1} \int_{t^n}^{t^{n+1}} g^2(t)dt + 2\sum_{n=0}^{N-1} \int_{t^n}^{t^{n+1}} h(t)dt \right).$$

*Proof.* Let $n \geq 0$ and $t \in [t^n, t^{n+1}]$. Applying the Young's inequality $ab \leq \frac{\varepsilon}{2}a^2 + \frac{1}{2\varepsilon}b^2$ to hypothesis $(iii)$ yields

$$\frac{1}{2}\frac{d}{dt}f^2(t) + H(t) \leq \frac{1}{2(T - t_0)}f^2(t) + \frac{T - t_0}{2}g^2(t) + h(t)$$

where we choose $\varepsilon = \frac{1}{T - t_0}$ . Multiplying the previous inequality by $\exp(-{(t-t_0)}/{T-t_0})$ and passing all the terms containing $f$ to the left hand side, we obtain

$$\frac{d}{dt}\left(f^2(t)\exp(-{(t-t_0)}/{T-t_0})\right) + 2H(t)\exp(-{(t-t_0)}/{T-t_0}) \\ \leq (T - t_0)g^2(t)\exp(-{(t-t_0)}/{T-t_0}) + 2h(t)\exp(-{(t-t_0)}/{T-t_0}).$$

Integrating between $t^n$ and $t^{n+1}$, we have

$$f^2(t^{n+1})\exp(-{(t^{n+1}-t_0)}/{T-t_0}) - f^2(t^n)\exp(-{(t^n-t_0)}/{T-t_0}) \\ + 2\int_{t^n}^{t^{n+1}} H(t)\exp(-{(t-t_0)}/{T-t_0})dt \leq (T - t_0)\int_{t^n}^{t^{n+1}} g^2(t)\exp(-{(t-t_0)}/{T-t_0})dt \\ + 2\int_{t^n}^{t^{n+1}} h(t)\exp(-{(t-t_0)}/{T-t_0})dt.$$

Observe that since $f$ is continuous in $[0, T]$, we can ensure that the sum

$$\sum_{n=0}^{N-1} \int_{t^n}^{t^{n+1}} \frac{d}{dt}\left(f^2(t)\exp(-{(t-t_0)}/{T-t_0})\right)dt$$

is telescopic. Therefore, summing up over $n$ the last inequality yields

$$f^2(T)\exp(-1) + 2\sum_{n=0}^{N-1}\int_{t^n}^{t^{n+1}} H(t)\exp(-{}^{(t-t_0)}/_{T-t_0})dt$$
$$\leq f^2(t_0) + (T-t_0)\sum_{n=0}^{N-1}\int_{t^n}^{t^{n+1}} g^2(t)\exp(-{}^{(t-t_0)}/_{T-t_0})dt$$
$$+ 2\sum_{n=0}^{N-1}\int_{t^n}^{t^{n+1}} h(t)\exp(-{}^{(t-t_0)}/_{T-t_0})dt$$
$$\leq f^2(t_0) + (T-t_0)\sum_{n=0}^{N-1}\int_{t^n}^{t^{n+1}} g^2(t)dt + 2\sum_{n=0}^{N-1}\int_{t^n}^{t^{n+1}} h(t)dt.$$

Finally, multiplying both sides by $\exp(1)$, we get

$$f^2(T) + 2\sum_{n=0}^{N-1}\int_{t^n}^{t^{n+1}} H(t)\exp(1-{}^{(t-t_0)}/_{T-t_0})dt$$
$$\leq \exp(1)\left(f^2(t_0) + (T-t_0)\sum_{n=0}^{N-1}\int_{t^n}^{t^{n+1}} g^2(t)dt + 2\sum_{n=0}^{N-1}\int_{t^n}^{t^{n+1}} h(t)dt\right).$$

Using that $\exp(1-{}^{(t-t_0)}/_{T-t_0}) \geq 1$ for all $t \in [t_0, T]$ and $H(t) \geq 0$ yields the result. □

**Remark A.4.**
We justify below the choice of the value of $\varepsilon$ in the proof above (we set $h = H = 0$ for simplicity). Assume that we apply the Young's inequality to hypothesis $(iii)$ where $\varepsilon$ is any strictly positive number, that we will set later one to get the suitable upper bound. We obtain

$$\frac{1}{2}\frac{d}{dt}f^2(t) \leq \frac{\varepsilon}{2}f^2(t) + \frac{1}{2\varepsilon}g^2(t)$$

Multiplying the previous inequality by $\exp(-\varepsilon(t-t_0))$ and passing all the terms containing $f$ to the left hand side, we obtain

$$\frac{d}{dt}\Big(f^2(t)\exp(-\varepsilon(t-t_0))\Big) \leq \frac{1}{\varepsilon}g^2(t)\exp(-\varepsilon(t-t_0)).$$

Continuing as in the proof, we integrate between $t^n$ and $t^{n+1}$ and sum up over $n$ yielding

$$f^2(T)\exp(-\varepsilon(T-t_0)) \leq f^2(t_0) + \frac{1}{\varepsilon}\sum_{n=0}^{N-1}\int_{t^n}^{t^{n+1}} g^2(t)\exp(-\varepsilon(t-t_0))dt$$
$$\leq f^2(t_0) + \frac{1}{\varepsilon}\sum_{n=0}^{N-1}\int_{t^n}^{t^{n+1}} g^2(t)dt.$$

Finally, multiplying both sides by $\exp(\varepsilon(T-t_0))$, we get

$$f^2(T) \leq \exp(\varepsilon(T-t_0))\left(f^2(t_0) + \frac{1}{\varepsilon}\sum_{n=0}^{N-1}\int_{t^n}^{t^{n+1}} g^2(t)dt\right).$$

Now, if we set for instance $\varepsilon = 1$, we obtain

$$f^2(T) \leq \exp((T-t_0))\left(f^2(t_0) + \sum_{n=0}^{N-1}\int_{t^n}^{t^{n+1}} g^2(t)dt\right),$$

which yields to nothing else than the classical Gronwall's Lemma where the estimate grows exponentially with the final time. To eliminate the exponential in the bound, and to obtain a linear increase, the idea is to set $\varepsilon = \frac{1}{T-t_0}$.

We also use the discrete versions of the Gronwall's Lemma, those proofs can be established following for instance the steps presented in [59], Lemma 5.1.

**Lemma A.5** (A discrete Gronwall's Lemma)**.**
*Let $N \geq 1$ be an integer. Let $a_n, b_n, c_n, \gamma_n, \mu_n$ be non-negative numbers for all $0 \leq n \leq N$ and $D \geq 0$ such that*

$$a_m + \sum_{n=0}^{m} b_n \leq \sum_{n=0}^{m-1} \gamma_n a_n + \sum_{n=0}^{m} \mu_n a_n + \sum_{n=0}^{m} c_n + D, \quad \forall 1 \leq m \leq N.$$

*Assume that $\mu_n < 1$ for all $0 \leq n \leq N$. Then*

$$a_m + \sum_{n=0}^{m} b_n \leq (a_0 + \sum_{n=0}^{m} c_n + D) \exp\left(\sum_{n=0}^{m-1} \gamma_n\right) \exp\left(\sum_{n=0}^{m} \frac{\mu_n}{1-\mu_n}\right), \quad \forall 1 \leq m \leq N.$$

We may use also this version of the previous Lemma, written in a difference form :

**Lemma A.6** (A discrete Gronwall's Lemma)**.**
*Let $N \geq 1$ be an integer. Let $a_n, \gamma_n, 0 \leq n \leq N$ and $b_n, c_n\mu_n, 1 \leq n \leq N$ be non-negative numbers such that*

$$a_m - a_{m-1} + b_m \leq \gamma_{m-1} a_{m-1} + \mu_m a_m + c_m \quad \forall 1 \leq m \leq N.$$

*Assume that $\mu_n < 1$ for all $1 \leq n \leq N$. Then*

$$a_m + \sum_{n=1}^{m} b_n \leq (a_0 + \sum_{n=1}^{m} c_n + D) \exp\left(\sum_{n=0}^{m-1} \gamma_n\right) \exp\left(\sum_{n=1}^{m} \frac{\mu_n}{1-\mu_n}\right), \quad \forall 1 \leq m \leq N.$$

**Remark A.7.**
In both Lemmas A.5 and A.6, observe that if $\mu_n = 0$ for all $n$, we obtain a bound without any size restriction on the coefficients.

## A.2 A Sobolev inequality for the Navier-Stokes equations

Here, we state several inequalities that are common tools to analyse the trilinear form

$$\int_\Omega ((\mathbf{u} \cdot \nabla)\mathbf{v}) \cdot \mathbf{w} d\mathbf{x}$$

that comes in the study of the Navier-Stokes equations. The proofs are standard and can be found in [21] or [99].

**Proposition A.8.**
*Let $d = 2, 3$ and $\Omega$ a bounded, open, Lipschitz subset of $\mathbb{R}^d$. Let $\mathbf{u}, \mathbf{v}, \mathbf{w} \in (H_0^1(\Omega))^d$. Then there exists a constant $C_{SOB} > 0$ depending only on $\Omega$ such that*

1. $\displaystyle\int_\Omega ((\mathbf{u} \cdot \nabla)\mathbf{v}) \cdot \mathbf{w} d\mathbf{x} \leq C_{SOB} \|\nabla \mathbf{v}\|_{L^2(\Omega)} \|\mathbf{u}\|_{L^2(\Omega)}^{1-d/4} \|\nabla \mathbf{u}\|_{L^2(\Omega)}^{d/4} \|\mathbf{w}\|_{L^2(\Omega)}^{1-d/4} \|\nabla \mathbf{w}\|_{L^2(\Omega)}^{d/4}.$
2. $\displaystyle\int_\Omega ((\mathbf{u} \cdot \nabla)\mathbf{v}) \cdot \mathbf{w} d\mathbf{x} \leq C_{SOB} \|\nabla \mathbf{u}\|_{L^2(\Omega)} \|\nabla \mathbf{v}\|_{L^2(\Omega)} \|\nabla \mathbf{w}\|_{L^2(\Omega)}.$
3. *For any $\varepsilon > 0$,*

$$\int_\Omega ((\mathbf{u} \cdot \nabla)\mathbf{v}) \cdot \mathbf{w} d\mathbf{x} \leq \frac{C_{SOB}}{\varepsilon} \frac{\|\nabla \mathbf{v}\|_{L^2(\Omega)}^{2(d-1)}}{2^{d-1}} \|\mathbf{u}\|_{L^2(\Omega)} \|\mathbf{w}\|_{L^2(\Omega)} + \frac{\varepsilon d}{4} \|\nabla \mathbf{u}\|_{L^2(\Omega)} \|\nabla \mathbf{w}\|_{L^2(\Omega)}.$$

4. *If $\mathbf{u}, \mathbf{w}$ are only in $(H^1(\Omega))^d$, then we have*

$$\int_\Omega ((\mathbf{u} \cdot \nabla)\mathbf{v}) \cdot \mathbf{w} d\mathbf{x} \leq C_{SOB} \|\mathbf{u}\|_{H^1(\Omega)} \|\nabla \mathbf{v}\|_{L^2(\Omega)} \|\mathbf{w}\|_{H^1(\Omega)}.$$

# Appendix B

# Stokes equations with variable coefficients

## B.1 A priori estimates for the Stokes equations with variable coefficients

In this section, we study the well-posedness and prove a priori estimates for Stokes equations with variable coefficients. We use in particular these estimates in Sections 3.1, 3.4 and 3.6 of Chapter 3 and in Section 4.2 of Chapter 4 to derive the a priori estimates for the dual problems. We focus on the two dimensional case, but the corresponding results for $\mathbb{R}^3$ can be obtained after a few modifications.

The main goal is to study the existence of solutions to a general saddle point problem of the form: find $(\mathbf{u}, p) \in (H_0^1(\Omega))^2 \times L_0^2(\Omega)$ that satisfy

$$\begin{cases} a(\mathbf{u}, \mathbf{v}) + b(\mathbf{v}, p) = F(\mathbf{v}), \forall v \in (H_0^1(\Omega))^2, \\ \\ -b(\mathbf{u}, q) = \int_\Omega gq, \forall q \in L_0^2(\Omega), \end{cases}$$

where $F \in (H^{-1}(\Omega))^2$, $g \in L_0^2(\Omega)$ and $a, b$ are bilinear forms of the type

$$a(u, v) = \int_\Omega \frac{\nabla \mathbf{u} A + A^T \nabla \mathbf{u}^T}{2} : \frac{\nabla \mathbf{v} A + A^T \nabla \mathbf{v}^T}{2} d\mathbf{x}$$

$$b(v, q) = -\int_\Omega q(B^T \nabla) \cdot \mathbf{v} d\mathbf{x}$$

where $A$ and $B$ are matrices. Note that some recent contributions were brought in [97] to the analysis of the differential operator

$$\nabla \mathbf{u} A + A^T \nabla \mathbf{u}^T.$$

We first established basic properties of the bilinear forms $a$ and $b$.

**Proposition B.1.**
*Let $\Omega \subset \mathbb{R}^2$ be a Lipschitz, connected, bounded, open set and $A \in (L^\infty(\Omega))^{2\times 2}$ a $2 \times 2$ matrix. Let $a : (H_0^1(\Omega))^2 \times (H_0^1(\Omega))^2 \to \mathbb{R}$ defined by*

$$a(\mathbf{u}, \mathbf{v}) = \int_\Omega \frac{\nabla \mathbf{u} A + A^T \nabla \mathbf{u}^T}{2} : \frac{\nabla \mathbf{v} A + A^T \nabla \mathbf{v}^T}{2} d\mathbf{x}, \quad \mathbf{u}, \mathbf{v} \in (H_0^1(\Omega))^2. \tag{B.1}$$

*We assume moreover that there exists $\alpha > 0$ such that*

$$a(\mathbf{u}, \mathbf{u}) \geq \alpha \int_\Omega D(\mathbf{u}) : D(\mathbf{u}) d\mathbf{x}, \text{ for all } \mathbf{u} \in (H_0^1(\Omega))^2. \tag{B.2}$$

*Then $a$ is bilinear, symmetric, continuous and coercive.*

*Proof.* Bilinearity and symmetry of $a$ are evident. We show the continuity and the coercivity. By the Cauchy-Schwartz inequality and the sub-multiplicability of the Frobenius product, we have that

$$a(\mathbf{u},\mathbf{v}) \leq \int_\Omega |\nabla\mathbf{u}A|_F|\nabla\mathbf{v}A|_F d\mathbf{x} \leq \int_\Omega |\nabla\mathbf{u}|_F|A|_F|\nabla\mathbf{v}|_F|A|_F d\mathbf{x} \leq \|A\|^2_{L^\infty(\Omega)}\|\nabla\mathbf{u}\|_{L^2(\Omega)}\|\nabla\mathbf{v}\|_{L^2(\Omega)},$$

where $|\cdot|_F$ stands for the norm induced by the Frobenius product. Moreover, using Korn's inequality and the hypothesis $(B.2)$, we obtain that

$$a(\mathbf{u},\mathbf{u}) \geq \frac{\alpha}{K^2}\|\nabla\mathbf{u}\|^2_{L^2(\Omega)},$$

where $K > 0$ is the Korn's constant of $\Omega$ satisfying

$$\|\nabla\mathbf{v}\|_{L^2(\Omega)} \leq K\|D(\mathbf{v})\|_{L^2(\Omega)}, \quad \forall\mathbf{v} \in (H^1_0(\Omega))^2.$$

□

**Remark B.2.**
Observe that the hypothesis $(B.2)$ is not necessary in the case where $A$ can be written as

$$A = |\det\nabla\Phi|^{1/2}(\nabla\Phi)^{-1},$$

where $\Phi : \overline{\Omega} \to \overline{\Omega}$ is a $C^1$-diffeomorphism such that the singular values $\sigma_i, i = 1, 2$ of $\nabla\Phi$ are uniformly bounded i.e. there exists two constants $C, c > 0$ such that

$$c \leq \sigma_i(\nabla\Phi(x)) \leq C, \quad \text{for all } x \in \Omega$$

Indeed, in this case, we can check that the bilinear form $a$ is coercive by applying the change of variable $x = \Phi(y)$ and $\mathbf{u} = \tilde{\mathbf{u}} \circ \Phi$

$$\begin{aligned}
\int_\Omega \left|\frac{\nabla\mathbf{u}A + A^T\nabla\mathbf{u}^T}{2}\right|^2_F d\mathbf{x} &= \int_\Omega |\det\nabla\Phi| \left|\frac{\nabla\mathbf{u}(\nabla\Phi)^{-1} + (\nabla\Phi)^{-T}\nabla\mathbf{u}^T}{2}\right|^2_F d\mathbf{x} \\
&= \int_\Omega |D(\tilde{\mathbf{u}})|^2_F dy \\
&\geq \frac{1}{K^2}\int_\Omega |\nabla\tilde{\mathbf{u}}|^2_F dy \\
&= \frac{1}{K^2}\int_\Omega |\det\nabla\Phi||\nabla\mathbf{u}(\nabla\Phi)^{-1}|^2_F d\mathbf{x} \\
&= \frac{1}{K^2}\int_\Omega |\det\nabla\Phi|\nabla\mathbf{u}(\nabla\Phi)^{-1}(\nabla\Phi)^{-T} : \nabla\mathbf{u}d\mathbf{x} \\
&\geq \frac{c^2}{K^2}\int_\Omega \lambda_{min}((\nabla\Phi)^{-1}(\nabla\Phi)^{-T})\nabla\mathbf{u} : \nabla\mathbf{u}d\mathbf{x} \\
&\geq \frac{c^2}{C^2K^2}\int_\Omega |\nabla\mathbf{u}|^2_F d\mathbf{x},
\end{aligned}$$

where $K$ is the Korn's constant and we use that

$$\det\nabla\Phi \geq \sigma_1(\nabla\Phi)\sigma_2(\nabla\Phi) \geq c^2, \quad \lambda_{min}((\nabla\Phi)^{-1}(\nabla\Phi)^{-T}) \geq \sigma_{min}(\nabla\Phi)^{-2} \geq C^{-2},$$

with $\lambda_{\min}$, respectively $\sigma_{\min}$ standing for the minimal eigenvalue, respectively the minimal singular value.

**Proposition B.3.**
*Let* $\Omega \subset \mathbb{R}^2$ *a Lipschitz, connected, bounded, open set and* $B \in (W^{1,\infty}(\Omega))^{2\times 2}$ *be an invertible* $2\times 2$ *matrix such that* $B^{-1} \in (W^{1,\infty}(\Omega))^{2\times 2}$*. Let assume moreover that* $\nabla \cdot B^T = 0$*. Let* $b : (H_0^1(\Omega))^2 \times L_0^2(\Omega) \to \mathbb{R}$ *be defined by*

$$b(\mathbf{v}, q) = -\int_\Omega q(B^T\nabla)\cdot \mathbf{v}d\mathbf{x}. \tag{B.3}$$

*Then* $b$ *is bilinear and continuous. Moreover, there exists a constant* $\beta > 0$ *depending only on* $\Omega$ *and* $\|B^{-1}\|_{W^{1,\infty}(\Omega)}$ *such that*

$$\inf_{q\in L_0^2(\Omega)} \sup_{\mathbf{v}\in(H_0^1(\Omega))^2} \frac{b(\mathbf{v}, q)}{\|q\|_{L^2(\Omega)}\|\nabla\mathbf{v}\|_{L^2(\Omega)}} \geq \beta. \tag{B.4}$$

*Proof.* Bilinearity of $b$ is obvious. To prove the continuity, we observe that thanks to Cauchy-Schwarz inequality

$$\begin{aligned} b(\mathbf{v}, q) = -\int_\Omega q(B^T\nabla)\cdot \mathbf{v}d\mathbf{x} = -\int_\Omega qB : \nabla\mathbf{v}d\mathbf{x} \\ \leq \int_\Omega |q||B|_F|\nabla\mathbf{v}|_F d\mathbf{x} \leq \|B\|_{L^\infty(\Omega)}\|q\|_{L^2(\Omega)}\|\nabla\mathbf{v}\|_{L^2(\Omega)}. \end{aligned}$$

To show $(B.4)$, it is sufficient to prove that there exists $C_1, C_2 > 0$ such that for all $q \in L_0^2(\Omega)$, there exists $\mathbf{v} \in (H_0^1(\Omega))^2$ such that

$$b(\mathbf{v}, q) \geq C_1\|q\|^2_{L^2(\Omega)}, \quad \|\nabla\mathbf{v}\|_{L^2(\Omega)} \leq C_2\|q\|_{L^2(\Omega)}.$$

Let $q \in L_0^2(\Omega)$. Using the standard inf-sup condition, there exists a constant $C > 0$ depending only on $\Omega$ and $\mathbf{w} \in (H_0^1(\Omega))^2$ such that $-\nabla\cdot\mathbf{w} = q$ and $\|\nabla\mathbf{w}\|_{L^2(\Omega)} \leq C\|q\|_{L^2(\Omega)}$. We set $\mathbf{v} = B^{-1}\mathbf{w}$. Then, using $\nabla \cdot B^T = 0$, we have

$$b(\mathbf{v}, q) = -\int_\Omega (B^T\nabla)\cdot \mathbf{v}qd\mathbf{x} = -\int_\Omega \nabla\cdot(B\mathbf{v})qd\mathbf{x} = -\int_\Omega \nabla\cdot\mathbf{w}qd\mathbf{x} = \|q\|^2_{L^2(\Omega)}.$$

Moreover,

$$\|\mathbf{v}\|_{L^2(\Omega)} = \|\nabla(B^{-1}\mathbf{w})\|_{L^2(\Omega)} \leq \|B^{-1}\|_{W^{1,\infty}(\Omega)}\|\nabla\mathbf{w}\|_{L^2(\Omega)} \leq \|B^{-1}\|_{W^{1,\infty}(\Omega)}C\|q\|_{L^2(\Omega)}.$$

Then the claim is fulfilled with $C_1 = 1$ and $C_2 = C\|B^{-1}\|_{W^{1,\infty}(\Omega)}$. □

**Theorem B.4.**
*Let* $\Omega \subset \mathbb{R}^2$ *be a Lipschitz, connected, bounded, open set and* $\mathbf{f} \in (H^{-1}(\Omega))^2, g \in L_0^2(\Omega)$*. Moreover let* $A, B$ *be* $2\times 2$ *matrices such that* $A \in (L^\infty(\Omega))^{2\times 2}$*,* $B, B^{-1} \in (W^{1,\infty}(\Omega))^{2\times 2}$ *and* $\nabla \cdot B^T = 0$*. Finally, let* $\beta$ *be the inf-sup constant associated to* $B$ *as given in* $(B.4)$*. We define the bilinear forms*

$$a(\mathbf{u}, \mathbf{v}) = \int_\Omega \frac{\nabla\mathbf{u}A + A^T\nabla\mathbf{u}^T}{2} : \frac{\nabla\mathbf{v}A + A^T\nabla\mathbf{v}^T}{2}d\mathbf{x}, \quad \mathbf{u}, \mathbf{v} \in (H_0^1(\Omega))^2,$$

*and*

$$b(\mathbf{v}, q) = -\int_\Omega q(B^T\nabla)\cdot \mathbf{v}d\mathbf{x}, \quad \mathbf{v} \in (H_0^1(\Omega))^2, q \in L_0^2(\Omega).$$

*Moreover, assume that there exists* $\alpha > 0$ *such that*

$$a(\mathbf{v}, \mathbf{v}) \geq \alpha \int_\Omega D(\mathbf{v}) : D(\mathbf{v})d\mathbf{x}, \text{ for all } \mathbf{v} \in (H_0^1(\Omega))^2.$$

*Then there exists a unique solution* $(\mathbf{u}, p) \in (H_0^1(\Omega))^2 \times L_0^2(\Omega)$ *of the Stokes problem*

$$\begin{cases} a(\mathbf{u}, \mathbf{v}) + b(\mathbf{v}, p) = F(\mathbf{v}), \forall \mathbf{v} \in (H_0^1(\Omega))^2, \\ \\ -b(\mathbf{u}, q) = \textstyle\int_\Omega gq, \forall q \in L_0^2(\Omega), \end{cases} \tag{B.5}$$

*where* $F(\mathbf{v}) = \langle \mathbf{f}, \mathbf{v} \rangle_{H^{-1}(\Omega), H_0^1(\Omega)}$. *Moreover, there exists a constant* $C > 0$ *depending only on* $\Omega$ *such that*

$$\|\nabla \mathbf{u}\|_{L^2(\Omega)} \le C \left( \frac{1}{\alpha} \|\mathbf{f}\|_{H^{-1}(\Omega)} + \left( \frac{1}{\beta} + \frac{\|A\|^2_{L^\infty(\Omega)}}{\alpha\beta} \right) \|g\|_{L^2(\Omega)} \right), \tag{B.6}$$

*and*

$$\|p\|_{L^2(\Omega)} \le C \left( \left( \frac{1}{\beta} + \frac{\|A\|^2_{L^\infty(\Omega)}}{\alpha\beta} \right) \|\mathbf{f}\|_{H^{-1}(\Omega)} + \left( \frac{\|A\|^2_{L^\infty(\Omega)}}{\beta^2} + \frac{\|A\|^4_{L^\infty(\Omega)}}{\alpha\beta^2} \right) \|g\|_{L^2(\Omega)} \right). \tag{B.7}$$

*Proof.* Let us define $V_g = \left\{ \mathbf{v} \in (H_0^1(\Omega))^2 : (B^T\nabla) \cdot \mathbf{v} = g \right\}$ and $V = \left\{ \mathbf{v} \in (H_0^1(\Omega))^2 : (B^T\nabla) \cdot \mathbf{v} = 0 \right\}$. Observe that if $\mathbf{u} \in V_g$ is a solution of

$$a(\mathbf{u}, \mathbf{v}) = F(\mathbf{v}), \quad \forall \mathbf{v} \in V, \tag{B.8}$$

then, from the inf-sup condition $(B.4)$, we can find a unique $p \in L_0^2(\Omega)$ such that

$$b(\mathbf{v}, p) = F(\mathbf{v}) - a(\mathbf{u}, \mathbf{v}), \quad \forall \mathbf{v} \in (H_0^1(\Omega))^2,$$

and

$$\|p\|_{L^2(\Omega)} \le \frac{1}{\beta} \left( \|\mathbf{f}\|_{H^{-1}(\Omega)} + \|A\|^2_{L^\infty(\Omega)} \|\nabla \mathbf{u}\|_{L^2(\Omega)} \right).$$

Moreover, we trivially obtain that

$$\int_\Omega q \ (B^T\nabla) \cdot \mathbf{u} d\mathbf{x} = \int_\Omega gq, \forall q \in L_0^2(\Omega).$$

So it is sufficient to prove that $(B.8)$ is uniquely solvable. Observe that $V \subset (H_0^1(\Omega))^2$ is an Hilbert space, since it is a close space. By the inf-sup condition $(B.4)$, there exists $\mathbf{u}_0 \in V^\perp$ such that $(B^T\nabla) \cdot \mathbf{u}_0 = g$, and $\|\nabla \mathbf{u}_0\|_{L^2(\Omega)} \le \frac{1}{\beta} \|g\|_{L^2(\Omega)}$. Now, we consider the variational problem : find $\mathbf{w} \in V$ the solution of

$$a(\mathbf{w}, \mathbf{v}) = F(\mathbf{v}) - a(\mathbf{u}_0, \mathbf{v}), \quad \forall \mathbf{v} \in V. \tag{B.9}$$

Proposition B.1 ensures that $(B.9)$ is well-posed by the Lax-Milgram Lemma. Moreover, standard elliptic theory ensures that the following a priori estimate holds

$$\|\nabla \mathbf{w}\|_{L^2(\Omega)} \le \frac{K^2}{\alpha} \left( C_p \|\mathbf{f}\|_{H^{-1}(\Omega)} + \|A\|^2_{L^\infty(\Omega)} \|\nabla \mathbf{u}_0\|_{L^2(\Omega)} \right).$$

Then $\mathbf{u} = \mathbf{w} + \mathbf{u}_0 \in V_g$ is the unique solution of $(B.8)$. Finally, using the estimate on $\mathbf{u}_0$, we finally obtain the following a priori bound for $\mathbf{u}$

$$\|\nabla \mathbf{u}\|_{L^2(\Omega)} \le \frac{K^2}{\alpha} \left( C_p \|\mathbf{f}\|_{H^{-1}(\Omega)} + \frac{\|A\|^2_{L^\infty(\Omega)}}{\beta} \|g\|_{L^2(\Omega)} \right) + \frac{1}{\beta} \|g\|_{L^2(\Omega)},$$

where $C_p$ stands for the Poincaré constant and $K$ for the Korn's constant of $\Omega$. This implies $(B.6)$. Combining the latter with the estimate for the pressure yields $(B.7)$. □

**Remark B.5.**
Observe that $g \in L_0^2(\Omega)$ is necessary for $(B.5)$ being well-posed. Indeed, if $\mathbf{u} \in (H_0^1(\Omega))^2$ satisfies $(B^T\nabla)\cdot\mathbf{u} = g$ then thanks to the divergence theorem, we must have

$$\int_\Omega g d\mathbf{x} = \int_\Omega (B^T\nabla)\cdot\mathbf{u} d\mathbf{x} = \int_\Omega \nabla\cdot(B\mathbf{u}) d\mathbf{x} = \int_{\partial\Omega} B\mathbf{u}\cdot\mathbf{n} d\mathbf{x} = 0,$$

where $\mathbf{n}$ stands for the unit outer normal of $\Omega$.

**Theorem B.6.**
*Let $\Omega \subset \mathbb{R}^2$ be a Lipschitz, connected, bounded, open set. Let $\mathbf{f}_1, \mathbf{f}_2 \in (L^2(\Omega))^2$, $A_1, A_2 \in (L^\infty(\Omega))^{2\times 2}$ be symmetric positive definite matrices, $B_1, B_2 \in (W^{1,\infty}(\Omega))^{2\times 2}$ such that $B_1^{-1}, B_2^{-1} \in (W^{1,\infty}(\Omega))^{2\times 2}$. Assume moreover that $\nabla\cdot B_1^T = \nabla\cdot B_2^T = 0$ and let us define for $i = 1, 2$, the bilinear and linear forms*

$$\begin{aligned}
a_i(\mathbf{u},\mathbf{v}) &= \int_\Omega \frac{\nabla\mathbf{u}A_i + A_i^T\nabla\mathbf{u}^T}{2} : \frac{\nabla\mathbf{v}A_i + A_i^T\nabla\mathbf{v}^T}{2} d\mathbf{x},\\
b_i(\mathbf{v},q) &= -\int_\Omega q(B_i^T\nabla)\cdot\mathbf{v} d\mathbf{x},\\
F_i(\mathbf{v}) &= \int_\Omega \mathbf{f}_i\cdot\mathbf{v} d\mathbf{x}.
\end{aligned}$$

*Finally, assume that there exists $\alpha_1, \alpha_2 > 0$ such that*

$$a_i(\mathbf{v},\mathbf{v}) \geq \alpha_i \int_\Omega D(\mathbf{v}) : D(\mathbf{v}) d\mathbf{x}, \text{ for all } \mathbf{v} \in (H_0^1(\Omega))^2.$$

*Then, for $i = 1, 2$, there exists unique solutions $(\mathbf{u}_i, p_i) \in (H_0^1(\Omega))^2 \times L_0^2(\Omega)$ of the variational problems*

$$\begin{cases} a_i(\mathbf{u}_i,\mathbf{v}) + b_i(\mathbf{v},p_i) = F_i(v), & \forall v \in (H_0^1(\Omega))^2,\\ -b_i(\mathbf{u}_i,q) = 0, & \forall q \in L_0^2(\Omega). \end{cases} \tag{B.10}$$

*Moreover, for $i = 1, 2$, let $\beta_i > 0$ be the inf-sup constant associate to the bilinear forms $b_i$. Then, there exists a constant $C > 0$ depending only on $\Omega$ such that*

$$\begin{aligned}
\|\nabla(\mathbf{u}_1 - \mathbf{u}_2)\|_{L^2(\Omega)} \leq C \Bigg( &\frac{1}{\alpha_1}\|\mathbf{f}_1 - \mathbf{f}_2\|_{L^2(\Omega)} + \frac{(\|A_1\|_{L^\infty(\Omega)} + \|A_2\|_{L^\infty(\Omega)})\|\nabla\mathbf{u}_2\|_{L^2(\Omega)}}{\alpha_1}\|A_1 - A_2\|_{L^\infty(\Omega)}\\
&+ \left(\|p_2\|_{L^2(\Omega)} + \left(\frac{1}{\beta_1} + \frac{\|A_1\|_{L^\infty(\Omega)}^2}{\alpha_1\beta_1}\right)\|\nabla\mathbf{u}_2\|_{L^2(\Omega)}\right)\|B_1 - B_2\|_{L^\infty(\Omega)}\Bigg),
\end{aligned} \tag{B.11}$$

*and*

$$\begin{aligned}
\|p_1 - p_2\|_{L^2(\Omega)} \leq C \Bigg( &\left(\frac{1}{\beta_1} + \frac{\|A_1\|_{L^\infty(\Omega)}^2}{\alpha_1\beta_1}\right)\|\mathbf{f}_1 - \mathbf{f}_2\|_{L^2(\Omega)}\\
&+ \left(\frac{1}{\beta_1} + \frac{\|A_1\|_{L^\infty(\Omega)}^2}{\alpha_1\beta_1}\right)(\|A_1\|_{L^\infty(\Omega)} + \|A_2\|_{L^\infty(\Omega)})\|\nabla\mathbf{u}_2\|_{L^2(\Omega)}\|A_1 - A_2\|_{L^\infty(\Omega)}\\
&+ \left(\left(\frac{1}{\beta_1} + \frac{\|A_1\|_{L^\infty(\Omega)}^2}{\alpha_1\beta_1}\right)\|p_2\|_{L^2(\Omega)} + \left(\frac{\|A_1\|_{L^\infty(\Omega)}^2}{\beta_1^2} + \frac{\|A_1\|_{L^\infty(\Omega)}^4}{\alpha_1\beta_1^2}\right)\|\nabla\mathbf{u}_2\|_{L^2(\Omega)}\right)\|B_1 - B_2\|_{L^\infty(\Omega)}\Bigg).
\end{aligned} \tag{B.12}$$

*Proof.* Observe that under the present hypothesis, the well-posedness of the problems $(B.10)$ is guaranteed for $i = 1, 2$ thanks to Theorem B.4. Taking the difference between $(B.10)$ with $i = 1$ and $(B.10)$ with $i = 2$, we get

$$\begin{cases} a_1(\mathbf{u}_1 - \mathbf{u}_2, v) + b_1(\mathbf{v}, p_1 - p_2) = F(\mathbf{v}), & \forall\mathbf{v} \in (H_0^1(\Omega))^2,\\ -b_1(\mathbf{u}_1 - \mathbf{u}_2, q) = (g, q), & \forall q \in L_0^2(\Omega), \end{cases} \tag{B.13}$$

where $(\cdot,\cdot)$ stands for the usual inner product between $L^2$ functions,

$$F(\mathbf{v}) = \int_\Omega (\mathbf{f}_1 - \mathbf{f}_2) v d\mathbf{x} - \int_\Omega \frac{\nabla \mathbf{u}_2 (A_1 - A_2) + (A_1 - A_2)^T \nabla \mathbf{u}_2^T}{2} : \frac{\nabla \mathbf{v} A_1 + A_1^T \nabla \mathbf{v}^T}{2} d\mathbf{x}$$
$$- \int_\Omega \frac{\nabla \mathbf{u}_2 A_2 + A_2^T \nabla \mathbf{u}_2^T}{2} : \frac{\nabla \mathbf{v}(A_1 - A_2) + (A_1 - A_2)^T \nabla \mathbf{v}^T}{2} d\mathbf{x} - \int_\Omega p_2((B_1 - B_2)^T \nabla) \cdot \mathbf{v} d\mathbf{x},$$

and

$$g = -((B_1 - B_2)^T \nabla) \cdot \mathbf{u}_2. \tag{B.14}$$

Then the estimates $(B.11), (B.12)$ are obtained observing that the problem $(B.13)$ satisfies the hypothesis of Theorem $B.4$ and that

$$\|F\|_{H^{-1}(\Omega)}$$
$$\leq C \|\mathbf{f}_1 - \mathbf{f}_2\|_{L^2(\Omega)} + \|A_1 - A_2\|_{L^\infty(\Omega)} (\|A_1\|_{L^\infty(\Omega)} + \|A_2\|_{L^\infty(\Omega)}) \|\nabla \mathbf{u}_2\|_{L^2(\Omega)} + \|B_1 - B_2\|_{L^\infty(\Omega)} \|p_2\|_{L^2(\Omega)},$$

$$\|g\|_{L^2(\Omega)} \leq \|B_1 - B_2\|_{L^\infty(\Omega)} \|\nabla \mathbf{u}_2\|_{L^2(\Omega)},$$

where $C > 0$ depends only on $\Omega$. □

**Remark B.7.**
In fact, we can prove the following general bound by combining (B.11) and (B.12) with the a priori estimates for $\mathbf{u}_2$ and $p_2$

$$\|\nabla(\mathbf{u}_1 - \mathbf{u}_2)\|_{L^2(\Omega)} + \|p_1 - p_2\|_{L^2(\Omega)}$$
$$\leq C \left( \|\mathbf{f}_1 - \mathbf{f}_2\|_{L^\infty(\Omega)} + \|A_1 - A_2\|_{L^\infty(\Omega)} + \|B_1 - B_2\|_{L^\infty(\Omega)} \right),$$

where $C$ depends on $\Omega, \|\mathbf{f}_1\|_{L^2(\Omega)}, \|\mathbf{f}_2\|_{L^2(\Omega)}, \|A_1\|_{L^\infty(\Omega)}, \|A_2\|_{L^\infty(\Omega)}, \alpha_1, \alpha_2, \beta_1, \beta_2$.

To conclude this section, we study the higher regularity of the solutions to the saddle point problem (B.5). In the case the coefficients of the matrices $A$ and $B$ are sufficiently smooth, it can be shown that the solutions belongs to $(H^2(\Omega))^2 \times H^1(\Omega)$.

We focus on a particular example, that we used in Chapter 3 and 4. In the notations introduced above, we consider now $\mathbf{f} \in (L^2(\Omega))^2$, $g = 0$, $B = I$ and $A = (2\mu)^{1/2} I$ where $\mu$ is a strictly positive function that belongs to $C^{0,1}(\overline{\Omega})$ (which is equivalent to be in $W^{1,\infty}(\Omega)$). In this situation, the Stokes problem (B.5) reads : find $(\mathbf{u}, p) \in (H_0^1(\Omega))^2 \times L_0^2(\Omega)$ the solutions of

$$\int_\Omega 2\mu D(\mathbf{u}) : D(\mathbf{v}) d\mathbf{x} - \int_\Omega p \operatorname{div} \mathbf{v} d\mathbf{x} = \int_\Omega \mathbf{f} \cdot \mathbf{v} d\mathbf{x}, \forall \mathbf{v} \in (H_0^1(\Omega))^2,$$
$$\int_\Omega q \operatorname{div} \mathbf{u} = 0, \forall q \in L_0^2(\Omega).$$

The last problem corresponds to the variational formulation of the PDE

$$-\operatorname{div}(2\mu D(\mathbf{u})) + \nabla p = \mathbf{f}$$
$$\operatorname{div} \mathbf{u} = 0.$$

In what follows, we show, under appropriate hypothesis on $\Omega$, that this problem has a unique $(H^2(\Omega))^2 \times H^1(\Omega)$ solution.

**Theorem B.8** ($H^2 - H^1$ regularity of solutions to Stokes equations with smooth variable coefficients)**.**
*Let $\Omega \subset \mathbb{R}^2$ be a Lipschitz, connected open set. Let $\mathbf{f} \in (H^{-1}(\Omega))^2$ and $\mu \in C^{0,1}(\overline{\Omega})$*

*such that* $0 < \mu_{\min} \leq \mu \leq \mu_{\max}$. *Then, there exists a unique weak solution* $(\mathbf{u}, p) \in (H_0^1(\Omega))^2 \times L_0^2(\Omega)$ *of the Stokes equations*

$$\begin{cases} -\operatorname{div}(2\mu D(\mathbf{u})) + \nabla p = \mathbf{f}, & \text{in } \Omega, \\ \operatorname{div} \mathbf{u} = 0, & \text{in } \Omega, \\ \mathbf{u} = 0, & \text{on } \partial\Omega, \end{cases} \tag{B.15}$$

*that satisfies the a priori estimate*

$$\mu_{\min} \|\nabla \mathbf{u}\|_{L^2(\Omega)} + \frac{\mu_{\min}}{\mu_{\max}} \|p\|_{L^2(\Omega)} \leq C \|\mathbf{f}\|_{H^{-1}(\Omega)}, \tag{B.16}$$

*where* $C > 0$ *depends only on* $\Omega$.

*Moreover, if we assume that* $\Omega$ *is a smooth domain or a convex polygon and* $\mathbf{f} \in (L^2(\Omega))^2$, *then* $(\mathbf{u}, p) \in (H^2(\Omega))^2 \times (H^1(\Omega))$ *and there exists* $C' > 0$ *depending only on* $\Omega$ *such that*

$$\mu_{\min} \|\mathbf{u}\|_{H^2(\Omega)} + \frac{\mu_{\min}}{\mu_{\max}} \|p\|_{H^1(\Omega)} \leq C' \left(1 + \|\mu^{-1}\nabla\mu\|_{L^\infty(\Omega)}\right) \frac{\mu_{\max}}{\mu_{\min}} \|\mathbf{f}\|_{L^2(\Omega)}. \tag{B.17}$$

*Proof.* In what follows, we denote by $C$ any positive constant that may depend only on $\Omega$, but which value can change from line to line. The existence and uniqueness of $(\mathbf{u}, p) \in (H_0^1(\Omega))^2 \times L_0^2(\Omega)$, as the a priori estimate (B.16), are direct consequences of Theorem B.4.

Under the additional hypothesis that $\Omega$ is smooth or a convex polygon, and $\mathbf{f}$ is a $L^2$ function, then one can prove that $(\mathbf{u}, p) \in (H^2(\Omega))^2 \times (H^1(\Omega))$, see for instance [21]. We briefly explain the main argument. Let us consider the weak formulation of (B.15). It reads

$$\int_\Omega 2\mu D(\mathbf{u}) : D(\mathbf{v}) d\mathbf{x} - \int_\Omega p \operatorname{div} \mathbf{v} d\mathbf{x} = \int_\Omega \mathbf{f} \cdot \mathbf{v} d\mathbf{x}, \forall \mathbf{v} \in (H_0^1(\Omega))^2,$$
$$\int_\Omega q \operatorname{div} \mathbf{u} d\mathbf{x} = 0, \forall q \in L_0^2(\Omega). \tag{B.18}$$

□

Now, since $\mu$ belongs in particular to $W^{1,\infty}(\Omega)$ and does not vanish, we can choose $v = \mu^{-1} w$ in (B.18) and we obtain that $(\mathbf{u}, \mu^{-1} p) \in (H_0^1(\Omega))^2 \times L^2(\Omega)$ are weak solutions of

$$\int_\Omega 2D(\mathbf{u}) : D(\mathbf{w}) d\mathbf{x} - \int_\Omega \mu^{-1} p \operatorname{div} \mathbf{w} d\mathbf{x}$$
$$= \int_\Omega \mathbf{f}(\mu^{-1} w) d\mathbf{x} - \int_\Omega 2\mu D(\mathbf{u}) \nabla \mu^{-1} \mathbf{w} d\mathbf{x} + \int_\Omega p \nabla \mu^{-1} \mathbf{w} d\mathbf{x}, \forall \mathbf{w} \in (H_0^1(\Omega))^2,$$
$$\int_\Omega q \operatorname{div} \mathbf{u} d\mathbf{x} = 0, \forall q \in L_0^2(\Omega). \tag{B.19}$$

Observe that (B.19) is nothing else than the variational formulation of the Stokes problem

$$\begin{cases} -\Delta \mathbf{u} + \nabla(\mu^{-1} p) = \mu^{-1} \mathbf{f} + 2\mu^{-1} D(\mathbf{u}) \nabla \mu + p \nabla \mu^{-1}, & \text{in } \Omega, \\ \operatorname{div} \mathbf{u} = 0, & \text{in } \Omega, \\ \mathbf{u} = 0, & \text{on } \partial\Omega, \end{cases} \tag{B.20}$$

where we use that $-\operatorname{div}(2D(\mathbf{u})) = -\Delta\mathbf{u}$ since $\operatorname{div}\mathbf{u} = 0$ and that $\mu\nabla\mu^{-1} = -\frac{\mu}{\mu^2}\nabla\mu = -\mu^{-1}\nabla\mu$. Moreover observe that

$$\mu^{-1}\mathbf{f} + 2\mu^{-1}D(\mathbf{u})\nabla\mu + p\nabla\mu^{-1} \in (L^2(\Omega)).$$

Thus, using the regularity results of [21] (for smooth domains) or [62] (for convex polygons), we have that $\mathbf{u} \in (H^2(\Omega))^2$ and $\mu^{-1}p \in H^1(\Omega)$, which implies that $p \in H^1(\Omega)$ since

$$\nabla p = \mu\left(\nabla(\mu^{-1}p) - \nabla\mu^{-1}p\right) \in (L^2(\Omega))^2.$$

So far, we have then proven that $(\mathbf{u}, p) \in (H^2(\Omega))^2 \times H^1(\Omega)$. To derive (B.17), we use again the strong formulation (B.20) for which the following a priori estimate is valid (see again the references pointed out above)

$$\|\mathbf{u}\|_{H^2(\Omega)} + \|\mu^{-1}p\|_{H^1(\Omega)} \le C\|\mathbf{g}\|_{L^2(\Omega)}$$

where $C$ depends only on $\Omega$ and we note

$$\mathbf{g} = \mu^{-1}\mathbf{f} + 2\mu^{-1}D(\mathbf{u})\nabla\mu + p\nabla\mu^{-1}.$$

Bounding the $L^2$ norm of $\mathbf{g}$ by using the $H^1 - L^2$ a priori estimate (B.16), we obtain that

$$\|\mathbf{u}\|_{H^2(\Omega)} \le C\left(1 + \|\mu^{-1}\nabla\mu\|_{L^\infty(\Omega)}\right)\|\mathbf{f}\|_{L^2(\Omega)}\frac{\mu_{\max}}{\mu_{\min}^2}. \tag{B.21}$$

Moreover we also have that

$$\|\mu^{-1}p\|_{H^1(\Omega)} \le C\left(1 + \|\mu^{-1}\nabla\mu\|_{L^\infty(\Omega)}\right)\|\mathbf{f}\|_{L^2(\Omega)}\frac{\mu_{\max}}{\mu_{\min}^2}.$$

Since again one can write

$$\nabla p = \mu\left(\nabla(\mu^{-1}p) - \nabla\mu^{-1}p\right),$$

and using a last time that $\nabla\mu{-}1 = \mu^{-2}\nabla\mu$ and the a priori estimate (B.16), we compute that

$$\|p\|_{H^1(\Omega)} \le C\left(1 + \|\mu^{-1}\nabla\mu\|_{L^\infty(\Omega)}\right)\|\mathbf{f}\|_{L^2(\Omega)}\frac{\mu_{\max}^2}{\mu_{\min}^2}. \tag{B.22}$$

Combining estimates (B.21) and (B.22) yields finally (B.17).

**Remark B.9.**
Observe that the strong formulation (B.20) is exactly the one that we obtain if we develop

$$-\operatorname{div}(2\mu D(\mathbf{u})) + \nabla p = \mathbf{f}$$

and then divide by $\mu$.

## B.2 Lipschitz continuity of steady Stokes flows around disks

In this section, we consider the following situation. Let $\Omega = ]0, a[^2$, $a > 0$, be a square in $\mathbb{R}^2$. Let $R > 0$ and $\mathbf{X} = (X_1, X_2)$, $\mathbf{Y} = (Y_1, Y_2) \in \Omega$. We denote by $\mathcal{B}(\mathbf{X})$, respectively $\mathcal{B}(\mathbf{Y})$ the open disks of radius $R$ centered at $\mathbf{X}$, respectively $\mathbf{Y}$. We assume that $\mathcal{B}(\mathbf{X}), \mathcal{B}(\mathbf{Y}) \subset\subset \Omega$ i.e. the disks are compactly included in $\Omega$. In particular, that means that $\partial\mathcal{B}(\mathbf{X}) \cap \partial\Omega \neq \emptyset$ and $\partial\mathcal{B}(\mathbf{Y}) \cap \partial\Omega \neq \emptyset$. For all $\mathbf{X}' \in \mathbb{R}^2$, we define then the piecewise constant coefficients

$$\mu_{\mathbf{X}'} = \mu_{\mathcal{B}}\chi_{\mathcal{B}(\mathbf{X}')} + \mu_{\mathcal{F}}(1 - \chi_{\mathcal{B}(\mathbf{X}')}), \qquad \rho_{\mathbf{X}'} = \rho_{\mathcal{B}}\chi_{\mathcal{B}(\mathbf{X}')} + \rho_{\mathcal{F}}(1 - \chi_{\mathcal{B}(\mathbf{X}')}), \tag{B.23}$$

where $\mu_\mathcal{B}, \mu_\mathcal{F}, \rho_\mathcal{B}, \rho_\mathcal{F} > 0$. To simplify the notation later, we note

$$\rho_{\min} = \min(\rho_\mathcal{B}, \rho_\mathcal{F}), \tag{B.24}$$

$$\rho_{\max} = \max(\rho_\mathcal{B}, \rho_\mathcal{F}), \tag{B.25}$$

$$\mu_{\min} = \min(\mu_\mathcal{B}, \mu_\mathcal{F}), \tag{B.26}$$

$$\mu_{\min} = \max(\mu_\mathcal{B}, \mu_\mathcal{F}). \tag{B.27}$$

The main result is the Theorem B.10 below, that is used in the proof of Proposition 4.28 in the second part of Chapter 4. It is the main tool to derive the a posteriori error estimate 4.84 for the falling disk experiment. The main result of Theorem B.10 is that the map $\mathbf{F}$ defined for $\mathbf{X}' \in \mathbb{R}^2$ by

$$\mathbf{F}(\mathbf{X}') = \int_{\mathcal{B}(\mathbf{X}')} \mathbf{u}_{\mathbf{X}'} d\mathbf{x}$$

, where $\mathbf{u}_{\mathbf{X}'}$ is the solution of a Stokes problem, is locally Lipschitz.

**Theorem B.10** (Lipschitz continuity of solutions to steady Stokes equations with variable coefficients)**.**
*Let* $(\mathbf{u}_\mathbf{X}, p_\mathbf{X}), (\mathbf{u}_\mathbf{Y}, p_\mathbf{Y}) \in (H_0^1(\Omega))^2 \times L_0^2(\Omega)$ *be the solutions of the problems*

$$\begin{cases} -\operatorname{div}(2\mu_\mathbf{X} D(\mathbf{u}_\mathbf{X})) + \nabla p_\mathbf{X} = \rho_\mathbf{X}\mathbf{g}, \\ \operatorname{div}\mathbf{u}_\mathbf{X} = 0, \end{cases} \tag{B.28}$$

$$\begin{cases} -\operatorname{div}(2\mu_\mathbf{Y} D(\mathbf{u}_\mathbf{Y})) + \nabla p_\mathbf{Y} = \rho_\mathbf{Y}\mathbf{g}, \\ \operatorname{div}\mathbf{u}_\mathbf{Y} = 0, \end{cases} \tag{B.29}$$

*where* $\mu_\mathbf{X}, \rho_\mathbf{X}, \mu_\mathbf{Y}$ *and* $\rho_\mathbf{Y}$ *are defined in* (B.23)*. If* $\dfrac{|\mathbf{X}-\mathbf{Y}|}{d(\mathcal{B}(\mathbf{X}); \partial\Omega)}$ *is small enough, then there exists a constant* $C > 0$ *depending only on* $\Omega$ *such that*

$$\left| \frac{1}{\pi R^2} \int_{\mathcal{B}(\mathbf{X})} \mathbf{u}_\mathbf{X} d\mathbf{x} - \frac{1}{\pi R^2} \int_{\mathcal{B}(\mathbf{Y})} \mathbf{u}_\mathbf{Y} d\mathbf{x} \right| \leq C \frac{\mu_{\max}\rho_{\max}|g|}{R\mu_{\min}^2} \frac{|\mathbf{X}-\mathbf{Y}|}{d(\mathcal{B}(\mathbf{X}); \partial\Omega)}. \tag{B.30}$$

**Remark B.11.**
Note that both problems $(B.28), (B.29)$ (in weak form) satisfy assumptions of Theorem B.4 and then are well posed in $(H_0^1(\Omega))^2 \times L_0^2(\Omega)$. Moreover, the following a priori estimate holds

$$\|\nabla \mathbf{u}_\mathbf{X}\|_{L^2(\Omega)}, \|\nabla \mathbf{u}_\mathbf{Y}\|_{L^2(\Omega)} \leq C \frac{\rho_{\max}}{\mu_{\min}} |\mathbf{g}|, \tag{B.31}$$

$$\|p_\mathbf{X}\|_{L^2(\Omega)}, \|p_\mathbf{Y}\|_{L^2(\Omega)} \leq C \frac{\rho_{\max}\mu_{\max}}{\mu_{\min}} |\mathbf{g}|, \tag{B.32}$$

where $C > 0$ depends only on $\Omega$.

The key point of the proof of Theorem B.10 consists to map $\mathcal{B}(\mathbf{X})$ into $\mathcal{B}(\mathbf{Y})$ with a suitable diffeomorphism. Reproducing what was done in [54] in the framework of random domains, we introduce the mapping $\Phi : \overline{\Omega} \to \overline{\Omega}$ defined by $(y_1, y_2) = \Phi(x_1, x_2)$ with

$$y_1 = x_1 + (Y_1 - X_1)\varphi_1(x_1)\varphi_2(x_2), \quad y_2 = x_2 + (Y_2 - X_2)\varphi_1(x_1)\varphi_2(x_2), \tag{B.33}$$

where for $i = 1, 2$ we note

$$\varphi_i(x_i) = \begin{cases} 1, \quad x_i \in [X_i - R, X_i + R], \\ \\ \dfrac{x_i}{X_i - R} - \dfrac{x_i(x_i - X_i + R)}{(X_i - R)^2}, \quad x_i \in [0, X_i - R], \\ \\ \dfrac{x_i - a}{X_i + R - a} - \dfrac{(x_i - a)(x_i - X_i - R)}{(X_i + R - a)^2}, \quad x_i \in [X_i + R, a]. \end{cases} \tag{B.34}$$

We shall observe that the boundary of $\Omega$ is fixed by $\Phi$.

**Proposition B.12.**
*Assume that* $\dfrac{|\mathbf{X}-\mathbf{Y}|}{d(\mathcal{B}(\mathbf{X});\partial\Omega)}$ *is small, then the mapping* $\Phi$ *defined by* $(B.33)$ *is a* $(C^1(\bar{\Omega}))^2 \cap (W^{2,\infty}(\Omega))^2$ *diffeomorphism from* $\overline{\Omega}$ *to* $\overline{\Omega}$. *Moreover, the jacobian matrix of* $\Phi$ *is given by*

$$\nabla\Phi = \nabla\Phi(x_1,x_2) = \begin{pmatrix} 1+\delta_1\varphi_1'\varphi_2 & \delta_1\varphi_1\varphi_2' \\ \delta_2\varphi_1'\varphi_2 & 1+\delta_2\varphi_1\varphi_2' \end{pmatrix}, \tag{B.35}$$

*where we note for* $i = 1,2$

$$\delta_i = Y_i - X_i, \quad \varphi_i = \varphi_i(x_i), \quad \varphi_i' = \varphi_i'(x_i). \tag{B.36}$$

*In particular, there exists* $c > 0$ *independent of* $\Omega, \mathbf{X}, \mathbf{Y}$ *and* $R$ *such that for all* $\mathbf{x} \in \overline{\Omega}$

$$\det \nabla\Phi(\mathbf{x}) \geq c. \tag{B.37}$$

*Proof.* We first prove that $\Phi \in (C^1(\bar{\Omega}))^2 \cap (W^{2,\infty}(\Omega))^2$. A direct computation yields

$$\varphi_i'(x_i) = \begin{cases} 0, \quad x_i \in [X_i - R, X_i + R], \\[2ex] \dfrac{2}{X_i - R} - \dfrac{2x_i}{(X_i-R)^2}, \quad x_i \in [0, X_i - R], \\[2ex] \dfrac{1}{X_i + R - a} - \dfrac{2x_i - X_i - R - a}{(X_i + R - a)^2}, \quad x_i \in [X_i + R, a], \end{cases} \tag{B.38}$$

and

$$\varphi_i''(x_i) = \begin{cases} 0, \quad x_i \in ]X_i - R, X_i + R[, \\[2ex] -\dfrac{2}{(X_i-R)^2}, \quad x_i \in ]0, X_i - R[, \\[2ex] -\dfrac{2}{(X_i + R - a)^2}, \quad x_i \in ]X_i + R, a[. \end{cases} \tag{B.39}$$

Since $\varphi_i' \in C^0[0,a], \varphi_i'' \in L^\infty(0,a), i = 1,2$, we necessarily obtain that $\Phi \in (C^1(\bar{\Omega}))^2 \cap (W^{2,\infty}(\Omega))^2$. A direct computation yield that

$$\nabla\Phi = \nabla\Phi(x_1,x_2) = \begin{pmatrix} 1+\delta_1\varphi_1'\varphi_2 & \delta_1\varphi_1\varphi_2' \\ \delta_2\varphi_1'\varphi_2 & 1+\delta_2\varphi_1\varphi_2' \end{pmatrix},$$

and

$$\det \nabla\Phi = 1 + \delta_1\varphi_1'\varphi_2 + \delta_2\varphi_1\varphi_2'.$$

Assuming that $\frac{|\mathbf{X}-\mathbf{Y}|}{d(\mathcal{B}(\mathbf{X});\partial\Omega)}$ is small enough, we can ensure that $\det \nabla\Phi \geq c$ in $\overline{\Omega}$ for a $c > 0$ independent of $\Omega, \mathbf{X}, \mathbf{Y}$ and $R$. Therefore, since its jacobian never vanishes, $\Phi$ is invertible and its inverse $\Phi^{-1}$ belongs to $(C^1(\bar{\Omega}))^2 \cap (W^{2,\infty}(\Omega))^2$. □

Since $\Phi$ is a diffeomorphism, then in particular the Piola's identity holds. It will be used in the proof of Theorem B.10 later. We recall it in the next proposition

**Proposition B.13.**
*Let* $\Phi$ *be the mapping defined by* $(B.33)$. *Then*

$$\nabla \cdot (\det \nabla\Phi(\nabla\Phi)^{-T}) = 0 \text{ almost everywhere in } \Omega. \tag{B.40}$$

*Proof.* A proof can be found in [33] and in [80]. □

**Proposition B.14.**
*If* $\dfrac{|\mathbf{X}-\mathbf{Y}|}{d(\mathcal{B}(\mathbf{X});\partial\Omega)}$ *is small enough, then there exists two constants* $c, C > 0$ *independent of* $\Omega, \mathbf{X}, \mathbf{Y}$ *and* $R$ *such that for all* $\mathbf{x} \in \overline{\Omega}$

*i)* $c \leq \det \nabla\Phi(\mathbf{x}) \leq 1 + C\dfrac{|\mathbf{X}-\mathbf{Y}|}{d(\mathcal{B}(\mathbf{X});\partial\Omega)}$,

*ii)* $c \leq \sigma_i(\nabla\Phi(\mathbf{x})) \leq C\left(1 + \dfrac{|\mathbf{X}-\mathbf{Y}|}{d(\mathcal{B}(\mathbf{X});\partial\Omega)}\right), \quad c \leq \sigma_i((\nabla\Phi(\mathbf{x}))^{-1}) \leq C\left(1 + \dfrac{|\mathbf{X}-\mathbf{Y}|}{d(\mathcal{B}(\mathbf{X});\partial\Omega)}\right)$,

*iii)* $c \leq \det\left((\nabla\Phi(\mathbf{x}))^{-1}\right) \leq 1 + C\dfrac{|\mathbf{X}-\mathbf{Y}|}{d(\mathcal{B}(\mathbf{X});\partial\Omega)}$,

*iv)* $|1 - \det \nabla\Phi(\mathbf{x})| \leq C\dfrac{|\mathbf{X}-\mathbf{Y}|}{d(\mathcal{B}(\mathbf{X});\partial\Omega)}$,

*v)* $\sigma_i(I - (\nabla\Phi)^{-1}(\mathbf{x})) \leq C\dfrac{|\mathbf{X}-\mathbf{Y}|}{d(\mathcal{B}(\mathbf{X});\partial\Omega)}, \sigma_i(I - (\nabla\Phi)(\mathbf{x})) \leq C\dfrac{|\mathbf{X}-\mathbf{Y}|}{d(\mathcal{B}(\mathbf{X});\partial\Omega)}$,

*where for a matrix* $A \in \mathbb{R}^{2\times 2}$, *we denote by* $\sigma_i(A), i = 1, 2$ *its singular values.*

*Proof.* In what follows, we will denote by $c$ or $C$ any positive constant, independent of $\Omega, R, \mathbf{X}, \mathbf{Y}$, but which values can change from line to line. We also omit to note the dependence on $x$. We only prove $i)$ and $ii)$. $iii), iv), v)$ can be obtained in the same way.

i) Observe that the lower bound is already proven in Proposition B.12. We only have to prove the upper one. Since $\det \nabla\Phi = 1 + \delta_1\varphi_1'\varphi_2 + \delta_2\varphi_1\varphi_2'$. Using the fact that

$$\varphi_i \leq 1, \quad |\varphi_i'| \leq 2\max\left(\frac{1}{|X_i - R|}, \frac{1}{|X_i - R + a|}\right) \leq 2\frac{1}{d(\mathcal{B}(\mathbf{X});\partial\Omega)},$$

yields the result.

ii) We recall that the singular values are given by

$$\sigma_i(\nabla\Phi) = (\lambda_i(\nabla\Phi\nabla\Phi^T))^{1/2},$$

where $\lambda_i, i = 1, 2$, satands for the eigenvalues. To get an upper bound for the singular values, we use the Gerschgorin's theorem. We have that

$$\lambda_i(\nabla\Phi\nabla\Phi^T) \leq \max_{i=1,2}\left(\sum_{j=1}^{2}|\nabla\Phi\nabla\Phi^T|_{ij}\right) \leq C\left(1 + \frac{|\mathbf{X}-\mathbf{Y}|}{d(\mathcal{B}(\mathbf{X});\partial\Omega)} + \left(\frac{|\mathbf{X}-\mathbf{Y}|}{d(\mathcal{B}(\mathbf{X});\partial\Omega)}\right)^2\right),$$

which implies that

$$\sigma_i(\nabla\Phi) \leq C\left(1 + \frac{|\mathbf{X}-\mathbf{Y}|}{d(\mathcal{B}(\mathbf{X});\partial\Omega)}\right)^{1/2} + C\frac{|\mathbf{X}-\mathbf{Y}|}{d(\mathcal{B}(\mathbf{X});\partial\Omega)}.$$

Using that $\sqrt{1+x} \leq 1 + x$ for all $x \geq 0$ yields the desired estimate. Recalling that

$$(\nabla\Phi)^{-1}(\nabla\Phi)^{-T} = \frac{1}{(\det\nabla\Phi)^2}\begin{pmatrix} (\nabla\Phi\nabla\Phi^T)_{22} & -(\nabla\Phi\nabla\Phi^T)_{12} \\ -(\nabla\Phi\nabla\Phi^T)_{12} & (\nabla\Phi\nabla\Phi^T)_{11} \end{pmatrix}.$$

We then obtain by the same argument that

$$\lambda_i((\nabla\Phi)^{-1}(\nabla\Phi)^{-T}) \leq c^{-2}C\left(1 + \frac{|\mathbf{X}-\mathbf{Y}|}{d(\mathcal{B}(\mathbf{X});\partial\Omega)} + \left(\frac{|\mathbf{X}-\mathbf{Y}|}{d(\mathcal{B}(\mathbf{X});\partial\Omega)}\right)^2\right)$$

which yields the upper bound for $\sigma_i((\nabla\Phi)^{-1})$. Finally, for the lower bounds, we recall that

$$\lambda_i(\nabla\Phi\nabla\Phi^T) = \frac{1}{\lambda_i((\nabla\Phi)^{-1}(\nabla\Phi)^{-T})}$$

implying that

$$\lambda_i(\nabla\Phi\nabla\Phi^T), \lambda_i((\nabla\Phi)^{-1}(\nabla\Phi)^{-T}) \geq c^2.$$

□

**Corollary B.15.**
*Under the assumption of Proposition B.14, there exists $C > 0$ independent of $\Omega, \mathbf{X}, \mathbf{Y}$ and $R$ such that*

*i)* $\|\det\nabla\Phi(\nabla\Phi)^{-1}\|_{L^\infty(\Omega)} \leq C\left(1 + \dfrac{|\mathbf{X}-\mathbf{Y}|}{d(\mathcal{B}(\mathbf{X});\partial\Omega)}\right)$,

*ii)* $\|I - \det\nabla\Phi(\nabla\Phi)^{-1}\|_{L^\infty(\Omega)} \leq C\dfrac{|\mathbf{X}-\mathbf{Y}|}{d(\mathcal{B}(\mathbf{X});\partial\Omega)}$,

*Proof.* *i)* is a direct consequence of the Proposition B.14, using the fact that for every matrix $A$

$$|A|_F \leq \sqrt{(2)}\max_{i=1,2}\sigma_i(A),$$

and that

$$\left(\frac{|\mathbf{X}-\mathbf{Y}|}{d(\mathcal{B}(\mathbf{X});\partial\Omega)}\right)^2 \leq \frac{|\mathbf{X}-\mathbf{Y}|}{d(\mathcal{B}(\mathbf{X});\partial\Omega)} \text{ if } \frac{|\mathbf{X}-\mathbf{Y}|}{d(\mathcal{B}(\mathbf{X});\partial\Omega)} \text{ is small .}$$

For *ii)* observe that

$$\|I - \det\nabla\Phi(\nabla\Phi)^{-1}\|_{L^\infty(\Omega)} \leq \|I - (\nabla\Phi)^{-1}\|_{L^\infty(\Omega)} + \|(1-\det\nabla\Phi)(\nabla\Phi)^{-1}\|_{L^\infty(\Omega)}.$$

We then conclude as previously. □

**Proposition B.16.**
*Let $\mathbf{v} \in (H_0^1(\Omega))^2, q \in L^2(\Omega)$. Let us define $\tilde{\mathbf{v}} = \mathbf{v}\circ\Phi, \tilde{q} = q\circ\Phi$ where $\Phi$ is given by (B.33). Under the assumption of Proposition B.14, we have that $\tilde{\mathbf{v}} \in (H_0^1(\Omega))^2, \tilde{q} \in L^2(\Omega)$. Moreover, the followings estimates hold*

*i)* $\|\nabla\tilde{\mathbf{v}}\|_{L^2(\Omega)} \leq C\left(1 + \dfrac{|\mathbf{X}-\mathbf{Y}|}{d(\mathcal{B}(\mathbf{X});\partial\Omega)}\right)\|\nabla\mathbf{v}\|_{L^2(\Omega)}$,

*ii)* $\|\tilde{p}\|_{L^2(\Omega)} \leq \left(1 + C\dfrac{|\mathbf{X}-\mathbf{Y}|}{d(\mathcal{B}(\mathbf{X});\partial\Omega)}\right)\|p\|_{L^2(\Omega)}$,

*where $C > 0$ is independent of $\Omega, \mathbf{X}, \mathbf{Y}$ and $R$.*

*Proof.*

In what follows, we will denote by $c$ or $C$ any positive constants, independent of $\Omega, R, \mathbf{X}, \mathbf{Y}$, but which values can change from line to line. Making the change of variables $\mathbf{x} = \Phi^{-1}(\mathbf{y})$

$$\|\nabla\tilde{\mathbf{v}}\|^2_{L^2(\Omega)} = \int_\Omega \nabla\tilde{\mathbf{v}} : \nabla\tilde{\mathbf{v}}d\mathbf{x} = \int_\Omega \nabla\mathbf{v}\nabla\Phi : \nabla\mathbf{v}\nabla\Phi|\det\nabla\Phi^{-1}|dy \leq C\int_\Omega |\nabla\Phi|_F^2|\nabla\mathbf{v}|_F^2 dy,$$

where we use that

$$\nabla\Phi^{-1}(y) = (\nabla\Phi)^{-1}(\Phi(y)), \quad \text{ and } \det(\nabla\Phi)^{-1} = \frac{1}{\det\nabla\Phi} \leq \frac{1}{c},$$

with $c$ as in Proposition B.14. Then, recalling that for all matrix $|A|_F \leq \sqrt{2}\sigma_{\max}(A)$ and using estimates of Proposition B.14 we finally obtain that

$$\|\nabla\tilde{\mathbf{v}}\|^2_{L^2(\Omega)} \leq C^2\left(1+\frac{|\mathbf{X}-\mathbf{Y}|}{d(\mathcal{B}(\mathbf{X});\partial\Omega)}\right)^2\|\nabla\mathbf{v}\|^2_{L^2(\Omega)},$$

where $C>0$ is independent of $\Omega,\mathbf{X},\mathbf{Y}$ and $R$. Therefore, we immediately obtain that $\tilde{\mathbf{v}} \in (H^1(\Omega))^2$. Moreover, since $\Phi$ fixes the boundary of $\Omega$, we have that $\tilde{\mathbf{v}} \in (H^1_0(\Omega))^2$.

By the same arguments, we have

$$\|\tilde{p}\|^2_{L^2(\Omega)} = \int_\Omega \tilde{p}^2 d\mathbf{x} = \int_\Omega p^2|\det\nabla\Phi^{-1}|dy \leq \left(1+C\frac{|\mathbf{X}-\mathbf{Y}|}{d(\mathcal{B}(\mathbf{X});\partial\Omega)}\right)^2\|p\|^2_{L^2(\Omega)},$$

where we use again that

$$\nabla\Phi^{-1}(\mathbf{y}) = (\nabla\Phi)^{-1}(\Phi(\mathbf{y})),$$

but this time we use the estimate

$$\det(\nabla\Phi)^{-1} \leq \left(1+C\frac{|\mathbf{X}-\mathbf{Y}|}{d(\mathcal{B}(\mathbf{X});\partial\Omega)}\right) \leq \left(1+C\frac{|\mathbf{X}-\mathbf{Y}|}{d(\mathcal{B}(\mathbf{X});\partial\Omega)}\right)^2.$$

□

We are now in position to prove the Theorem B.10.

*Proof of Theorem B.10.* For the whole proof, we will denote by $C$ any positive constant, which value can change from line to line and depends only on $\Omega$. We first write both problems in a weak form. $(\mathbf{u}_\mathbf{X}, p_\mathbf{X}), (\mathbf{u}_\mathbf{Y}, p_\mathbf{Y}) \in (H^1_0(\Omega))^2 \times L^2_0(\Omega)$ are solutions of the variational problems

$$\begin{cases} \int_\Omega 2\mu_\mathbf{X} D(\mathbf{u}_\mathbf{X}) : D(\mathbf{v})d\mathbf{x} - \int_\Omega p_\mathbf{X}\operatorname{div}\mathbf{v}d\mathbf{x} = \int_\Omega \rho_\mathbf{X}\mathbf{g}\cdot\mathbf{v}d\mathbf{x}, \forall\mathbf{v}\in(H^1_0(\Omega))^2, \\ \int_\Omega \operatorname{div}(\mathbf{u}_\mathbf{X})qd\mathbf{x} = 0, \forall q\in L^2_0(\Omega), \end{cases} \tag{B.41}$$

$$\begin{cases} \int_\Omega 2\mu_\mathbf{Y} D(\mathbf{u}_\mathbf{Y}) : D(\mathbf{v})d\mathbf{y} - \int_\Omega p_\mathbf{Y}\operatorname{div}\mathbf{v}d\mathbf{y} = \int_\Omega \rho_\mathbf{X}\mathbf{g}\cdot\mathbf{v}d\mathbf{y}, \forall\mathbf{v}\in(H^1_0(\Omega))^2, \\ \int_\Omega \operatorname{div}(\mathbf{u}_\mathbf{Y})qd\mathbf{y} = 0, \forall q\in L^2_0(\Omega). \end{cases} \tag{B.42}$$

*Part 1.* We do the change of variable $\mathbf{y} = \Phi(\mathbf{x})$ in $(B.42)$, where $\Phi$ is the mapping defined in $(B.33)$. Observe that we have for $\mathbf{u} \in (H^1(\Omega))^2$

$$\nabla_y = (\nabla\Phi)^{-T}\nabla_x, \quad \nabla_y\mathbf{u} = \nabla_x\tilde{\mathbf{u}}(\nabla\Phi)^{-1}, \quad \operatorname{div}_y\mathbf{u} = ((\nabla\Phi^{-T})\nabla)\cdot\tilde{\mathbf{u}},$$

where $\tilde{\mathbf{u}} = \mathbf{u}\circ\Phi$. Noting $\tilde{\mathbf{u}}_\mathbf{Y} = \mathbf{u}_\mathbf{Y}\circ\Phi, \tilde{p}_\mathbf{Y} = p_\mathbf{Y}\circ\Phi, \tilde{\mathbf{v}} = \mathbf{v}\circ\Phi, \tilde{q} = q\circ\Phi$, the equations of Problem $(B.42)$ can be written as

$$\int_\Omega 2\mu_\mathbf{X}\det\nabla\Phi\frac{\nabla\tilde{\mathbf{u}}_\mathbf{Y}(\nabla\Phi)^{-1}+(\nabla\Phi)^{-T}\nabla\tilde{\mathbf{u}}_\mathbf{Y}^T}{2} : \frac{\nabla\tilde{\mathbf{v}}(\nabla\Phi)^{-1}+(\nabla\Phi)^{-T}\nabla\tilde{\mathbf{v}}^T}{2}d\mathbf{x}$$
$$-\int_\Omega \tilde{p}_\mathbf{Y}\det\nabla\Phi((\nabla\Phi)^{-T}\nabla)\cdot\tilde{\mathbf{v}}d\mathbf{x} = \int_\Omega \det\nabla\Phi\rho_\mathbf{X}\mathbf{g}\cdot\tilde{\mathbf{v}}d\mathbf{x}, \tag{B.43}$$

$$\int_\Omega \tilde{q}\det\nabla\Phi((\nabla\Phi)^{-T}\nabla)\cdot\tilde{\mathbf{u}}_\mathbf{Y}d\mathbf{x} = 0. \tag{B.44}$$

The main step of the proof consists to reproduce the strategy of the one of Theorem B.6 applied to the problems $(B.41)$ and $(B.43), (B.44)$. To do so, test functions must be taken in the same spaces. By Proposition B.16, $\tilde{\mathbf{u}}_{\mathbf{Y}}, \tilde{\mathbf{v}} \in (H_0^1(\Omega))^2$. Nevertheless, we do not have that $\tilde{p}_{\mathbf{Y}}, \tilde{q} \in L_0^2(\Omega)$. In fact they belong to the following subspace of $L^2(\Omega)$

$$L_\Phi^2(\Omega) = \left\{ \tilde{q} \in L^2(\Omega) : \int_\Omega \tilde{q} \det(\nabla\Phi)^{-1} d\mathbf{x} = 0 \right\}. \tag{B.45}$$

Observe that if $\tilde{q} = q \circ \Phi, q \in L_0^2(\Omega)$, then the mean value of $\tilde{q}$ can be estimated by

$$\frac{1}{\Omega}\int_\Omega \tilde{q} d\mathbf{x} = \frac{1}{\Omega}\int_\Omega q \det(\nabla\Phi)^{-1} d\mathbf{x} \le C\frac{|\mathbf{X}-\mathbf{Y}|}{d(\mathcal{B}(\mathbf{X});\partial\Omega)}\int_\Omega |q| d\mathbf{x} \le C\frac{|\mathbf{X}-\mathbf{Y}|}{d(\mathcal{B}(\mathbf{X});\partial\Omega)}\|q\|_{L^2(\Omega)} \tag{B.46}$$

since $\det((\nabla\Phi)^{-1}) = (\det\nabla\Phi)^{-1}$ can be written as $1 + g(x_1, x_2)$ where $g$ is bounded by $C\dfrac{|\mathbf{X}-\mathbf{Y}|}{d(\mathcal{B}(\mathbf{X});\partial\Omega)}$. We translate the problem to $L_0^2(\Omega)$ observing the following. First of all, we recall that $\operatorname{div}\mathbf{u}_{\mathbf{Y}} = 0$ almost everywhere in $\Omega$. By change of variable, we get that, noting $\tilde{q} = q \circ \Phi$,

$$\int_\Omega \tilde{q} \det\nabla\Phi((\nabla\Phi)^{-T}\nabla)\cdot\tilde{\mathbf{u}}_{\mathbf{Y}} d\mathbf{x} = \int_\Omega q \operatorname{div}\mathbf{u}_{\mathbf{Y}} d\mathbf{x} = 0 \text{ for all } \tilde{q} \in L^2(\Omega), \tag{B.47}$$

so in particular

$$\int_\Omega q \det\nabla\Phi((\nabla\Phi)^{-T}\nabla)\cdot\tilde{\mathbf{u}}_{\mathbf{Y}} d\mathbf{x} = 0, \text{ for all } q \in L_0^2(\Omega).$$

Moreover, letting $\bar{p}_{\mathbf{Y}} = \tilde{p}_{\mathbf{Y}} - \dfrac{1}{\Omega}\displaystyle\int_\Omega \tilde{p}_{\mathbf{Y}} d\mathbf{x} \in L_0^2(\Omega)$, we have for all $\mathbf{v} \in (H_0^1(\Omega))^2$

$$\begin{aligned}\int_\Omega \bar{p}_{\mathbf{Y}} \det\nabla\Phi((\nabla\Phi)^{-T}\nabla)\cdot\mathbf{v} d\mathbf{x} &= \int_\Omega \tilde{p}_{\mathbf{Y}} \det\nabla\Phi((\nabla\Phi)^{-T}\nabla)\cdot\mathbf{v} d\mathbf{x} \\ &- \frac{1}{\Omega}\int_\Omega \tilde{p}_{\mathbf{Y}} d\mathbf{x}\int_\Omega \det\nabla\Phi((\nabla\Phi)^{-T}\nabla)\cdot\mathbf{v} d\mathbf{x} = \int_\Omega \tilde{p}_{\mathbf{Y}} \det\nabla\Phi((\nabla\Phi)^{-T}\nabla)\cdot\mathbf{v} d\mathbf{x},\end{aligned}$$

where we use that, thanks to Proposition $B.13$ and divergence theorem,

$$\int_\Omega \det\nabla\Phi((\nabla\Phi)^{-T}\nabla)\cdot\mathbf{v} d\mathbf{x} = \int_\Omega \nabla\cdot(\det\nabla\Phi(\nabla\Phi)\mathbf{v}) d\mathbf{x} = \int_{\partial\Omega} \det\nabla\Phi(\nabla\Phi)\mathbf{v}\cdot\mathbf{n} ds = 0.$$

Consequently, $(\tilde{\mathbf{u}}_{\mathbf{Y}}, \tilde{p}_{\mathbf{Y}}) \in (H_0^1(\Omega))^2 \times L_\Phi^2(\Omega)$ is a solution to $(B.43), (B.44)$ if and only if $(\tilde{\mathbf{u}}_{\mathbf{Y}}, \bar{p}_{\mathbf{Y}}) \in (H_0^1(\Omega))^2 \times L_0^2(\Omega)$ is a solution to $(B.48), (B.49)$. We will then consider the following equivalent problem to $(B.42)$ (we omit the tilde in the test functions)

$$\begin{aligned}&\int_\Omega 2\mu_{\mathbf{X}} \det\nabla\Phi \frac{\nabla\tilde{\mathbf{u}}_{\mathbf{Y}}(\nabla\Phi)^{-1} + (\nabla\Phi)^{-T}\nabla\tilde{\mathbf{u}}_{\mathbf{Y}}^T}{2} : \frac{\nabla\mathbf{v}(\nabla\Phi)^{-1} + (\nabla\Phi)^{-T}\nabla\mathbf{v}^T}{2} d\mathbf{x} \\ &- \int_\Omega \bar{p}_{\mathbf{Y}} \det\nabla\Phi((\nabla\Phi)^{-T}\nabla)\cdot\mathbf{v} d\mathbf{x} = \int_\Omega \det\nabla\Phi\rho_{\mathbf{X}}\mathbf{g}\cdot\mathbf{v} d\mathbf{x}, \text{ for all } \mathbf{v} \in (H_0^1(\Omega))^2,\end{aligned} \tag{B.48}$$

$$\int_\Omega q \det\nabla\Phi((\nabla\Phi)^{-T}\nabla)\cdot\tilde{\mathbf{u}}_{\mathbf{Y}} d\mathbf{x} = 0, \text{ for all } q \in L_0^2(\Omega). \tag{B.49}$$

We now proceed as in the proof of Theorem B.6. We take the difference between $(B.41)$ and $(B.48), (B.49)$ and adding/subtracting the appropriate terms to obtain the following

$$\begin{aligned}\int_\Omega 2\mu_{\mathbf{X}} D(\mathbf{u}_{\mathbf{X}} - \tilde{\mathbf{u}}_{\mathbf{Y}}) : D(\mathbf{v}) d\mathbf{x} - \int_\Omega (p_{\mathbf{X}} - \bar{p}_{\mathbf{Y}}) \operatorname{div}\mathbf{v} d\mathbf{x} &= \rho_{\mathcal{F}} \int_{\Omega\setminus\overline{\mathcal{B}(\mathbf{X})}} (1 - \det\nabla\Phi)\mathbf{g}\cdot\mathbf{v} d\mathbf{x} \\ &+ \int_{\Omega\setminus\overline{\mathcal{B}(\mathbf{X})}} \bar{p}_{\mathbf{Y}}((I - \det\nabla\Phi(\nabla\Phi)^{-1})\nabla)\cdot\mathbf{v} d\mathbf{x} \\ &- 2\mu_{\mathcal{F}} \int_{\Omega\setminus\overline{\mathcal{B}(\mathbf{X})}} (I - (\nabla\Phi)^{-1})\nabla\tilde{\mathbf{u}}_{\mathbf{Y}} : D(\mathbf{v}) d\mathbf{x} \\ - 2\mu_{\mathcal{F}} \int_{\Omega\setminus\overline{\mathcal{B}(\mathbf{X})}} \frac{\nabla\tilde{\mathbf{u}}_{\mathbf{Y}}(\nabla\Phi)^{-1} + (\nabla\Phi)^{-T}\nabla\tilde{\mathbf{u}}_{\mathbf{Y}}^T}{2} &: (I - \det\nabla\Phi(\nabla\Phi)^{-1})\nabla\mathbf{v} d\mathbf{x},\end{aligned} \tag{B.50}$$

$$\int_\Omega q \operatorname{div}(\mathbf{u_X} - \tilde{\mathbf{u}}_\mathbf{Y}) d\mathbf{x} = -\int_{\Omega\setminus\overline{\mathcal{B}(\mathbf{X})}} q((I - \det\nabla\Phi(\nabla\Phi)^{-T})\nabla)\cdot\tilde{\mathbf{u}}_\mathbf{Y} d\mathbf{x}. \tag{B.51}$$

Observe that the right hand sides in both above equations are computed only on $\Omega\setminus\overline{\mathcal{B}(\mathbf{X})}$ since $\nabla\Phi = I$ in $\mathcal{B}(\mathbf{X})$. To conclude, we apply a priori estimates of Theorem $B.4$ with

$$\begin{aligned} F(v) = \rho_\mathcal{F}\int_{\Omega\setminus\overline{\mathcal{B}(\mathbf{X})}}(1-\det\nabla\Phi)\mathbf{g}\cdot\mathbf{v}d\mathbf{x} + \int_{\Omega\setminus\overline{\mathcal{B}(\mathbf{X})}}\bar{p}_\mathbf{Y}((I-\det\nabla\Phi(\nabla\Phi)^{-1})\nabla)\cdot\mathbf{v}d\mathbf{x}\\ -2\mu_\mathcal{F}\int_{\Omega\setminus\overline{\mathcal{B}(\mathbf{X})}}(I-(\nabla\Phi)^{-1})\nabla\tilde{\mathbf{u}}_\mathbf{Y} : D(\mathbf{v})d\mathbf{x}\\ -2\mu_\mathcal{F}\int_{\Omega\setminus\overline{\mathcal{B}(\mathbf{X})}}\frac{\nabla\tilde{\mathbf{u}}_\mathbf{Y}(\nabla\Phi)^{-1} + (\nabla\Phi)^{-T}\nabla\tilde{\mathbf{u}}_\mathbf{Y}^T}{2} : (I-\det\nabla\Phi(\nabla\Phi)^{-1})\nabla\mathbf{v}d\mathbf{x}, \end{aligned}$$

and

$$g = -((I-\det\nabla\Phi(\nabla\Phi)^{-T})\nabla)\cdot\tilde{\mathbf{u}}_\mathbf{Y}.$$

In the notations of Theorem $B.4$ we have $\alpha = 2\mu_{\min}, A = \sqrt{2\mu_\mathbf{X}}I$ and $\beta$ depends only on $\Omega$. Therefore, there exists a constant $C > 0$ depending only on $\Omega$ such that

$$\begin{aligned} &\|\nabla\mathbf{u_X} - \nabla\tilde{\mathbf{u}}_\mathbf{Y}\|_{L^2(\Omega)}\\ &\quad\le \frac{C}{\mu_{\min}}\left(\|1-\det\nabla\Phi\|_{L^\infty(\Omega)}\rho_\mathcal{F}|\mathbf{g}| + \left\|I-\det\nabla\Phi(\nabla\Phi)^{-1}\right\|_{L^\infty(\Omega)}\|\bar{p}_\mathbf{Y}\|_{L^2(\Omega)}\right.\\ &\qquad +\mu_\mathcal{F}\left\|I-(\nabla\Phi)^{-1}\right\|_{L^\infty(\Omega)}\|\nabla\tilde{\mathbf{u}}_\mathbf{Y}\|_{L^2(\Omega)}\\ &\qquad \left.+(\mu_\mathcal{F}+\mu_{\min}+\mu_{\max})\left\|I-\det\nabla\Phi(\nabla\Phi)^{-1}\right\|_{L^\infty(\Omega)}\|\nabla\tilde{\mathbf{u}}_\mathbf{Y}\|_{L^2(\Omega)}\right). \end{aligned} \tag{B.52}$$

Note that we have using Proposition B.16 and a priori estimate $(B.31), (B.32)$ that

$$\begin{aligned} \|\nabla\tilde{\mathbf{u}}_\mathbf{Y}\|_{L^2(\Omega)} &\le C\left(1+\frac{|\mathbf{X}-\mathbf{Y}|}{d(\mathcal{B}(\mathbf{X});\partial\Omega)}\right)\|\nabla\mathbf{u_Y}\|_{L^2(\Omega)}\\ &\le C\left(1+\frac{|\mathbf{X}-\mathbf{Y}|}{d(\mathcal{B}(\mathbf{X});\partial\Omega)}\right)\frac{\rho_{\max}}{\mu_{\min}}|\mathbf{g}|, \end{aligned} \tag{B.53}$$

and

$$\begin{aligned} \|\bar{p}_\mathbf{Y}\|_{L^2(\Omega)} \le 2\|\tilde{p}_\mathbf{Y}\|_{L^2(\Omega)} &\le C\left(1+\frac{|\mathbf{X}-\mathbf{Y}|}{d(\mathcal{B}(\mathbf{X});\partial\Omega)}\right)\|p_\mathbf{Y}\|_{L^2(\Omega)}\\ &\le C\left(1+\frac{|\mathbf{X}-\mathbf{Y}|}{d(\mathcal{B}(\mathbf{X});\partial\Omega)}\right)\frac{\rho_{\max}\mu_{\max}}{\mu_{\min}}|\mathbf{g}|. \end{aligned} \tag{B.54}$$

Recalling that we assume $\frac{|\mathbf{X}-\mathbf{Y}|}{d(\mathcal{B}(\mathbf{X});\partial\Omega)}$ small, so we can bound all the high order terms by $\frac{|\mathbf{X}-\mathbf{Y}|}{d(\mathcal{B}(\mathbf{X});\partial\Omega)}$, we finally obtain

$$\|\nabla\mathbf{u_X} - \nabla\tilde{\mathbf{u}}_\mathbf{Y}\|_{L^2(\Omega)} \le C\frac{\mu_{\max}\rho_{\max}|g|}{\mu_{\min}^2}\frac{|\mathbf{X}-\mathbf{Y}|}{d(\mathcal{B}(\mathbf{X});\partial\Omega)}. \tag{B.55}$$

*Part 2.*

We prove $(B.30)$. By change of variable, we have

$$\begin{aligned} \frac{1}{\pi R^2}\left(\int_{\mathcal{B}(\mathbf{X})}\mathbf{u_X}d\mathbf{x} - \int_{\mathcal{B}(\mathbf{Y})}\mathbf{u_Y}d\mathbf{x}\right) &= \frac{1}{\pi R^2}\left(\int_{\mathcal{B}(\mathbf{X})}\mathbf{u_X}d\mathbf{x} - \int_{\mathcal{B}(\mathbf{Y})}\tilde{\mathbf{u}}_\mathbf{Y}\det\nabla\Phi d\mathbf{x}\right)\\ &= \frac{1}{\pi R^2}\left(\int_{\mathcal{B}(\mathbf{X})}(\mathbf{u_X}-\tilde{\mathbf{u}}_\mathbf{Y})d\mathbf{x} + \int_{\mathcal{B}(\mathbf{Y})}\tilde{\mathbf{u}}_\mathbf{Y}(1-\det\nabla\Phi)d\mathbf{x}\right). \end{aligned}$$

Using Cauchy-Schwarz and Poincaré inequalities yields

$$\frac{1}{\pi R^2}\left(\int_{\mathcal{B}(\mathbf{X})}\mathbf{u}_{\mathbf{X}}d\mathbf{x}-\int_{\mathcal{B}(\mathbf{Y})}\mathbf{u}_{\mathbf{Y}}d\mathbf{x}\right)\leq\frac{C}{\sqrt{\pi}R}\left(\|\nabla\mathbf{u}_{\mathbf{X}}-\nabla\tilde{\mathbf{u}}_{\mathbf{Y}}\|_{L^2(\Omega)}+\|1-\det\nabla\Phi\|_{L^\infty(\Omega)}\|\nabla\tilde{\mathbf{u}}_{\mathbf{Y}}\|_{L^2(\Omega)}\right).$$

Finally, by estimate *iv*) of Proposition $B.14$, ($B.53$) and ($B.55$), we finally obtain that

$$\frac{1}{\pi R^2}\left(\int_{\mathcal{B}(\mathbf{X})}\mathbf{u}_{\mathbf{X}}d\mathbf{x}-\int_{\mathcal{B}(\mathbf{Y})}\mathbf{u}_{\mathbf{Y}}d\mathbf{x}\right)\leq C\frac{\mu_{\max}\rho_{\max}|g|}{R\mu_{\min}^2}\frac{|\mathbf{X}-\mathbf{Y}|}{d(\mathcal{B}(\mathbf{X});\partial\Omega)},$$

where all the higher order terms in $\frac{|\mathbf{X}-\mathbf{Y}|}{d(\mathcal{B}(\mathbf{X});\partial\Omega)}$ were bounded by $\frac{|\mathbf{X}-\mathbf{Y}|}{d(\mathcal{B}(\mathbf{X});\partial\Omega)}$. □

**Remark B.17.**
Note that if, for $\mathbf{X}'\in\mathbb{R}^2$, the function $\mu_{\mathbf{X}'},\rho_{\mathbf{X}'}$ given by (B.23) are Lipschitz functions with respect to the position of the center $\mathbf{X}'$ (for instance by using a regularization of the characteristic functions $\chi_{\mathcal{B}(\mathbf{X}')}$), then the proof is easier. By taking directly the difference between the problems (B.41) and (B.42) and using the Lipschitz continuity of the coefficients, one can prove that there exists a constant $K$ that does not depend on $\mathbf{X}$ and $\mathbf{Y}$ such that

$$\|\nabla(\mathbf{u}_{\mathbf{X}}-\mathbf{u}_{\mathbf{Y}})\|_{L^2(\Omega)}\leq K|\mathbf{X}-\mathbf{Y}|, \tag{B.56}$$

that is to say the flow are Lipschitz continuous with respect to the position of the center of the disks (compared with (B.55) in the proof above where we obtain a similar result for $\mathbf{u}_{\mathbf{X}}$ and $\tilde{\mathbf{u}}_{\mathbf{Y}}$). Then, we can easily estimate that

$$\begin{aligned}\left|\int_{\mathcal{B}(\mathbf{X})}\mathbf{u}_{\mathbf{X}}d\mathbf{x}-\int_{\mathcal{B}(\mathbf{Y})}\mathbf{u}_{\mathbf{Y}}d\mathbf{x}\right|&\leq\left|\int_{\mathcal{B}(\mathbf{X})}\mathbf{u}_{\mathbf{X}}d\mathbf{x}-\int_{\mathcal{B}(\mathbf{X})}\mathbf{u}_{\mathbf{Y}}d\mathbf{x}\right|+\left|\int_{\mathcal{B}(\mathbf{X})}\mathbf{u}_{\mathbf{Y}}d\mathbf{x}-\int_{\mathcal{B}(\mathbf{Y})}\mathbf{u}_{\mathbf{Y}}d\mathbf{x}\right|\\&\leq\int_{\mathcal{B}(\mathbf{X})}|\mathbf{u}_{\mathbf{X}}-\mathbf{u}_{\mathbf{Y}}|d\mathbf{x}+\int_{\mathcal{B}(\mathbf{X})\setminus\mathcal{B}(\mathbf{X})\cap\mathcal{B}(\mathbf{Y})}|\mathbf{u}_{\mathbf{Y}}|d\mathbf{x}+\int_{\mathcal{B}(\mathbf{Y})\setminus\mathcal{B}(\mathbf{X})\cap\mathcal{B}(\mathbf{Y})}|\mathbf{u}_{\mathbf{Y}}|d\mathbf{x}\\&\leq C\|\nabla(\mathbf{u}_{\mathbf{X}}-\mathbf{u}_{\mathbf{Y}})\|_{L^2(\Omega)}+\|\mathbf{u}_{\mathbf{Y}}\|_{L^\infty(\Omega)}|\mathcal{B}(\mathbf{X})\setminus\mathcal{B}(\mathbf{X})\cap\mathcal{B}(\mathbf{Y})|+\|\mathbf{u}_{\mathbf{Y}}\|_{L^\infty(\Omega)}|\mathcal{B}(\mathbf{Y})\setminus\mathcal{B}(\mathbf{X})\cap\mathcal{B}(\mathbf{Y})|,\end{aligned}$$

where $C$ depends only on $\Omega$ and we use the fact $\mathbf{u}_{\mathbf{Y}}$ is bounded, since it belongs to $(H^2(\Omega))^2$ (see Theorem B.8) due to the smoothness of the coefficients. Then, computing that $|\mathcal{B}(\mathbf{X})\setminus\mathcal{B}(\mathbf{X})\cap\mathcal{B}(\mathbf{Y})|,|\mathcal{B}(\mathbf{Y})\setminus\mathcal{B}(\mathbf{X})\cap\mathcal{B}(\mathbf{Y})|\leq C'|\mathbf{X}-\mathbf{Y}|$ where $C'$ depends only on the radius $R$ and using (B.56), we can conclude finally that

$$\left|\int_{\mathcal{B}\mathbf{X}}\mathbf{u}_{\mathbf{X}}d\mathbf{x}-\int_{\mathcal{B}\mathbf{Y}}\mathbf{u}_{\mathbf{Y}}d\mathbf{x}\right|\leq C''|\mathbf{X}-\mathbf{Y}|,$$

$C''$ depends on $\Omega, R, \mathbf{u}_{\mathbf{Y}}$ and $K$.

These manipulations (in particular to prove (B.56)) are unfortunately not possible in the case of non-smooth coefficients. This is why we use the diffeomorphism $\Phi$ to define every quantities on $\mathcal{B}(\mathbf{X})$.

# Bibliography


[1] M. Ainsworth and J. T. Oden. A posteriori error estimation in finite element analysis. *Computer Methods in Applied Mechanics and Engineering*, 142(1):1–88, 1997.

[2] G. Akrivis and P. Chatzipantelidis. A posteriori error estimates for the two-steps backward differentiation formula method for parabolic equations. *SIAM J. Num. Analysis*, 48:109–132, 2010.

[3] G. Akrivis, C. Makridakis, and R. H. Nochetto. A posteriori error estimates for the Crank-Nicolson method for parabolic equations. *Math. Comp*, 75:511–531, 2006.

[4] Georgios Akrivis, Charalambos Makridakis, and Ricardo H. Nochetto. Optimal order a posteriori error estimates for a class of Runge–Kutta and Galerkin methods. *Numerische Mathematik*, 114(1):133, Aug 2009.

[5] F. Alauzet and M. Mehrenberger. $P^1$-conservative solution interpolation on unstructured triangular meshes. *Int. J. Numer. Meth. Engng*, 84:1552–1588, 2010.

[6] Frédéric Alauzet and Adrien Loseille. A decade of progress on anisotropic mesh adaptation for computational fluid dynamics. *Comput.-Aided Des.*, 72:13–39, 2016.

[7] I. Babushka and A. Aziz. On the angle condition in the finite element method. *SIAM Journal on Numerical Analysis*, 13(2):214–226, 1976.

[8] I. Babushka, J. Chandra, and J.E. Flaherty. *Adaptive Methods for Partial Differential Equations*. Proceedings in Applied Mathematics. Society for Industrial and Applied Mathematics, 1989.

[9] I. Babushka, R. Durán, and R. Rodríguez. Analysis of the efficiency of an a posteriori error estimator for linear triangular finite elements. *SIAM Journal on Numerical Analysis*, 29(4):947–964, 1992.

[10] I. Babushka and W. C. Rheinboldt. A-posteriori error estimates for the finite element method. *International Journal for Numerical Methods in Engineering*, 12(10):1597–1615, 1978.

[11] E Bänsch, F Karakatsani, and Ch. Makridakis. The effect of mesh modification in time on the error control of fully discrete approximations for parabolic equations. *Applied Numerical Mathematics*, 67:35–63, 2013.

[12] C. Bardos. Problèmes aux limites pour les équations aux dérivées partielles du premier ordre à coefficients réels; théorèmes d'approximations; application à l'équation du transport. *Annales scientifiques de l' É.N.S*, tome 3(2):185–233, 1970.

[13] T.J. Barth and H. Deconinck. *Error Estimation and Adaptive Discretization Methods in Computational Fluid Dynamics*. Lecture Notes in Computational Science and Engineering. Springer Berlin Heidelberg, 2002.

[14] C. Bernardi and E. Süli. Time and space adaptivity for the second-order wave equation. *Mathematical Models and Methods in Applied Sciences*, 15(02):199–225, 2005.

[15] C. Bernardi and R. Verfürth. Adaptive finite element methods for elliptic equations with non-smooth coefficients. *Numer. Math.*, 85:579–608, 2000.

[16] C. Bernardi and R. Verfürth. A posteriori error analysis of the fully discretized time-dependent Stokes equations. *Math. Model. Numer. Anal.*, 38:437–455, 2004.

[17] Stefano Berrone. Adaptive discretization of stationary and incompressible Navier–Stokes equations by stabilized finite element methods. *Computer Methods in Applied Mechanics and Engineering*, 190(34):4435–4455, 2001.

[18] Edward Boey, Yves Bourgault, and Thierry Giordano. Anisotropic space-time adaptation for reaction-diffusion problems. 2017.

[19] H. Borouchaki and P.-L. George. *Triangulation de Delaunay et maillage.* HERMES, 1997.

[20] Y. Bourgault and M. Picasso. Anisotropic error estimates and space adaptivity for a semidiscrete finite element approximation of the transient transport equation. *SIAM J. Sci. Comput.*, 35(2):A1192–A1211, 2013.

[21] F. Boyer and P. Fabrie. *Mathematical Tools for the Study of the Incompressible Navier-Stokes Equations and Related Models*, volume 183 of *Applied Mathematical Sciences.* Springer, 2013.

[22] E. Burman. Consistent SUPG-method for transient transport problems : Stability and convergence. *Comput. Methods Appl. Mech. Engrg.*, 199:1114–1123, 2010.

[23] E. Bänsch and A. Brenner. A posteriori error estimates for pressure-correction schemes. *SIAM J. Num. Analysis*, 54:2323–2358, 2016.

[24] E. Bänsch, F. Karakatsani, and C. Makridakis. A posteriori error control for fully discrete crank–nicolson schemes. *SIAM Journal on Numerical Analysis*, 50(6):2845–2872, 2012.

[25] G. Caloz and J. Rappaz. *Numerical analysis for nonlinear and bifurcation problems*, volume 5, pages 487–637. North Holland, 1997.

[26] A. Cangiani, E. Gerogoulis, and S. Metcalfe. Adaptive discontinuous galerkin methods for nonstationnary convection-diffusion problems. *IMA Journal of Numerical Analysis*, pages 1–20, 2013.

[27] Weiming Cao. Superconvergence analysis of the linear finite element method and a gradient recovery postprocessing on anisotropic meshes. *Math. Comput.*, 84:89–117, 2014.

[28] C. Carstensen and R. Verfürth. Edge Residuals Dominate a Posteriori Error Estimates for Low Order Finite Element Methods. *SIAM J. Numer. Anal*, 36(5):1571–1587, 1999.

[29] M. J. Castro-Diaz, F. Hecht, B. Mohammadi, and O. Pironneau. Anisotropic unstructured mesh adaption for flow simulations. *Internat. J. Numer. Methods Fluids*, 25(4):475–491, 1997.

[30] S. Chandrasekhar. *Hydrodynamic and Hydromagnetic Stability.* Dover Books on Physics. Dover Publications, 2013.

[31] Y. C. Chang, T. Y. Hou, B. Merriman, and S. Osher. A Level Set Formulation of Eulerian Interface Capturing Methods for Incompressible Fluid Flows. *J. Comput. Phys.*, 124:449–463, 1996.

[32] Y.C. Chang, T.Y. Hou, B. Merriman, and S. Osher. A level set formulation of eulerian interface capturing methods for incompressible fluid flows. *Journal of Computational Physics*, 124(2):449 – 464, 1996.

[33] P.G. Ciarlet. *Mathematical Elasticity, Volume I: Three-Dimensional Elasticity*, volume 20 of *Stud. Math. Appl.* North-Holland, 1988.

[34] P.G. Ciarlet. *The Finite Element Method for Elliptic Problems.* Classics in Applied Mathematics. Society for Industrial and Applied Mathematics, 2002.

[35] P. Clément. Approximation by finite element functions using local regularization. *RAIRO Annal. Numér.*, 9(R2):77–84, 1975.

[36] Bernardo Cockburn and Pierre-Alain Gremaud. Error estimates for finite element methods for scalar conservation laws. *SIAM J. Numer. Anal.*, 33(2):522–554, 1996.

[37] T. Coupez. Metric construction by length distribution tensor and edge based error for anisotropic adaptive meshing. *J. Comput. Phys.*, 230(7):2391–2405, 2011.

[38] J. Crank and P. Nicolson. A practical method for numerical evaluation of solutions of partial differential equations of the heat-conduction type. *P. Adv. Comput.Math.*, 6, 1996.

[39] Willy Dörfler. A time- and space adaptive algorithm for the linear time-dependent Schrödinger equation. *Numerische Mathematik*, 73(4):419–448, 1996.

[40] P. G. Drazin and W. H. Reid. *Hydrodynamic Stability.* Cambridge Mathematical Library. Cambridge University Press, 2 edition, 2004.

[41] S. Dubuis and M. Picasso. An Adaptive Algorithm for the Time Dependent Transport Equation with Anisotropic Finite Elements and the Crank-Nicolson Scheme. *J. Sci. Comput.*, 75(1):350–375, 2018.

[42] Willy Dörfler. A convergent adaptive algorithm for poisson's equation. *Siam Journal on Numerical Analysis - SIAM J NUMER ANAL*, 33, 06 1996.

[43] P. E. Farell, M. D. Piggott, C. C. Pain, G. J. Gorman, and C. R. Wilson. Conservative interpolation between unstructured meshes via supermesh construction. *Comput. Methods Appl. Mech. Engrg.*, 198:2632–2642, 2009.

[44] L. Formaggia and S. Perotto. New anisotropic a priori error estimates. *Numer. Math.*, 89:641–667, 2001.

[45] L. Formaggia and S. Perotto. Anisotropic error estimates for elliptic problems. *Numer. Math.*, 94:67–92, 2003.

[46] Luca Formaggia, Stefano Micheletti, and Simona Perotto. Anisotropic mesh adaptation in computational fluid dynamics: Application to the advection–diffusion–reaction and the Stokes problems. *Applied Numerical Mathematics*, 51(4):511–533, 2004.

[47] Luca Formaggia, Simona Perotto, and Paolo Zunino. An anisotropic a-posteriori error estimate for a convection-diffusion problem. *Computing and Visualization in Science*, 4(2):99–104, Dec 2001.

[48] L. P. Franca and S. L. Frey. Stabilized finite elements methods: II. The incompressible Navier-Stokes equations. *Comput. Methods Appl. Mech. Engrg.*, 99:209–233, 1992.

[49] P. J. Frey and P.-L. George. *Maillages.* HERMES, 1999.

[50] R. Glowinski. *Numerical Methods for Fluids.* Number Part 3 in Handbook of Numerical Analysis. North Holland, 2003.

[51] O. Gorynina. *Eléments finis adaptatifs pour l'équation des ondes instationnaires.* PhD thesis, Université ouverte de Franche-Comté, 2018.

[52] P. Grisvard. *Elliptic Problems in Nonsmooth Domains.* Classics in Applied Mathematics. Society for Industrial and Applied Mathematics, 2011.

[53] J.-L. Guermond and A. Salgado. A splitting method for incompressible flows with variable density based on pressure poisson equation. *Journal of Computational Physics*, 228:2834–2846, 2009.

[54] D. Guignard, F. Nobile, and M. Picasso. *A posteriori* error estimation for the steady navier-stokes equations in random domains. *Comput. Methods Appl. Mech. Engrg.*, 313:483–511, 2017.

[55] Thomas Frédéric Hilke. *Méthodes numériques liées à la distribution d'alumine dans une cuve d'électrolyse d'aluminium.* PhD thesis, EPFL, 2019.

[56] M. Hillairet. Lack of collision between solid bodies in a 2D incompressible viscous flow. *Communications in Partial Differential Equations*, 32(9), 2007.

[57] J. Janela, A. Lefebvre, and B. Maury. A penalty method for the simulation of fluid-rigid body interaction. *ESSAIM Proc*, 14:115–123, 2005.

[58] J.Heywood and R.Rannacher. Finite-element approximation of the nonstationary Navier-Stokes problem. part i: Regularity of solutions and second-order error estimates for spatial discretization. *SIAM J. Numer. Anal*, 19(2):275–311, 1982.

[59] J.Heywood and R.Rannacher. Finite-element approximation of the nonstationary Navier-Stokes problem. part iv: Error analysis for second-order time discretization. *SIAM J. Numer. Anal*, 27(2):353–384, 1990.

[60] C. Johnson, U. Nävert, and J. Pitkäranta. Finite Element Methods For Linear Hyperbolic Problems. *Comput. Methods Appl. Mech. Engrg.*, 45:285–312, 1984.

[61] F. Karakatsani and C. Makridakis. A posteriori estimates for approximations of time-dependent Stokes equations. *IMA Journal of Numerical Analysis*, 27:741–764, 2006.

[62] R. B. Kellogg and J. E. Osborn. A Regularity Result for the Stokes Problem in a Convex Polygon. *Journal of functional analysis*, 21:397–431, 1976.

[63] G. Kunert. An a posteriori residual error estimator for the finite element method on anisotropic tetrahedral meshes. *Numer. Math.*, 86(3):471–490, 2000.

[64] G. Kunert and S. Nicaise. Zienkiewicz-Zhu error estimatos on anisotropic tetrahedral and triangular finite element meshes. *M2AN Math. Model. Numer. Anal.*, 37(6):1013–1043, 2003.

[65] O. Lakkis and C. Makridakis. Elliptic reconstruction and a posteriori error estimates for fully discretized linear parabolic problems. *Mathematics of Computation*, 75(256):1627–1658, 2006.

[66] S. Larsson and E. D. Svensson. Pointwise a posteriori error estimates for the Stokes equations in polyhedral domains. Preprint, 2006.

[67] P. Laug and H. Borouchaki. The BL2D Mesh Generator: Beginner's Guide, User's and Programmer's Manual. *Technical report RT-0194, Institut National de Recherche en Informatique et Automatique (INRIA), Rocquencourt, Le Chesnay, France*, 1996.

[68] V. Laurmaa. *An octree-based adaptive semi-Lagrangian free surface flow solver*. PhD thesis, Ecole polytechnique fédérale de Lausanne, 2016.

[69] P.-L. Lions. *Mathematical Topics in Fluid Mechanics. Volume 1 Incompressible Models*. Oxford, 1996.

[70] C. Liu and N. Walkington. Convergence of numerical approximations of the incompressible navier-stokes equations with variable density and viscosity. *SIAM J. Numerical Analysis*, 45:1287–1304, 2007.

[71] A. Loseille and A. Löhner. Anisotropic mesh generation for high-fidelity simulations in cfd. INRIA Preprint, 2014.

[72] A. Lozinski, M. Picasso, and V. Prachittham. An anisotropic error estimator for the Crank-Nicolson method : application to a parabolic problem. *SIAM J. Sci. Comput.*, 31(2):2757–2783, 2009.

[73] Alexei Lozinski, Olga Gorynina, and Marco Picasso. Time and space adaptivity of the wave equation discretized in time by a second-order scheme. *IMA Journal of Numerical Analysis*, 00:1–34, 2018.

[74] C. Makridakis and R. H. Nochetto. Elliptic reconstruction and a posteriori error estimates for parabolic problems. *SIAM J. Numer. Anal*, 41:1585–1594, 2003.

[75] V. Maronnier. *Simulation numérique d'écoulements de fluides incompressibles avec surface libre*. PhD thesis, Ecole polytechnique fédérale de Lausanne, 2000.

[76] J. Alonso San Martin, V. Starovoitov, and M. Tucsnak. Global Weak Solutions for the Two-Dimensional Motion of Several Rigid Bodies in an Incompressible Viscous Fluid. *Arch. Rational Mech. Anal.*, 161:113–147, 2002.

[77] B. Maury. Numerical analysis of a finite element/volume penalty method. *SIAM J. Numer. Anal*, 47(2):1126–1148, 2009.

[78] S. Micheletti, S. Perotto, and M.Picasso. Stabilized finite elements on anisotropic meshes : a priori error estimates for the advection-diffusion and the Stokes problems. *SIAM J. Numer. Anal*, 41(3):1131–1162, 2003.

[79] R. H. Nochetto, A. Schmidt, and C. Verdi. A posteriori error estimation and adaptivity for degenerate parabolic problems. *Mathematics of Computation*, 69(229):1–24, 2000.

[80] R. W. Ogden. *Non-Linear Elastic Deformations.* Mathematics and Its Applications. Ellis Horwood, 1984.

[81] R. Rannacher P. Houston and E. Süli. A posteriori error analysis for stabilised finite element approximations of transport problems. *Computer Methods in Applied Mechanics and Engineering*, 190(11):1483–1508, 2000.

[82] M. Picasso. Adaptive finite elements for a linear parabolic problem. *Comput. Methods Appl. Mech. Engrg.*, 167:223–237, 1998.

[83] M. Picasso. A stopping criterion for the conjugate gradient algorithm in the framework of anisotropic adaptive finite elements. *Commun. Numer. Meth. Engng.*, 00:1-6, 2000.

[84] M. Picasso. Numerical study of the effectivity index for an anisotropic error indicator based on Zienkiewicz-Zhu error estimator. *Commun. Numer. Meth. Engng*, 19(1):13–23, 2002.

[85] M. Picasso. An anisotropic error estimator indicator based on Zienkiewicz-Zhu error estimator : application to elliptic and parabolic problems. *SIAM J. Sci. Comput.*, 24(4):1328–1355, 2003.

[86] M. Picasso. An adaptive algorithm for the Stokes problem unsing continuous, piecewise linear stabilized finite elements and meshes with high aspect ratio. *Applied Numerical Mathematics*, 54:470–490, 2005.

[87] M. Picasso. Adaptive finite elements with large aspect ratio based on an anisotropic error estimator involving first order derivatives. *Comput. Methods Appl. Mech. Engrg.*, 196:14–23, 2006.

[88] M. Picasso. Numerical study of an anisotropic error estimator in the $L^2(H^1)$ norm for the finite element discretization of the wave equation. *SIAM J. Sci. Comput.*, 32:2213–2234, 2010.

[89] M. Picasso and J. Rappaz. Stability of Time-Splitting Schemes for the Stokes Problem with Stabilized Finite Elements. *Numer Methods Partial Differential Eq*, 17:632–656, 2001.

[90] Marco Picasso and Virabouth Prachittham. An adaptive algorithm for the Crank–Nicolson scheme applied to a time-dependent convection–diffusion problem. *Journal of Computational and Applied Mathematics*, 233(4):1139–1154, 2009.

[91] A. Quarteroni. *Numerical Models for Differential Problems.* MS&A. Springer Milan, 2010.

[92] A. Quarteroni and A. Valli. *Numerical Approximation of Partial Differential Equations.* Springer, 2008.

[93] Jonathan Rochat. *Approximation numérique des écoulements turbulents dans des cuves d'électrolyse de l'aluminium.* PhD thesis, EPFL, 2016.

[94] N. Sauerwald. An adaptive method for solving stokes' flow around a falling sphere. Master's thesis, EPFL, 2014.

[95] H.M. Soner, W. Bangerth, R. Rannacher, H. Foellmer, and L.C.G. Rogers. *Adaptive Finite Element Methods for Differential Equations.* Adaptive Finite Element Methods for Differential Equations. Springer, 2003.

[96] Victor N. Starovoitov. Behavior of a rigid body in an incompressible viscous fluid near a boundary. In Pierluigi Colli, Claudio Verdi, and Augusto Visintin, editors, *Free Boundary Problems*, pages 313–327. Birkhäuser Basel, 2004.

[97] D. Strütt. *Sur quelques équations aux dérivées partielles en lien avec le lemme de Poincaré*. PhD thesis, Ecole polytechnique fédérale de Lausanne, 2018.

[98] Endre Süli and Paul Houston. *Adaptive Finite Element Approximation of Hyperbolic Problems*, pages 269–344. Springer Berlin Heidelberg, 2003.

[99] R. Temam. *Navier-Stokes Equations : Theory and Numerical Analysis*. North-Holland, 1977.

[100] G. Tryggvason. Numerical simulations of the Rayleigh-Taylor instability. *Journal of Computational Physics*, 75:253–282, 1988.

[101] R. Verfürth. A posteriori error estimates for finite element discretizations of the heat equation. *Calcolo*, 40(3):195–212, dec 2003.

[102] R. Verfürth. *A Posteriori Error Estimation Techniques for Finite Element Methods*. A Posteriori Error Estimation Techniques for Finite Element Methods. OUP Oxford, 2013.

[103] R. Verfürth. A Posteriori Error Estimates for Nonlinear Problems. Finite Element Discretizations of Elliptic Equations. *Mathematics of Computation*, 62(206):445–475, 1994.

[104] R Verfürth. A posteriori error estimation and adaptive mesh-refinement techniques. *J. Comput. Appl. Math*, 50:67–83, 1994.

[105] R Verfürth. *A review of A Posteriori Error Estimation and Adaptive Mesh-Refinement Techniques*. Wiley-Teubner, 1996.

[106] R. Verfürth. A posteriori error estimates for nonlinear problems: $L^r, (0, T; W^r, \rho(\Omega))$-error estimates for finite element discretizations of parabolic equations. *Numerical Methods for Partial Differential Equations*, 14(4):487–518, 1998.

[107] T. Zhang and S. Li. A posteriori error estimates of finite element method for the time-dependent navier-stokes equations. *Appl. Math. Comp.*, 315:13–26, 2017.

[108] O. C. Zienkiewicz and J. Z. Zhu. A simple error estimator and adaptive procedure for practical engineering analysis. *Int. J. Numer. Mehtods Engrg.*, 24(2):337–357, 1987.

[109] O. C. Zienkiewicz and J. Z. Zhu. Analysis of the Zienkiewicz-Zhu a posteriori error estimator in the finite element method. *Int. J. Numer. Mehtods Engrg.*, 28(9):2161–2174, 1989.

[110] O. C. Zienkiewicz and J. Z. Zhu. The superconvergent patch recovery and a posteriori error estimates. I. the recovery technique. *Int. J. Numer. Mehtods Engrg.*, 33(7):1331–1364, 1992.

# Curriculum Vitae

## Samuel Dubuis

EPFL

Phone : +41 21 693 25 13

Email: samuel.dubuis@epfl.ch

Born: May 21, 1988-Martigny, Switzerland

### Education

2008-2014: MSc in Mathematics, EPFL Lausanne
2014-2019: PhD in Mathematics, EPFL Lausanne

### Publications

S. Dubuis and M. Picasso, An Adaptive Algorithm for the Time Dependent Transport Equation with Anisotropic Finite Elements and the Crank-Nicolson Scheme, *J. Sci. Comput.* 75: 350–375, 2018

### Teaching

2014-2019 : Teaching assistant for analysis and numerical analysis